1990 ANNUAL TROPICAL CYCLONE REPORT

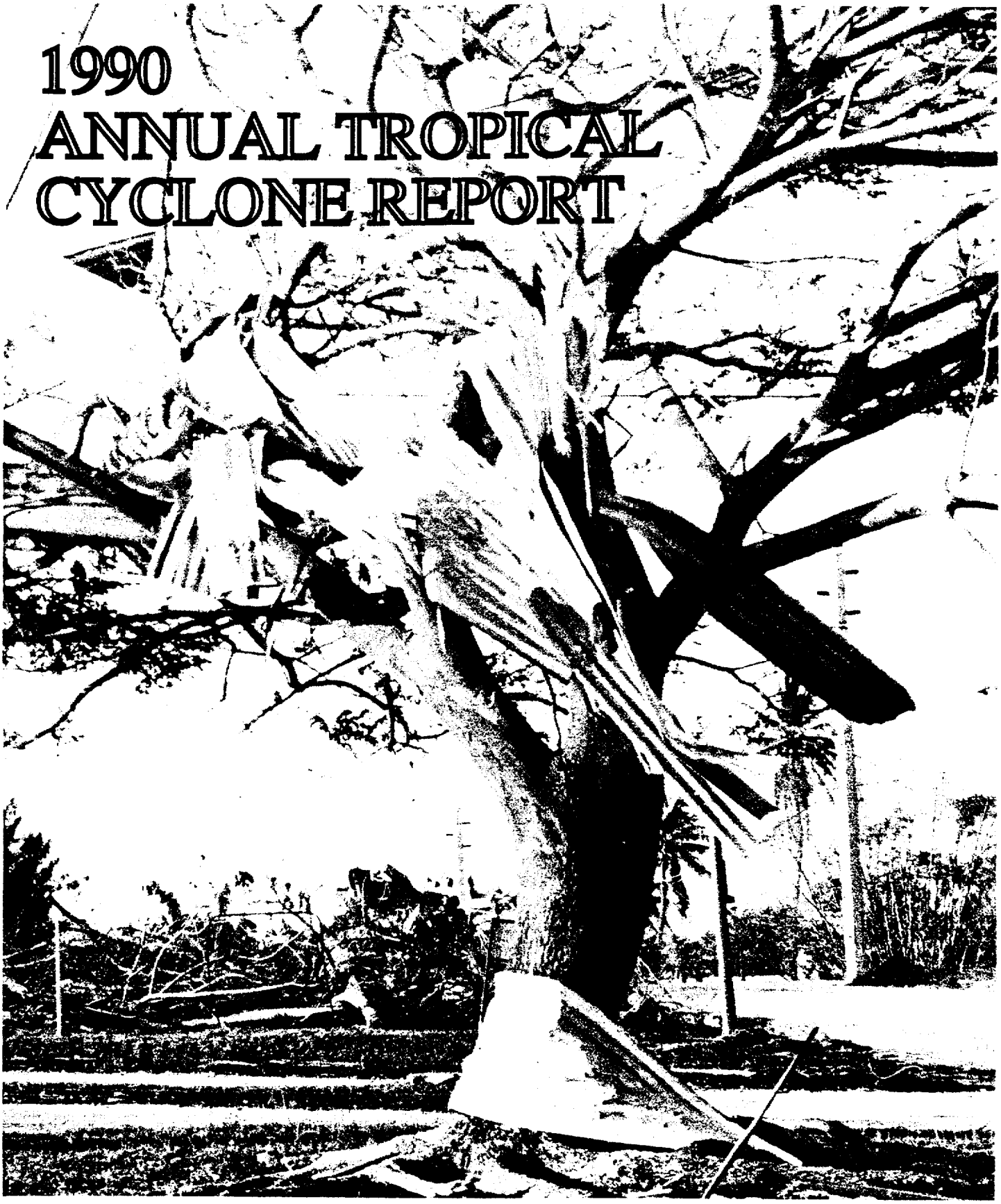

JOINT TYPHOON WARNING CENTER
GUAM, MARIANA ISLANDS

COVER CAPTION: Corrugated sheet iron roofing material wrapped around a splintered flame tree at commissary junction, Guam, bears mute testimony to the fury of Typhoon Russ' passage just four days before Christmas (Photo courtesy of NOCC/JTWC/Mr. F. H. Wells).

U. S. NAVAL OCEANOGRAPHY COMMAND CENTER
JOINT TYPHOON WARNING CENTER
COMNAVMARIANAS BOX 12
FPO SAN FRANCISCO, CA 96630-2926

DIETER K. RUDOLPH

CAPTAIN, UNITED STATES NAVY
COMMANDING OFFICER

CHARLES P. GUARD

LIEUTENANT COLONEL, UNITED STATES AIR FORCE
DIRECTOR, JOINT TYPHOON WARNING CENTER
COMMANDER, DETACHMENT 1, 1ST WEATHER WING

STAFF

JOINT TYPHOON WARNING CENTER

	LCDR	NICHOLAS D. GURAL	USN	DEPUTY DIRECTOR
	LCDR	LESTER E. CARR, III	USN	DEPUTY DIRECTOR, TECH DEVLP
	LCDR	ROBERT L. BEARD	USN	TDO
*	LCDR	RICHARD H. BOUCHARD	USN	TDO, EDITOR
	CAPT	DAN B. MUNDELL	USAF	TDO
	CAPT	ANN R.GOETZ	USAF	TDO, BEST TRACKS
	CAPT	BRUCE W. THOMPSON	USAF	TDO
	LT	STACY R. STEWART	USNR	TDO **
	LTJG	RICHARD A. JEFFRIES	USN	TDO
	AGCS	PATRICK J. HENDRICKS	USN	LCPO
	AG2	BARRY F. BROCKMAN	USN	TDA, LPO
*	SSGT	JAMES B. WIEMANN	USAF	TDA, GRAPHICS NCOIC
*	AG3	JEREMY D. WILLIAMS	USN	TDA, STATISTIC PO
*	SGT	HOLLY A. JENNINGS	USAF	TDA, GRAPHICS
*	AG3	KIMBERLEY J. WOODS	USN	TDA
	AG3	JEFFREY B. ARMBRUSTER	USN	TDA, STATISTICS
	AG3	HOLLY L. HOULIHAN	USN	TDA
	AG3	TRACEY R. MARTIN	USN	TDA, STATISTICS
*	SRA	PATRICIO M. HERNANDEZ JR.	USAF	TDA
	SRA	LANCE W. CASHMAN	USAF	TDA
*	AGAN	LAURA A. MASTERS	USN	TDA
	A1C	TIMOTHY J. GALLAGHER	USAF	TDA
	AGAA	GEORGE P. JOHNSON	USN	TDA
	AGAA	GLENDA D. SCAGGS	USN	TDA
	AMN	JEREMY A. ENTWISTLE	USAF	TDA

DET 1, 1WW

*	MAJ	JOEL D. MARTIN	USAF	TDO, TECHNIQUE DEVELOPMENT
	CAPT	DANIEL N. SHOEMAKER	USAF	TDO, TECHNIQUE DEVELOPMENT
*	CAPT	TIM D. HUTCHISON	USAF	MSC
*	CAPT	ROBERT J. FALVEY	USAF	TDO, DATA DEVELOPMENT
	1LT	ROBERT G. HUDSON	USAF	MSC
	1LT	JOSEPH A. HANSER	USAF	DATA DEVELOPMENT
	MSGT	CHARLES P. BONINI	USAF	TECHNIQUE DEVELOPMENT, NCOIC
	TSGT	DANILO O. MONTILLANO	USAF	INFORMATION MANAGEMENT, CHIEF
	TSGT	BRIAN P. BURKE	USAF	ANALYST, NCOIC
	SSGT	MICHELLE R. TIMPERIO	USAF	ANALYST
	SSGT	PAUL F. HARPER	USAF	ANALYST
	SSGT	RAYMOND L. SOUZA, JR.	USAF	ANALYST
	SSGT	WAYNE I. GENTRY	USAF	ANALYST
	SSGT	DANIEL T. EBBERT	USAF	ANALYST

ATCR STAFF

LT	DIANNE K. EDSON	USN	TDO, STATISTICS OFFICER, EDITOR
MR	FRANK H. WELLS	CIV	TECHNICAL EDITOR
SGT	BRIAN L. McDONALD	USAF	SENIOR TDA, GRAPHICS
SGT	CARLOS A. DELANUEZ	USAF	TDA, GRAPHICS, STATISTICS NCOIC
SGT	RAY O. BELEW	USAF	TDA, GRAPHICS NCOIC

ONR POST - DOCTORATE FELLOW

DR	MARK A. LANDER	UNIVERSITY OF HAWAII

* TRANSFERRED DURING 1990
** ACTIVE DUTY TRAINING

FOREWORD

The Annual Tropical Cyclone Report is prepared by the staff of the Joint Typhoon Warning Center (JTWC), a combined Air Force/Navy organization operating under the command of the Commanding Officer, U.S. Naval Oceanography Command Center/Joint Typhoon Warning Center, Guam. JTWC was founded 1 May 1959 when USCINCPAC directed that a single tropical cyclone warning center be established for the western North Pacific region. The operations of JTWC are guided by CINCPACINST 3140.1T.

The mission of the Joint Typhoon Warning Center is multi-faceted and includes:

1. Continuous monitoring of all tropical weather activity in the Northern and Southern Hemispheres, from 180 degrees longitude westward to the east coast of Africa, and the prompt issuance of appropriate advisories and alerts when tropical cyclone development is anticipated.

2. Issuance of warnings on all significant tropical cyclones in the above area of responsibility.

3. Determination of requirements for tropical cyclone reconnaissance and assignment of appropriate priorities.

4. Post-storm analysis of significant tropical cyclones occurring within the western North Pacific and North Indian Oceans, which includes an in-depth analysis of tropical cyclones of note and all typhoons.

5. Cooperation with the Naval Oceanographic and Atmopheric Research Laboratory (NOARL), Monterey, California, on the operational evaluation of tropical cyclone models and forecast aids, and the development of new techniques to support operational forecast scenarios.

The JTWC staff constantly strives to improve the quality of the Annual Tropical Cyclone Report. Last year we sent out questionaires requesting recommendations for improvement. This 1991 edition of the Report contains changes in format and content that represent our attempt to incorporate your recommendations. We hope you find the changes beneficial. In any case, we would like to hear your comments.

Changes in this year's publication include: addition of an Executive Summary; movement of contractions and distribution to Appendices; western North Pacific write-ups included more synoptic details and photos; Tropical cyclone support summary expanded to include local studies; and tropical cyclone warning statistics as well as track and fix data are available upon request to be copied on to user provided diskettes.

JTWC has seen many changes over the past year. Perhaps the most significant was Air Force funding for the Det 1, 1WW Automation Project which should improve satellite reconnaissance support to JTWC.

Special thanks to: Captain Robert J. Plante for his significant contributions and support; the men and women of the 27th Communications Squadron, Operating Location Charlie and the Operations and Equipment Support departments of the Naval Oceanography Command Center, Guam for the high quality real-time satellite imagery support; personnel of the Pacific Fleet Audio-Visual Center, Guam for their assistance in the reproduction of satellite data for this report; the people of the Navy Publications and Printing Service Branch Office, Guam; Dr. Bob Abbey and the Office of Naval Research for their support to the University of Hawaii for the Post Doctorate Fellow at JTWC and their sponsorship of the largest typhoon experiment ever held in the western North Pacific, TCM-90; and Dr. Mark Lander for his training efforts and suggestions.

EXECUTIVE SUMMARY

The following information summarizes the 1990 tropical cyclone season in terms of JTWC's workload, reconnaissance support, forecast errors, and support to the Tropical Cyclone Motion (TCM-90) field experiment which was sponsored by the Office of Naval Research.

In 1990, JTWC issued 794 warnings on 32 tropical cyclones in the western North Pacific Ocean, 46 warnings on four in the North Indian Ocean and 298 warnings on 29 in the Southern Hemisphere, making it the center's busiest year in its history. The following summary shows JTWC's workload in each ocean basin and for the total area of responsibility (AOR):

	NWP	SH	NIO	AOR
Tropical cyclones	32	29	4	65
Days in warning status	165	98	15	239
Days in multiple warning status	54	29	0	83
Total Warnings	**794**	**298**	**47**	**1139**

Almost 5000 satellite fixes supported the tropical cyclone warning mission. In addition, several land-based radar stations in the western North Pacific provided nearly 1000 radar fixes. The NASA DC-8 research aircraft used in TCM-90 provided four aircraft fixes. The following table summarizes the reconnaissance support received at JTWC in 1990:

	NWP	SH	NIO	AOR
Satellite fixes	3140	1702	80	4922
Radar fixes	994	0	0	994
Aircraft fixes	4	0	0	4

JTWC's performance during 1990 resulted in the lowest 24-hr, the third lowest 48-hr, and the fourth lowest 72-hr forecast position errors ever in the Northwest Pacific. This performance was remarkable, considering that 65% of the tropical cyclones took recurving tracks. Of the 32 tropical cyclones in the western North Pacific, four were super typhoons, 17 were less intense typhoons, 10 were tropical storms and one was a tropical depression. 1990 also saw the second lowest intensity forecast errors ever at all verifying times. In the western North Pacific JTWC also reduced the false alarm rate in forecasting tropical cyclone development from 32% in 1989 to 9% in 1990, while increasing the probability of detection from 91% to 97%. The following statistical summary shows JTWC's forecast errors in each ocean basin and in the total AOR:

	NWP	SH	NIO	AOR
Position errors				
24hr	103nm	143nm	101nm	114nm
48hr	203nm	263nm	146nm	217nm
72hr	310nm	--------	185nm	305nm
Intensity errors				
24hr	10 kt	10 kt	9 kt	10 kt
48hr	16 kt	16 kt	24 kt	16 kt
72hr	20 kt	------	48 kt	21 kt

JTWC acted as the operations center for TCM-90. More than 30 research scientists from several countries worked closely with Typhoon Duty Officers and other JTWC personnel during the busiest part of the western North Pacific tropical cyclone season. The Center dedicated over 3000 man-hours in support of TCM-90, resulting in closer ties between operational forecasters and the research community. The resulting data base was the most complete and finest ever collected on western North Pacific cyclones and will support decades of tropical cyclone research.

TABLE OF CONTENTS

INDIVIDUAL TROPICAL CYCLONES

1. OPERATIONAL PROCEDURES

1.1 GENERAL

The Joint Typhoon Warning Center (JTWC) provides a variety of routine products and services to the organizations within its area of responsibility, including:

1.1.1 SIGNIFICANT TROPICAL WEATHER ADVISORIES — Issued daily or as needed, to describe all tropical disturbances and their potential for further development during the advisory period.

1.1.2 TROPICAL CYCLONE FORMATION ALERTS — Issued when synoptic or satellite data indicate the development of a tropical cyclone is likely within 24 hours in a specified area.

1.1.3 TROPICAL CYCLONE/ TROPICAL DEPRESSION WARNINGS — Issued periodically throughout each day to provide forecasts of position, intensity, and wind distribution for tropical cyclones in JTWC's area of responsibility (AOR).

1.1.4 PROGNOSTIC REASONING MESSAGES — Issued with warnings for tropical depressions, tropical storms, typhoons and super typhoons in the western North Pacific to discuss the rationale for the content of JTWC's warnings.

1.1.5 PRODUCT CHANGES — The contents and availability of the above JTWC products are set forth in USCINCPACINST 3140.1 (series). Changes to USCINCPACINST 3140.1 and JTWC products and services are proposed and discussed at the Annual Tropical Cyclone Conference. Significant changes this year to the warning system include: more involved procedures for intensity forecasting and a redefiniition of the boundary between ocean basins in the Southern Hemisphere from 100° east to 135° east longitude for the significant tropical weather advisories.

1.2 DATA SOURCES

1.2.1 COMPUTER PRODUCTS — Numerical and statistical guidance are available from the USN Fleet Numerical Oceanography Center (FNOC) at Monterey, California. These products along with selected ones from the National Meteorological Center (NMC) are received through the Naval Environmental Data Network (NEDN), the Naval Environmental Satellite Network (NESN), and by microcomputer dial-up connections using military and commercial telephone lines. Numerical guidance is also received from Air Force Global Weather Center (AFGWC) at Omaha, Nebraska via the Pacific Digital Information Graphics System (PACDIGS), and from indigenous sources within our AOR.

1.2.2 CONVENTIONAL DATA — These data sets are comprised of land and shipboard surface observations, and enroute meteorological observations from commercial and military aircraft (AIREPS) recorded within six hours of synoptic times, and cloud-motion winds derived from satellite data . The conventional data is hand- and computer-plotted, and hand-analyzed in the tropics for the surface/gradient and 200-mb levels. These analyses are prepared twice daily from 0000Z and 1200Z synoptic data. Also, FNOC supplies JTWC with computer generated analyses and prognoses, from 0000Z and 1200Z synoptic data, at the surface, 850-mb, 700-mb, 500-mb, 400-mb, 200-mb levels, and deep layer mean winds.

1.2.3 SATELLITE RECONNAISSANCE — Meteorological satellite imagery recorded at USAF/USN ground sites and USN ships supply day and night coverage in JTWC's area of responsibility. Interpretation of these satellite data provides tropical cyclone positions and estimates of current and forecast intensities (Dvorak, 1984). The USAF tactical satellite sites and Air Force Global Weather Central

currently receive and analyze special sensor microwave/imager (SSM/I) data to provide estimates of 30-knot wind radii near tropical cyclones. Use of satellite reconnaissance is discussed further in section 2. Reconnaissance and Fixes.

1.2.4 RADAR RECONNAISSANCE — Land-based radar observations are used to position tropical cyclones. Once a well-defined tropical cyclone moves within the range of land-based radar sites, radar reports are invaluable for determination of position and movement. Use of radar reports during 1990 is discussed in section 2. Reconnaissance and Fixes.

1.2.5 AIRCRAFT RECONNAISSANCE – In support of the Tropical Cyclone Motion (TCM-90) experiment the NASA DC-8 aircraft provided a limited number of fixes. These were the first high-level fixes from aircraft ever provided to JTWC and used in support of the official warnings.

1.2.6 DRIFTING METEOROLOGICAL BUOYS - In 1990, 18 mini-drifting buoys were specifically deployed in the western North Pacific for tropical cyclone warning support. Twelve buoys were deployed by the JTWC in support of the TCM90 experiment. Six buoys were deployed from Cubi Point NAS during the last part of the year. Several of these buoys took direct hits from typhoons. In 1989 Commander, Naval Oceanography Command put into action the NAVOCEANCOM Integrated Drifting Buoy Plan 1989-1994 to provide mini-drifting buoys to meet USCINCPACFLT requirements including tropical cyclone warning support.

JTWC acquires drifting buoy data directly through its Local User Terminal (LUT). The buoys transmit data to the TIROS-N polar orbiting satellites, which in turn relay the data to JTWC's LUT. JTWC transmits buoy data on the AWN under the header SSVE 01 PGTW. Additionally, the data stored aboard the satellites are recovered via Service ARGOS at NOAA/NESDIS in Suitland, Maryland. NOAA/NESDIS processes and distributes the Meteorological data to users via the Global Telecommunications System (GTS) and the Automated Weather Network (AWN).

1.2.7 AUTOMATIC WEATHER OBSERVING STATIONS (AMOS) — Through a cooperative effort between the Naval Oceanography Command, the Department of the Interior, and NOAA, a network of 20 AMOS stations are being installed in the Micronesian islands. In the Commonwealth of the Northern Mariana Islands, there are now stations on Saipan, Rota, and Pagan. In the Federated States of Micronesia, there is a station on Kosrae. In the Republic of the Marshall Islands,there are now stations on Ujae,

Table 1-1. AUTOMATIC WEATHER OBSERVING STATIONS SUMMARY

Site	Location	Callsign	ID#	Type	System	Installed
Saipan	(15.2°N, 145.7°E)	15D151D2	-----	HANDAR	ARC	1986
Rota	(14.2°N, 145.2°E)	15D16448	-----	HANDAR	ARC	1987
Faraulep*	(8.6°N, 144.6°E)	FARP2	52005	AMOS	C-MAN/ARGOS	1988
Ujae	(8.9°N, 165.8°E)	UJAP2	91365	AMOS	C-MAN	1989
Enewetak	(11.4°N, 162.3°E)	ENIP2	91251	AMOS	C-MAN	1989
Pagan	(18.1°N, 145.8°E)	PAGP2	91222	AMOS	C-MAN	1990
Kosrae	(5.3°N, 163.0°E)	KOSP2	91356	AMOS	C-MAN	1990
Mili	(6.1°N, 171.8°E)	MILP2	91377	AMOS	C-MAN	1990

* Prototype site, which was destroyed in November, will not be reestablished.

ARC = Automated Remote Collection system (via GOES West)
ARGOS = System ARGOS data collection (via TIROS-N)
C-MAN = Coastal-Marine Automated Network (via GOES West)

Enewetak, and Mili. JTWC receives AMOS data from all sites via the AWN under the bulletin headers SMPW01 KWBC, SIPW01 KWBC, and SNPW01 KWBC. The prototype site on Faraulep was destroyed during Super Typhoon Owen on 28 November. An AMOS summary appears in Table 1.1.

1.3 COMMUNICATIONS

Primary communications support is provided by the Naval Telecommunications Center (NTCC), Nimitz Hill, a component of the Naval Communications Area Master Station, Western Pacific (NAVCAMS WESTPAC). JTWC uses the following communications systems:

1.3.1 AUTOMATED DIGITAL NETWORK (AUTODIN) — AUTODIN is used for dissemination of warnings, alerts and other related bulletins to Department of Defense (DOD) and other US Government installations. These messages are relayed for further transmission over Navy Fleet Broadcasts, and Coast Guard continuous wave Morse code and voice broadcasts. AUTODIN messages can be relayed to commercial telecommunications for delivery to non-DOD users. Inbound message traffic for JTWC is received via AUTODIN addressed to NAVOCEANCOMCEN GQ//JTWC// or DET 1 1WW NIMITZ HILL GQ//CC//.

1.3.2 AUTOMATED WEATHER NETWORK (AWN) - The AWN provides weather data over the Pacific Meteorological Data System (PACMEDS). The PACMEDS, operational at JTWC since April 1988, allows Pacific-Theater agencies to receive weather information at 1200 baud. JTWC uses a software package called AWNCOM/WINDS on a microcomputer to send and receive data via the PACMEDS. This system will eventually provide effective storage and manipulation of the large volume of meteorological reports available from throughout JTWC's vast Area of Responsibility (AOR). Through the AWN, JTWC has access to data available on the Global Telecommunications System (GTS). JTWC's AWN station identifier is PGTW

1.3.3 DEFENSE SWITCHED NETWORK (DSN) — DSN, formerly AUTOVON, is a world-wide general purpose switched telecommunications network for the DOD. The network provides a rapid and vital voice link for JTWC to communicate tropical cyclone information to DOD installations. The DSN telephone numbers for JTWC are 344-4224 or 321-2345.

1.3.4 NAVAL ENVIRONMENTAL DATA NETWORK (NEDN) — The NEDN is the primary link to FNOC to obtain computer generated analyses and prognoses. It is also a backup communication line for requesting and receiving the objective tropical cyclone forecast aids from FNOC's mainframe computers. The NEDN allows JTWC to communicate directly to the other Naval Oceanography Command Centers around the world.

1.3.5 PUBLIC DATA NETWORK (PDN) — A commercial packet switching network that provides low-speed interactive transmission to users of FNOC products. The PDN is now the primary method for JTWC to request and receive FNOC produced objective tropical cyclone forecast aids. The PDN allows direct access of FNOC products via the Automated Tropical Cyclone Forecast (ATCF) system. The PDN also serves as an alternate method of obtaining FNOC analyses and forecast fields. TYMNET is the contractor providing PDN services to FNOC.

1.3.6 DEFENSE DATA NETWORK (DDN) —The DDN is a DOD computer communications network utilized to exchange data files. Because the DDN has links, or gateways, to non-military information networks, it is primarily used to exchange data with the research community. JTWC's address is 1WW JTWC @ SACEMNET .AF. MIL

1.3.7 TELEPHONE FACSIMILE (TELEFAX) — TELEFAX provides the

capability to rapidly scan and transmit, or receive, documents over commercial telephone lines or DSN. TELEFAX is used to disseminate tropical cyclone advisories and warnings to key agen-cies on Guam and, in special situations, the other Micronesian Islands. Inbound documents for JTWC are received via commercial telephone at (671) 477-6186. If inbound through DSN, the Guam DSN operator 322-1110 can transfer the call to the commercial number 477-6186.

1.3.8 NAVAL ENVIRONMENTAL SATELLITE NETWORK (NESN) — The NESN's primary function is to pass satellite data from the satellite global data base at FNOC to regional centers. Similarly, it can pass satellite data from NOCC/JTWC to FNOC or other regional centers. It can also provide a limited back-up for the NEDN.

1.3.9 AIRFIELD FIXED TELECOMMUNICATIONS NETWORK (AFTN) — AFTN was installed at JTWC in January 1990. Though AFTN is primarily for the exchange of aviation information; weather information and warnings are also distributed via this network. AFTN also provides point-to-point communication with other warning agencies. JTWC's AFTN identifier is PGUMYMYT.

1.3.10 LOCAL USER TERMINAL (LUT) — JTWC uses a LUT, provided by the Naval Oceanographic Office, as the primary means of receiving real-time data from drifting meteorological buoys and ARGOS-equipped AMOS via the polar orbiting NOAA satellites.

1.3.11 COMPUTER FACSIMILE - The JTWC Rapid Response Team (RRT) uses a microcomputer to transmit facsimile messages to agencies on Guam and the Northern Marianas when a typhoon threatens the Mariana Islands. The RRT can be reached at (671)-344-7116 or (671)-344-7119.

1.4 DATA DISPLAYS

1.4.1 NAVAL ENVIRONMENTAL DISPLAY STATION (NEDS) — The NEDS receives, processes, stores, displays and prints copies of FNOC environmental products. It drives the fleet facsimile broadcast and can also be used to generate the requests for objective tropical cyclone forecast techniques.

1.4.2 AUTOMATED TROPICAL CYCLONE FORECAST SYSTEM (ATCF) — The ATCF cuts message preparation time and reduces the number of corrections to JTWC's alerts and warnings. The ATCF automatically computes the myriad of statistics calculated by JTWC. Links have been established through a Local Area Network (LAN) to the NOCC Operations watch team to facilitate the generation of tropical cyclone warning graphics for the fleet facsimile broadcasts and their local metwatch and warning products for Micronesia. A module permits satellite reconnaissance fixes to be input from Det 1, 1WW into the LAN. Several other modules are still under development including: direct links to NTCC, the LUT, and AWNCOM/WINDS.

1.4.3 PACIFIC DIGITAL INFORMATION GRAPHICS SYSTEM (PACDIGS) — The PACDIGS is a communications circuit that was expanded to include JTWC in 1988. Air Force Global Weather Central (AFGWC) at Omaha, Nebraska provides a standard set of numerical products to the PACDIGS circuit which can be used for additional evaluation in the development of tropical cyclone warnings.

1.4.4 NAVAL SATELLITE DISPLAY SYSTEM (NSDS) — The NSDS functions as a display of FNOC stored Defense Meteorological Satellite Program (DMSP) imagery and low resolution geostationary imagery . It is the primary means for JTWC to observe areas of cloudiness in the Indian Ocean.

1.4.5 NAVAL SATELLITE DISPLAY SYSTEM-GEOSTATIONARY(NSDS-G) — The NSDS-G is the primary system used to process high resolution geostationary imagery for tropical cyclone positioning and intensity estimates for the western Pacific Ocean. Its built-in sectorizer allows scale expansion and downloading of electronic files to evaluate the

data effectively, and monitor several cyclones or suspect areas at once.

1.5 ANALYSES

The JTWC Typhoon Duty Officer (TDO) routinely performs manual streamline analyses of composite surface/gradient-level (3000 ft (914 m)) and upper-tropospheric (centered on the 200-mb level) data for 0000Z and 1200Z each day. Manual sea-level pressure analyses concentrating on the mid-latitudes are available from the NOCC Operations watch team. Computer analyses of the surface, 850-, 700-, 500-, 400-, and 200-mb levels, deep layer mean winds, and frontal boundaries are available from the 0000Z and 1200Z FNOC data bases. Additional sectional charts at intermediate synoptic times and auxiliary charts, such as station-time plot diagrams and pressure-change charts, are analyzed during periods of significant tropical cyclone activity.

1.6 FORECAST PROCEDURES

1.6.1 INITIAL POSITIONING — The warning position is the best estimate of the center of the surface circulation at synoptic time. It is estimated from an analysis of all fix information received from one hour before to one and one-half hours after that synoptic time. The analysis is aided by a computer-generated objective best track scheme that weights fix information based on its statistical accuracy. The TDO includes synoptic observations and other information to adjust the position, testing consistency with the past direction, speed of movement and the influence of the different scales of motions. If the fix data are not available due to reconnaissance platform malfunction or communication problems, or are considered unrepresentative, synoptic data and/or extrapolation from previous fixes are used.

1.6.2 TRACK FORECASTING — In preparing the JTWC official forecast, the TDO evaluates a wide variety of information, and employs a number of objective and subjective techniques. Because tropical cyclone track forecasting has and continues to require a significant amount of subjective input from the TDO, detailed aspects of the forecast-development process will vary somewhat from TDO to TDO, particularly with respect to the weight given to any of the available guidance. However, throughout 1990, JTWC has developed a standardized, three phase tropical cyclone motion forecasting process to improve not only forecast accuracy, but also forecast-to-forecast consistency.

1.6.2.1 Field Analysis Phase — NOGAPS analyses and prognoses at various levels are evaluated for position, development, and movement of not only the tropical cyclone, but also relevant synoptic features such as: i) subtropical ridge circulations, ii) mid-latitude short/long-wave troughs and associated weaknesses in the subtropical ridge, iii) monsoon surges, and iv) other tropical cyclones. This process permits the TDO to develop an initial impression of the environmental steering influences to which the tropical cyclone is and will be subjected as depicted by NOGAPS. The NOGAPS analyses are then compared to the hand-plotted and analyzed charts prepared by the TDO and to the latest satellite imagery in order to determine how well the NOGAPS-initialization process has conformed to the available synoptic data, and how well the resultant analysis fields agree with the synoptic situation inferred from the imagery. Finally, the TDO compares both the computer and hand-analyzed charts to monthly climatology in order to make a preliminary determination of to what degree the tropical cyclone is and will continue to be (according to NOGAPS) subjected to a climatological or aclimatological synoptic environment. Noting latitudinal and longitudinal displacements of subtropical ridge and long-wave midlatitude features is of particular importance, and will partially determine the relative weights given to climatologically or dynamically-based objective forecast guidance.

1.6.2.2 Objective Techniques Analysis Phase — After displaying latest set of forecasts given

by JTWC's suite of objective techniques, the TDO then evaluates the pattern produced by the set of forecasts according to the following principles. First, the degree to which the current situation is considered to be and will continue to be climatological is further refined by comparing the forecasts of the climo-based objective techniques, dynamically-based techniques, and past motion of the present storm. This assessment partially determines the relative weighting given the different classes of objective techniques. Second, the spread of the pattern determined by the set of objective forecasts is used to provide a measure of the predictability of subsequent motion, and the advisability of including a low or moderate probability alternate forecast scenario in the prognostic reasoning message or warning (outside the western North Pacific). The spread of the objective techniques pattern is typically small well-before or well-after recurvature (providing high forecast confidence) and large near recurvature or during a quasi-stationary phase (increasing likelihood of alternate scenarios).

1.6.2.3 Construct Forecast Phase — The TDO then constructs the JTWC official forecast giving due consideration to the: i) extent to which the synoptic situation is and is expected to remain climatological, ii) past statistical performance of the various objective techniques on the current storm, and iii) known properties of individual objective techniques given the present synoptic situation. The following guidance for weighting the objective techniques is applied:

a) Weight persistence strongly in the first 12 to 24 hours of the forecast period.
b) Give significant weight to the last JTWC forecast at all forecast times, unless there is significant evidence to warrant a departure. (Also utilize latest forecasts from regional warning centers, if applicable.)
c) Give more weight to the techniques that have been performing well on the current storm and/or are expected to perform well in the current and expected synoptic situation.
d) Stay within the "envelope" determined by the spread of objective techniques forecasts unless there is a specific reason for not doing so (eg., all objective forecasts start out at a significant angle relative to past motion of the current storm.

1.6.3 INTENSITY FORECASTING—The empirically derived Dvorak (1984) technique is used as a first guess for the intensity forecast. The TDO then adjusts the forecast after evaluating climatology and the synoptic situation. An interactive climatology scheme allows the TDO to define a situation similar to the system being forecast in terms of location, time of year, and current intensity. Synoptic influences such as the location of major troughs and ridges, and the position and intensity of the Tropical Upper Tropospheric Trough (TUTT) all play a large part in intensifying or weakening a tropical cyclone. JTWC incorporates a checklist into the intensity forecast procedure. Such criteria as upper-level outflow patterns, neutral points, sea-surface temperatures, enhanced monsoonal or cross-equatorial flow, and vertical wind shear are evaluated for their tendency to enhance or inhibit normal development. In addition to climatology and synoptic influences, the first guess is modified for interactions with land, with other tropical cyclones, and with extratropical features.

1.6.4 WIND-RADII FORECASTING — After the loss of aircraft reconnaissance, JTWC began over-estimating the extent of damaging winds by as much as 100%. The algorithm previously used at JTWC involved knowledge of the intensity and radius of maximum winds derived from aircraft data and based on a statistical average. Det 1 Techniques Development incorporated techniques from various sources, leading to development of the Martin-Holland wind radii technique. Wei and Gray, in an unpublished study, showed that cloud shield size related to the extent of

damaging winds - tropical cyclones with large cloud shields generally had damaging winds much further from the center than tropical cyclones with small cloud shields. Holland (1980) described an analytic model of tropical cyclone wind profiles which could estimate extent of damaging wind. Holland's equation uses a logarithmic wind profile outside the radius of maximum winds. It is based on size and shape parameters. The size parameter uses the cloud shield size (based on the size of the minus 65°C isotherm outside the central convection) to determine the areal extent of damaging winds. The shape parameter uses the Dvorak intensity estimate to determine the maximum wind intensity. Asymmetry is added based on system motion and latitude.

1.6.5 EXTRATROPICAL TRANSITION — When a tropical cyclone is forecast to become an extratropical system, JTWC coordinates the transfer of warning responsibility with the appropriate Naval Oceanography Command Regional Center, which assumes warning responsibilities for the extratropical system.

1.6.6 TRANSFER OF WARNING RESPONSIBILITIES — JTWC coordinates the transfer of tropical warning responsibility for tropical cyclones entering or exiting its AOR. For tropical cyclones crossing the dateline in the North Pacific Ocean, JTWC coordinates with the Central Pacific Hurricane Center (CPHC), Honolulu via the Naval Western Oceanography Center (NWOC), Pearl Harbor, Hawaii. For the South Pacific Ocean, JTWC coordinates with NWOC.

In the event JTWC should become incapacitated, the Alternate Joint Typhoon Warning Center (AJTWC), collocated with NWOC assumes JTWC's functions. Assistance in determining satellite reconnaissance requirements, and in obtaining the resultant data, is provided by the PACAF Weather Support Unit, Hickam AFB, Hawaii.

1.7 WARNINGS

JTWC issues two types of warnings: Tropical Cyclone Warnings and Tropical Depression Warnings.

Tropical Cyclone Warnings — are issued when a closed circulation is evident and maximum sustained winds are forecast to reach 34 kt (18 m/sec) within 48 hours, or when the tropical cyclone is in such a position that life or property may be endangered within 72 hours.

Each Tropical Cyclone Warning is numbered sequentially and includes the following information: the current position of the surface center; estimate of the position accuracy and the supporting reconnaissance (fix) platforms; the direction and speed of movement during the past six hours (past 12 hours in the Southern Hemisphere); and the intensity and radial extent of over 30-, 50-, and 100-kt surface winds, when applicable. At forecast intervals of 12, 24, 48, and 72 hours (12, 24, and 48 hours in the Southern Hemisphere), information on the tropical cyclone's anticipated position, intensity and wind radii is provided. Vectors indicating the mean direction and mean speed between forecast positions are included in all warnings. In addition, a 3-hour extrapolated position is provided in the remarks section.

Warnings in the western North Pacific and North Indian Oceans are issued every six hours valid at standard times: 0000Z, 0600Z, 1200Z and 1800Z (every 12 hours: 0000Z, 1200Z or 0600Z, 1800Z in the Southern Hemisphere). All warnings are released to the communications network no earlier than synoptic time and no later than synoptic time plus two and one-half hours, so that recipients are assured of having all warnings in hand by synoptic time plus three hours (0300Z, 0900Z, 1500Z and 2100Z). By area, the warning bulletin headers are: WTIO31-35 PGTW for northern latitudes from 35° to 100° east longitude, WTPN31-36 PGTW for northern latitudes from 100° to 180° east longitude, WTXS31-36 PGTW for southern latitudes from 35° to 135° east longitude, and WTPS31-35

PGTW for southern latitudes from 135° to 180° east longitude.

Tropical Depression Warnings — are issued only for western North Pacific tropical depressions that are not expected to reach the criteria for Tropical Cyclone Warnings, as mentioned above. The depression warning contains the same information as a Tropical Cyclone Warning except the Tropical Depression Warning is issued every 12 hours at standard synoptic times and extends only to the 36-hour forecast period.

Both Tropical Cyclone and Tropical Depression Warning forecast positions are later verified against the corresponding best track positions (obtained during detailed post-storm analyses) to determine the most probable path and intensity of the cyclone. A summary of the verification results for 1990 is presented in section 5. Summary of Forecast Verification.

1.8 PROGNOSTIC REASONING MESSAGES

The plain language messages provide meteorologists with the rationale for the forecasts for tropical cyclones in the western North Pacific Ocean. They also discuss alternate forecast scenarios. Prognostic reasoning messages (WDPN21-26 PGTW) are prepared to complement warnings. In addition to these messages, prognostic reasoning information is provided in the remarks section of warnings when significant forecast changes are made or when deemed appropriate by the TDO.

1.9 TROPICAL CYCLONE FORMATION ALERTS

Tropical Cyclone Formation Alerts are issued whenever interpretation of satellite imagery and other meteorological data indicates that the formation of a significant tropical cyclone is likely. These alerts will specify a valid period not to exceed 24 hours and must either be cancelled, reissued, or superseded by a warning prior to expiration. By area, the alert bulletin headers are: WTIO21-25 PGTW for northern latitudes from 35° to 100° east longitude, WTPN21-26 PGTW for northern latitudes from 100° to 180° east longitude, WTXS21-25 PGTW for southern latitudes from 35° to 135° east longitude, and WTPS21-25 PGTW for southern latitudes from 135° to 180° east longitude.

1.10 SIGNIFICANT TROPICAL WEATHER ADVISORIES

This product contains a description of all tropical disturbances in JTWC's area of responsibility (AOR) and their potential for further (tropical cyclone) development. In addition, all tropical cyclones in warning status are briefly discussed.

Two separate messages are issued daily and each is valid for a 24-hour period. The Significant Tropical Weather Advisory for the Western Pacific Ocean is issued by 0600Z. The Significant Tropical Weather Advisory for the Indian Ocean is issued by 1800Z. These are reissued whenever the situation warrants. For each suspect area, the words "poor", "fair", or "good" are used to describe the potential for development. "Poor" will be used to describe a tropical disturbance in which the meteorological conditions are currently unfavorable for development. "Fair" will be used to describe a tropical disturbance in which the meteorological conditions are favorable for development, but significant development has not commenced. "Good" will be used to describe the potential for development of a disturbance covered by an alert. By area, the advisory bulletin headers are: ABPW10 PGTW for northern latitudes from 100° to 180° east longitude and southern latitudes from 135° to 180° east longitude and ABIO10 PGTW for northern latitudes from 35° to 100° east longitude and southern latitudes from 35° to 135° east longitude.

2. RECONNAISSANCE AND FIXES

2.1 GENERAL

The Joint Typhoon Warning Center depends on reconnaissance to provide necessary, accurate, and timely meteorological information in support of advisories, alerts and warnings. JTWC relies primarily on two reconnaissance platforms: satellite and radar. In data rich areas, synoptic data are also used to supplement the above. As in past years, the optimum use of all available reconnaissance resources to support JTWC's products remains a primary concern. Weighing the specific capabilities and limitations of each reconnaissance platform, and the tropical cyclone's threat to life and property both afloat and ashore, continue to be important factors in careful product preparation.

2.2 RECONNAISSANCE AVAILABILITY

2.2.1 SATELLITE — Fixes from Air Force/Navy ground sites and Navy ships provide day and night coverage in JTWC's area of responsibility. Interpretation of this satellite imagery yields tropical cyclone positions and estimates of current and forecast intensities through the Dvorak technique. The Special Sensor Microwave/Imager (SSM/I) data is used to determine the extent of the 30-kt winds around the tropical cyclone and to aid in tropical cyclone positioning.

2.2.2 RADAR — Land-based radar remotely senses and maps precipitation within tropical cyclones in the proximity (usually within 175 nm (325 km) of radar sites in the Philippine Islands, Taiwan, Hong Kong, China, Japan, South Korea, Kwajalein and Guam. The next DOD radar upgrade will be the arrival of the next generation Doppler radars in the early 1990's.

2.2.3 SYNOPTIC — JTWC also determines tropical cyclone positions based on the analysis of surface/gradient-level synoptic data. These positions are an important supplement to fixes provided by remote sensing platforms and become invaluable in situations where neither satellite nor radar fixes are available.

2.3 SATELLITE RECONNAISSANCE SUMMARY

The Air Force provides satellite reconnaissance support to JTWC through the DMSP Tropical Cyclone Reporting Network (DMSP Network), which consists of tactical sites and a centralized facility. The personnel of Det 1, 1WW, collocated with JTWC at Nimitz Hill, Guam, coordinate the satellite acquisitions and tropical cyclone reconnaissance with the following units:

Det 4 , 20 WS, Hickam AFB, Hawaii
Det 5, 20 WS, Clark AB, Republic of the Philippines
Det 8, 20 WS, Kadena AB, Okinawa, Japan
Det 15, 30 WS, Osan AB, Republic of Korea
Air Force Global Weather Central, Offutt AFB, Nebraska

These sites provide a combined coverage that includes most of the western North Pacific, from near the date line westward to the Malay Peninsula. For the remainder of its AOR, JTWC relies on AFGWC to provide coverage using stored satellite data. The Naval Oceanography Command Detachment, Diego Garcia, furnishes interpretation of low resolution NOAA polar orbiting coverage in the central Indian Ocean, and USN ships equipped for direct satellite readout contribute supplementary support. Additionally, civilian contractors with the U.S. Army at Kwajalein Atoll provide satellite fixes on tropical cyclones in the Marshall Islands to supplement Det 1, 1WW's satellite coverage. An additional source of satellite data is DMSP satellite mosaics available from the Fleet Numerical Oceanography Center via the NEDN and NESN lines. These valuable data are used to metwatch the areas not in the DMSP tactical site satellite coverage and provide forecasters the capability to monitor tropical cyclones that AFGWC satellite analysts are fixing.

In addition to polar orbiter imagery, Det 1, 1 WW uses geostationary imagery to support the reconnaissance mission. Low resolution imagery is received, displayed and animated by microcomputers at the DMSP tactical sites. The animation of these images is invaluable in depicting cloud systems in their formative stages and determining coarse motion vectors. Animation is also valuable in assessing environmental changes affecting tropical cyclone behavior. In addition to this capability, Det 1, 1WW receives high resolution digital geostationary data through the Naval Satellite Dissemination System-Geostationary (NSDS-G). The new Det 1 Automation system is being developed and installed by the National Aeronautics and Space Administration (NASA). Phase 1 of Det 1 Automation, installed in December 1990, consists of a minicomputer and large screen work station which provides advanced graphic and enhancement capabilities for geostationary data. Phase 2, scheduled for September 1991, will injest NOAA and DMSP polar orbiter images, SSM/I and satellite sounder data, plus conventional meteorological data already available on site.

AFGWC is the centralized member of the DMSP network. In support of JTWC, AFGWC processes stored imagery from DMSP and NOAA spacecraft. Stored imagery is recorded onboard the spacecraft as they pass over the earth and is later down-linked to AFGWC via a network of command readout sites and communication satellites. This enables AFGWC to obtain the coverage necessary to fix all tropical cyclones within JTWC's AOR. AFGWC has the primary responsibility to provide tropical cyclone reconnaissance over the entire Indian Ocean, southwest Pacific, and the area near the dateline in the northwest Pacific Ocean. Additionally, AFGWC can be tasked to provide tropical cyclone support in the northwest Pacific as backup to coverage routinely available in that region.

The hub of the DMSP network is Det 1, 1WW, collocated with JTWC at Nimitz Hill, Guam. Based on available satellite coverage, Det 1, 1WW is responsible for coordinating satellite reconnaissance requirements with JTWC and tasking the individual network sites for the necessary tropical cyclone fixes, current intensity estimates and forecast intensities. When a particular satellite pass is selected to support the development of JTWC's next tropical cyclone warning, two sites are tasked to fix the tropical cyclone from the same pass. This "dual-site" concept provides the necessary redundancy that virtually guarantees JTWC a satellite fix to support each warning.

The network provides JTWC with several products and services. The main service is to monitor the AOR for indications of tropical cyclone development. If development is detected, JTWC is notified. Once JTWC issues either a Tropical Cyclone Formation Alert or a warning, the network provides three products: tropical cyclone positions, current intensity estimates and forecast intensities. Each satellite tropical cyclone position is assigned a Position Code Number (PCN), which is a measure of positioning confidence. The PCN is determined by a combination of the availability of visible landmarks in the image that can be used as references for precise gridding and the degree of organization of the tropical cyclone's cloud system (Table 2-1). Once the tropical cyclone reaches 50 kt (25 m/sec), information on the distribution of 30-kt (15-m/sec) winds is provided using SSM/I data.

Det 1, 1 WW provides a minimum of one estimate of the tropical cyclone's current intensity every 12 hours once JTWC is in alert status and every 6 hours when in warning status. Current intensity estimates and 24-hour intensity forecasts are made using the Dvorak technique (NOAA Technical Report NESDIS 11) for both visual and enhanced infrared imagery (Figure 2-1). The enhanced infrared

TABLE 2-1 **POSITION CODE NUMBERS (PCN)**

PCN	METHOD FOR CENTER DETERMINATION/GRIDDING
1	EYE/GEOGRAPHY
2	EYE/EPHEMERIS
3	WELL DEFINED CIRCULATION CENTER/GEOGRAPHY
4	WELL DEFINED CIRCULATION CENTER/EPHEMERIS
5	POORLY DEFINED CIRCULATION CENTER/GEOGRAPHY
6	POORLY DEFINED CIRCULATION CENTER/EPHEMERIS

technique is preferred due to its increased objectivity and accuracy, however, the visual technique is used to supplement this information during the daylight hours. The standard relationship between tropical cyclone "T-number", maximum sustained surface wind speed (Dvorak, 1984) and minimum sea-level pressure (Atkinson and Holliday, 1977) for the Pacific is shown in Table 2-2. For subtropical cyclones, intensity estimates are made using the Hebert and Poteat technique (NOAA Technical Memorandum NWS SR-83, 1975).

2.3.1 SATELLITE PLATFORM SUMMARY --- Figure 2-2 shows the status of operational polar orbiting spacecraft. Two DMSP spacecraft, 19543 (F8) and 20542 (F9), were operational during 1990. The SSM/I on spacecraft F8 experienced increasing noise problems on its horizontally polarized 85 gigahertz channel during the year. A new DMSP spacecraft 21544 (F10), which was launched on 1 December 1990, became operational on 15 January 1991 and will be ready for 1991 tropical cyclones. With regard to the NOAA spacecraft, NOAA 9 remained in standby and NOAA 10 and NOAA 11 spacecraft were operational throughout 1990.

2.3.2 STATISTICAL SUMMARY — During 1990, the DMSP network was the primary input

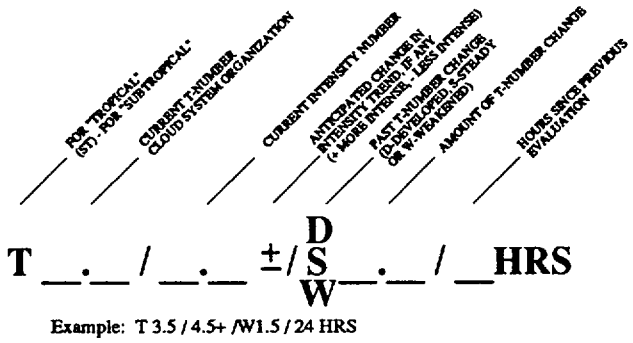

Figure 2-1. Dvorak code for communicating estimates of current and forecast intensity derived from satellite data. In the example, the current "T-number" is 3.5, but the current intensity is 4.5. The cloud system has weakened by 1.5 "T-numbers" since the previous evaluation conducted 24-hours earlier. The plus (+) symbol indicates an expected reversal of the weakening trend or very little further weakening of the tropical cyclone during the next 24-hour period.

to JTWC for operational warnings and post analysis best tracks in the entire 53 million square mile area of responsibility for the warning center. Almost all the warnings were based on satellite reconnaissance. JTWC received a total of 2834 satellite fixes from the DMSP network on 31 tropical cyclones in the western North Pacific Ocean. Of this, 51 percent were from polar orbiters, while 49 percent were from geostationary. Another 306 fixes were received from non-network sites. In addition, 64 network and 16 non-network fixes were made on tropical cyclones in the North Indian Ocean and 1342 network and 360 non-network fixes on cyclones in the Southern Hemisphere. A comparison of satellite fixes from all data sources with their corresponding best track positions is shown in Tables 2-3A and 2-3B. For the western North Pacific, the total mean error was comparable to the multi-year average and has essentially remained constant.

2.3.3 NEW TECHNIQUES — The Det 1 Automation system was installed just two weeks prior to year's end and provided Det 1, 1 WW satellite analysts with the capability to rapidly make or modify satellite image enhancements.

The SSM/I, mounted on the F8 DMSP spacecraft, was operational throughout 1990. Four tactical sites in the Pacific: Nimitz Hill, Hickam AFB, Kadena AB, and Clark AB; as well as AFGWC received the Mission Sensor Tactical Imaging Computer (MISTIC) during the summer of 1990. As in 1989, extensive SSM/I support was provided by analysts in the AFGWC Tropical Section. Both AFGWC and Det 1, 1 WW provided bulletins to JTWC

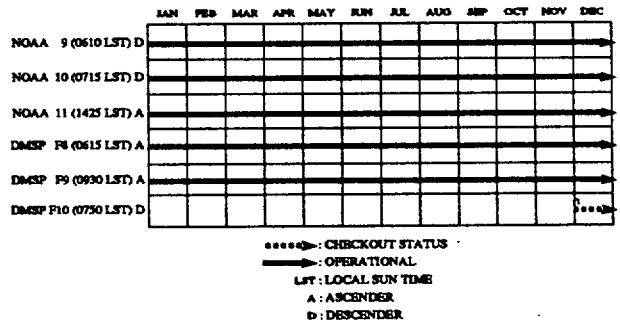

Figure 2-2. Polar orbiters for 1990.

describing the extent of 30-kt winds surrounding the tropical cyclone for all systems with maximum sustained winds of 50 kt or greater. Because Det 1 can only receive realtime DMSP data directly down linked to its tracking antenna, SSM/I coverage is limited to within approximately 20 degrees longitude of Guam. While Operating Line Scan (OLS) imagery can be obtained at a distance of 28 degrees longitude, such low elevation angles prevent retrieval of sufficient quantities of SSM/I data to produce an image. Winds can only be obtained in rain-free areas and areas free of deep moisture. If the cloud system center was rain free, analysts provided center/eye positions based on the 85 GHz microwave channel display. These positions provided a comparison with those made using visual and infrared spectral windows. However, limitations of the computer's ephemeris program caused geolocation errors varying up to 1.4 degrees. The tactical sites compensated by comparing the locations of conservative convective features on the microwave image with those on the OPS imagery.

2.3.4 FUTURE OF SATELLITE RECONNAISSANCE — Det 1 Automation will be 100 percent operational by the summer of 1991 and it will provide JTWC with the enhanced satellite support. At Det 1, 1 WW, the goal is to have a fully integrated satellite system, capable of ingesting data from both geostationary and polar satellites and then overlaying graphics from and interfacing with multiple data sources, e.g., Automated Weather Distribution System (AWDS), NEXRAD Doppler radar, and the advanced tactical terminal(Mark IVB). The Mark IVB is scheduled to replace the Mark III and Mark IV satellite ingest and display systems during the 1992-1993 time frame.

Until the installation of AWDS in 1993, data will be retrieved via the Automated Weather Network (AWN) and then overlaid on Satellite Imagery. With GEMPAC software developed by NASA, analysts will be able to overlay SSM/I, doppler, wind, temperature, pressure and height fields on visual or infrared imagery. Det 1, 1 WW/JTWC will have the capability to integrate large volumes of data more efficiently and effectively than ever before. Additionally,

TABLE 2-2

MAXIMUM SUSTAINED WIND SPEED (KT) AS A FUNCTION OF DVORAK CURRENT AND FORECAST INTENSITY NUMBER AND MINIMUM SEA-LEVEL PRESSURE (MSLP)

TROPICAL CYCLONE INTENSITY NUMBER	WIND SPEED	MSLP (NW PACIFIC)
0.0	<25	- - - -
0.5	25	- - - -
1.0	25	- - - -
1.5	25	- - - -
2.0	30	1000
2.5	35	997
3.0	45	991
3.5	55	984
4.0	65	976
4.5	77	966
5.0	90	954
5.5	102	941
6.0	115	927
6.5	127	914
7.0	140	898
7.5	155	879
8.0	170	858

TABLE 2-3A **MEAN DEVIATION (NM) OF ALL SATELLITE DERIVED TROPICAL CYCLONE POSITIONS FROM JTWC BEST TRACK POSITIONS IN THE NORTHWEST PACIFIC AND NORTH INDIAN OCEANS (NUMBER OF CASES IN PARENTHESES)**

	NORTHWEST PACIFIC OCEAN				NORTH INDIAN OCEAN			
PCN	1979-1989 AVERAGE		1990 AVERAGE		1980-1989 AVERAGE		1990 AVERAGE	
1	13.8	(1848)	13.6	(232)	14.7	(64)	8.6	(16)
2	14.4	(3653)	12.9	(519)	13.3	(33)	12.9	(7)
3	20.9	(2415)	21.0	(275)	23.9	(47)	47.4	(2)
4	21.3	(2991)	18.1	(654)	33.7	(39)	78.5	(1)
5	36.3	(4141)	37.0	(317)	37.4	(375)	24.9	(41)
6	35.2	(7587)	40.2	(1143)	40.0	(496)	58.6	(13)
1&2	13.8	(5501)	13.1	(751)	14.2	(97)	9.9	(23)
3&4	21.2	(5406)	19.0	(929)	28.4	(86)	57.8	(3)
5&6	35.6	(11728)	39.5	(1460)	38.9	(871)	33.0	(54)
1,3&5	27.0	(8404)	25.1	(824)	33.2	(486)	21.2	(59)
2,4&6	26.9	(14231)	27.8	(2316)	38.0	(568)	44.3	(21)
Totals:	**26.9**	**(22635)**	**27.1**	**(3140)**	**35.7**	**(1054)**	**27.3**	**(80)**

TABLE 2-3B **MEAN DEVIATION (NM) OF ALL SATELLITE DERIVED TROPICAL CYCLONE POSITIONS FROM JTWC BEST TRACK POSITIONS IN THE WESTERN SOUTH PACIFIC AND SOUTH INDIAN OCEANS (NUMBER OF CASES IN PARENTHESES)**

PCN	1985 - 1989 AVERAGE		1990 AVERAGE	
1	15.8	(211)	15.5	(153)
2	16.1	(804)	19.0	(162)
3	31.0	(170)	26.2	(79)
4	26.5	(631)	24.6	(168)
5	37.9	(758)	30.3	(362)
6	36.5	(4386)	33.9	(778)
1&2	16.1	(1015)	17.3	(315)
3&4	27.5	(801)	25.1	(247)
5&6	36.8	(5144)	32.8	(1140)
1,3&5	32.7	(1139)	25.9	(594)
2,4&6	32.6	(5821)	30.3	(1108)
Totals:	**32.6**	**(6960)**	**28.8**	**(1702)**

procedures for post storm reviews will be simplified. Archived hard copy imagery will be replace by loops and sectorized images archived on 4 mm, 1.2 gigabyte tapes. When unarchived, the data can again be enhanced for further detailed analysis. Det 1 and NASA are working together to explore the possible use of optical disks and other large storage devices for instantaneous access of short term archived data. The Mark IVB will also have powerful graphic and enhancement capabilities. Therefore, it is essential that the two systems are integrated in order to exploit their full potential.

2.4 RADAR RECONNAISSANCE

Twenty-one of the thirty-two significant tropical cyclones in the western North Pacific during 1990 passed within range of land-based radar with sufficient cloud pattern organization to be fixed. A total of 994 land-based radar fixes were obtained and logged at JTWC. Four airborne radar fixes were obtained by a research aircraft associated with the 1990 Office of Naval Research Tropical Cyclone Motion Experiment (TCM-90).

The WMO radar code defines three categories of accuracy: good (within 10 km (5 nm)), fair (within 10-30 km (5-16 nm)), and poor (within 30-50 km (16-27 nm)). Of the 1073 radar fixes encoded in this manner; 314 were good, 341 were fair, and 418 were poor. Compared to JTWC's best track, the mean vector deviation for land-based radar sites was 20 nm (37 km). Excellent support from the radar network through timely and accurate radar fix positioning allowed JTWC to track and forecast tropical cyclone movement during even the most erratic track changes.

No radar reports were received on Southern Hemisphere or North Indian Ocean tropical cyclones. However, a projected GTS circuit between Melbourne, Australia and Hickam AFB, Hawaii should provide access to radar reports from the South Pacific and Indian Oceans.

2.5 TROPICAL CYCLONE FIX DATA

A total of 4139 fixes on thirty-two northwest Pacific tropical cyclones and 80 fixes on four North Indian Ocean tropical cyclones were logged at JTWC. Table 2-4A delineates the number of fixes per platform for each individual tropical cyclone for the western North Pacific and North Indian Oceans. Season totals and percentages are also indicated. Table 2-4B provides similar information for the 1702 fixes in the South Pacific and South Indian Oceans.

TABLE 2-4A

1990 NORTHWEST PACIFIC AND NORTH INDIAN OCEAN FIX PLATFORM SUMMARY

NORTHWEST PACIFIC		SATELLITE	RADAR	SYNOPTIC	TOTAL
TY Koryn	(01W)	97	26	0	123
TS Lewis	(02W)	75	0	0	75
TY Marian	(03W)	60	0	0	60
TD 04W	(04W)	19	0	0	19
TS Nathan	(05W)	75	0	0	75
TY Ofelia	(06W)	136	59	0	195
TY Percy	(07W)	126	0	0	126
TS Robyn	(08W)	108	13	0	121
TY Steve	(09W)	107	1	0	108
TY Tasha	(10W)	60	5	0	65
TY Vernon	(11W)	159	35	0	194
TY Winona	(12W)	87	70	0	157
TS Aka	(01C)	30	0	0	30
TY Yancy	(13W)	131	84	0	215
TY Zola	(14W)	96	66	0	162
TY Abe	(15W)	123	98	0	221
TY Becky	(16W)	92	11	0	103
TY Dot	(17W)	82	32	0	114
TY Cecil	(18W)	22	13	0	35
TY Ed	(19W)	175	30	0	205
STY Flo	(20W)	102	76	0	182 *
TY Gene	(21W)	145	250	0	395
TY Hattie	(22W)	125	80	0	205
TS Ira	(23W)	23	0	0	23
TS Jeana	(24W)	19	0	0	19
TY Kyle	(25W)	102	2	0	104
TS Lola	(26W)	34	0	0	34
STY Mike	(27W)	177	0	0	177
TS Nell	(28W)	22	0	0	22
STY Page	(29W)	180	15	0	195
STY Owen	(30W)	174	2	0	176
TY Russ	(31W)	177	26	0	203
Totals NWP:		**3140**	**994**	**0**	**4138***
Percentage of Total:		**76 %**	**24 %**	**0 %**	**100 %**

NORTH INDIAN OCEAN		SATELLITE	RADAR	SYNOPTIC	TOTAL
TC 01B	(01B)	5	0	0	5
TC 02B	(02B)	48	0	0	118
TC 03B	(03B)	13	0	0	13
TC 04B	(04B)	14	0	0	14
Totals NIO:		**80**	**0**	**0**	**80**
Percentage of Total:		**100 %**	**0 %**	**0 %**	**100 %**

* Four airborne radar fixes were received.

TABLE 2-4B **1990 SOUTH PACIFIC AND SOUTH INDIAN OCEANS FIX PLATFORM SUMMARY**

TROPICAL CYCLONES		SATELLITE	SYNOPTIC	RADAR	TOTAL
TC 01S	- - - -	18	0	0	18
TC 02S	- - - -	38	0	0	38
TC 03S	- - - -	16	0	0	16
TC 04S	- - - -	26	0	0	26
TC 05S	- - - -	26	0	0	26
TC 06S	Pedro	71	0	0	71
TC 07P	Felicity	67	0	0	67
TC 08S	Alibera	178	0	0	178
TC 09S	Baomavo	61	0	0	61
TC 10S	Sam	80	0	0	80
TC 11S	Tina	40	0	0	40
TC 12P	Nancy	61	0	0	61
TC 13P	Ofa	61	0	0	61
TC 14S	Cezera	85	0	0	85
TC 15S	Dety	68	0	0	68
TC 16P	Peni	20	0	0	20
TC 17S	Vincent	64	0	0	64
TC 18S	Edisaona	63	0	0	63
TC 19P	Greg	41	0	0	41
TC 20S	Walter	39	0	0	39
TC 21P	Hilda	55	0	0	55
TC 22S	Felana	60	0	0	60
TC 23S	Gregoara	98	0	0	98
TC 24S	Alex	108	0	0	108
TC 25P	Ivor	94	0	0	94
TC 26P	Rae	42	0	0	42
TC 27S	- - - -	19	0	0	19
TC 28S	Bessi	26	0	0	26
TC 29S	Ikonjo	77	0	0	77
Total Number of Fixes:		**1702**	**0**	**0**	**1702**

3. SUMMARY OF WESTERN NORTH PACIFIC AND NORTH INDIAN OCEAN TROPICAL CYCLONES

3.1 GENERAL

For the western North Pacific 1990 became the busiest in JTWC's history - 794 warnings were issued on 32 tropical cyclones (Table 3-1). This was slightly more than the climatological mean of 31 tropical cyclones noted in Table 3-2. The North Indian Ocean was moderately active with 4 tropical cyclones which is just below the average of five per year. During the year a record 841 warnings were issued on 36 tropical cyclones in the Northern Hemisphere. A chronology of the activity is provided in Figure 3-1.

In the western North Pacific, JTWC was in warning status 165 days compared to 154 in 1989 and 114 in 1988. Again, considering only the western North Pacific, there were 54 days when the Center issued warnings on two cyclones and 3 days when it warned on three cyclones (Table 3-3). There were no days with warnings were issued on four or more tropical cyclones at once. When the North Indian Ocean is included in the total, there were 180 days with warnings on one cyclone and 10 days with warnings on two. Thirty-three initial Tropical Cyclone Formation Alerts were issued on western North Pacific tropical disturbances (Table 3-4) and 8 on disturbances in the North Indian Ocean. Alerts preceded warnings on all significant tropical cyclones in the western North Pacific and North Indian Oceans with the exception of Tropical Depression 04W.

TABLE 3-1

NORTHWEST PACIFIC OCEAN
SIGNIFICANT TROPICAL CYCLONES
FOR 1990

TROPICAL CYCLONE	PERIOD OF WARNING	NUMBER OF WARNINGS ISSUED	MAXIMUM SURFACE WINDS KT (M/SEC)	ESTIMATED MSLP (MB)
(01W) TY Koryn	12 Jan - 17 Jan	19	75(39)	967
(02W) TS Lewis	29 Apr - 03 May	15	35(18)	997
(03W) TY Marian	15 May - 19 May	17	90(46)	954
(04W) TD 04W	14 Jun - 15 Jun	4	30(15)	1000
(05W) TS Nathan	15 Jun - 19 Jun	14	55(28)	984
(06W) TY Ofelia	17 Jun - 25 Jun	31	90(46)	954
(07W) TY Percy	21 Jun - 30 Jun	36	115(59)	927
(08W) TS Robyn	07 Jul - 11 Jul	18	45(23)	991
(09W) TY Steve	25 Jul - 02 Aug	31	115(59)	927
(10W) TS Tasha	28 Jul - 31 Jul	12	55(28)	984
(11W) TY Vernon	29 Jul - 07 Aug	39	95(49)	948
(12W) TY Winona	06 Aug - 11 Aug	20	65(33)	976
(01C) TS Aka*	07 Aug - 15 Aug	32	45(23)	991
(13W) TY Yancy	13 Aug - 21 Aug	31	90(46)	954
(14W) TY Zola	17 Aug - 23 Aug	23	100(51)	944
(15W) TY Abe	24 Aug - 01 Sep	36	90(46)	954
(16W) TY Becky	24 Aug - 30 Aug	25	70(36)	972
(17W) TY Dot	03 Sep - 09 Sep	25	80(41)	963
(18W) TS Cecil	04 Sep - 05 Sep	5	45(23)	991
(19W) TY Ed	10 Sep - 20 Sep	40	90(46)	954
(20W) STY Flo	12 Sep - 20 Sep	31	145(75)	891 **
(21W) TY Gene	23 Sep - 30 Sep	30	80(41)	963
(22W) TY Hattie	30 Sep - 08 Oct	31	90(46)	954
(23W) TS Ira	02 Oct - 03 Oct	7	35(18)	997
(24W) TS Jeana	13 Oct - 15 Oct	6	35(18)	997
(25W) TY Kyle	16 Oct - 22 Oct	28	90(46)	954
(26W) TS Lola	17 Oct - 18 Oct	7	40(21)	994
(27W) STY Mike	07 Nov - 18 Nov	43	150(77)	885
(28W) TS Nell	10 Nov - 12 Nov	7	50(26)	987
(29W) STY Page	19 Nov - 30 Nov	45	140(72)	898
(30W) STY Owen	21 Nov - 03 Dec	48	140(72)	898
(31W) TY Russ***	14 Dec - 24 Dec	38	125(64)	916

TOTAL: 794

* 24 WARNINGS ISSUED BY NWOC
** BASED ON AIRCRAFT DATA.
*** TWO WARNINGS ISSUED BY AJTWC.

The criteria used in Table 3-2 are as follows:

1. If a tropical cyclone was first warned on during the last two days of a particular month and continued into the next month for longer than two days, then that system was attributed to the second month.

2. If a tropical cyclone was warned on prior to the last two days of a month, it was attributed to the first month, regardless of how long the system lasted.

3. If a tropical cyclone began on the last day of the month and ended on the first day of the next month, that system was attributed to the first month. However, if a tropical cyclone began on the last day of the month and continued into the next month for only two days, then it was attributed to the second month.

TABLE 3-2 LEGEND

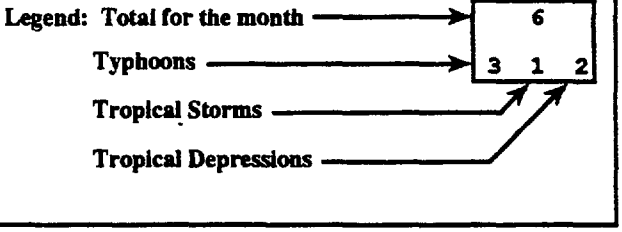

TABLE 3-2 **WESTERN NORTH PACIFIC TROPICAL CYCLONE DISTRIBUTION**

YEAR	JAN	FEB	MAR	APR	MAY	JUN	JUL	AUG	SEP	OCT	NOV	DEC	TOTALS
1960	1	0	1	1	1	3	3	9	5	4	1	1	30
	001	000	001	100	010	210	210	810	041	400	100	100	19 8 3
1961	1	1	1	1	4	6	5	7	6	7	2	1	42
	010	010	100	010	211	114	320	313	510	322	101	100	20 11 11
1962	0	1	0	1	3	0	8	8	7	5	4	2	39
	000	010	000	100	201	000	512	701	313	311	301	020	24 6 9
1963	0	0	1	1	0	4	5	4	4	6	0	3	28
	000	000	001	100	000	310	311	301	220	510	000	210	19 6 3
1964	0	0	0	0	3	2	8	8	8	7	6	2	44
	000	000	000	000	201	200	611	350	521	331	420	101	26 13 5
1965	2	2	1	1	2	4	6	7	9	3	2	1	40
	110	020	010	100	101	310	411	322	531	201	110	010	21 13 6
1966	0	0	0	1	2	1	4	9	10	4	5	2	38
	000	000	000	100	200	100	310	531	532	112	122	101	20 10 8
1967	1	0	2	1	1	1	8	10	8	4	4	1	41
	010	000	110	100	010	100	332	343	530	211	400	010	20 15 6
1968	0	1	0	1	0	4	3	8	4	6	4	0	31
	000	001	000	100	000	202	120	341	400	510	400	000	20 7 4
1969	1	0	1	1	0	0	3	3	6	5	2	1	23
	100	000	010	100	000	000	210	210	204	410	110	010	13 6 4
1970	0	1	0	0	0	2	3	7	4	6	4	0	27
	000	100	000	000	000	110	021	421	220	321	130	000	12 12 3
1971	1	0	1	2	5	2	8	5	7	4	2	0	37
	010	000	010	200	230	200	620	311	511	310	110	000	24 11 2
1972	1	0	1	0	0	4	5	5	6	5	2	3	32
	100	000	001	000	000	220	410	320	411	410	200	210	22 8 2
1973	0	0	0	0	0	0	7	6	3	4	3	0	23
	000	000	000	000	000	000	430	231	201	400	030	000	12 9 2
1974	1	0	1	1	1	4	5	7	5	4	4	2	35
	010	000	010	010	100	121	230	232	320	400	220	020	15 17 3
1975	1	0	0	1	0	0	1	6	5	6	3	2	25
	100	000	000	001	000	000	010	411	410	321	210	002	14 6 5
1976	1	1	0	2	2	2	4	4	5	0	2	2	25
	100	010	000	110	200	200	220	130	410	000	110	020	14 11 0
1977	0	0	1	0	1	1	4	2	5	4	2	1	21
	000	000	010	000	001	010	301	020	230	310	200	100	11 8 2
1978	1	0	0	1	0	3	4	8	4	7	4	0	32
	010	000	000	100	000	030	310	341	310	412	121	000	15 13 4
1979	1	0	1	1	2	0	5	4	6	3	2	3	28
	100	000	100	100	011	000	221	202	330	210	110	111	14 9 5
1980	0	0	1	1	4	1	5	3	7	4	1	1	28
	000	000	001	010	220	010	311	201	511	220	100	010	15 9 4
1981	0	0	1	1	1	2	5	8	4	2	3	2	29
	000	000	100	010	010	200	230	251	400	110	210	200	16 12 1
1982	0	0	3	0	1	3	4	5	6	4	1	1	28
	000	000	210	000	100	120	220	500	321	301	100	100	19 7 2
1983	0	0	0	0	0	1	3	6	3	5	5	2	25
	000	000	000	000	000	010	300	231	111	320	320	020	12 11 2
1984	0	0	0	0	0	2	5	7	4	8	3	1	30
	000	000	000	000	000	020	410	232	130	521	300	100	16 11 3
1985	2	0	0	0	1	3	1	7	5	5	1	2	27
	020	000	000	000	100	201	100	520	320	410	010	110	17 9 1
1986	0	1	0	1	2	2	2	5	2	5	4	3	27
	000	100	000	100	110	110	200	410	200	320	220	210	19 8 0
1987	1	0	0	1	0	2	4	4	7	2	3	1	25
	100	000	000	010	000	110	400	310	511	200	120	100	18 6 1
1988	1	0	0	0	1	3	2	5	8	4	2	1	27
	100	000	000	000	100	111	110	230	260	400	200	010	14 12 1
1989	1	0	0	1	2	2	6	8	4	6	3	2	35
	010	000	000	100	200	110	231	332	220	600	300	101	21 10 4
1990	1	0	0	0	2	4	4	5	5	5	4	1	32
	100	000	000	000	110	211	220	500	410	230	310	100	21 10 1
(1960-1990)													
MEAN:	0.6	0.2	0.5	0.7	1.3	2.2	4.5	6.1	5.5	4.6	2.8	1.4	30.8
CASES:	19	8	17	22	41	68	141	190	172	144	88	44	954

Figure 3-1. Chronology of western North Pacific and North Indian Ocean tropical cyclones for 1990.

TABLE 3-3 **WESTERN NORTH PACIFIC TROPICAL CYCLONES**

TYPHOONS
(1945 - 1959)

	JAN	FEB	MAR	APR	MAY	JUN	JUL	AUG	SEP	OCT	NOV	DEC	TOTALS
MEAN:	0.3	0.1	0.3	0.4	0.7	1.0	2.9	3.1	3.3	2.4	2.0	0.9	16.4
CASES:	5	1	4	6	10	15	29	46	49	36	30	14	245

(1960 - 1990)

	JAN	FEB	MAR	APR	MAY	JUN	JUL	AUG	SEP	OCT	NOV	DEC	TOTALS
MEAN:	0.3	0.1	0.2	0.5	0.7	1.1	2.7	3.2	3.2	3.1	1.7	0.6	17.5
CASES:	9	2	6	15	23	34	84	99	100	97	54	20	543

TROPICAL STORMS AND TYPHOONS
(1945 - 1959)

	JAN	FEB	MAR	APR	MAY	JUN	JUL	AUG	SEP	OCT	NOV	DEC	TOTALS
MEAN:	0.4	0.1	0.5	0.5	0.8	1.6	2.9	4.0	4.2	3.3	2.7	1.2	22.2
CASES:	6	2	7	8	11	22	44	60	64	49	41	18	332

(1960 - 1990)

	JAN	FEB	MAR	APR	MAY	JUN	JUL	AUG	SEP	OCT	NOV	DEC	TOTALS
MEAN:	0.6	0.3	0.4	0.7	1.1	1.9	4.2	5.3	4.9	4.2	2.6	1.2	27.3
CASES:	18	8	13	21	35	58	129	165	153	130	82	38	850

1990 FORMATION ALERTS: 30 OF 33 INITIAL FORMATION ALERTS DEVELOPED INTO SIGNIFICANT TROPICAL CYCLONES. NO TROPICAL CYCLONE FORMATION ALERT WAS ISSUED FOR TROPICAL CYCLONE 04W.

WARNINGS DAYS:
NUMBER OF CALENDAR WARNING DAYS: 165
NUMBER OF CALENDAR WARNING DAYS WITH TWO TROPICAL CYCLONES: 54
NUMBER OF CALENDAR WARNING DAYS WITH THREE TROPICAL CYCLONES: 3

TABLE 3-4 **TROPICAL CYCLONE FORMATION ALERTS**
WESTERN NORTH PACIFIC OCEAN

YEAR	INITIAL TCFAS	TROPICAL CYCLONES WITH TCFAS	TOTAL TROPICAL CYCLONES	FALSE ALARM RATE	PROBABILITY OF DETECTION
1976	34	25	25	26%	100%
1977	26	20	21	23%	95%
1978	32	27	32	16%	84%
1979	27	23	28	15%	82%
1980	37	28	28	24%	100%
1981	29	28	29	3%	96%
1982	36	26	28	28%	93%
1983	31	25	25	19%	100%
1984	37	30	30	19%	100%
1985	39	26	27	33%	96%
1986	38	27	27	29%	100%
1987	31	24	25	23%	96%
1988	33	26	27	21%	96%
1989	51	32	35	32%	91%
1990	33	30	31	9%	97%
(1976-1990) MEAN:	34.3	26.5	27.9	21%	95%

3.2 WESTERN NORTH PACIFIC TROPICAL CYCLONES

1990 was an average year with 31 tropical cyclones - 4 super typhoons, 17 typhoons, 10 tropical storms and one tropical depression. This was above average for the number of typhoons and super typhoons, similar to 1989, but below in tropical depressions. All the tropical cyclones formed in the monsoon, or near-equatorial, trough even though the TUTT was much in evidence during the summer.

The year started off with a bang with Typhoon Koryn (01W) forming below 5° north latitude in a near-equatorial trough the second week of January. After a three month break in activity, Lewis (02W) flared up in low latitudes the last week of April, and Marian (03W) followed, finishing up by mid-May. The rest of May and first half of June were quiet, then Tropical Depression 04W formed in the South China Sea. As the monsoon trough extended eastward, so did the area for development of the next four tropical cyclones. First Nathan (05W) started just east of Mindanao, then Ofelia (06W) a little farther east, and Percy (07W), and finally, the last two days of June, Robyn (08W) in the eastern Caroline Islands.

During the first two weeks of July, a change took place in the synoptic pattern. A large TUTT low became dominant just west of the date line and drifted westward. Deep convection extended in a hook-like pattern south and east of the TUTT low and the low level monsoon trough became oriented northeast to southwest. A three-storm multiple outbreak followed during the third week of July. Three small tropical cyclones - Steve (09W), Tasha (10W) and Vernon (11W) - formed as the trough continued moving northwestward towards Asia. By the first week of August, the trough axis was near 25° north latitude and supported Winona's (12W) development near Okinawa.

After Winona (12W) the monsoon trough reestablished a normal orientation, extending southeastward from Asia in the southern Philippine Sea and large tropical cyclones generated one at a time, starting with Yancy (13W) in the second week of August. The process continued through Hattie (22W) which started the last week of September. Cecil (18W), a midget tropical storm, was the only exception. During the second week of October northeasterly low-level flow surged into the northern South China Sea, as Hattie (22W) recurved. Three South China Sea cyclones - Ira (23W), Jeana (24W) and Lola (26W) - followed. After Kyle (25W), which began the middle of October, recurved just east of Iwo Jima, the summer monsoon weakened as winter set in and the axis of the monsoon trough shifted equatorward.

Following a two week break in activity, Mike (27W) formed in the eastern Caroline Islands at the end of the first week of November and became the first of three super typhoons to occur during the month. Nell (28W) developed in the South China Sea in association with the enhanced monsoonal flow into Mike (27W). The winter monsoon became established across Southeast Asia, however activity continued in the near-equatorial trough to the east. Initially tropical cyclone development was slow with both Page (29W) and Owen (30W) remaining as tropical disturbances for over a week. The pair intensified as Sina (03P) generated in the Southern Hemisphere near the date line. Almost two weeks of relative quiet followed before Russ (31W) formed in the near-equatorial trough below 5° north latitude with a twin, Joy (06P) forming in the Southern Hemisphere.

JANUARY THROUGH MAY

The first tropical cyclone of 1990 in the western North Pacific, **Koryn (01W)** also became the third typhoon to occur in January in the past eleven years. Unlike Typhoon Jack (1989), which two weeks earlier came to an abrupt halt and rapidly dissipated just east of Guam, this typhoon turned northward and tracked through the Mariana Islands. Koryn brought the strongest sustained winds to the Marianas since Roy (1988), another January typhoon. After a three month lull, **Lewis (02W)** developed 200 nm south of Chuuk and moved

north, passing directly over the island. After continuing its northward trek for four more days, it was sheared apart by a digging midlatitude trough, and the low-level remnants of the tropical cyclone drifted west-northwestward for several more days before completely dissipating. **Marian (03W)** followed and persisted in low latitudes for almost a week before intensifying to become the second typhoon of 1990 and the only significant tropical cyclone to form in May. It tracked from the Philippine Sea across the Philippine Islands and into the South China Sea, where recurved and merged with a frontal system to form an extratropical low.

JUNE

Following a one month break in tropical cyclone activity, **Tropical Depression 04W**, became the first significant tropical cyclone to form in the South China Sea this year. Because satellite and synoptic fix positions disagreed throughout the depression's life, the depression proved to be very difficult to locate and forecast. As **Tropical Storm Nathan (05W)** crossing into the South China Sea, Tropical Depression 04W was drawn into the larger circulation and absorbed. Nathan, then executed an abrupt track change and stalled before tracking off to the north. Both the track and intensity of TD04W and Nathan were dominated by a larger monsoon circulation in the South China Sea. **Ofelia (06W)** became the third typhoon of 1990 and the first for the month of June. It moved toward the Philippine Islands, then slowed and turned to the northwest. It was the second tropical cyclone of the year to strike Taiwan and the first to affect the east coast of China. After recurvature, the extratropical remnants of Ofelia crossed Korea; an unusual characteristic for a June system. **Percy (07W)** followed as the fourth and last tropical cyclone in June. After forming southeast of Guam, it turned on an unusual track to the southwest for 36 hours before paralleling Ofelia's (06W) track to the west-northwest around the western periphery of the subtropical ridge. Percy damaged the western Caroline Islands and became the second typhoon within a week to batter northern Luzon before recurving over eastern China.

JULY THROUGH OCTOBER

The first significant tropical cyclone of July, **Robyn (08W)** followed what at first glance might appear to be a typical recurvature track. However, Robyn's motion was actually a classic example of the response of a tropical cyclone to the establishment of an omega block in the westerlies to the north, and thus was significant as a case study of an infrequent, but complex, synoptic influence on tropical cyclone motion. The monsoon trough activity substantially increased and **Steve (09W)** along with Tropical Storm Tasha (10W) and Typhoon Vernon (11W) combined into the only three storm tropical cyclone outbreak to occur in the northwest Pacific this year. Steve persisted on an atypical northeastward track throughout its existence. **Tasha (10W)**, the third of four western Pacific tropical cyclones to occur in July, developed in the monsoon trough, but instead of following Steve (09W) and Vernon (11W) to the northeast, it made only a brief start in that direction before curving to the west and entering the South China Sea. After erratic motion and slow intensification, Tasha finally reached tropical storm intensity before slamming into the southern coast of China. **Vernon (11W)**, the last of four tropical cyclones to develop during July, followed Steve's northward-oriented track, as the monsoon trough underwent a major displacement to the north. The first typhoon of 1990 to hit Japan, **Winona (12W)** was the only tropical cyclone to form poleward of 25°north latitude this year. It formed in August from the remnants of Tropical Storm Tasha (10W) in a monsoon trough that was displaced northward of its normal location. Winona had an unusual track to the southeast before it turned northward to cross the southern portion of the Kanto Plain. In the central Pacific, **Aka (01C)** developed and remained embedded in the trade wind trough. It tracked steadily west-northwestward and never developed beyond tropical storm intensity. Aka

was the only tropical cyclone of 1990 to be in warning status when it crossed the date line from the Central into the Western Pacific Ocean. As Aka was dissipating, **Yancy (13W)** generated in the monsoon trough. It became JTWC's best forecast tropical cyclone of the year, and although the track was generally toward the northwest, it contained several interesting features, including interaction with a strengthening subtropical ridge, the effects of a passing mid-latitude shortwave trough and land interaction with the mountainous terrain of Taiwan. In the wake of Typhoon Yancy (13W), a surge in the southwesterly monsoon flow developed and **Zola (14W)** formed west of Guam in the monsoon trough. The depression initially tracked northeastward in response to a monsoon surge and slowly intensified. Zola then broke away from the monsoon trough and intensified to a typhoon. The typhoon recurved over western Honshu, moved into the Sea of Japan and accelerated east-northeastward. **Typhoon Abe (15W)**, the fourth of five tropical cyclones in August, caused
extensive damage from the Republic of the Philippines to northern China during its nine day life. Abe was also noteworthy as a classic example of the erratic motion and rapid reorganization that can occur in association with an intense monsoon surge. **Becky (16W)**, a midget typhoon and the eleventh typhoon of 1990, generated in the monsoon trough and tracked south of the subtropical ridge throughout its existence. After initially moving west-northwestward, the storm took a southwestward track across the northwestern tip of Luzon before heading westward across the South China Sea. Becky hit northern Luzon with typhoon-force winds and later slammed into northern Vietnam as a severe tropical storm. **Dot (17W)** developed in the monsoon trough at the same time as Tropical Storm Cecil (18W) and brought enhanced southwesterly wind flow and heavy rains across Guam. Later, as Dot crossed central Taiwan, torrential monsoon rains from the associated monsoon surge caused extensive flooding in northern Luzon. During its passage across Taiwan and the Fujian Province of China, surface winds in the Formosa Strait exceeded 50 kt (26 m/sec) for 30 hours. **Tropical Storm Cecil (18W)** was a short-lived, midget tropical cyclone that formed in the wake of Typhoon Abe (15W). As Abe raced poleward, the monsoon trough reestablished itself over northern Luzon, and Cecil formed at the northeast end of the trough. Cecil tracked northward and skirted the northern coast of Taiwan before making landfall in southeastern China. **Ed (19W)**, which had the second longest track (3150 nm (5830 km)) of any "straight runner" in 1990, formed in the Marshall Islands and continued westward for nearly two weeks before finally making landfall in northern Vietnam. It was the third of six tropical cyclones to form in September. **Flo (20W)** was the fourth of six tropical cyclones to develop in September, the first of four super typhoons this year, and the object of over three consecutive days of upper-tropospheric aircraft reconnaissance missions during the TCM-90 field experiment. Flo formed in the wake of Typhoon Ed (19W), passed close by Guam, then rapidly intensified into a super typhoon as it approached Okinawa. Recurvature was slow before the tropical cyclone accelerated northeastward towards the Japanese mainland where it was called the most powerful typhoon to hit Honshu in 19 years. At least 38 people were reported dead or missing, and damage was estimated in the millions of dollars. Transportation, communications and power were also disrupted. **Gene (21W)** was the fifth significant tropical cyclone to form in September and the fifteenth of the year to reach typhoon intensity. The initial disturbance formed 250 nm (465 km) west-southwest of Guam and tracked westward for three days before turning northwestward. Gene followed a classic recurvature pattern, passing west of Okinawa and skirting southern Japan. The orientation of Gene's recurvature track resulted in sustained radar contact from 251400Z to 300400Z and an excellent, high quality set of 250 position reports from land radar sites in the islands nearby. **Hattie (22W)**, the last of six tropical cyclones to form in September, was the fourth tropical cyclone in a six-week period to affect Okinawa and southern Japan. It also

followed a classic recurvature track. **Ira (23W)** was the eighth tropical cyclone to hit Vietnam in 1990 and the last in a series of weak, highly sheared tropical systems in the South China Sea. It formed in a broad area of convection near Palawan Island. The convective cloud mass tracked steadily westward in the deep easterly flow and made landfall at Qui Nhon, Vietnam on the third of October. **Jeana (24W)**, the second of four tropical cyclones to form in October, was the fifth to churn across the South China Sea in 1990. This minimal tropical storm proved to be as difficult to estimate intensity for, as it was to position. **Kyle (25W)** generated from a disturbance in the monsoon trough 600 nm (1110 km) east of Guam. Separating from the trough, the cloud system gained organization and began to track along the southern edge of the subtropical ridge to its northeast. The subtropical ridge and a series of fast moving mid-latitude short-wave troughs strongly influenced Kyle's track. The tropical cyclone passed through the northern Mariana Islands, causing minimal damage, intensified into a typhoon, and recurved. **Lola (26W)**, the last of four tropical cyclones to develop in October, formed in the South China Sea. It tracked westward along the same path taken by Tropical Storm Jeana (24W) four days earlier.

NOVEMBER THROUGH DECEMBER

Mike (27W), one of the most intense and destructive tropical cyclones of 1990, caused havoc in western Carolines and in the central Philippine islands. Although basically a west-northwestward "straight runner," it posed numerous forecast challenges due to frequent direction, speed and intensity changes. As a result of the devastation and death in the Republic of the Philippines, Super Typhoon Mike's name was retired from the JTWC list of tropical cyclone names. **Nell (28W)**, the second of four November tropical cyclones, intensified in the South China Sea and tracked westward, making landfall in Vietnam. **Page (29W)** was the third of four tropical cyclones to form in November, the second super typhoon of the month, and part of the three-storm outbreak which included a pair of tropical cyclones near the dateline: Owen (30W) in the northern hemisphere and Sina (TC 03P) in the southern hemisphere. Persisting as a discrete disturbance for nearly two weeks before the first warning was issued, Page took only three days to intensify to 140 kt (70 m/sec) once development commenced. **Owen (30W)** was both the longest lasting and one of the most interesting tropical cyclones of 1990. It started to rapidly intensify while still a tropical depression, explosively deepened to super typhoon intensity, weakened and then reintensified to a super typhoon. Owen started as a discrete cloud mass southwest of Hawaii, maintained its integrity as it tracked westward in the trade wind trough, but did not intensify until it crossed the dateline and passed north of Kwajalein in the Marshall Islands. It then reached typhoon intensity in less than 18 hours and continued westward over the central Caroline Islands until its deep convection was sheared away southeast of Ulithi Island in the western Carolines. The exposed low-level remained organized for six more days as it moved north, then west, and finally southwestward before dissipating over the Celebes Sea after crossing Mindanao. **Russ (31W)**, the last western North Pacific tropical cyclone of 1990, was the most severe to strike Guam in 14 years. Damage was estimated as high as 120 million dollars. Russ formed in the Marshall Islands, tracked west-northwestward and intensified to near super typhoon intensity as it approached Guam. The typhoon passed within 30 nm (55 km) of the southern tip of Guam and brought typhoon force winds which caused extensive damage, especially to the southern portion of the island. After leaving Guam, Russ slowly weakened, recurved and became an extratropical cyclone.

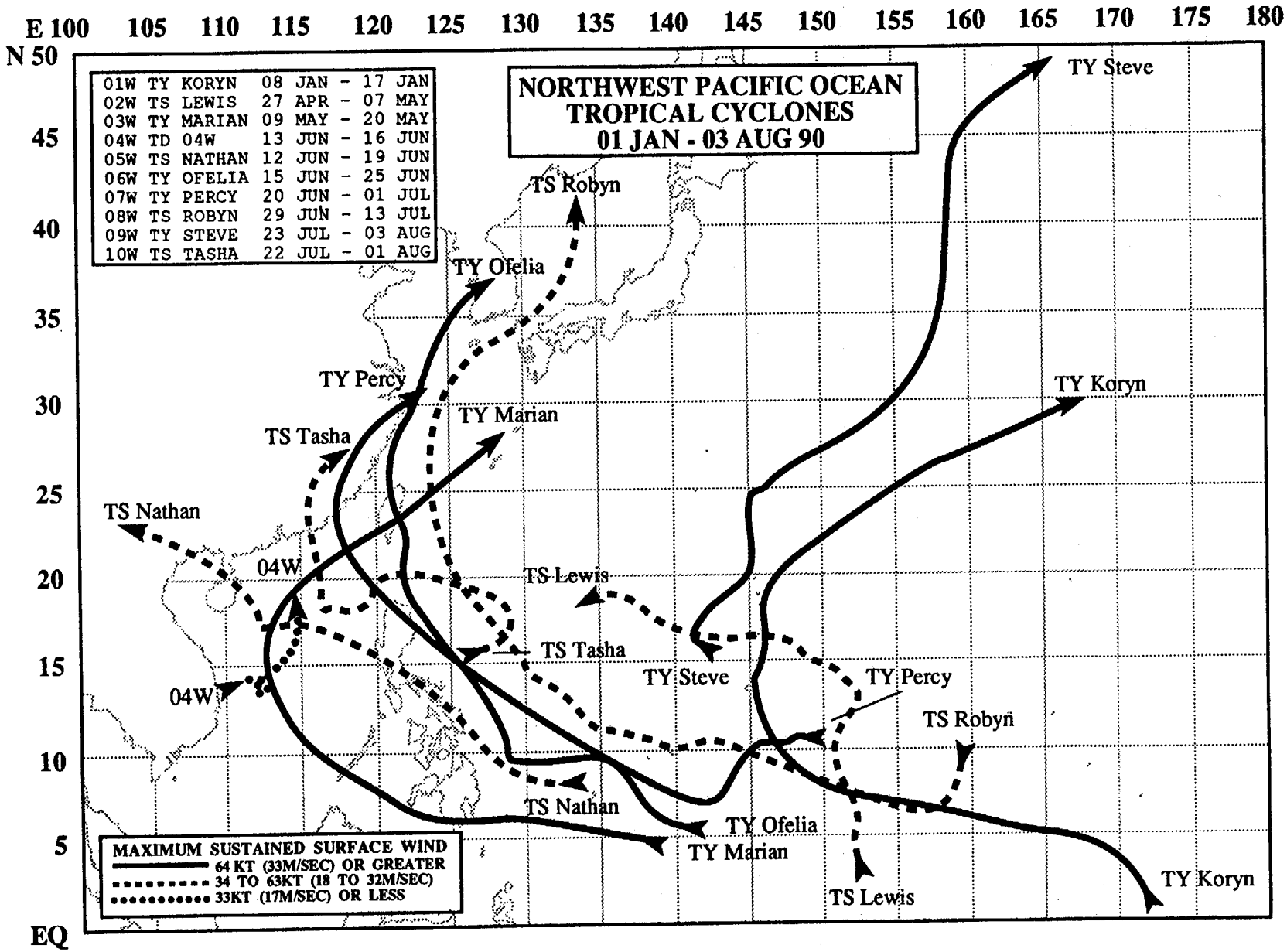
NORTHWEST PACIFIC OCEAN
TROPICAL CYCLONES
01 JAN - 03 AUG 90
01W TY KORYN 08 JAN - 17 JAN
02W TS LEWIS 27 APR - 07 MAY
03W TY MARIAN 09 MAY - 20 MAY
04W TD 04W 13 JUN - 16 JUN
05W TS NATHAN 12 JUN - 19 JUN
06W TY OFELIA 15 JUN - 25 JUN
07W TY PERCY 20 JUN - 01 JUL
08W TS ROBYN 29 JUN - 13 JUL
09W TY STEVE 23 JUL - 03 AUG
10W TS TASHA 22 JUL - 01 AUG
MAXIMUM SUSTAINED SURFACE WIND
64 KT (33M/SEC) OR GREATER
34 TO 63KT (18 TO 32M/SEC)
33KT (17M/SEC) OR LESS
E 100
105
110
115
120
125
130
135
140
145
150
155
160
165
170
175
180
N 50
45
40
35
30
25
20
15
10
5
EQ
TS Robyn
TY Ofelia
TY Percy
TY Marian
TS Tasha
TS Nathan
04W
04W
TS Lewis
TS Tasha
TY Steve
TY Percy
TS Robyn
TS Nathan
TY Ofelia
TY Marian
TS Lewis
TY Steve
TY Koryn
TY Koryn

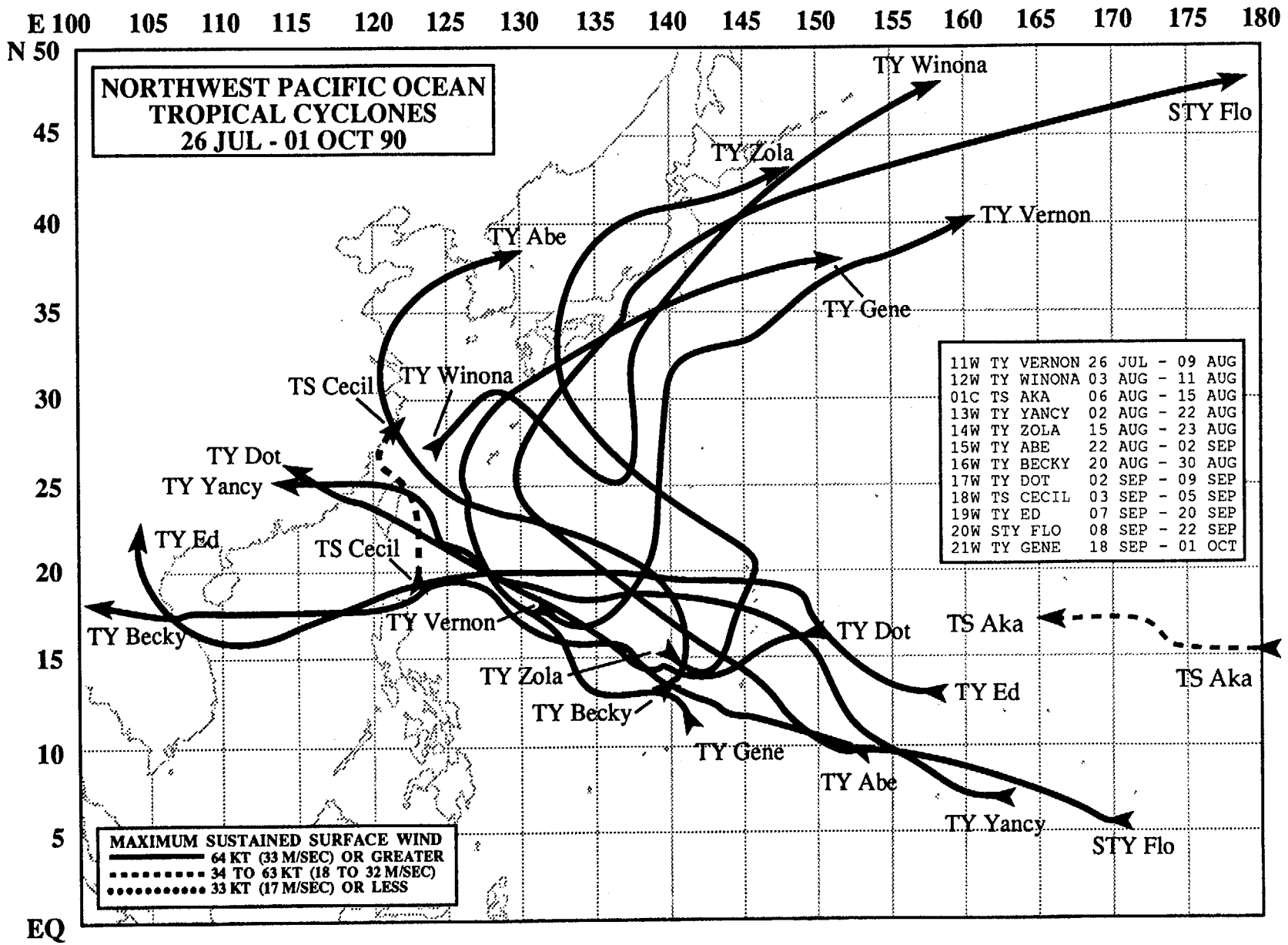
NORTHWEST PACIFIC OCEAN
TROPICAL CYCLONES
26 JUL - 01 OCT 90
E 100 105 110 115 120 125 130 135 140 145 150 155 160 165 170 175 180
N 50 45 40 35 30 25 20 15 10 5 EQ
TY Winona
STY Flo
TY Zola
TY Vernon
TY Abe
TY Gene
TS Cecil
TY Winona
TY Dot
TY Yancy
TY Ed
TS Cecil
TY Becky
TY Vernon
TY Dot
TS Aka
TS Aka
TY Zola
TY Ed
TY Becky
TY Gene
TY Abe
TY Yancy
STY Flo
11W TY VERNON 26 JUL - 09 AUG
12W TY WINONA 03 AUG - 11 AUG
01C TS AKA 06 AUG - 15 AUG
13W TY YANCY 02 AUG - 22 AUG
14W TY ZOLA 15 AUG - 23 AUG
15W TY ABE 22 AUG - 02 SEP
16W TY BECKY 20 AUG - 30 AUG
17W TY DOT 02 SEP - 09 SEP
18W TS CECIL 03 SEP - 05 SEP
19W TY ED 07 SEP - 20 SEP
20W STY FLO 08 SEP - 22 SEP
21W TY GENE 18 SEP - 01 OCT
MAXIMUM SUSTAINED SURFACE WIND
64 KT (33 M/SEC) OR GREATER
34 TO 63 KT (18 TO 32 M/SEC)
33 KT (17 M/SEC) OR LESS

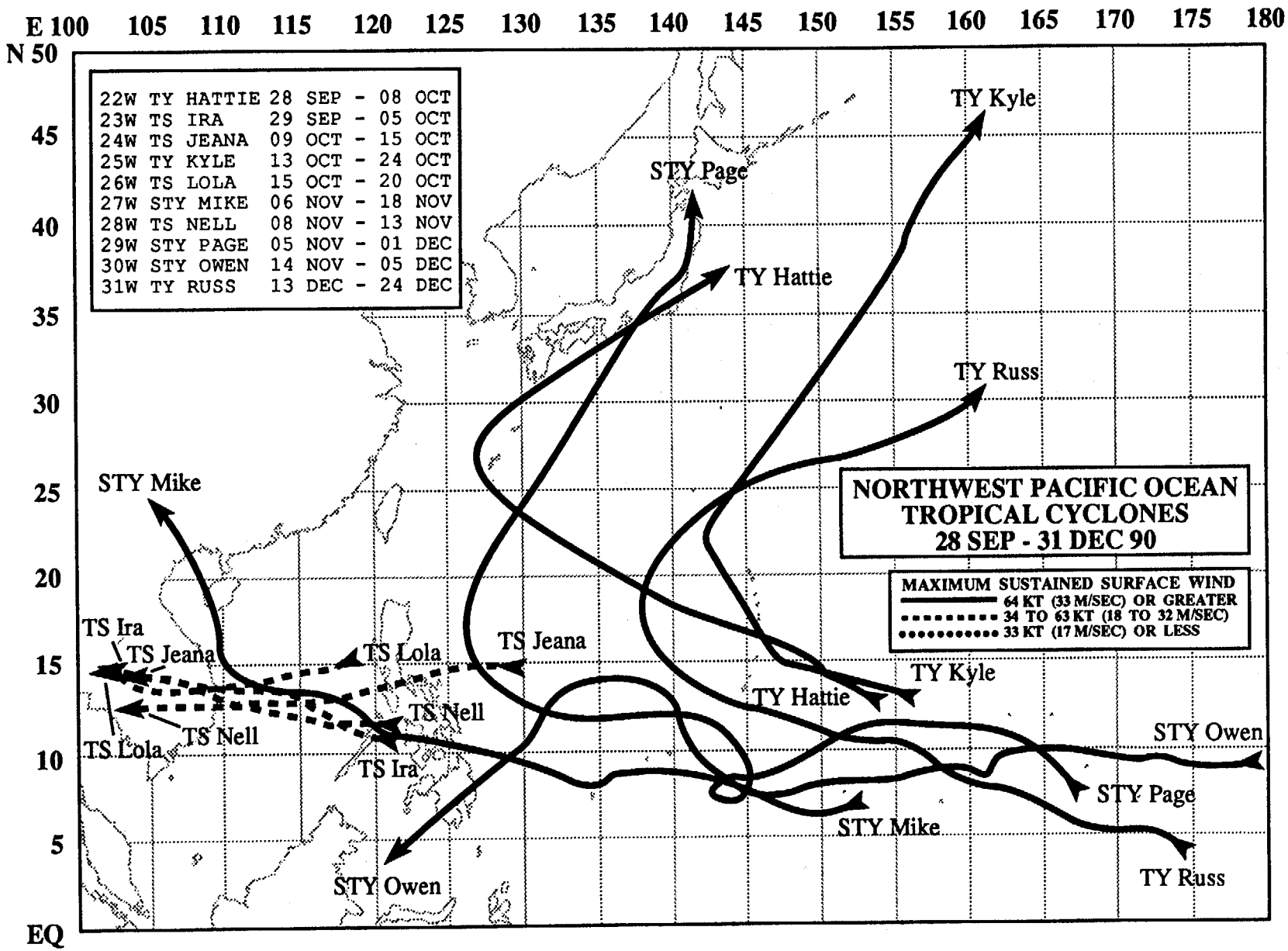
E 100 105 110 115 120 125 130 135 140 145 150 155 160 165 170 175 180
N 50 45 40 35 30 25 20 15 10 5 EQ
22W TY HATTIE 28 SEP - 08 OCT
23W TS IRA 29 SEP - 05 OCT
24W TS JEANA 09 OCT - 15 OCT
25W TY KYLE 13 OCT - 24 OCT
26W TS LOLA 15 OCT - 20 OCT
27W STY MIKE 06 NOV - 18 NOV
28W TS NELL 08 NOV - 13 NOV
29W STY PAGE 05 NOV - 01 DEC
30W STY OWEN 14 NOV - 05 DEC
31W TY RUSS 13 DEC - 24 DEC
NORTHWEST PACIFIC OCEAN
TROPICAL CYCLONES
28 SEP - 31 DEC 90
MAXIMUM SUSTAINED SURFACE WIND
64 KT (33 M/SEC) OR GREATER
34 TO 63 KT (18 TO 32 M/SEC)
33 KT (17 M/SEC) OR LESS
STY Page
TY Kyle
TY Hattie
TY Russ
STY Mike
TS Ira
TS Jeana
TS Lola
TS Nell
STY Owen

Intentionally left blank.

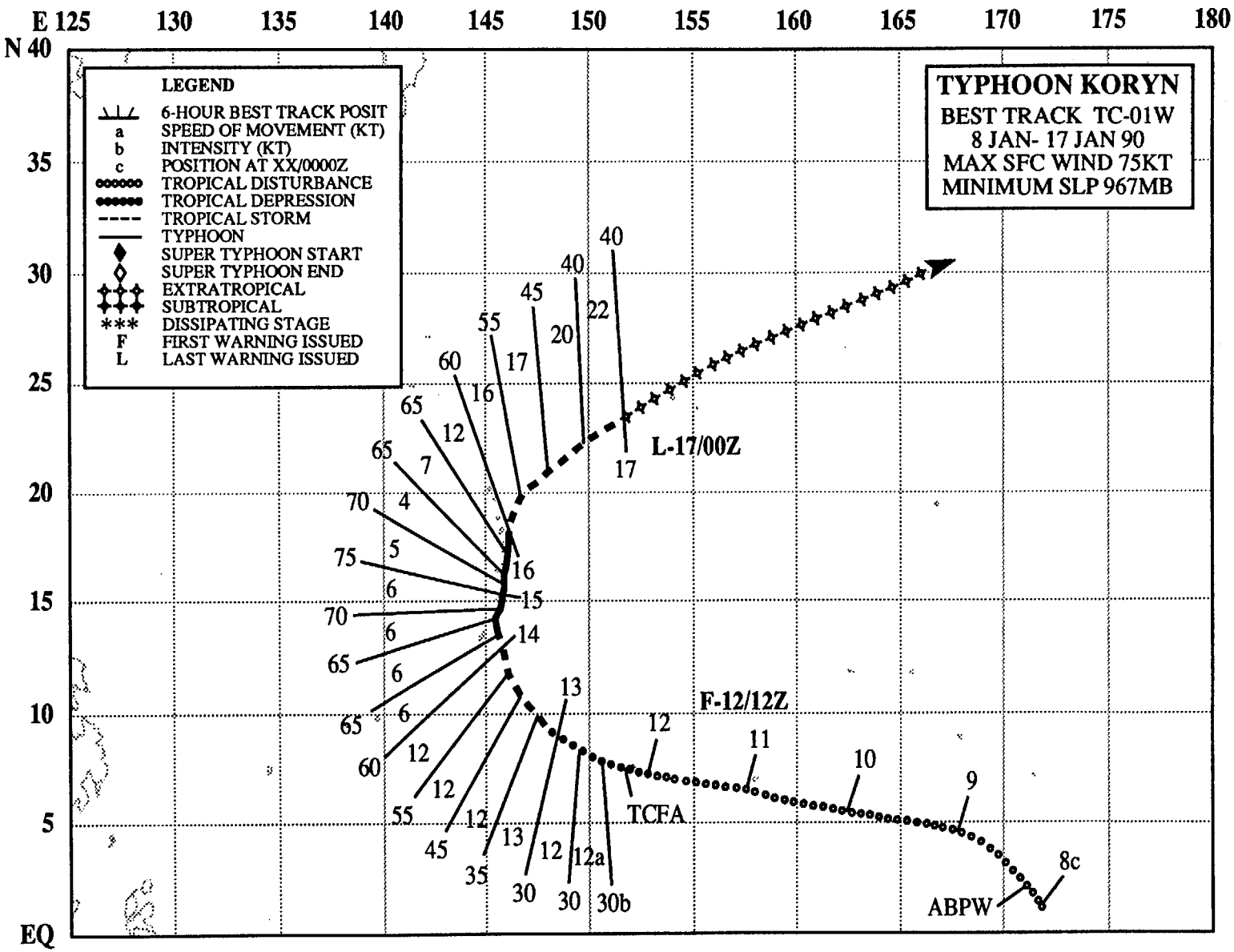
E 125
130
135
140
145
150
155
160
165
170
175
180
N 40
35
30
25
20
15
10
5
EQ
LEGEND
6-HOUR BEST TRACK POSIT
a SPEED OF MOVEMENT (KT)
b INTENSITY (KT)
c POSITION AT XX/0000Z
TROPICAL DISTURBANCE
TROPICAL DEPRESSION
TROPICAL STORM
TYPHOON
SUPER TYPHOON START
SUPER TYPHOON END
EXTRATROPICAL
SUBTROPICAL
*** DISSIPATING STAGE
F FIRST WARNING ISSUED
L LAST WARNING ISSUED
TYPHOON KORYN
BEST TRACK TC-01W
8 JAN- 17 JAN 90
MAX SFC WIND 75KT
MINIMUM SLP 967MB
L-17/00Z
F-12/12Z
TCFA
ABPW
8c
30b
12a

TYPHOON KORYN (01W)

I. HIGHLIGHTS

Koryn, the first tropical cyclone of 1990 in the western North Pacific, became the third typhoon to occur in January in the past eleven years. It developed at an unusually low latitude. Unlike Typhoon Jack (1989), which two weeks earlier came to an abrupt halt and rapidly dissipated just east of Guam, this typhoon turned northward and tracked through the Mariana Islands. Koryn brought the strongest sustained winds to the Marianas since Roy (1988), another January typhoon.

II. CHRONOLOGY OF EVENTS

081500Z - First mentioned on the Significant Tropical Weather Advisory due to persistence of convection.

120430Z - Tropical Cyclone Formation Alert followed 4 mb pressure falls with strong easterly flow to the north, weak westerlies to the south and a CI 1.5.

121200Z - First warning based on increased convective curvature and outflow aloft.

130600Z - Upgraded to tropical storm intensity following improved organization of convection and good outflow aloft in all quadrants which resulted in a CI 2.5.

140600Z - Upgraded to typhoon based on the appearance of an eye and a CI 4.0.

150000Z - Peak intensity 75 kt (39 m/sec) with a ragged eye and a CI 4.5.

160000Z - Downgraded to tropical storm with signs of extratropical transition, shearing-type cloud pattern and restricted outflow.

170000Z - Final warning. Koryn extratropical with exposed low-level circulation center displaced to southwest of central cloud mass.

III. TRACK AND MOTION

Koryn originated as a disturbance (Figure 3-01-1) near the Gilbert Islands. The cyclonic circulation formed in sympathetic response to enhanced westerly monsoonal flow extending from the Solomon Islands eastward along 5° south latitude to a low pressure system near the Fiji Islands. While Koryn was embedded in the flow south of the subtropical ridge, it moved west-northwestward to Chuuk (Truk) in the eastern Caroline Islands. The subtropical ridge was north of the tropical cyclone along 20°

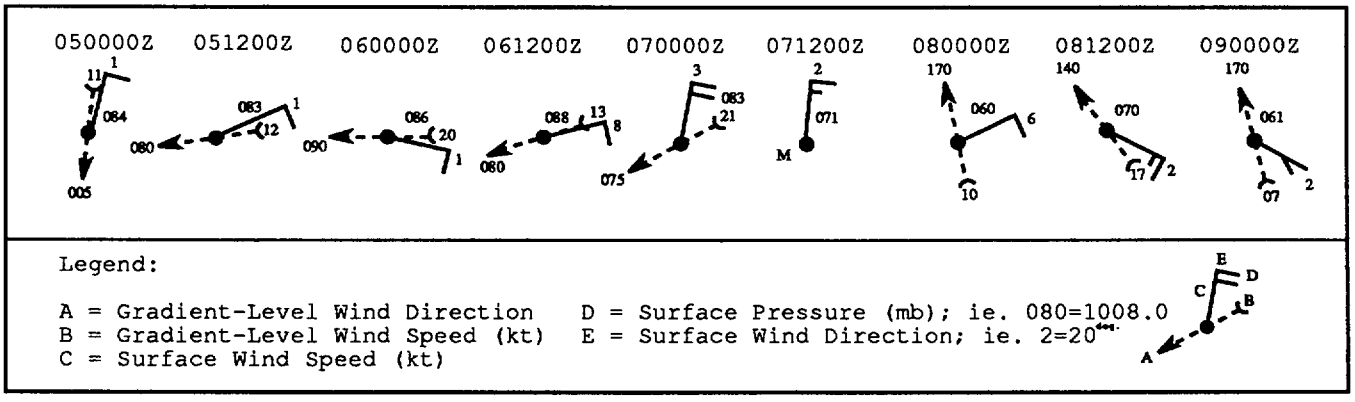

Figure 3-01-1. Surface pressure, gradient and surface wind reports for Tarawa (WMO 91610) in the Gilbert Islands reflect the formation of Koryn just to the west of the station. From 050000Z until 071200Z, the gradient-level wind is the normal cross-equatorial flow from the Northern Hemisphere, around a buffer system on the equator to the monsoon westerlies farther south. Note that on 8 January, the pressure in the past 24 hours fell over 2 mb and the gradient-level flow abruptly shifted to south-southeasterly. This supports the formation of a cyclonic circulation just to the west of the station.

north latitude; but lower pressures aloft in the northern Marianas indicated a break in the ridge. Koryn turned to a more northward track toward this break in the ridge and Guam. The typhoon slowed, passed just east of Guam and directly over Saipan. The slow forward motion and prolonged northward track appear related to the weaker steering flow associated with the break in the ridge and with the relative broad character of the ridge itself (Figure 3-01-2). Strong zonal westerlies aloft resulted in recurvature and a northeastward acceleration. Koryn's residual circulation and associated cloudiness continued northeastward along the edge of the maritime polar air and linked up to a passing short wave.

IV. INTENSITY

Koryn's weak low-level circulation first appeared just to the north of a broad area of cloudiness that stretched along and south of the equator. As this circulation moved west-northwestward, convection flared-up to its north and east. This enhanced cloudiness (Figure 3-01-3) became more organized and developed into a tropical cyclone as the low-level circulation center moved beneath an area of upper-level divergence. The synoptic scale upper-level anticyclone remained displaced to the east. Although upper tropospheric southeasterlies restricted Koryn's outflow to the southeast, the upper-level anticyclone of the typhoon continued to provide good outflow until the system reached its peak intensity (Figure 3-01-4). As Koryn moved northward, increasing vertical wind shear in the mid-

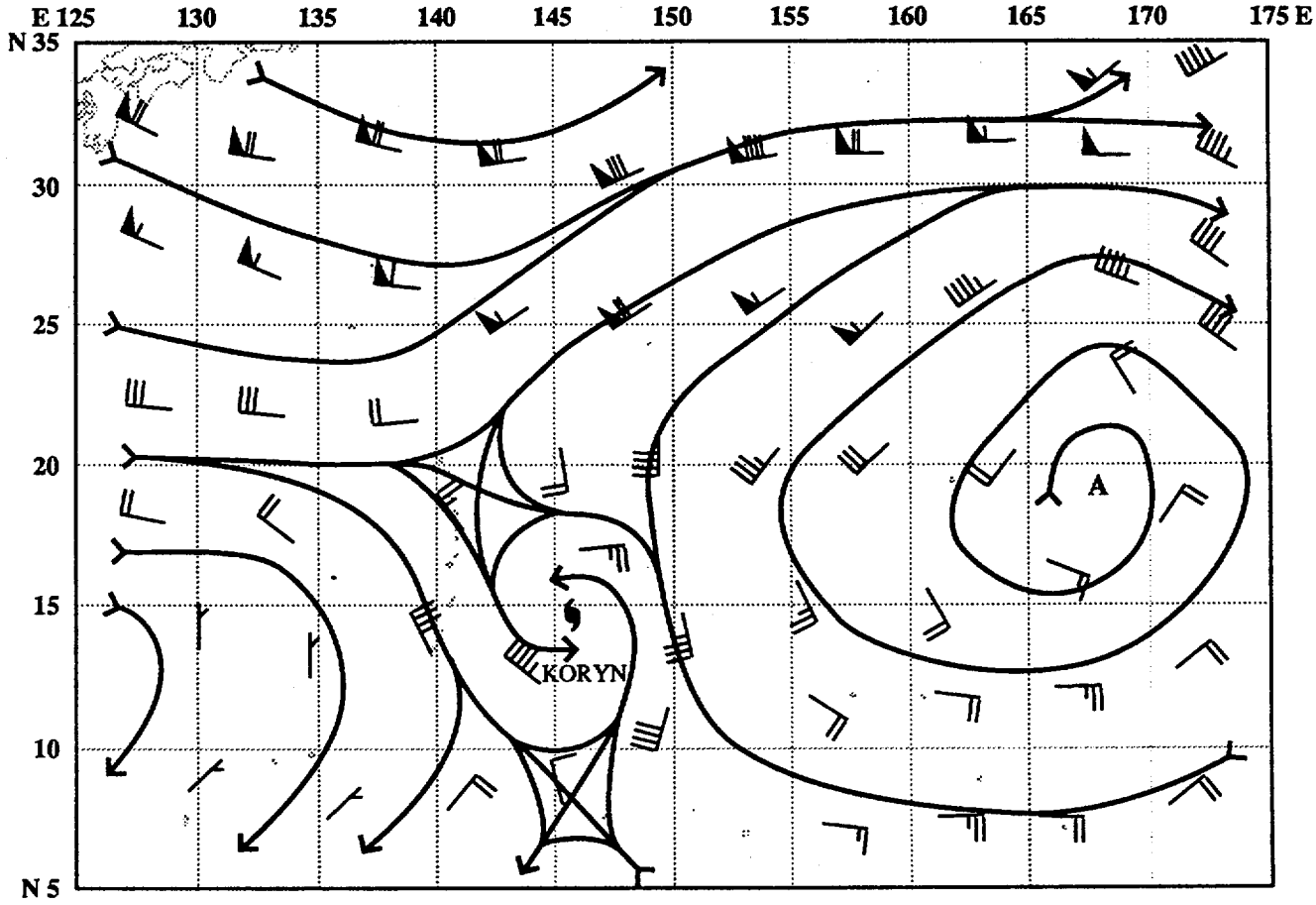

Figure 3-01-2. NOGAPS 500 mb analysis for 141200Z January shows the typhoon in the relative broad subtropical ridge. The ridge axis is at approximately 20° north latitude.

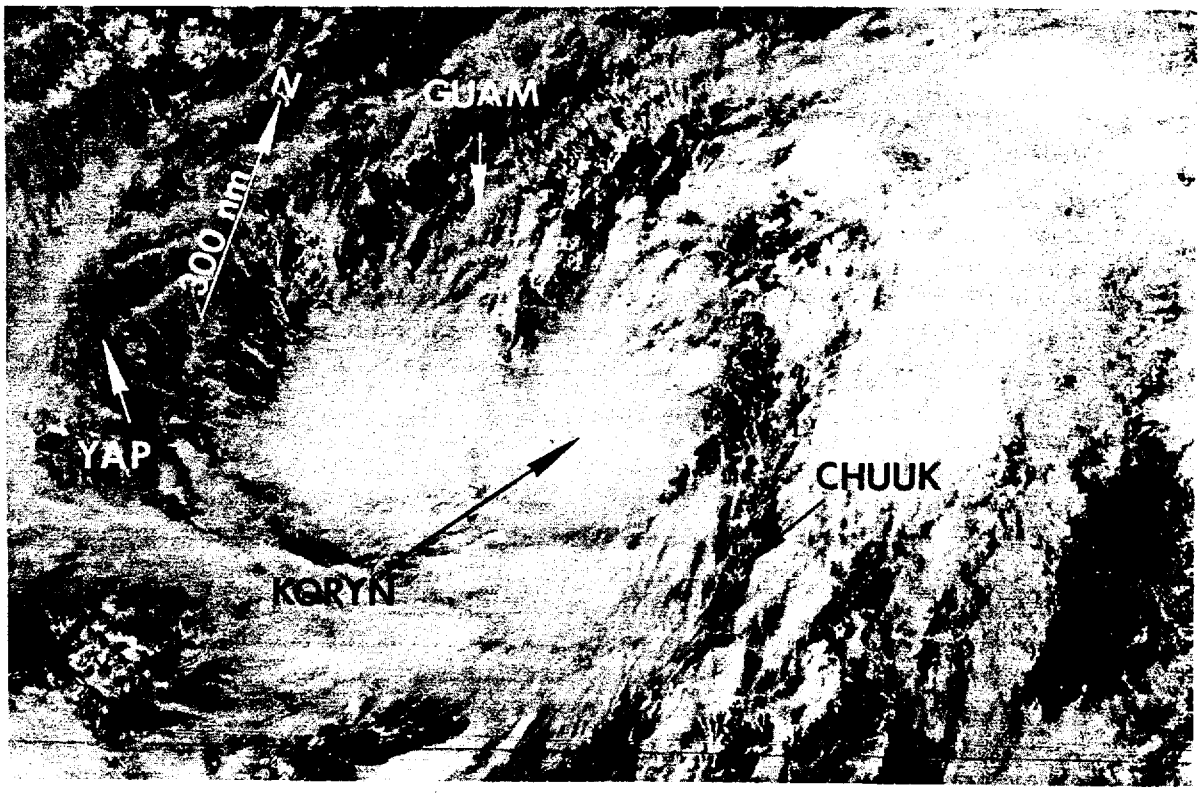

Above: Figure 3-01-3. Tropical Depression 01W's poorly defined cloudiness southeast of Guam (122330Z January DMSP visual imagery).

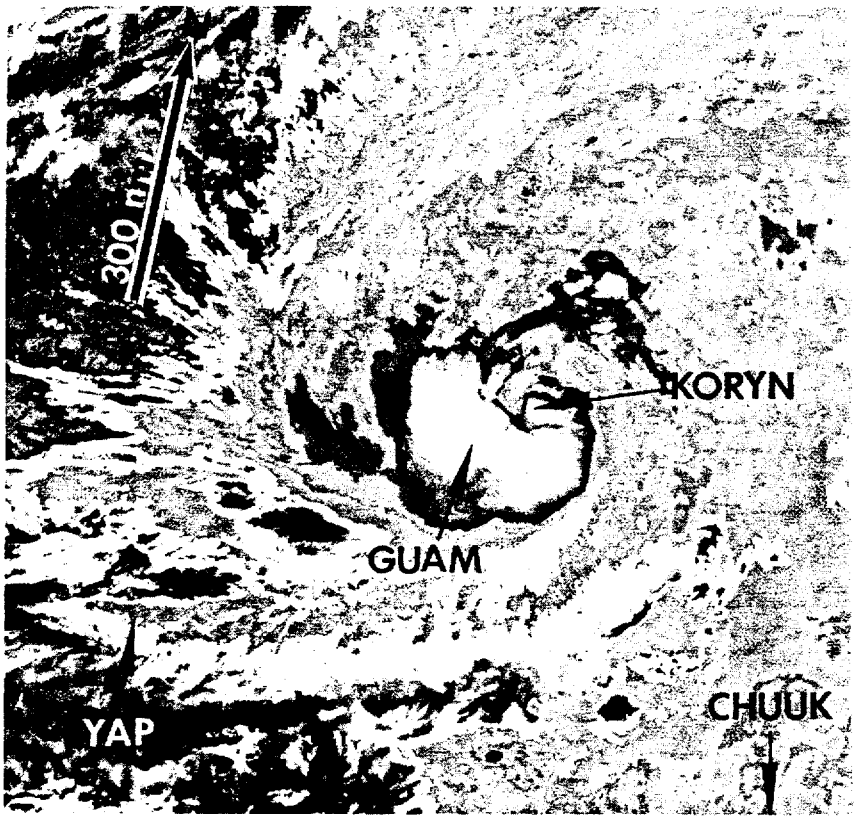

Left: Figure 3-01-4. Typhoon Koryn near peak intensity and just before maximum surface wind gusts to 70 kt (36 m/sec) were recorded on Guam (140958Z January NOAA enhanced infrared imagery).

latitude westerlies weakened the system. After recurvature, the cyclone's acceleration retarded the penetration of cooler low-level air into the center maintaining the intensity. Extratropical transition was completed a day after recurvature started.

V. FORECASTING PERFORMANCE

Overall JTWC forecast performance is shown in Figure 3-01-5. Initially, the weakness in the subtropical ridge was not expected to influence the track. As a result, JTWC forecast a westward track instead of recurvature near Guam. OTCM guidance (Figure 3-01-6) at first indicated a west-northwest track. However, on 13 January OTCM began to hint at recurvature. At 131800Z, JTWC included recurvature (Figure 3-01-7) as an alternate scenario, and it became the primary on the next warning. The forecast track might have been adjusted sooner, but disagreement among radar and satellite fixes resulted in the initial working best track being more westward and slower than the actual track as the system approached Guam.

VI. IMPACT

The forecasting difficulties mentioned above reduced on-island preparation time for Koryn's closest approach to Guam. Andersen AFB suspended aircraft evacuation and only one Navy ship sortied from Apra Harbor. The aircraft and ships remaining in Guam did not sustain any damage. Although Koryn passed within 50 nm (93 km) east of Guam, the island suffered only slight damage. Maximum winds reported at Andersen AFB were 40 kt (21 m/sec) gusting to 55 kt (28 m/sec). NAS Agana reported 54 kt (28 m/sec) gusting to 70 kt (36 m/sec). Koryn passed directly over Saipan, which also sustained only minor damage. Maximum winds at the Saipan Airport were 32 kt (16 m/sec), and the minimum sea-level pressure was 981 mb.

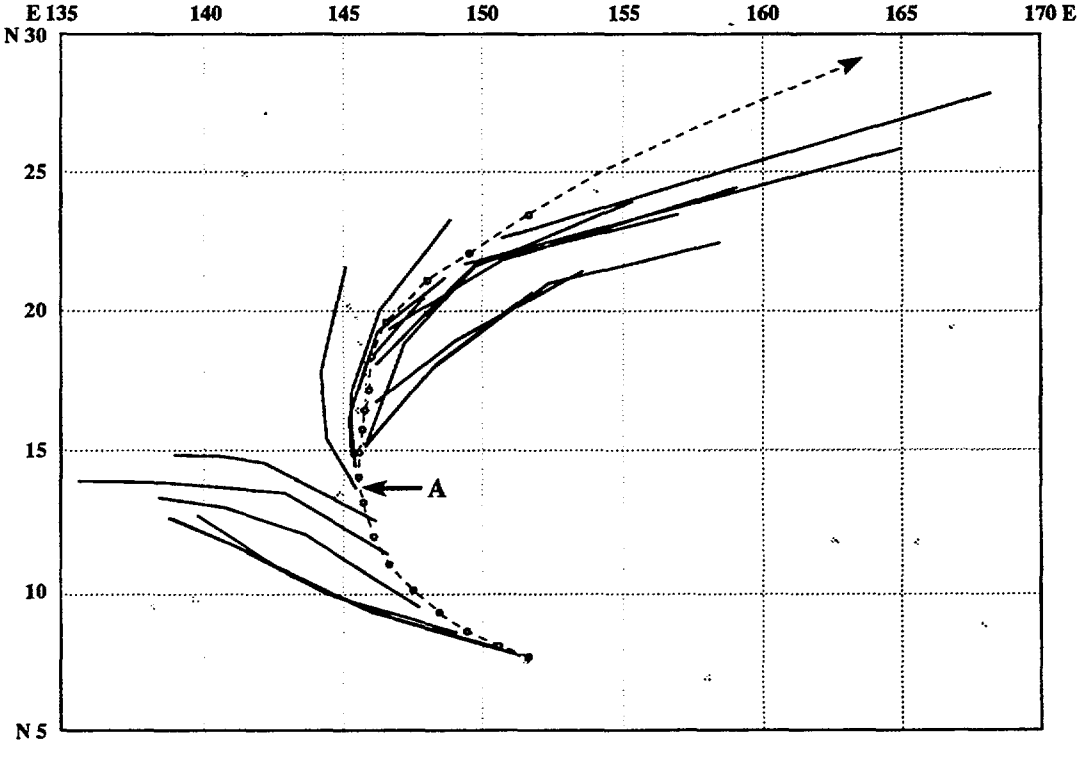

Figure 3-01-5. Summary of forecasts (solid lines) for Koryn superimposed on the final best track (dashed line). Point A identifies the first recurvature forecast at 140000Z.

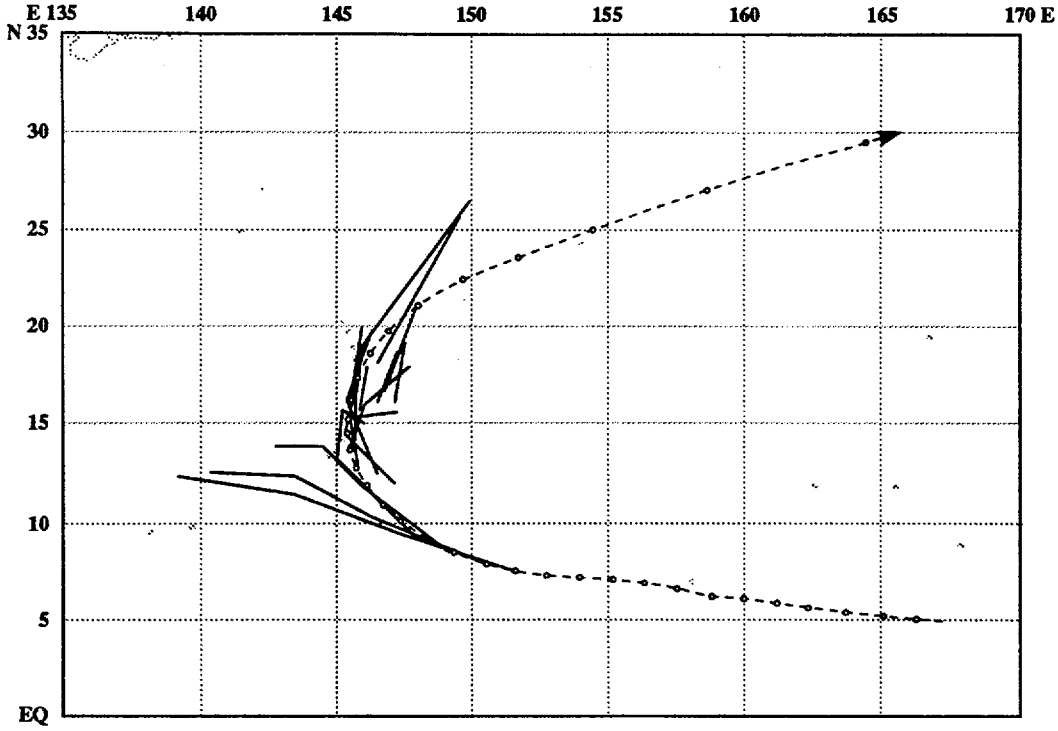

Figure 3-01-6. OTCM guidance (solid lines) superimposed on the final best track for Koryn (dashed line). OTCM started to hint at recurvature early on 13 January.

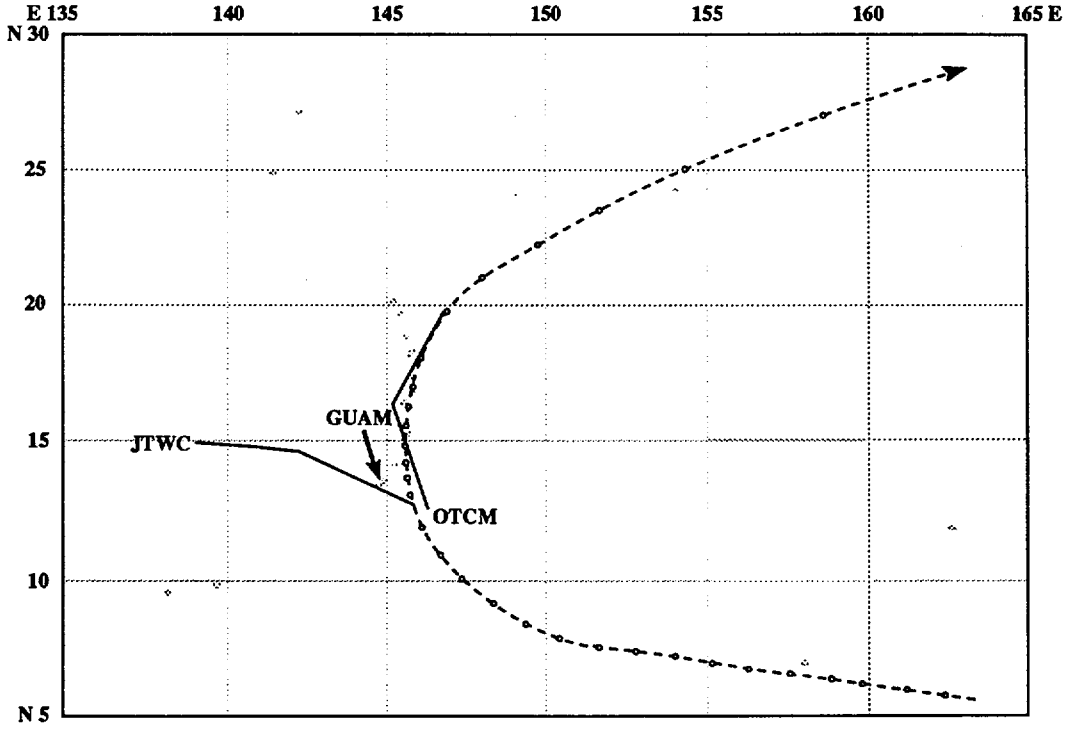

Figure 3-01-7. Comparison of the JTWC forecast (solid line) and OTCM guidance (solid line) at 131800Z.

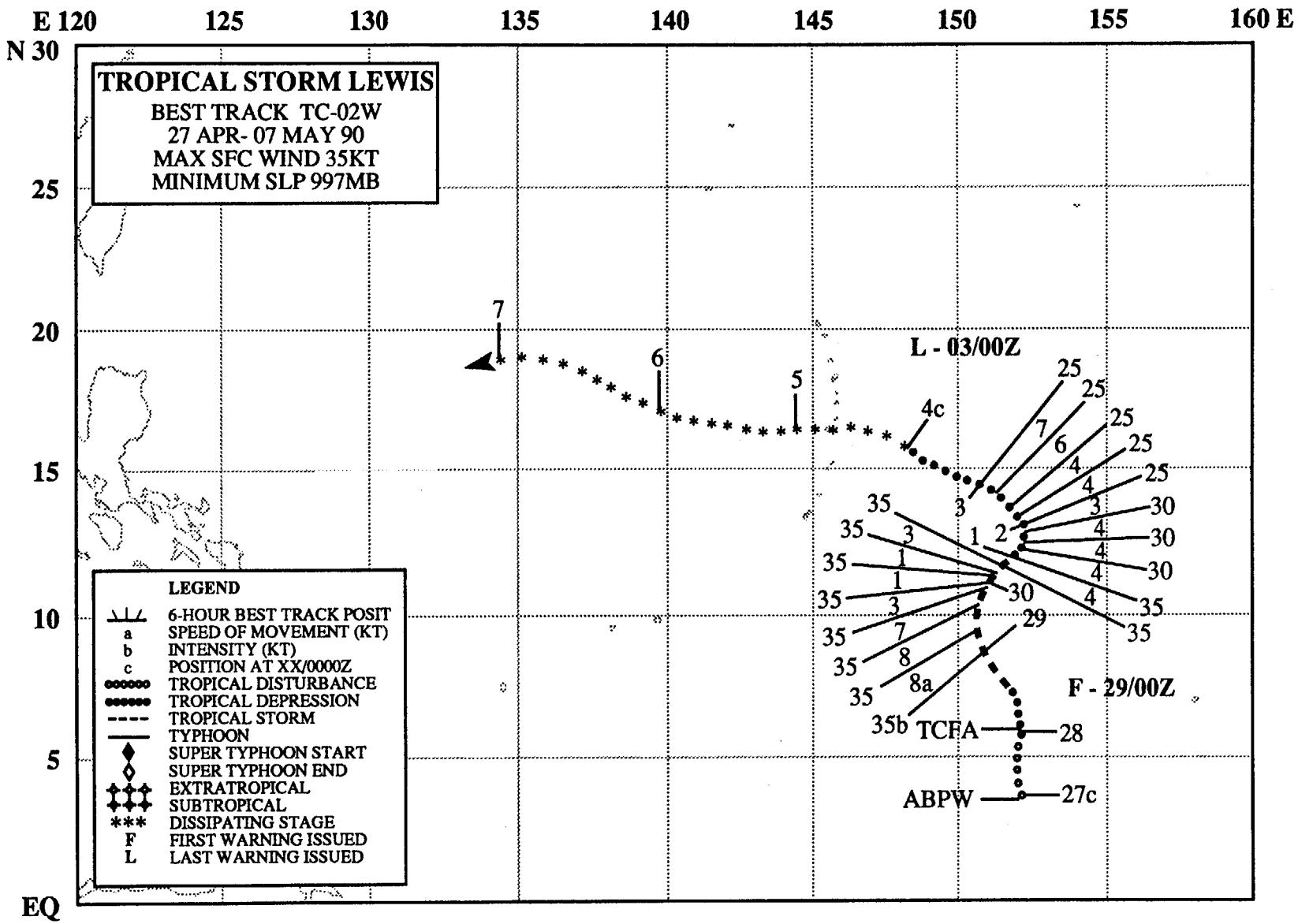
E 120
125
130
135
140
145
150
155
160 E
N 30
25
20
15
10
5
EQ
TROPICAL STORM LEWIS
BEST TRACK TC-02W
27 APR- 07 MAY 90
MAX SFC WIND 35KT
MINIMUM SLP 997MB
LEGEND
6-HOUR BEST TRACK POSIT
a SPEED OF MOVEMENT (KT)
b INTENSITY (KT)
c POSITION AT XX/0000Z
TROPICAL DISTURBANCE
TROPICAL DEPRESSION
TROPICAL STORM
TYPHOON
SUPER TYPHOON START
SUPER TYPHOON END
EXTRATROPICAL
SUBTROPICAL
*** DISSIPATING STAGE
F FIRST WARNING ISSUED
L LAST WARNING ISSUED
L - 03/00Z
F - 29/00Z
TCFA
ABPW
4c
35b
8a
27c
28
29
30

TROPICAL STORM LEWIS (02W)

I. HIGHLIGHTS

Lewis ended the two and a half month lull in northern hemisphere tropical cyclone activity that followed Typhoon Koryn (01W) in January. Developing from a tropical disturbance 200 nm south of Chuuk in the central Caroline Islands, Lewis passed directly over Chuuk while still a tropical depression and continued a northward trek for four more days. After being sheared apart by a digging midlatitude trough, the low-level remnants of the tropical cyclone drifted west-northwestward for several more days before completely dissipating.

II. CHRONOLOGY OF EVENTS

262330Z - The Significant Tropical Weather Advisory was reissued to address the redevelopment of an area of persistent convection with an estimated minimum sea-level pressure of 1009 mb.

280300Z - Tropical Cyclone Formation Alert based on increased convection, organization, and outflow aloft.

290000Z - First warning due to continued improvement in organization of the convection. Initial intensity based on synoptic data vice Dvorak intensity which had been CI 2.5 for approximately six hours.

290600Z - Upgrade to tropical storm prompted by improved upper-level organization. Peak intensity never exceeded 35 knots.

011800Z - Downgrade to tropical depression based on visual satellite imagery which showed partially exposed low-level.

030000Z - Final warning - dissipating over water - due to fully exposed low-level circulation.

III. TRACK AND MOTION

During initial development, Lewis tracked northward due to southerly flow associated with a mid-level anticyclone over the Marshall Islands. The anticyclone was separate from the subtropical ridge that was located near 20°north lattitude. The initial northward motion changed to northwestward at 281200Z (Figure 3-02-1). This synoptic adjustment resulted in Lewis passing directly over Chuuk. As a midlatitude trough began to dig to the northwest of Lewis, the steering flow veered from southeasterly to southwesterly (Figure 3-02-2) and caused the tropical cyclone to begin recurving at

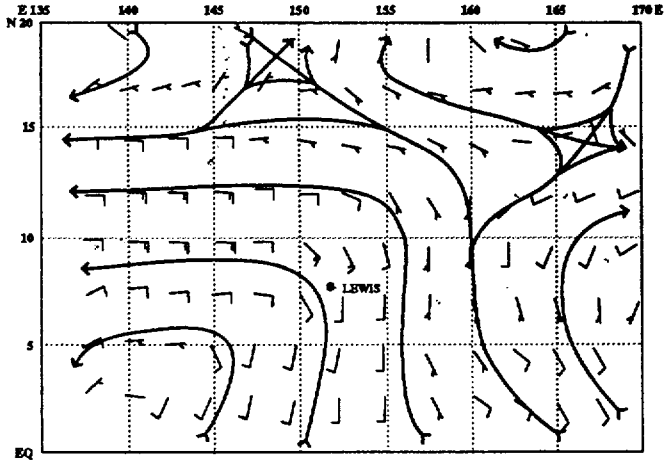

Figure 3-02-1. Lewis' turn to the northwest appears related to the subtle change of the steering flow from south to southeast on the 281200Z deep layer mean analysis.

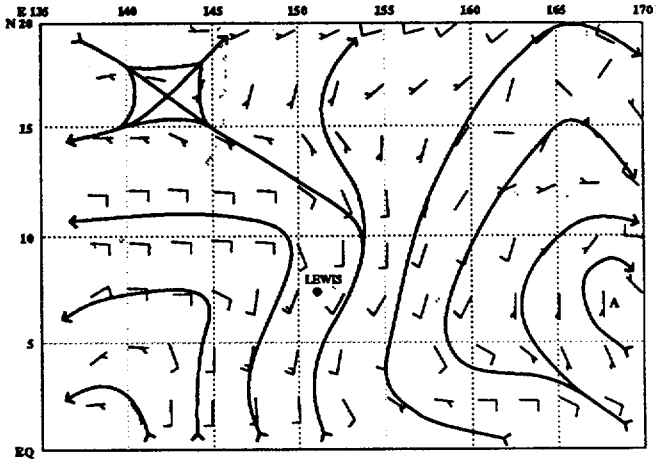

Figure 3-02-2. The 290000Z deep layer mean analysis shows the weakening of the ridge north-northeast of Lewis and maintenance of the anticyclonic circulation east of the tropical cyclone. This synoptic change, plus Lewis' continued movement to the north, brought Lewis into an area of light southwesterly steering flow.

291200Z. However, by 300000Z, the upper-level trough dug so far equatorward (to 10° north latitude) that the top of Lewis was sheared off by stronger westerlies aloft. Although Lewis' central convective activity intermittently flared up, the low-level circulation became exposed at 020000Z, and the low-level remnants of the cyclonic circulation drifted west-northwestward in response to the steering flow under the 850-mb ridge.

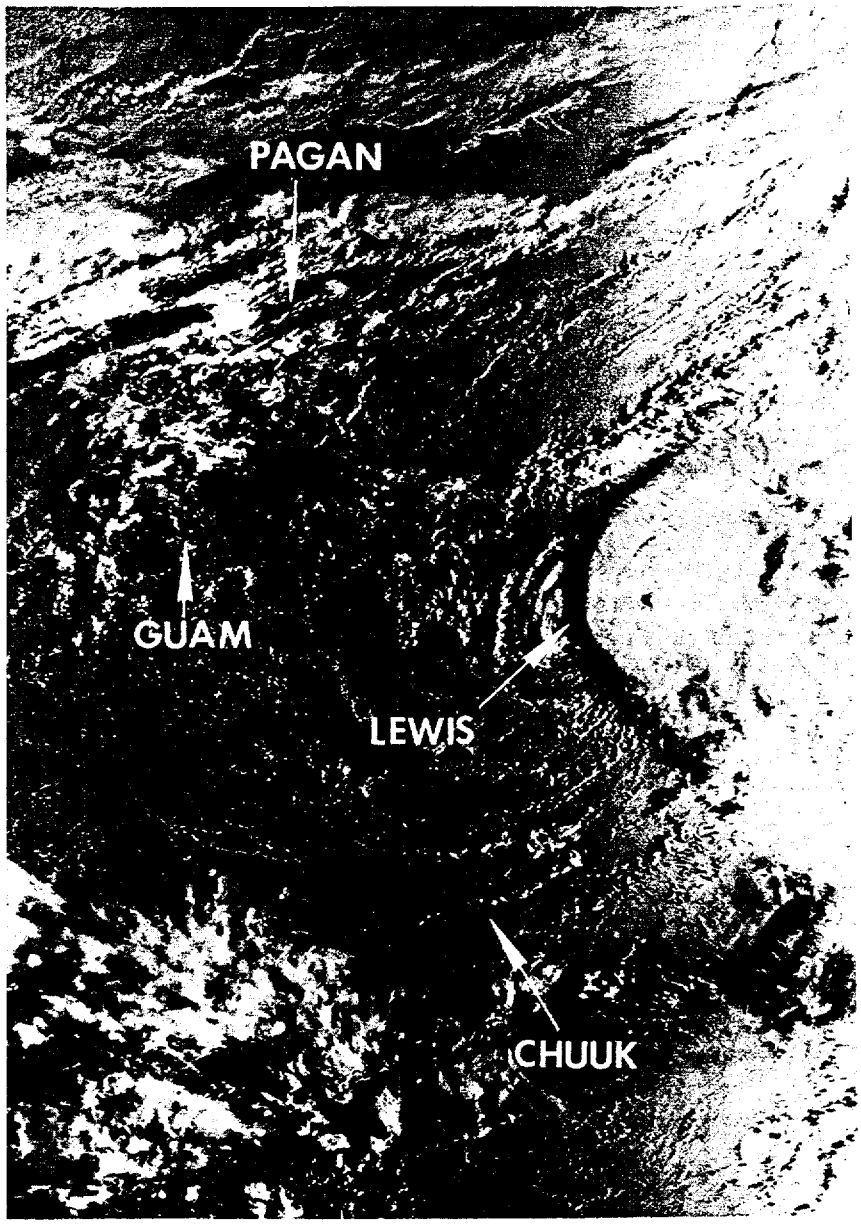

Figure 3-02-3. The sheared condition of Lewis (02W) is strikingly emphasized by the low sun-angle (012022Z May DMSP visual imagery).

IV. INTENSITY

In the early stages of its development, Lewis exhibited sufficient outflow to support moderate development. However, after reaching minimal tropical storm intensity, Lewis' further development was arrested by the encroaching 200-mb westerlies associated with the digging midlatitude trough (Figure 3-02-3). Two days later, the system began to slowly dissipate.

V. FORECASTING PERFORMANCE

Figure 3-02-4 shows the JTWC forecast performance for Lewis. Although the early forecasts anticipated the track change to the northwest followed by a change to the northeast, the forecasts were slow to anticipate the recurving effect of the digging midlatitude trough. Since neither subjective guidance nor the objective forecast aids available to JTWC were able to precisely address a shear-induced decoupling of the low-level circulation from its upper-level, the official forecasts incorrectly presumed continued recurvature. However, as early as 300600Z forecasters included an alternate scenario of shear-induced decoupling followed by west-northwestward movement of the low-level circulation in the prognostic reasoning.

VI. IMPACT

No information received.

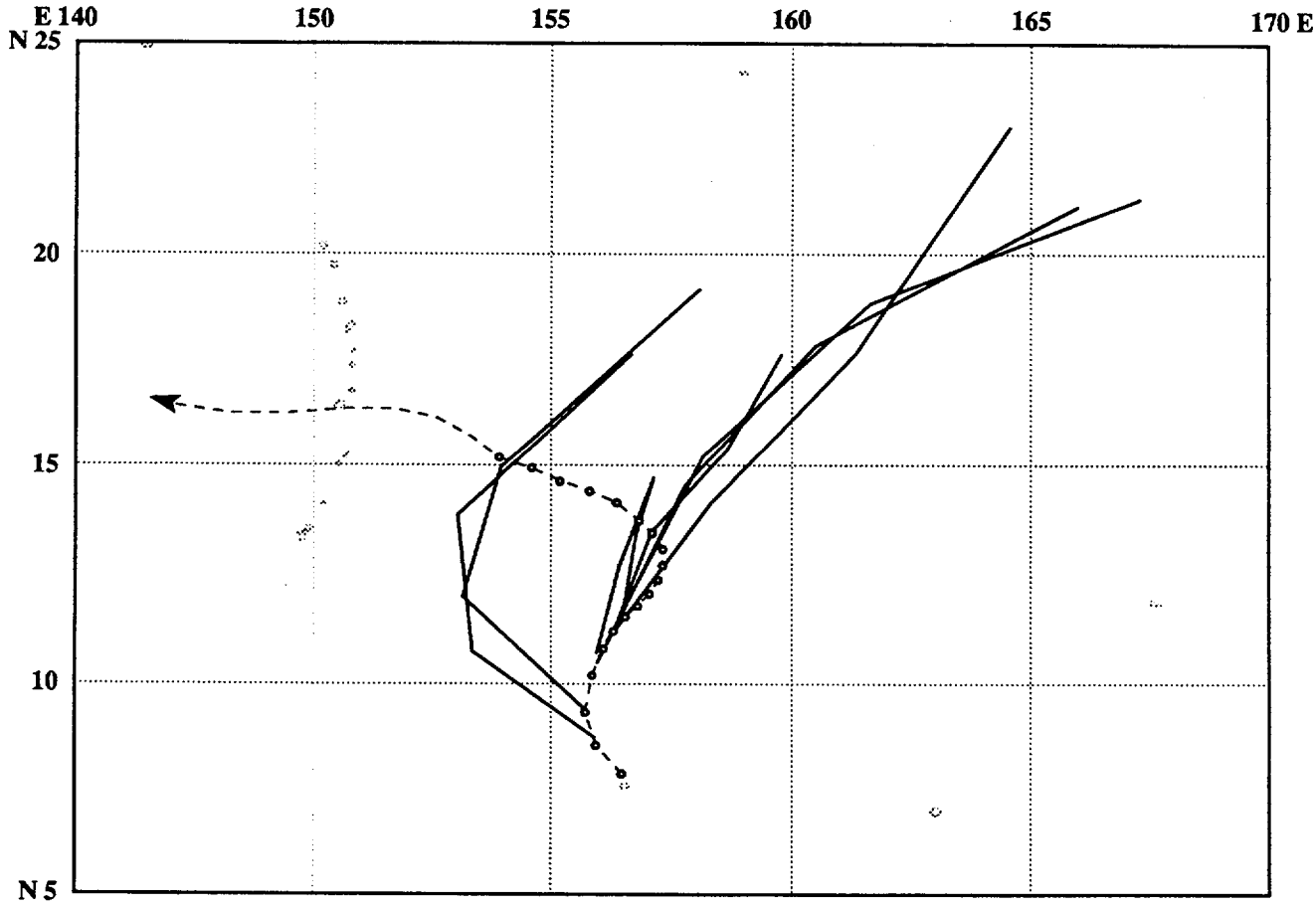

Figure 3-02-4. Summary of JTWC forecasts (solid lines) for Lewis (02W) superimposed on the final best track (dashed line).

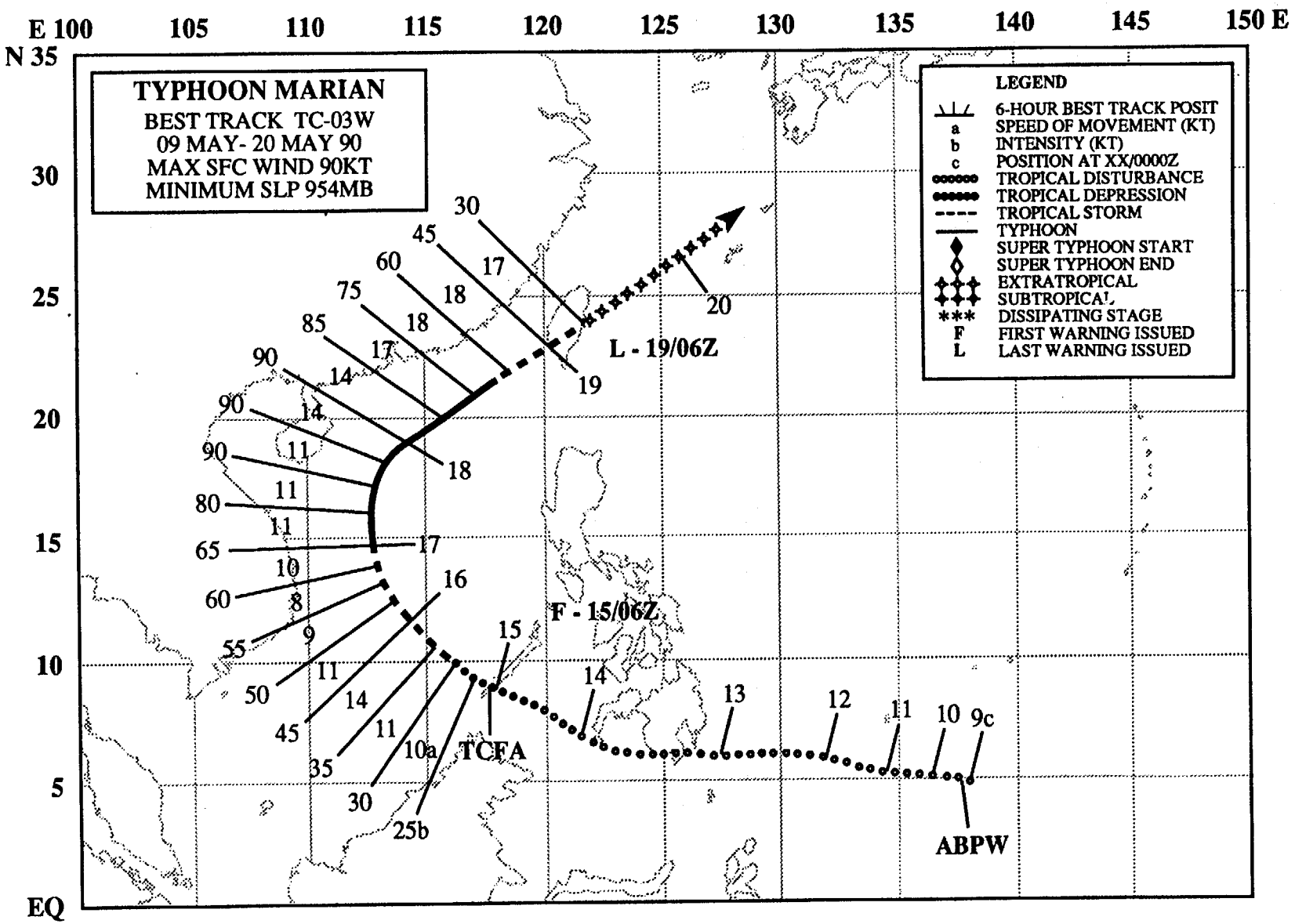
E 100
105
110
115
120
125
130
135
140
145
150 E
N 35
30
25
20
15
10
5
EQ
TYPHOON MARIAN
BEST TRACK TC-03W
09 MAY- 20 MAY 90
MAX SFC WIND 90KT
MINIMUM SLP 954MB
LEGEND
6-HOUR BEST TRACK POSIT
a SPEED OF MOVEMENT (KT)
b INTENSITY (KT)
c POSITION AT XX/0000Z
TROPICAL DISTURBANCE
TROPICAL DEPRESSION
TROPICAL STORM
TYPHOON
SUPER TYPHOON START
SUPER TYPHOON END
EXTRATROPICAL
SUBTROPICAL
*** DISSIPATING STAGE
F FIRST WARNING ISSUED
L LAST WARNING ISSUED
L - 19/06Z
F - 15/06Z
TCFA
ABPW
30
45
60
75
85
90
90
90
80
65
60
55
50
45
35
30
25b
10a
90
90
90
80
65
60
55
50
45
35
30
25b
10a
9c
10
11
12
13
14
15
16
17
18
19
20
17
18
18
17
14
14
11
11
11
10
8
9
11
14
11

TYPHOON MARIAN (03W)

I. HIGHLIGHTS

Marian, the second typhoon of 1990 in the western North Pacific and the only significant tropical cyclone to form in May, persisted in low latitudes for almost a week before intensifying. Its convective cloud mass tracked westward initially, passing south of Yap and Palau in the western Caroline Islands. After entering the South China Sea, the system finally developed into a typhoon. Marian then recurved and merged with a frontal system to form an extratropical low.

II. CHRONOLOGY OF EVENTS

090600Z - First mentioned on Significant Tropical Weather Advisory as an area of persistent convection with an estimated minimum sea-level pressure of 1006 mb.

150230Z - Tropical Cyclone Formation Alert based on better convective organization with increased low-level inflow and outflow aloft.

150600Z - First warning due to increased amount of central convection and cloud organization.

151800Z - Upgraded to a tropical storm prompted by steady intensification, favorable outflow aloft in all quadrants and the first intensity estimate of CI 2.5.

170000Z - Upgraded to typhoon following improved outflow, expected formation of an eye and the first CI 4.0.

171800Z - Peak intensity - 90 kt (46 m/sec) - coincident with visible eye with intensity estimate of CI 5.0.

181800Z - Downgraded to tropical storm because of increased vertical wind shear and start of extratropical transition. Convection decreased in amount and organization.

190600Z - Final warning - (extratropical) - followed interaction with rugged mountains of Taiwan. Principle low-level circulation center passed east of the island.

III. TRACK AND MOTION

The system developed in low latitudes in the central Caroline Islands and tracked slowly westward on the south side of the subtropical ridge. After passing over Mindanao in the southern Philippine Islands, Marian tracked around the western end of the subtropical ridge (Figure 3-03-1). As

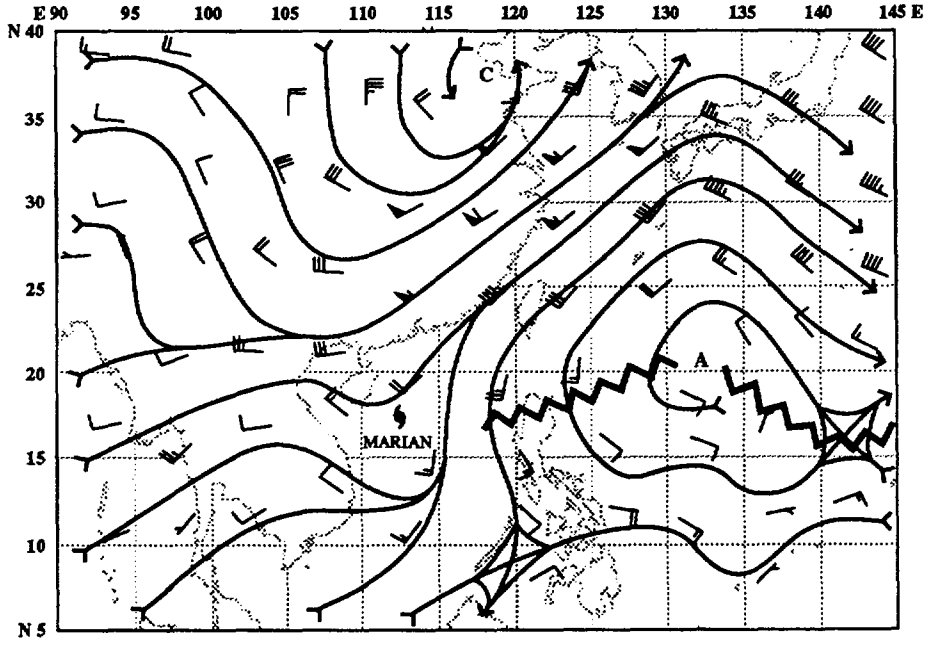

Figure 3-03-1. 500 mb NOGAPS analysis from 171200Z May, showing the cutoff low over eastern China, subtropical ridge to the east of Marian's surface position. The tropical cyclone, is tracking around the western periphery of the subtropical ridge and beginning to accelerate.

the tropical cyclone approached the south coast of China, increased southwesterlies aloft accelerated Marian northeastward along the edge of the modifying polar air.

IV. INTENSITY

The convective cloud mass that eventually developed into Typhoon Marian remained intact, but relatively unorganized, for almost a week. Brisk easterly trade winds (Figure 3-03-2) to the north and light cross-equatorial flow to the south supported the circulation, but outflow aloft was restricted by zonal westerly winds to the north. As the disturbance passed over the southern islands of the Philippine archipelago, interaction with land further inhibited low-level development. Upper-level conditions became favorable for intensification as a new outflow channel to the north combined with the preexisting weak one to the south and west. As the cyclone entered the South China Sea, it developed into Tropical Storm Marian. Steady intensification continued until an eye formed (Figure 3-03-3). After reaching peak intensity on 17 May, increased southwesterly flow aloft ahead of a shortwave trough began to strip away the convection. As the system recurved, it was caught up in the approaching cold front and commenced extratropical transition (Figure 3-03-4).

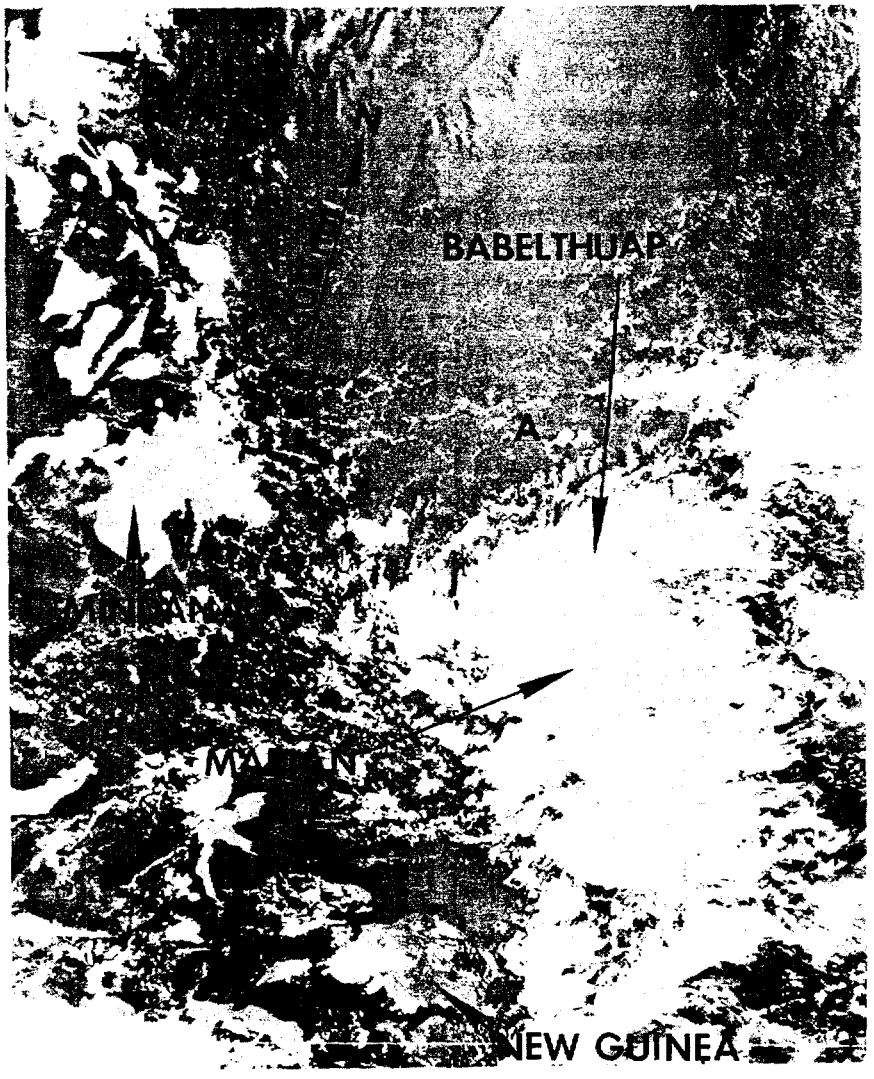

Figure 3-03-2. Marian approaches the southern Philippine Islands. To the north of the central cloud mass at point A, low-level cloud arcs can be seen in the brisk easterly trade flow. Towering cumulus and cumulonimbus forming on these arcs were sheared away by westerly winds aloft (110051Z May DMSP visual imagery).

V. FORECASTING PERFORMANCE

Overall JTWC forecast performance is shown in Figure 3-03-5. The initial forecasts did not call for recurvature. The NOGAPS prognostic series retained a weak mid-level ridge over the South China Sea, suggesting continued west-northwestward motion and eventual landfall in Vietnam. Because of the proximity of the shortwave trough over China, an alternate scenario was developed to weaken the subtropical ridge, allowing Marian to recurve. This alternate soon became the primary forecast, as the ridge did weaken and Marian recurved.

VI. IMPACT

No information was received.

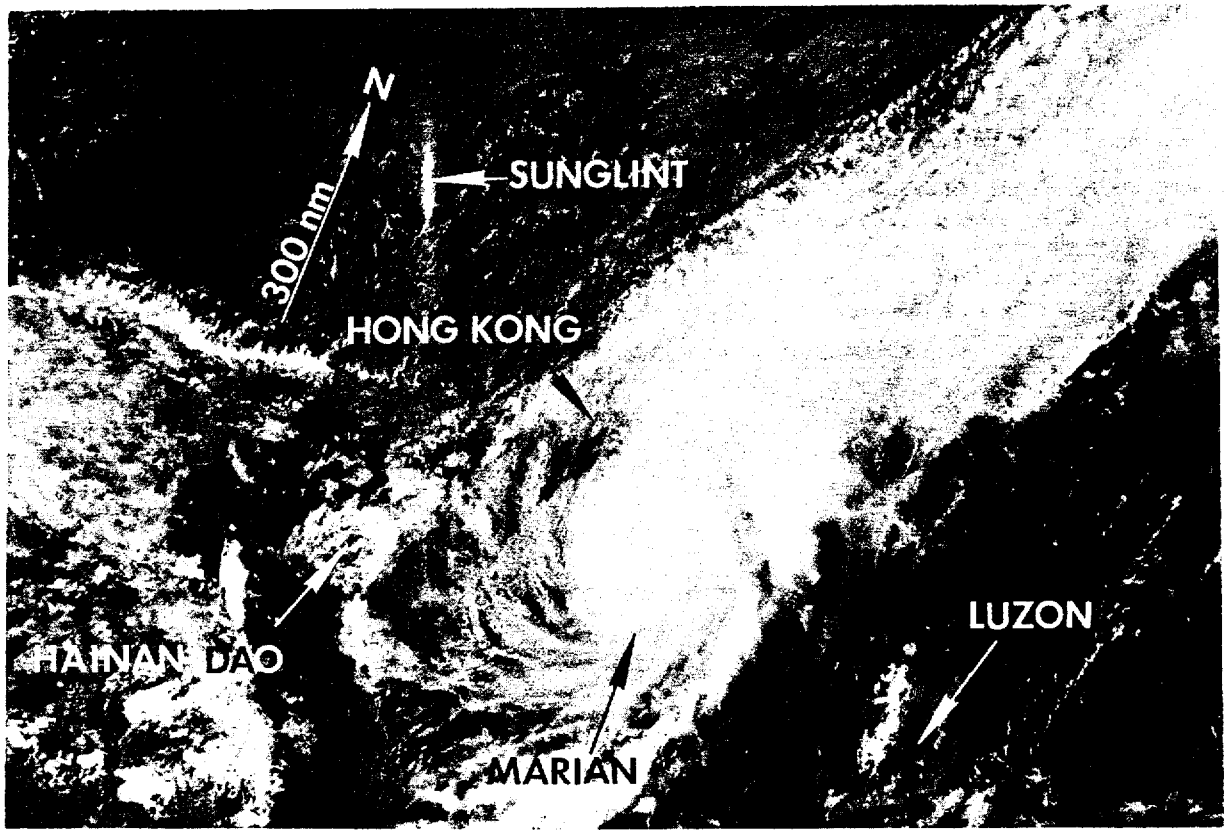

Figure 3-03-3. Typhoon Marian with a small eye interacts with a frontal system that is moving seaward from eastern Asia (180608Z May NOAA visual imagery).

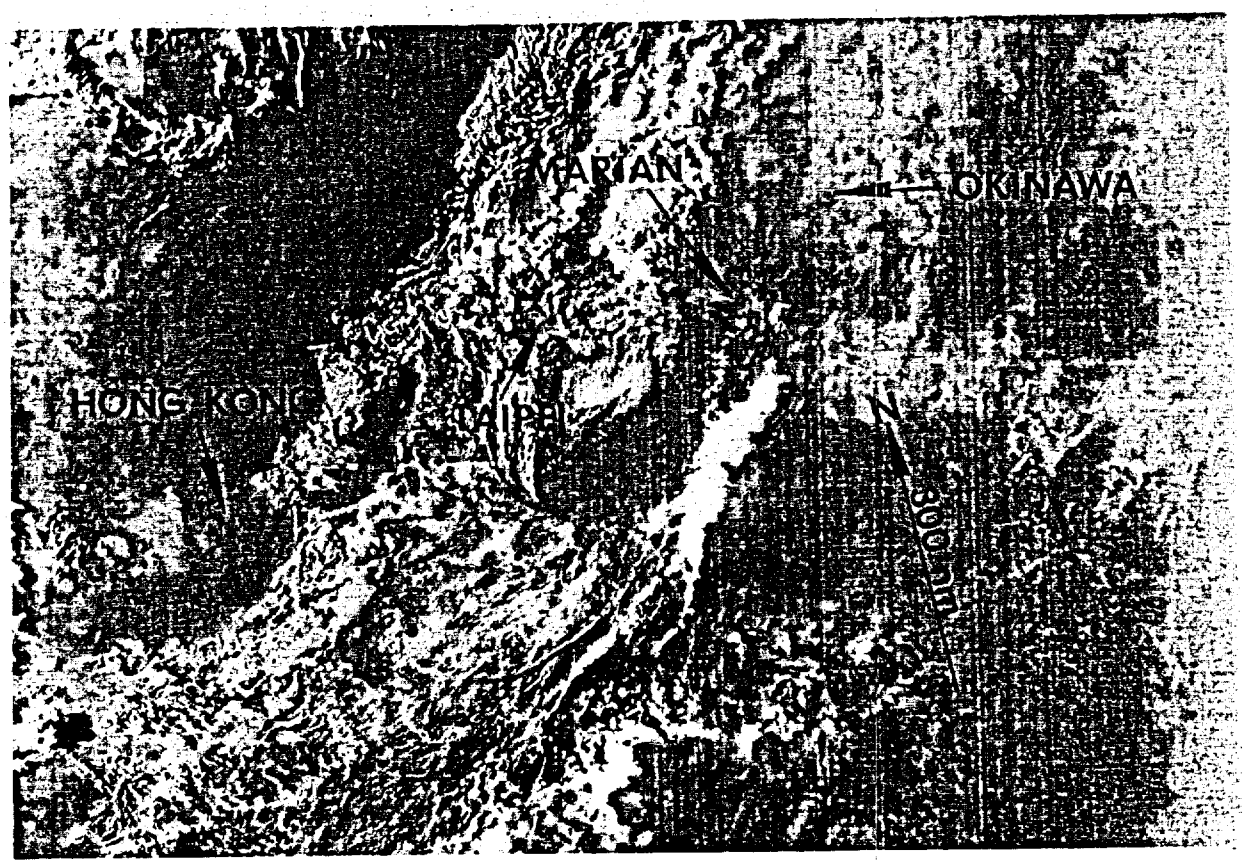

Figure 3-03-4. The remnants of Marian are embedded in the frontal zone just east of Taiwan. There appears to be no middle or high cloud in the subsiding air over the center of the vortex (191022Z May DMSP visual imagery).

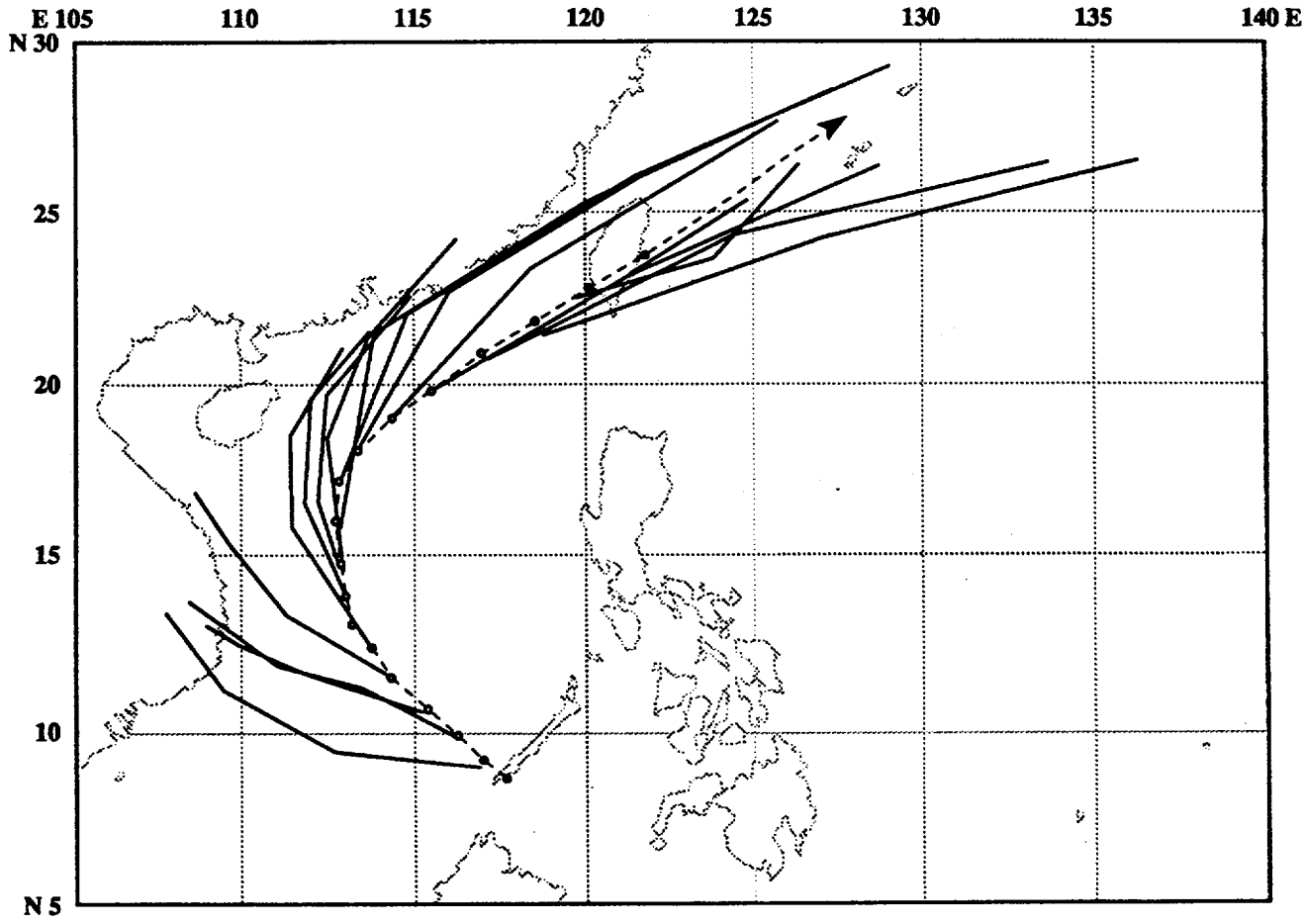

Figure 3-03-5. Summary of JTWC forecasts (solid lines) for Marian is superimposed on the final best track (dashed line).

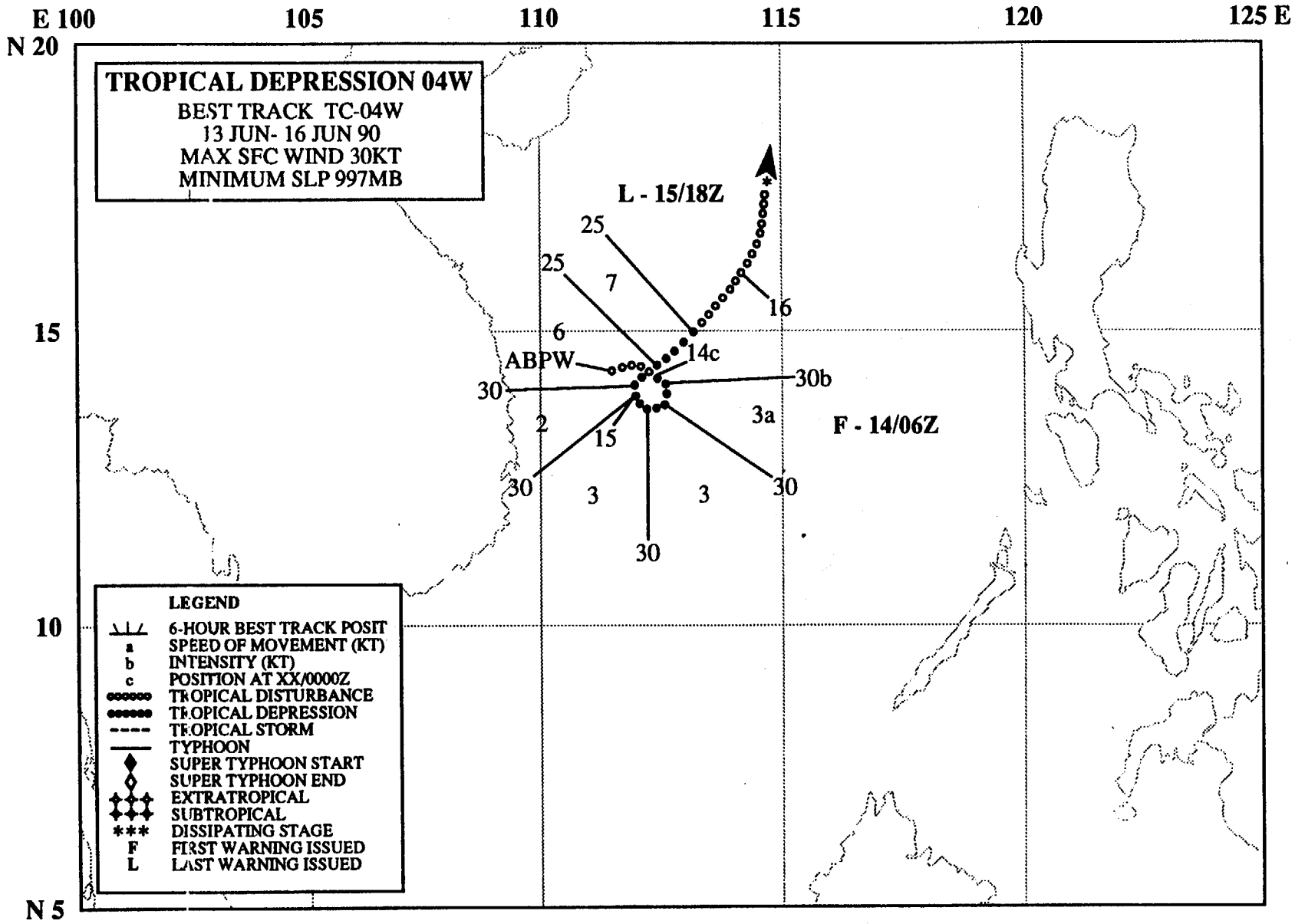
E 100
105
110
115
120
125 E
N 20
15
10
N 5
TROPICAL DEPRESSION 04W
BEST TRACK TC-04W
13 JUN- 16 JUN 90
MAX SFC WIND 30KT
MINIMUM SLP 997MB
L - 15/18Z
F - 14/06Z
25
25
7
16
6
14c
ABPW
30
30b
2
15
3a
30
3
3
30
30
LEGEND
6-HOUR BEST TRACK POSIT
a SPEED OF MOVEMENT (KT)
b INTENSITY (KT)
c POSITION AT XX/0000Z
TROPICAL DISTURBANCE
TROPICAL DEPRESSION
TROPICAL STORM
TYPHOON
SUPER TYPHOON START
SUPER TYPHOON END
EXTRATROPICAL
SUBTROPICAL
*** DISSIPATING STAGE
F FIRST WARNING ISSUED
L LAST WARNING ISSUED

TROPICAL DEPRESSION 04W

I. HIGHLIGHTS

Tropical Depression 04W, the first significant tropical cyclone to form in the South China Sea this year, proved to be very difficult to locate and forecast. Satellite and synoptic fix positions disagreed throughout the depression's life. As the convection flared near the center of the system, the mid-level and upper-level prevailing east-northeasterly flow moved the convection toward the coast of Vietnam. The satellite analysts tracked the convection onto the coast of Vietnam. However, as the area of convection over Vietnam dissipated a new area of convection developed near the circulation center indicated in the synoptic data. As Tropical Storm Nathan (05W) continued to develop, Tropical Depression 04W was drawn into the larger circulation and absorbed.

II. CHRONOLOGY OF EVENTS

130600Z - First mentioned on Significant Tropical Weather Advisory due to weak low-level circulation center in the synoptic data and 1004 mb pressure.

140600Z - First Warning based on the low-level circulation center exposed to the east of the poorly organized central cloud mass. Synoptic data indicated the presence of 20-30 kt (10-15 m/sec) winds.

140600Z - Peak Intensity of 30 kt (15 m/sec) established in synoptic data.

151200Z - Final warning followed the loss of convective signature as the low level circulation was absorbed by Nathan (05W).

III. MOTION

Tropical Depression 04W proved to be a significant motion forecast problem. From the beginning, the 850 mb wind patterns in the area indicated that the vortex was located along the western side of the low-level mean wind flow of approximately 30 kt (15 m/sec) from the west-southwest associated with the summer monsoon. The depression remained quasi-stationary for the first two days. As Tropical Storm Nathan (05W) moved into the South China Sea, strong southwesterly monsoon flow began to feed into it. Tropical Depression 04W (Figure 3-04-1) became involved in the associated broad scale flow and was absorbed by the larger cyclone.

IV. INTENSITY

The strong vertical wind shear always restricted Tropical Depression 04W development. The 200-mb winds over the area were 30 to 35 kt (15 to 18 m/sec) and the low-level monsoonal flow was of equal intensity and opposing direction. As a result of the strong shear, JTWC did not expect intensification above 30 kt (15 m/sec) and issued only 36-hour tropical depression warnings.

V. FORECASTING PERFORMANCE

Superimposed on the final best track are the JTWC forecasts (Figure 3-04-2). Due to the lack of synoptic data in the early portions of the forecast scenario, JTWC depended primarily on satellite fixes to determine Tropical Depression 04W's location. In this high vertical wind shear environment the satellite fixes indicated an apparent westward motion of the system. Thus, JTWC forecast aids and the official forecast track indicated westward motion for most of the life of the depression.

VI. IMPACT

No impact was reported in association with Tropical Depression 04W.

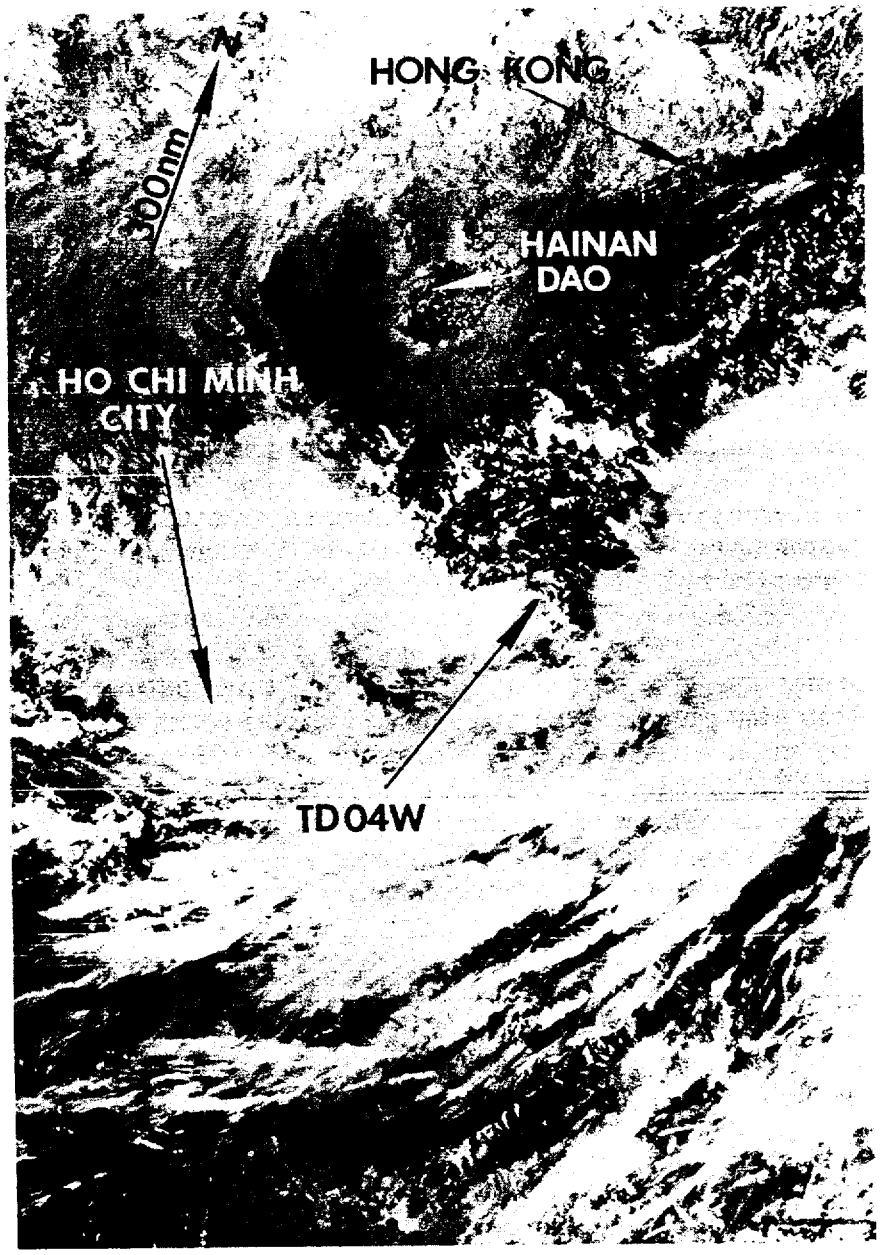

Figure 3-04-1. Tropical Depression 04W, which is south-southeast of Hainan Dao, becomes involved with Tropical Storm Nathan (05W) (150210Z June DMSP visual imagery).

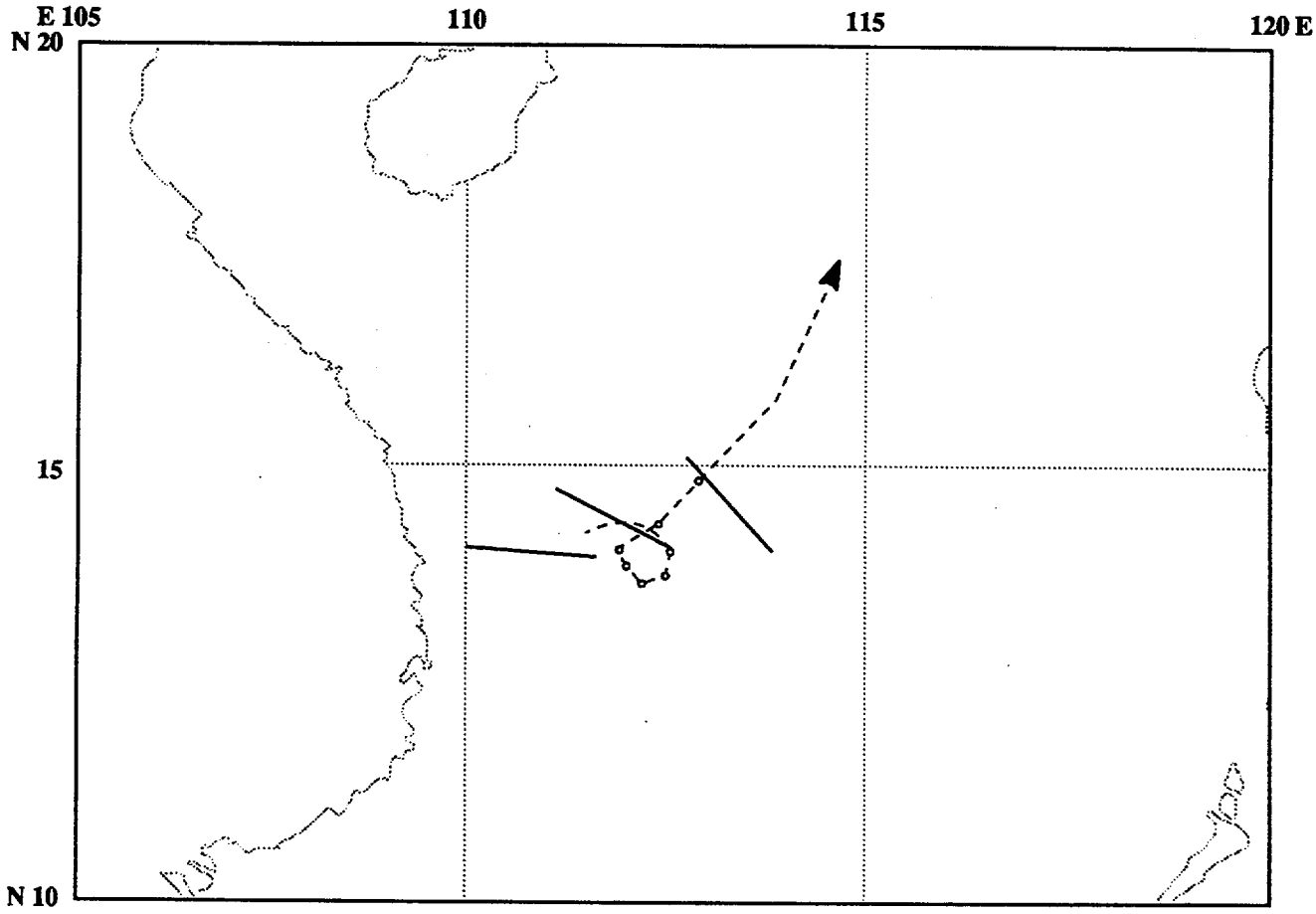

Figure 3-04-2. Summary of JTWC forecasts (solid lines) superimposed on the final best track (dashed line).

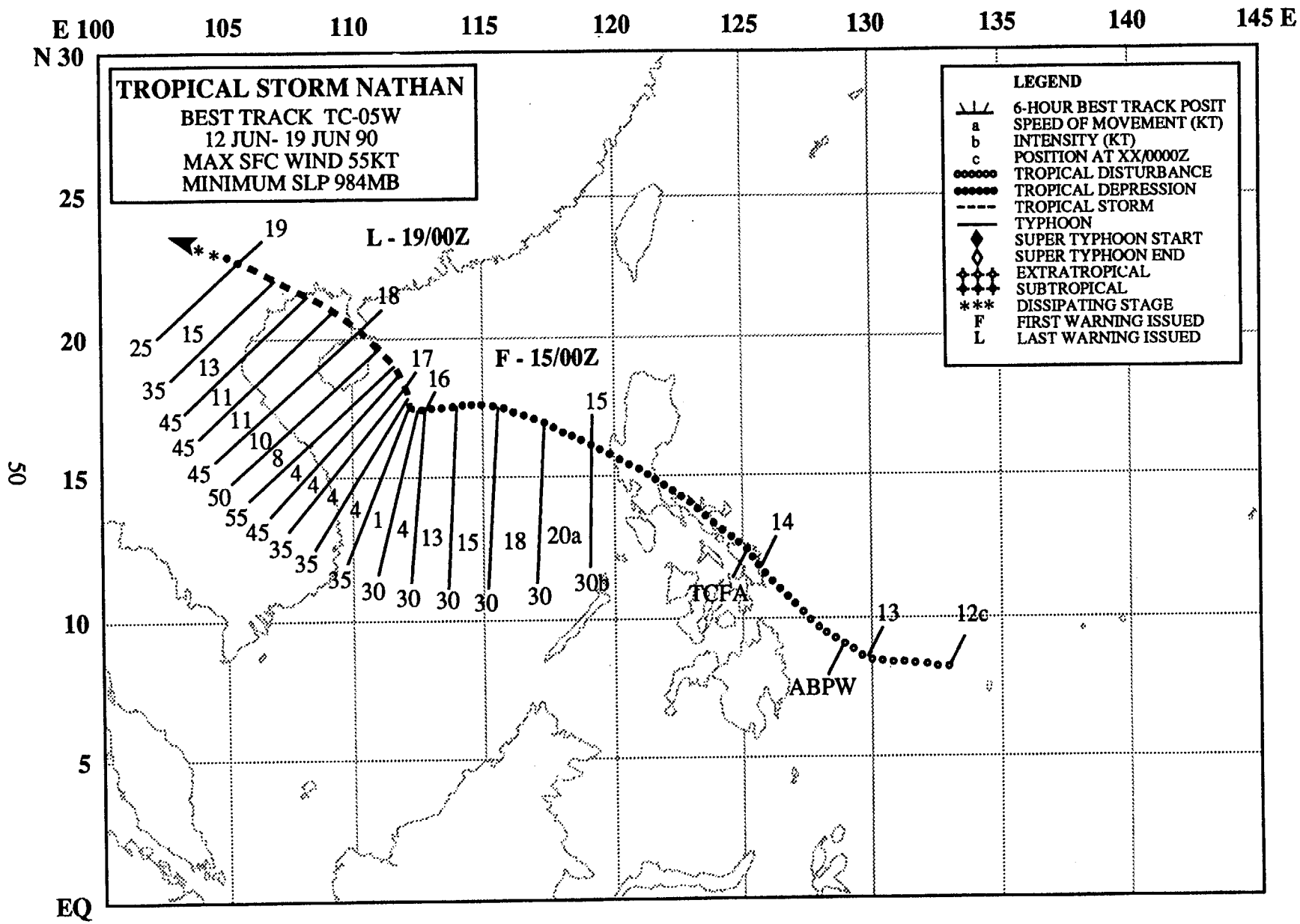
TROPICAL STORM NATHAN
BEST TRACK TC-05W
12 JUN- 19 JUN 90
MAX SFC WIND 55KT
MINIMUM SLP 984MB
LEGEND
6-HOUR BEST TRACK POSIT
a SPEED OF MOVEMENT (KT)
b INTENSITY (KT)
c POSITION AT XX/0000Z
TROPICAL DISTURBANCE
TROPICAL DEPRESSION
TROPICAL STORM
TYPHOON
SUPER TYPHOON START
SUPER TYPHOON END
EXTRATROPICAL
SUBTROPICAL
*** DISSIPATING STAGE
F FIRST WARNING ISSUED
L LAST WARNING ISSUED
L - 19/00Z
F - 15/00Z
TCFA
ABPW
E 100
105
110
115
120
125
130
135
140
145 E
N 30
25
20
15
10
5
EQ
50

TROPICAL STORM NATHAN (05W)

I. HIGHLIGHTS

Nathan, the second tropical cyclone to form in June, crossed the Philippine island of Luzon as a disturbance, executed an abrupt track change and stalled in the South China Sea. Both the track and intensity of TD04W and Nathan were dominated by a larger monsoon circulation in the South China Sea.

II. CHRONOLOGY OF EVENTS

130600Z - First mentioned on Significant Tropical Weather Advisory as an area of weak circulation with an estimated minimum sea-level pressure of 1004 mb embedded in the monsoon trough .

140300Z - Tropical Cyclone Formation Alert based on improved organization with increased low-level inflow and increased outflow aloft.

150000Z - First warning due to increased winds as the system came off Luzon and entered the warm waters of the South China Sea.

161200Z - Upgraded to tropical storm after system became quasi-stationary and the exposed low-level became more aligned with the deep convection; the first intensity estimate of CI 2.5 received.

171200Z - Peak intensity - 55 kt (28 m/sec) -based on a ship report of 50 kt (26 m/sec) winds within 55 nm (100 km) of cloud system center.

181200Z - Landfall along Chinese/Vietnamese border, 100 nm (185 km) east-northeast of Hanoi.

190000Z - Final warning - (dissipated over land)- followed rapid weakening as Nathan encountered the mountains of northern Vietnam.

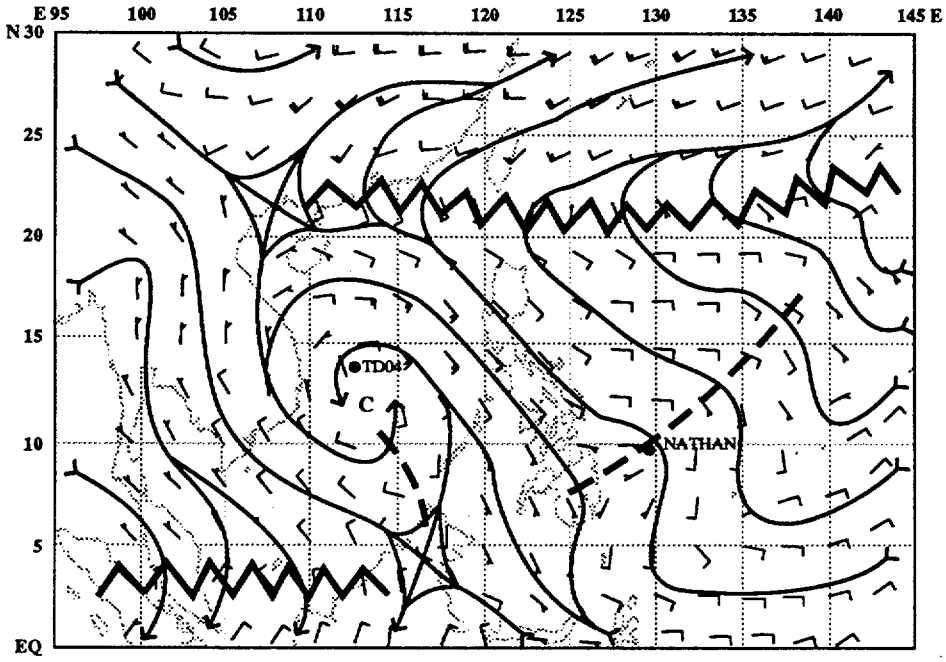

Figure 3-05-1. The 131200Z June deep layer mean analysis shows the large monsoon circulation (LMC) near 11° north latitude in the South China Sea and the subtropical ridge near 20° north latitude. Tropical Depression 04W is northwest of the center of the LMC and Nathan appears as an inverted trough east of Mindanao.

III. TRACK AND MOTION

A large monsoon circulation (hereafter called LMC) in the South China Sea and the subtropical ridge along 20° north latitude set the stage for Nathan's unusual track. Initially Nathan was reflected in the deep layer mean analysis (Figure 3-05-1) as a wave in the easterlies. Farther to the west Tropical Depression 04W was a smaller shallow circulation embedded within the synoptic scale LMC. As Nathan moved northwestward and crossed southern Luzon, both the subtropical ridge and the LMC began shifting

northward (Figure 3-05-2). The curved best track reflects both Nathan's westward movement into the LMC in the South China Sea and the displacement to the north of the entire synoptic pattern. For a time, Tropical Depression 04W was expected to be drawn into Nathan; however, as Nathan sped by, Tropical Depression 04W dissipated. Nathan's abrupt track change and stall on 16 June was the result of a binary interaction with the LMC. The tropical cyclone separated from the LMC core and continued northwestward (Figure 3-05-3).

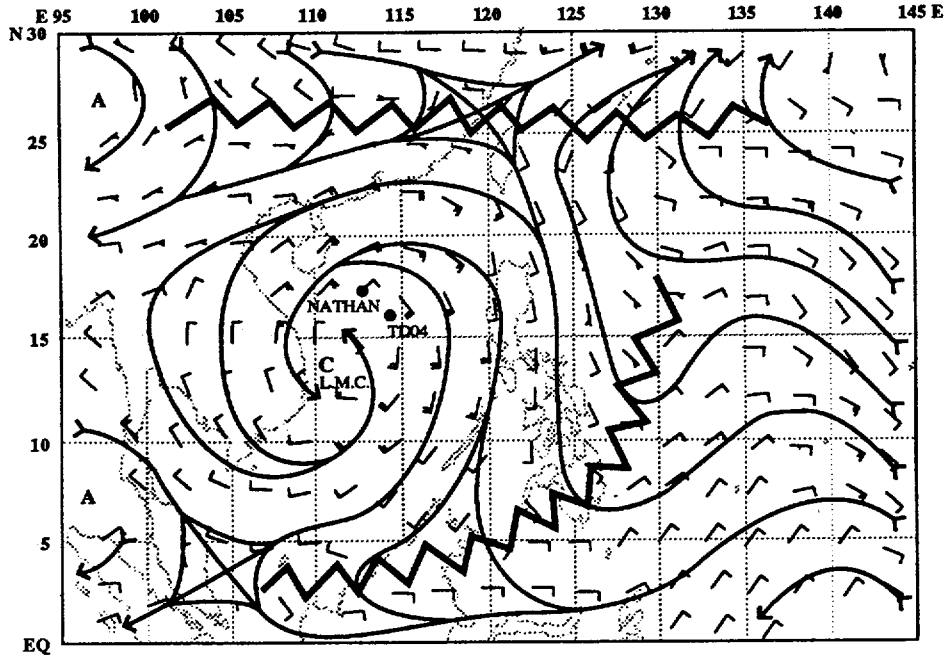

Figure 3-05-2. Both TD04W and Nathan are embedded in the flow near the center of the LMC on the 160000Z June deep layer mean analysis.

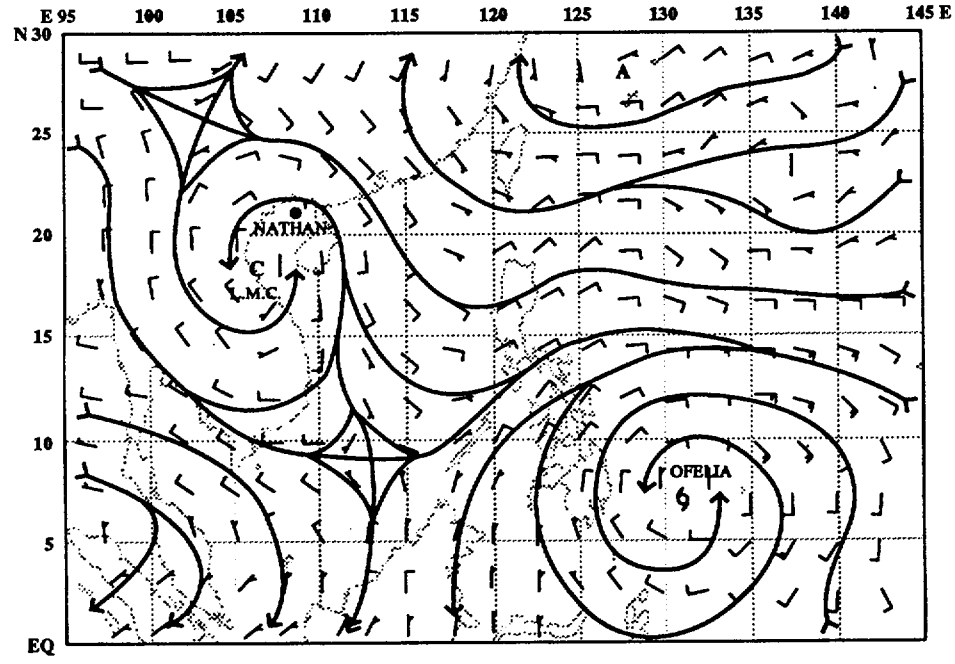

Figure 3-05-3. The 181200Z June deep layer mean analysis shows Nathan north-northeast of the center of the LMC.

IV. INTENSITY

Nathan slowly consolidated from multiple low-level circulations in an area of poorly organized convection. Convection continued to increase in amount and organization as the system approached the Philippine Islands (Figure 3-05-4). Nevertheless, passage across Luzon, rapid motion toward the LMC in the South China Sea and strong vertical wind shear all kept Nathan below tropical storm intensity. Intensification finally occurred when Nathan entered the core of the LMC on 16 June. The shear-type cloud pattern with its exposed low-level circulation center gave way to a central dense overcast, and

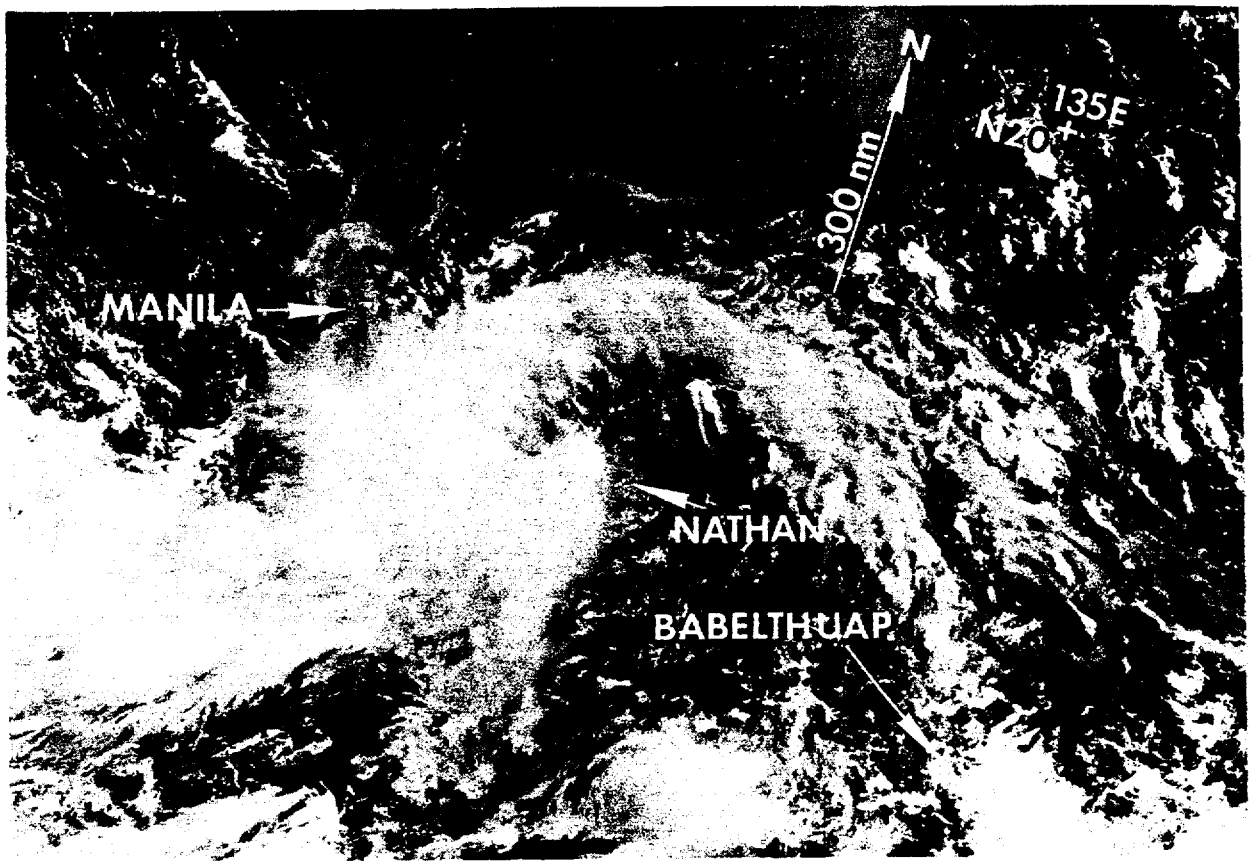

Figure 3-05-4. Nathan consolidates as it approaches the Philippine Islands (140049Z June DMSP visual imagery).

Nathan intensified into a tropical storm (Figure 3-05-5). Slow intensification continued until the tropical cyclone began interacting with land. Nathan weakened and dissipated rapidly after crossing Hainan Dao and making landfall on the coast of Vietnam on 18 June.

V. FORECASTING PERFORMANCE

Plots of JTWC's forecasts on the best track are presented in Figure 3-05-6. JTWC had a difficult time with this tropical cyclone in the South China Sea. Nathan's interaction with the center of the LMC and the northward shift of the entire synoptic pattern became apparent only after the fact. OTCM had a better handle on the overall northwestward track (Figure 3-05-7), but it did not reflect the interaction with the core of the LMC, as can be seen by the OTCM guidance to the south on 15 June.

VI. IMPACT

In Hong Kong, according to the "Monthly Weather Summary June 1990" published by the Royal Observatory, 13 people were killed, 5 were missing and 15 injured as a result of Nathan. Minor mudslides were reported throughout the area and scaffoldings collapsed in Kowloon. The cargo ship "Tien Fu" sank in the South China Sea on the night of 16 June with the loss of the captain and three of its crew. Along China's southern coast, torrential rain associated with Nathan caused 10 deaths and flooded 5,000 hectares of farmland in eastern Guangdong. In Zhanjiang, 100,000 hectares of paddy fields were destroyed. Two men were reported missing in Macao after being swept overboard from a dredger on 17 June.

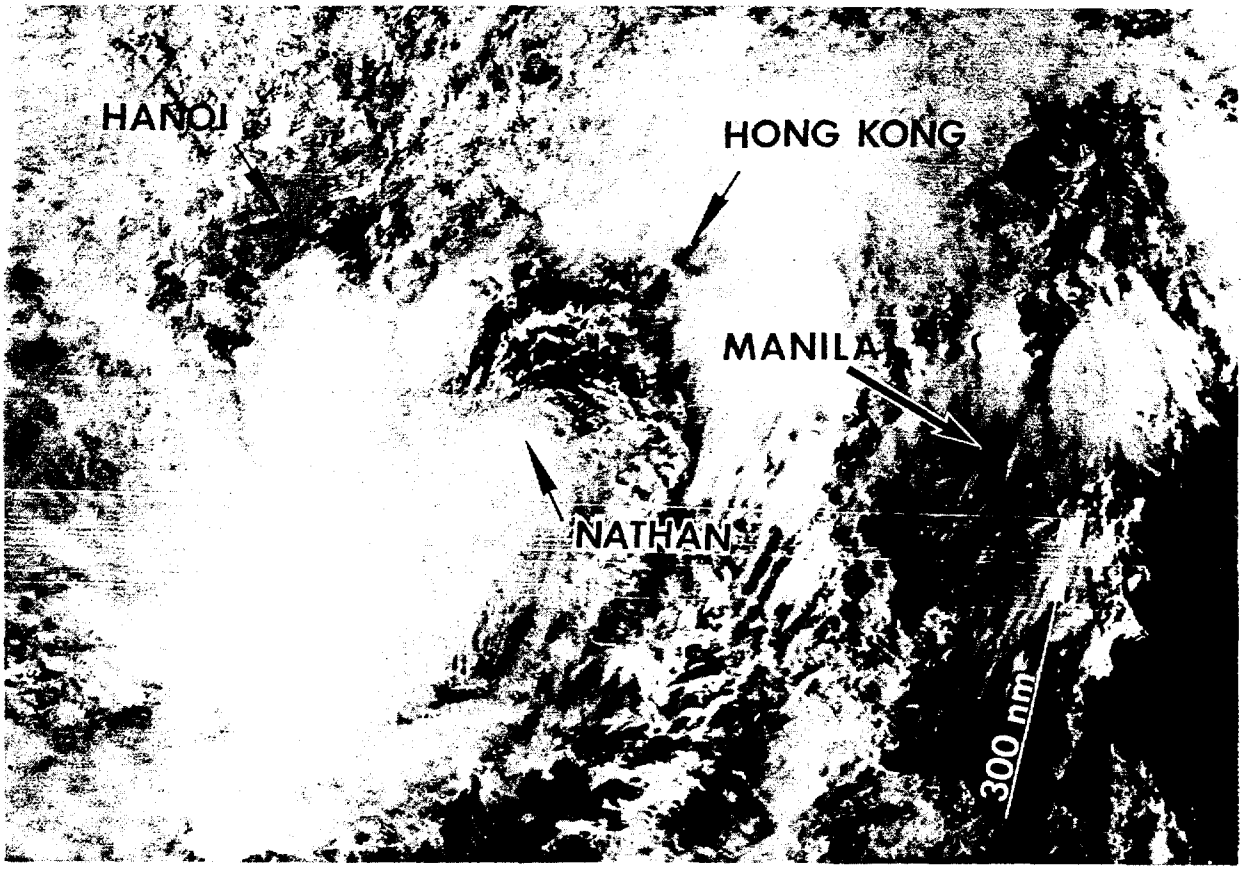

Figure 3-05-5. Tropical Storm Nathan with a ragged central dense overcast churns towards Hainan Dao (170128Z June DMSP visual imagery).

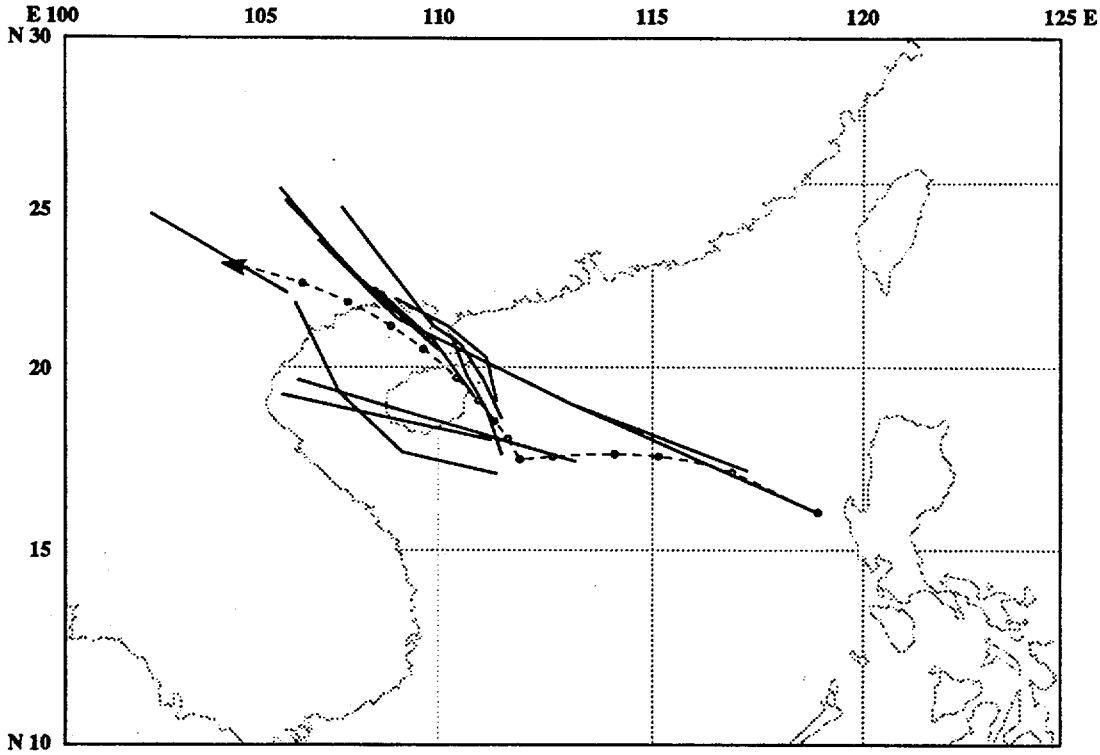

Figure 3-05-6. JTWC forecasts (solid lines) for Nathan are superimposed on the final best track (dashed line). The abrupt track change and stall in the South China Sea were difficult to forecast.

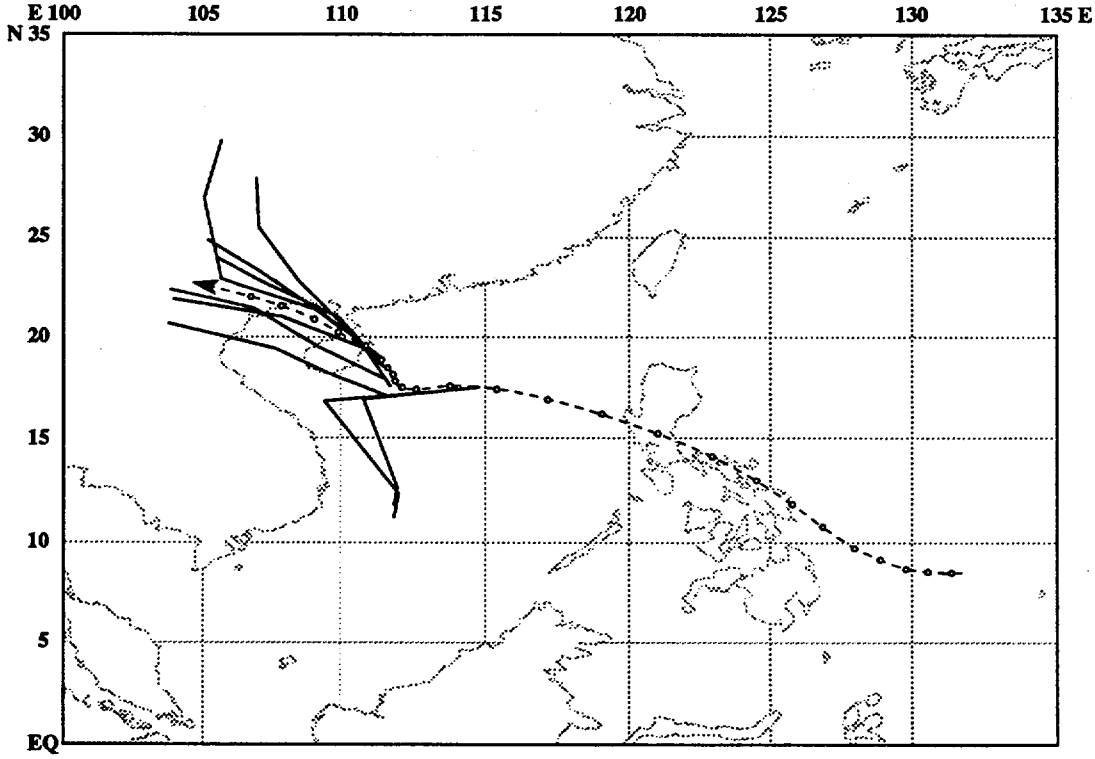

Figure 3-05-7. When Nathan interacted with the core of the LMC, OTCM guidance had difficulties, as indicated by the two solid lines that abruptly turn southward on 15 June.

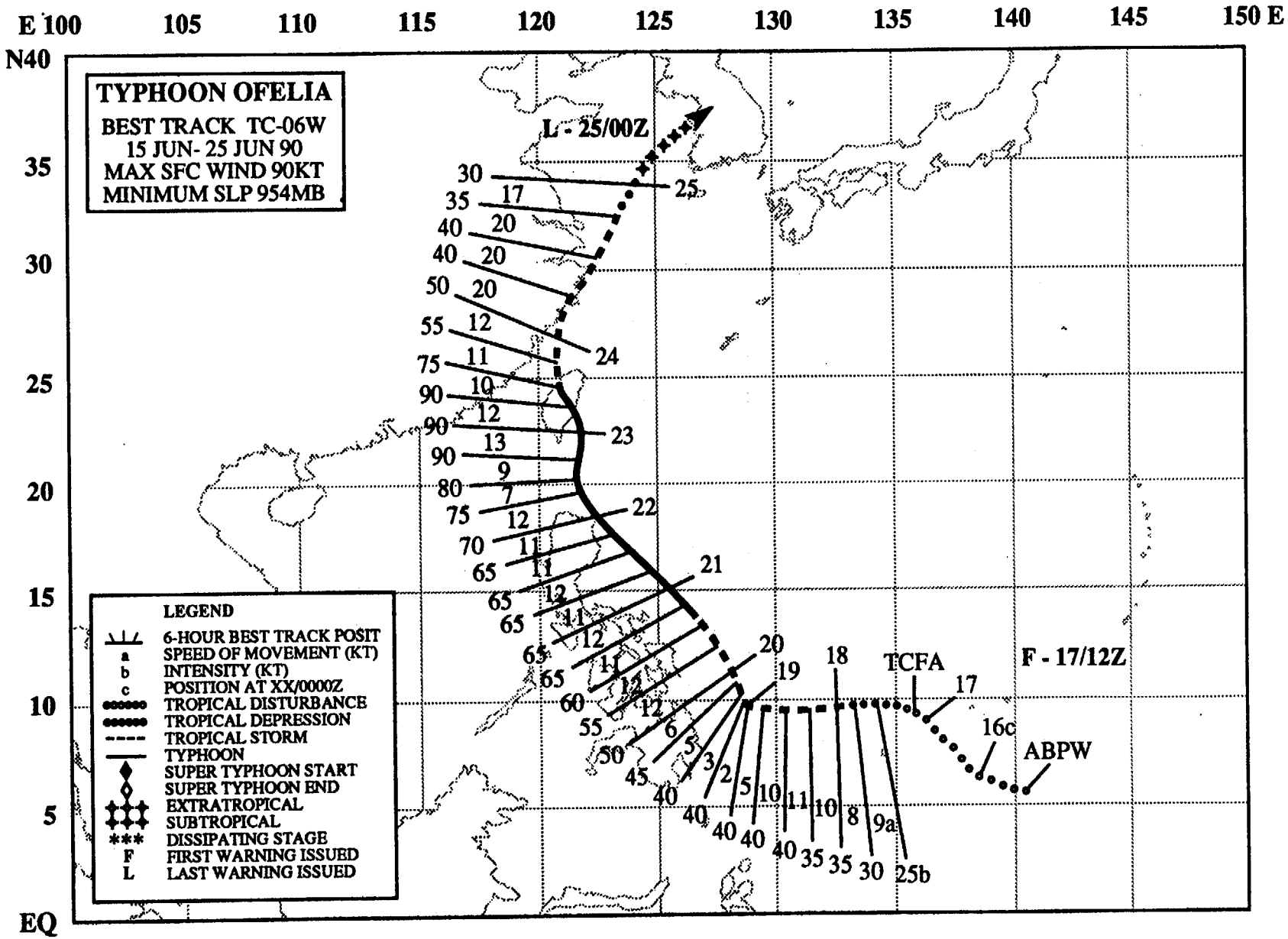
E 100
105
110
115
120
125
130
135
140
145
150 E
N40
35
30
25
20
15
10
5
EQ
TYPHOON OFELIA
BEST TRACK TC-06W
15 JUN- 25 JUN 90
MAX SFC WIND 90KT
MINIMUM SLP 954MB
L - 25/00Z
F - 17/12Z
TCFA
ABPW
LEGEND
6-HOUR BEST TRACK POSIT
a SPEED OF MOVEMENT (KT)
b INTENSITY (KT)
c POSITION AT XX/0000Z
TROPICAL DISTURBANCE
TROPICAL DEPRESSION
TROPICAL STORM
TYPHOON
SUPER TYPHOON START
SUPER TYPHOON END
EXTRATROPICAL
SUBTROPICAL
*** DISSIPATING STAGE
F FIRST WARNING ISSUED
L LAST WARNING ISSUED

TYPHOON OFELIA (06W)

I. HIGHLIGHTS

Ofelia was the third western North Pacific typhoon of 1990 and the first for the month of June. It moved toward the Philippine Islands, then slowed and turned to the northwest. Ofelia became the second tropical cyclone of the year to hit Taiwan and the first to affect the east coast of China. After recurvature, the extratropical remnants of Ofelia crossed Korea, unusual for a June system.

II. CHRONOLOGY OF EVENTS

150600Z - First mentioned on Significant Tropical Weather Advisory as an area of persistent convection with estimated maximum winds of 15 kt.

170430Z- Tropical Cyclone Formation Alert based on increased convection during diurnal minimum, more curvature to the cloud bands, and better outflow aloft.

171200Z- First warning due to improved cloud signature.

180000Z- Upgraded to tropical storm prompted by an intensity estimate of CI 2.5.

201800Z- Upgraded to typhoon based on well-defined central dense overcast and overshooting cloud tops.

230000Z- Peak intensity - 90 kt (46 m/sec) - based on appearance of an eye and a CI 5.0 estimate.

231800Z- Downgraded to tropical storm after crossing Taiwan and weakening due to land effects.

250000Z- Final warning - (extratropical) - as cyclone merged with a frontal boundary while approaching the Korean Peninsula.

III. TRACK AND MOTION

Ofelia developed in the monsoon trough in the central Caroline Islands and tracked westward along the periphery of the subtropical ridge. On 19 June the tropical cyclone slowed and executed an abrupt track change to the northwest. Although the NOGAPS 500-mb analysis (Figure 3-06-1) at 190000Z June failed to show any significant reason for the track anomaly, the 850-mb analysis (Figure 3-06-2) revealed the presence of 30 to 40 kt (15 to 21 m/sec) southwesterly flow. Since the heights and

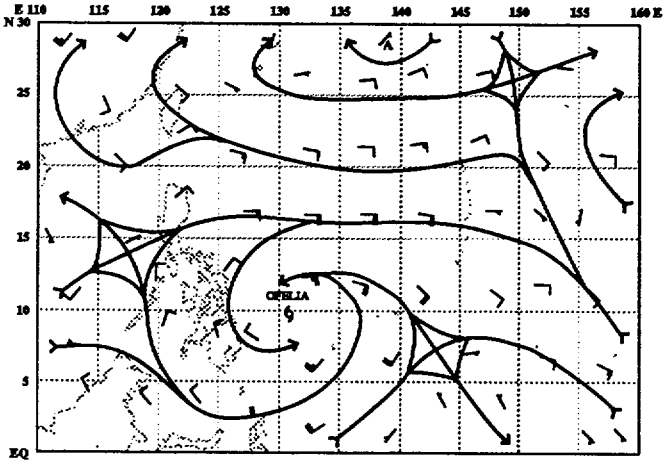

Figure 3-06-1. The 190000Z June NOGAPS 500-mb analysis shows a roughly balanced flow around Ofelia.

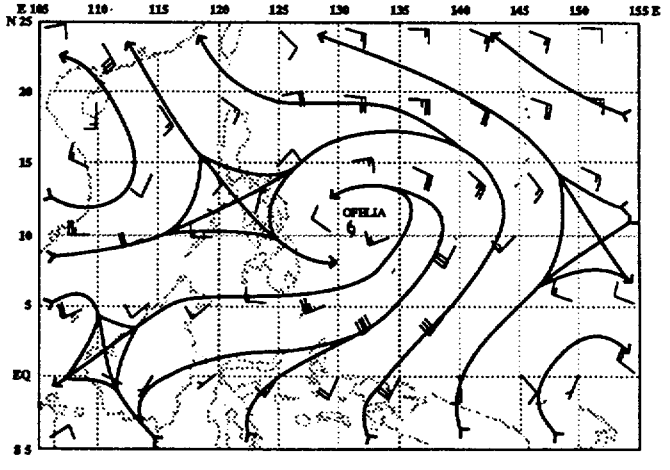

Figure 3-06-2. The 190000Z June NOGAPS 850-mb analysis reveals a stronger southwesterly inflow into the tropical cyclone.

patterns of the subtropical ridge to the north were relatively unchanged, it appears that the start of a shallow monsoon surge from the southwest into Ofelia disrupted the normal steering current. By 20 June a balance between the monsoon steering and the ridge steering had returned, and the tropical cyclone continued tracking around the ridge. On 22 June, when Ofelia was in the Bashi Channel between Luzon and Taiwan, the southwesterly monsoon flow at 850mb (Figure 3-06-3) broadened and reached 50 kt (26 m/sec) over the central Philippine Islands. This flow also deepened through the middle troposphere, where 40 kt (21 m/sec) winds appeared on the 500-mb analysis (Figure 3-06-4). It appears that as Ofelia approached 20° north latitude, the strength of the surge temporarily resulted in a more northward track. Soon after, the typhoon took a northwestward slide across Taiwan, then reached the axis of the subtropical ridge and began recurving toward Korea.

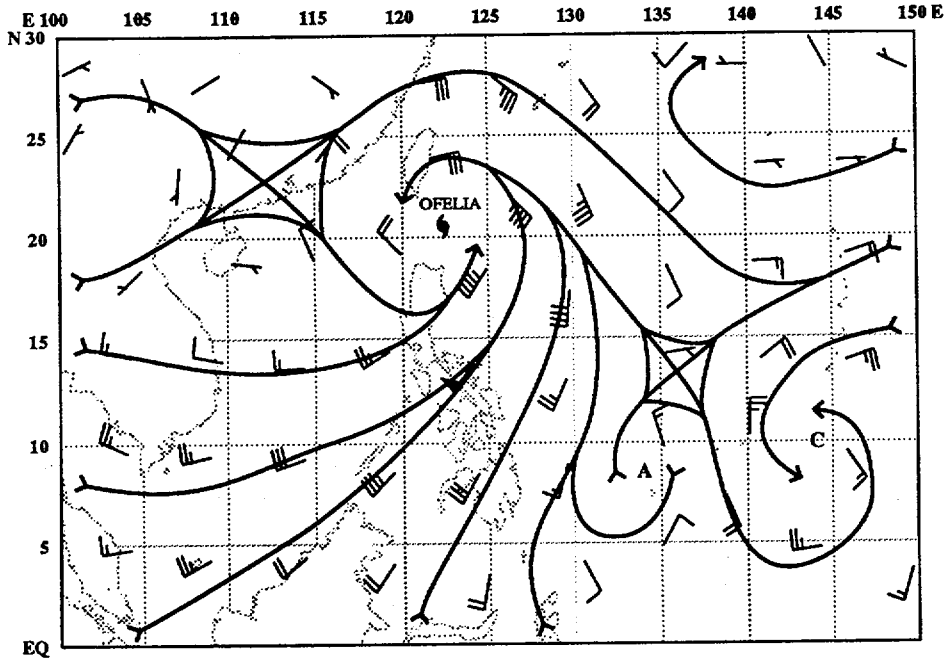

Figure 3-06-3. The 221200Z June NOGAPS 850-mb analysis shows the broad southwest monsoon flow with 50 kt (26 m/sec) across the central Philippine Islands.

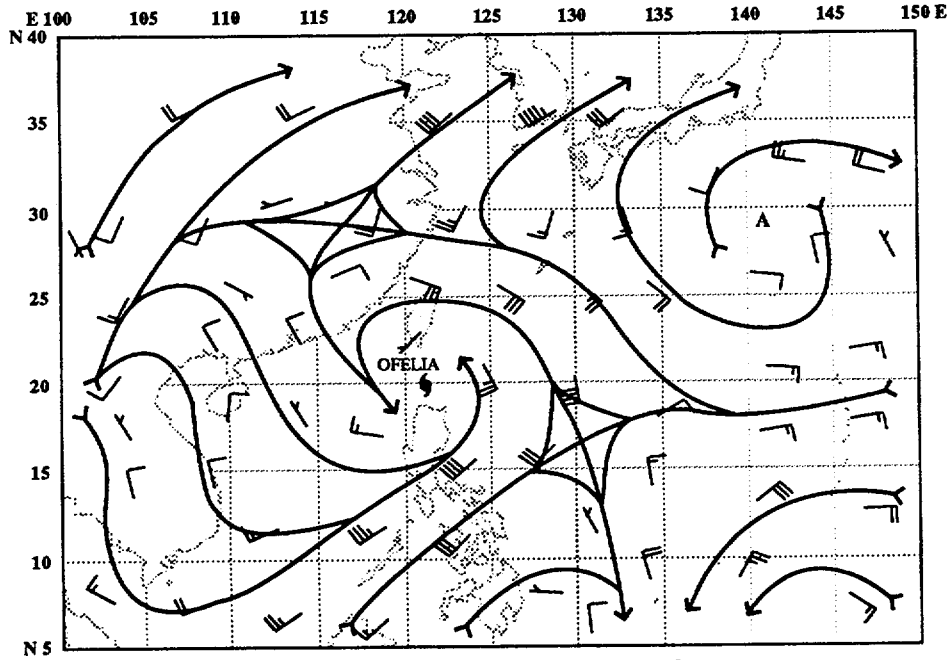

Figure 3-06-4. The 221200Z June NOGAPS 500-mb analysis indicates that the southwesterly flow extends well up into the middle troposphere.

IV. INTENSITY

The tropical depression which was to become Ofelia was initially slow to develop due to vertical wind shear from the northeast. As the southwesterly inflow into the tropical cyclone increased and deepened, an anticyclone formed aloft and the vertical wind shear decreased. Ofelia (Figure 3-06-5) intensified at a slower than average rate and peaked at 90 kt (46 m/sec) (Figure 3-06-6), five days after reaching tropical storm intensity. Part of this slower than average rate was caused by land influences from the Philippine Islands to the west of track. Rapid weakening after 230000Z was caused by land interaction, as the cloud system crossed the mountainous island of Taiwan and moved northward over the China coast.

V. FORECASTING PERFORMANCE

The NOGAPS series kept the subtropical ridge across the Philippine Sea north of the cloud system and linked it to the ridge over central China. JTWC initially expected a more westward track for the system, and continued to forecast the track too far to the west until the system approached Taiwan (Figure 3-06-7). The bias to the west of track appeared in the NOGAPS guidance and suggests that the influence of the strength and depth of the southwest monsoonal flow on Ofelia may not have been correctly addressed by the NOGAPS model.

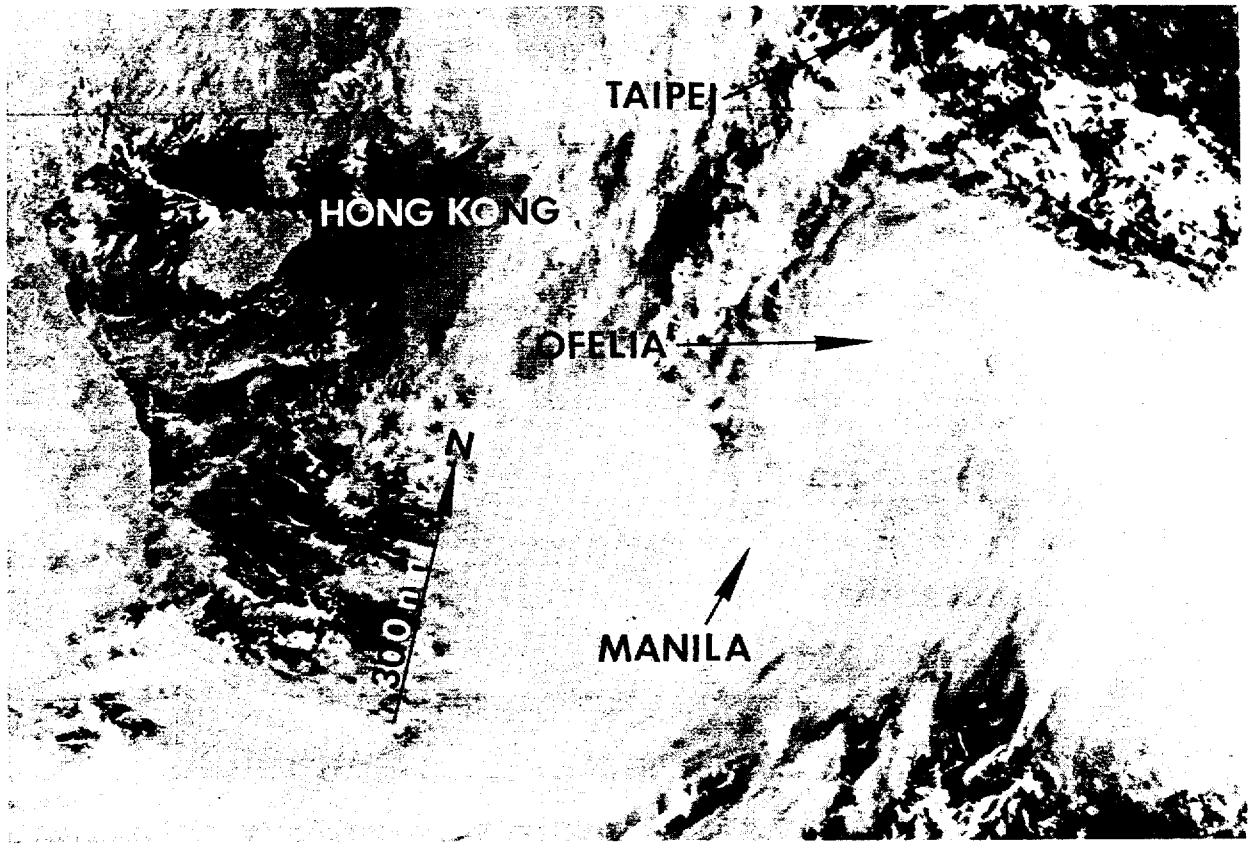

Figure 3-06-5. Typhoon Ofelia is located north of Luzon. The overcast conditions over the Philippine Islands are associated with the deep southwesterly inflow into the typhoon (220124Z June DMSP visual imagery).

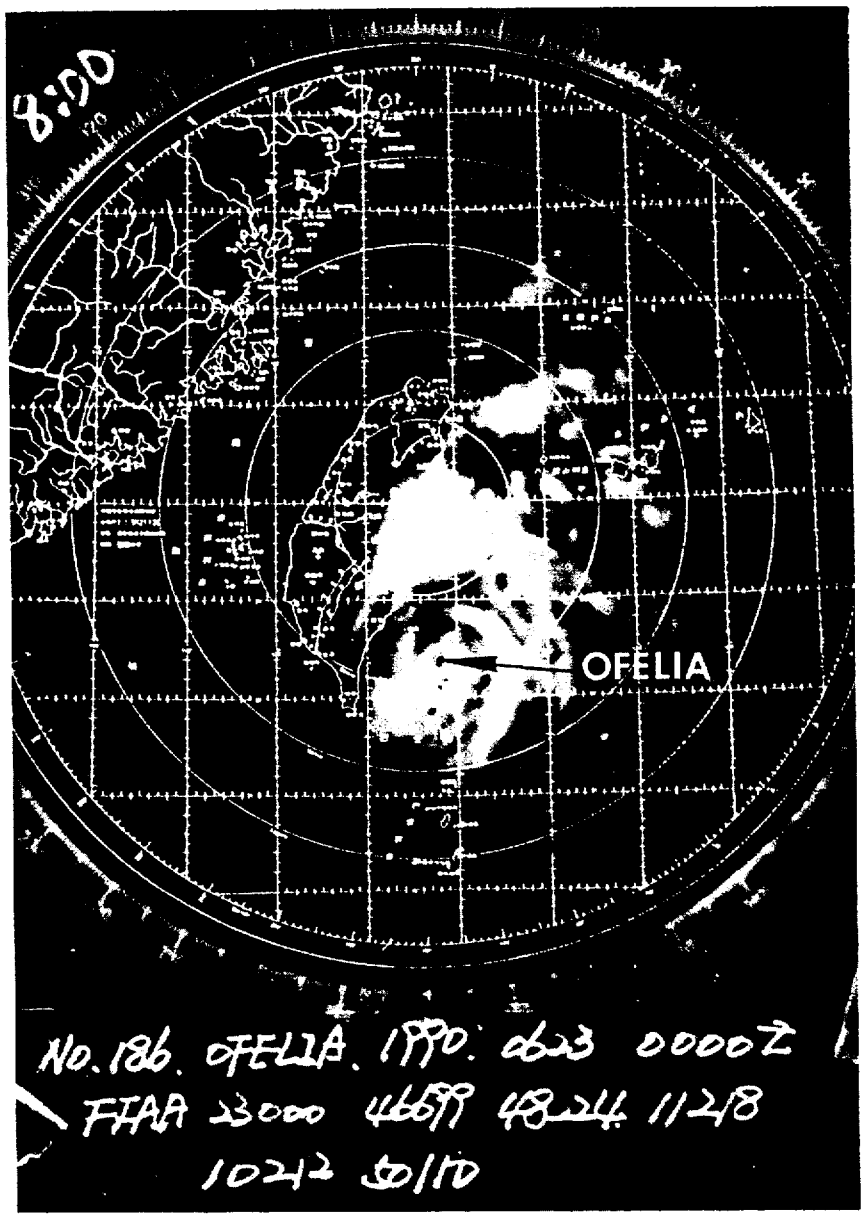

Figure 3-06-6. The 230000Z June radar image from Haulien, Taiwan (WMO 46699) of Ofelia at peak intensity. A small eye is present (radar photo courtesy of the Central Weather Bureau, Taipei, Taiwan).

VI. IMPACT

Ofelia was a destructive system. Although it didn't cross directly over northern Luzon, the system caused a surge in the southwest monsoon which resulted in torrential rains and widespread flooding in the northern Philippine Islands. Newspaper reports indicated that more than 25 people died and over 84,000 were forced to flee their homes. Taiwan took a direct hit from Ofelia. Media releases said the storm was the worst to hit eastern Taiwan in 30 years. Seventeen people died and 23 were missing due to floods and mud slides. In central China, at least 22 were killed as Ofelia, which caused flooding to low-lying provinces, moved up the coast.

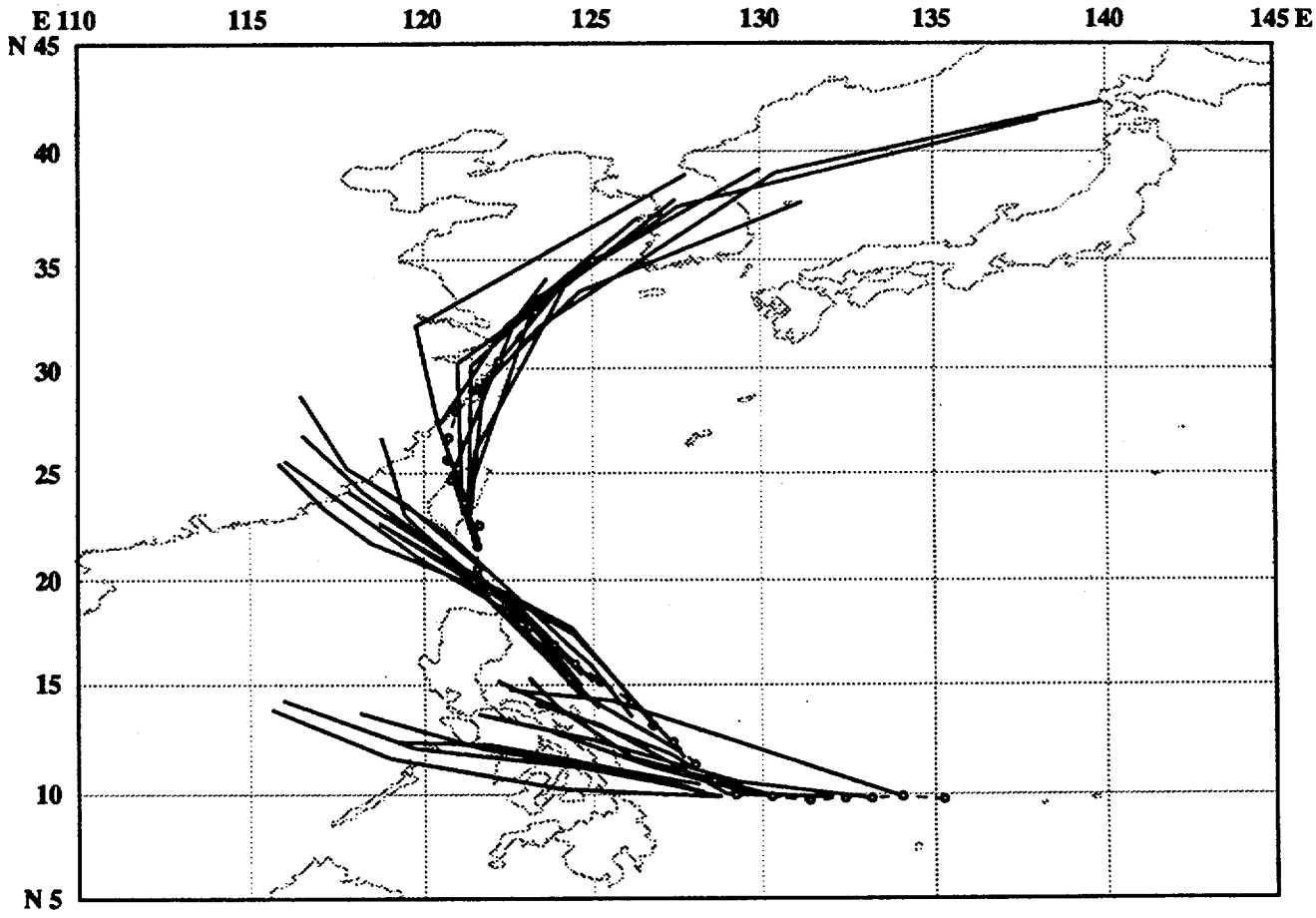

Figure 3-06-7. Summary of JTWC forecasts (solid lines) for Ofelia are superimposed on the final best track (dashed line).

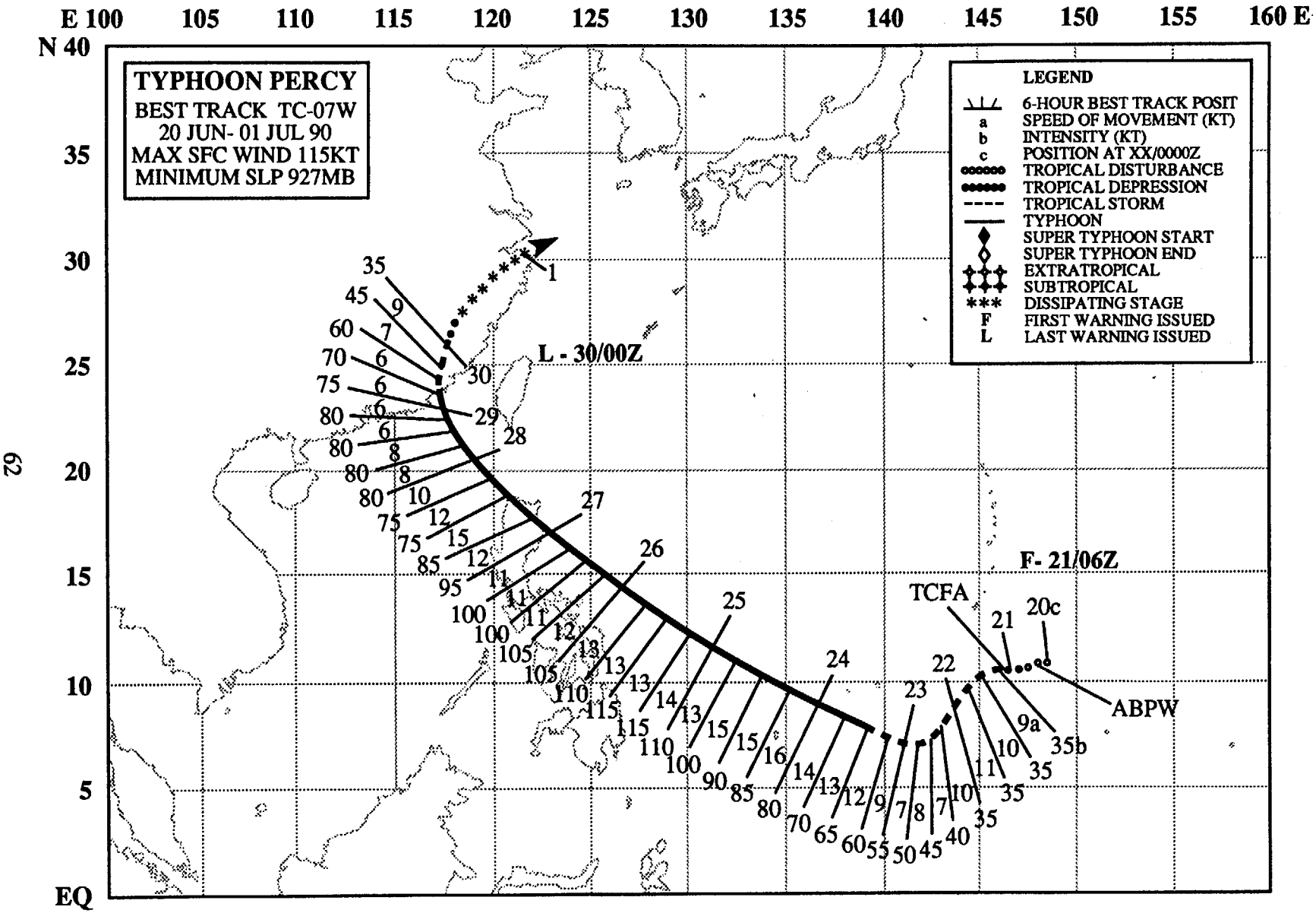
TYPHOON PERCY
BEST TRACK TC-07W
20 JUN- 01 JUL 90
MAX SFC WIND 115KT
MINIMUM SLP 927MB
LEGEND
6-HOUR BEST TRACK POSIT
SPEED OF MOVEMENT (KT)
INTENSITY (KT)
POSITION AT XX/0000Z
TROPICAL DISTURBANCE
TROPICAL DEPRESSION
TROPICAL STORM
TYPHOON
SUPER TYPHOON START
SUPER TYPHOON END
EXTRATROPICAL
SUBTROPICAL
DISSIPATING STAGE
FIRST WARNING ISSUED
LAST WARNING ISSUED
L - 30/00Z
F- 21/06Z
TCFA
ABPW
E 100
105
110
115
120
125
130
135
140
145
150
155
160 E
N 40
35
30
25
20
15
10
5
EQ

TYPHOON PERCY (07W)

I. HIGHLIGHTS

Percy was the fourth and last tropical cyclone in June. After forming southeast of Guam, it executed an unusual track to the southwest for 36 hours before paralleling Ofelia's (06W) track to the west-northwest around the western periphery of the subtropical ridge. Percy damaged the western Caroline Islands and became the second typhoon within a week to batter northern Luzon before recurving over eastern China.

II. CHRONOLOGY OF EVENTS

200600Z - First mentioned on the Significant Tropical Weather Advisory as an area of convection that had persisted for 12 hours. A cyclonic circulation was present in the low-level wind field under weakly divergent flow aloft.

202230Z - Advisory reissued to upgrade system's potential for development from poor to fair as outflow and cloud signature improved.

210300Z - Tropical Cyclone Formation Alert due to significant increase in organized convection and improved outflow aloft during the past 24 hours.

210600Z - First warning and upgrade to tropical storm prompted by receipt of 35 kt (18m/sec) ship report.

231800Z - Upgraded to typhoon followed initial signs of eye formation within the central dense overcast and first intensity estimate of T4.0.

250600Z - Peak intensity - 115 kt (59 m/sec) - with 25 nm (46 km) diameter eye and T6.0.

291200Z - Downgraded to tropical storm resulted from weakened convective signature following cyclone's interaction with the coast of southeastern China.

300000Z - Final warning - (dissipating over land) - followed further loss of convective organization as system underwent increased vertical wind shear and loss of latent and sensible heat.

III. TRACK AND MOTION

After initially tracking westward, Percy turned and tracked southwestward for approximately 36 hours. Since the extent of the subtropical ridge and its axis along 28°N remained relatively unchanged during this period, the track change must have resulted from activity near the monsoon trough. An anticyclone had formed southeast of Typhoon Ofelia (06W) and was tracking west-northwestward in tandem with it. As Percy formed, subsidence associated with the converging outflow aloft from both Percy and Ofelia strengthened the anticyclone which resulted in northerly steering flow across Percy (Figure 3-07-1). Percy tracked around the east side of this anticyclone until approximately 221200Z. As Ofelia moved northwestward away from Percy, the anticyclone between them tracked northwestward, weakened and merged with the subtropical ridge to its north. By 231200Z it was only evident as a southwestward extension of the subtropical ridge between Ofelia and Percy (Figure 3-07-2), and by 251200Z it was no longer discernible. Percy then tracked west-northwestward around the subtropical ridge (Figure 3-07-3). After making landfall on the southeast coast of China, Percy was picked up by a mid-latitude short wave trough and finally dissipated as it recurved over eastern China.

IV. INTENSITY

Starting as a low-level circulation at the eastern end of the monsoon trough, Percy quickly developed into a tropical storm as it moved into an area of upper-level divergence. An upper-level anticyclone soon developed over the low-level circulation center. The vertically aligned system intensified into a typhoon as it obtained an outflow channel to the south. As Percy cleared the western Caroline Islands, it developed an additional outflow channel to the north and further intensified, reaching its maximum intensity of 115 kt (59 m/sec) at 250600Z (Figure 3-07-4). The typhoon

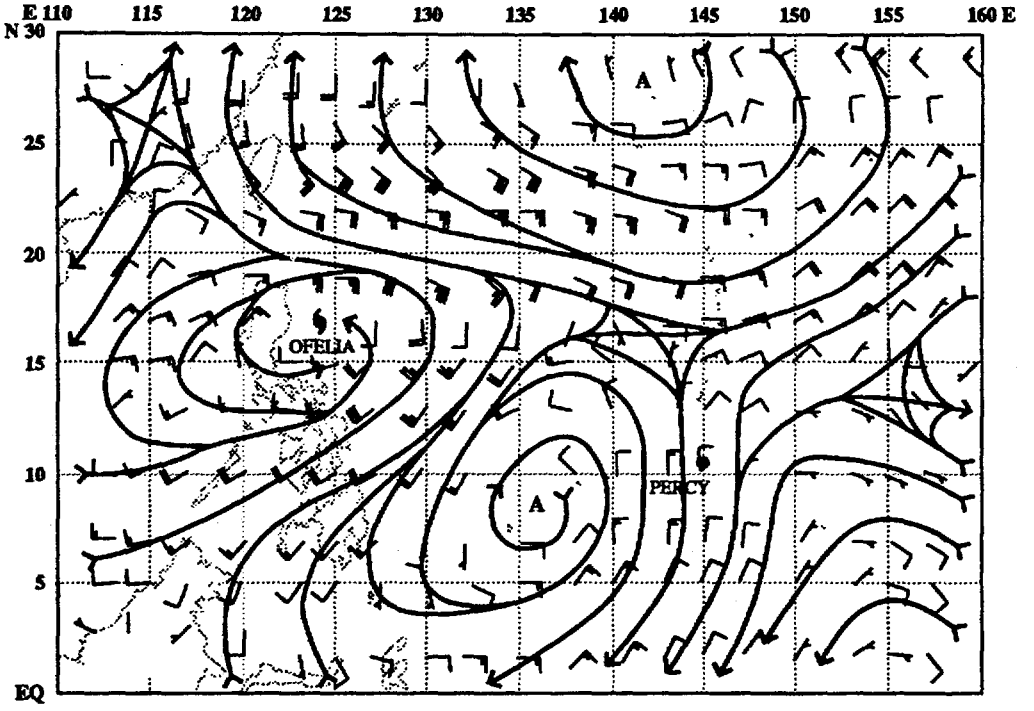

Figure 3-07-1. The 211200Z June deep layer mean analysis shows Percy embedded in northerly flow with a anticyclone to its west. Ofelia's (06W) circulation is located to the northwest of the anticyclone.

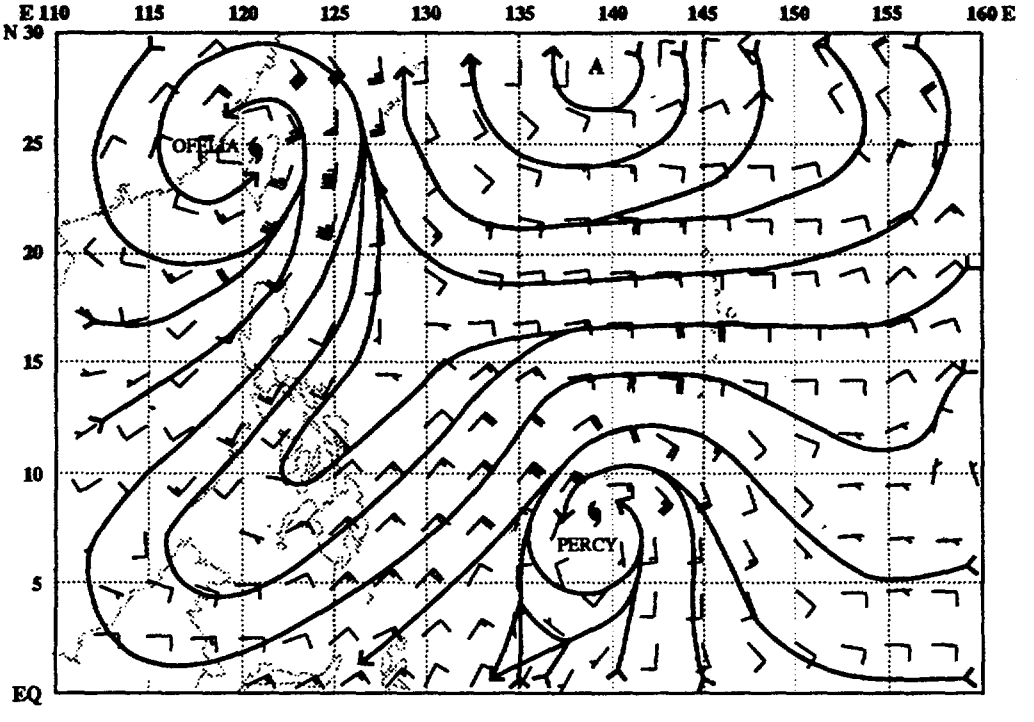

Figure 3-07-2. The 231200Z June deep layer mean analysis indicates the ridge between Ofelia (06W) and Percy has weakened and become a southwestward extension of the subtropical ridge.

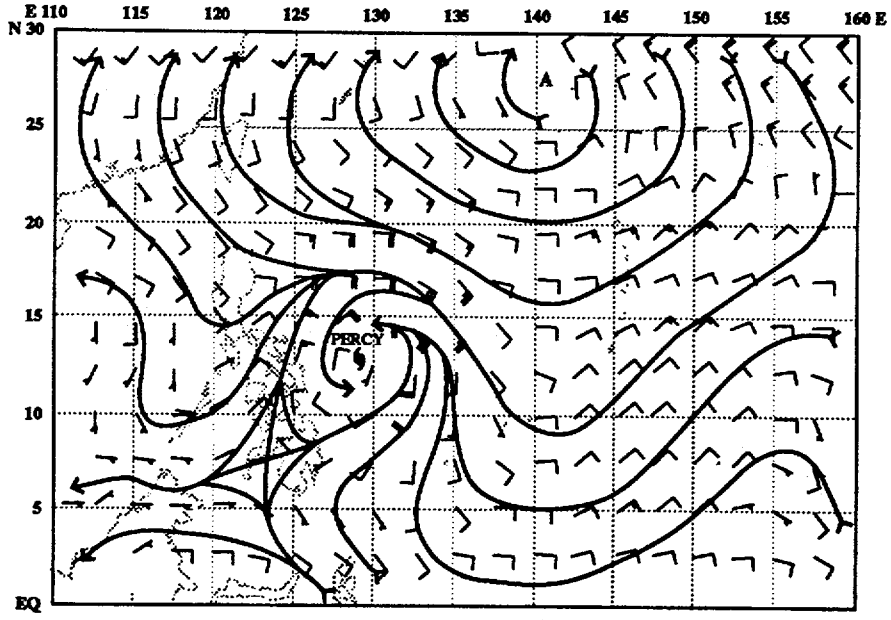

Figure 3-07-3. The 251200Z June deep layer mean analysis shows Percy embedded in the flow around the western end of the subtropical ridge.

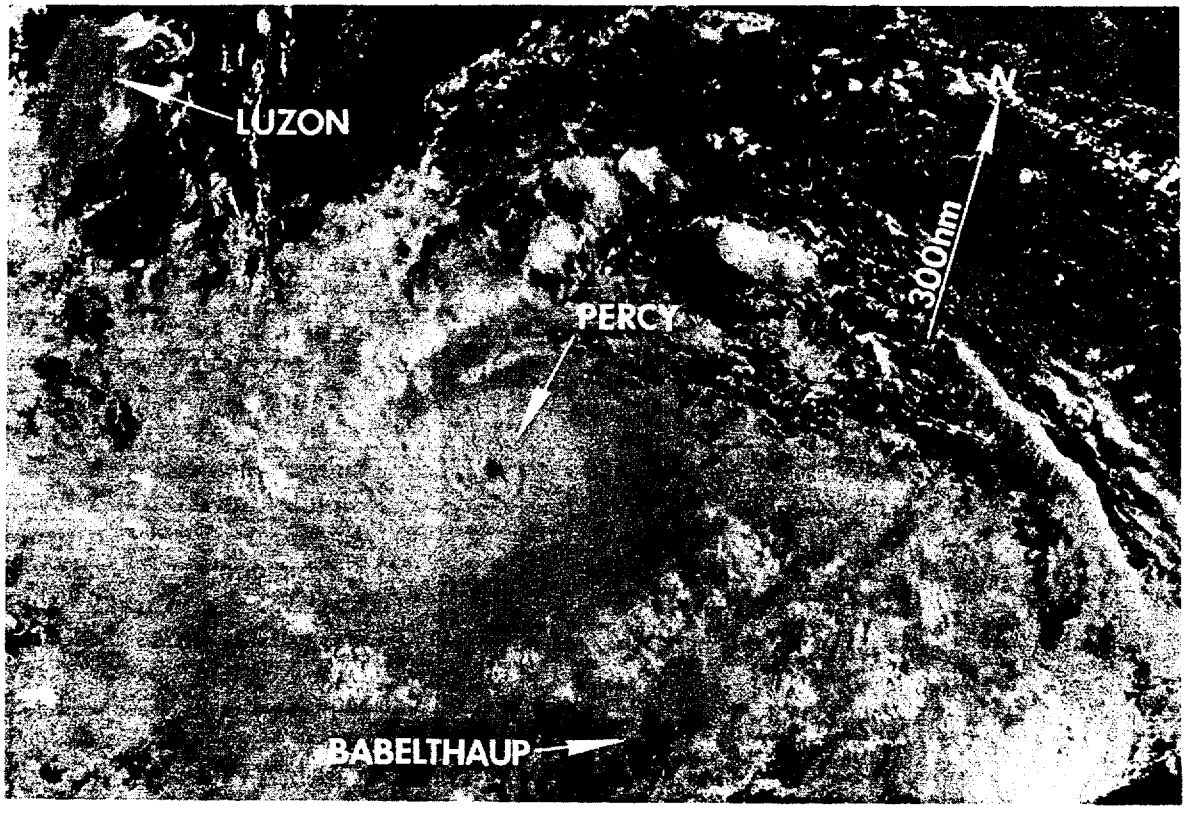

Figure 3-07-4. Typhoon Percy just prior to reaching maximum intensity. Northern Luzon is visible at the top left of the image (250021Z June DMSP visual imagery).

weakened initially due to increasing vertical wind shear from the northeast, and later, from land interactions with northern Luzon (Figure 3-07-5). After moving into the South China Sea and reintensifying slightly, Percy's eye wall (Figure 3-07-6) assumed a polygonal structure (Lewis and Hawkins, 1982). Further weakening resulted from additional vertical wind shear and passage over China.

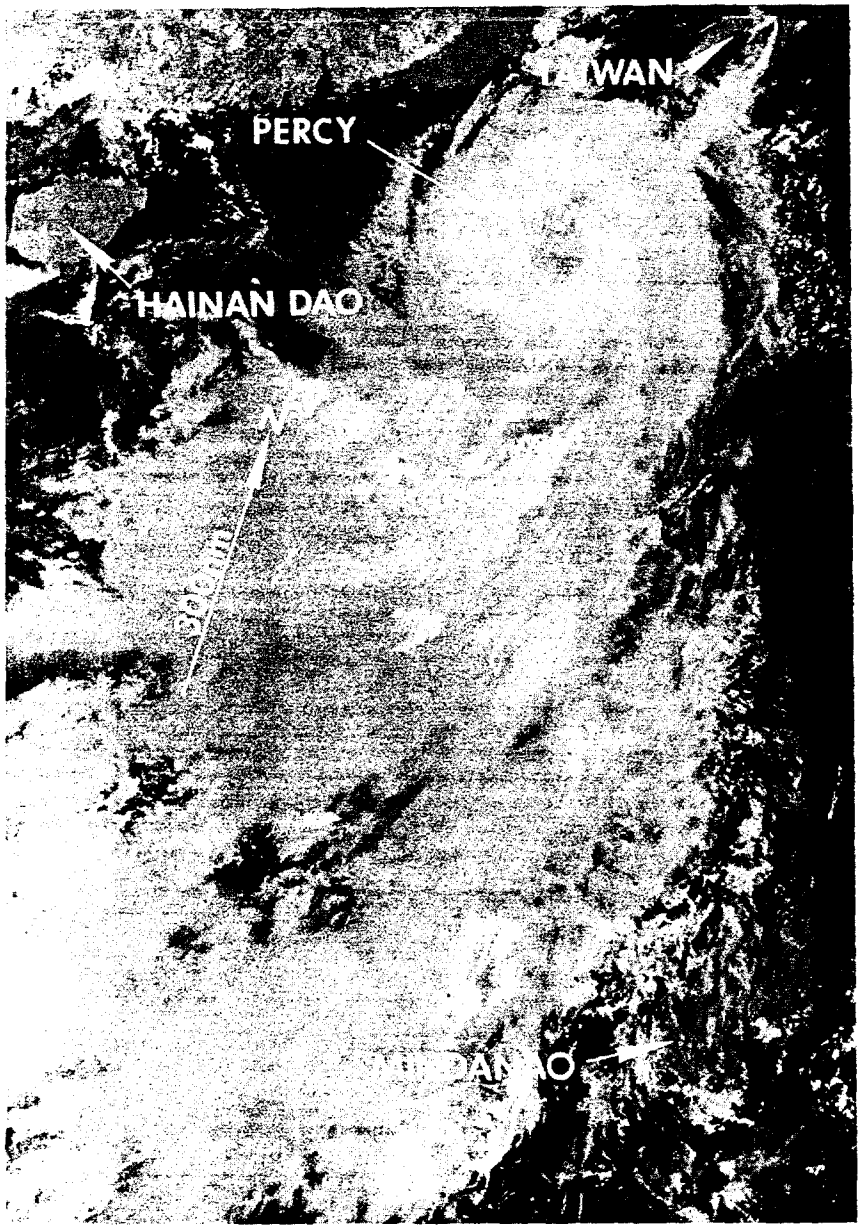

Figure 3-07-5. A ragged, cloud-filled eye reformed after the typhoon collided with northern Luzon. Percy is one day before making landfall in southeastern China. Taiwan is at top right and Hainan Dao at top left (280100Z June DMSP enhanced infrared imagery).

V. FORECASTING PERFORMANCE

Of particular interest was the southwestward portion of Percy's track. Initially, JTWC thought the dynamic high pressure system between Ofelia (06W) and Percy was too weak to influence Percy's track. Forecasters favored persistence and climatology for a west-northwestward track. Forecasters assumed that any departure from this track would be short lived as a result of interactions with a vorticity center associated with a mass of convection to the southeast of Percy. A binary interaction (Figure 3-07-7), when added to the translation of the overall system, would cause a net displacement of Percy to the southwest. This would only last until the two vortices merged. In contrast, OTCM guidance (Figure 3-07-8), which agreed with the deep layer mean, suggested a track south of west which turned out to be accurate. Later, as Percy approached Luzon, another forecast problem arose. The NOGAPS prognostic series indicated that the subtropical ridge would weaken and allow Percy to recurve east of Taiwan. As a result, JTWC and a number of the objective aids forecast recurvature at that longitude. However, the subtropical ridge

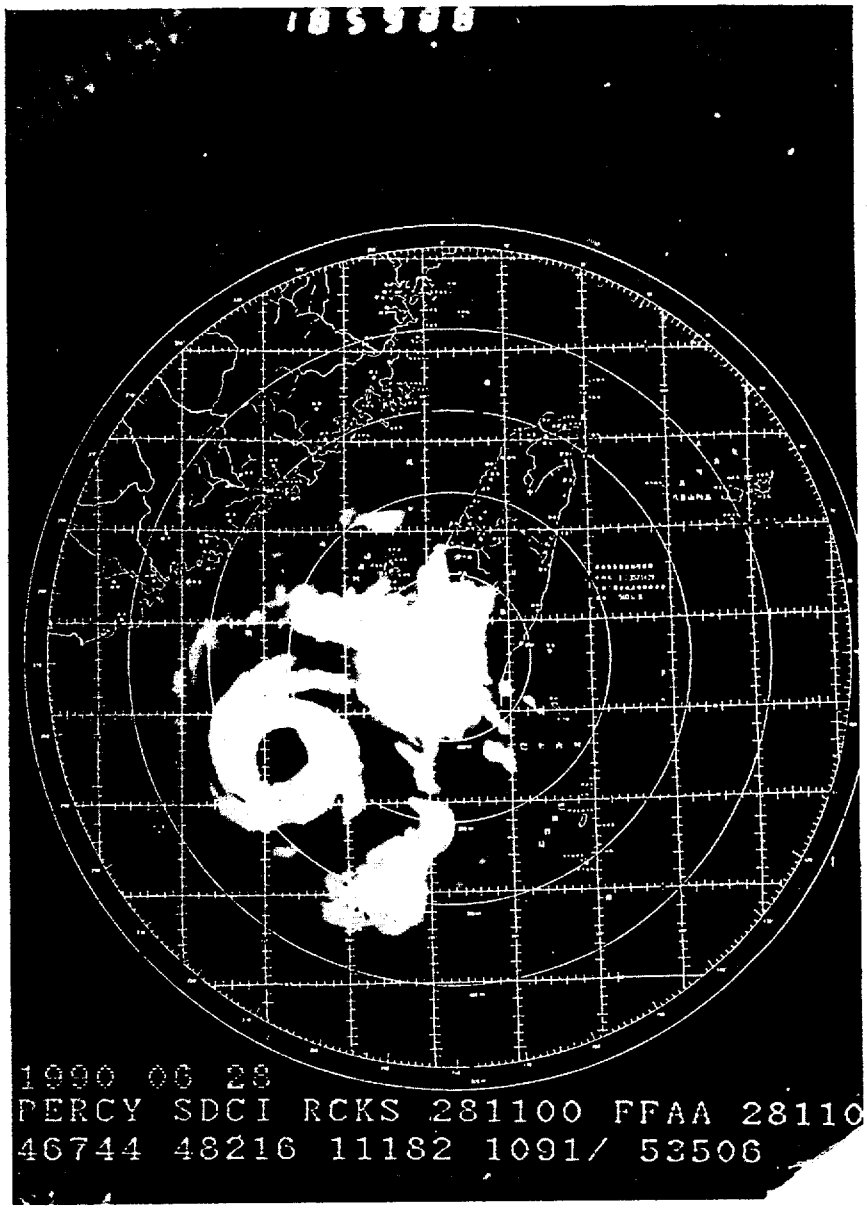

Figure 3-07-6. The polygonal structure of Percy's eye wall at 281100Z June as viewed by the zohsiung (WMO 46744) radar (photograph courtesy of the Central Weather Bureau, Taipei, Taiwan).

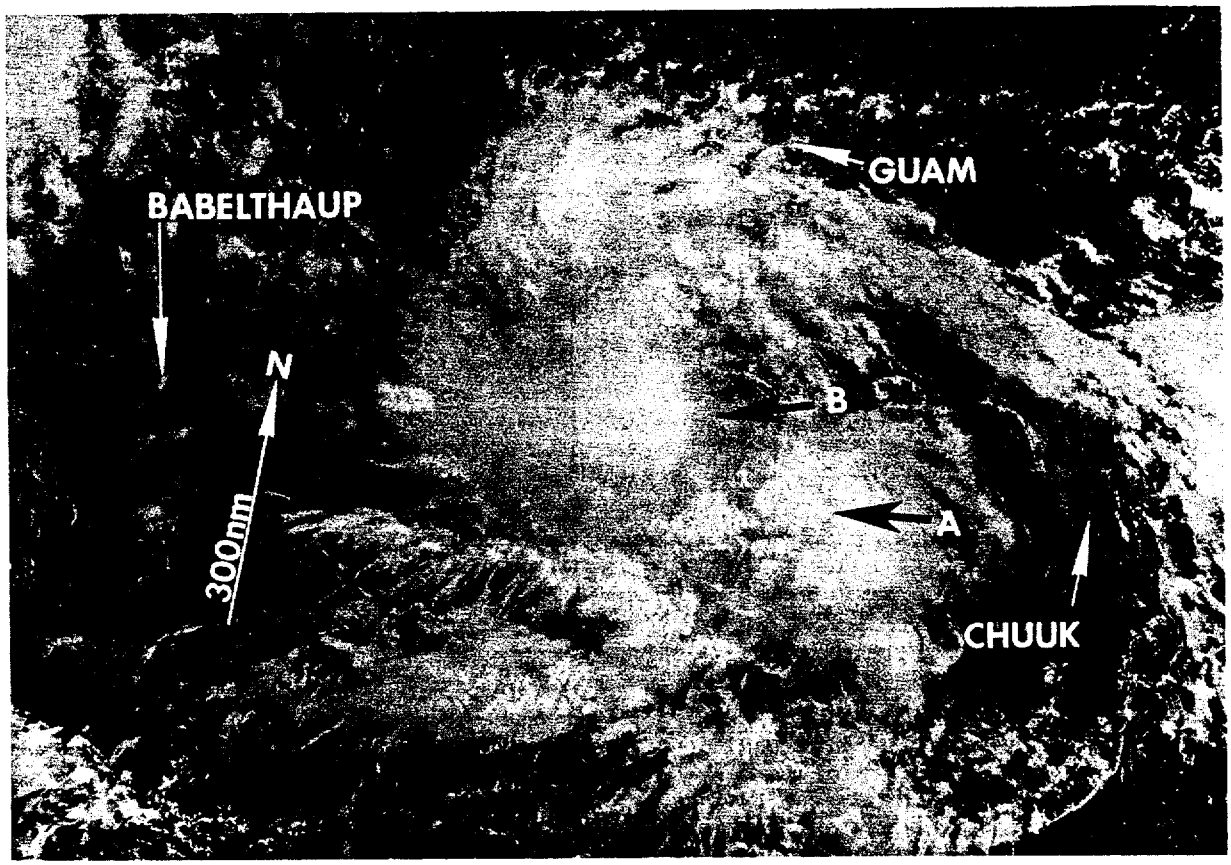

Figure 3-07-7. The vorticity associated with the convective mass (at point A) may have joined with the vorticity associated with the low-level circulation center (at point B), to interact as a binary pair. Babelthaup in the Palau Islands can be seen to the west of Percy's cloudiness (212343Z June DMSP visual imagery).

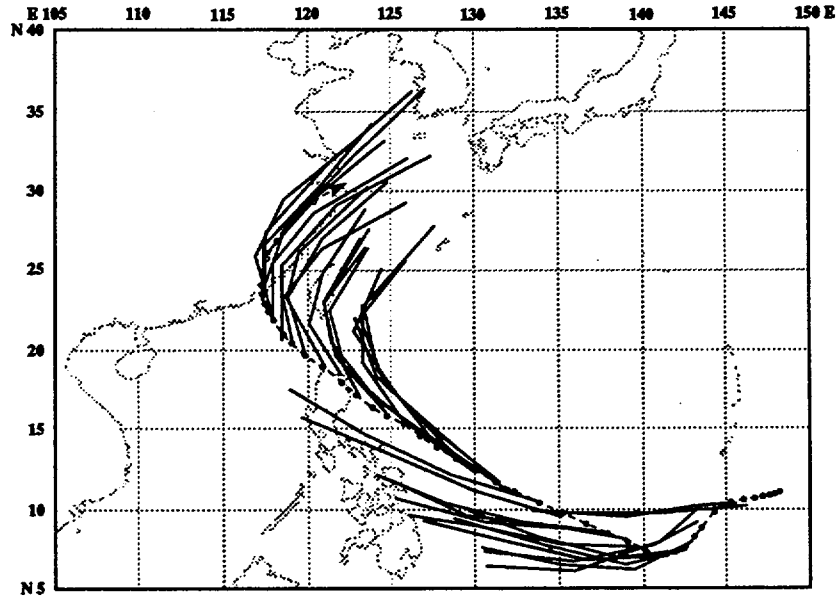

Figure 3-07-8. OTCM guidance and the JTWC forecasts compared to the final best track near the start of the unusual southwesterly motion.

did not weaken and Percy tracked further west before recurving. All the JTWC forecasts are plotted on the best track in Figure 3-07-9.

VI. IMPACT

Percy seriously affected several islands in the western Carolines. The first of these was Sorol, an atoll located 150 nm (280 km) southeast of Yap. As the tropical storm passed 40 nm (75 km) to the south of Sorol, the second largest island in the lagoon, Pegelmol, was almost cut in half and another island lost one third of its area due to wave action. Taro patches, coconut trees and other vital crops were essentially wiped out and will take take years to replace. After reaching typhoon intensity, Percy passed 55 nm (100 km) south-southwest of Yap, which received sustained winds of 35-45 kt (18-23 m/sec) with gusts to 55 kt (28 m/sec). In addition, Yap suffered extensive flooding along its eastern shore. Most roads were blocked by water and later by debris and flooding from the unusually high tide. Nugulu, 60 nm (110 km) to the south-southwest of Yap, took the brunt of the typhoon. Maximum gusts estimated at 70 kt (35 m/sec) totally destroyed all crops. Seven homes were completely demolished; others lost their roofs. Fortunately there were no fatalities. Palau was not as lucky; one child's death was attributed to the typhoon as Percy passed 125 nm (230 km) to the north-northeast of Koror. Power, radio and TV were knocked out as winds ripped off tin roofs and snapped power poles. Broken limbs took out power lines. Once past the Caroline islands, Percy became the second storm in less then a week to devastate northern Luzon. The resulting landslides and floods left at least 8 people dead and 31,206 homeless, adding to the misery left behind by Ofelia (06W).

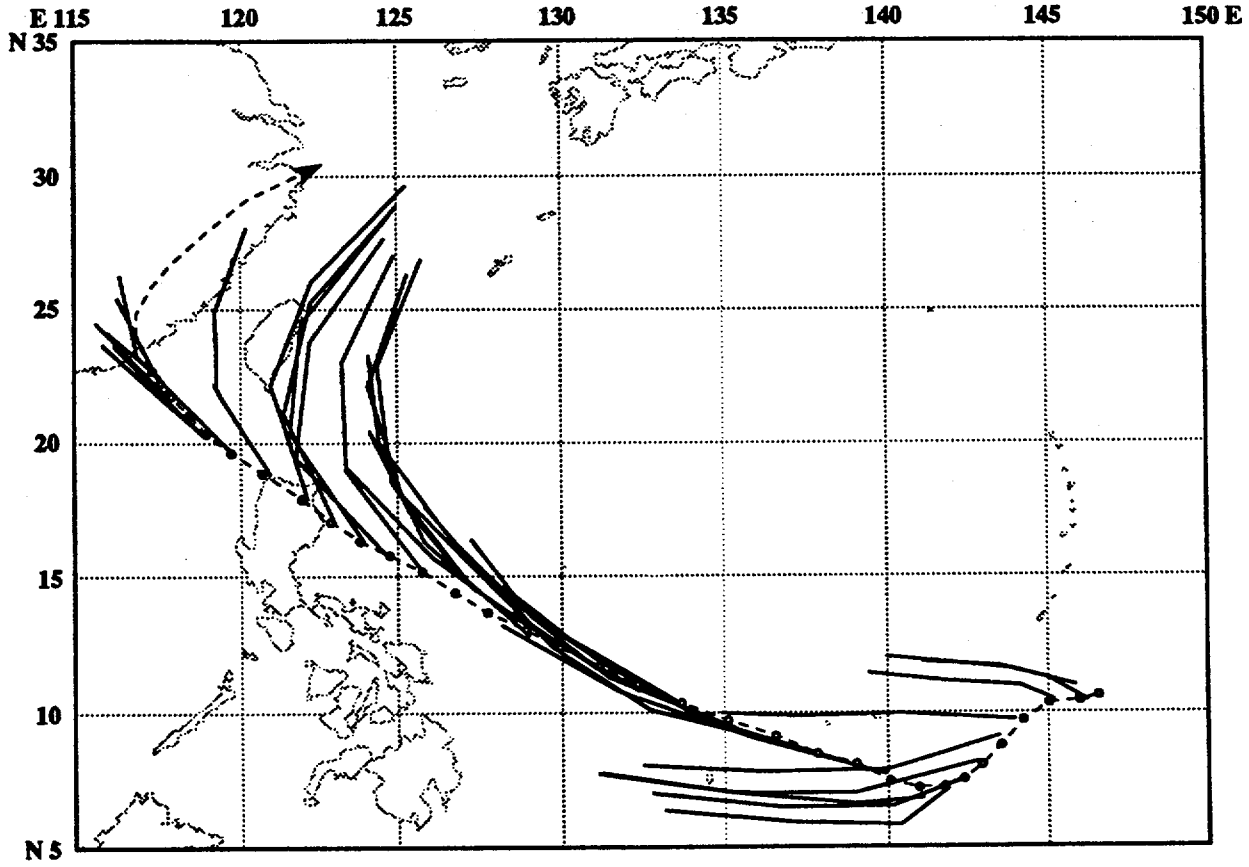

Figure 3-07-9. A plot of all the JTWC forecasts (solid lines) with the best track (dashed lines).

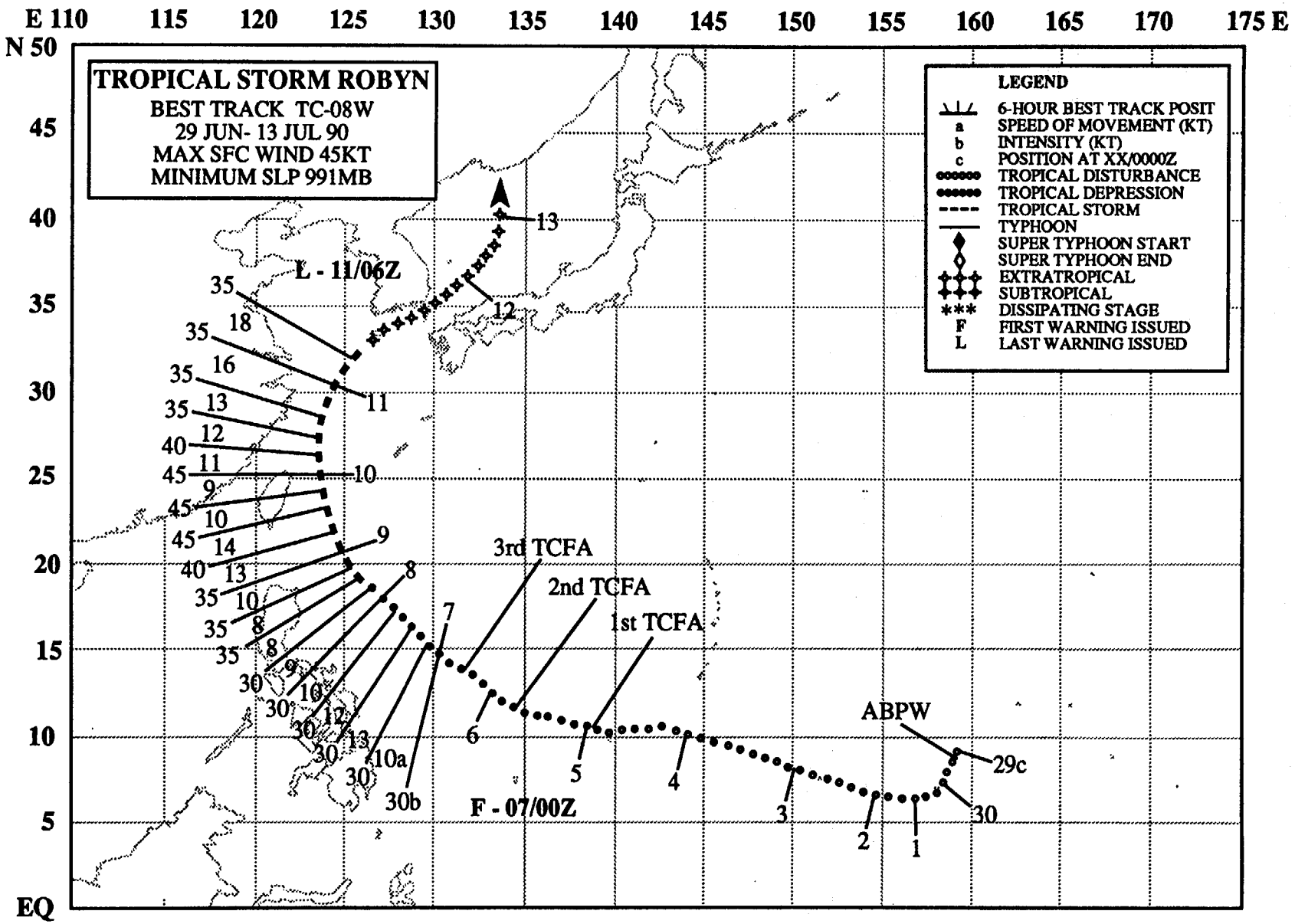
TROPICAL STORM ROBYN
BEST TRACK TC-08W
29 JUN- 13 JUL 90
MAX SFC WIND 45KT
MINIMUM SLP 991MB
LEGEND
6-HOUR BEST TRACK POSIT
SPEED OF MOVEMENT (KT)
INTENSITY (KT)
POSITION AT XX/0000Z
TROPICAL DISTURBANCE
TROPICAL DEPRESSION
TROPICAL STORM
TYPHOON
SUPER TYPHOON START
SUPER TYPHOON END
EXTRATROPICAL
SUBTROPICAL
DISSIPATING STAGE
FIRST WARNING ISSUED
LAST WARNING ISSUED
L - 11/06Z
F - 07/00Z
3rd TCFA
2nd TCFA
1st TCFA
ABPW
E 110
115
120
125
130
135
140
145
150
155
160
165
170
175 E
N 50
45
40
35
30
25
20
15
10
5
EQ

70

TROPICAL STORM ROBYN (08W)

I. HIGHLIGHTS

Robyn, the first significant tropical cyclone of July, followed what at first glance might appear to be a typical recurvature track. However, Robyn's motion was actually a classic example of the response of a tropical cyclone to the establishment of an omega block, and thus is significant as a case study of an infrequent, but complex, synoptic influence on tropical cyclone motion.

II. CHRONOLOGY OF EVENTS

290600Z - (June) First mentioned on Significant Tropical Weather Advisory as an area of persistent convection with an estimated minimum sea-level pressure of 1006 mb.
042300Z - (July) First Tropical Cyclone Formation Alert based on increased convection, organization, and outflow aloft.
051530Z - Second Tropical Cyclone Formation Alert issued. Organization temporarily delayed due to upper-level wind shear.
061530Z - Third Tropical Cyclone Formation Alert issued. Convection still consolidating during diurnal fluctuations.
070000Z - First warning based on improved outflow to the southeast and anticipated reduction of vertical wind shear.
081800Z - Upgraded to tropical storm based on enhanced convection and improved organization.
091800Z - Peak intensity of 45 kt (23 m/sec) based on synoptic data.
110000Z - Downgraded to tropical depression .
110600Z - Final warning - (extratropical) - due to the loss of persistent central convection.

III. TRACK AND MOTION

From the initial mention on the Significant Tropical Weather Advisory until the first warning at 070000Z, Robyn tracked essentially west-northwestward under the subtropical ridge. However, on 6 July an omega block began to form with the digging lows located about 49°N 117°E and 51°N 153°E as shown in Figure 3-08-1a. The 5880 meter height contour identified significant ridging poleward of Robyn, which under normal circumstances would imply continued westward movement. As shown in Figure 3-08-1b, the omega block was firmly established at 080000Z, and the digging lows had dramatically eroded the ridge north of Robyn causing the increase in its northward motion component. At 100000Z, the ridge was fully eroded permitting Robyn to pass Taiwan to the east (Figure 3-08-1c). The downwind digging low had penetrated more equatorward than its upwind counterpart causing the omega block to tilt eastward. This shift signaled the beginning of the breakdown of the block. Still, the ridging directly east of Robyn, associated with the central axis of the block, was sufficient to keep Robyn on a northward track, delaying recurvature. At 120000Z, the central ridging of the omega block (Figure 3-08-1d) had broken down sufficiently for Robyn to recurve and significantly accelerate as it moved into the Sea of Japan as an extratropical low.

IV. INTENSITY

The delayed development of Robyn and its subsequent intensification to only a nominal tropical storm (Figure 3-08-2) was due to moderate but persistent vertical wind shear associated with the eastern periphery of the summertime 200-mb easterly jet over southern Asia. In addition, the ridging to the north of Robyn for much of its life-cycle restricted outflow. When the ridge broke down, Robyn briefly intensified to 45 kt (23 m/sec) in response to outflow into the midlatitude westerlies.

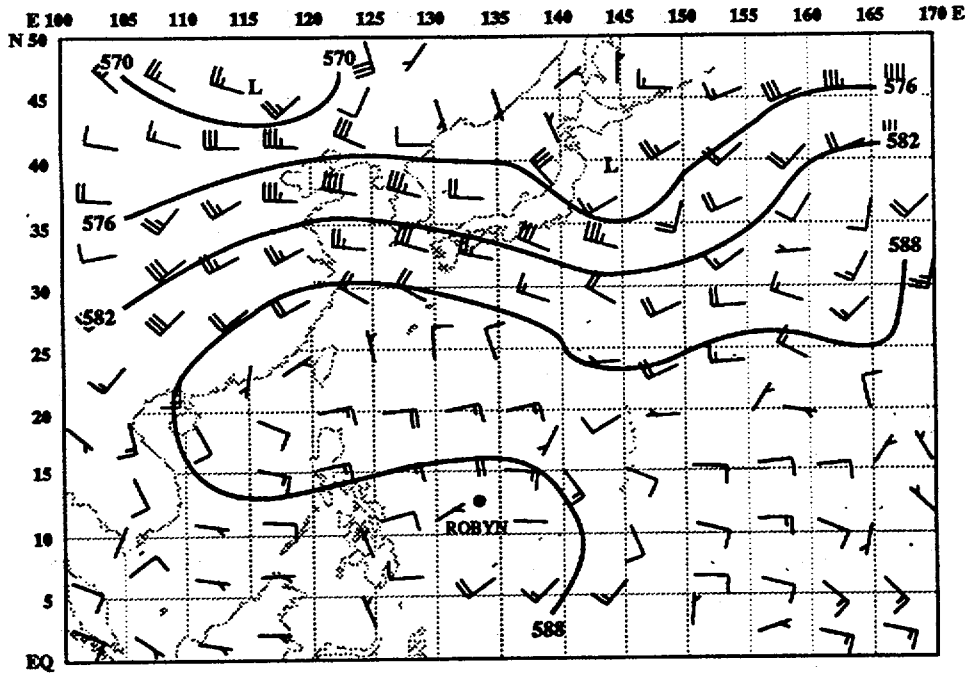

a.

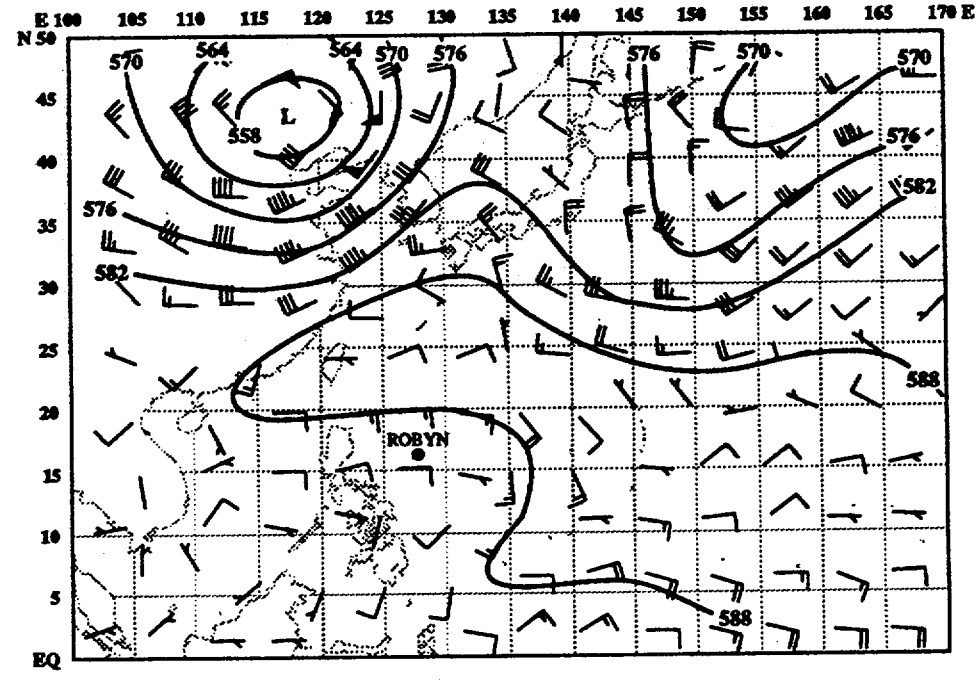

b.

Figure 3-08-1 a, b. NOGAPS 500-mb height analyses (in decameters) with the corresponding positions of Robyn for valid times a.) 060000Z and b.) 080000Z

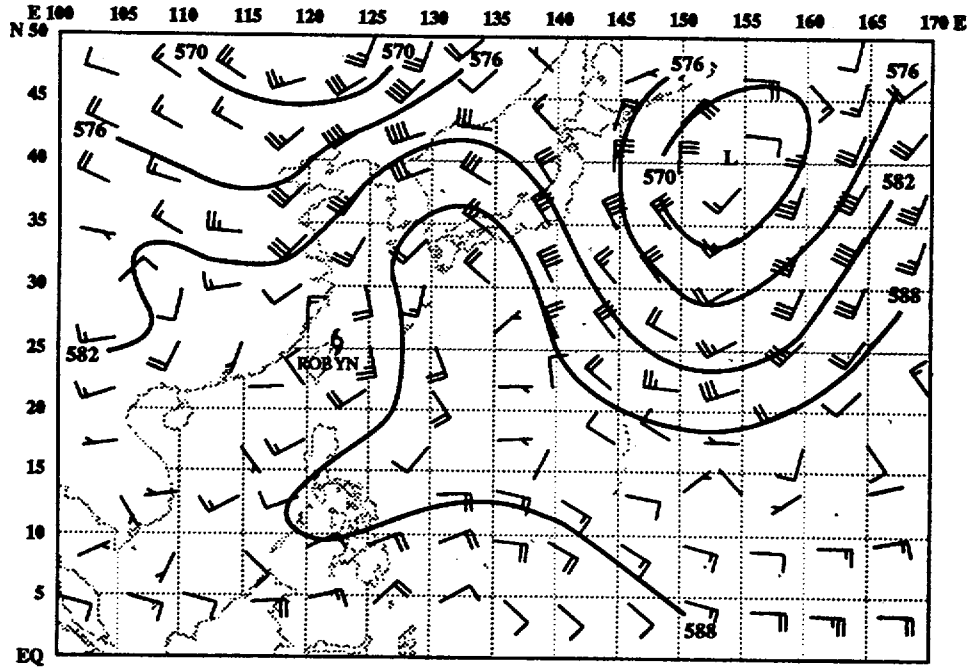

c.

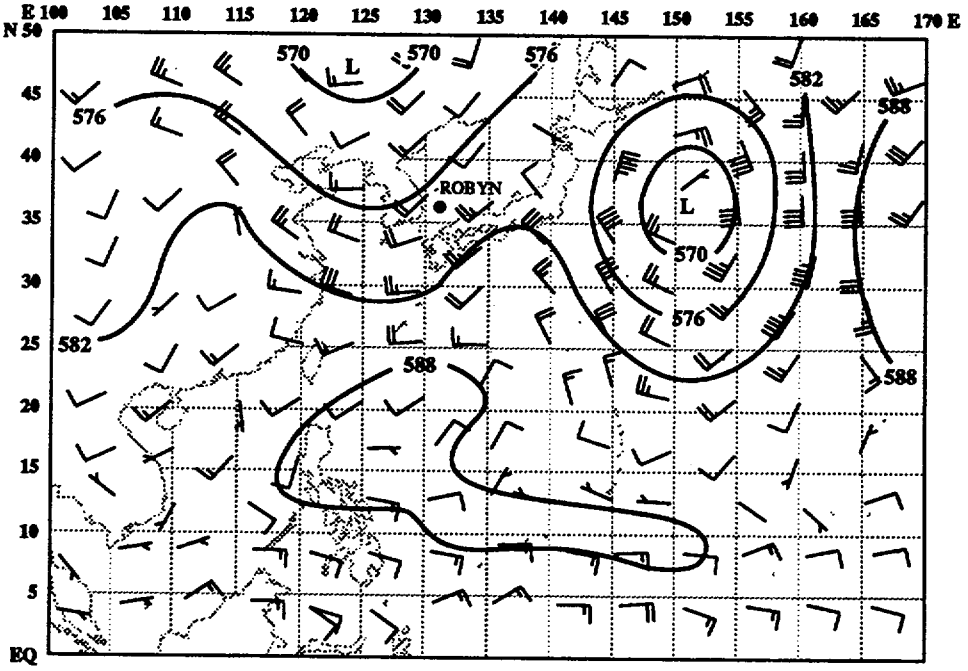

d.

Figure 3-08-1 c, d. NOGAPS 500-mb height analyses (in decameters) with the corresponding positions of Robyn for valid times c.) 100000Z and d.) 120000Z.

V. FORECASTING PERFORMANCE

The key variable in forecasting the motion of Robyn was the rapidity with which the low upwind of the omega block would break down the mid-level ridge to the north of Robyn. As Figure 3-08-3 illustrates, guidance available to JTWC between 070000Z and 080000Z did not indicate that the breakdown would proceed in time to permit Robyn to recurve east of Taiwan. JTWC relies heavily on the dynamic models OTCM and FBAM, the accuracies of which in turn depend heavily on the accuracy of the NOGAPS prognoses. By comparing Figure 3-08-3 with Figure 3-08-1c, it is evident that the NOGAPS 500-mb 72-hour prognosis for 100000Z had prematurely weakened the upwind low of the omega block. As a result, the NOGAPS 500-mb 72-hour prognoses that verified between 090000Z and 100000Z retained ridging north of Robyn that did not verify. This, in turn, caused NOGAPS-dependent objective techniques such as OTCM and FBAM to forecast continued west-northwestward movement for Robyn, which contributed to JTWC's left-of-track bias during that same period.

VI. IMPACT

No information received.

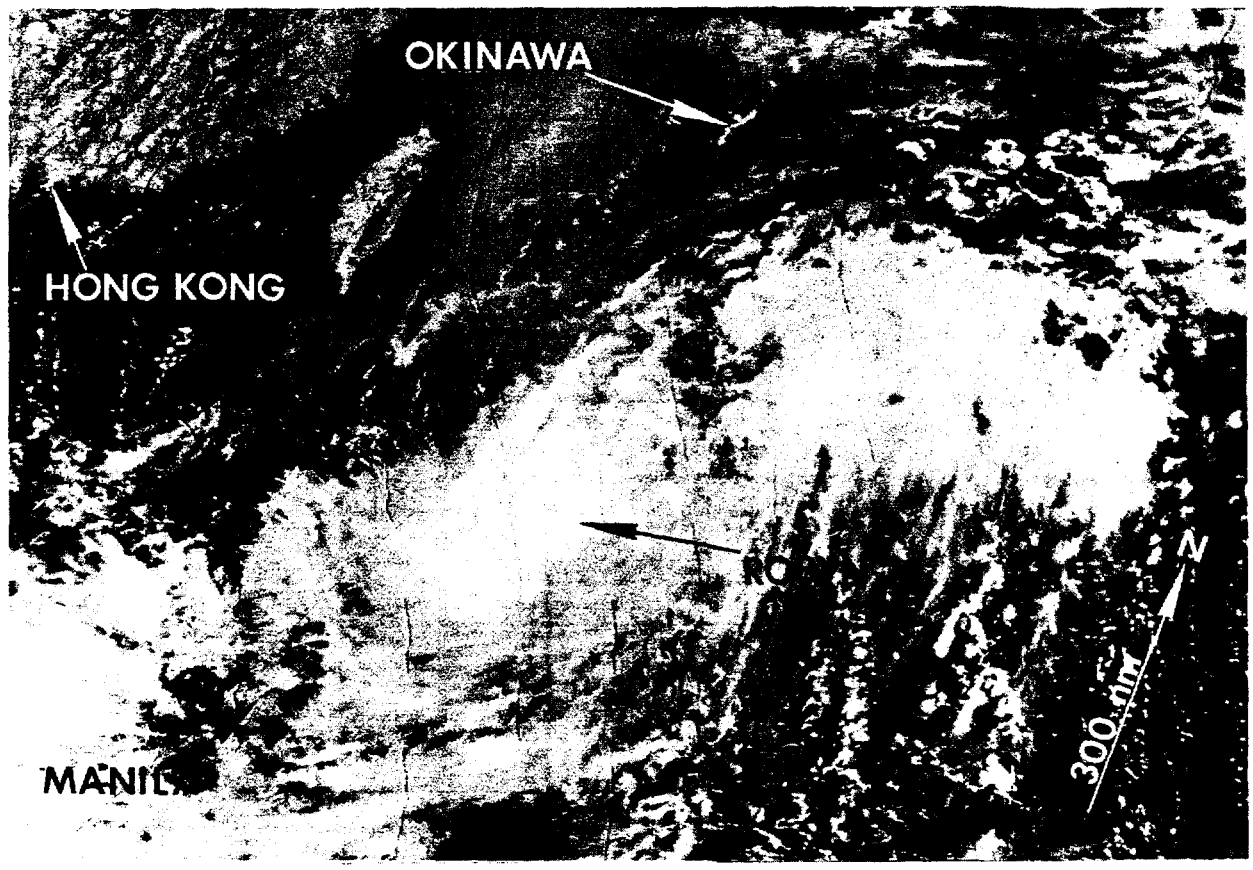

Figure 3-08-2. Robyn just before reaching tropical storm intensity (080514Z July NOAA visual imagery).

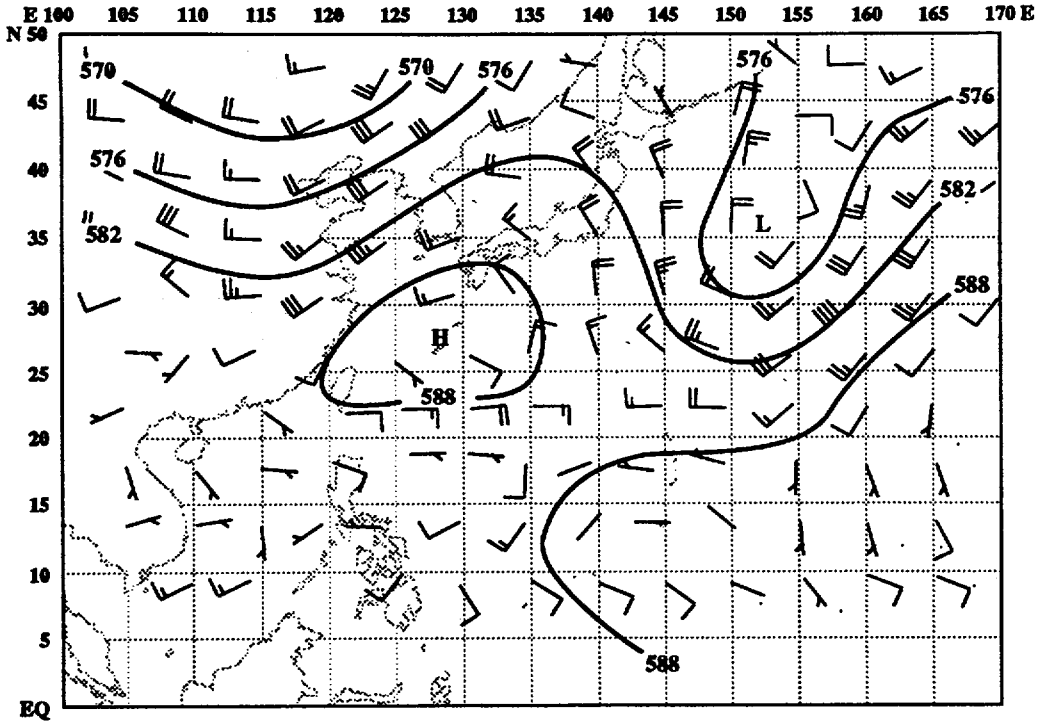

Figure 3-08-3. NOGAPS 500-mb 72-hr prognosis in decameters valid at 100000Z July.

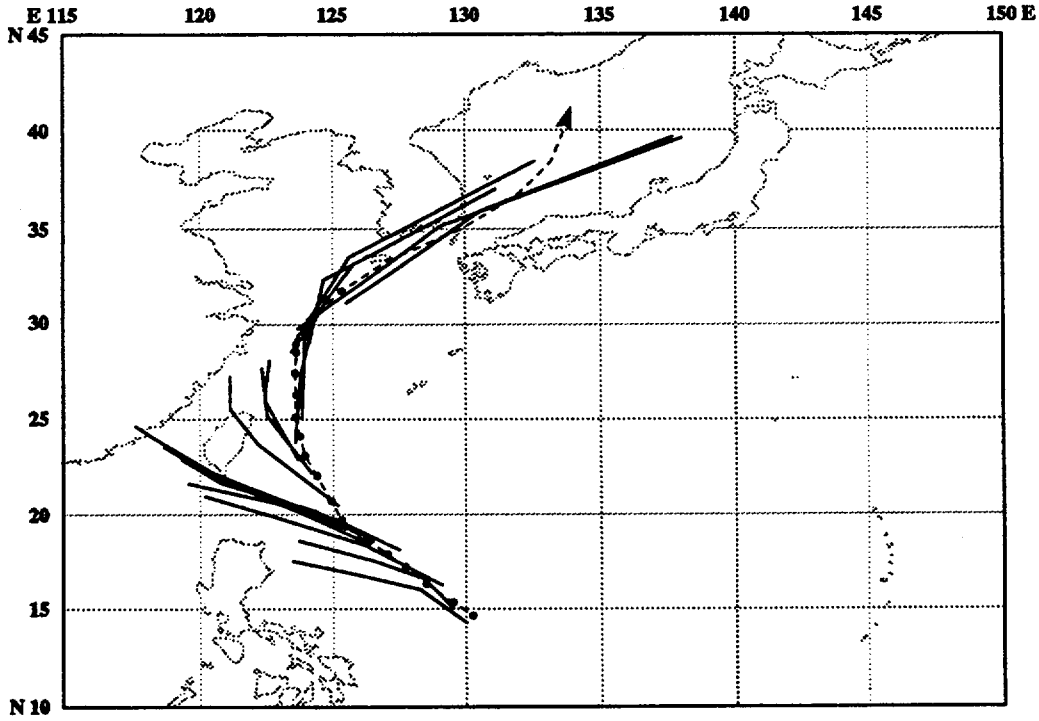

Figure 3-08-4. Summary of JTWC forecasts (solid lines) for Robyn superimposed on the best track (dashed line).

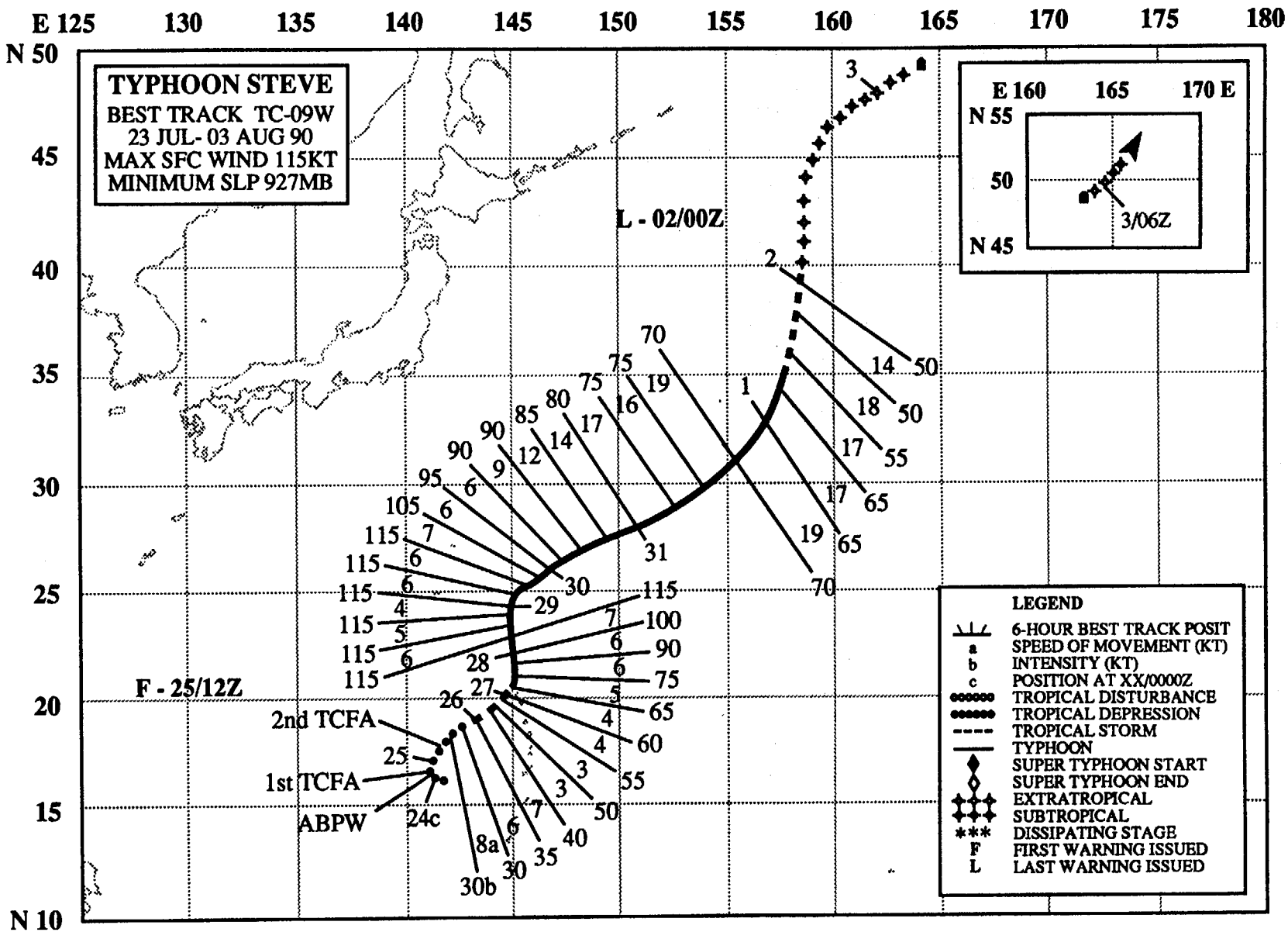
TYPHOON STEVE
BEST TRACK TC-09W
23 JUL- 03 AUG 90
MAX SFC WIND 115KT
MINIMUM SLP 927MB
E 125
130
135
140
145
150
155
160
165
170
175
180
N 50
45
40
35
30
25
20
15
N 10
L - 02/00Z
F - 25/12Z
2nd TCFA
1st TCFA
ABPW
24c
E 160
165
170 E
N 55
50
N 45
3/06Z
LEGEND
6-HOUR BEST TRACK POSIT
SPEED OF MOVEMENT (KT)
INTENSITY (KT)
POSITION AT XX/0000Z
TROPICAL DISTURBANCE
TROPICAL DEPRESSION
TROPICAL STORM
TYPHOON
SUPER TYPHOON START
SUPER TYPHOON END
EXTRATROPICAL
SUBTROPICAL
DISSIPATING STAGE
FIRST WARNING ISSUED
LAST WARNING ISSUED

TYPHOON STEVE (09W)

I. HIGHLIGHTS

Steve, with Tropical Storm Tasha (10W) and Typhoon Vernon (11W), made up the only three storm tropical cyclone outbreak to occur in the northwest Pacific this year. Steve persisted on an atypical northeastward track throughout its existence. The orientations of the monsoon trough and the subtropical ridge influenced the track of this system.

II. CHRONOLOGY OF EVENTS

240600Z - First mentioned on Significant Tropical Weather Advisory as an area of persistent convection with an estimated minimum sea-level pressure of 1004 mb.
240800Z - First Tropical Cyclone Formation Alert based on continued development of the convection.
250800Z - Tropical Cyclone Formation Alert reissued due to slow development.
251200Z - First warning based on development of persistent central convection.
260000Z - Upgraded to tropical storm after restriction to outflow eased.
270600Z - Upgraded to typhoon based on eye formation.
281800Z - Peak intensity - 115 kt (59 m/sec) - restricted outflow to the west, preventing further intensification.
011200Z - Downgraded to tropical storm because of decreased convection and increased vertical wind shear.
020000Z - Final warning - (extratropical) - based on the loss of central convection.

III. TRACK AND MOTION

On 19 July, several days before Steve formed, a large TUTT low appeared near the dateline and was reflected in the deep-layer mean analysis (Figure 3-09-1) as an inverted trough. By 23 July, the TUTT low became associated with the eastern extension of the Asian monsoon trough in the deep layer mean analysis (Figure 3-09-2). This synoptic-scale trough segmented the subtropical ridge into an

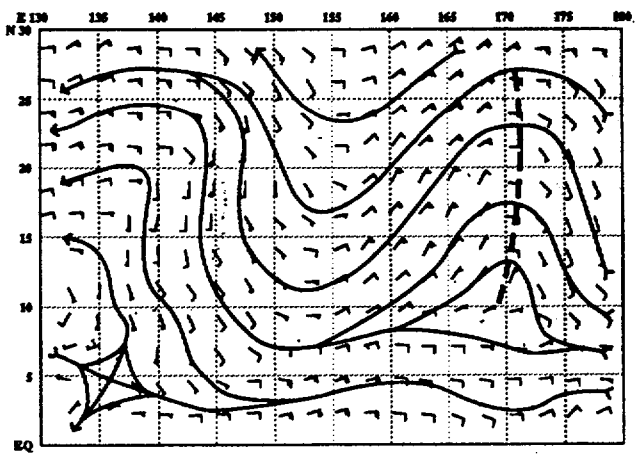

Figure 3-09-1. Deep-layer mean analysis at 190000Z July, showing the reflection of the TUTT low as an inverted trough oriented north-south along 170° East longitude.

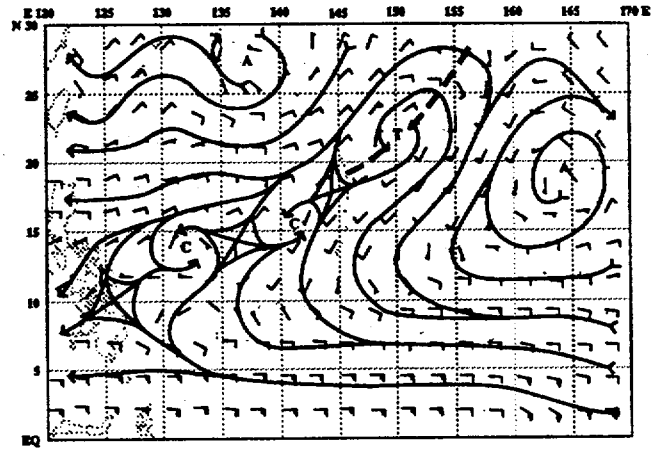

Figure 3-09-2. Deep layer mean analysis at 231200Z July indicates that the TUTT low at point T has elongated northeast-southwest and appears as an eastward extension of the Asian monsoon.

Asian cell, extending eastward from Asia, and a maritime cell, southeast of and parallel to the trough axis. Once Steve formed in the low-level monsoon trough, its basic track was to the northeast, roughly parallel to the axis of the monsoon trough. Short term speed and direction changes appeared to be related to the interaction between Steve, a midget typhoon, and the larger cyclonic circulation in the trough. Note in Figure 3-09-3 that Steve was east of a large cyclonic circulation as shown on the deep layer mean analysis for 261200Z. It was also under southwesterly mid-tropospheric flow. The track change to the north at 271200Z was related to the change in steering from southwesterly to southerly on the analysis (Figure 3-09-4). After Steve reached higher latitudes and began to weaken, it became the dominant cyclonic circulation. As the system took on extratropical characteristics and increased in size, it filled and accelerated northeastward.

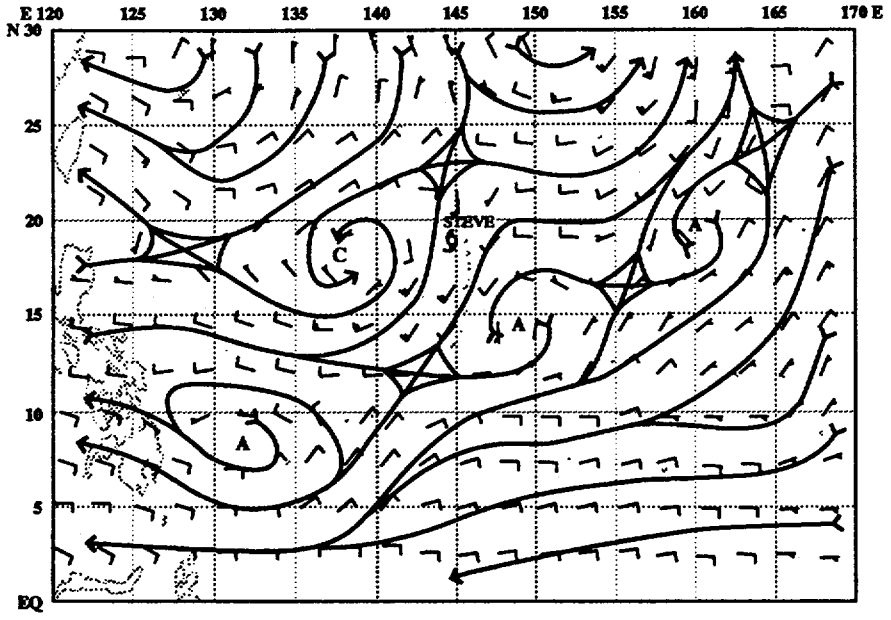

Figure 3-09-3. Deep layer mean analysis at 261200Z July depicts Steve east of a larger cyclonic circulation in the monsoon trough, embedded in southwesterly flow.

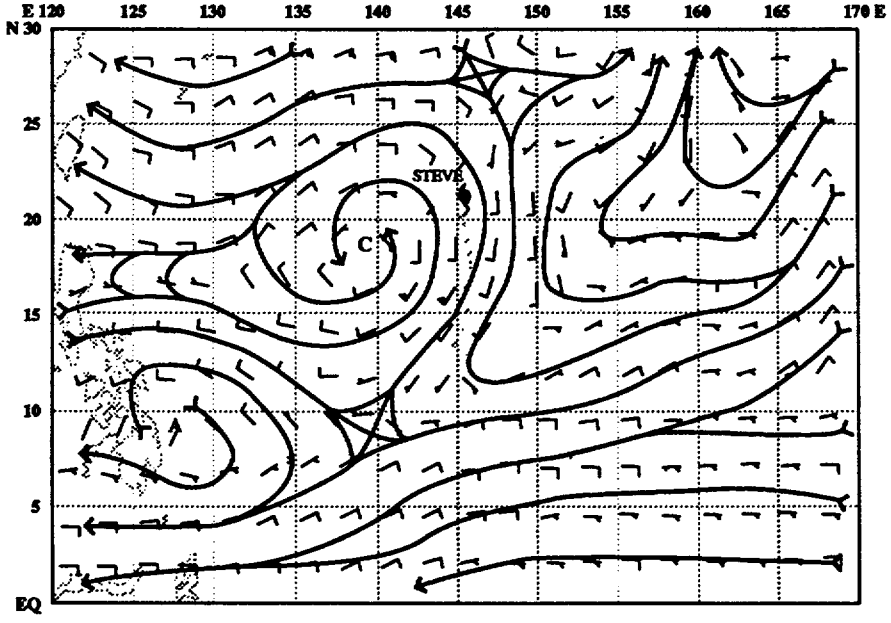

Figure 3-09-4. Deep layer mean analysis at 271200Z July shows Steve embedded in southerly flow.

IV. INTENSITY

The area of convection that eventually became Typhoon Steve formed in the monsoon trough and moved under strong upper-level divergence. Once the convection consolidated, the system (Figure 3-09-5) developed rapidly but remained relatively small -- its deep convection was confined to within 90 nm (165 km) of the center. With no restriction to its outflow, Steve quickly developed an eye and reached typhoon intensity. The typhoon intensified to 115 kt (59 m/sec) and remained at peak intensity

Figure 3-09-5. Steve intensifies as it tracks northward (280811Z July DMSP visual imagery).

for 24 hours until upper-level outflow from Tropical Storm Vernon (11W) to the southwest began to restrict Steve's outflow to the west (Figure 3-09-6). Steve weakened slowly as its deep convection gradually decreased. Its circulation expanded in size and retained storm-force winds as an extratropical system.

V. FORECAST PERFORMANCE

Steve's atypical track produced a difficult forecasting situation. The synoptic features that influenced the track, the monsoon trough and subtropical ridge, were themselves difficult to forecast. To further complicate matters, Steve was one of three tropical cyclones active in the Northwest Pacific at the same time. JTWC's track forecasts were based on Steve's location relative to the subtropical ridge to the northwest. Steve's northeastward movement put the JTWC forecasts significantly left of the actual track (Figure 3-09-7). Dynamical, statistical and climatological objective aids all predicted initial northwestward motion for Steve. The 72-hour forecast errors for Steve averaged 556 nm (1030 km).

VI. IMPACT

No information was received.

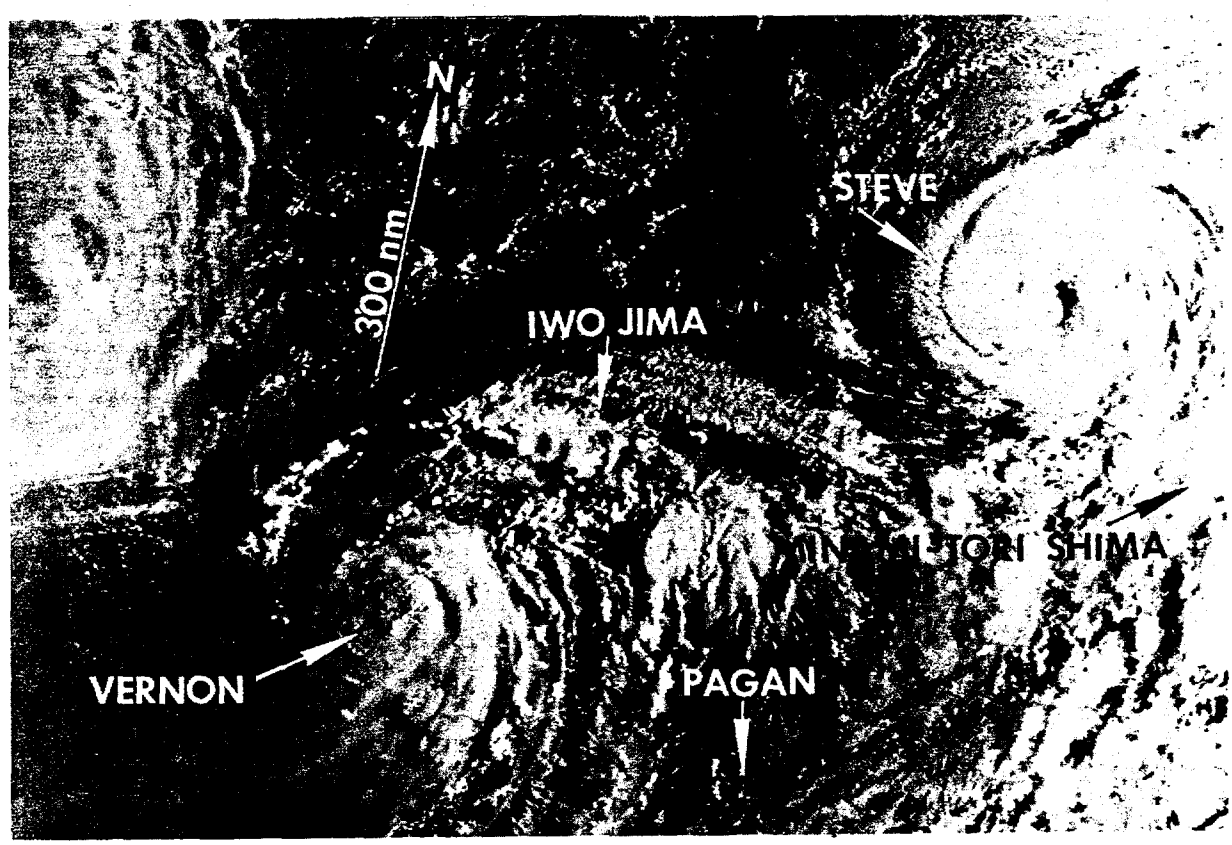

Figure 3-09-6. As Steve weakens, Tropical Storm Vernon (11W) intensifies to the southwest (302028Z July DMSP visual imagery).

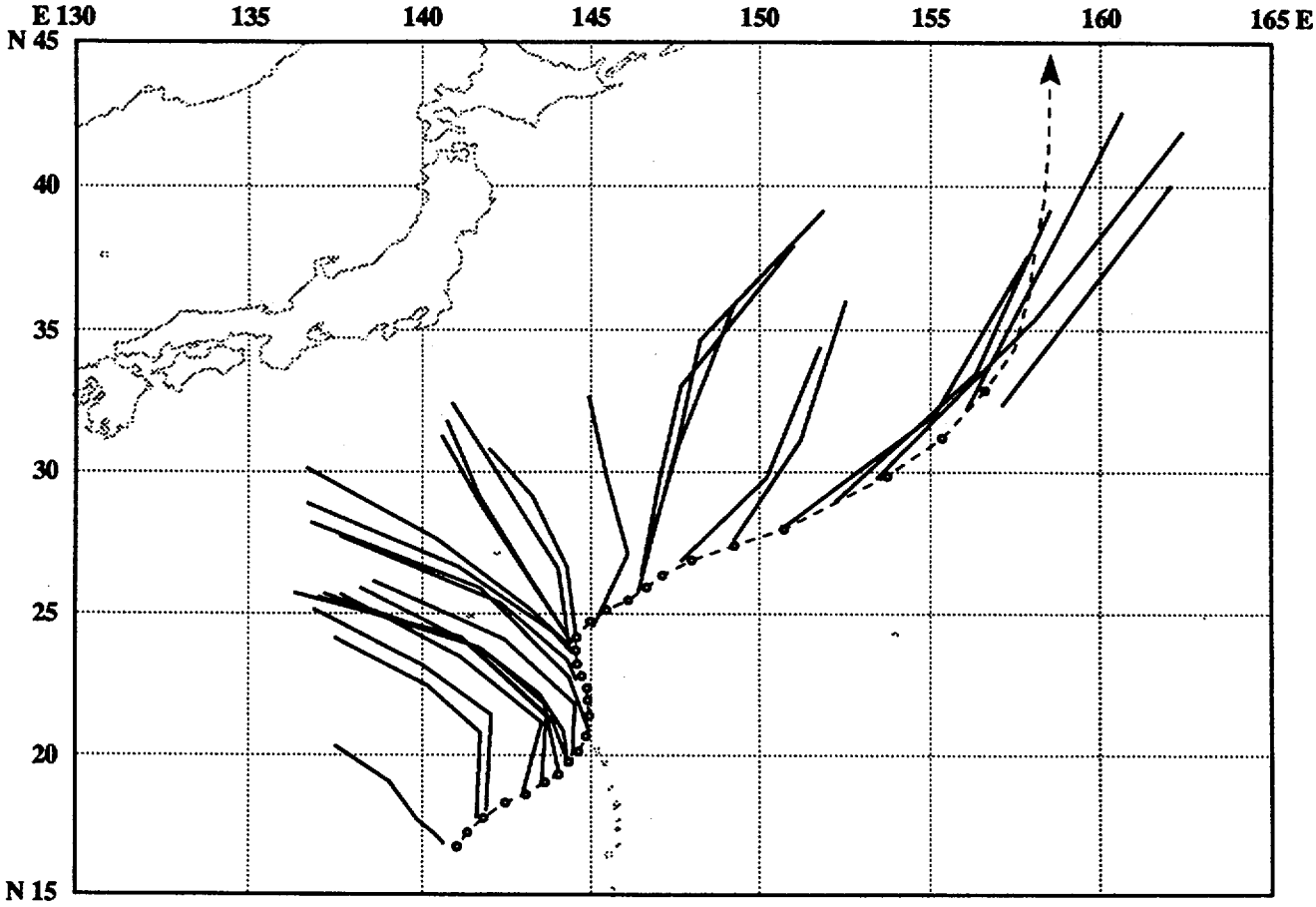

Figure 3-09-7. Summary of JTWC forecasts (solid lines) for Steve is superimposed on the best track (dashed line).

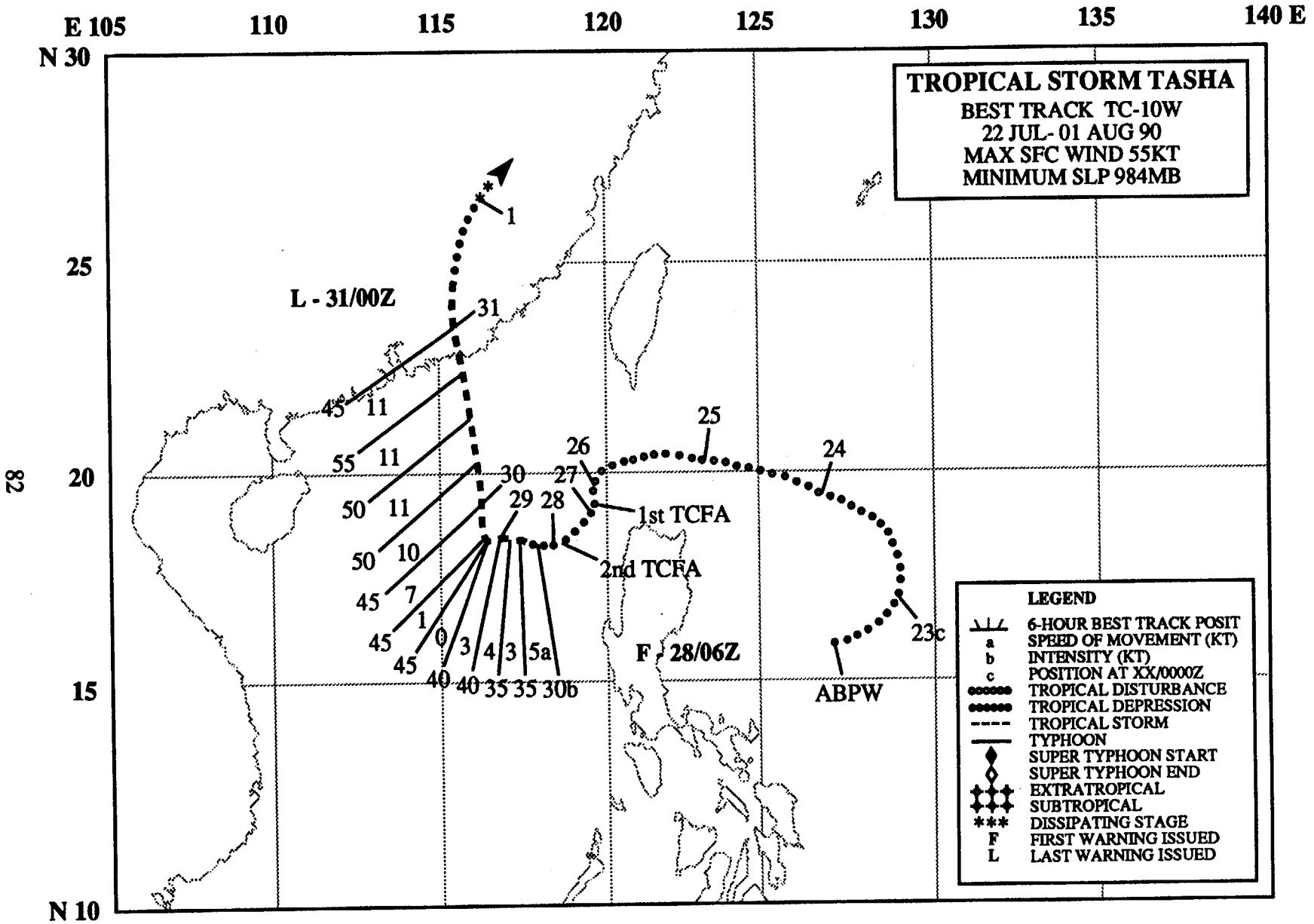
E 105
110
115
120
125
130
135
140 E
N 30
25
20
15
N 10
82
TROPICAL STORM TASHA
BEST TRACK TC-10W
22 JUL- 01 AUG 90
MAX SFC WIND 55KT
MINIMUM SLP 984MB
L - 31/00Z
F - 28/06Z
1st TCFA
2nd TCFA
ABPW
LEGEND
6-HOUR BEST TRACK POSIT
SPEED OF MOVEMENT (KT)
INTENSITY (KT)
POSITION AT XX/0000Z
TROPICAL DISTURBANCE
TROPICAL DEPRESSION
TROPICAL STORM
TYPHOON
SUPER TYPHOON START
SUPER TYPHOON END
EXTRATROPICAL
SUBTROPICAL
DISSIPATING STAGE
FIRST WARNING ISSUED
LAST WARNING ISSUED

TROPICAL STORM TASHA (10W)

I. HIGHLIGHTS

Tasha, the third of four western Pacific tropical cyclones to occur in July, developed in the monsoon trough. Instead of following Steve (09W) and Vernon (11W) to the northeast, it made only a brief start in that direction before curving to the west and entering the South China Sea. After erratic motion and slow intensification, Tasha finally reached tropical storm intensity before slamming into the southern coast of China.

II. CHRONOLOGY OF EVENTS

220600Z - First mentioned on Significant Tropical Weather Advisory as an area of persistent convection with an estimated minimum sea-level pressure of 1006 mb.

262000Z - Tropical Cyclone Formation Alert issued based on indications in the synoptic data of increased organization of the low-level circulation and upper-level outflow.

272000Z - Tropical Cyclone Formation Alert reissued based on increased central convection and falling surface pressures.

280600Z - First warning issued due to preliminary appearance of a central dense overcast.

281200Z - Upgraded to tropical storm based on a ship report of 35 kt (20 m/sec) and a minimum sea-level pressure of 995 mb.

301800Z - Peak intensity of 55 kt (28 m/sec) coincident with increased size of the central dense overcast and an intensity estimate of CI 3.5.

310000Z - Final warning - dissipating over land - followed landfall 75 nm (140 km) east of Hong Kong.

III. TRACK AND MOTION

Tasha, developed in the monsoon trough over the warm 84°F (29°C) waters of the Philippine Sea. The low-level cyclonic circulation initially tracked northeastward in response to shallow southwesterly wind flow that extended up to 700 mb (Figure 3-10-1). As the pre-Tasha disturbance

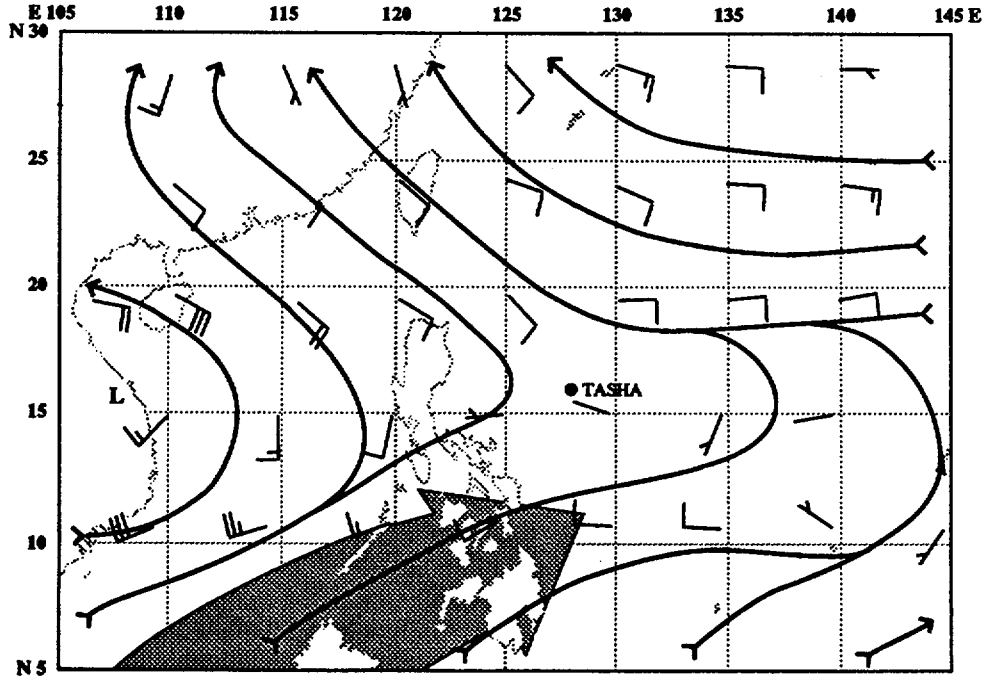

Figure 3-10-1. 700-mb NOGAPS streamline analysis at 221200Z July, showing the southwesterly steering flow over the southern Philippine Sea.

continued to develop, it turned westward in response to easterly flow associated with the an extension of the subtropical ridge centered over the East China Sea (Figure 3-10-2). For the next several days, the disturbance drifted slowly westward and passed through the Luzon Strait. At this point, Tasha moved slowly southward and westward, interacting with a larger, synoptic-scale cyclonic circulation to the southwest in the monsoon trough (Figure 3-10-3). By 29 July, Tasha had intensified and become the dominant vortex in the South China Sea. After a 12-hour period of quasi-stationary motion, Tasha then commenced a northward track at 291800Z in response to a moderately strong (up to 35 kt (18 m/sec) surface winds) and deep (1000 to 700 mb) surge in the monsoonal flow to the south (Figure 3-10-4) which was accompanied by a northward shift of the synoptic-scale monsoon trough axis (Figure 3-10-5). Tasha ultimately made landfall just east of Hong Kong.

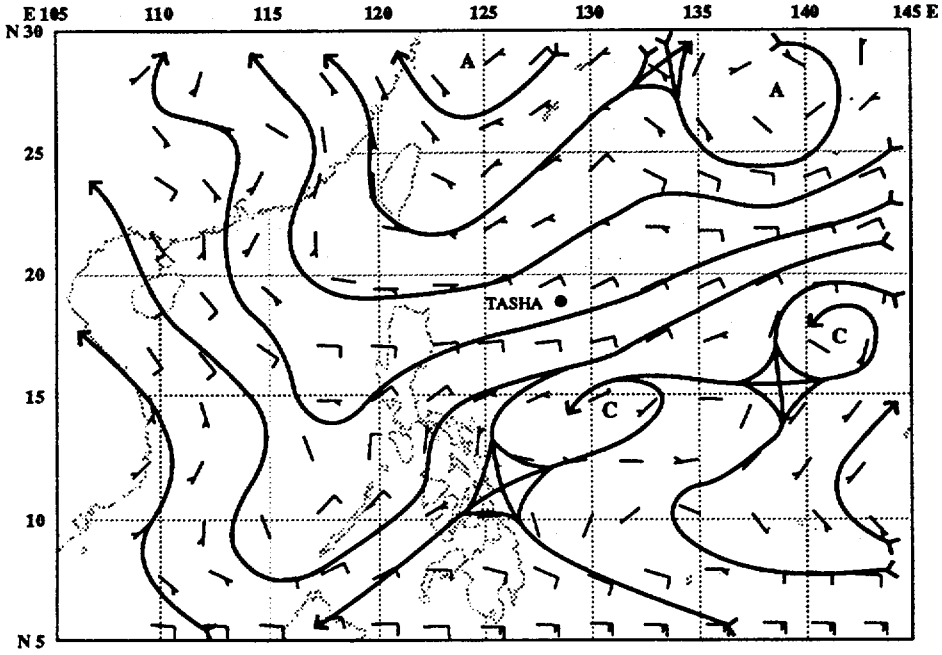

Figure 3-10-2. Deep layer mean analysis at 231200Z July, showing the mean position of the subtropical ridge over the East China Sea and weak easterly steering flow over Tasha.

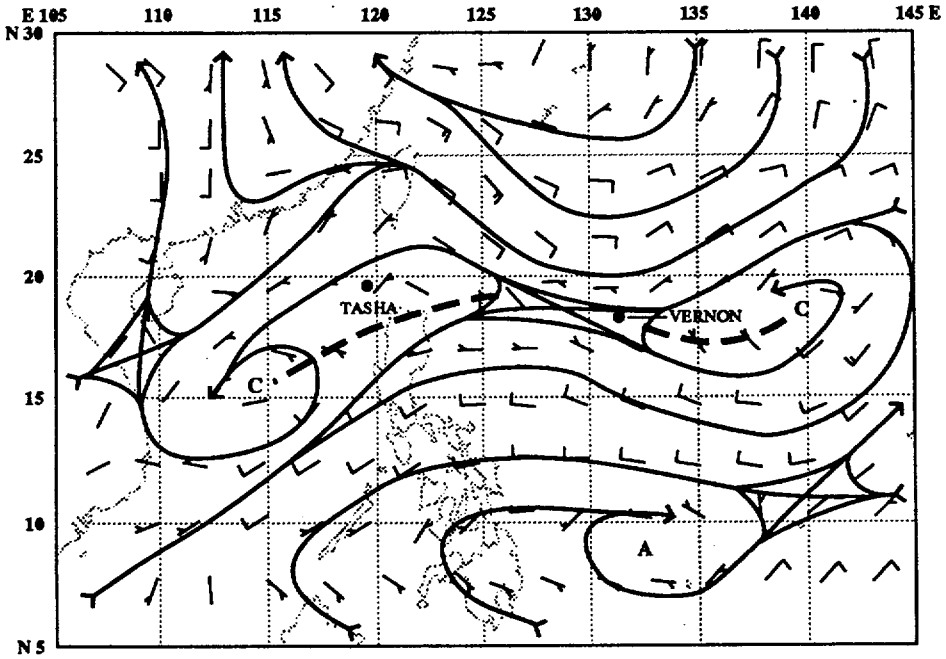

Figure 3-10-3. Deep layer mean analysis at 261200Z July with Tasha beginning to interact with the large cyclonic circulation to the southwest.

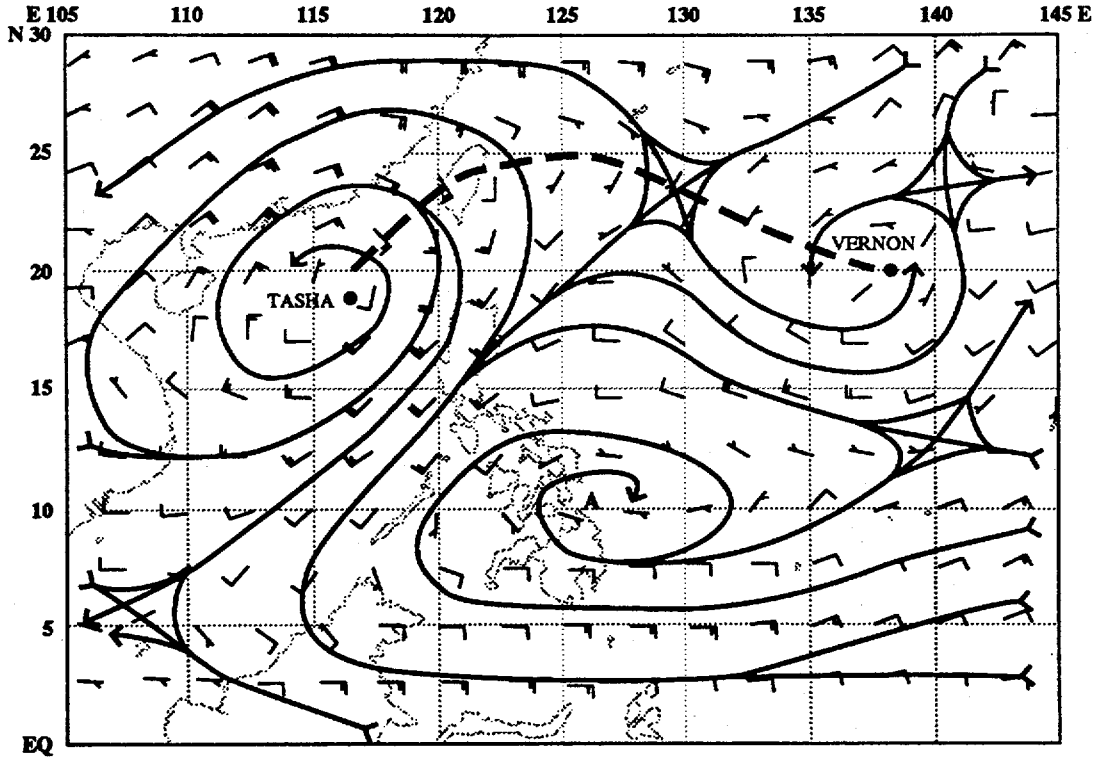

Figure 3-10-4. Deep layer mean analysis at 301200Z July depicting the moderate monsoon surge to the south of Tasha (compare with Figure 3-10-3).

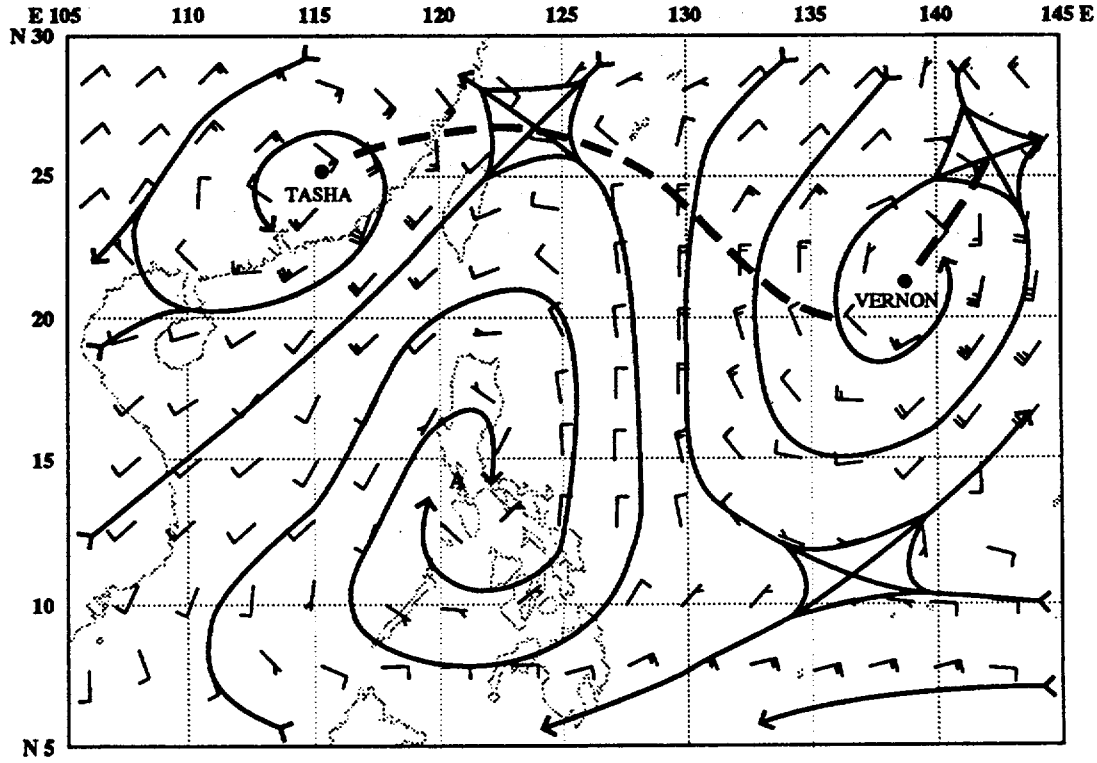

Figure 3-10-5. Deep layer mean analysis at 311200Z July, when compared with Figure 3-10-3, reveals that the axis of the monsoon trough with Tasha embedded has shifted northward over China.

IV. INTENSITY

For several days before significant development occurred, the persistent, but poorly organized, convection remained embedded in the monsoon trough, undergoing large diurnal fluctuations. During this time, the upper-level winds over the system were in excess of 30 kt (15 m/sec). However, after passing through the Luzon Strait, the tropical disturbance moved into a more favorable environment with less vertical shear near the eastern end of the tropical easterly jet. The cyclone reached peak intensity on 30 July, just prior to landfall (Figure 3-10-6). Once inland, the system dissipated due to the influence of rugged terrain in southeastern China and the loss of its oceanic source of heat and moisture.

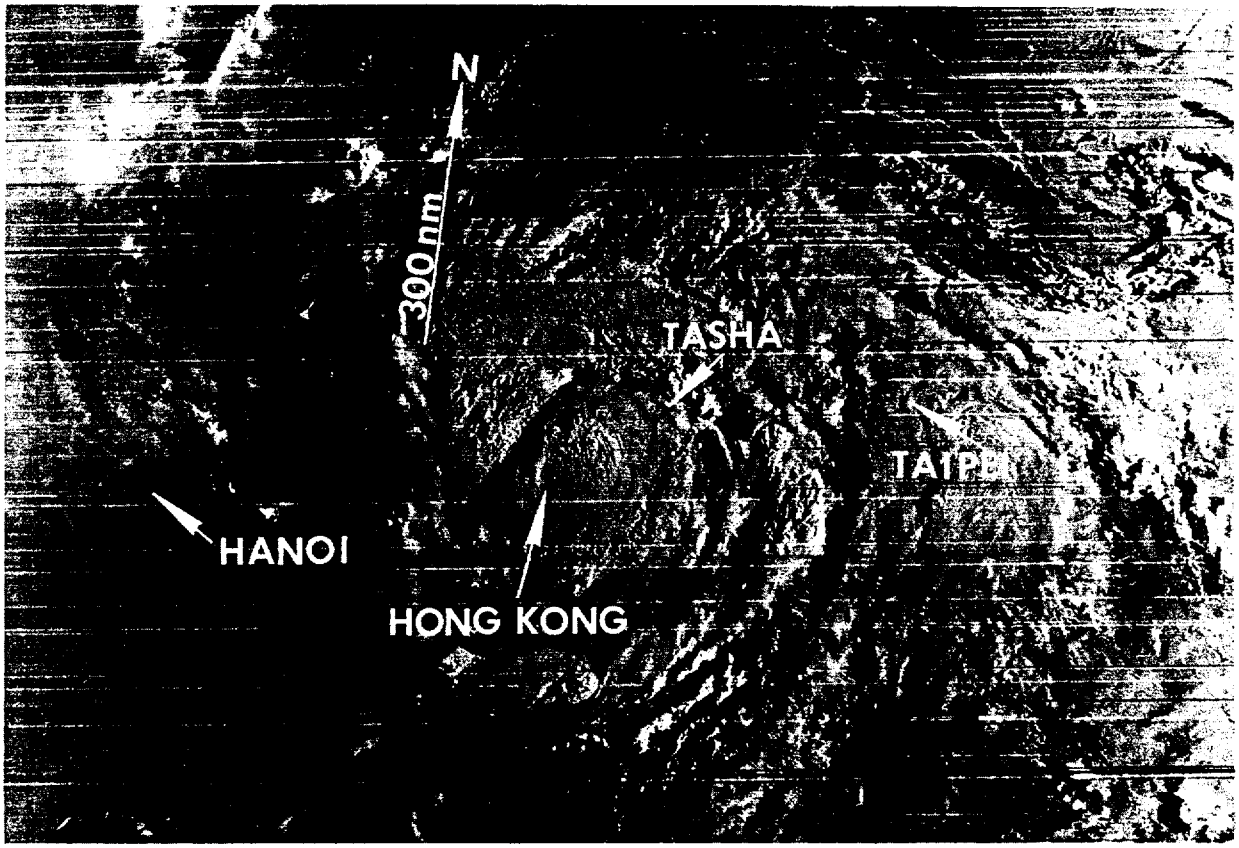

Figure 3-10-6. Tropical Storm Tasha at peak intensity moves into southern China (302210Z July DMSP visual imagery).

V. FORECASTING PERFORMANCE

Tasha's eventual northward track was not forecast initially (Figure 3-10-7). The NOGAPS prognoses maintained a weak subtropical ridge over southern China, which was expected to steer the system west-northwestward between Hainan Dao and Hong Kong. However, due to the weak steering flow depicted by the models, an alternate scenario for erratic motion was developed. On 29 July, after satellite imagery indicated that the previously mentioned monsoonal surge was beginning, the track was modified to initial northeastward movement followed by a turn to the north. If the surge turned out to be weaker than anticipated, an alternate scenario of steady northward movement was included. The alternate scenario turned out to be correct. Throughout Tasha's life, the guidance provided by the numerical forecast aids was practically useless. The major northward shift of the axis of the monsoon trough was not depicted well in the NOGAPS prognoses, and the complex and rapidly changing synoptic environment was not amenable to subjective analysis by the forecaster.

VI. IMPACT

Tasha landed 75 nm (140 km) east of Hong Kong at 312100Z and caused widespread damage due to torrential rains and flooding in Fujian and Guangdong provinces. In Fujian Province in southeastern China, 69 people were killed and 10,000 houses destroyed. Irrigation facilities were damaged, and approximately 5 million acres of farmland were flooded, with rainfall amounts reported in excess of 12 inches (305 mm). In Guangdong Province in southern China, 39 people died, 335 were injured and 25,200 houses were destroyed. Rainfall in some areas exceeded 14 inches (355 mm) with 5.3 million acres of farmland flooded. In contrast, damage in Hong Kong was relatively minor. Ferries to outlying islands, Macau and many parts of Guangdong were suspended or canceled. Seven emergency shelters were opened and many social activities were disrupted, but no serious flooding or landslides occurred.

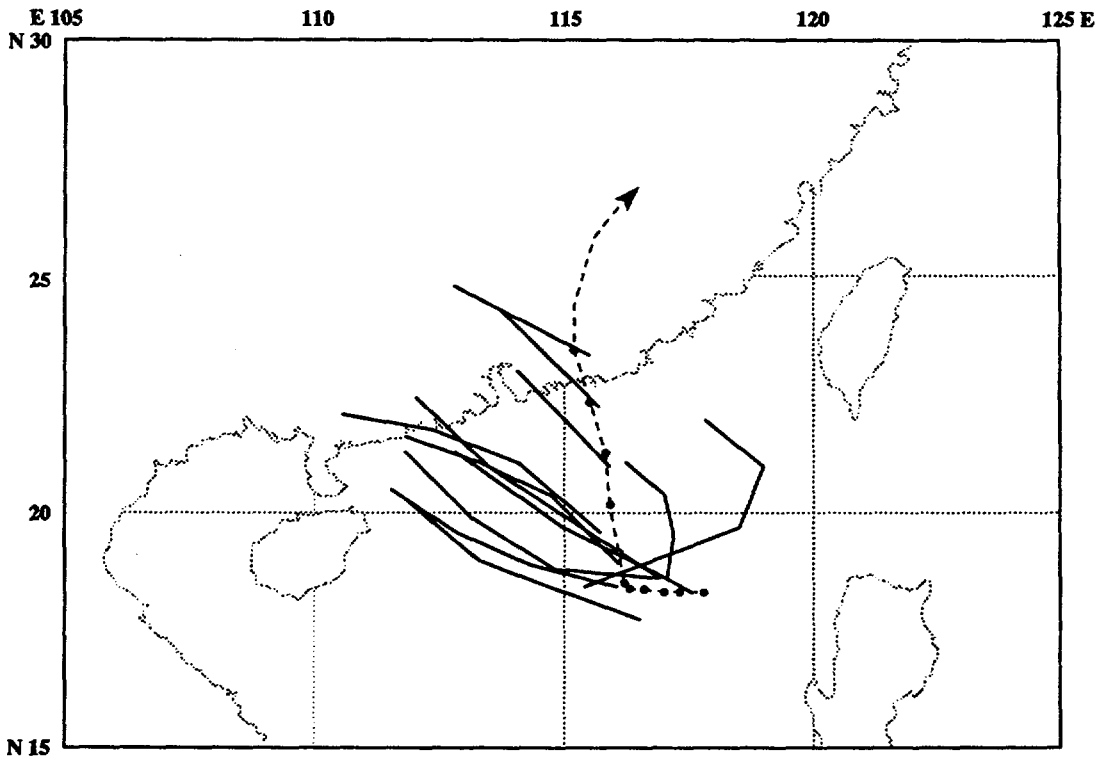

Figure 3-10-7. Summary of JTWC forecasts (solid lines) for Tasha is superimposed on the final best track (dashed line).

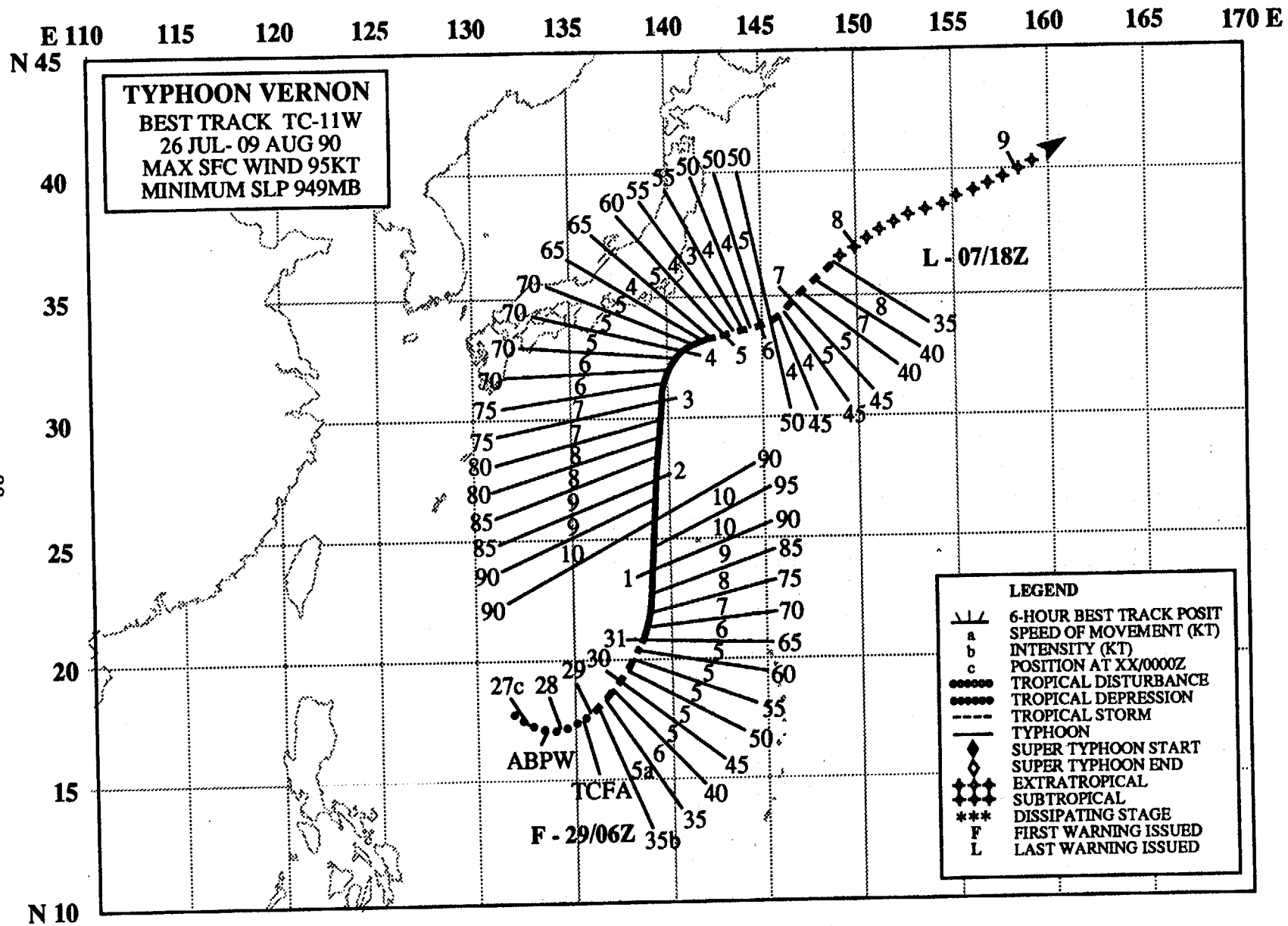
TYPHOON VERNON
BEST TRACK TC-11W
26 JUL- 09 AUG 90
MAX SFC WIND 95KT
MINIMUM SLP 949MB
E 110
115
120
125
130
135
140
145
150
155
160
165
170 E
N 45
40
35
30
25
20
15
N 10
L - 07/18Z
F - 29/06Z
ABPW
TCFA
LEGEND
6-HOUR BEST TRACK POSIT
SPEED OF MOVEMENT (KT)
INTENSITY (KT)
POSITION AT XX/0000Z
TROPICAL DISTURBANCE
TROPICAL DEPRESSION
TROPICAL STORM
TYPHOON
SUPER TYPHOON START
SUPER TYPHOON END
EXTRATROPICAL
SUBTROPICAL
DISSIPATING STAGE
FIRST WARNING ISSUED
LAST WARNING ISSUED

88

TYPHOON VERNON (11W)

I. HIGHLIGHTS

Vernon, the last of four tropical cyclones to develop during July, was the last of a series of storms that included Tropical Storm Tasha (10W) and Typhoon Steve (09W) to form the only three-storm outbreak in the western North Pacific during 1990. Vernon followed Steve's northward-oriented track, as the monsoon trough underwent a major displacement to the north.

II. CHRONOLOGY OF EVENTS

271700Z - Significant Tropical Weather Advisory reissued to include a low-level cyclonic circulation in the monsoon trough with persistent convection and an estimated minimum sea-level pressure of 1004 mb.

282200Z - Tropical Cyclone Formation Alert issued for increased outflow and improved convective curvature.

290600Z - First warning followed consolidation of convection into two interlocking cloud bands.

291200Z - Upgraded to tropical storm after appearance of a ragged central dense overcast.

310000Z - Upgraded to typhoon based on eye development.

010600Z - Peak intensity - 95 kt (48 m/sec) - based on intensity estimate of CI 5.5 at 010300Z.

050000Z - Downgraded to tropical storm intensity due to the loss of central convection.

071800Z - Final warning - extratropical - issued as Vernon continued to lose its supporting convection.

III. TRACK AND MOTION

During the last week of July, the western portion of the active monsoon trough was anchored in Asia by Tasha (10W). The trough extended eastward across the Philippine Sea through Steve (09W) and north-northeastward to a mid-level cyclonic circulation east of Honshu (Figure 3-11-1). Vernon developed in the monsoon trough between these two tropical cyclones and moved slowly eastward along the trough axis on the edge of the deep southwesterly flow. The eastward track along the trough axis became more northward as the entire monsoon trough shifted northward throughout the week. As Vernon approached Japan, the Asian High persisted across Honshu, and Vernon was forced to slow and

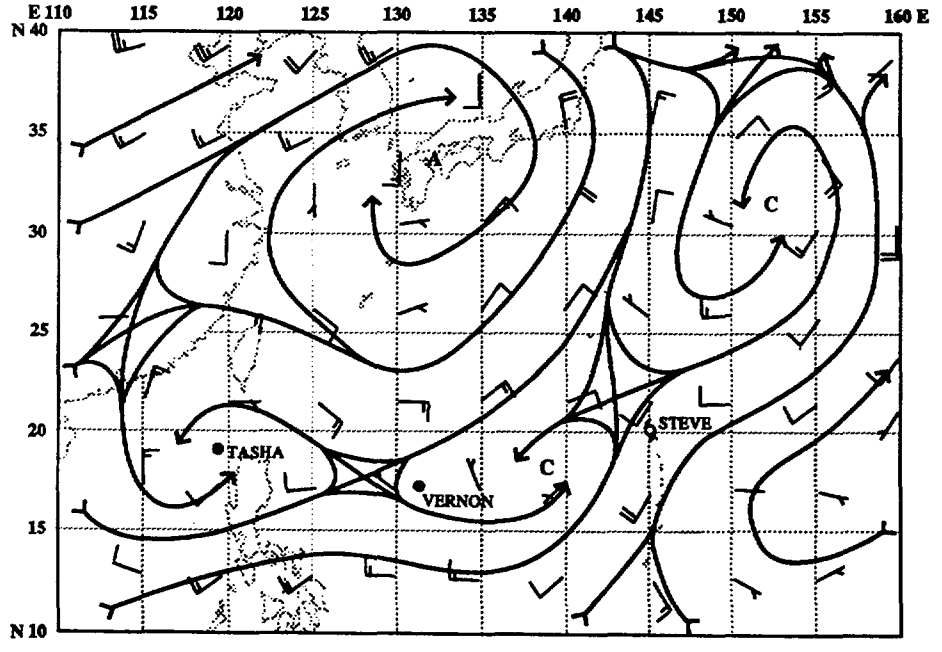

Figure 3-11-1. The 270000Z July NOGAPS 500-mb analysis shows the monsoon trough, extending eastward from Tasha (10W) through Steve (09W) to a low east of Honshu. Equatorward of the trough axis the deep southwesterly flow extends up through the middle troposphere. 84

track around the southern portion of the High. Vernon and Steve (09W) moved in a similar manner and maintained a separation of approximately 800 nm (1480 km) until Steve accelerated northeastward.

IV. INTENSIFICATION

Typhoon Vernon (Figure 3-11-2) intensified steadily despite the proximity to both Steve (09W) and Tasha (10W). The upper-level outflow from Tropical Storm Tasha, however, disrupted Vernon's vertical alignment. Only after Tasha dissipated over China on 31 July was Vernon able to develop into a typhoon (Figure 3-11-3). Approaching Honshu on 3 August, the eye of the typhoon became elongated along an east-west axis and lost much of its definition. After turning northeastward, Vernon (Figure 3-11-4) began a slow extratropical transition.

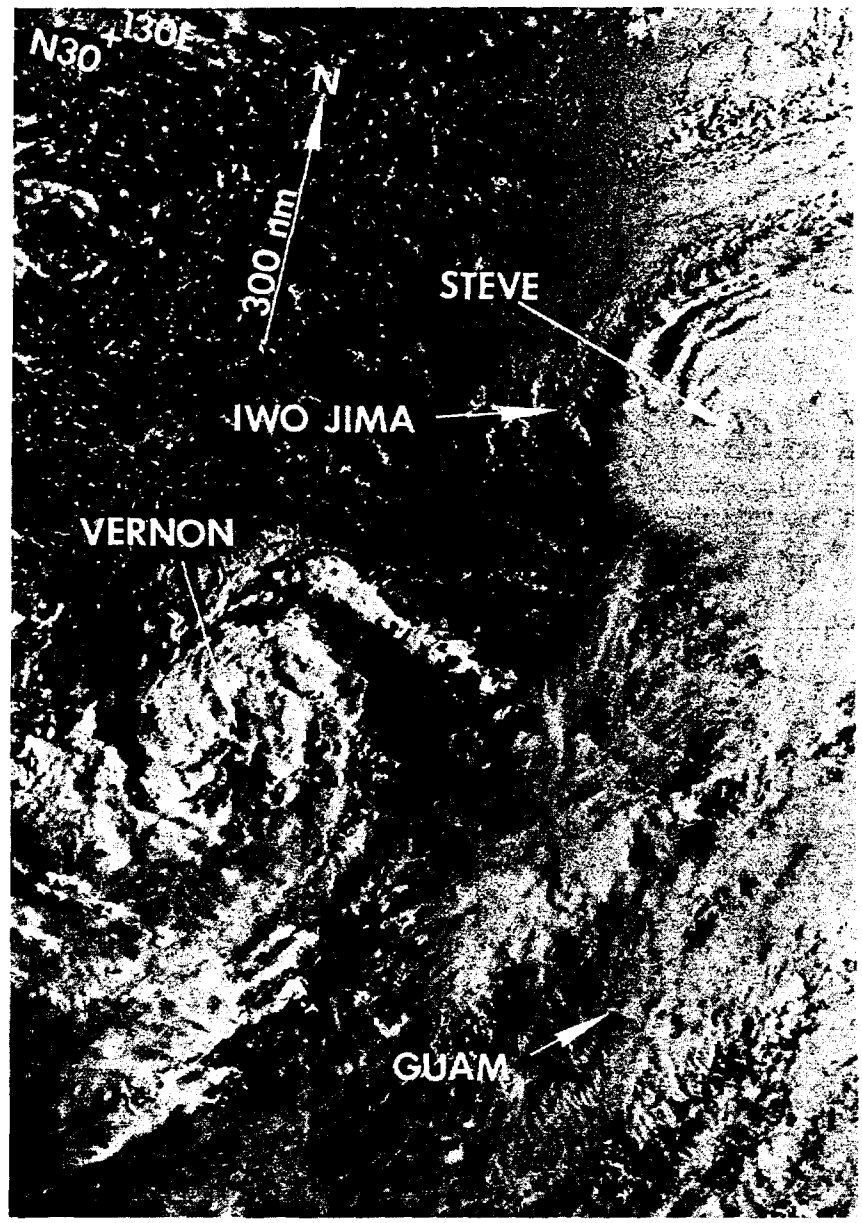

Figure 3-11-2. The tropical disturbance which became Typhoon Vernon develops approximately 700 nm (1300 km) southwest of Typhoon Steve (09W). The curved convective bands indicate the system is developing. A Tropical Cyclone Formation Alert was issued one hour after this image was received (282055Z July DMSP visual imagery).

V. FORECASTING PERFORMANCE

Due to their close proximity, forecasters initially considered the possibility of binary interaction between Vernon and Steve (09W). However, after rotation around a common midpoint was not observed, the binary interaction scenario was discarded in favor of a north-oriented forecast track similar to that taken by Steve three days earlier. The first nine forecasts (Figure 3-11-5) using this scenario were extremely accurate and had 72-hour mean forecast errors of less than 100 nm (185 km). As Vernon moved further north, forecasters experienced the same dilemma as with Steve (09W). The NOGAPS prognostic series indicated the subtropical ridge would build from the east, displacing the cyclone further west with landfall in the heavily populated areas of Japan. The forecasts were based on this guidance. As Vernon moved northward, the ridge built in from the east as forecast, but further to the south. At 040600Z August, it became evident that the mid-level ridge would hold across Honshu, and the forecast track was changed from northward to northeastward and away from Japan.

As a point of interest, the NOGAPS and JMA models had totally different prognostic solutions for the ridge motion across Japan. JMA retained the ridge and let Vernon move north-northeastward. NOGAPS linked the ridge over Japan with the maritime subtropical ridge to the east, and then moved the ridge off the island and over the Pacific. The NOGAPS guidance was used for the forecasts and the JMA guidance became the alternate scenario. In retrospect, the alternate scenario proved to be correct.

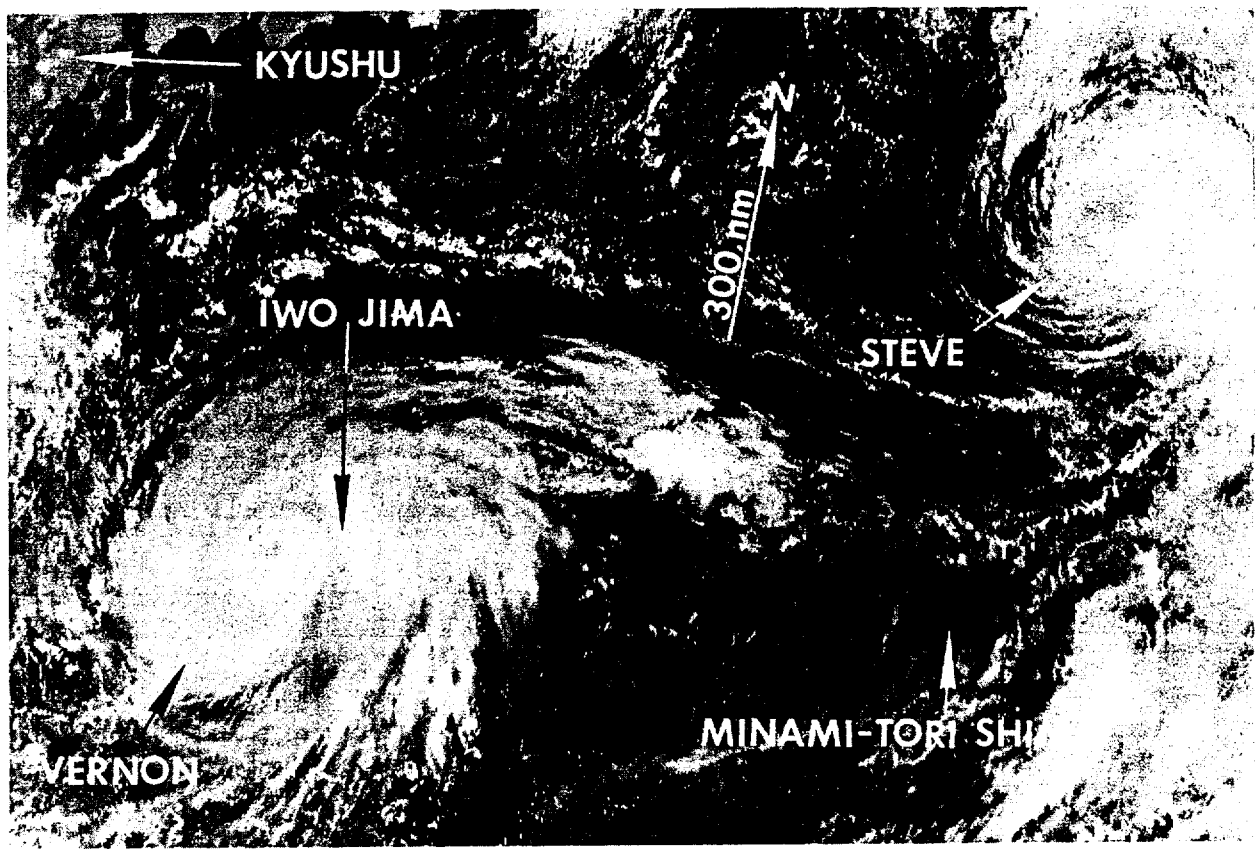

Figure 3-11-3. Typhoon Vernon near maximum intensity of 95 kt (48 m/sec). At this point, Vernon has a well-defined, but cloud-filled eye, and Typhoon Steve is weakening over water (312316Z July DMSP visual imagery).

VI. IMPACT

Although Typhoon Vernon threatened the Tokyo metropolitan area, it veered northeastward, passing within 120 nm (220 km) of the Japanese coast. There were no deaths or significant damage reports related to Vernon.

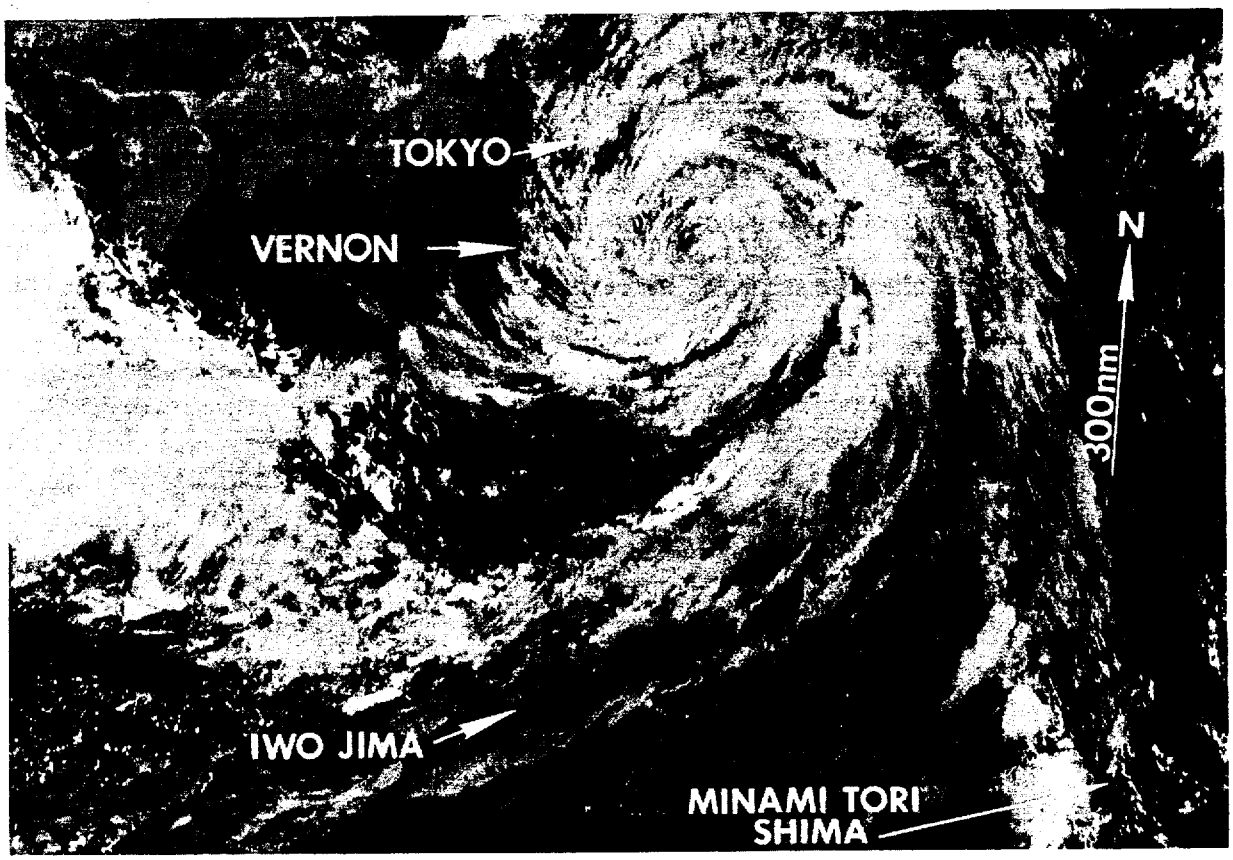

Figure 3-11-4. Vernon as it was downgraded to a tropical storm. Most of the deep central convection has diminished, leaving a well-defined low level circulation of stratocumulus and cumulus clouds (042333Z August DMSP visual imagery).

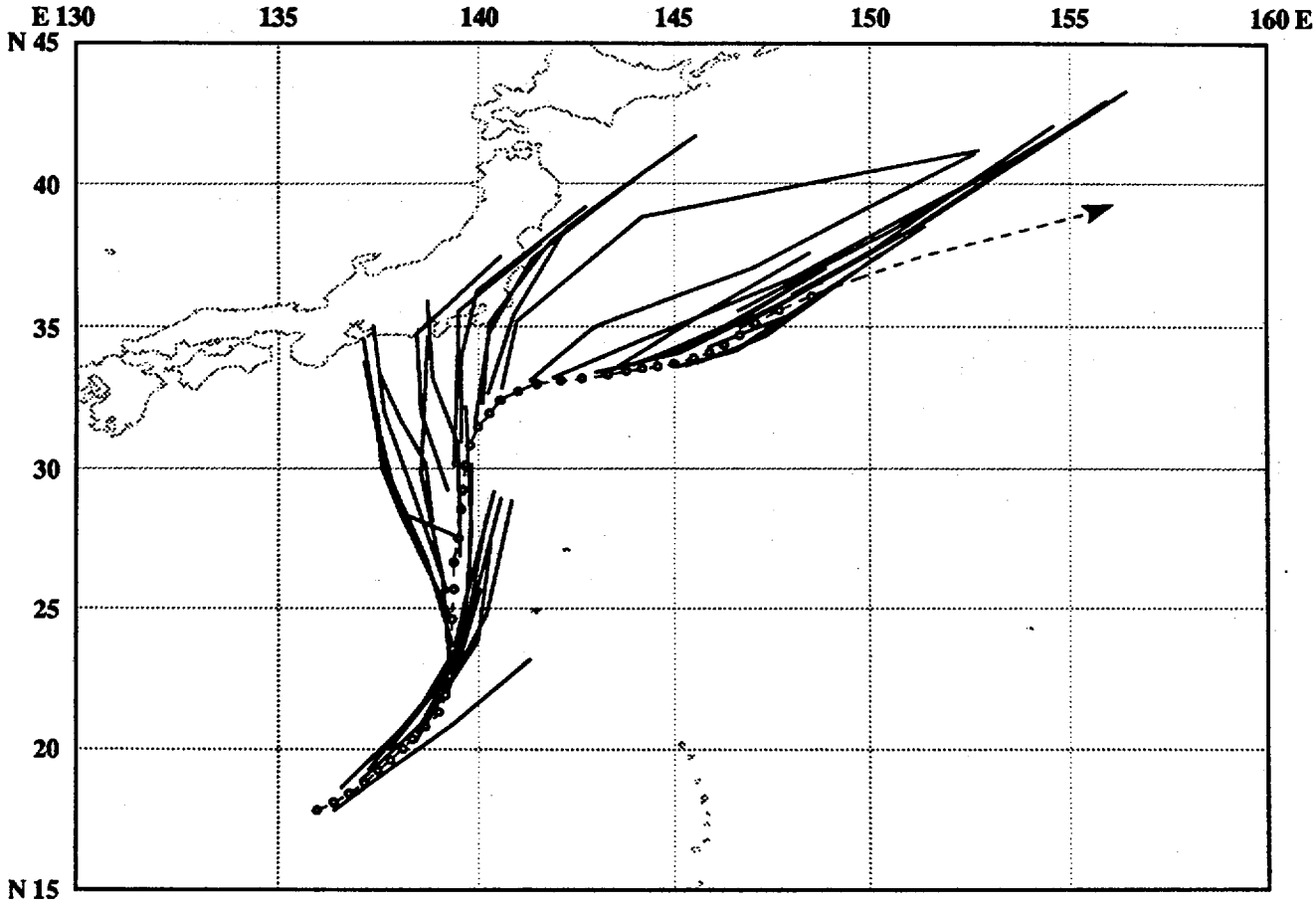

Figure 3-11-5. Summary of JTWC forecasts (solid lines) for Vernon (11W) is superimposed on the final best track (dashed lines).

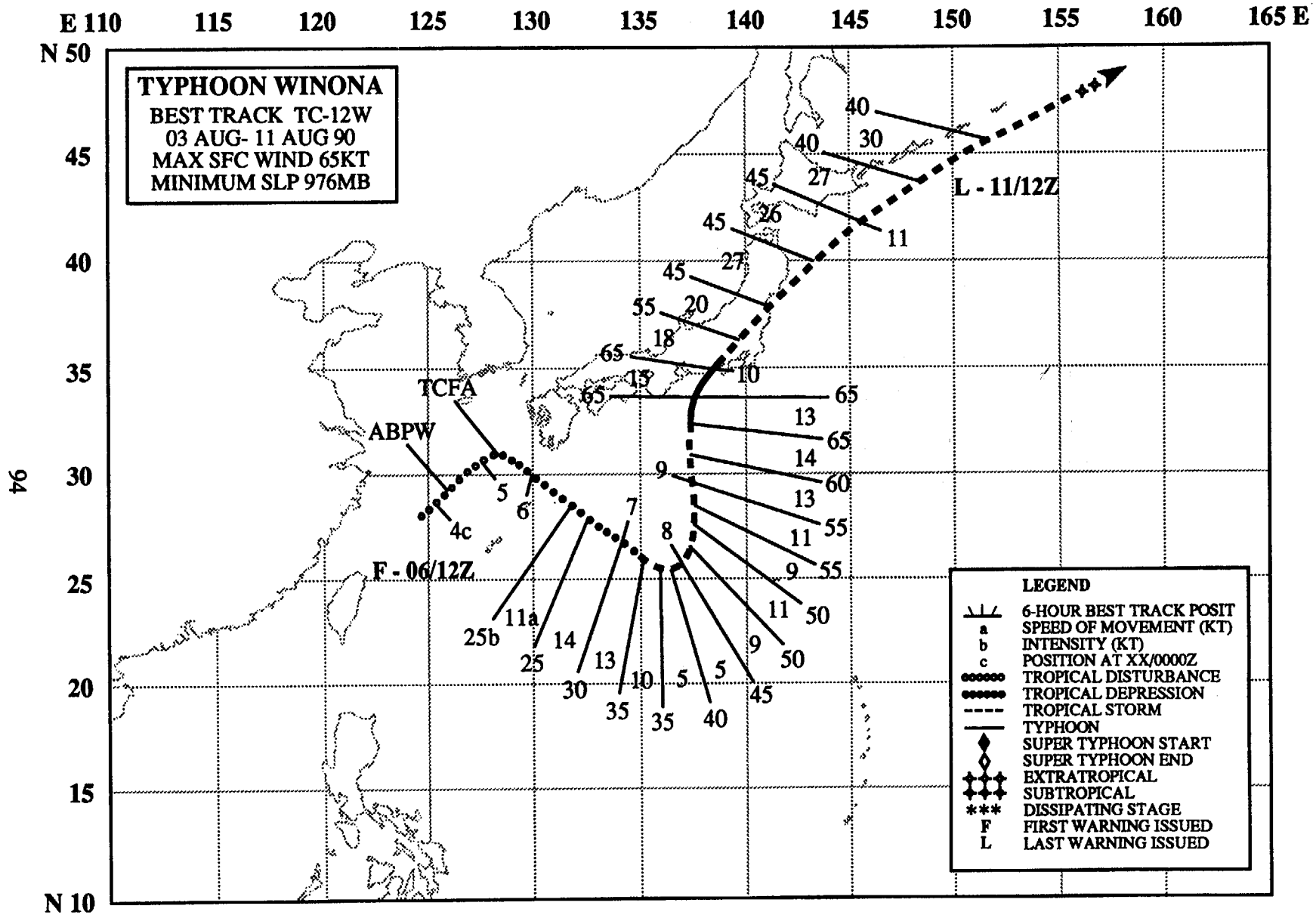
E 110
115
120
125
130
135
140
145
150
155
160
165 E
N 50
45
40
35
30
25
20
15
N 10
TYPHOON WINONA
BEST TRACK TC-12W
03 AUG- 11 AUG 90
MAX SFC WIND 65KT
MINIMUM SLP 976MB
TCFA
ABPW
F - 06/12Z
L - 11/12Z
LEGEND
6-HOUR BEST TRACK POSIT
SPEED OF MOVEMENT (KT)
INTENSITY (KT)
POSITION AT XX/0000Z
TROPICAL DISTURBANCE
TROPICAL DEPRESSION
TROPICAL STORM
TYPHOON
SUPER TYPHOON START
SUPER TYPHOON END
EXTRATROPICAL
SUBTROPICAL
DISSIPATING STAGE
FIRST WARNING ISSUED
LAST WARNING ISSUED

TYPHOON WINONA (12W)

I. HIGHLIGHTS

Winona was the first typhoon of 1990 to hit Japan and the only tropical cyclone to form poleward of 25 degrees north latitude. It formed from the remnants of Tropical Storm Tasha (10W) in a monsoon trough displaced northward of its normal location. Winona tracked across the southern portion of the Kanto Plain, was caught in the westerlies, and completed extratropical transition as it swept just south of the Kurils.

II. CHRONOLOGY OF EVENTS

040600Z - First mentioned on the Significant Tropical Weather Advisory as remnants of Tropical Storm Tasha moving off China and reforming as a weak circulation in the East China Sea.

051100Z - Tropical Cyclone Formation Alert issued based on improved convective organization and Dvorak analysis of CI 1.0.

061200Z - First warning issued as a tropical depression. Although both convection and organization had improved, vertical shear from the northwest inhibited further development.

070600Z - Upgraded to tropical storm as vertical shear decreased and circulation center and convection became better aligned.

091200Z - Upgrade to typhoon and peak intensity - 65 kt (33 m/sec)- based on a ragged eye and first intensity estimate of CI 4.0.

100000Z - Landfall on Japan 20 nm (35 km) east of Hamamatsu, a city 110 nm (205 km) southwest of Tokyo. Downgraded to tropical storm.

111200Z - Final warning - extratropical - issued as Winona became embedded in mid-latitude westerlies.

III. TRACK AND MOTION

Winona was unique in regard to both its genesis and its movement. The system formed in the monsoon trough, which was displaced 300 nm (555 km) north of its normal location. The initial southeastward movement almost directly opposed the expected climatological track. Winona typified the complex interaction that can occur among tropical cyclones, the deep monsoon southwesterlies, and the subtropical ridge. Winona later moved north, then northeast, in response to a well-developed mid-latitude trough.

Enhanced convection became prevalent in the East China Sea as the low pressure area associated with the remnants of Tropical Storm Tasha (10W) moved out to sea by 040000Z August. This area of enhanced convection developed into Winona. The system tracked northeastward initially, then southeastward along the edge of the deep monsoon westerlies. The 500-mb analysis at 070000Z (Figure 3-12-1) shows Winona embedded in a complex flow pattern with Tropical Storm Vernon (11W) to the northeast. The subtropical ridge had split, with one cell centered in the Luzon Strait, and the other south of Vernon. Winona tracked toward the neutral point between the two cells.

By 080000Z, Vernon (11W) had tracked northeastward and become extratropical. At the same time, Winona slowed to 4 kt (7 km/hr) and turned sharply northward as the ridge to the southeast built poleward. As Vernon (11W) completed its extratropical transition at 090000Z near the Kamchatka Peninsula, the ridge strengthened north and northeast of Winona in response to the extratropical cyclone's rapid deepening. In response, Winona maintained a northward track until it made landfall near Hamamatsu, Japan. After landfall, it began to accelerate northeastward, and by 101200Z, Winona was embedded in the mid-latitude westerlies, beginning its extratropical transition. Winona finished its extratropical transition by 111200Z as it skirted south of the Kuril Islands.

IV. INTENSITY

Winona developed as the remnants of Tasha (10W) moved off the coast of China into the East China Sea. The disturbance generated persistent convection, but it was subject to strong upper-level northerly flow (Figure 3-12-2). The strong vertical wind shear left Winona's circulation center exposed north of the deep convection.

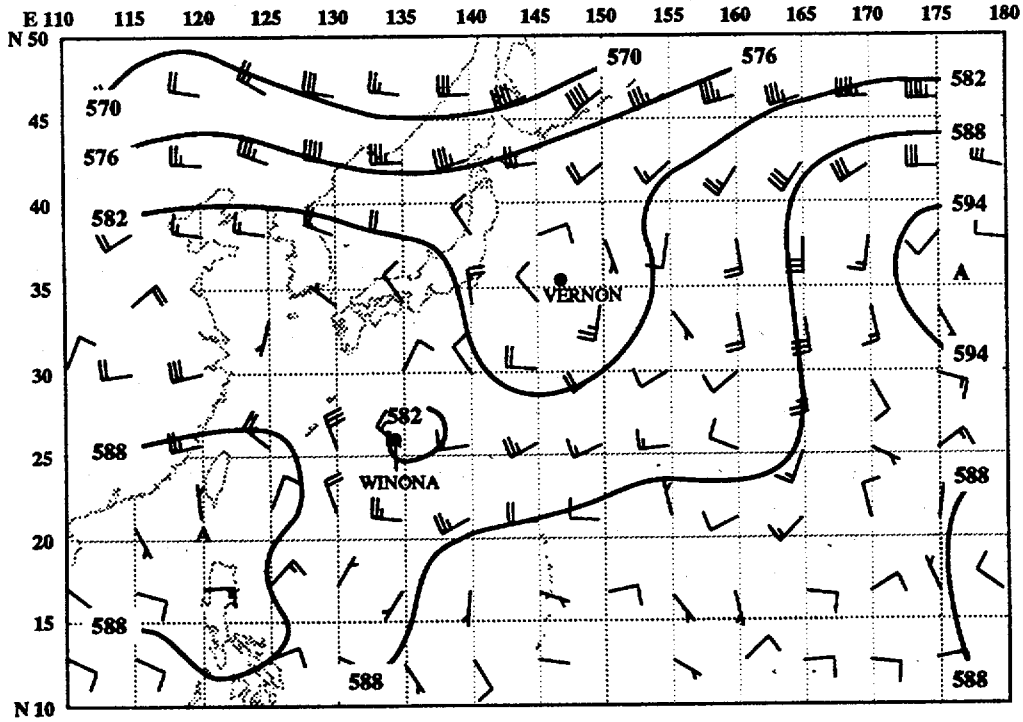

Figure 3-12-1. The 500-mb NOGAPS analysis for 070000Z August depicts Winona tracking between the two subtropical highs. Tropical Storm Vernon (11W) northeast of Winona. Note: heights are in decameters.

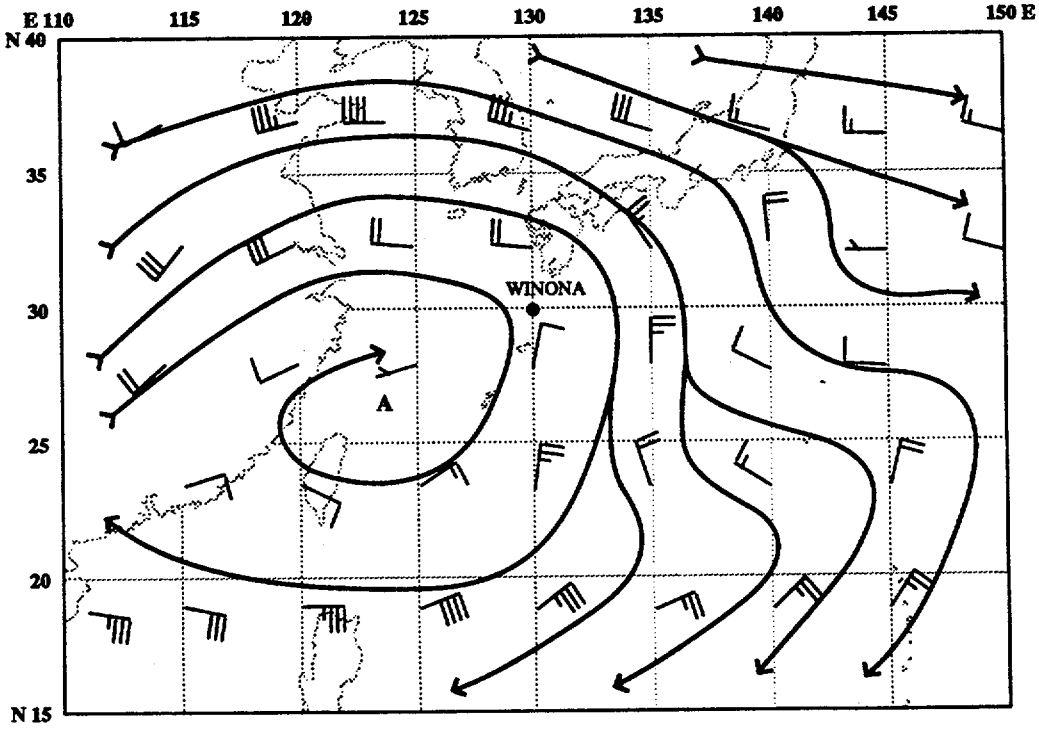

Figure 3-12-2. The 200-mb analysis for 060000Z August shows Winona is under the influence of unidirectional flow from the north.

As the shear decreased, the LLCC moved under the deep convection, and the system began to intensify. On 070000Z, a ship (call sign JFYD) approximately 215 nm (400 km) south of the center reported 35 kt (18 m/sec) southwesterly winds. At 070448Z (Figure 3-12-3), satellite analysts provided the first CI 2.5 Dvorak analysis, and the system was upgraded to a tropical storm. Winona continued to move southwestward toward a col and away from the shear, as it intensified. As Winona tracked northward, after an abrupt turn, it intensified further and developed dual upper-level outflow channels: one to the northeast and southwest. By 091200Z, Winona reached its maximum intensity of 65 kt (33 m/sec) and maintained it until making landfall 12 hours later. Winona weakened but managed to retain some strength and organization throughout its track over land. Yokota Air Base (WMO 47642) received peak winds of 40 kt (21 m/sec) with gusts to 57 kt (29 m/sec) at 100322Z and nearby Camp Zama had gusts up to 63 kt (32 m/sec) recorded at 100250Z. Winona got caught up in the westerlies as it reentered the water east of the Kanto Plain and became extratropical.

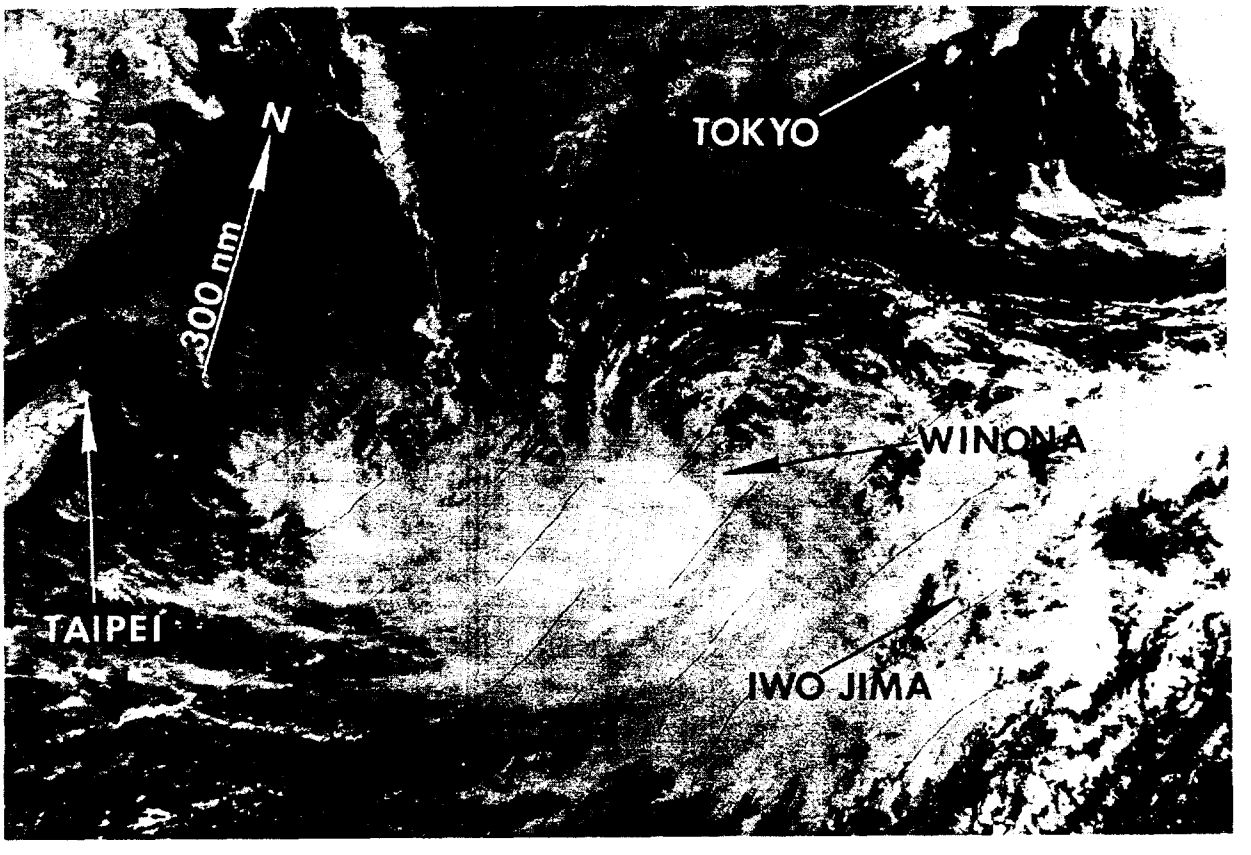

Figure 3-12-3. Winona's low-level circulation center is moving underneath the deep convection. This was the first good indication that Winona would intensify. Vernon (11W) is northeast of Winona (070448Z August NOAA visual imagery).

V. FORECASTING PERFORMANCE

The overall JTWC forecast performance is shown in Figure 3-12-4. The initial forecasts on Winona predicted a weak, disorganized system that would be short lived. Reorganization of the system as the center moved under the deep convection caused the track to be relocated on the third warning. By then, JTWC had a much better handle on the system and correctly forecast the sharp 120 degree turn to the north. This was 12 hours ahead of other agencies. Forecasters were slow in developing the system until it made the turn. After the LLCC moved under the deep convection, JTWC correctly predicted the effect that dual outflow channels would have in rapidly deepening the system. The objective aids FBAM and CSUM had problems with Winona's track. FBAM continued to move Winona south around the ridge until the system made the turn, then it caught on and went due north. CSUM started the turn too early and made it too tight, coming in west of the actual track. NOGAPS correctly built the ridge northward, which caused the push to the north. In addition to the accurate northward forecast, JTWC accurately forecast landfall. Forecasters then expected Winona to track northeastward north of the subtropical high and get caught up in the westerlies. A big decision centered around which way the storm would track around Mt. Fuji-san. JTWC did not predict the ridge flattening overnight and opted for an initial track through central Honshu west of Mt. Fuji-san, then skirting northern Honshu just off the coast in the Sea of Japan. As a short wave trough passed to the north, the ridge damped, and Winona turned sooner than forecast. Both JTWC and the Japan Meteorological Agency brought their tracks further south once it was obvious that Winona would track south of Mt. Fuji-san. Both agencies also kept their forecast tracks over the northeastern edge of Japan, skirting along or just south of the Kurils. Winona tracked just south of these forecasts. Both agencies, however, correctly forecast the acceleration of the system as it became embedded in the westerlies and subsequently became extratropical.

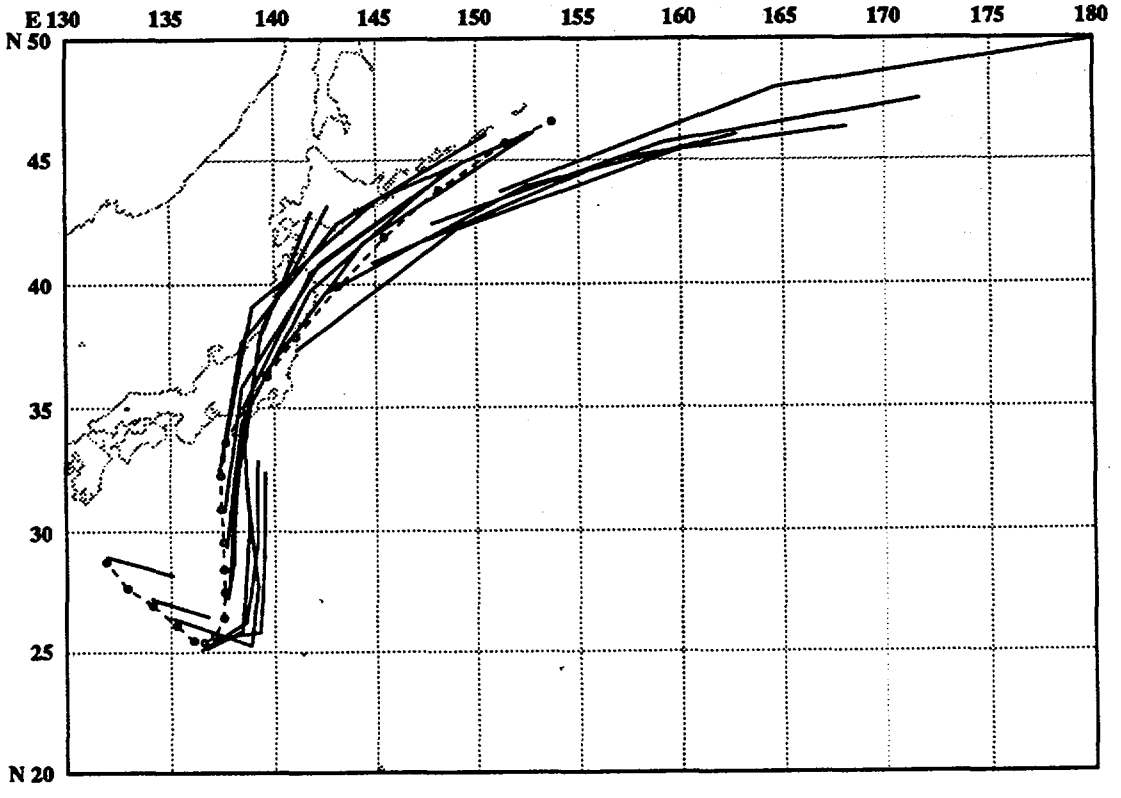

Figure 3-12-4. Summary of JTWC forecasts (solid lines) for Winona is superimposed on the final best track (dashed lines).

VI. IMPACT

Damages to U.S. military installations in Japan were minimal. Trees on bases were uprooted, tiles were blown off roofs, and there were isolated power outages.

The rest of Japan did not fare as well. According to reports from various Japanese newspapers, there were 13 typhoon related injuries but no deaths. In southeast Japan over 7000 homes in the Shizuoka Prefecture cities of Yaizu, Hamamatsu and Shimoda lost electricity as trees fell on the power lines. There were 686 homes flooded and 43 landslides. Transportation was disrupted, and over 500,000 travelers were affected by either the cancellation of 62 domestic flights from Tokyo's Haneda Airport or the many trains that were halted or delayed. All Tokaido Shinkansen bullet trains between Tokyo and Osaka were stopped. The teams scheduled to play in the Tokyo Dome could not find transportation, resulting in the first "rained out" game since the stadium was built in 1987.

The much needed rainfall poured more than 20 million tons of water into Japanese reservoirs, pushing them up to 36 percent of their total capacity. This allowed the lifting of water restrictions which had gone into effect earlier in the year.

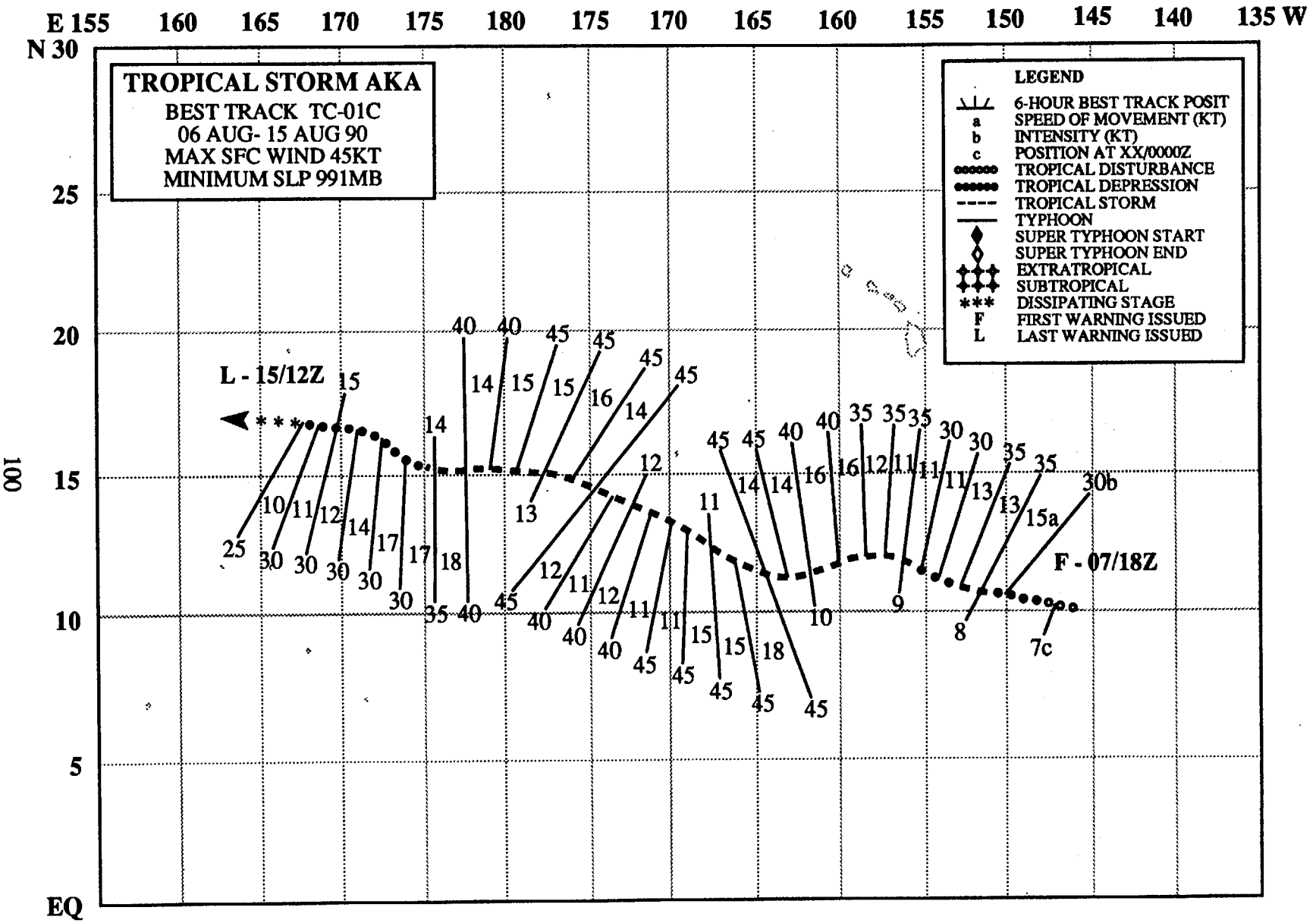
E 155 160 165 170 175 180 175 170 165 160 155 150 145 140 135 W
N 30
25
20
15
10
5
EQ
100
TROPICAL STORM AKA
BEST TRACK TC-01C
06 AUG- 15 AUG 90
MAX SFC WIND 45KT
MINIMUM SLP 991MB
LEGEND
6-HOUR BEST TRACK POSIT
a SPEED OF MOVEMENT (KT)
b INTENSITY (KT)
c POSITION AT XX/0000Z
TROPICAL DISTURBANCE
TROPICAL DEPRESSION
TROPICAL STORM
TYPHOON
SUPER TYPHOON START
SUPER TYPHOON END
EXTRATROPICAL
SUBTROPICAL
*** DISSIPATING STAGE
F FIRST WARNING ISSUED
L LAST WARNING ISSUED
L - 15/12Z
F - 07/18Z

TROPICAL STORM AKA (01C)

I. HIGHLIGHTS

Aka was the only tropical cyclone of 1990 to be in warning status when it crossed the date line from the central into the western North Pacific Ocean. It remained embedded in the trade wind trough, tracked steadily west-northwestward and never developed beyond tropical storm intensity.

II. CHRONOLOGY OF EVENTS

071800Z - First advisory issued by the Central Pacific Hurricane Center (CPHC) due to increased organization and amount of deep central convection.

090000Z - Upgraded to tropical storm intensity after convective organization improved and the first Dvorak intensity estimate of 2.5.

131500Z - Final advisory issued by CPHC and responsibility for Aka passed to the Joint Typhoon Warning Center (JTWC).

131800Z - First warning on Aka issued by JTWC.

140600Z - Downgraded to a tropical depression due to the loss of central convection resulting from persistent vertical wind shear.

151200Z - Final warning (dissipating over water) followed further weakening from vertical shear associated with a vigorous TUTT low to the northwest.

III. TRACK AND MOTION

Aka formed in the trade wind trough southeast of Hawaii (Figure 3-01C-1), remained embedded in the broad low-latitude easterlies and tracked steadily west-northwestward.

IV. INTENSITY

Although Aka persisted for nine days, its convection never became well organized. The system was maintained by low-level easterlies converging into the trade wind trough. However, the upper-level outflow pattern was continually disrupted by vertical wind shear. On 15 August, the low-level flow carried Aka westward under a vigorous TUTT low near the dateline. The upper level sheared away, the low level circulation dissipated and only the TUTT low remained (Figure 3-01C-2).

V. FORECASTING PERFORMANCE

Overall JTWC forecast performance is shown in Figure 3-01C-3. The NOGAPS prognostic series correctly maintained a mid- and low-level ridge north of Aka. Forecasters were uncertain about how long the tropical cyclone would persist as it approached the TUTT low. When dissipation became obvious, the forecast period was truncated and the final warning issued.

VI. IMPACT

No information available.

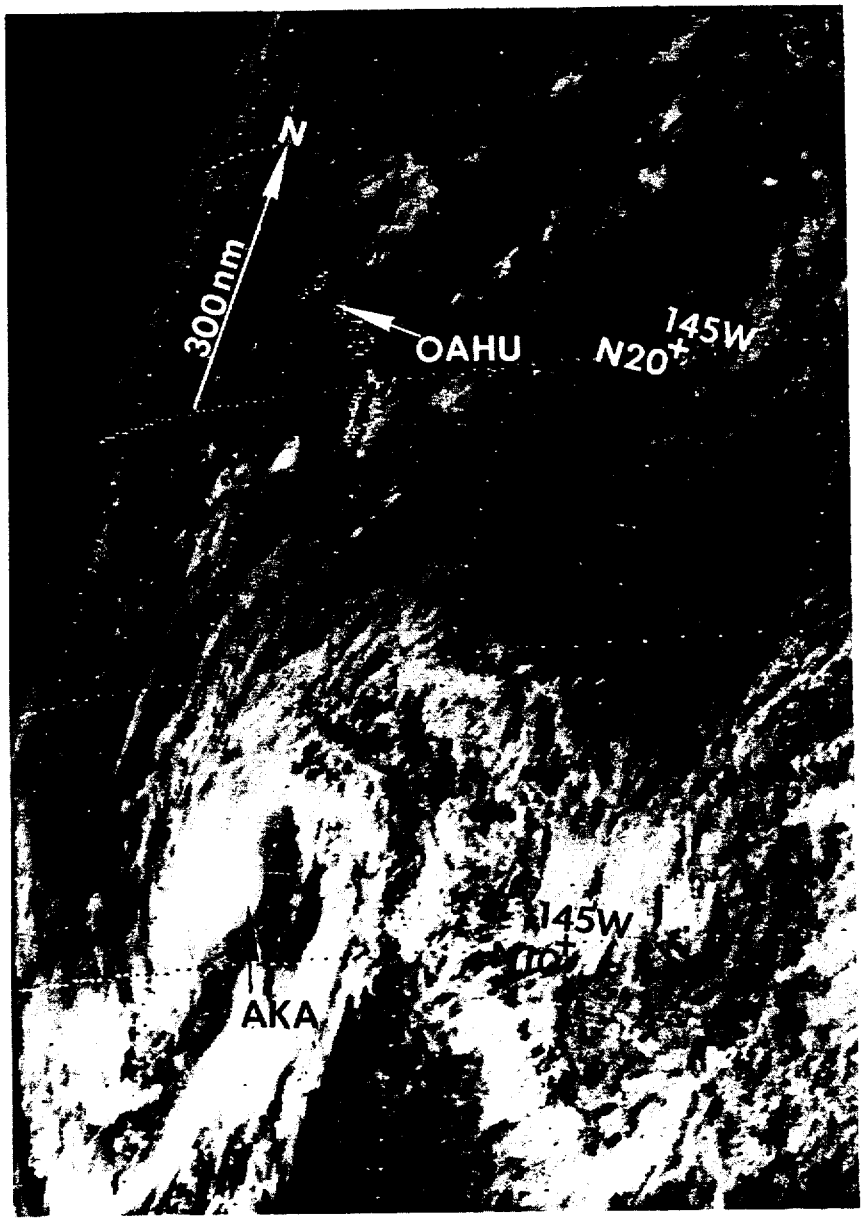

Figure 3-01C-1. Aka reaches tropical storm intensity south of the Hawaiian Islands (090101Z August GOES Central visual imagery - photo courtesy of the National Weather Service Forecast Office, Honolulu, Hawaii).

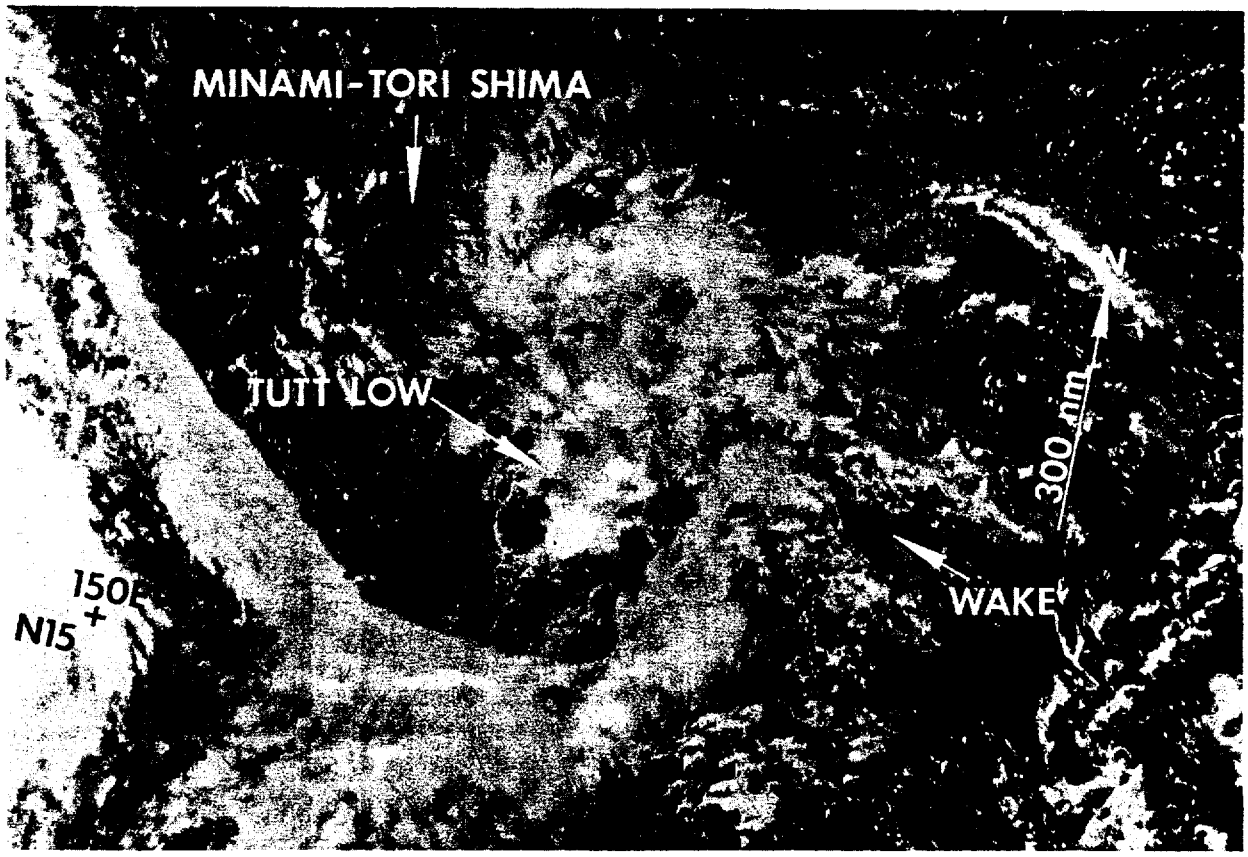

Figure 3-01C-2. The vigorous TUTT low with its random convective elements dominate the area where Aka dissipated 15 hours before (160308Z August NOAA visual imagery).

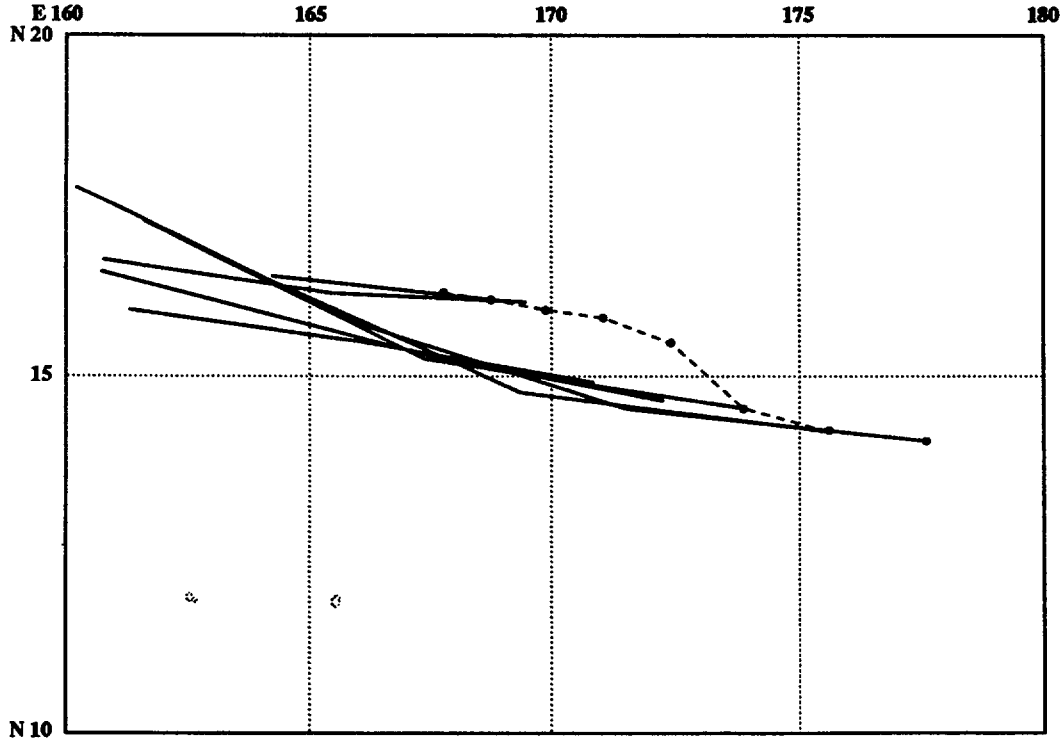

Figure3-01C-3. Summary of JTWC forecasts (solid lines) for Aka is superimposed on the final best track (dashed line).

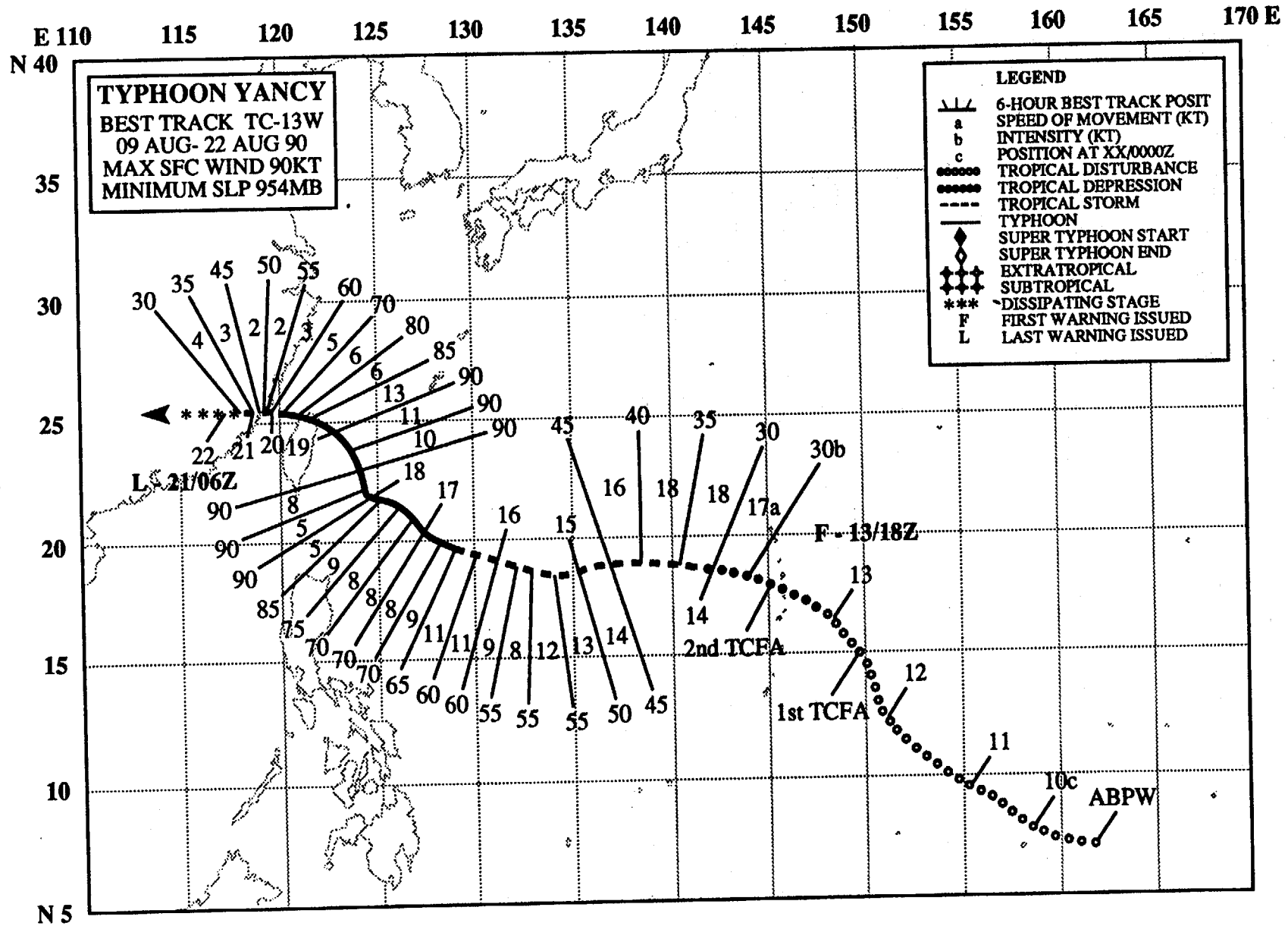
TYPHOON YANCY
BEST TRACK TC-13W
09 AUG- 22 AUG 90
MAX SFC WIND 90KT
MINIMUM SLP 954MB
LEGEND
6-HOUR BEST TRACK POSIT
SPEED OF MOVEMENT (KT)
INTENSITY (KT)
POSITION AT XX/0000Z
TROPICAL DISTURBANCE
TROPICAL DEPRESSION
TROPICAL STORM
TYPHOON
SUPER TYPHOON START
SUPER TYPHOON END
EXTRATROPICAL
SUBTROPICAL
DISSIPATING STAGE
FIRST WARNING ISSUED
LAST WARNING ISSUED
L - 21/06Z
F - 13/18Z
2nd TCFA
1st TCFA
ABPW
E 110
115
120
125
130
135
140
145
150
155
160
165
170 E
N 40
35
30
25
20
15
10
N 5

TYPHOON YANCY (13W)

I. HIGHLIGHTS

Yancy, JTWC's best forecast tropical cyclone of the year, was one of a series of August storms that generated in the monsoon trough. Although the track was generally toward the northwest, it contained several interesting features, including interaction with a strengthening subtropical ridge, the effects of a passing mid-latitude shortwave trough and land interaction with the mountainous terrain of Taiwan.

II. CHRONOLOGY OF EVENTS

090600Z - First mentioned on the Significant Tropical Weather Advisory as an area of persistent convection with an estimated minimum sea-level pressure of 1008 mb.

112100Z - First Tropical Cyclone Formation Alert based on an increase in central convection, more pronounced upper-level outflow and surface pressure decreases at several nearby land stations.

121400Z - Second Tropical Cyclone Formation Alert based on a northward shift of a consolidating low-level center and continued drops in surface pressure at several nearby land stations.

131400Z - Third Tropical Cyclone Formation Alert based on a continued increase in organization, deep central convection and an approaching surge in southwest monsoon flow.

131800Z - First warning due to increased consolidation of central convection and improvements in the upper-level outflow.

141200Z - Upgrade to tropical storm prompted by increased convective curvature, consolidation of the cyclonic center and the first intensity estimate of CI 2.5.

161200Z - Upgrade to typhoon prompted by a decrease in vertical wind shear, improved organization in the deep central convection, improved upper-level outflow and intensity estimates of CI 4.0.

180000Z - Peak intensity - 90 kt (46 m/sec) - based on intensity estimate of CI 5.0.

200000Z - Downgraded to tropical storm based on radar reports, synoptic reports and satellite imagery which indicated significant weakening due to land interaction as the system crossed Taiwan.

210600Z - Downgraded to tropical depression due to the effects of land interaction and increased vertical wind shear.

210600Z - Final warning - dissipated - based on a combination of land interaction and increased vertical wind shear as the system moved into mainland China.

III. TRACK AND MOTION

The LLCC which developed into Yancy generated on the eastern side of a broad monsoon depression. A series of vortices persisted at low latitudes for four days before consolidating into Yancy. In its formative stages, Yancy moved erratically as mesoscale convective elements developed, decayed, and were replaced by new elements. The resulting large monsoon depression moved generally westward at 8 to 10 kt (15 to 20 km/hr) until 13 August. A 48-hour period of rapid westward movement followed as Yancy moved into an area dominated by a strengthening subtropical ridge to the north (Figure 3-13-1). This westward track continued until a mid-latitude shortwave trough moving off the coast of China weakened the subtropical ridge over the East China Sea (Figure 3-13-2), resulting in an 18-hour period of north-northwestward movement. The system resumed its westward track across Taiwan as the subtropical ridge reestablished itself. Yancy executed a mesoscale trochoidal oscillation (wobble) about a smoothed track as it moved past Taiwan as depicted by radar position reports from Hualein (WMO 46699), Taiwan in Figure 3-13-3.

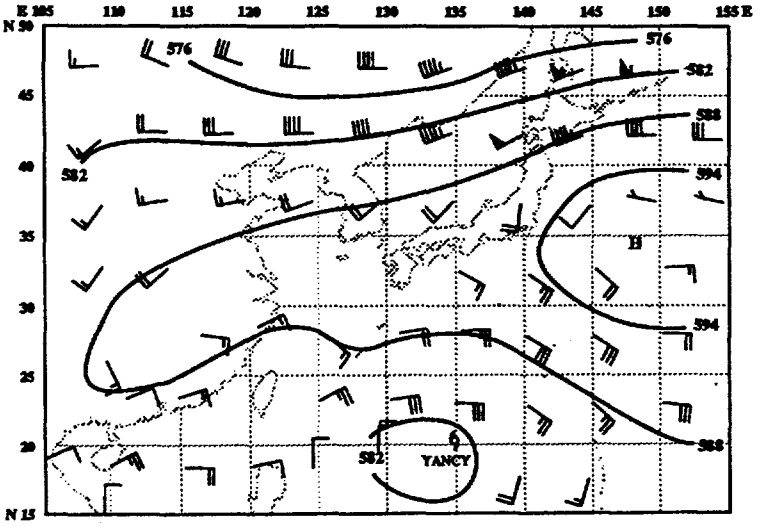

Figure 3-13-1. 500-mb NOGAPS analysis from 150000Z August, showing the strengthening of the mid-level ridge north of Yancy which resulted in the westward track.

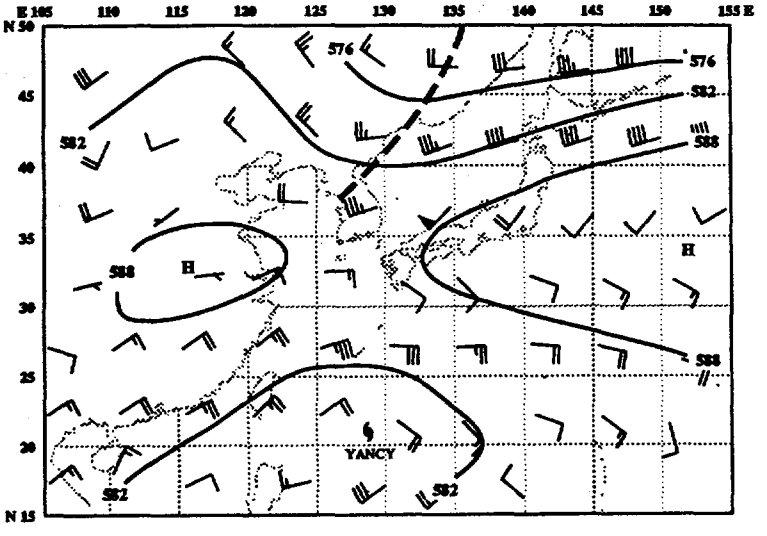

Figure 3-13-2. 500-mb NOGAPS analysis from 170000z August, showing a passing shortwave trough weakening the mid-level subtropical ridge, which resulted in a jog in the track to the north-northwestward.

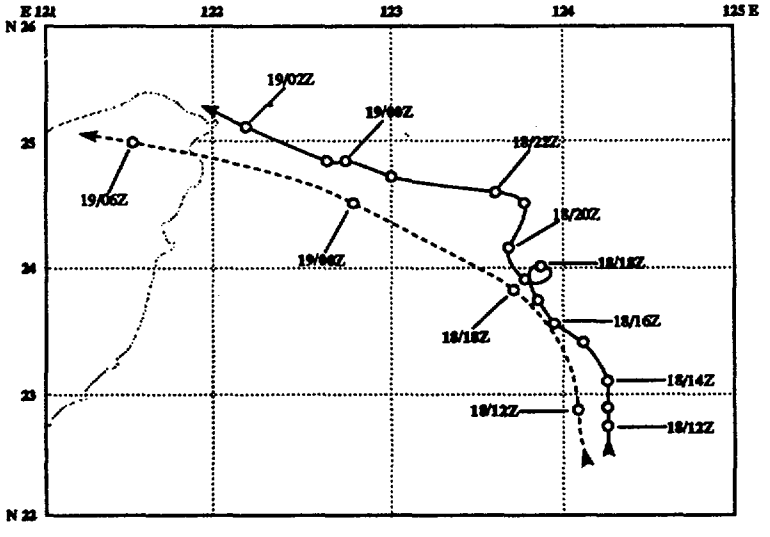

Figure 3-13-3. Plots of hourly radar positions from Hualein (WMO 46699), Taiwan compared to the smoothed best track (dashed line) show Yancy's wobble.

IV. INTENSITY

At 150000Z August, Yancy had a distinct low-level circulation center on the poleward side of the monsoon cloud mass (Figure 3-13-4). The poleward dislocation was attributed to strong upper-level flow from the north and east that apparently inhibited rapid development. A strongly divergent flow became established over the system on August 17, with outflow branches into the equatorial easterlies and into the major TUTT cell to the east-northeast (Figure 3-13-5). Fairly slow deepening to maximum intensity followed and Yancy developed an eye on 18 August (Figure 3-13-6). Weakening and decay were directly attributable to the close approach to the Taiwan mountains, followed by landfall on mainland China.

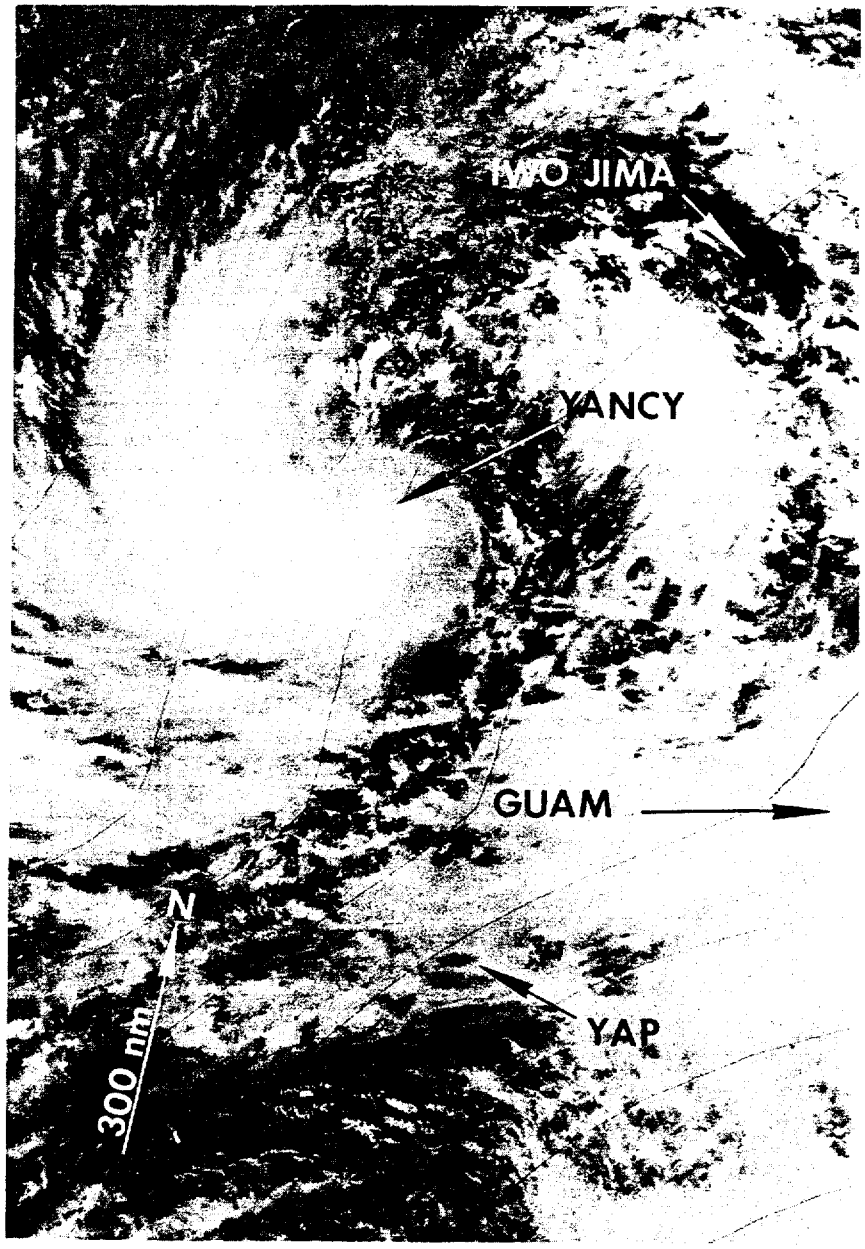

Figure 3-13-4. Tropical Storm Yancy (13W) as it separates from the convection associated with the monsoon trough. Note the area of strong low-level convergence southeast of the system. This area was associated with a strong surge in the monsoon flow from which Yancy separated (150504Z August NOAA visual imagery).

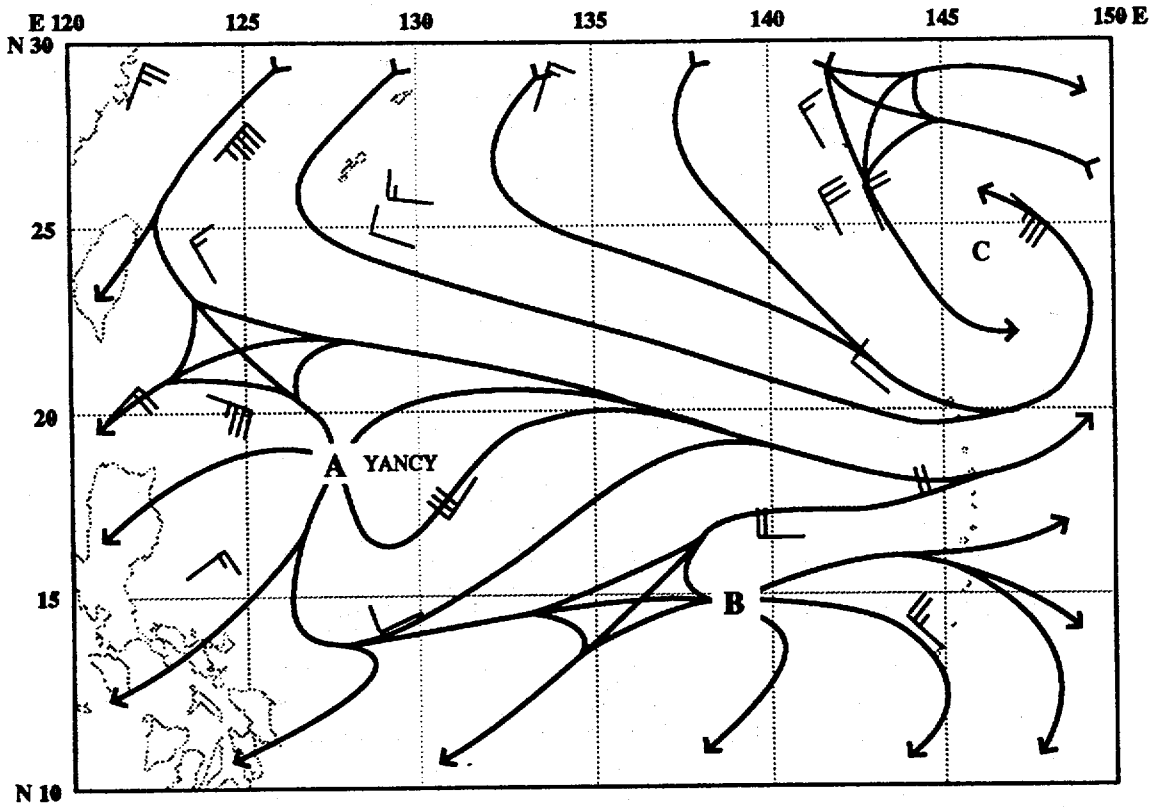

Figure 3-13-5. The 170000z August 200-mb analysis, with Yancy at point A, showing the upper-level outflow channel to the southwest and eastward into the large TUTT cell at point C. The outdraft at point B is over deep convection associated with the formation of Zola (14W).

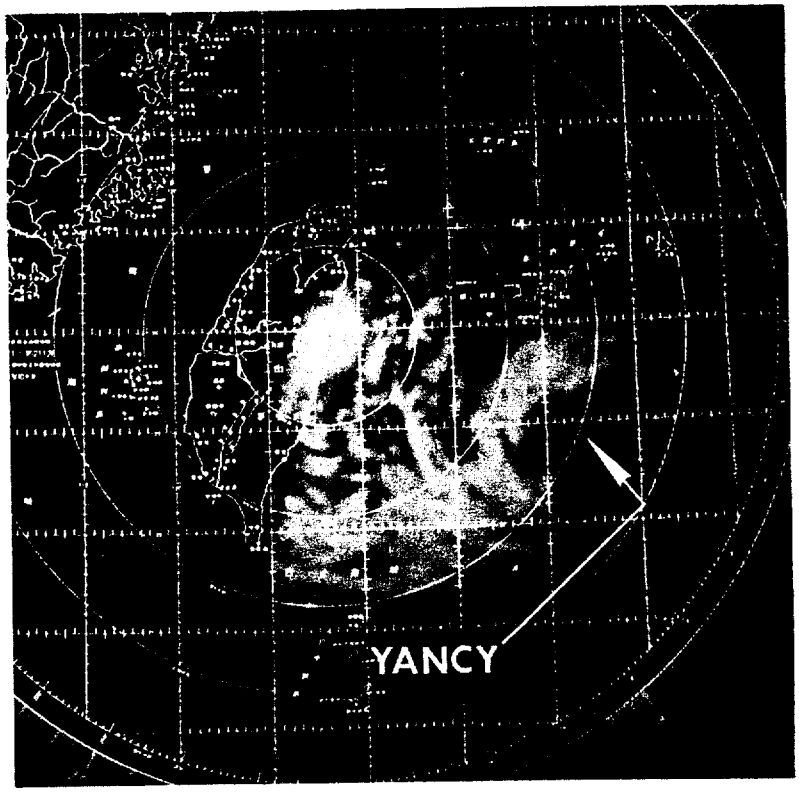

Figure 3-13-6. Yancy's eye appears at the edge of the radar scope at Hualein (WMO 46699), Taiwan (181200Z August photo courtesy of the Central Weather Bureau, Taipei, Taiwan).

V. FORECASTING PERFORMANCE

Although Yancy followed what might appear to be a simple northwestward track, it proved to be a difficult forecast scenario. At two key points during the forecast cycle, the forecast aids and NOGAPS prognostic charts were not in agreement as to the final storm track. As the tropical storm passed through the northern Mariana Islands, the statistical forecast aids indicated that the storm would recurve, while the dynamic forecast aids and the NOGAPS model indicated the system would move westward in response to a building mid-level ridge to the north. The second difficult forecast decision came as the storm approached Taiwan. The statistical forecast aids, the ECMWF model, the NMC model and the Japanese model all called for the system to recurve in response to a passing mid-latitude shortwave trough. The dynamic forecast aids and the NOGAPS model forecast the system to track westward toward a col in the mid-level subtropical ridge over eastern China. As Figure 3-13-7 indicates, JTWC chose the correct forecast at each of these key forecast points. Yancy proved to be JTWC's best forecast storm of the year, with errors of 97nm (180km) at 24 hours, 98nm (182km) at 48 hours and 108nm (200km) at 72 hours.

VI. IMPACT

Yancy passed through the northern Philippine Sea, triggering a deep monsoon surge that resulted in heavy rains and flooding on northern Luzon, leaving at least six people dead and more than 60,000 people fleeing to evacuation centers. Yancy's next impact was felt on Taiwan as it brought heavy winds and torrential rains to the northern half of the island before moving into mainland China. There, the death toll climbed to 216 people, with an additional 59 reported missing and an estimated economic loss of approximately 170 million dollars.

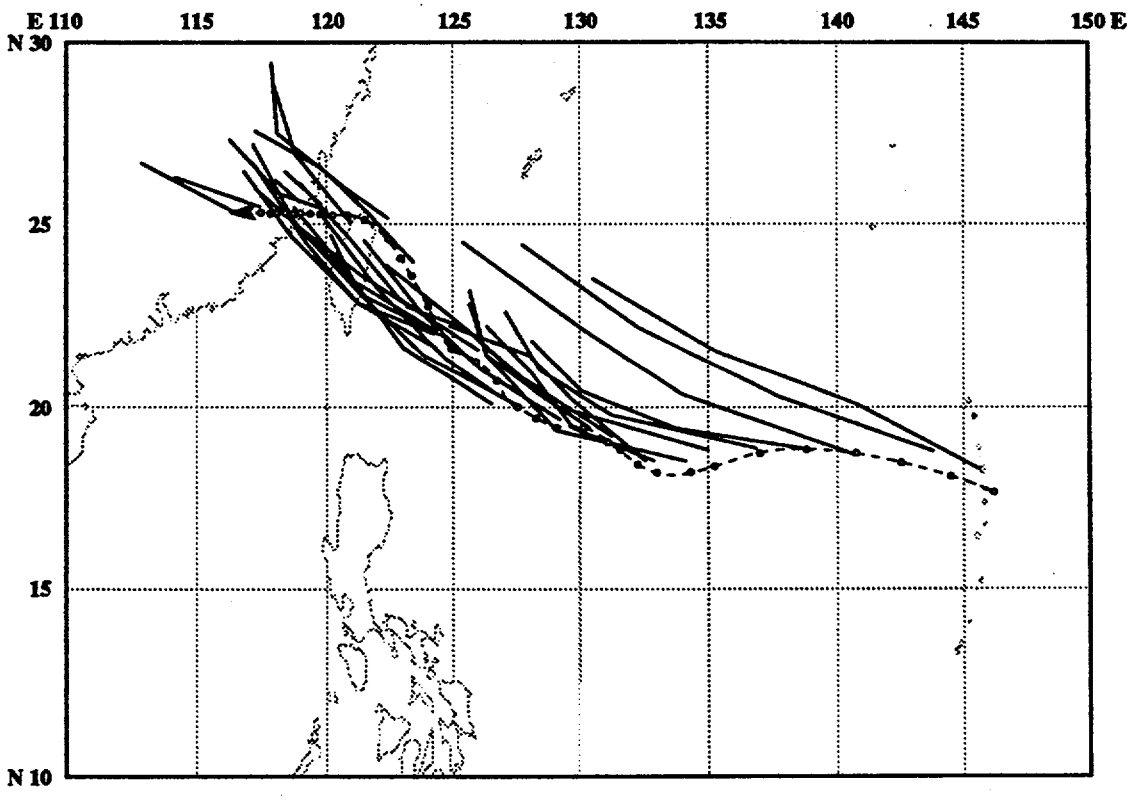

Figure 3-13-7. Summary of JTWC forecasts (solid lines) for Yancy is superimposed on the final best track (dashed line).

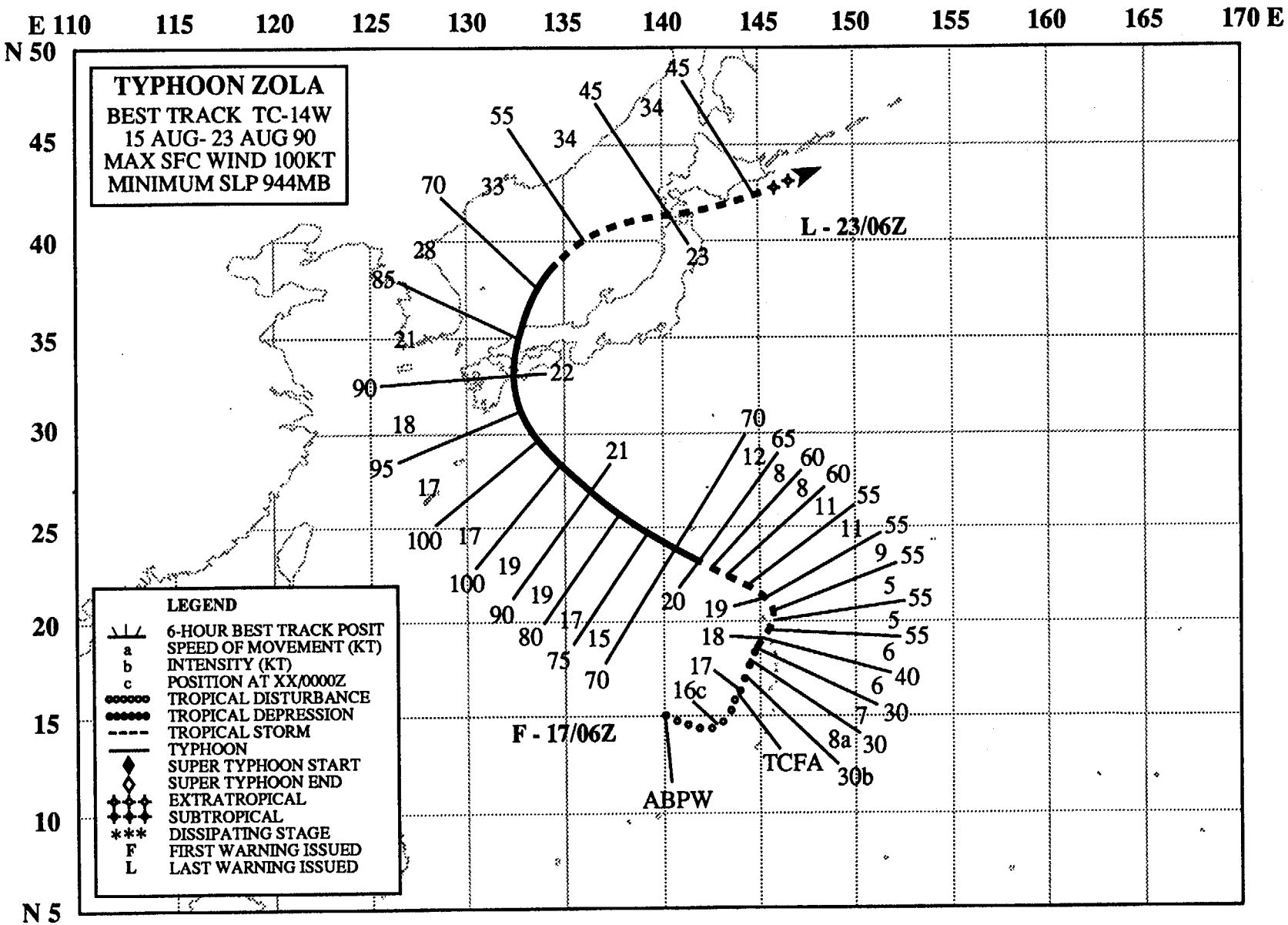
TYPHOON ZOLA
BEST TRACK TC-14W
15 AUG- 23 AUG 90
MAX SFC WIND 100KT
MINIMUM SLP 944MB
E 110
115
120
125
130
135
140
145
150
155
160
165
170 E
N 50
45
40
35
30
25
20
15
10
N 5
110
L - 23/06Z
F - 17/06Z
ABPW
TCFA
LEGEND
6-HOUR BEST TRACK POSIT
a SPEED OF MOVEMENT (KT)
b INTENSITY (KT)
c POSITION AT XX/0000Z
TROPICAL DISTURBANCE
TROPICAL DEPRESSION
TROPICAL STORM
TYPHOON
SUPER TYPHOON START
SUPER TYPHOON END
EXTRATROPICAL
SUBTROPICAL
*** DISSIPATING STAGE
F FIRST WARNING ISSUED
L LAST WARNING ISSUED

TYPHOON ZOLA (14W)

I. HIGHLIGHTS

In the wake of Typhoon Yancy (13W), a surge in the southwesterly monsoon flow developed and Zola formed west of Guam in the monsoon trough. The depression initially tracked northeastward with the movement of the monsoon surge and slowly intensified. Then, Zola broke away from the monsoon trough and intensified into a typhoon. The typhoon recurved over western Honshu into the Sea of Japan and accelerated to the east-northeastward.

II. CHRONOLOGY OF EVENTS

150600Z - First mentioned on the Significant Tropical Weather Advisory as a persistent area of convection which extended eastward from Tropical Storm Yancy (13w). The estimated minimum sea-level pressure was 1000 mb.

162200Z - Tropical Cyclone Formation Alert based on a transient band of convection wrapping around the low-level circulation center.

170600Z - First Tropical Depression Warning prompted by the persistence of deep convection associated with a surge in the monsoonal flow just to the south of the circulation center.

180600Z - Upgraded to a tropical storm after receipt of a ship report of 55 kt (27 m/sec) and a 998 mb sea-level pressure indicating increased periphery winds and a tightened pressure gradient to the south and east.

200000Z - Upgraded to typhoon based on the appearance of a 25 nm (45 km) diameter ragged eye and the first CI 4.0.

210600Z - Peak intensity - 100 kt (51 m/sec) - followed an increase in organization, outflow, and intensity estimate of CI 5.5.

221800Z - Downgraded to tropical storm due to increased vertical wind shear and the start of extratropical transition.

230600Z - Final warning - extratropical - issued as Zola transitioned into a mid-latitude low due to strong vertical shear associated with the mid-latitude westerlies.

III. TRACK AND MOTION

After briefly tracking eastward during its formative stages, Typhoon Zola tracked north-northeastward just west of the Northern Mariana Islands along the western side of the subtropical high to the northeast. The tropical cyclone continued to track towards the north-northeast for the next three days as a short wave trough tracked slowly eastward, north of the system. Once the shortwave passed, the subtropical high built westward and combined with a dynamic high that moved off the coast of China to Japan reestablishing the subtropical ridge over Japan (Figure 3-14-1 through Figure 3-14-3). As this happened, Zola turned sharply and started tracking northwestward around the ridge. It recurved over southern Honshu and accelerated northeastward into the Sea of Japan.

IV. INTENSITY

Starting in the monsoon trough, Zola spun up as a result of a surge in the southwest monsoon associated with Typhoon Yancy (13W). For the first several days, the tropical cyclone developed slowly, remaining a tropical depression, primarily due to vertical wind shear. As Zola continued to track northeastward, the system intensified to 55 kt (28 m/sec) as it moved into an area of upper-level divergence southeast of a Tropical Upper Tropospheric Trough (TUTT) low. However, it remained a tropical storm until breaking away from the monsoon trough (Figure 3-14-4). Once separated from the monsoon trough, Zola intensified as it developed an outflow channel to the south. Intensification continued due to enhanced outflow to the north associated with a TUTT low to the northwest. The tropical cyclone reached a peak intensity of 100 kt (51 m/sec) on 21 August (Figure 3-14-5). At

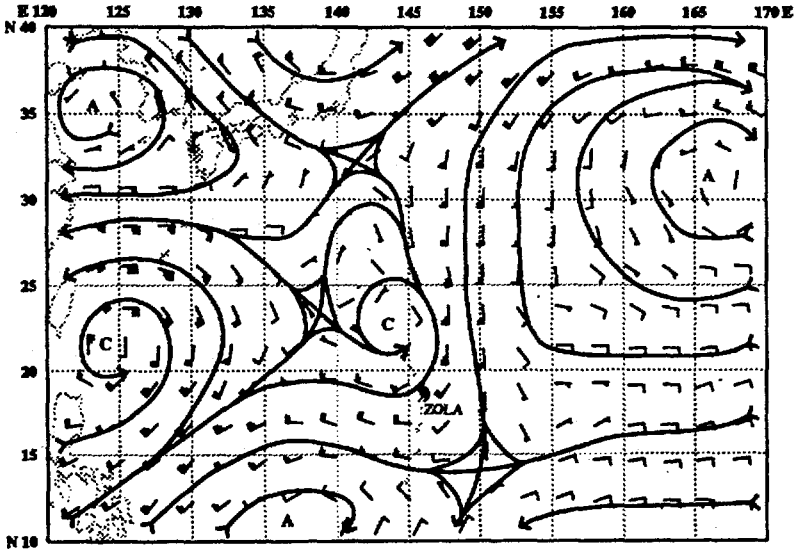

Figure 3-14-1. The 180000Z August NOGAPS deep layer mean analysis shows Zola's surface position, the subtropical high to the northeast, the mid-latitude trough to the north-northwest, and the dynamic high over the Yellow Sea. At this time, Zola was moving north-northeastward along the southwest side of the subtropical high

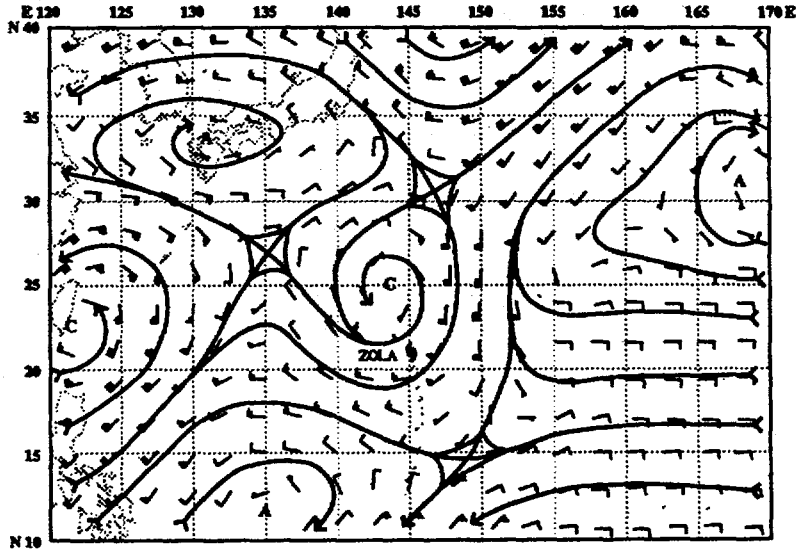

Figure 3-14-2. The 190000Z August NOGAPS deep layer mean circulation analysis depicts the mid-latitude trough in a position north-northeast of Zola. The dynamic high has moved to a location over southern Japan.

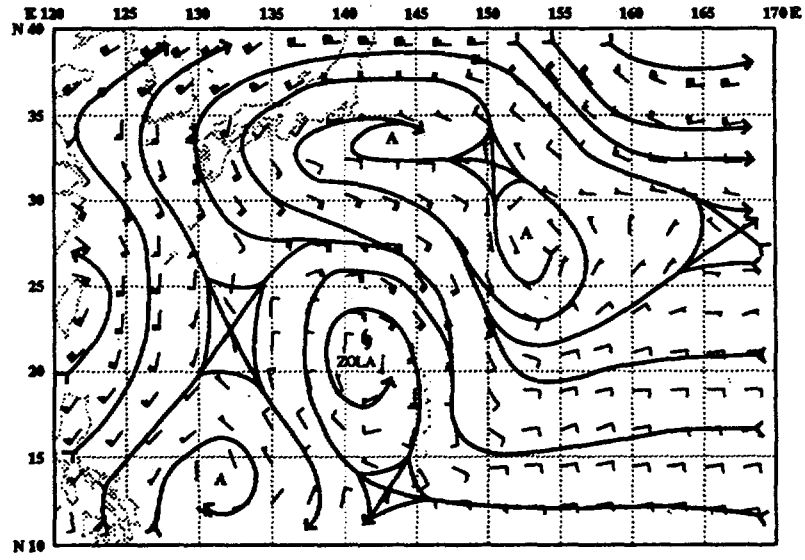

Figure 3-14-3. The 200000Z August NOGAPS deep layer mean circulation analysis shows the dynamic high and the subtropical high merging north of Zola.

211800Z, the typhoon started to weaken due to increasing vertical wind shear associated with the mid-latitude westerlies and land interaction with Japan. After recurving Zola quickly transitioned into an extratropical system.

V. FORECASTING PERFORMANCE

Overall JTWC forecast performance is shown in Figure 3-14-6. The initial warnings did not forecast Zola's sharp turn and track to the northwest. The NOGAPS prognostic series did not indicate a dynamic high moving off the coast of eastern Asia and combining with the subtropical high, reestablishing the ridge further to the west. JTWC also forecast Zola to recurve further to the east. The recurvature farther to the west may have been caused by the advection of warm, moist air from the tropics which strengthened the subtropical high to the tropical cyclone's northeast.

VI. IMPACT

No information received.

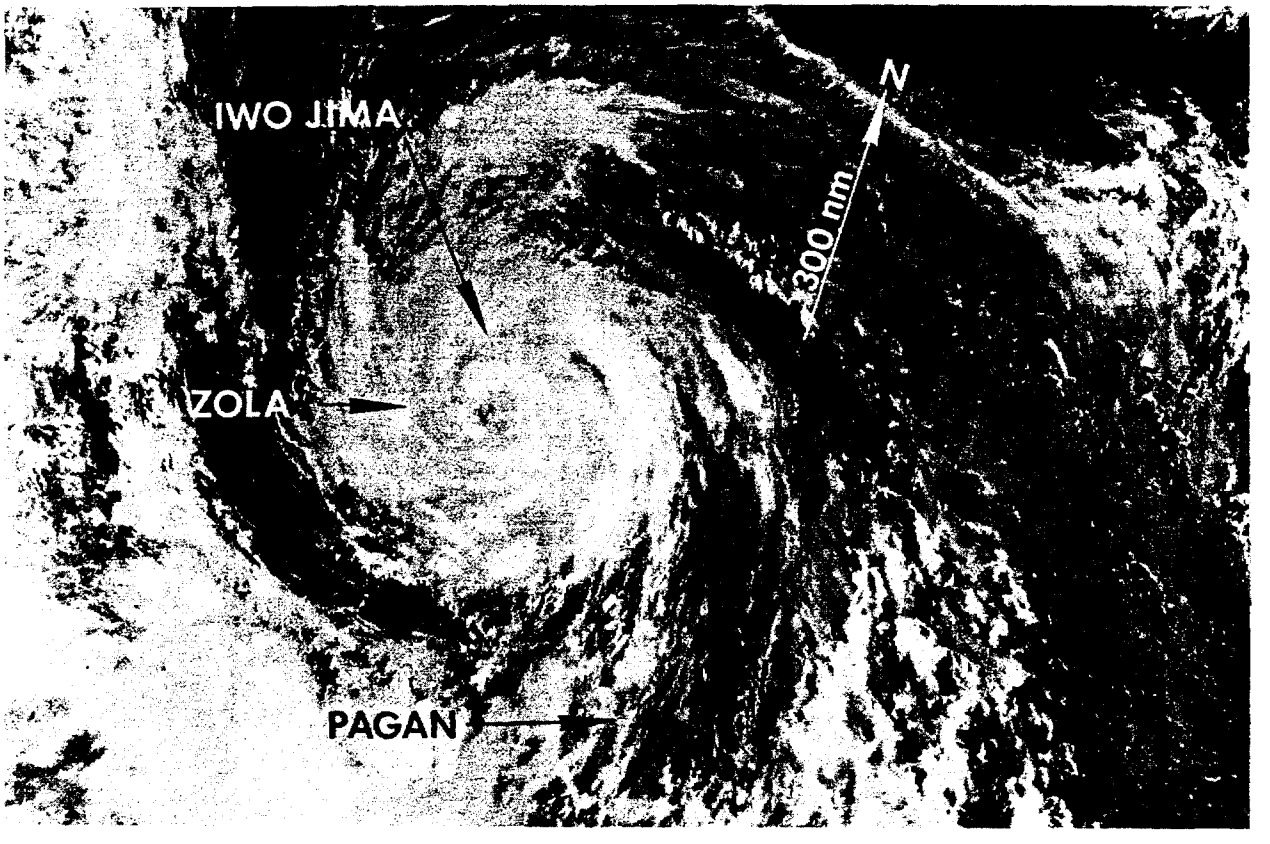

Figure 3-14-4. Zola just after breaking away from the monsoon trough. A distinct separation can be seen between Zola and the cloud mass to its south (192322Z August DMSP visual imagery).

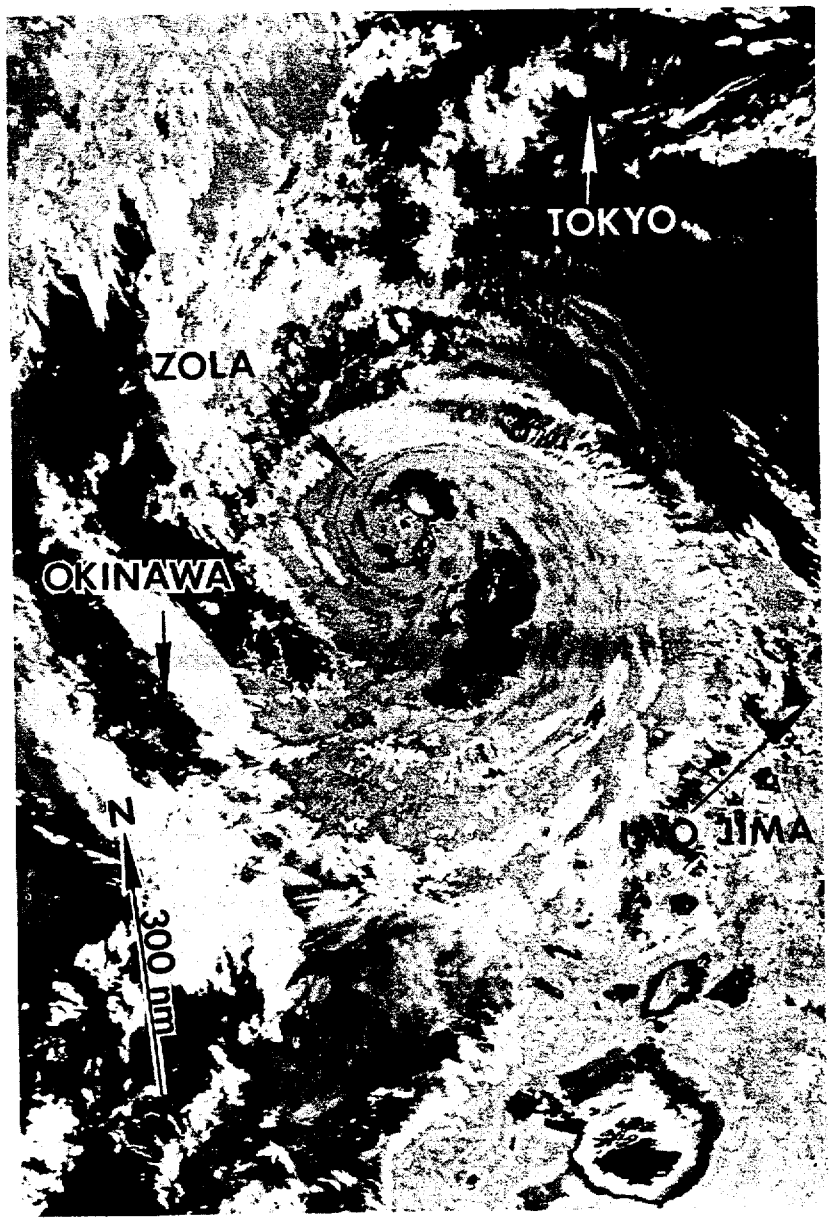

Figure 3-14-5. Zola, with a small eye and at maximum intensity, is moving northwestward towards southern Japan (210933Z August DMSP enhanced infrared imagery).

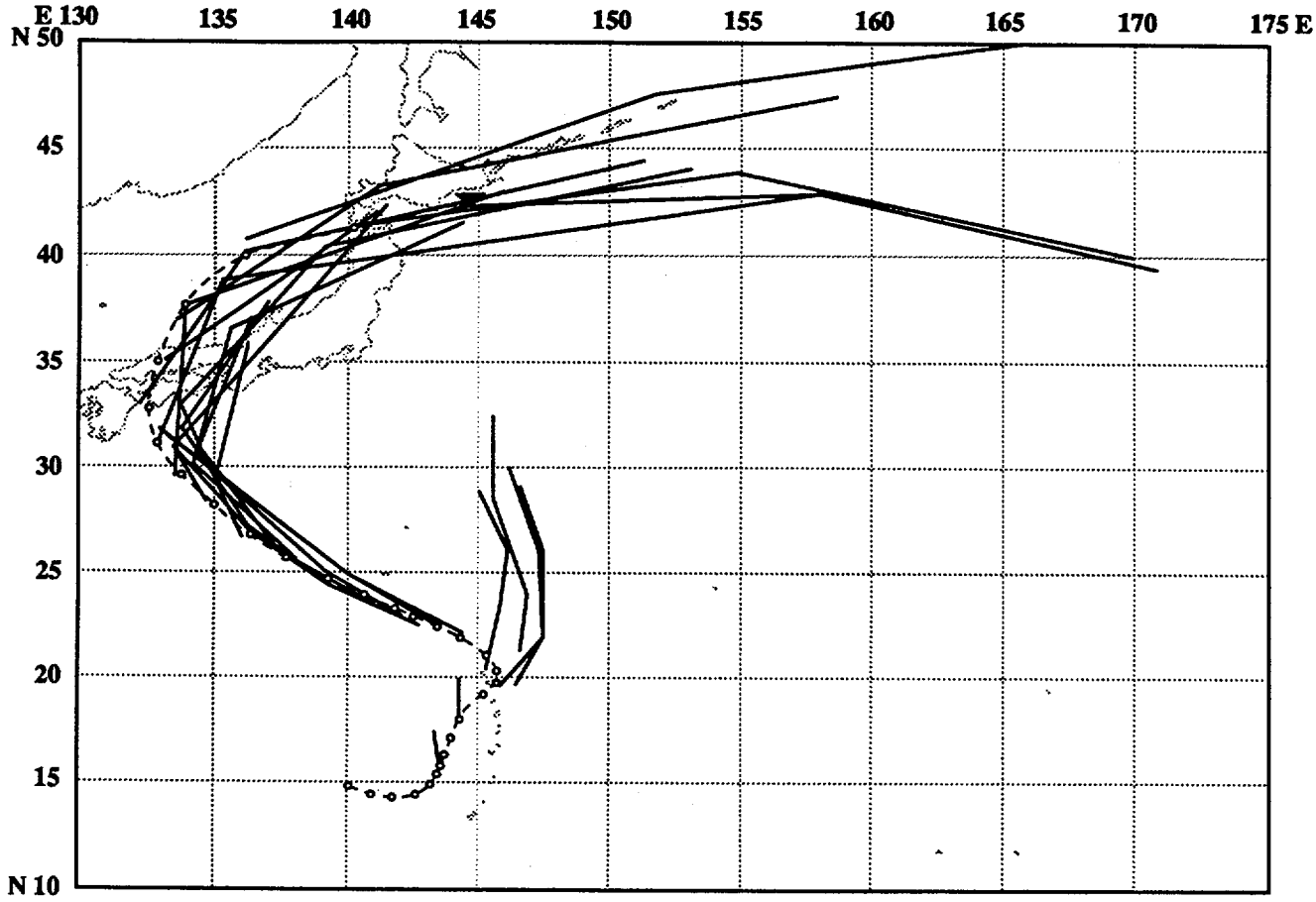

Figure 3-14-6. Summary of JTWC forecasts (solid lines) for Zola is superimposed on the final best track (dashed line).

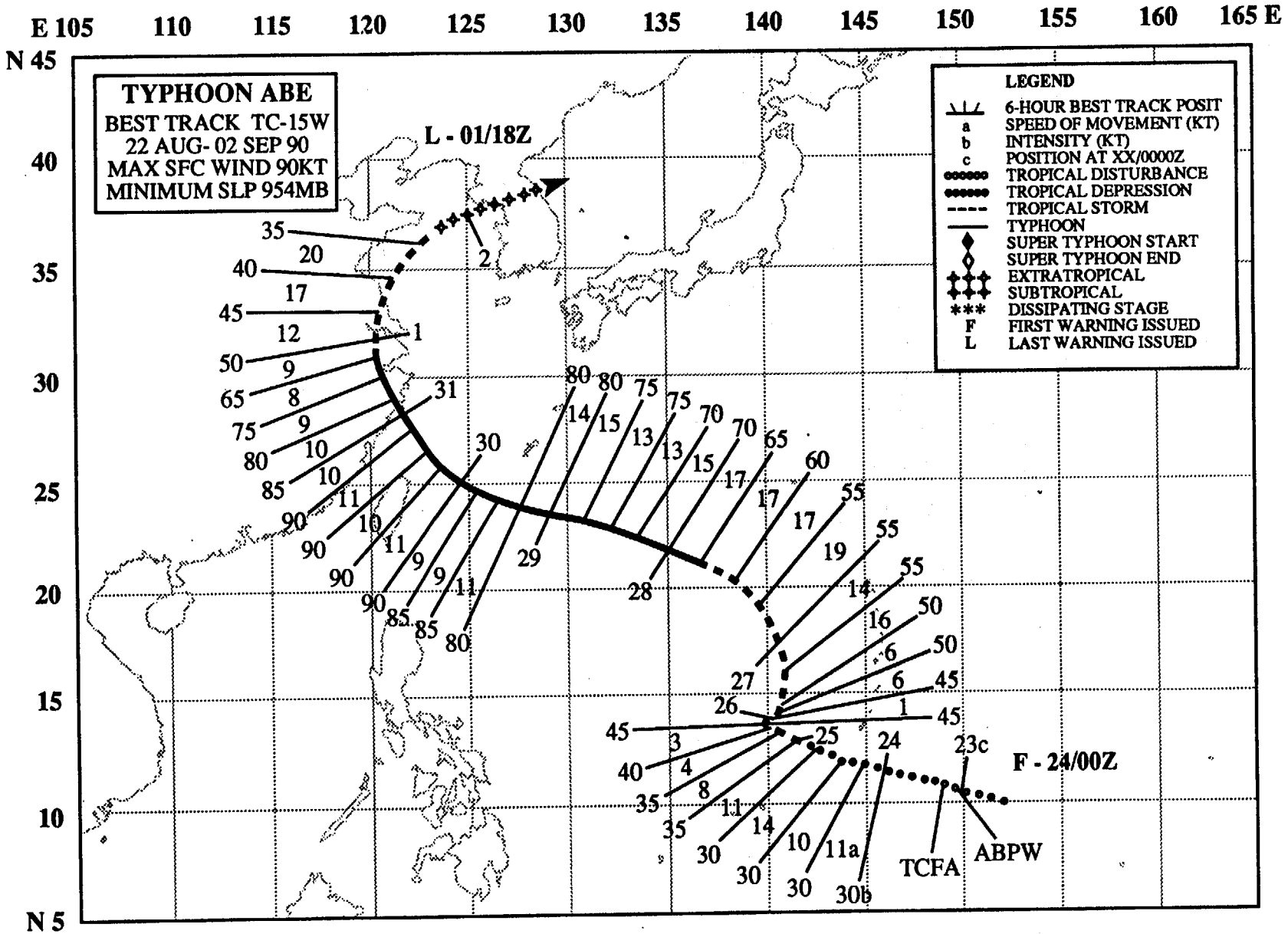
E 105
110
115
120
125
130
135
140
145
150
155
160
165 E
N 45
40
35
30
25
20
15
10
N 5
TYPHOON ABE
BEST TRACK TC-15W
22 AUG- 02 SEP 90
MAX SFC WIND 90KT
MINIMUM SLP 954MB
L - 01/18Z
F - 24/00Z
TCFA
ABPW
LEGEND
6-HOUR BEST TRACK POSIT
SPEED OF MOVEMENT (KT)
INTENSITY (KT)
POSITION AT XX/0000Z
TROPICAL DISTURBANCE
TROPICAL DEPRESSION
TROPICAL STORM
TYPHOON
SUPER TYPHOON START
SUPER TYPHOON END
EXTRATROPICAL
SUBTROPICAL
DISSIPATING STAGE
FIRST WARNING ISSUED
LAST WARNING ISSUED

TYPHOON ABE (15W)

I. HIGHLIGHTS

Typhoon Abe, the fourth of five tropical cyclones in August, caused extensive damage from the Republic of the Philippines through eastern China during its nine day life. Abe was also noteworthy as a classic example of the erratic motion and rapid reorganization that can occur in association with an intense monsoon surge.

II. CHRONOLOGY OF EVENTS

230100Z - First mentioned on Significant Tropical Weather Advisory as an area of persistent convection at the end of an active monsoon trough. Minimum sea-level pressure estimated to be 1007 mb.
230600Z - First Tropical Cyclone Formation Alert based on increased convection, organization, and outflow aloft.
240000Z - First warning issued due to continued development.
250000Z - Upgraded to a tropical storm based on increased central convection.
271200Z - Upgraded to a typhoon after detection of a ragged eye.
300000Z - Peak intensity - 90 knots (46 m/sec) - based on intensity estimate of CI 5.0
311200Z - Downgraded to tropical storm as convection decreased due to land interaction.
011800Z - Final warning issued due to extratropical transition.

III. TRACK AND MOTION

From its initial mention on the Significant Tropical Weather Advisory until 250000Z, Abe tracked steadily west-northwestward under a well-developed subtropical ridge. By 251200Z, an intense, deep surge in the monsoon westerlies began to develop south of Abe, arresting its westward motion. The enhanced convection associated with the surge (Figures 3-15-1a, 3-15-1b and 3-15-1c) initially formed east of Abe's convective cloud mass and grew as it wrapped around to the north. Eventually, Abe's circulation center reorganized to the north, between the competing convective masses. The intensity and horizontal extent of the monsoon surge is illustrated by the time sequence of gradient level winds recorded at the National Weather Service Observatory at Taguac, Guam (WMO 91217) and shown in Figure 3-15-2. During the timeframe of the figure, Abe was located between 270 and 540 nm (500 to 1000 km) from Guam. Following the monsoon surge event that pushed the system on a brief eastward then northward track, Abe resumed a west-northwestward track along the periphery of the subtropical ridge. The typhoon eventually recurved through a weakness in the subtropical ridge associated with a passing short-wave trough. The recurvature track took Abe along the coasts of the Zhejtang and Jiangsu Provinces of China, into the Yellow Sea, and across the middle portion of South Korea.

IV. INTENSITY

From the initial warning at 240000Z until 270600Z, Abe intensified by only 25 kt (13 m/sec) due to the disruptive shearing effects of the monsoon surge. The subsequent three days of intensification to its peak of 90 kt (46 m/sec) at 300000Z was also slower than normal. The slow intensification may be attributed to some restriction of Abe's outflow into the tropical upper-level easterlies caused by the outflow of Typhoon Becky (16W). Any additional intensification that might have resulted from the eventual establishment of good outflow into the midlatitude westerlies at 310000Z was negated by the terrain effects as Abe approached China.

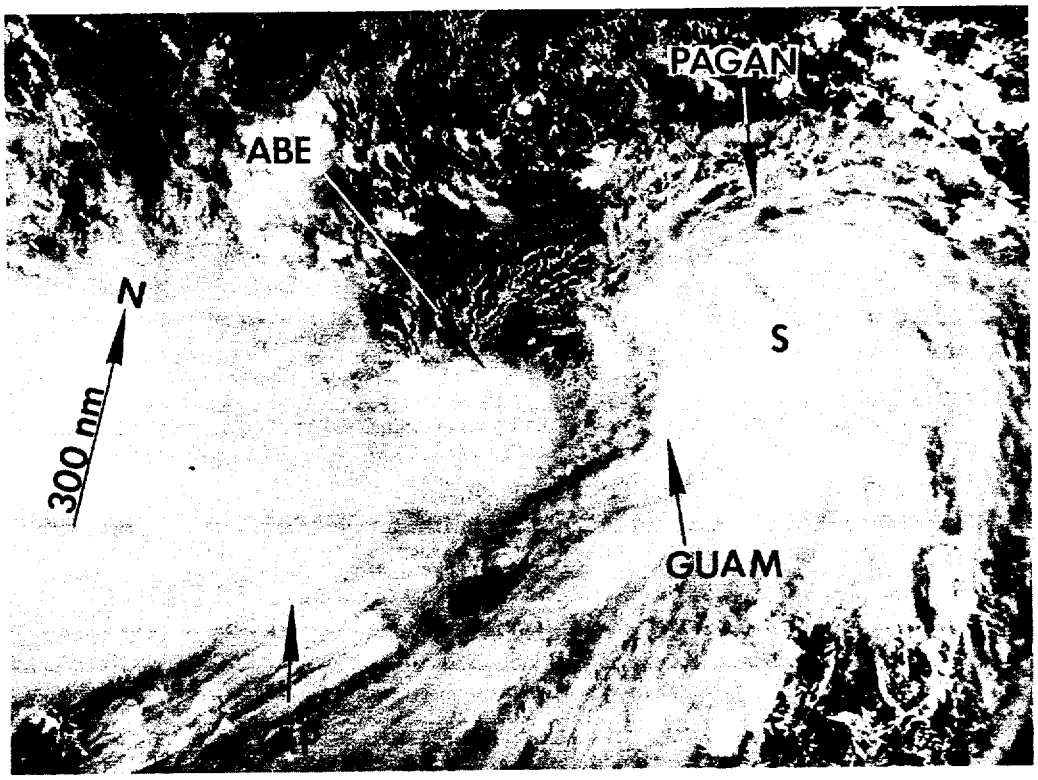

Figure 3-15-1a. The comma-shaped cloudiness (at Point S) to the northeast of Guam is associated with a monsoon surge that is wrapping around Abe's center (260441Z August NOAA visual imagery).

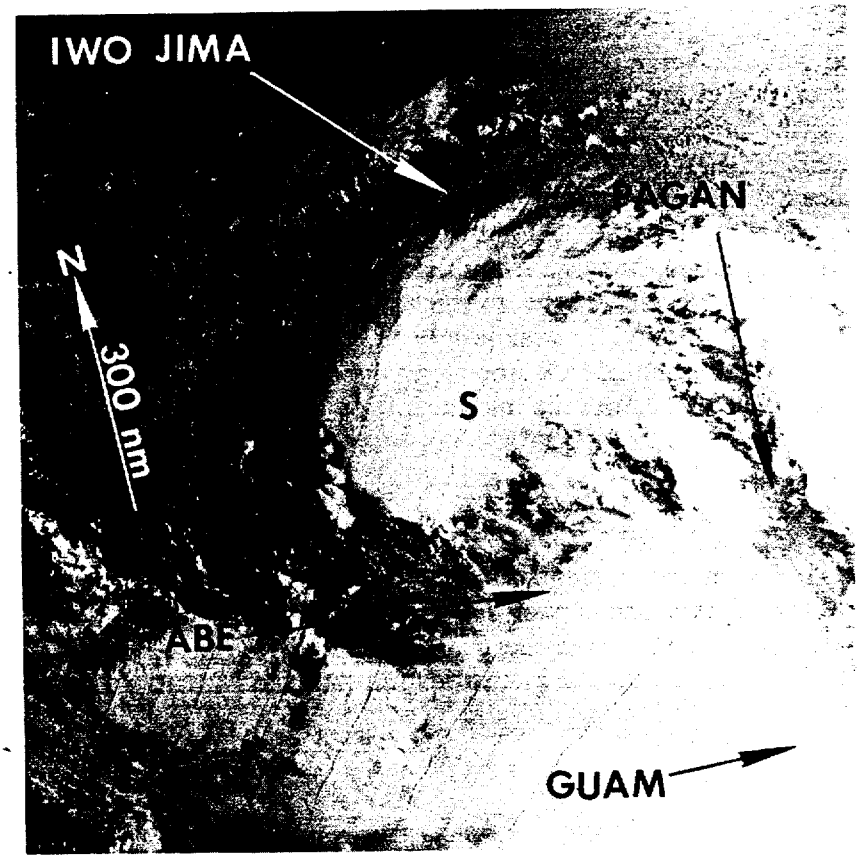

Figure 3-15-1b. The comma-shaped cloudiness (at Point S) has rotated counterclockwise around Abe's center during the past 18 hours, and is to the north (262238Z August NOAA visual imagery).

Figure 3-15-1c. The area of broken cloudiness (at Point S) which has rotated around to the west of Abel's center in the past 6 hours is associated with the monsoon surge mentioned in Figures 3-15-1a and 3-15-1b (270430Z August NOAA visual imagery).

V. FORECASTING PERFORMANCE

As illustrated by Figure 3-15-3, the overall forecast performance of JTWC for Abe was quite good with the exception of the period when Abe made the sharp turn northward due to the monsoon surge-induced reorganization. JTWC has no objective guidance that can reliably forecast the onset of deep monsoon surges or the associated track changes that might be induced. Theoretically-based synoptic reasoning that can assist forecasters in subjectively anticipating either the onset of the monsoon surge or its effects is limited. The best tool for short-range forecast intelligence is meteorological satellite imagery.

VI. IMPACT

The impact from Abe was extensive. Monsoon rains from the surge feeding into Abe caused extensive flooding in Luzon, killing 12 people in Manila. Landslides from the heavy rains resulted in 32 deaths in the provinces of Benguet, Nueva Viscaya and Nueva Ecija to the north of Manila. According to the Red Cross, the death toll in the Philippines due to the combined effects of Abe and Becky (16W) was 85. Okinawa experienced winds as high as 60 kt (31 m/sec), and high surf conditions there swept one person out to sea. Flooding in Taiwan resulted in one death and six injuries, and landfall in China resulted in 51 deaths and 250 injuries near Shanghai.

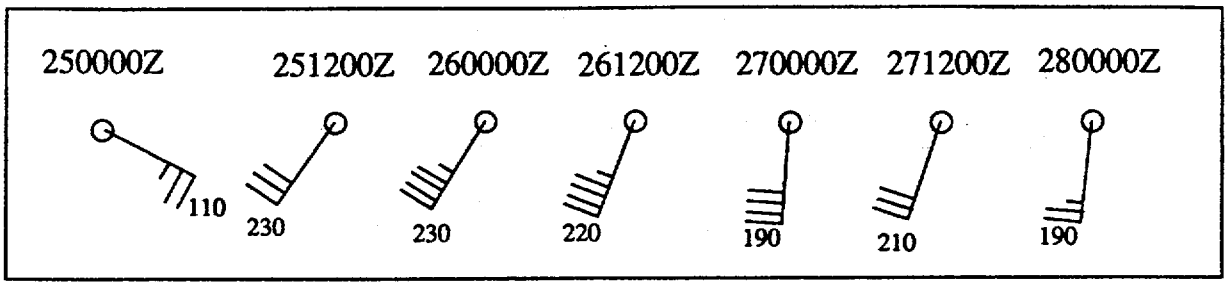

Figure 3-15-2. Gradient level winds recorded at Guam (WMO 91212) during monsoon surge associated with Abe.

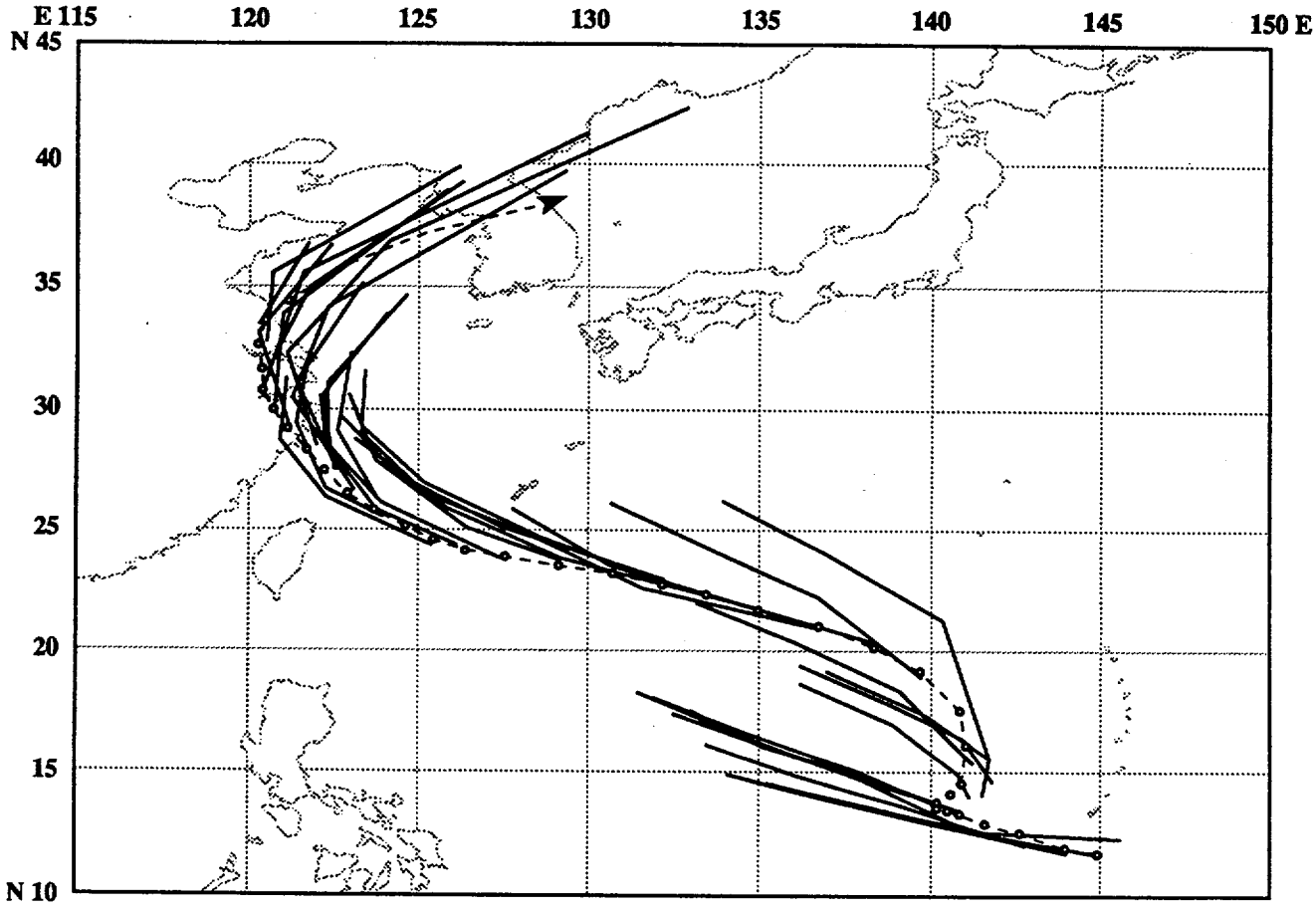

Figure 3-15-3. Summary of JTWC forecasts (solid lines) for Abe superimposed on the final best track (dashed line).

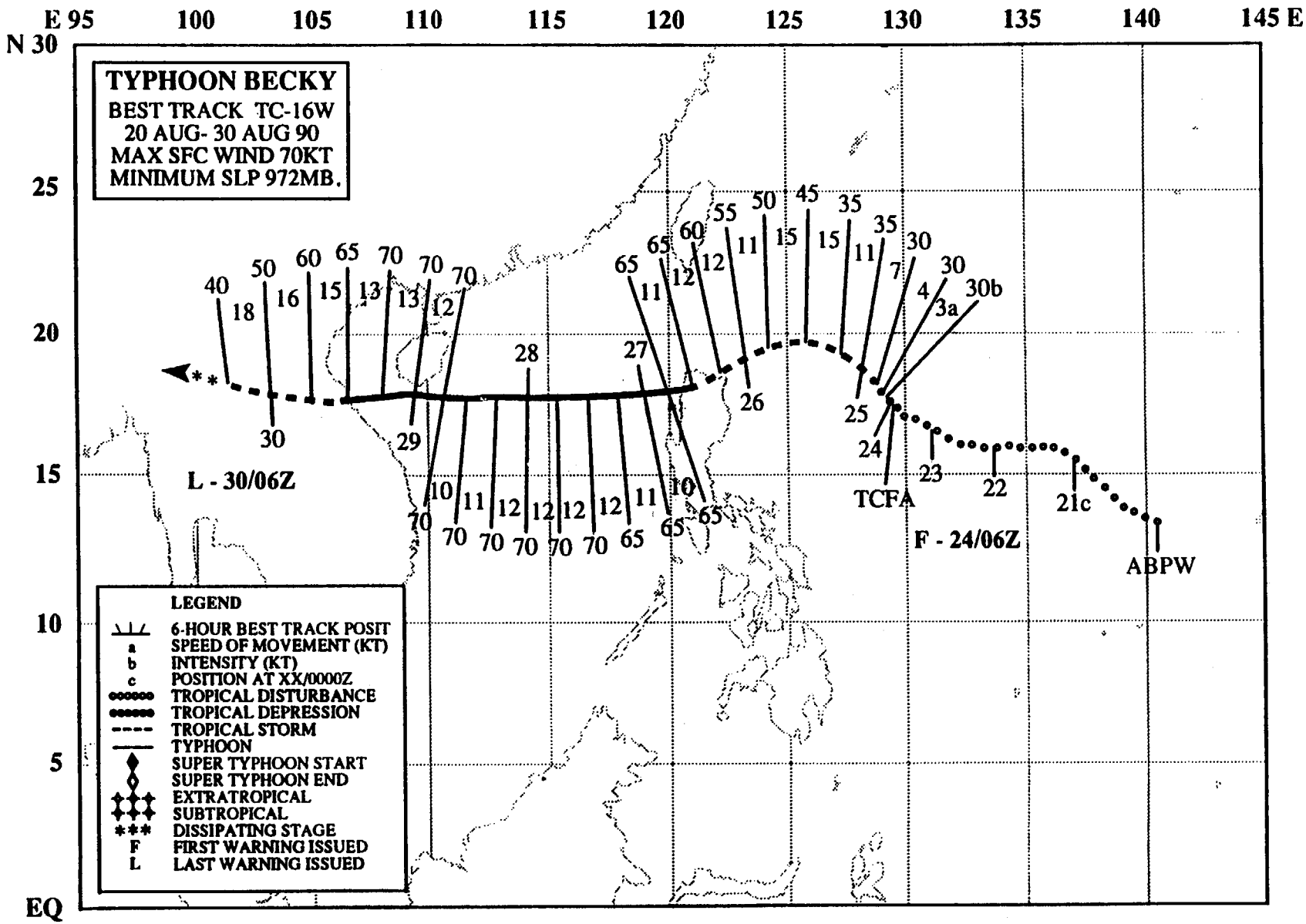
TYPHOON BECKY
BEST TRACK TC-16W
20 AUG- 30 AUG 90
MAX SFC WIND 70KT
MINIMUM SLP 972MB.
E 95
100
105
110
115
120
125
130
135
140
145 E
N 30
25
20
15
10
5
EQ
L - 30/06Z
TCFA
F - 24/06Z
ABPW
LEGEND
6-HOUR BEST TRACK POSIT
SPEED OF MOVEMENT (KT)
INTENSITY (KT)
POSITION AT XX/0000Z
TROPICAL DISTURBANCE
TROPICAL DEPRESSION
TROPICAL STORM
TYPHOON
SUPER TYPHOON START
SUPER TYPHOON END
EXTRATROPICAL
SUBTROPICAL
DISSIPATING STAGE
FIRST WARNING ISSUED
LAST WARNING ISSUED

TYPHOON BECKY (16W)

I. HIGHLIGHTS

Becky, a midget typhoon and the eleventh typhoon of 1990, generated in the monsoon trough and tracked south of the subtropical ridge throughout its existence. After initially moving west-northwestward, the storm took a southwestward track across the northwestern tip of Luzon before heading westward across the South China Sea. Becky hit northern Luzon with typhoon-force winds and later slammed into northern Vietnam as a severe tropical storm.

II. CHRONOLOGY OF EVENTS

200600Z - First mentioned on Significant Tropical Weather Advisory as an area of persistent convection with a minimum sea-level pressure of 1007 mb.

232200Z - Tropical Cyclone Formation Alert based on increased convective organization, a steady drop in sea-level pressure, and a corresponding increase in surface winds.

240600Z - First warning based on appearance of a well-developed low-level circulation center on the edge of the deep convection.

250000Z - Upgrade to tropical storm based on tighter spiral band curvature and first intensity estimate of CI 2.5.

261200Z - Upgraded to typhoon after appearance of a 10 nm (19 km) diameter eye and the first CI 4.0 satellite signature.

271200Z - Peak intensity - 70 kt (36 m/sec) - accompanied the reappearance of a small 8 nm (15 km) diameter ragged eye.

291800Z - Downgraded to tropical storm intensity after the central dense overcast degenerated into a poorly defined spiral cloud band.

300600Z - Final warning - dissipated over land.

III. TRACK AND MOTION

After forming 275 nm (510 km) west of Guam, Becky tracked slowly west-northwestward under the influence of the subtropical ridge (Figure 3-16-1) that was building westward across the wake of Typhoon Zola (14W) which was moving through the Sea of Japan. While Becky approached northern

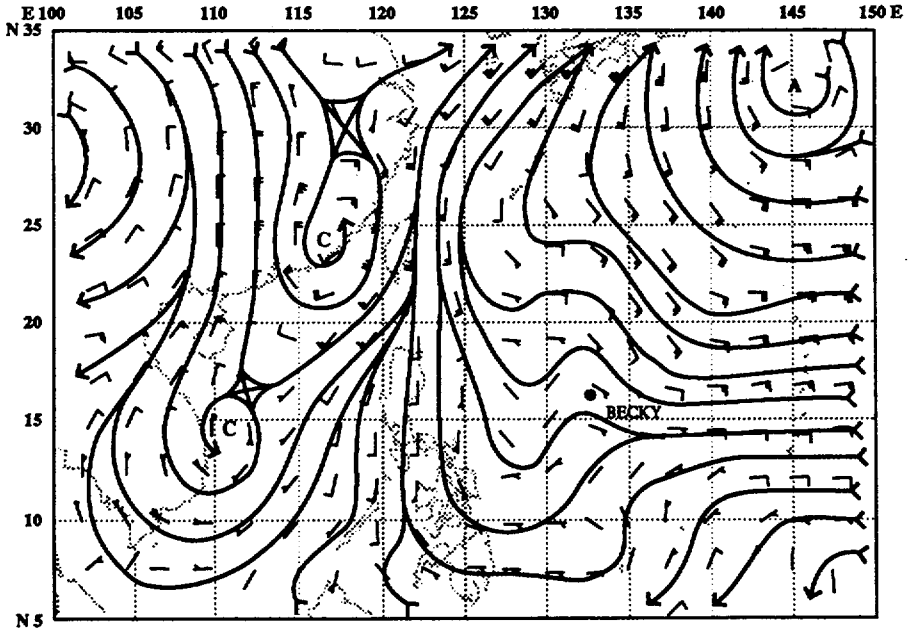

Figure 3-16-1. Deep layer mean circulation analysis from 221200Z August shows ridging north of Becky and troughing over the east coast of China.

Luzon, the trough shown over eastern China in Figure 3-16-1 moved eastward and filled (Figure 3-16-2). Subsequently, Becky accelerated as the steering flow strengthened and tracked to the west-southwest for the next day-and-a-half. With the high established to the north, the typhoon tracked due west and made landfall in northern Vietnam.

IV. INTENSITY

The disturbance that developed into Typhoon Becky originated in the low-level monsoon trough and the cloudiness left behind after Typhoon Zola (14W) separated from the trough. Strong northerly upper-level outflow from Zola slowed early development of Becky. Reestablishment of the TUTT to the north of the tropical cyclone effectively reduced the vertical shear and allowed the tropical cyclone to reach tropical storm intensity on 25 August. Becky attained minimal typhoon intensity and exhibited a 10 nm (19 km) diameter eye just as it crossed the northwestern tip of Luzon (Figure 3-16-3). After entering the South China Sea, Becky (Figure 3-16-4) maintained minimum typhoon intensity until it made landfall in northern Vietnam and rapidly dissipated.

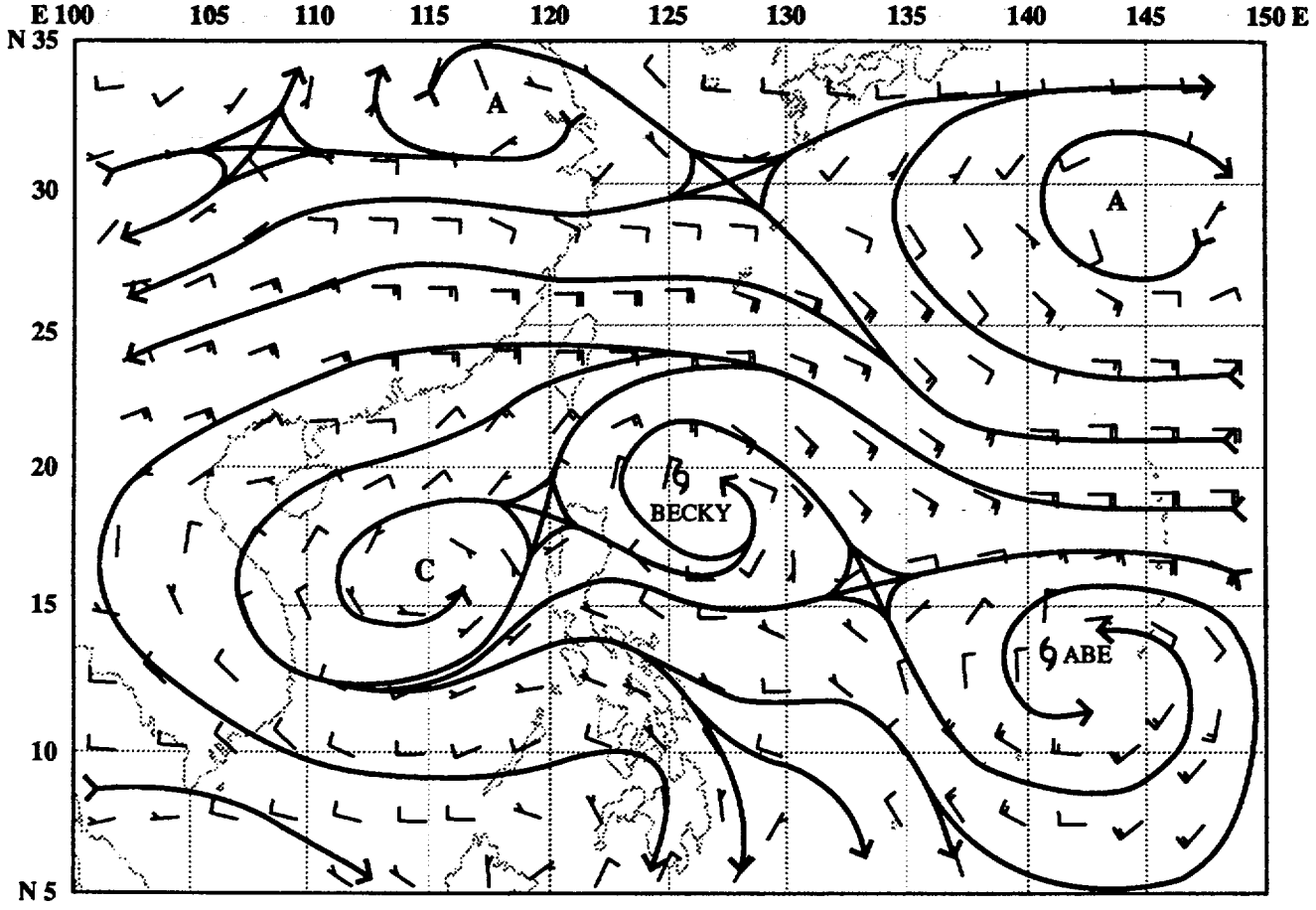

Figure 3-16-2. Deep layer mean circulation analysis for 251200Z August shows ridging over northeast China.

Figure 3-16-3. Becky reaches minimum typhoon intensity just as it hits northern Luzon (260039Z August DMSP visual imagery).

V. FORECASTING PERFORMANCE

Except for the first two warnings, JTWC correctly anticipated that Becky would turn and accelerate onto a more west-northwestward heading as it passed northern Luzon in response to the building ridge over eastern Asia (Figure 3-16-5). However, the strength of the ridge development was underestimated, resulting in a delay in forecasting the west-southwest portion of Becky's track.

VI. IMPACT

Becky crossed northern Luzon as it reached typhoon intensity, killing 32 people and forcing the evacuation of thousands due to heavy flooding. News reports from Vietnam stated that the northern province of Nghe Tinh experienced winds greater than 60 kt (30 m/sec) which severely damaged 400,000 acres of rice paddy and many homes. Three boats with a total of 20 fishermen aboard were reported missing.

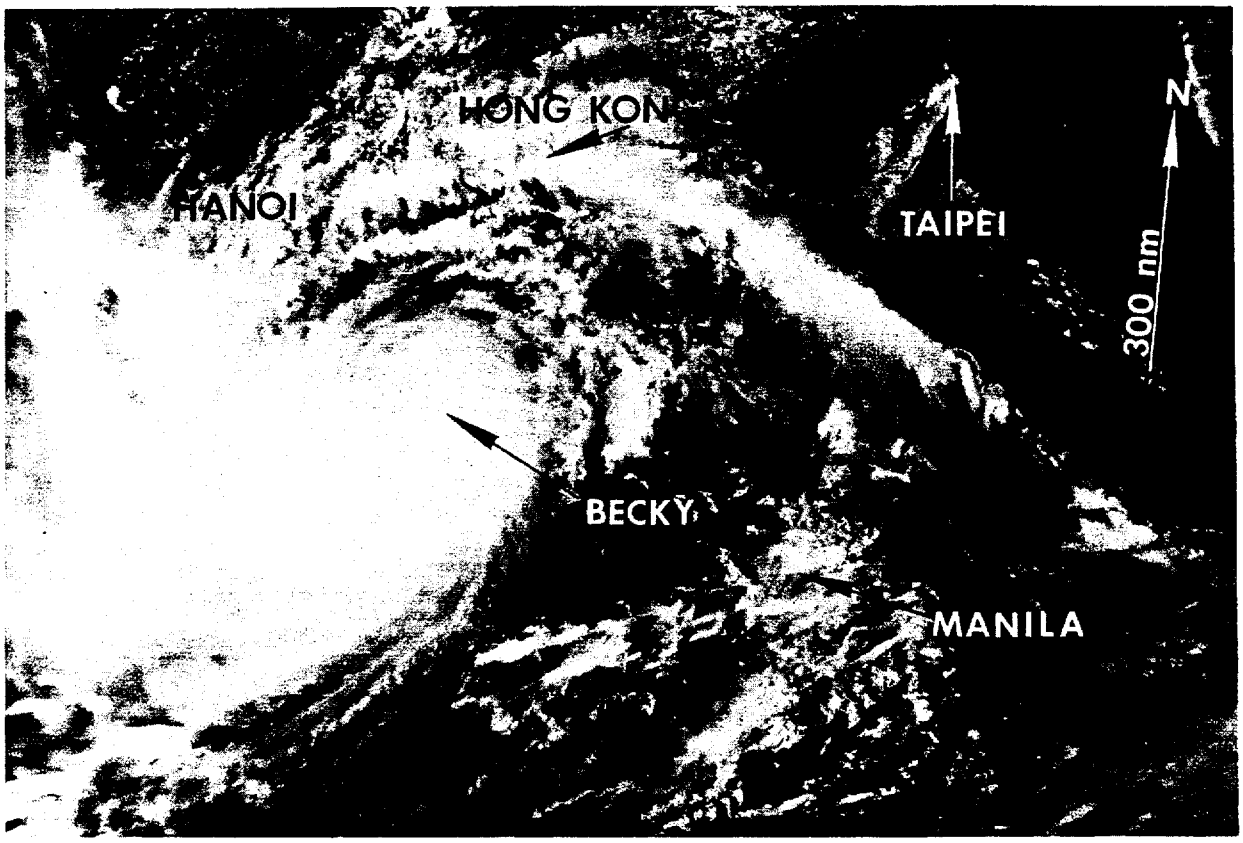

Figure 3-16-4. Becky at peak intensity of 70 kt (36 m/sec) before making landfall in northern Vietnam (280600Z August NOAA visual imagery).

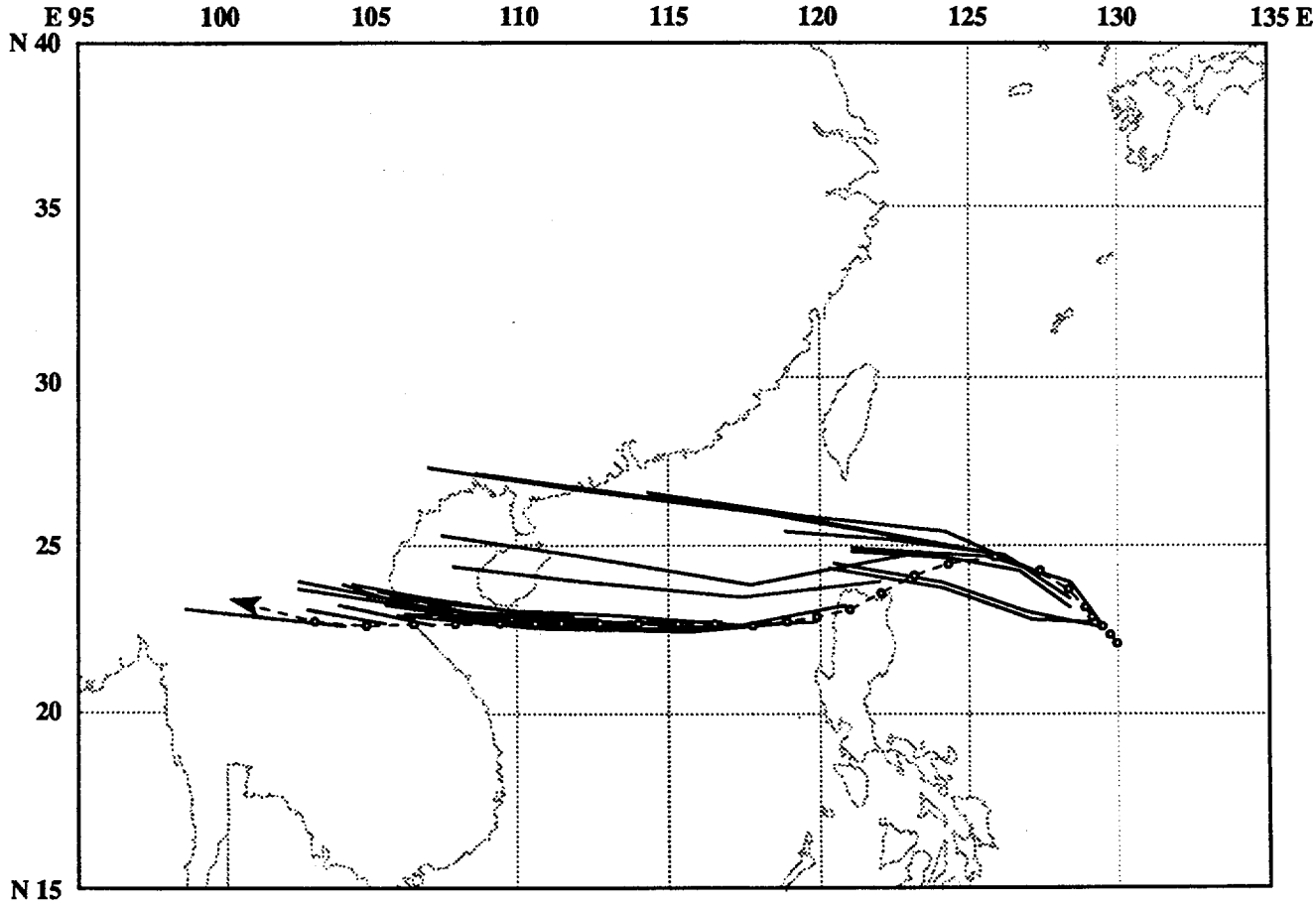

Figure 3-16-5. Summary of JTWC forecasts (solid lines) for Becky superimposed on the final best track (dashed line).

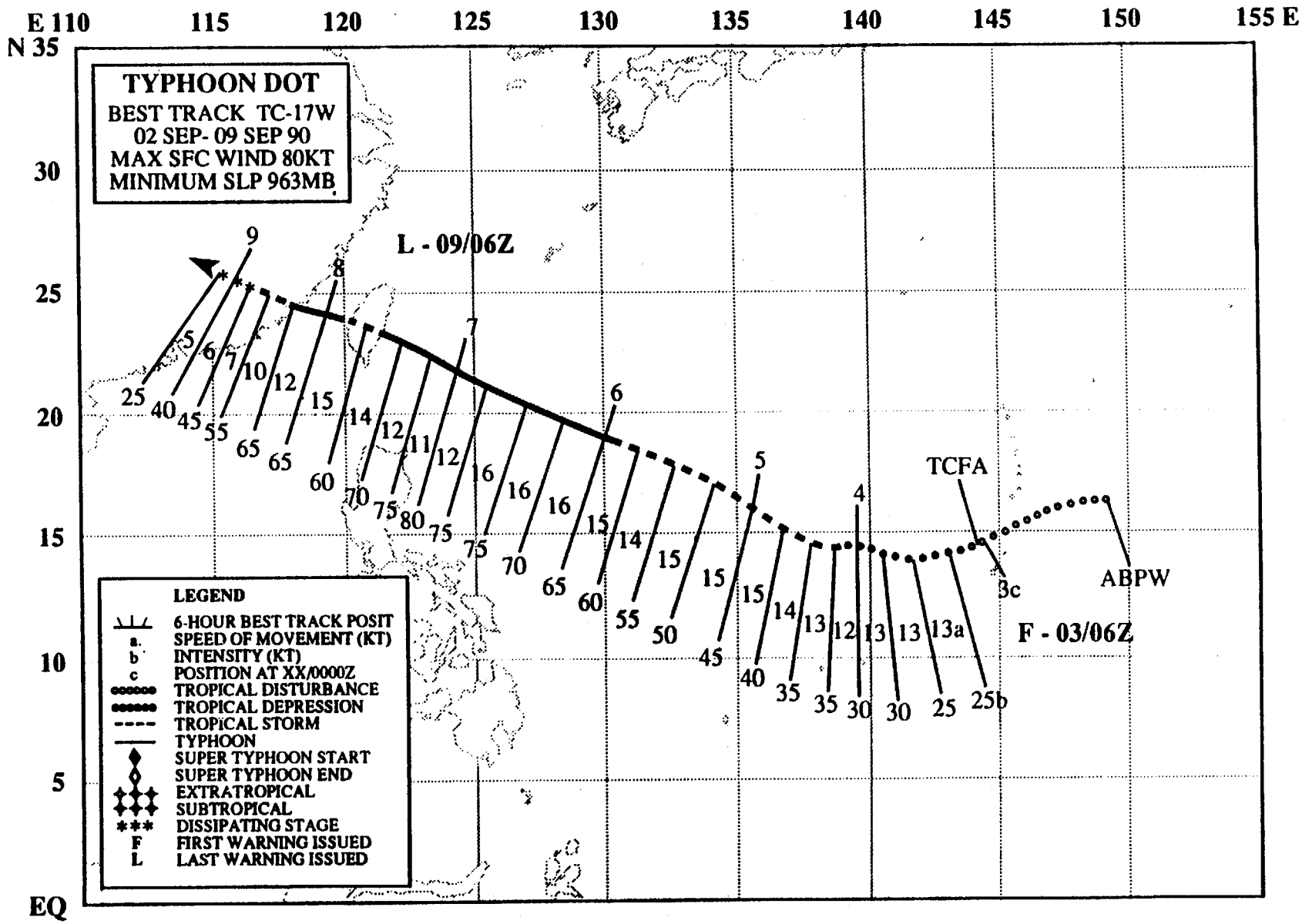
E 110
115
120
125
130
135
140
145
150
155 E
N 35
30
25
20
15
10
5
EQ
TYPHOON DOT
BEST TRACK TC-17W
02 SEP- 09 SEP 90
MAX SFC WIND 80KT
MINIMUM SLP 963MB
L - 09/06Z
F - 03/06Z
TCFA
3c
ABPW
25b
LEGEND
6-HOUR BEST TRACK POSIT
a. SPEED OF MOVEMENT (KT)
b INTENSITY (KT)
c POSITION AT XX/0000Z
TROPICAL DISTURBANCE
TROPICAL DEPRESSION
TROPICAL STORM
TYPHOON
SUPER TYPHOON START
SUPER TYPHOON END
EXTRATROPICAL
SUBTROPICAL
DISSIPATING STAGE
F FIRST WARNING ISSUED
L LAST WARNING ISSUED

TYPHOON DOT (17W)

I.HIGHLIGHTS

Dot developed in the monsoon trough at the same time as Tropical Storm Cecil (18W) and brought enhanced southwesterly wind flow and heavy rains across Guam. Later, as Dot crossed central Taiwan, torrential monsoon rains from the associated monsoon surge caused extensive flooding in northern Luzon. During its passage across Taiwan and the Fujian Province of China, surface winds in the Formosa Strait exceeded 50 kt (26 m/sec) for 30 hours.

II. CHRONOLOGY OF EVENTS

300600Z - (August) First mentioned on the Significant Tropical Weather Advisory as a weak cyclonic circulation.
030100Z - (September) Tropical Cyclone Formation Alert issued due to improved vertical alignment between the low level circulation and the convection.
030600Z - First warning prompted by increased convective cloud organization.
040600Z - Upgrade to tropical storm based on consolidation of central cloud mass.
060000Z - Upgrade to typhoon based on formation of a banding-type eye.
070000Z - Peak intensity - 80 kt (41 m/sec) - as deep convection around a ragged eye increased.
071800Z - Downgraded to tropical storm due to the effects of mountainous terrain in central Taiwan.
080000Z - Upgraded to typhoon as eye redeveloped over the Formosa Strait.
081200Z - Final warning - dissipated - after Dot moved over land.

III. TRACK AND MOTION

The disturbance which later became Dot generated in the eastern extension of an active monsoon trough. Initially, Dot's cloud system center remained poorly organized and difficult to position. Consequently, six of the first seven warnings on the tropical cyclone were relocated as the convection fluctuated between the multiple circulation centers in the broad monsoon trough (Figure 3-17-1). After

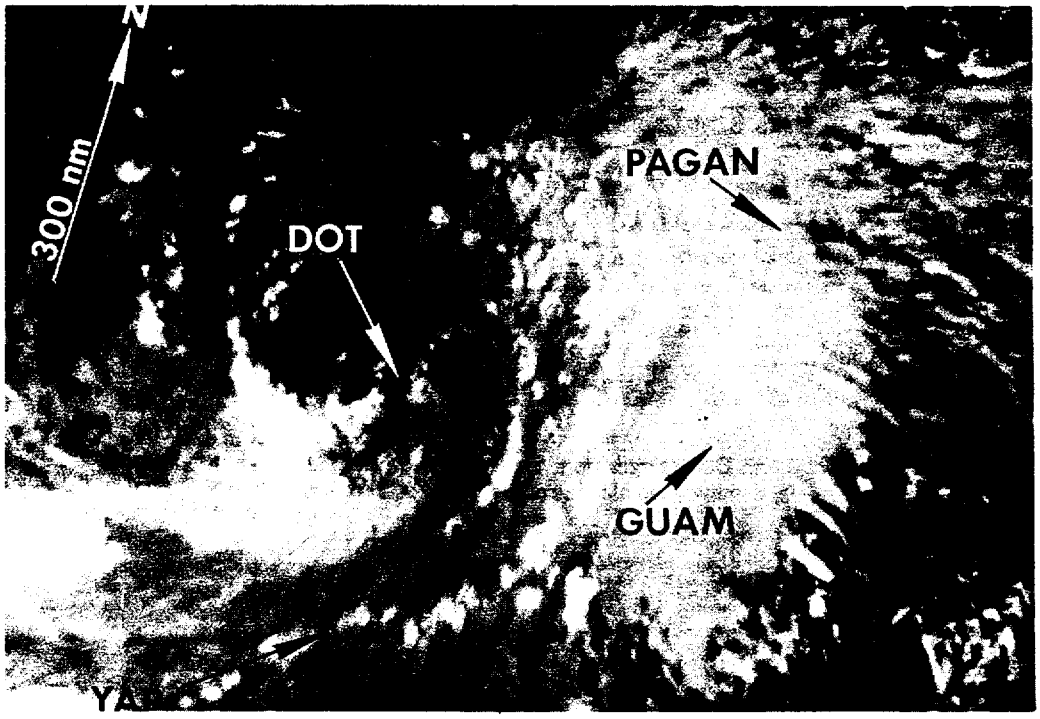

Figure 3-17-1. The broad circulation associated with Tropical Depression 17W extends over 300 nm (483 km) from its poorly defined circulation center (040423Z September NOAA visual imagery).

consolidation took place on 5 September (Figure 3-17-2), Dot tracked steadily west-northwestward south of the subtropical ridge, crossed central Taiwan and dissipated over Fujian Province in southeastern China.

Figure 3-17-2. Tropical Storm Dot emerges from the monsoon trough and begins to consolidate around a single, dominant circulation center (042232Z September NOAA visual imagery).

IV. INTENSITY

As a broad monsoon depression, Dot intensified at a rate of only 5 kt (3 m/sec) per day in its early stage of development. As the upper-level shear across the system diminished, convection increased around the circulation center, and a faster rate of intensification commenced. After becoming a tropical, Dot intensified at a steady rate of 20 kt (10 m/sec) per day prior to landfall in Taiwan. At maximum intensity, Typhoon Dot had a ragged eye approximately 25 nm (40 km) in diameter (Figure 3-17-3).

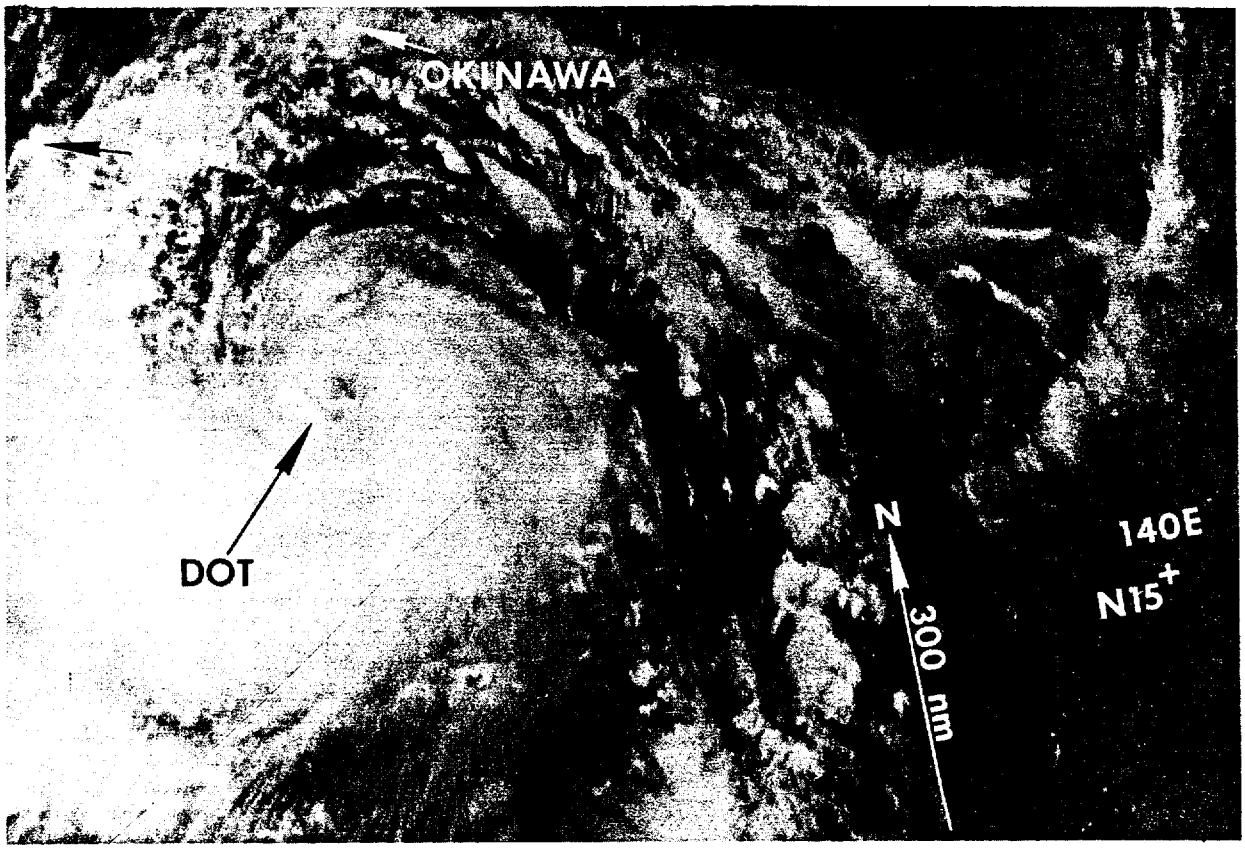

Figure 3-17-3. Typhoon Dot 11 hours prior to reaching maximum intensity east of Taiwan (061251Z September DMSP visual imagery)

Dot weakened significantly over the mountainous terrain of central Taiwan, then reintensified in the Formosa Strait. Dot's ragged eye was visible on radar (Figure 3-17-4) prior to landfall south of Zhangzhou in southern China.

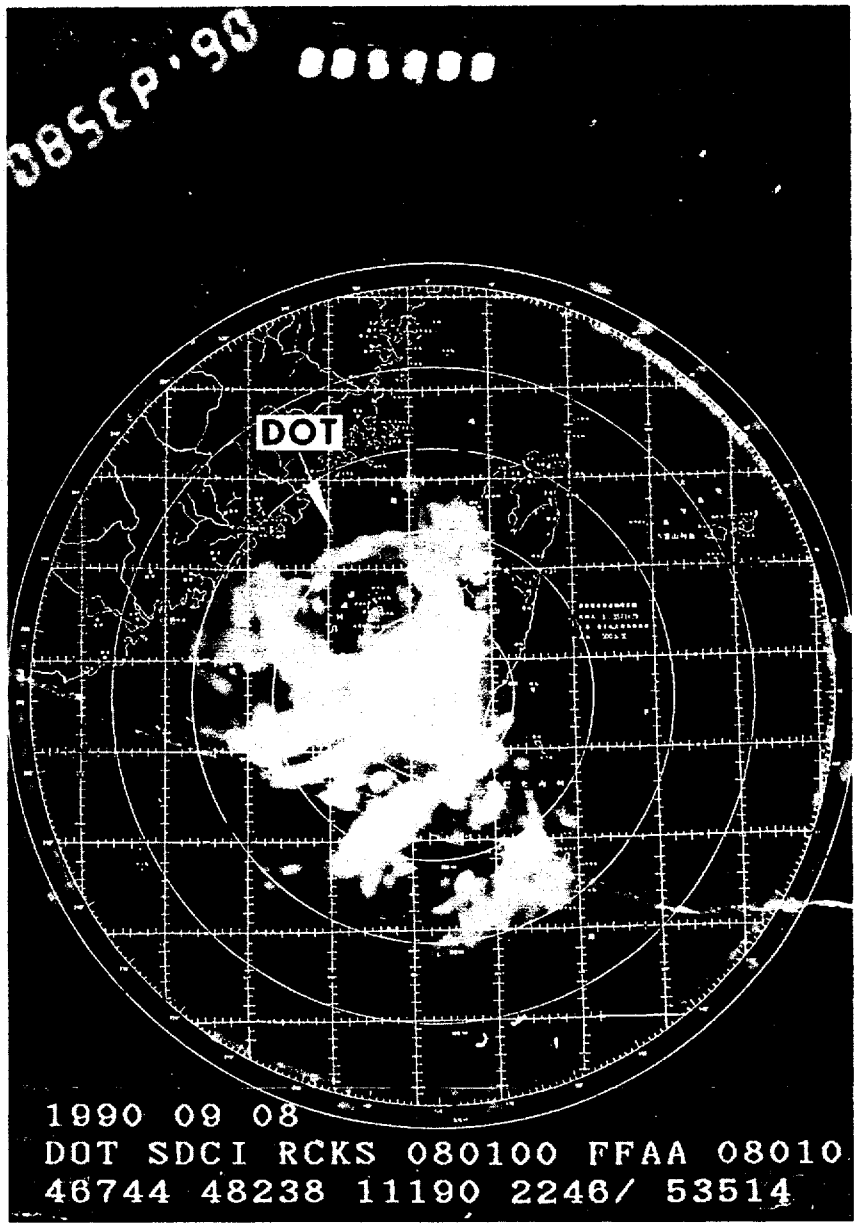

Figure 3-17-4. Evidence of redevelopment of an eye after Typhoon Dot passed across central Taiwan as seen by radar at Kaohsiung (WMO 46744) at 080100Z September (Photograph courtesy of Central Weather Bureau, Taipei, Taiwan).

V. FORECASTING PERFORMANCE

The overall JTWC forecast performance is shown in Figure 3-17-5. Uncertainty about Dot's motion on 4 September resulted in larger forecast errors, but once its motion was more clearly established, JTWC forecast a west-northwestward track south of the subtropical ridge.

VI. IMPACT

Heavy rains from convergent low-level wind flow into Dot caused flooding on Guam, Luzon and Taiwan. The floods in northern Luzon caused the deaths of four people and the evacuation of an estimated 65,000 more. At least three deaths were reported in Taiwan.

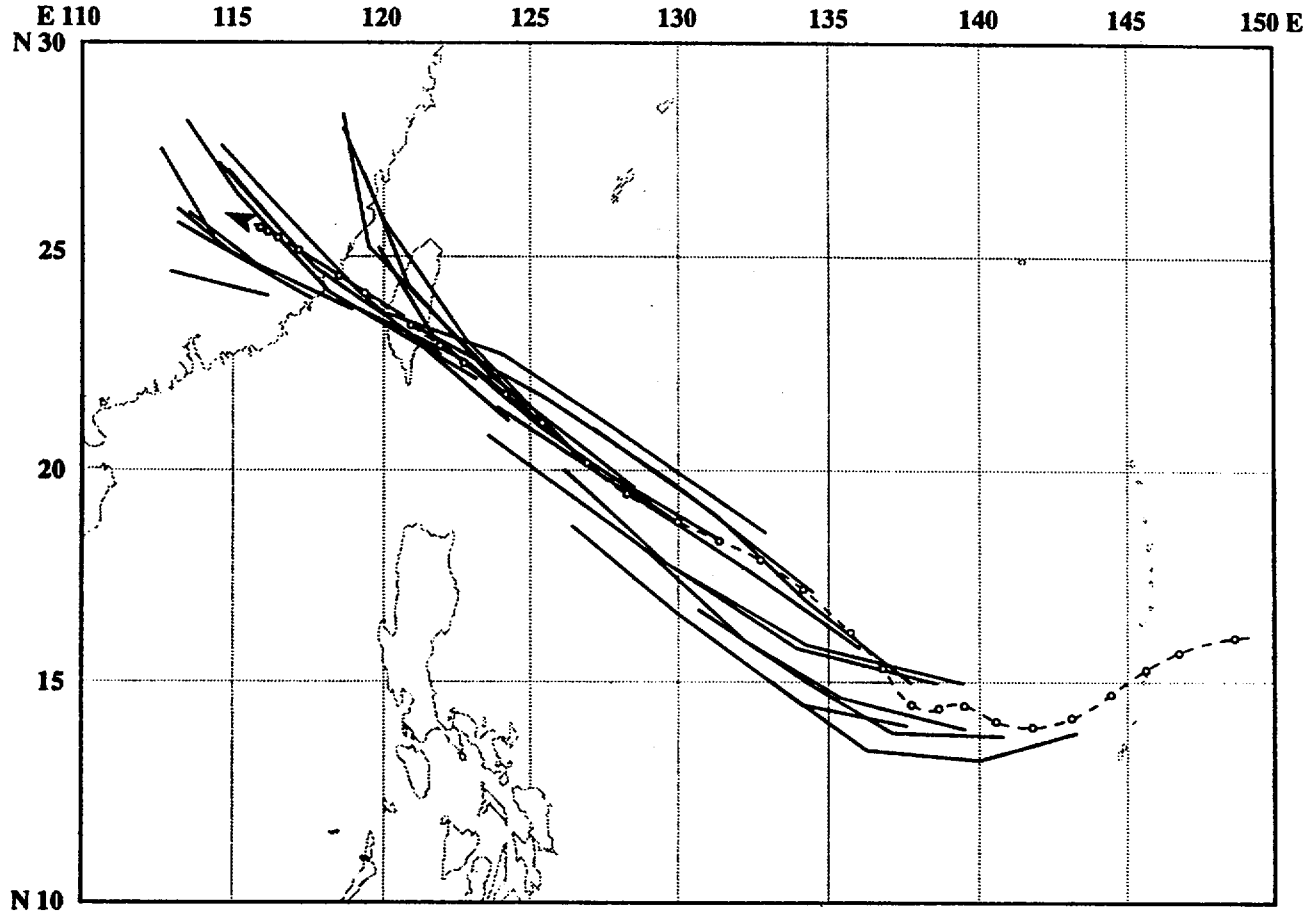

Figure 3-17-5. Summary of JTWC forecasts (solid lines) for Dot superimposed on the final best track (dashed line).

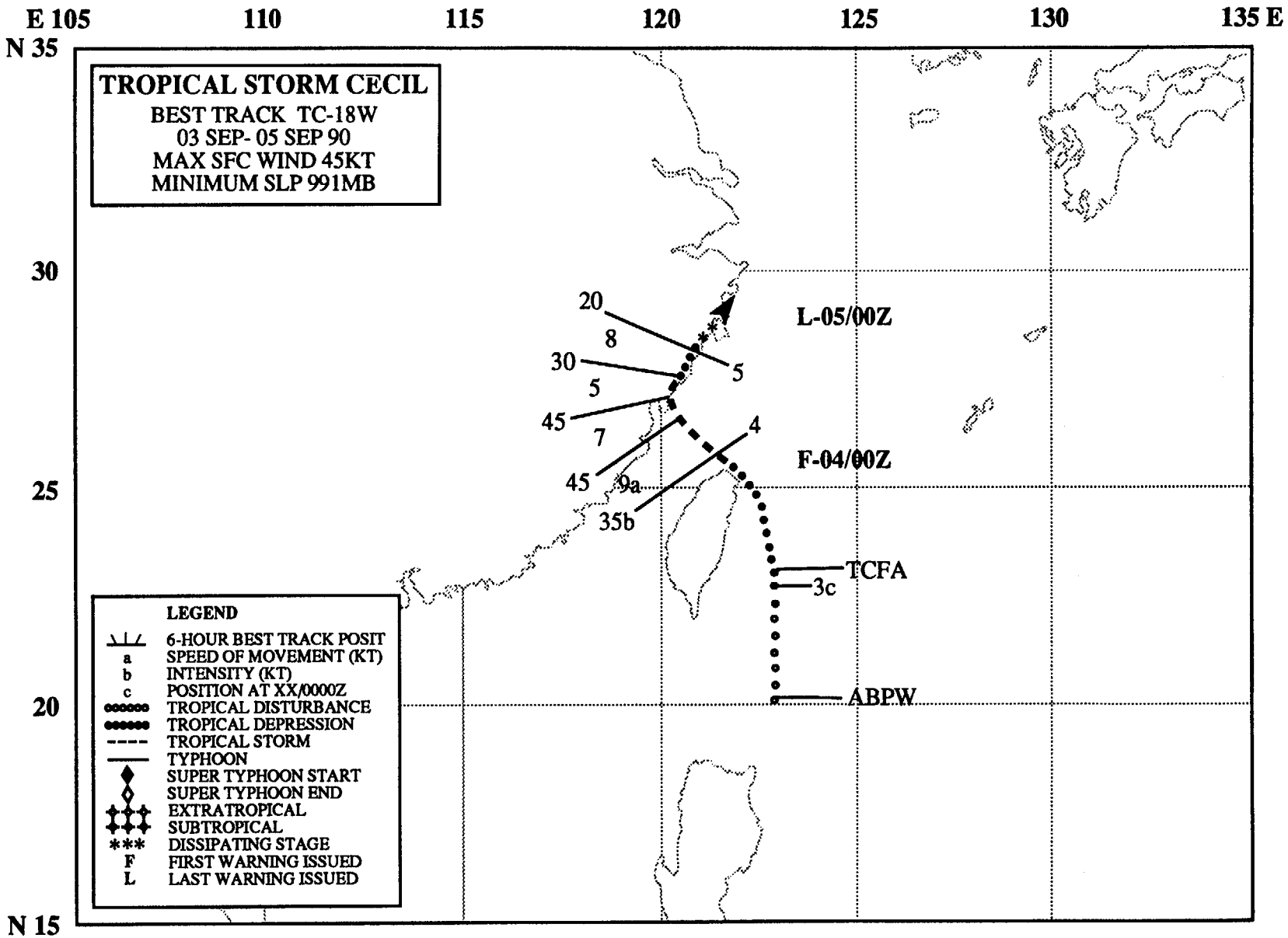
E 105
110
115
120
125
130
135 E
N 35
30
25
20
N 15
TROPICAL STORM CECIL
BEST TRACK TC-18W
03 SEP- 05 SEP 90
MAX SFC WIND 45KT
MINIMUM SLP 991MB
20
8
30
5
45
7
45
9a
35b
4
5
L-05/00Z
F-04/00Z
TCFA
3c
ABPW
LEGEND
6-HOUR BEST TRACK POSIT
a SPEED OF MOVEMENT (KT)
b INTENSITY (KT)
c POSITION AT XX/0000Z
TROPICAL DISTURBANCE
TROPICAL DEPRESSION
TROPICAL STORM
TYPHOON
SUPER TYPHOON START
SUPER TYPHOON END
EXTRATROPICAL
SUBTROPICAL
*** DISSIPATING STAGE
F FIRST WARNING ISSUED
L LAST WARNING ISSUED

TROPICAL STORM CECIL (18W)

I. HIGHLIGHTS

Tropical Storm Cecil was a short-lived, midget tropical cyclone that formed in the wake of Typhoon Abe (15W). As Abe raced poleward, the monsoon trough reestablished itself over northern Luzon, and Cecil formed at the northeast end of the trough. Cecil tracked northward and skirted the northern coast of Taiwan before making landfall in southeastern China.

II. CHRONOLOGY OF EVENTS

020600Z - First mentioned on Significant Tropical Weather Advisory as a low level cyclonic circulation in the monsoon trough.
030400Z - Tropical Cyclone Formation Alert issued due to Dvorak intensity estimate of CI 1.5.
040000Z - First tropical storm warning issued after Dvorak analysis jumped up to CI 2.5.
040600Z - Peak intensity - 45 kt (23 m/sec) - based on synoptic report.
050000Z - Final warning issued as Cecil moved over land and dissipated.

III. TRACK AND MOTION

After Abe (15W) moved inland and northward over China, Cecil formed northeast of Luzon in association with a surge in the monsoon. Cecil tracked northward around the western periphery of the maritime subtropical ridge. As the tropical cyclone approached northern Taiwan, it turned northwestward and made landfall over southeastern China.

IV. INTENSITY

The mountainous terrain of Taiwan inhibited Cecil's development, however the tropical cyclone consolidated on a smaller than normal scale to become a midget tropical storm. The peak intensity of 45 kt (23 m/sec) was attained while crossing the Formosa Strait. Cecil (Figure 3-18-1) dissipated rapidly after making landfall over mainland China.

V. FORECASTING PERFORMANCE

The overall JTWC forecast performance is shown in Figure 3-18-2. Forecasters initially expected Cecil to continue to track northward around the western side of the subtropical ridge. Subsequent forecasts reflected the northwestward track across the Formosa Strait and dissipation over land.

VI. IMPACT

No information was received.

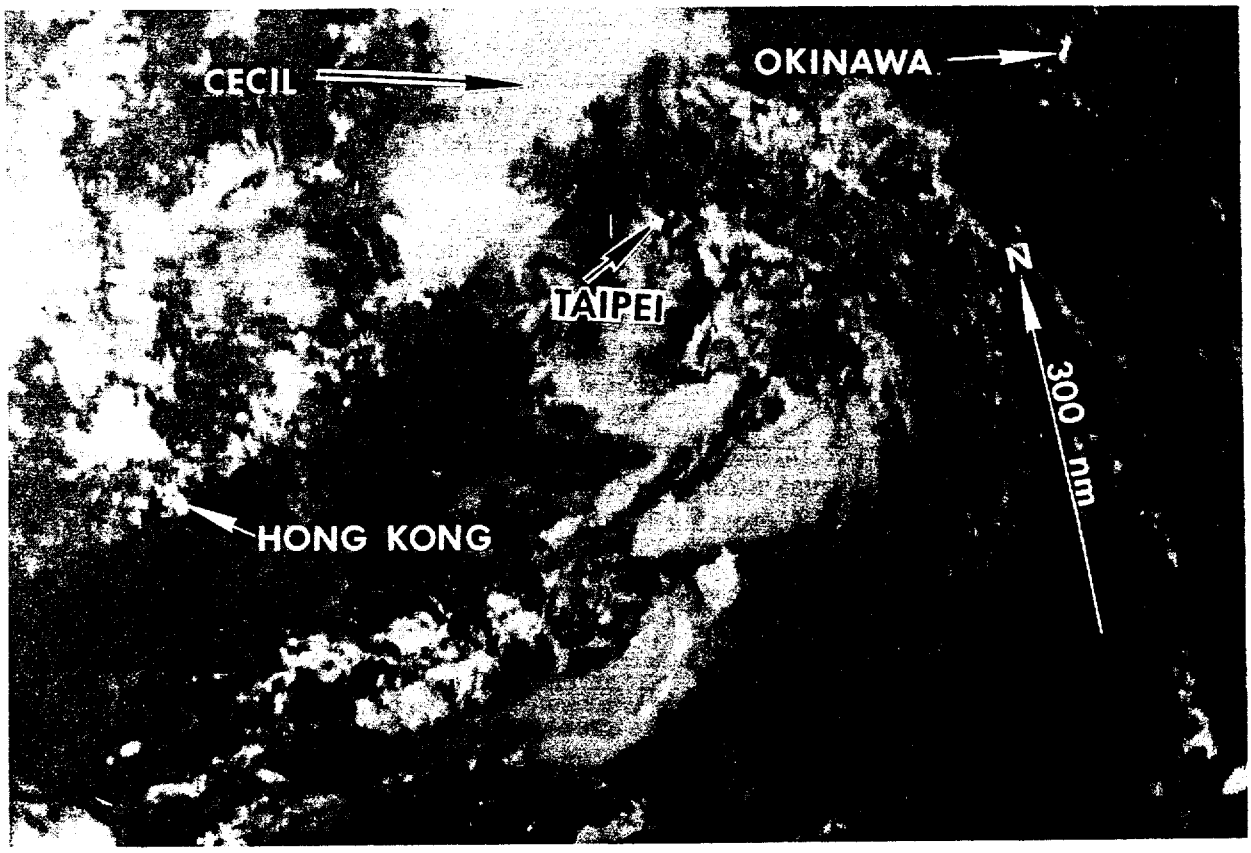

Figure 3-18-1. Moonlight photo of Cecil's small central dense overcast just on the coast of southeastern China. There is another tropical disturbance just southeast of Taipei. Note the bright city lights of Hong Kong, Taipei and Okinawa (041333Z September DMSP visual imagery).

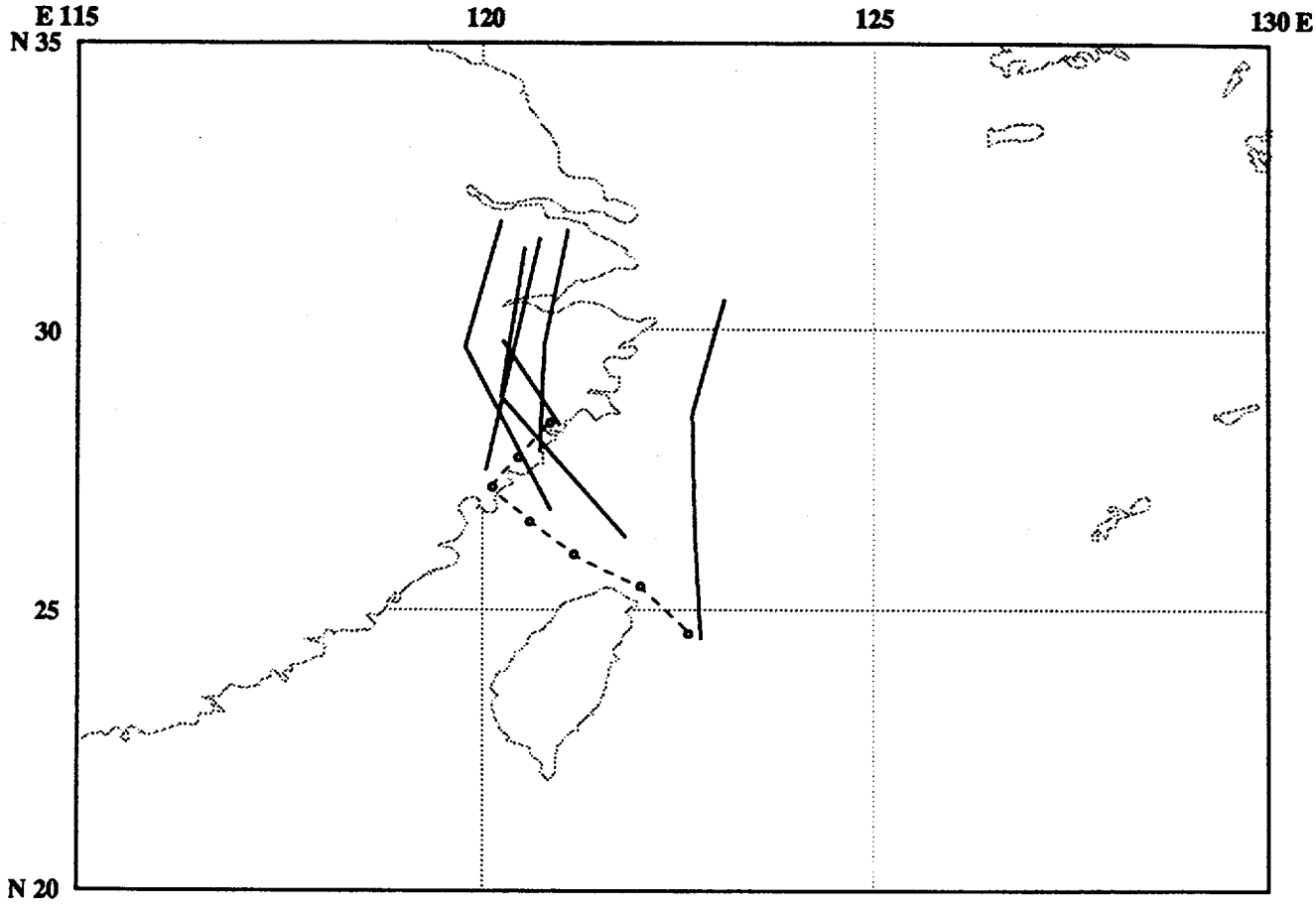

Figure 3-18-2. Summary of JTWC forecasts (solid lines) for Cecil are superimposed on the best track (dashed line).

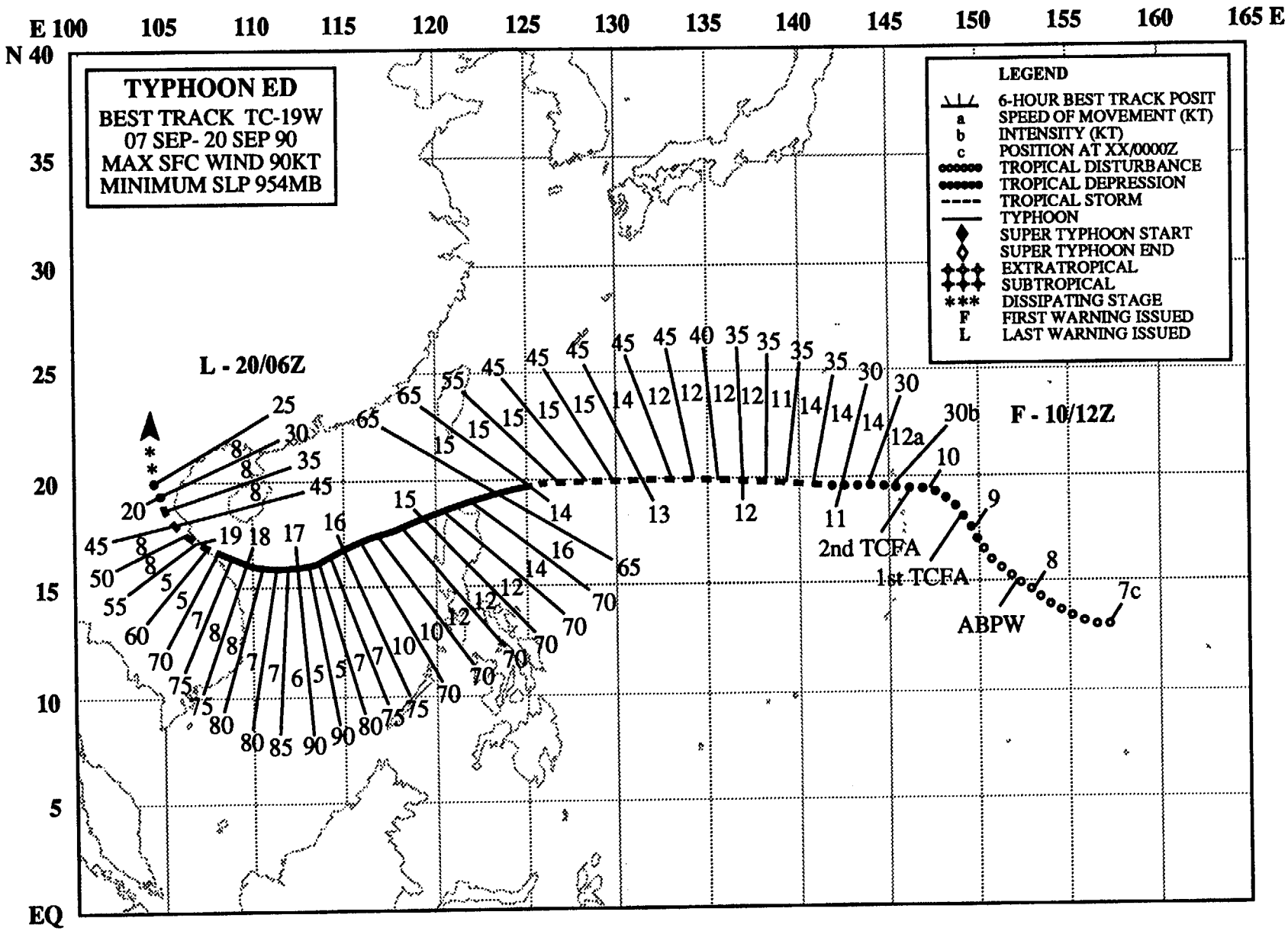
TYPHOON ED
BEST TRACK TC-19W
07 SEP- 20 SEP 90
MAX SFC WIND 90KT
MINIMUM SLP 954MB
LEGEND
6-HOUR BEST TRACK POSIT
a SPEED OF MOVEMENT (KT)
b INTENSITY (KT)
c POSITION AT XX/0000Z
TROPICAL DISTURBANCE
TROPICAL DEPRESSION
TROPICAL STORM
TYPHOON
SUPER TYPHOON START
SUPER TYPHOON END
EXTRATROPICAL
SUBTROPICAL
*** DISSIPATING STAGE
F FIRST WARNING ISSUED
L LAST WARNING ISSUED
L - 20/06Z
F - 10/12Z
2nd TCFA
1st TCFA
ABPW
E 100
105
110
115
120
125
130
135
140
145
150
155
160
165 E
N 40
35
30
25
20
15
10
5
EQ

TYPHOON ED (19W)

I. HIGHLIGHTS

Ed, which had the second longest track (3150 nm (5835 km)) of any "straight runner" in 1990, formed in the Marshall Islands and continued westward for nearly two weeks before finally making landfall in northern Vietnam. It was the third of six tropical cyclones to form in September.

II. CHRONOLOGY OF EVENTS

080600Z - First mentioned on Significant Tropical Weather Advisory as an area of persistent convection with an estimated minimum sea-level pressure of 1008 mb.

090730Z - First Tropical Cyclone Formation Alert based on increased in convective organization; synoptic data in the area indicating a small compact surface circulation; and favorable outflow conditions aloft.

100600Z - Second Tropical Cyclone Formation Alert based on persistent, well developed low-level circulation indicated by synoptic data.

101200Z - First warning followed improved organization in the convection, fair upper-level outflow in all quadrants and the first intensity estimate of CI 2.0.

121200Z - Upgrade to a tropical storm based on synoptic data, consolidation of the convection, improved upper-level outflow and the first intensity estimate of CI 2.5.

140000Z - Upgraded to typhoon due to better definition in the spiral banding, development of a partial eye wall and the first intensity estimate of CI 4.0.

181800Z - Downgraded to tropical storm based on a decrease in central convection, and an intensity estimate of CI 3.5.

200000Z - Downgraded to a tropical depression after a decrease in organization, land interaction and an intensity estimate of CI 2.0.

200600Z - Final warning - dissipated over land - issued as Ed moved inland over northern Vietnam.

III. TRACK AND MOTION

As a disturbance, Ed initially tracked northwestward in response to the deep layer flow around the subtropical anticyclone to the northeast (Figure 3-19-1). The tropical cyclone became involved in a

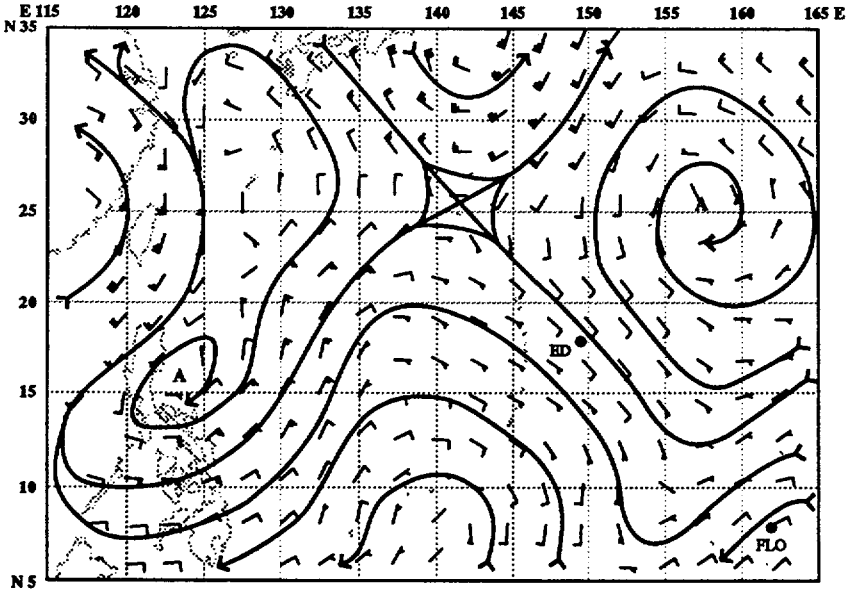

Figure 3-19-1. NOGAPS deep layer mean analysis from 090000Z September showing Ed embedded in southeasterly flow associated with the anticyclone to the northeast. Flo (20W) is located to the southeast of Ed.

ridge building process to the north and took a more westerly track on 10 September. Then the mid-level ridge strengthened to the north (Figure 3-19-2) and the typhoon turned west-southwestward at 140000Z. For four days Ed continued to track to the west-southwest before turning northwestward along the coast of Vietnam. The northwestward turn appeared to be the combined result of the steering flow becoming southerly when a mid-level ridge formed between Ed and Flo (20W)(Figure 3-19-3), and the barrier

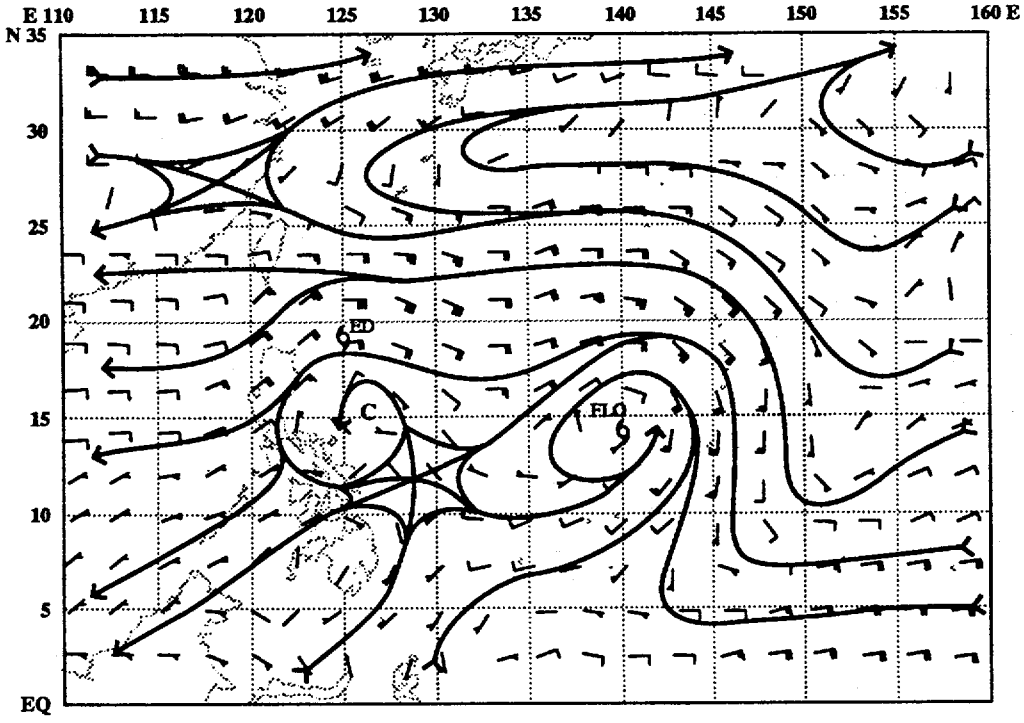

Figure 3-19-2. NOGAPS deep layer mean analysis from 140000Z September shows the increased wind flow between Ed and the building subtropical ridge to the north. Flo (20W) is located to the east-southeast of Ed.

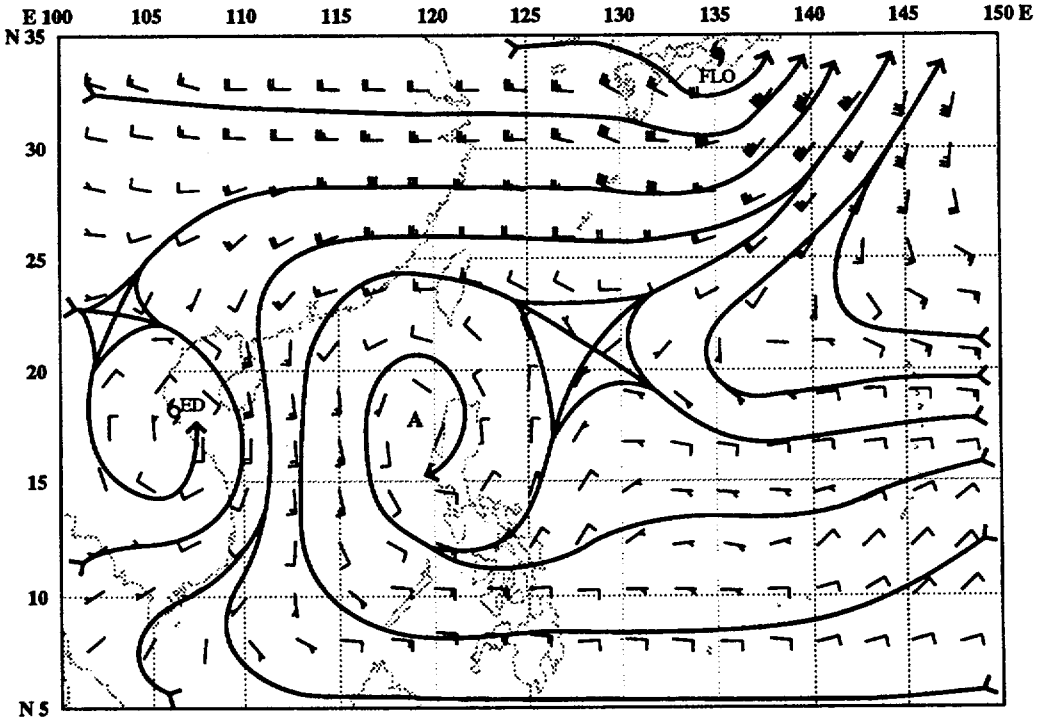

Figure 3-19-3. NOGAPS deep layer mean analysis from 191200Z September shows a mid-level anticyclone over the Philippine Islands producing southerly flow across the South China Sea.

effect of the coastal mountains of Vietnam.

IV. INTENSITY

On 10 September, Ed's compact cluster of cumulonimbus clouds moved into a more favorable upper-level environment with low vertical wind shear. At the same time, the disturbance which would later become Flo (20W), was rapidly taking shape southeast of Guam (Figure 3-19-4). The 20-30 kt (10-15 m/sec) low-level monsoonal southwesterlies to the south aided the development of both systems. Intensification continued at a normal rate of one T-number per day, and Ed became a typhoon on 14 September (Figure 3-19-5). The tropical cyclone maintained typhoon intensity until it struck the Vietnamese coast on 18 September.

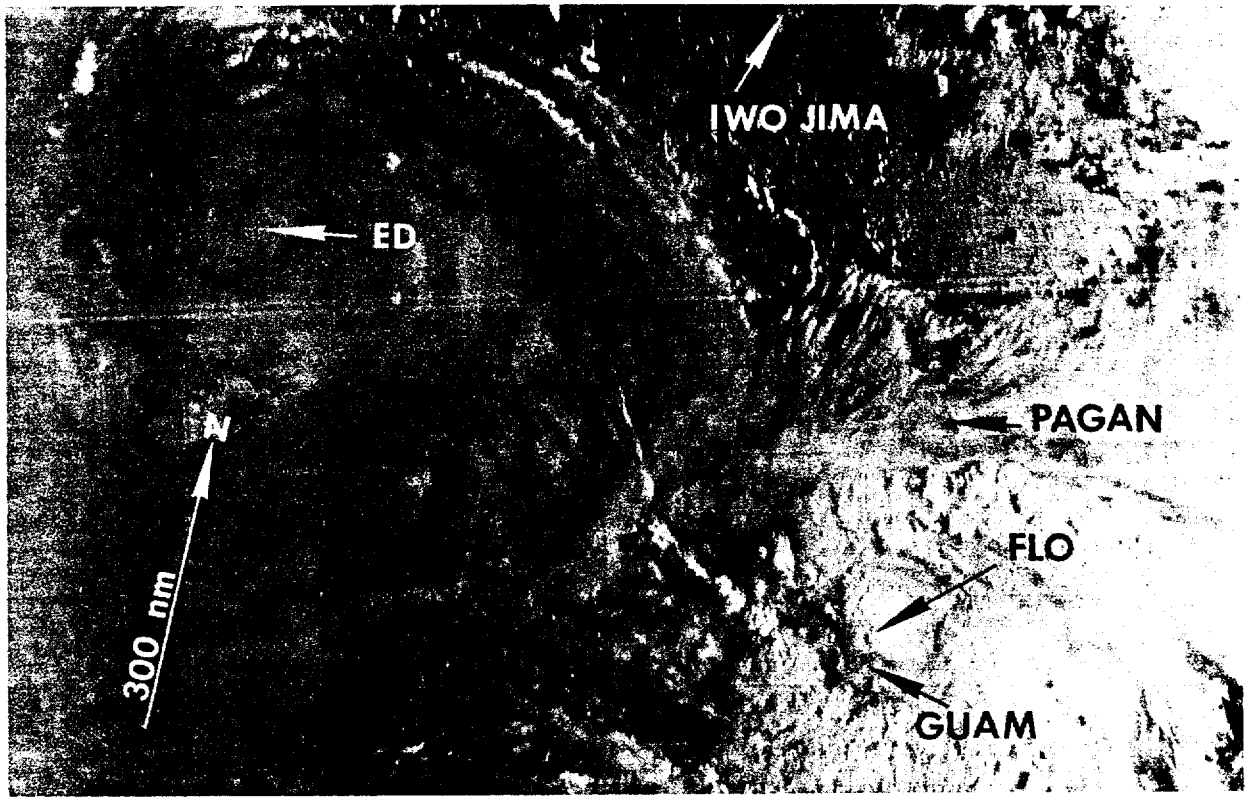

Figure 3-19-4. Tropical Storm Ed as it moves westward across the Philippine Sea. Tropical Storm Flo is rapidly developing to the southeast near Guam (122042Z September DMSP visual imagery).

V. FORECASTING PERFORMANCE

The overall JTWC forecast performance is shown in Figure 3-19-6. The initial forecasts were to the right of Ed's westward track and were influenced by the NOGAPS 500-mb prognostic series, which continued to forecast significant weakening of the mid-level ridge over the East China Sea. The ridge actually strengthened, keeping the tropical cyclone on a more westward track. JTWC was strongly influenced by the dynamic aid, OTCM, which forecast a west-northwestward track throughout Ed's life. Of interest, the dynamic aid FBAM, which used the smoothed deep layer mean fields for steering, correctly forecast Ed's turn to the southwest, but missed the track change off Vietnam.

VI. IMPACT

No information was received.

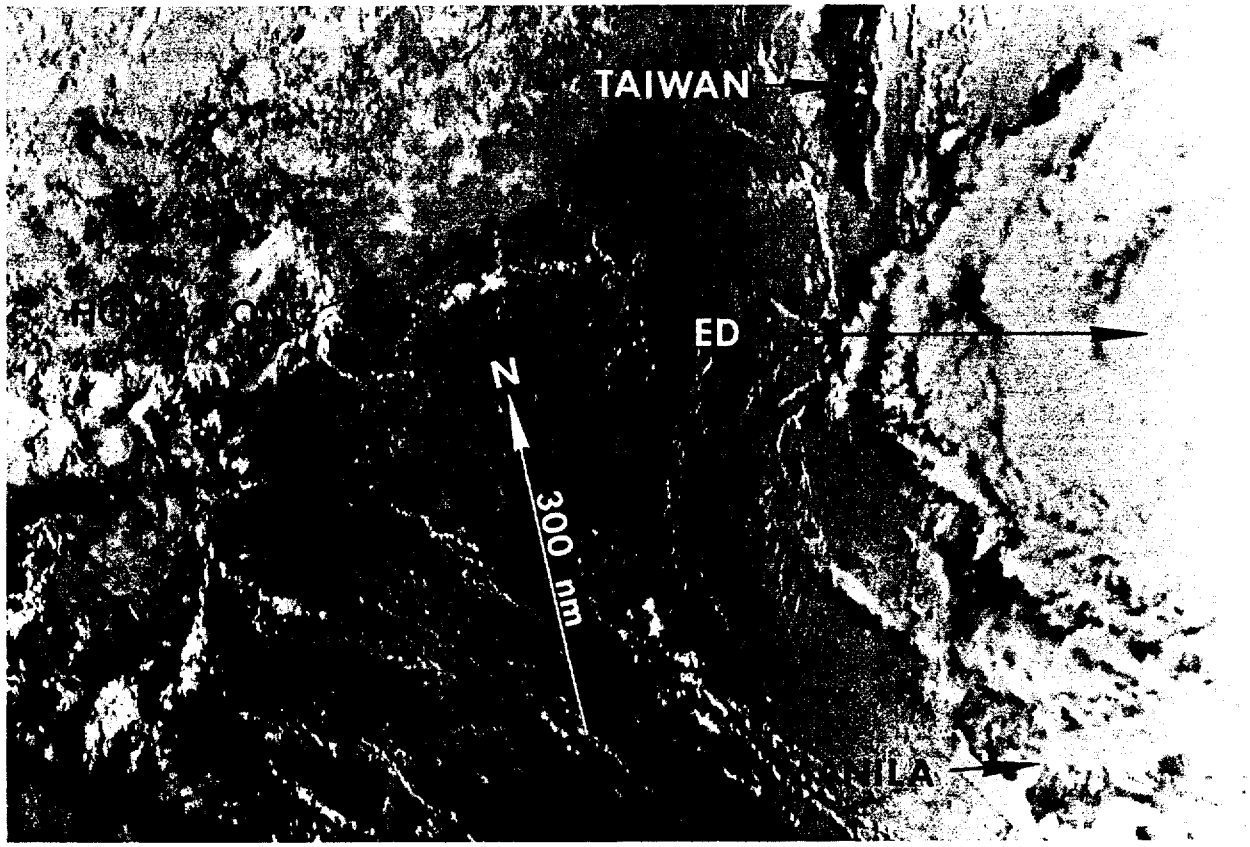

Figure 3-19-5. Typhoon Ed approaches the Straits of Luzon (140007Z September NOAA visual imagery).

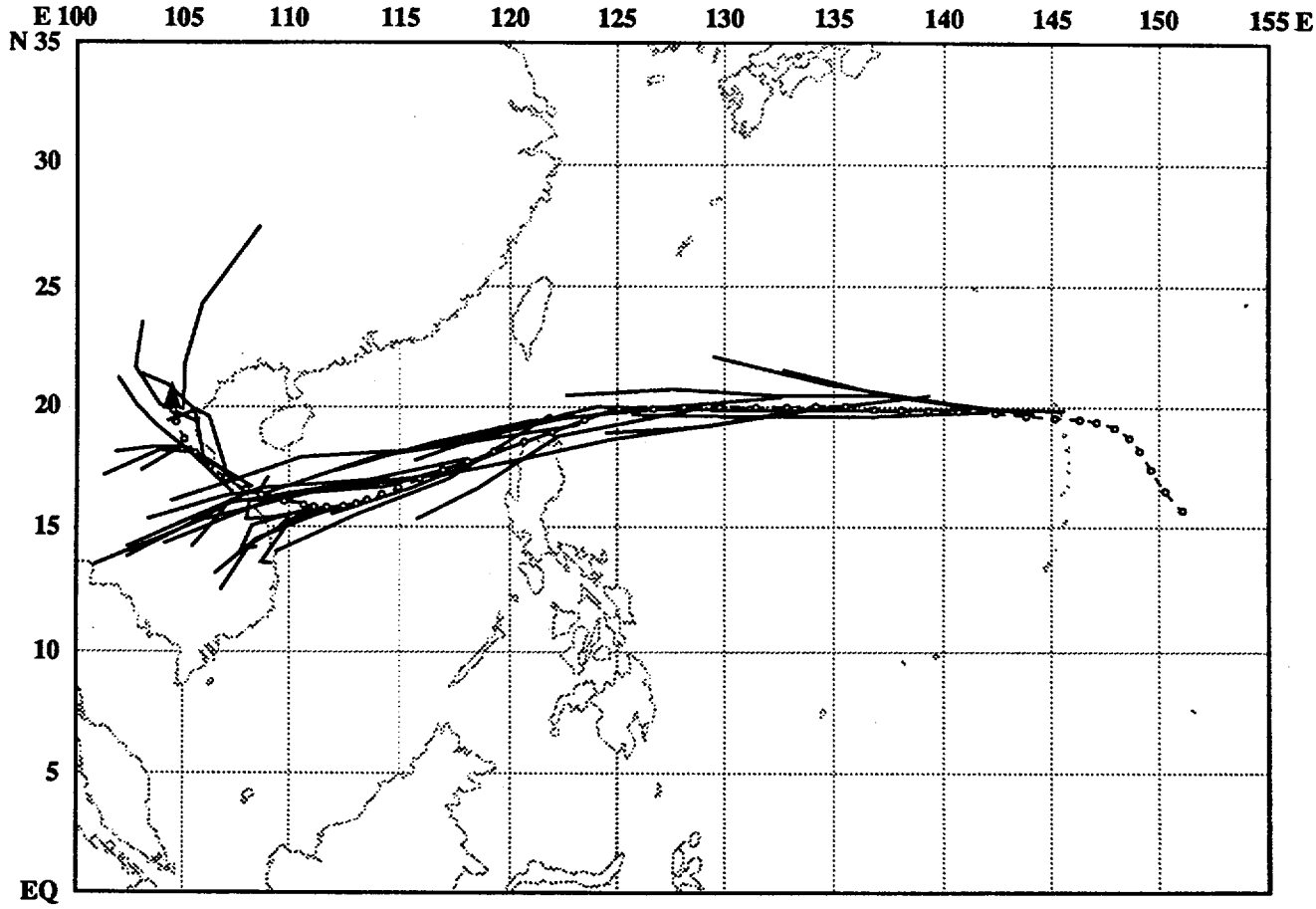

Figure 3-19-6. Summary of JTWC forecasts (solid lines) for Ed superimposed on the final best track (dashed line).

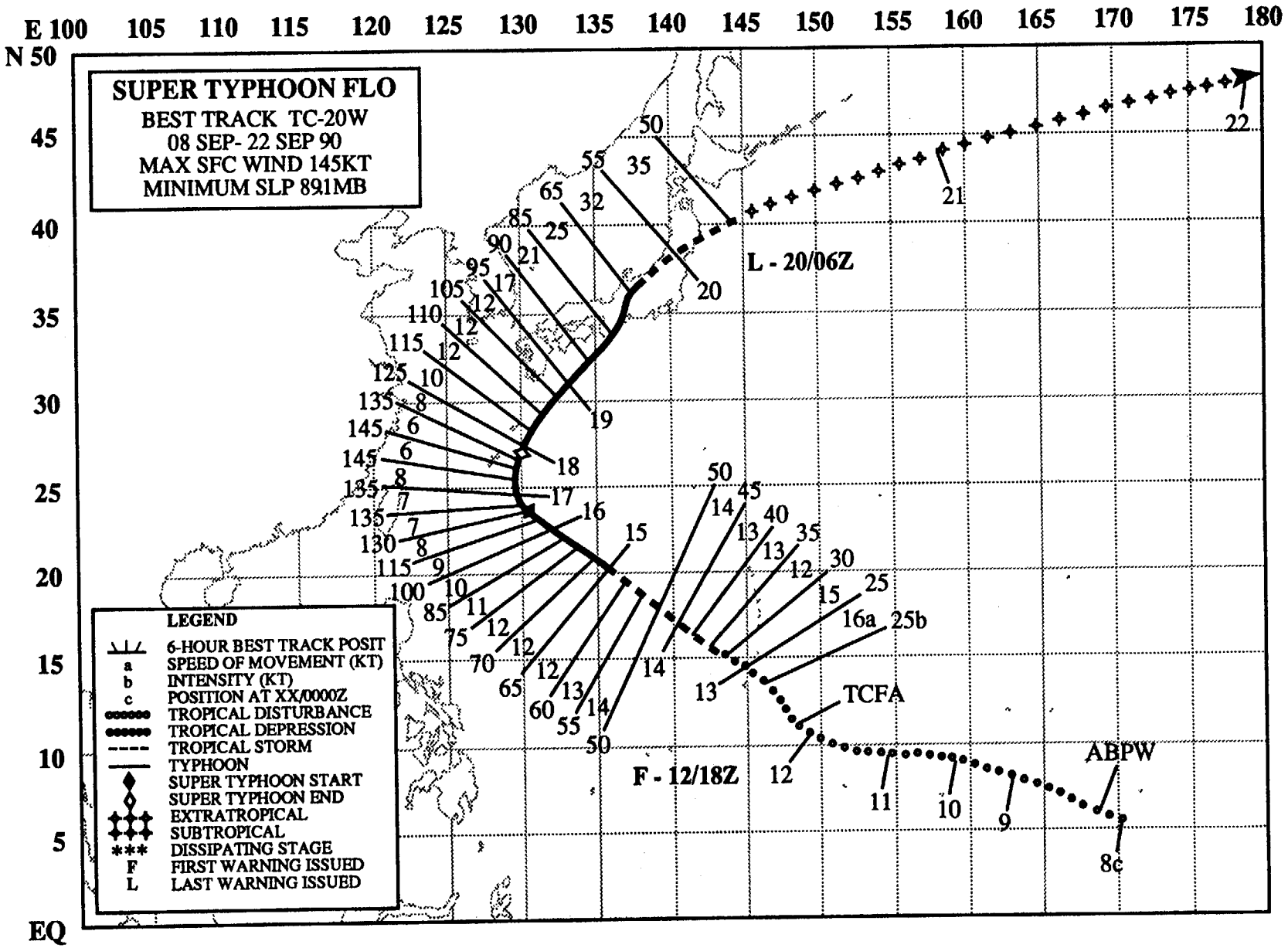
SUPER TYPHOON FLO
BEST TRACK TC-20W
08 SEP- 22 SEP 90
MAX SFC WIND 145KT
MINIMUM SLP 891MB
E 100 105 110 115 120 125 130 135 140 145 150 155 160 165 170 175 180
N 50 45 40 35 30 25 20 15 10 5 EQ
L - 20/06Z
F - 12/18Z
TCFA
ABPW
LEGEND
6-HOUR BEST TRACK POSIT
SPEED OF MOVEMENT (KT)
INTENSITY (KT)
POSITION AT XX/0000Z
TROPICAL DISTURBANCE
TROPICAL DEPRESSION
TROPICAL STORM
TYPHOON
SUPER TYPHOON START
SUPER TYPHOON END
EXTRATROPICAL
SUBTROPICAL
DISSIPATING STAGE
FIRST WARNING ISSUED
LAST WARNING ISSUED

SUPER TYPHOON FLO (20W)

I. HIGHLIGHTS

Flo was the fourth of six tropical cyclones to develop in September, the first of four super typhoons this year, and the object of over three consecutive days of upper-tropospheric aircraft reconnaissance missions during the TCM-90 field experiment. Flo formed in the wake of Typhoon Ed (19W), passed close by Guam, then rapidly intensified into a super typhoon as it approached Okinawa. Recurvature was slow before the tropical cyclone accelerated northeastward towards the Japanese mainland where it was called the most powerful typhoon to hit Honshu in 19 years. At least 38 people were reported dead or missing, damage was estimated in the millions of dollars, and transportation, communications and power were disrupted.

II. CHRONOLOGY OF EVENTS

080600Z - First mentioned on the Significant Tropical Weather Advisory as an area of convection in the monsoon trough with an estimated sea-level pressure of 1008 mb.
120530Z - Tropical Cyclone Formation Alert based on increased organization associated with well defined upper-level circulation center.
121800Z - First warning issued due to a continued increase in convective organization.
131800Z - Upgraded to tropical storm after a Dvorak intensity estimate of CI 2.5.
150600Z - Upgrade to typhoon based on the appearance of a small circular eye and the first CI 4.0.
161200Z - Reached super typhoon intensity after undergoing a period of rapid deepening: intensity estimate of CI 7.0.
170600Z - Peak intensity - 145 kt (75 m/sec) - based on the 891 mb report from a TCM-90 aircraft reconnaissance dropsonde.
180000Z - Downgraded to typhoon intensity after eye became ragged and intensity estimate of CI 6.0.
200000Z - Downgraded to a tropical storm due to increased vertical wind shear and the start of extratropical transition.
200600Z - Final warning issued as Flo transformed into an extratropical low.

III. TRACK AND MOTION

Within a day after Ed (19W) began to consolidate on 7 September in the monsoon trough 750 nm (1390 km) east of Guam, a persistent area of convection that would become Flo developed farther to the east in the southern Marshall Islands. Under the steering influence of the subtropical ridge to the north, Flo drifted west-northwestward for the next eight days at approximately 12 kt (22 km/hr). As the tropical cyclone approached Okinawa on 15 September, a mid-latitude short wave trough deepened to the northwest and induced a break in the subtropical ridge. On 17 September, Flo slowed and started to recurve around the western periphery of the ridge. It slowly accelerated in response to the passing trough. Finally, on 19 September, the typhoon accelerated northeastward across Honshu, as it became embedded in the stronger mid-latitiude westerlies aloft. Flo subsequently transitioned to an extratropical system east of Japan on 20 September.

IV. INTENSITY

Flo existed as a weak disturbance for four and a half days (8 - 12 September) before it started to intensify. Nearing Guam on 12 September, the disturbance's convection and low-level circulation appeared to consolidate (Figure 3-20-1). This consolidation process seemed related to the availability of deeper monsoonal southwesterly flow that was enhanced by the presence of Ed (19W) to the west. During the subsequent intensification process, the TCM-90 Doppler radar profiler on the island of

Saipan, 100 nm (185 km) to the north-northeast of Guam, recorded an interesting event. A time-height cross-section of meridional wind speed for 13 September revealed a mid-tropospheric 50 kt (25 m/sec) wind maximum (Figure 3-20-2) that extended around the eastern edge of Flo. The presence of the mid-level jet was concurrent with the intensification of Flo into a tropical storm.

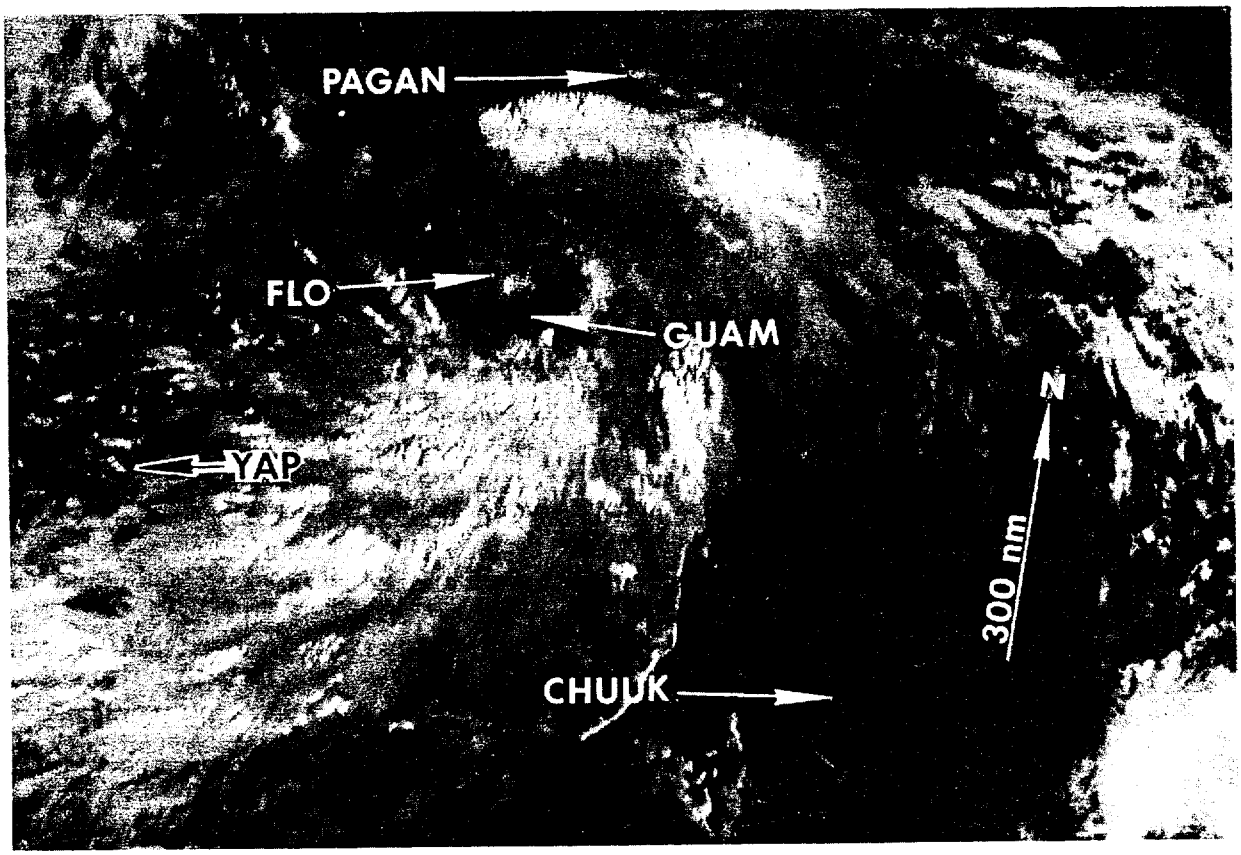

Figure 3-20-1. Flo as a tropical depression near Guam. The relatively clear area northeast of Guam is related to subsidence from Ed (19W), which is just off the top left edge of the photo (122325Z September DMSP visual imagery).

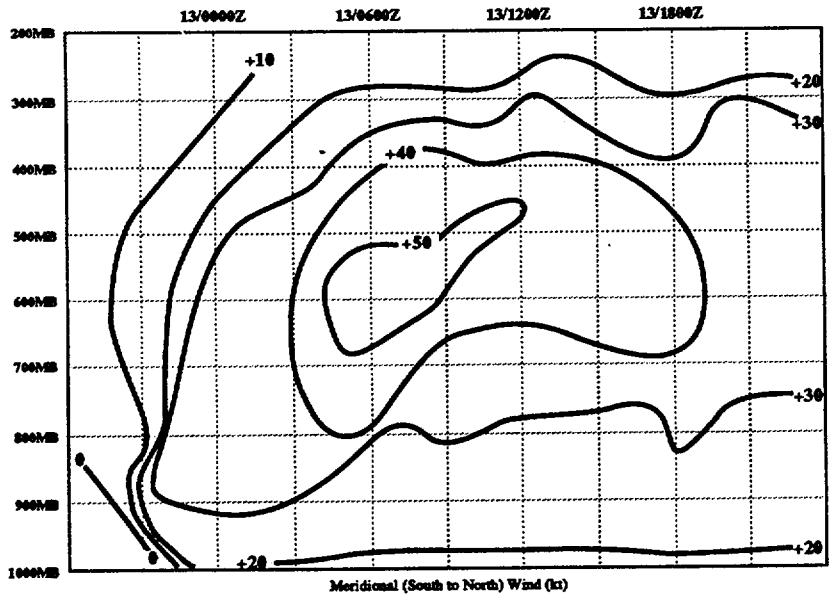

Figure 3-20-2. Time-height cross-section of the meridional wind speed for 13 September from the TCM-90 Doppler radar profiler on Saipan. The analysis shows the mid-level wind maximum that was observed on the east side of Flo.

Subsequently, the tropical cyclone intensified at a normal rate of one T-number per day until it reached typhoon intensity on 15 September (Figure 3-20-3). Then Flo rapidly intensified for the next 36 hours. On 16 September, as Flo was becoming a super typhoon, it also was the subject of an Intensive Observing Period (IOP) as part of the TCM-90 experiment. During the IOP, the NASA DC-8 reconnaissance aircraft provided JTWC with invaluable information on the location, structure, and intensity of Flo as the storm approached Okinawa (Figures 3-20-4 and 3-20-5). These data were the first-ever upper tropospheric (near 200 mb) winds from a western North Pacific tropical cyclone to be collected and used operationally. As a result of the information provided, JTWC increased the maximum winds from 135 kt (69 m/sec) to 145 kt (75 m/sec) at 170600Z September (Figure 3-20-6). The flight level for the reconnaissance missions ranged from 37,000 to 43,000 ft (11.3 km to 13.1 km), approximately the 200-mb level. These data revealed that there was intense cyclonic flow around. Flo's core with what appeared to be very little direct outflow evident close to the eye. Flight-level winds of 110 kt (55 m/sec) were recorded just east of the eye on 17 September. In addition, the presence of an anticyclonic eddy to the southeast of the eye was documented. A central pressure of 891 mb obtained via the dropsonde on the same day correlated well with both the Dvorak (1984) estimates of current intensity and the Atkinson-Holliday (1977) pressure-wind relationship.

As Flo began to recurve, it remained over the warm waters of the Kuroshio Current. Vertical wind shear weakened the typhoon, but it still had 90 kt (45 m/sec) sustained surface winds when it slammed into southern Honshu on 19 September. Interaction with land further weakened the tropical cyclone, and it transitioned to an extratropical cyclone the following day.

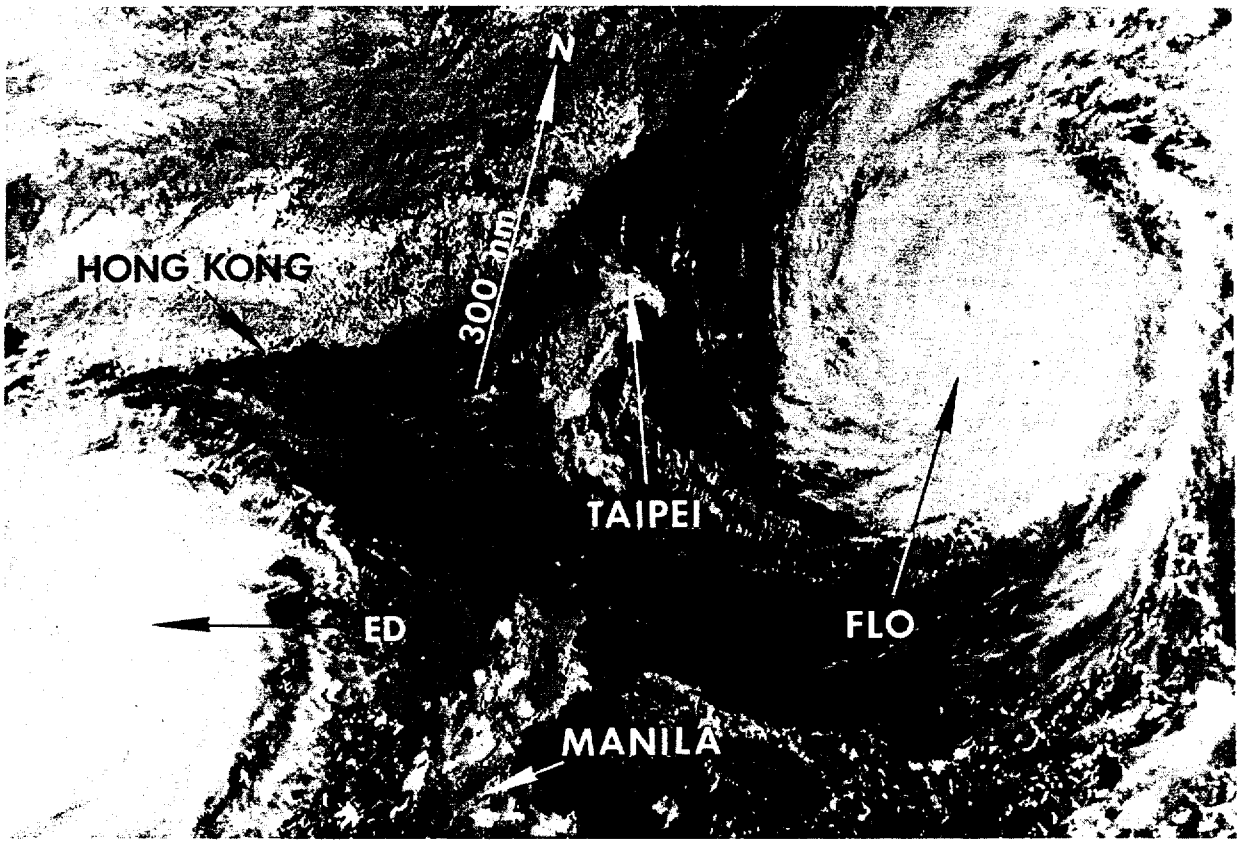

Figure 3-20-3. Flo at maximum intensity is starting to recurve just east of Okinawa while Typhoon Ed (19W) approaches Vietnam (170541Z September DMSP visual imagery).

Figure 3-20-4. Photograph of Flo from the NASA DC-8 reconnaissance aircraft flying near 200 mb on 17 September shows the top and side of the wall cloud (Photo courtesy of Mr. Franz Wen-Ching Yeh, TCM-90 experiment).

V. FORECASTING PERFORMANCE

The overall JTWC forecast performance is shown in Figure 3-20-7. Although the overall 72-hour position error was well below average at 215 nm (395 km), some forecast problems were encountered. Twenty-four hours prior to recurvature, JTWC forecast Flo to make landfall in southern Kyushu whereas the actual landfall was farther east on southern Honshu. A mid-latitude short wave moving off the coast of Asia, deepened more rapidly than anticipated; thus, the forecasts were too far to the west.

VI. IMPACT

Flo passed only 60 nm (110 km) east of Okinawa - close enough to break the drought with 5 to 10 inches (125 to 255 mm) of rain, but just far enough away to spare the island from the most extreme winds near the eye. The maximum wind gusts reported at Naha, Okinawa were 66 kt (35 m/sec). Futenma Marine Corps Air Station and Kadena Air Base reported 64 kt (35 m/sec) and 60 kt (30 m/sec), respectively. The crew of the NASA DC-8 estimated that 100 kt (50 m/sec) winds were just off the east coast of Okinawa. Damage to Okinawa was minor; however, there were news reports that four people died and three were missing in landslides. Flo made landfall on Honshu, 60 nm (110 km) south of Osaka with an intensity of 90 kt (45 m/sec). It was the most powerful typhoon to hit Honshu in 19 years according to news releases. The typhoon brought widespread flooding and caused 115 landslides in Honshu, leaving at least 32 people dead, six missing and 90 people injured. Property and crop damage were estimated in the millions of dollars, and communications, power, and transportation systems were interrupted. A tornado also occurred, injuring 12 people, damaging or destroying 200 homes and other buildings, and downing power lines.

Figure 3-20-5. Photograph of Flo from NASA DC-8 reconnaissance aircraft flying near 200mb on 17 September showing the stratocumulus cloud spirals that define the low-level center (Photo courtesy of Mr. Franz Wen-Ching Yeh, TCM-90 experiment).

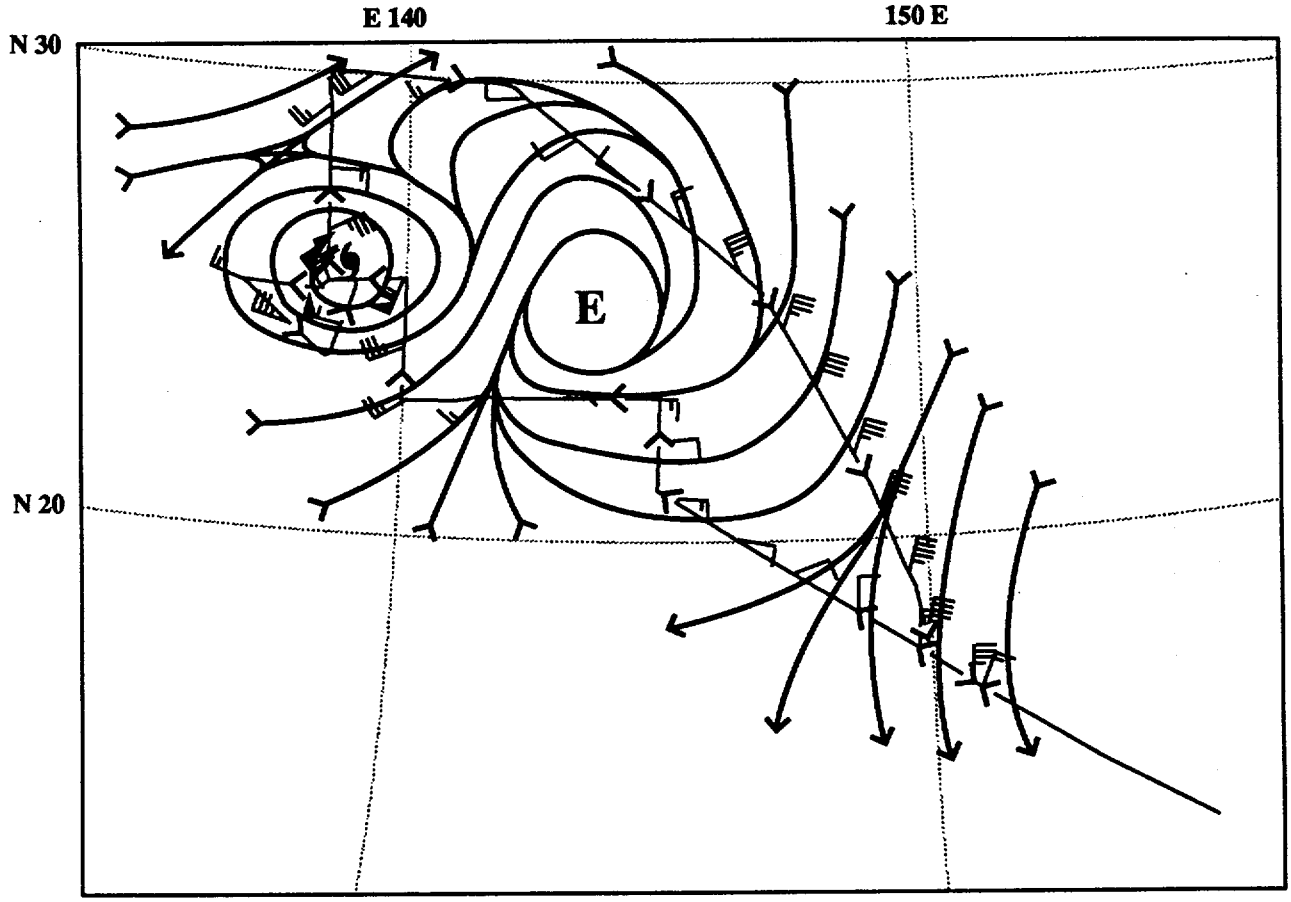

Figure 3-20-6. Flight-level winds reports from aircraft reconnaissance at 37,000-43,000ft for the period 170204Z to 170904Z September show the intense cyclonic circulation near Flo's eye and the anticyclonic eddy to the southeast.

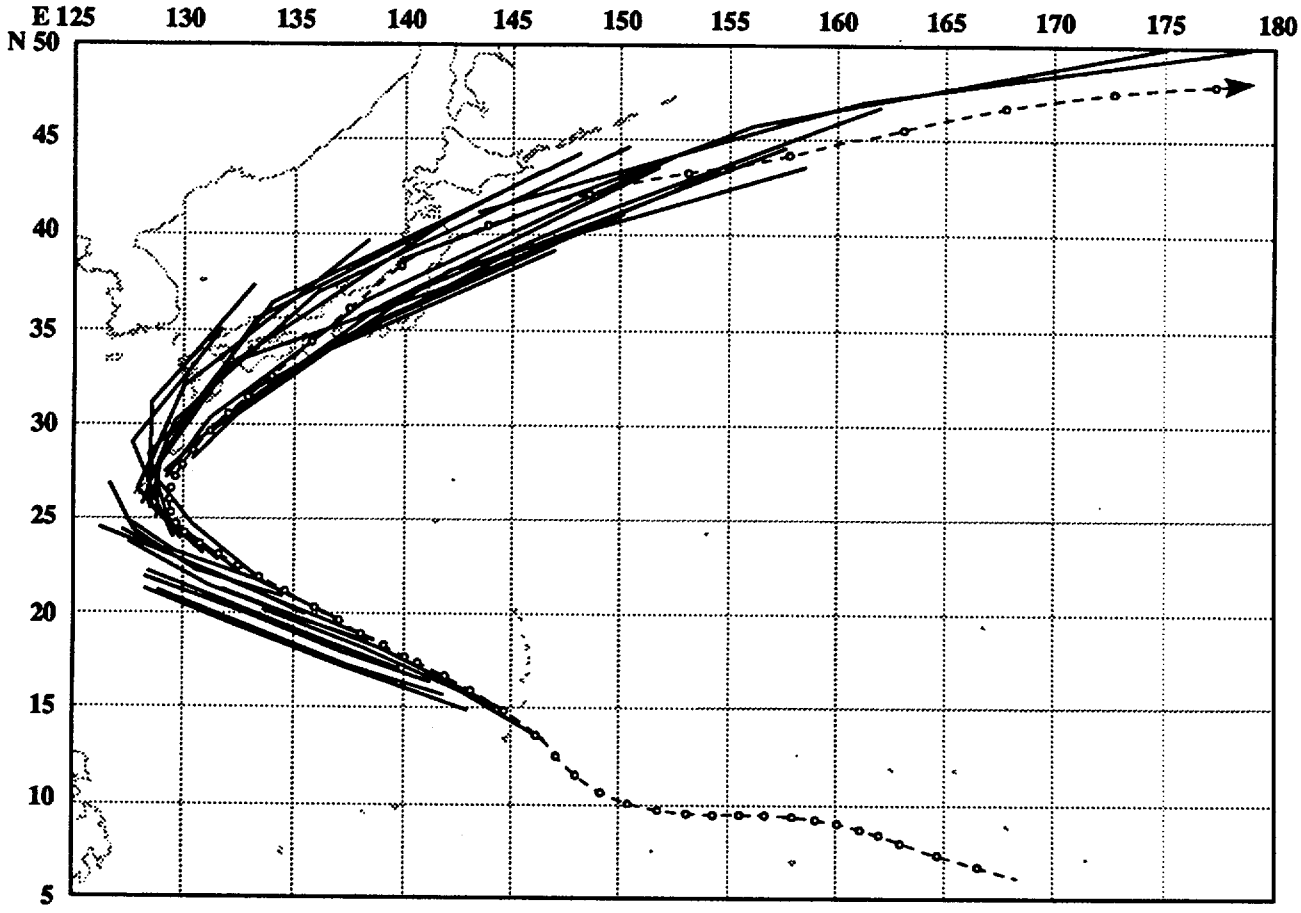

Figure 3-20-7. Summary of JTWC forecasts (solid lines) for Flo is superimposed on the final best track (dashed line).

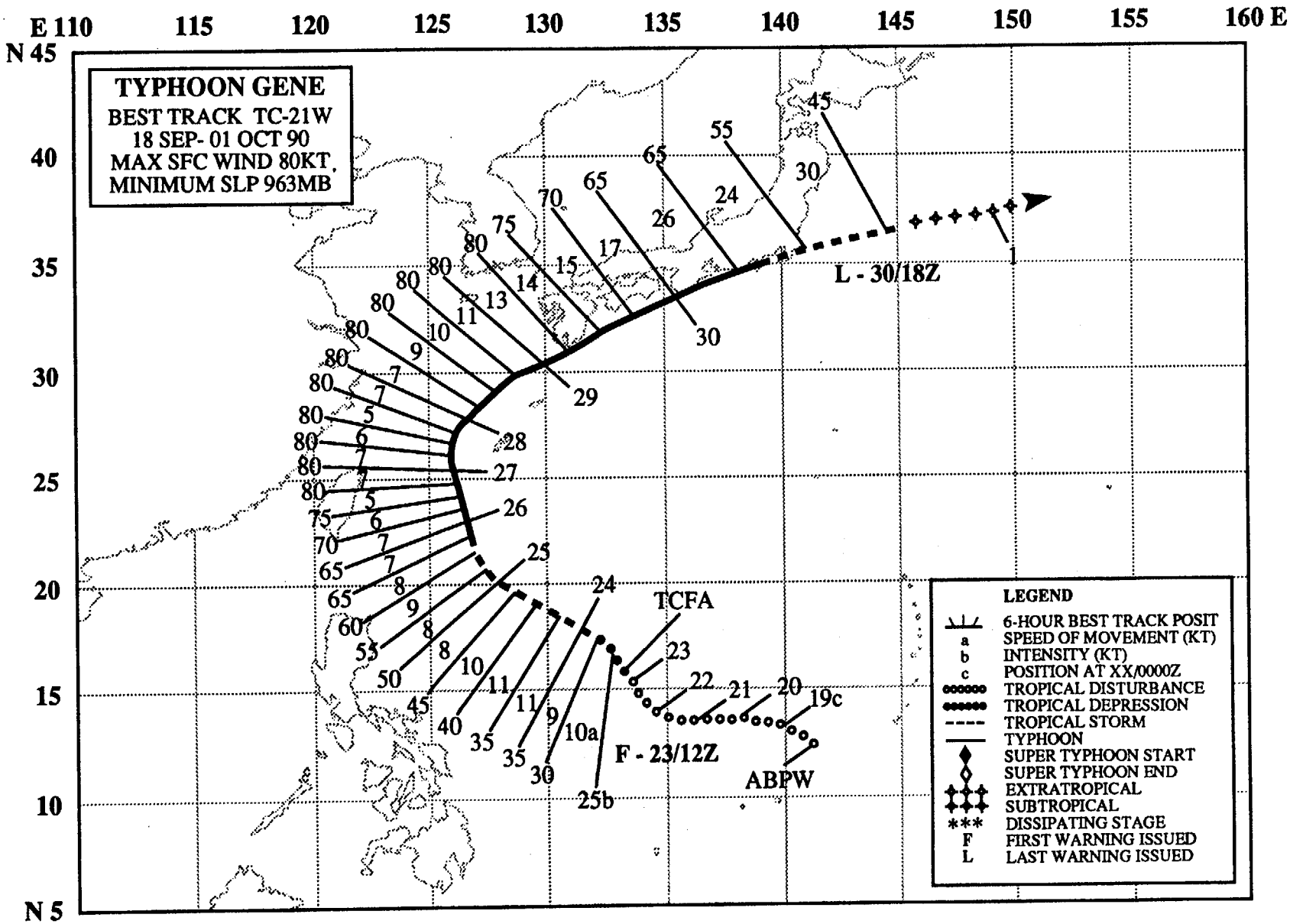
TYPHOON GENE
BEST TRACK TC-21W
18 SEP- 01 OCT 90
MAX SFC WIND 80KT,
MINIMUM SLP 963MB
E 110
115
120
125
130
135
140
145
150
155
160 E
N 45
40
35
30
25
20
15
10
N 5
L - 30/18Z
TCFA
F - 23/12Z
ABPW
LEGEND
6-HOUR BEST TRACK POSIT
SPEED OF MOVEMENT (KT)
INTENSITY (KT)
POSITION AT XX/0000Z
TROPICAL DISTURBANCE
TROPICAL DEPRESSION
TROPICAL STORM
TYPHOON
SUPER TYPHOON START
SUPER TYPHOON END
EXTRATROPICAL
SUBTROPICAL
DISSIPATING STAGE
FIRST WARNING ISSUED
LAST WARNING ISSUED

TYPHOON GENE (21W)

I. HIGHLIGHTS

Gene was the fifth significant tropical cyclone to form in September and the fifteenth of the year to reach typhoon intensity. The initial disturbance formed 250 nm (465 km) west-southwest of Guam and tracked westward for three days before turning northwestward. Gene followed a classic recurvature pattern, passing west of Okinawa and skirting southern Japan. The orientation of Gene's recurvature track resulted in sustained radar contact from 251400Z to 300400Z and an excellent, high quality set of 250 position reports from land radar sites in the islands nearby.

II. CHRONOLOGY OF EVENTS

180600Z - First mentioned on Significant Tropical Weather Advisory as an area of persistent convection with an estimated minimum sea-level pressure of 1008 mb.
230600Z - First Tropical Cyclone Formation Alert issued in response to increased organization induced by TUTT cell to the west.
231200Z - First warning prompted by a Dvorak current intensity estimate of 2.0 and an increase in total convection.
240600Z - Upgrade to tropical storm based on improved organization and enhanced outflow.
251800Z - Upgrade to typhoon based on a CI 4.0.
271200Z - Peak intensity of 80 kt (40 m/sec) maintained until 290600Z.
300600Z - Downgraded to tropical storm based on synoptic data.
301800Z - Final warning issued due to extratropical transition.

III. TRACK AND MOTION

Gene followed a typical recurvature track. The tropical cyclone initially tracked along the equatorward side of the mid-level subtropical ridge, then turned northwestward to approach a break in the axis in the ridge. Recurvature occurred on 27 October 100 nm (185 km) west of Okinawa in conjunction with a passing short-wave trough. Now under the influence of stronger westerly winds aloft, Gene accelerated east-northeastward and changed into an extratropical low 300 nm (555 km) east of Tokyo.

IV. INTENSITY

For five days Gene's winds remained less than 25 kt (13 m/sec). However, on 23 September, assisted by a TUTT cell to the west, normal intensification of one T-number per day started. Although the track followed the warm Kuroshio ocean current, restricted outflow aloft limited development. Nevertheless, after attaining peak intensity, Gene (Figure 3-21-1) maintained 80 kt (40 m/sec) for two and a half days before slowly weakening.

V. FORECASTING PERFORMANCE

Figure 3-21-2, provides an overview of the forecasts. It illustrates two points: first, when NOGAPS prognoses are slow to weaken the mid-level subtropical ridge in response to the passing short-wave, JTWC's dynamic aids were slow (Figure 3-21-3); and second, if the initial forecast philosophy is for a "straight runner," there is a reluctance to shift to recurvature at the first indication of a change.

VI. IMPACT

There were no reports of damage on Okinawa, but as Gene moved along the southern coastlines of the Kyushu and Honshu, it caused four deaths, 12 injuries, and localized flooding. Wind speeds of 70 kt (36 m/sec) were measured on Kyushu, but weakened to 38 kt (20 m/sec) as Gene brushed by Tokyo.

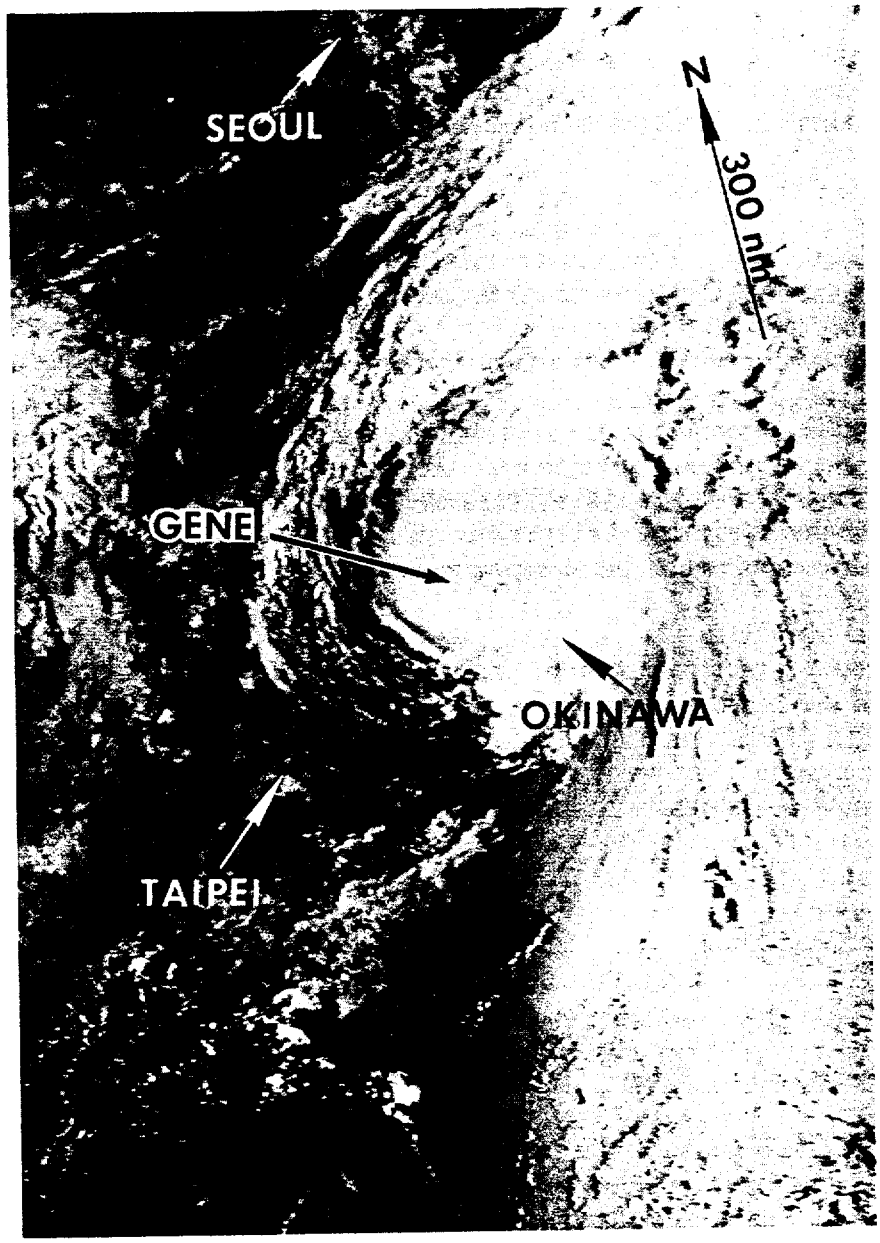

Figure 3-21-1. Gene at peak intensity (272346Z September NOAA visual imagery).

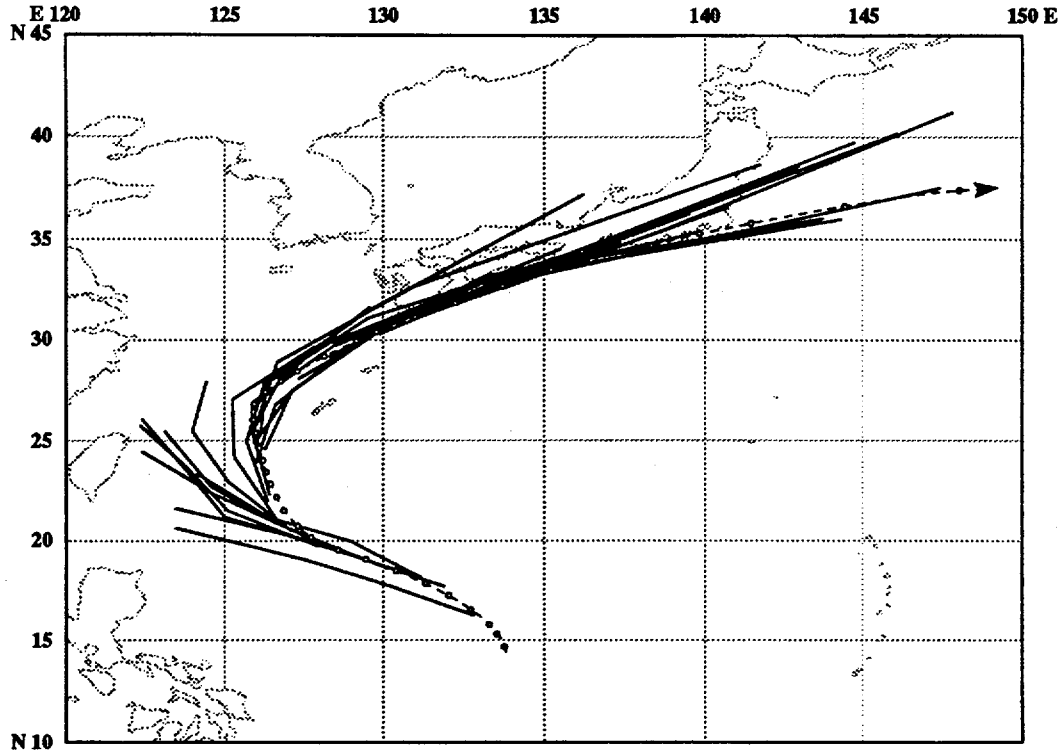

Figure 3-21-2. Summary of JTWC forecasts (solid lines) for Gene superimposed on the final best track (dashed line).

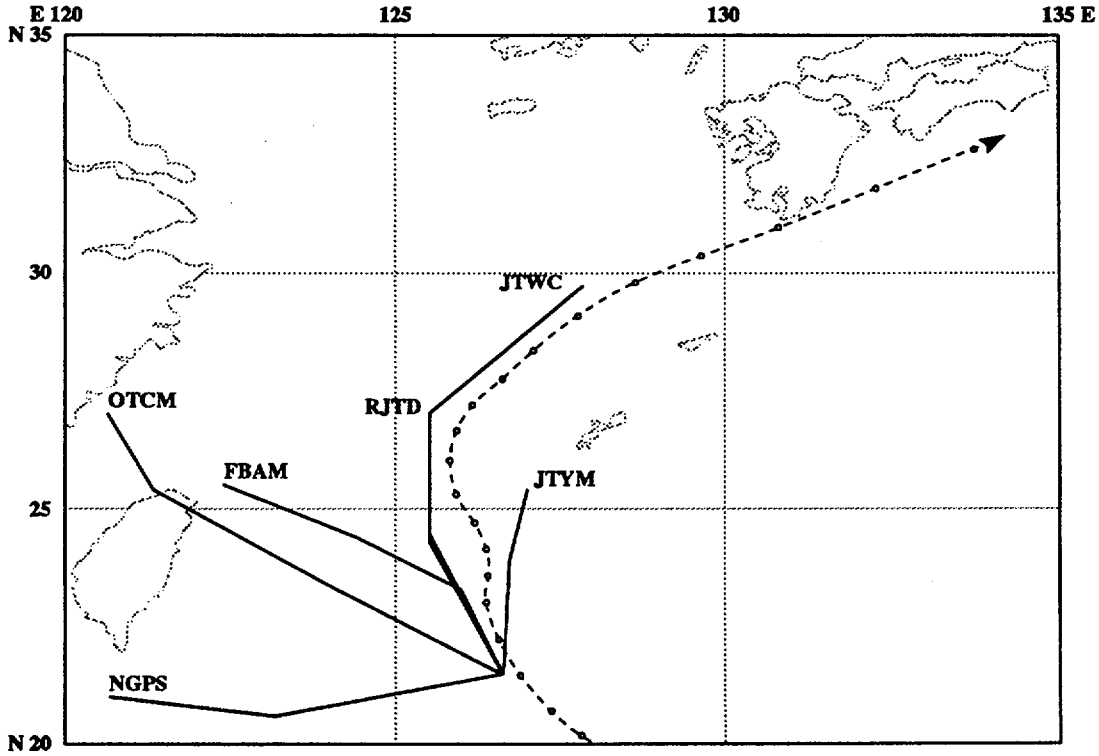

Figure 3-21-3. Comparison of 251200Z September forecasts by JTWC and supporting dynamic aids NGPS, FBAM and OTCM. Also shown are forecasts by the Japan Meteorological Agency (RJTD) and the Japanese Typhoon Model (JTYM).

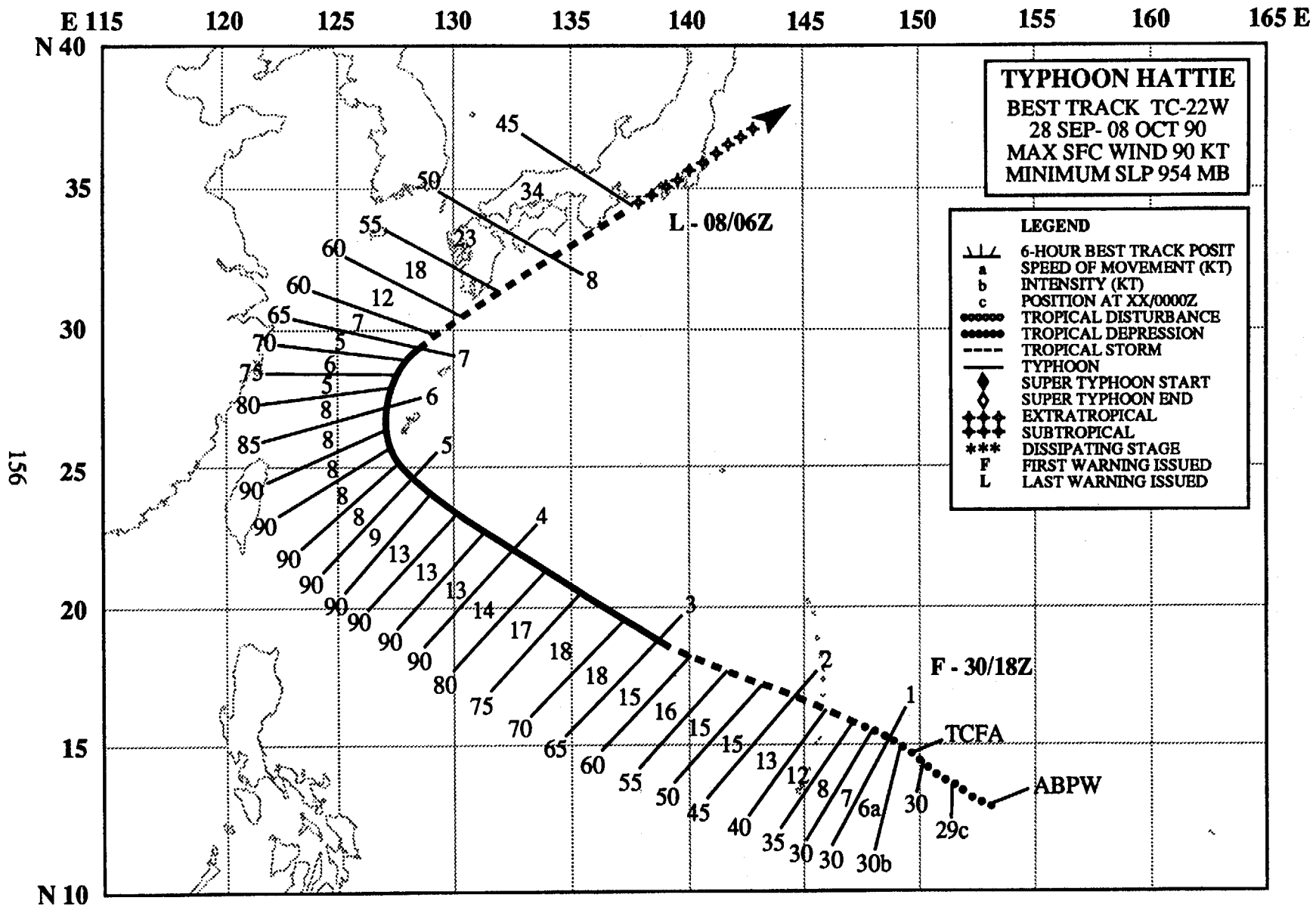
E 115
120
125
130
135
140
145
150
155
160
165 E
N 40
35
30
25
20
15
N 10
156
TYPHOON HATTIE
BEST TRACK TC-22W
28 SEP- 08 OCT 90
MAX SFC WIND 90 KT
MINIMUM SLP 954 MB
LEGEND
6-HOUR BEST TRACK POSIT
a SPEED OF MOVEMENT (KT)
b INTENSITY (KT)
c POSITION AT XX/0000Z
TROPICAL DISTURBANCE
TROPICAL DEPRESSION
TROPICAL STORM
TYPHOON
SUPER TYPHOON START
SUPER TYPHOON END
EXTRATROPICAL
SUBTROPICAL
*** DISSIPATING STAGE
F FIRST WARNING ISSUED
L LAST WARNING ISSUED
L - 08/06Z
F - 30/18Z
TCFA
ABPW

TYPHOON HATTIE (22W)

I. HIGHLIGHTS

Hattie, the last of six tropical cyclones to form in September, was the fourth tropical cyclone a in six-week period to affect Okinawa and southern Japan. It's track was a classic example of recurvature.

II. CHRONOLOGY OF EVENTS

280600Z - First mentioned on Significant Tropical Weather Advisory as an area of persistent convection with an estimated minimum sea-level pressure of 1010 mb.

300730Z - Tropical Cyclone Formation Alert followed a flare up of deep convection and the first Dvorak intensity estimate of 1.0.

301800Z - First warning based on intensification manifested by the cirrus outflow layer showing signs of rapid growth, appearance of overshooting cumulonimbus tops, and a CI 2.0.

011200Z - Upgraded to tropical storm due to increase in convective extent and organization.

030000Z - Upgrade to typhoon based on the formation of a small eye on satellite imagery and a CI 4.0.

040000Z - Peak intensity - 90 kt (46 m/sec) - based on a decrease in eyewall cloud top temperatures and a CI 5.0.

071200Z - Downgraded to a tropical storm due to increased upper-level westerly wind shear and loss of central convection.

080600Z - Final warning issued following Hattie's transformation into an extratropical cyclone.

III. TRACK AND MOTION

As Typhoon Gene (21W), which had just recurved, accelerated towards the main islands of Japan on 28 September, Hattie formed in the monsoon trough 100 nm (185 km) east of Guam. Hattie followed a smooth track west-northwestward, slowed late on 4 October as it approached the lighter winds near the axis of the subtropical ridge, and recurved just to the west of Okinawa late on 5 October. Then on 7 October, Hattie accelerated northeastward in the strong southwesterly flow and churned by Tokyo, Japan on 8 October.

IV. INTENSITY

For a three-day period, 29 September to 1 October, Hattie's intensification was arrested by westerly winds aloft and to the north. On 1 October, anticyclonically curved cirrus outflow was observed to push northward from the depression's cloud system center (Figure 3-22-1), and Hattie began to intensify at a normal rate of one T-number per day. This steady intensification continued until 4 October, when the typhoon peaked at 90 kt (45 m/sec)(Figure 3-22-2). Hattie maintained its peak intensity for almost two days before moving into the strong vertical shear region north of the subtropical ridge axis. The typhoon weakened as it lost central convection and transitioned to an extratropical system on 8 October.

V. FORECASTING PERFORMANCE

The first three warnings issued by JTWC were based on Hattie's poorly defined cloud system center and verified significantly south of track (Fig 3-22-3). Then warning 04 relocated Hattie's center to the north as the convection consolidated the low-level circulation. All subsequent track forecasts verified well. In particular, three consecutive warnings beginning 48 hours prior to the recurvature point achieved exceptionally low 72-hour forecast errors near 90 nm (165 km).

VI. IMPACT

Typhoon Hattie passed 30 nm (55 km) west of Okinawa, causing damage in excess of $1.7 million to U.S. military bases. Roof damage and beach erosion were extensive. Maximum wind gusts as high as 75 kt (38 m/sec) were recorded on Okinawa. On a positive note, the water rationing in since mid-September was lifted. Total rainfall from Flo (20W), Gene (21W) and Hattie provided 15-20 inches (380-510 mm) to fill up the almost empty reservoirs.

After Hattie recurved, it tracked along the south coast of Japan, bringing heavy rains and strong winds. Three people in Shikoku were killed and 14 injured as the bus they were riding in was struck by a landslide.

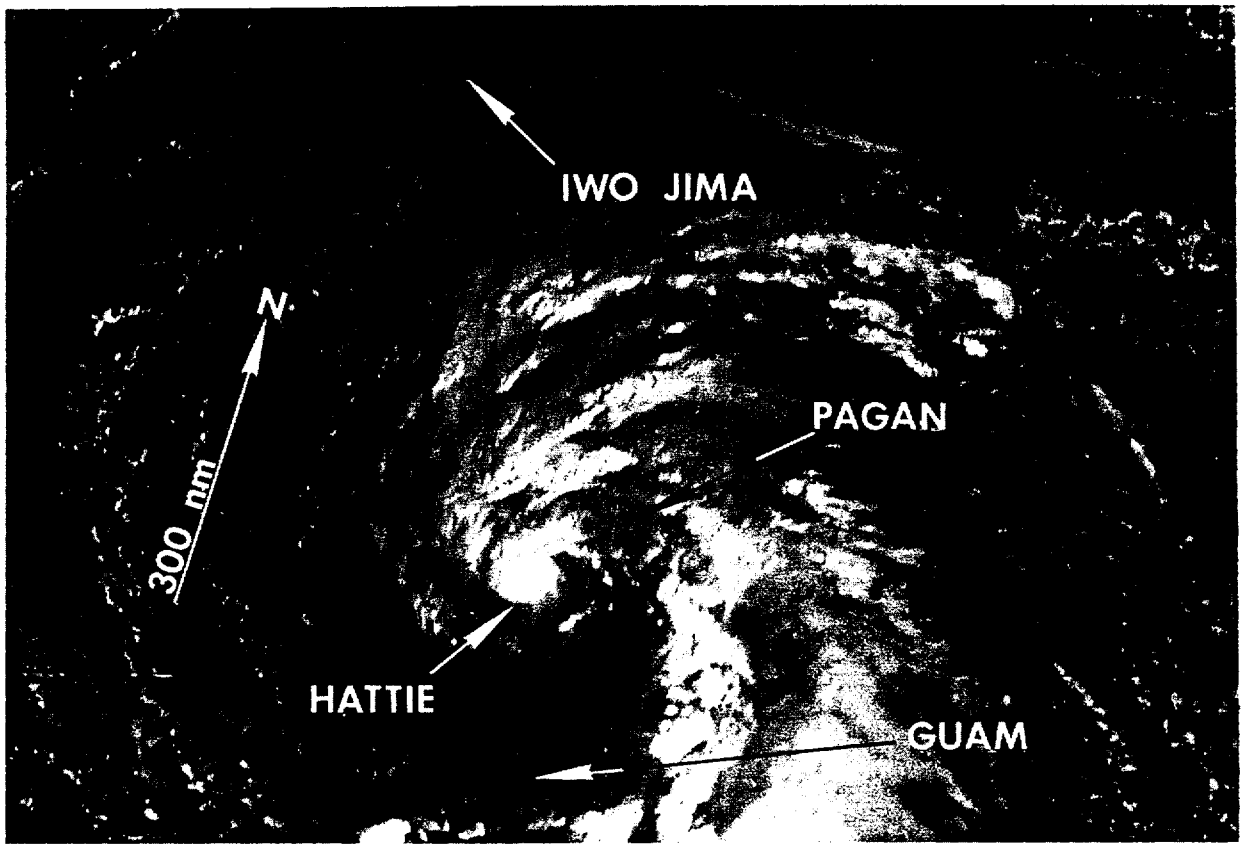

Figure 3-22-1. Hattie intensifies and its cirrus outflow pushes northward (012330Z October DMSP visual imagery).

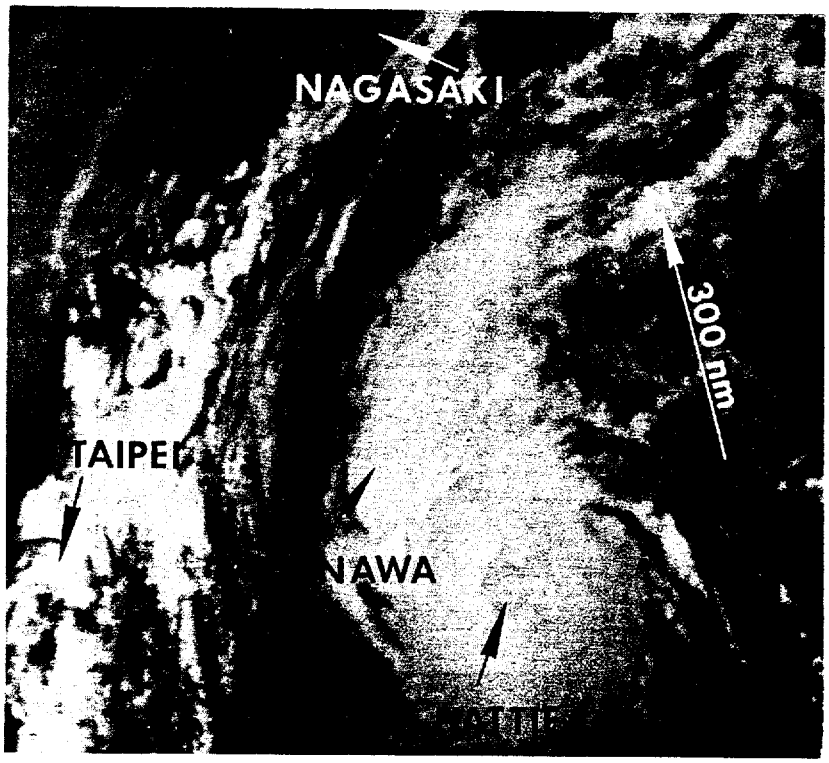

Figure 3-22-2. Typhoon Hattie at peak intensity (041307 October DMSP nighttime visual imagery).

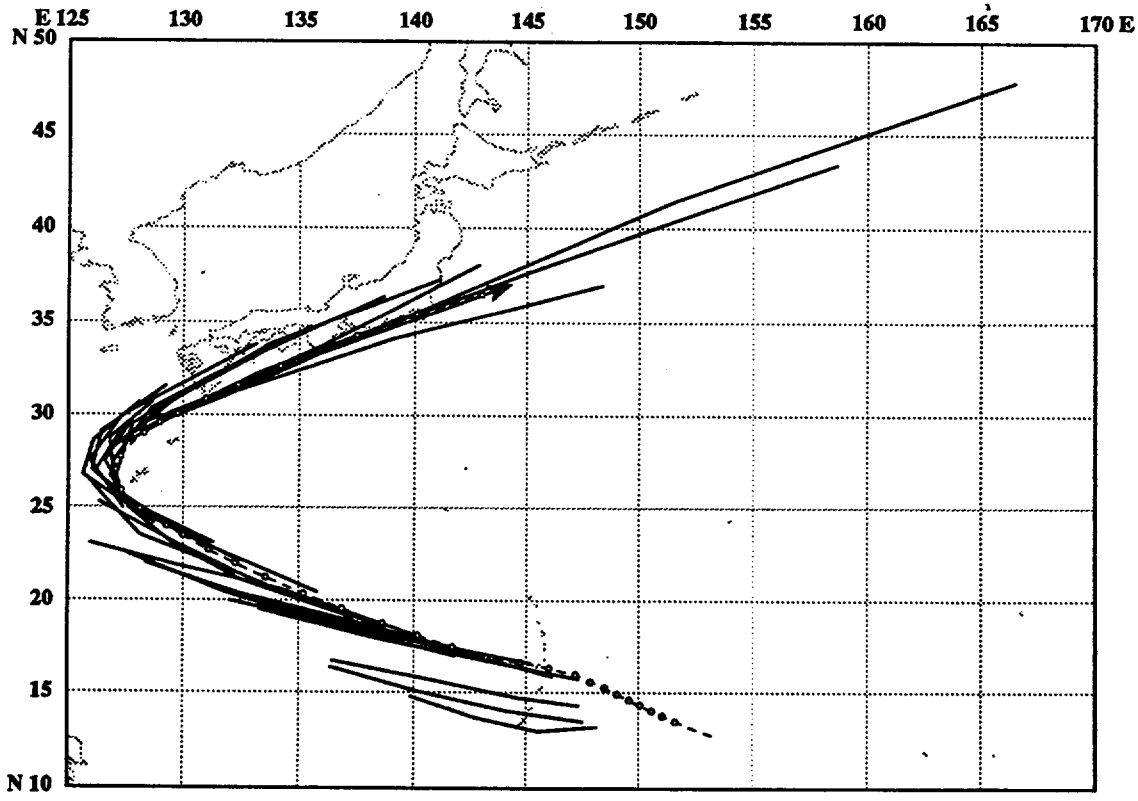

Figure 3-22-3. Summary of JTWC forecasts (solid lines) for Hattie is superimposed on the final best track (dashed line).

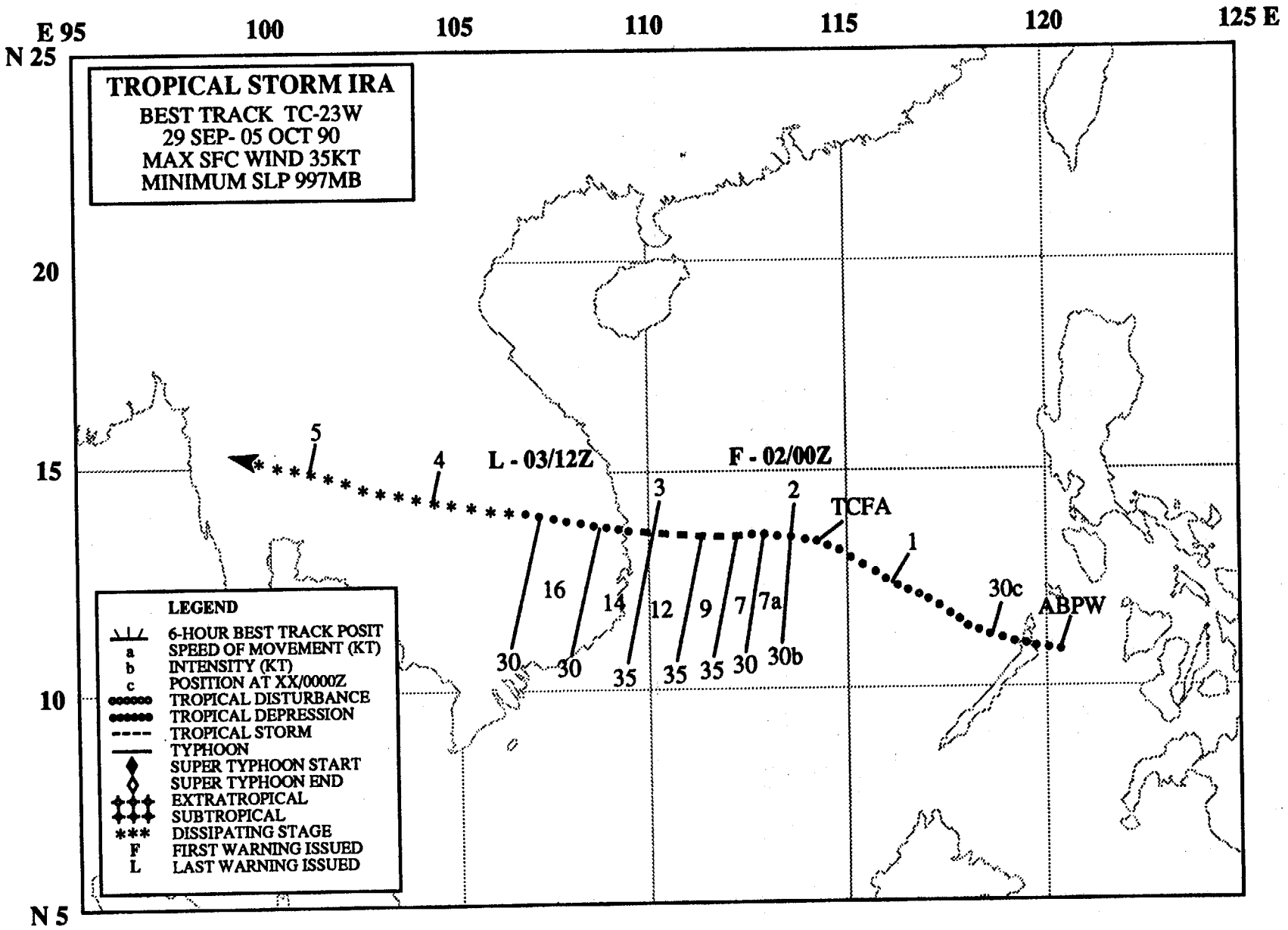
E 95
100
105
110
115
120
125 E
N 25
20
15
10
N 5
160
TROPICAL STORM IRA
BEST TRACK TC-23W
29 SEP- 05 OCT 90
MAX SFC WIND 35KT
MINIMUM SLP 997MB
L - 03/12Z
F - 02/00Z
TCFA
ABPW
5
4
3
2
1
30c
16
14
12
9
7
7a
30b
30
30
35
35
35
30
LEGEND
6-HOUR BEST TRACK POSIT
a SPEED OF MOVEMENT (KT)
b INTENSITY (KT)
c POSITION AT XX/0000Z
TROPICAL DISTURBANCE
TROPICAL DEPRESSION
TROPICAL STORM
TYPHOON
SUPER TYPHOON START
SUPER TYPHOON END
EXTRATROPICAL
SUBTROPICAL
*** DISSIPATING STAGE
F FIRST WARNING ISSUED
L LAST WARNING ISSUED

TROPICAL STORM IRA (23W)

I. HIGHLIGHTS

Ira, the eighth tropical cyclone to hit Vietnam in 1990 and the last in a series of weak, highly sheared tropical systems in the South China Sea, formed in a broad area of convection near Palawan Island. The convective cloud mass tracked steadily westward in the deep easterly flow and made landfall at Qui Nhon Vietnam on the third of October.

II. CHRONOLOGY OF EVENTS

290600Z - First mentioned on the Significant Tropical Weather Advisory as an area of persistent convection with an estimated minimum sea-level pressure of 1009 mb.

011800Z - Tropical Cyclone Formation Alert based on 12 hours of persistent cirrus outflow,the consolidation of the central convection and first CI 1.0 estimate.

020000Z - First warning issued due to increased deep central convection and upper-level outflow.

021200Z - Upgraded to tropical storm because of a continued increase in central convection.

030600Z - Downgraded to tropical depression based on synoptic reports along the Vietnamese coast.

031200Z - Final warning issued due to land interaction, and severing of the low-level overwater moisture source.

III. TRACK AND MOTION

Ira developed in the monsoon trough near the southern Philippine island of Palawan on 29 September and tracked steadily westward on the south side of a persistent mid-level ridge centered over southern China (Figure 3-23-1). On 2 October, as the tropical cyclone approached the coast of Vietnam, increased mid- and low-level easterly flow accelerated Ira on shore over Vietnam.

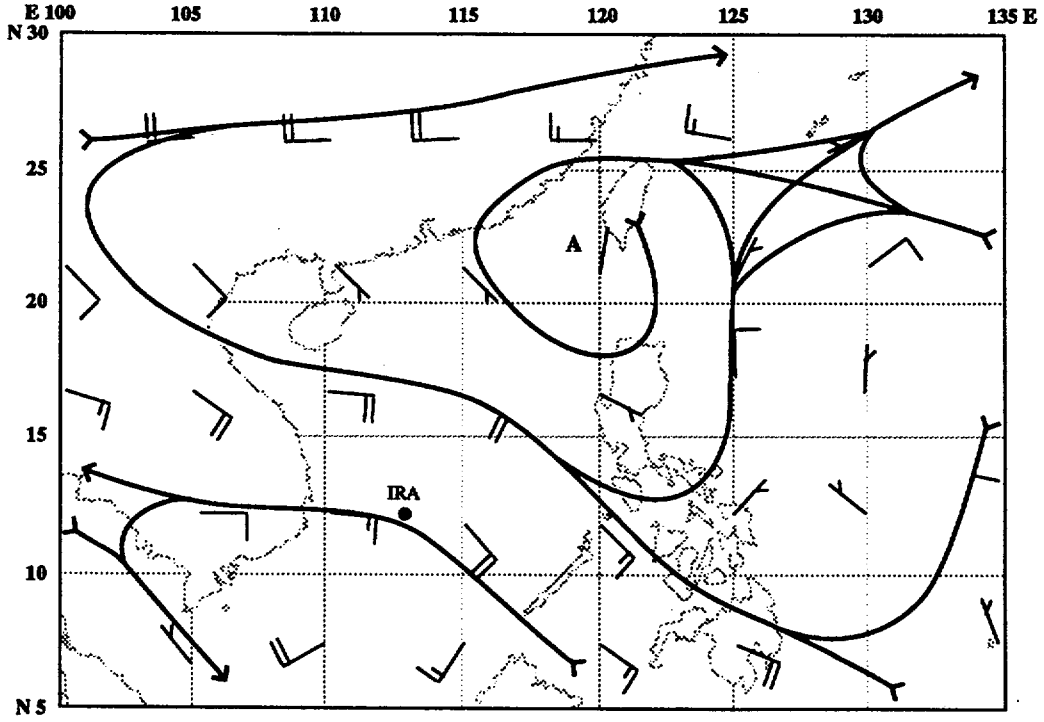

Figure 3-23-1. 500-mb NOGAPS analysis from 020000Z October, showing a persistent mid-level ridge positioned along the coast of southern China.

IV. INTENSITY

Ira's convective cloud mass was poorly organized throughout the life of the storm. The cloud system was embedded in an unfavorable environment of strong upper-level unidirectional southeasterly flow (Figure 3-23-2). Therefore, Ira was unable to develop an efficient outflow pattern during its early stages of development (Figure 3-23-3). Later, after the tropical cyclone moved over land on 3 October , its remnants tracked westward across virtually all of Indochina. There was even brief mention on the Significant Tropical Weather Advisory of a possible regeneration if the remnants moved into the Bay of Bengal.

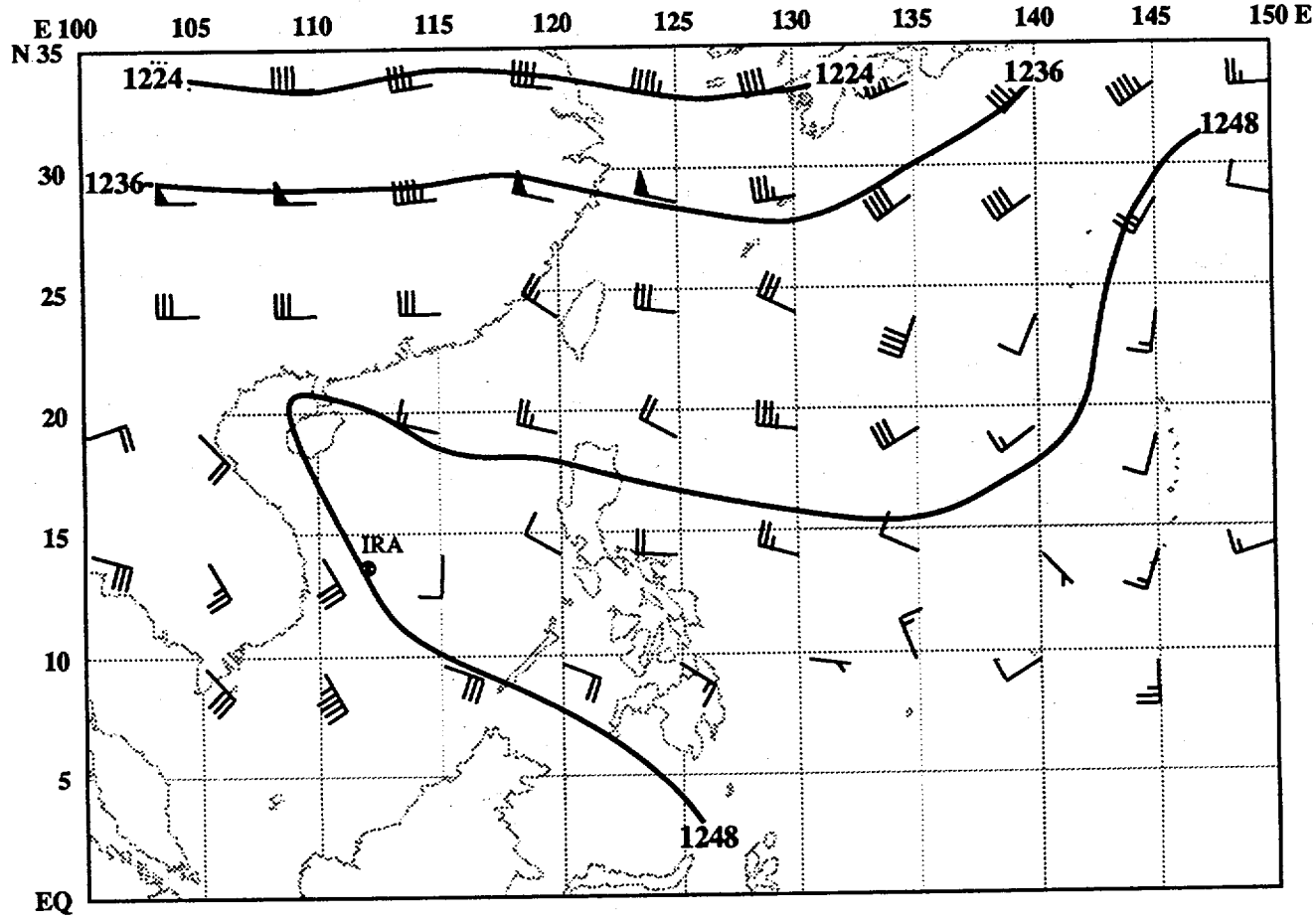

Figure 3-23-2. The 200-mb NOGAPS analysis with heights in decameters at 020000Z October, showing strong unidirectional southeasterly flow over the South China Sea which restricted the development of an efficient upper-level outflow pattern above Ira.

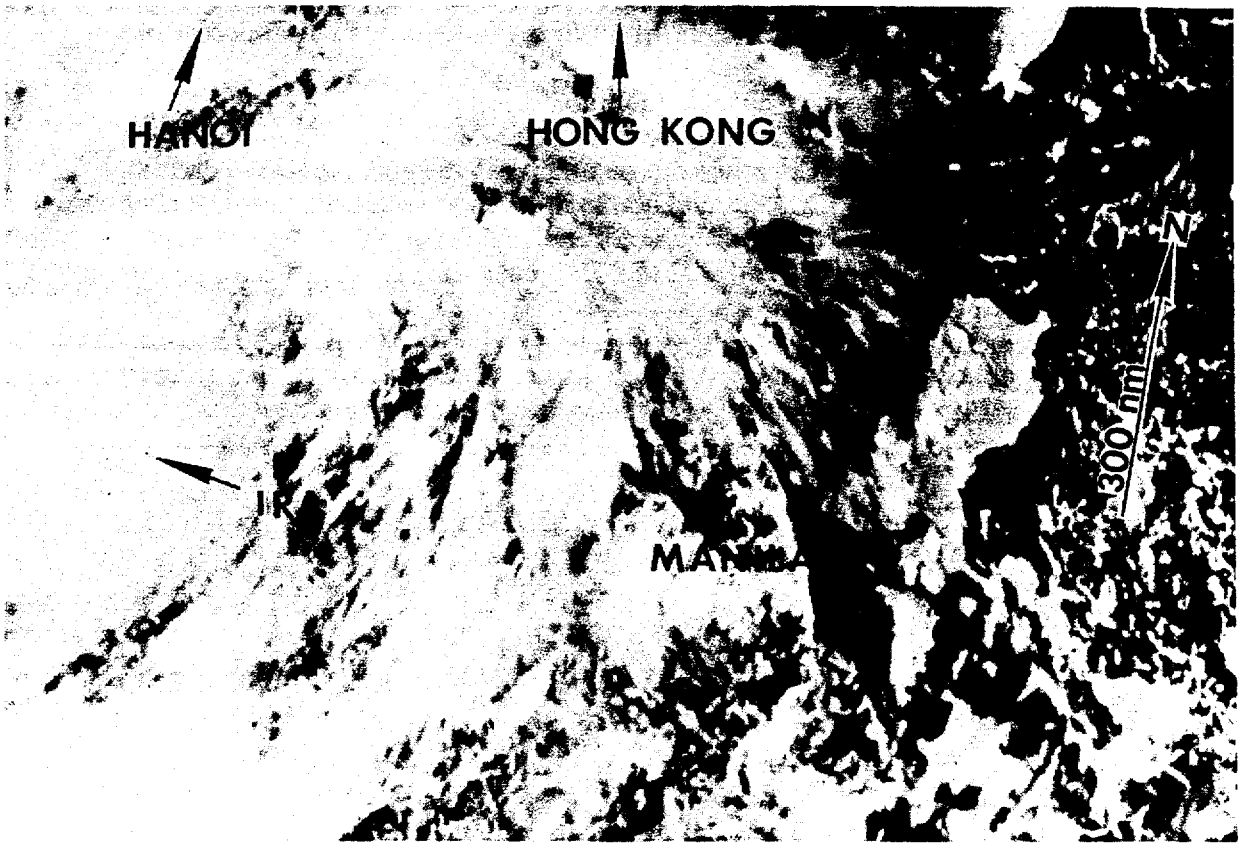

Figure 3-23-3. Ira approaches the coast of Vietnam (030607Z October NOAA visual imagery).

V. FORECASTING PERFORMANCE

The overall JTWC forecast performance is shown in Figure 3-23-4. The only major problems encountered were the result of conflicts between synoptic reports and satellite fixes. JTWC biased the initial warning positions toward the synoptic reports after the second warning, and the accuracy of the initial motion forecasts quickly improved.

VI. IMPACT

The following report was released by the **United Press International** in Bangkok,

A typhoon damaged 110,000 houses and killed seven people in the coastal provinces of Vietnam, official Radio Hanoi reported.

The radio, in a broadcast Monday, said the Central Flood and Typhoon Control Committee has reported that the eigth typhoon to hit Vietnam this year caused heavy rainfall in Thua Thien-Hue Province, 320 miles south of Hanoi.

"The average rainfall was between 12 to 27.5 inches," the broadcast said, according to a translation made available Wednesday.

"Heavy rains submerged 110 of the 145 villages and more than 110,000 houses, (and) killed seven people," the radio said.

The radio did not give the exact date when the storm hit the country.

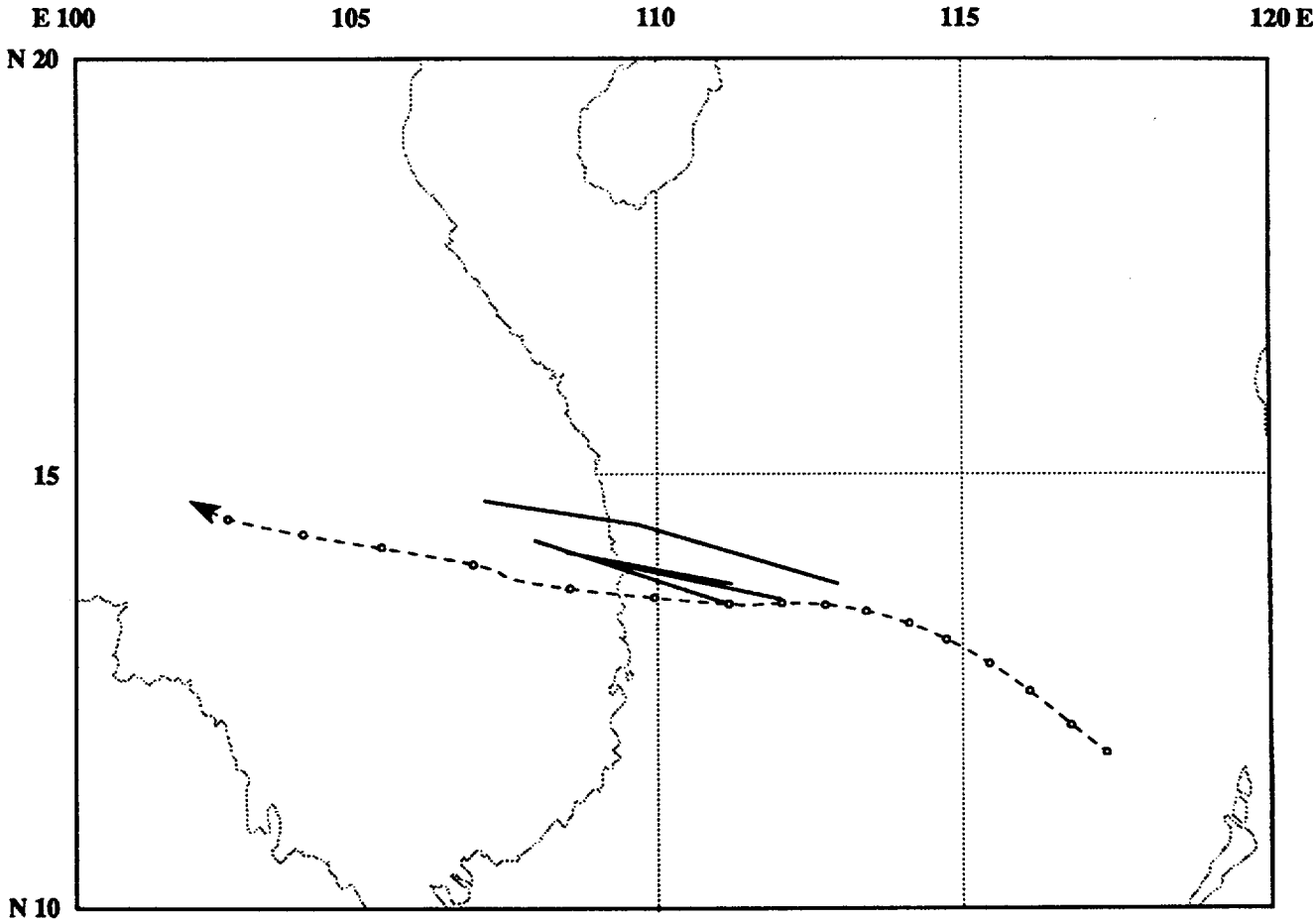

Figure 3-24-4. Summary of JTWC forecasts (solid lines) for Ira superimposed on the final best track (dashed line).

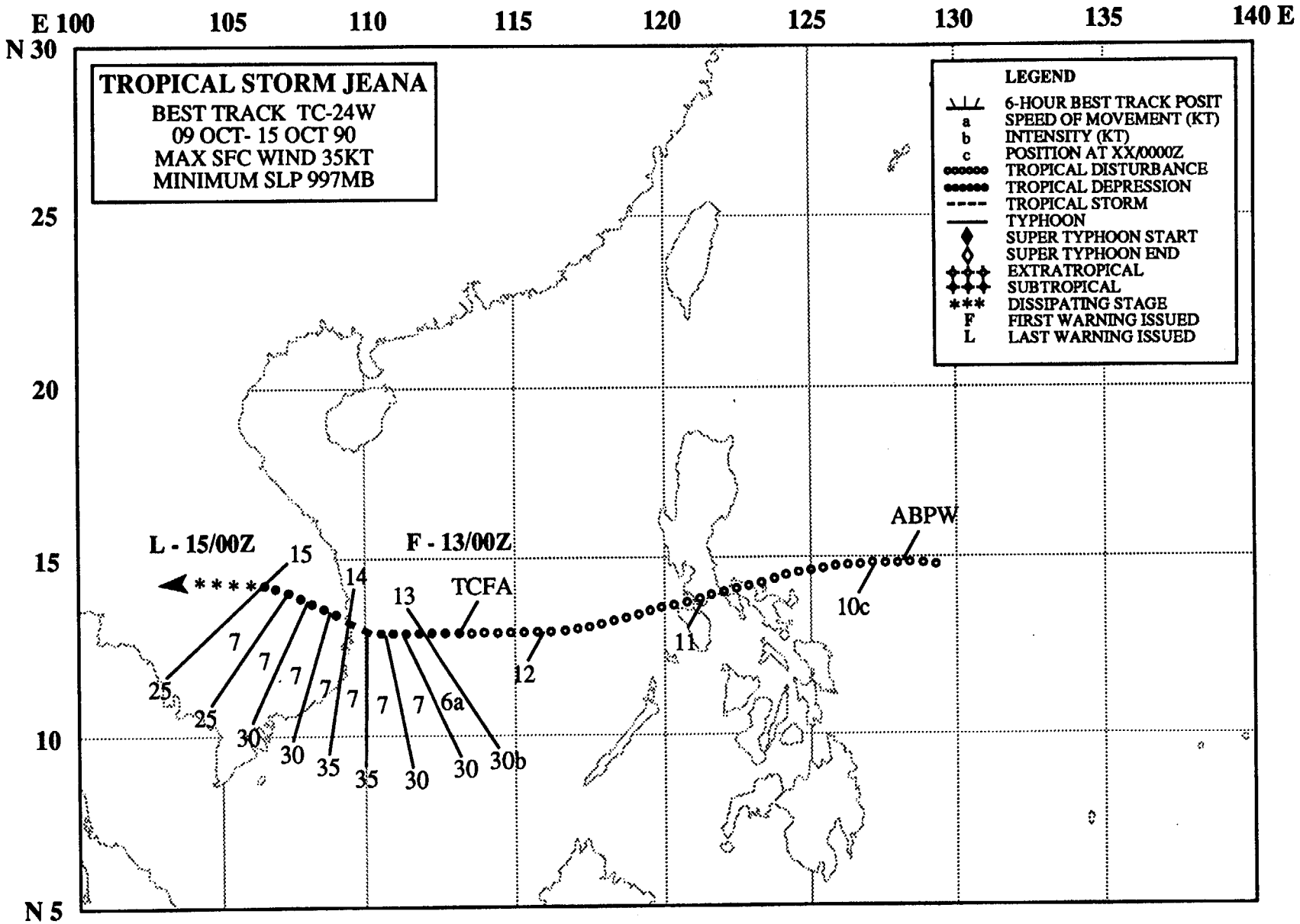
E 100
105
110
115
120
125
130
135
140 E
N 30
25
20
15
10
N 5
TROPICAL STORM JEANA
BEST TRACK TC-24W
09 OCT- 15 OCT 90
MAX SFC WIND 35KT
MINIMUM SLP 997MB
LEGEND
6-HOUR BEST TRACK POSIT
a SPEED OF MOVEMENT (KT)
b INTENSITY (KT)
c POSITION AT XX/0000Z
TROPICAL DISTURBANCE
TROPICAL DEPRESSION
TROPICAL STORM
TYPHOON
SUPER TYPHOON START
SUPER TYPHOON END
EXTRATROPICAL
SUBTROPICAL
*** DISSIPATING STAGE
F FIRST WARNING ISSUED
L LAST WARNING ISSUED
L - 15/00Z
F - 13/00Z
TCFA
ABPW
15
14
13
12
11
10c
6a
30b
7
25
30
35

TROPICAL STORM JEANA (24W)

I. HIGHLIGHTS

Jeana, the second of four tropical cyclones to form in October, was the fifth to churn across the South China Sea in 1990. This minimal tropical storm proved as difficult to estimate intensity for, as it was to position.

II. CHRONOLOGY OF EVENTS

091900Z - First mentioned on the Significant Tropical Weather Advisory as a weak cyclonic circulation associated with a shear zone in the Philippine Sea.

121330Z - Tropical Cyclone Formation Alert issued based on the presence of a 1005 mb minimum sea-level pressure, a well defined surface cyclone, brisk northeasterly trade winds of 25-30 kt (13-15 m/sec) extending 200-400 nm (350-750 km) to the north, and a CI 1.0.

130000Z - First warning issued due to continued development and a CI 2.0.

141200Z - Upgrade to tropical storm based on synoptic ship reports of 35 to 40 kt (17-20 m/sec) and an CI 2.5.

141800Z - Downgraded to a tropical depression after moving over land.

150000Z - Final warning issued based on Jeana's movement further inland and dissipation.

III. TRACK AND MOTION

On 9 October, Jeana developed in the Philippine Sea 540 nm (1000 km) southeast of Manila. For the next six days, the tropical cyclone tracked westward, south of a narrow subtropical ridge that extended across southern China and eastward along 25° north latitude. On 13 and 14 October, because of the poorly defined cloud system center (Figure 3-24-1), the exact location of Jeana as it approached the coast of Vietnam was difficult to fix. Synoptic and satellite fixes differed, which resulted in relocations for warnings number 02 and 03 and holding Jeana quasi-stationary for number 04. Only after the 15 October data became available and the low-level circulation located well inland in Laos, was the final best track constructed.

IV. INTENSITY

On 12 October intensification started in the South China Sea. An extensive area of peripheral northeasterly gales developed to the north of Jeana because of the tightening surface pressure gradient. On 14 October, ships reported 35-40 kt (17-20 m/sec) southerly winds 80-100 nm (150-185 km) east of Jeana's apparent center. It appeared that Jeana had most likely intensified into an tropical storm just before landfall on 14 October and the gale force winds remained overwater as the center of the circulation moved inland.

V. FORECASTING PERFORMANCE

The JTWC forecasts are superimposed on the final best track in Figure 3-24-2. Jeana's westward direction was correctly forecast.

VI. IMPACT

None reported.

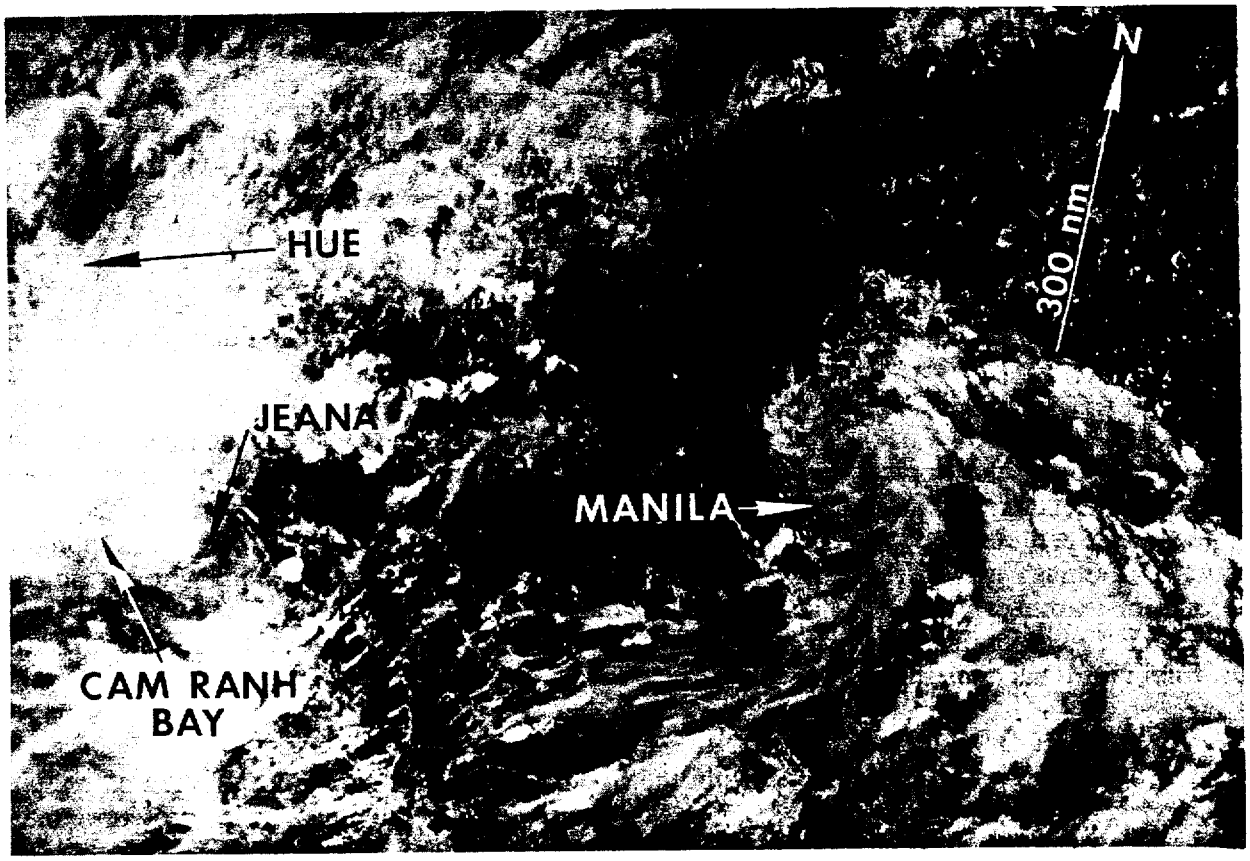

Figure 3-24-1. The partially exposed low-level circulation center of Tropical Depression 24W (Jeana) 12 hours prior to maximum intensity (130557Z October NOAA visual imagery).

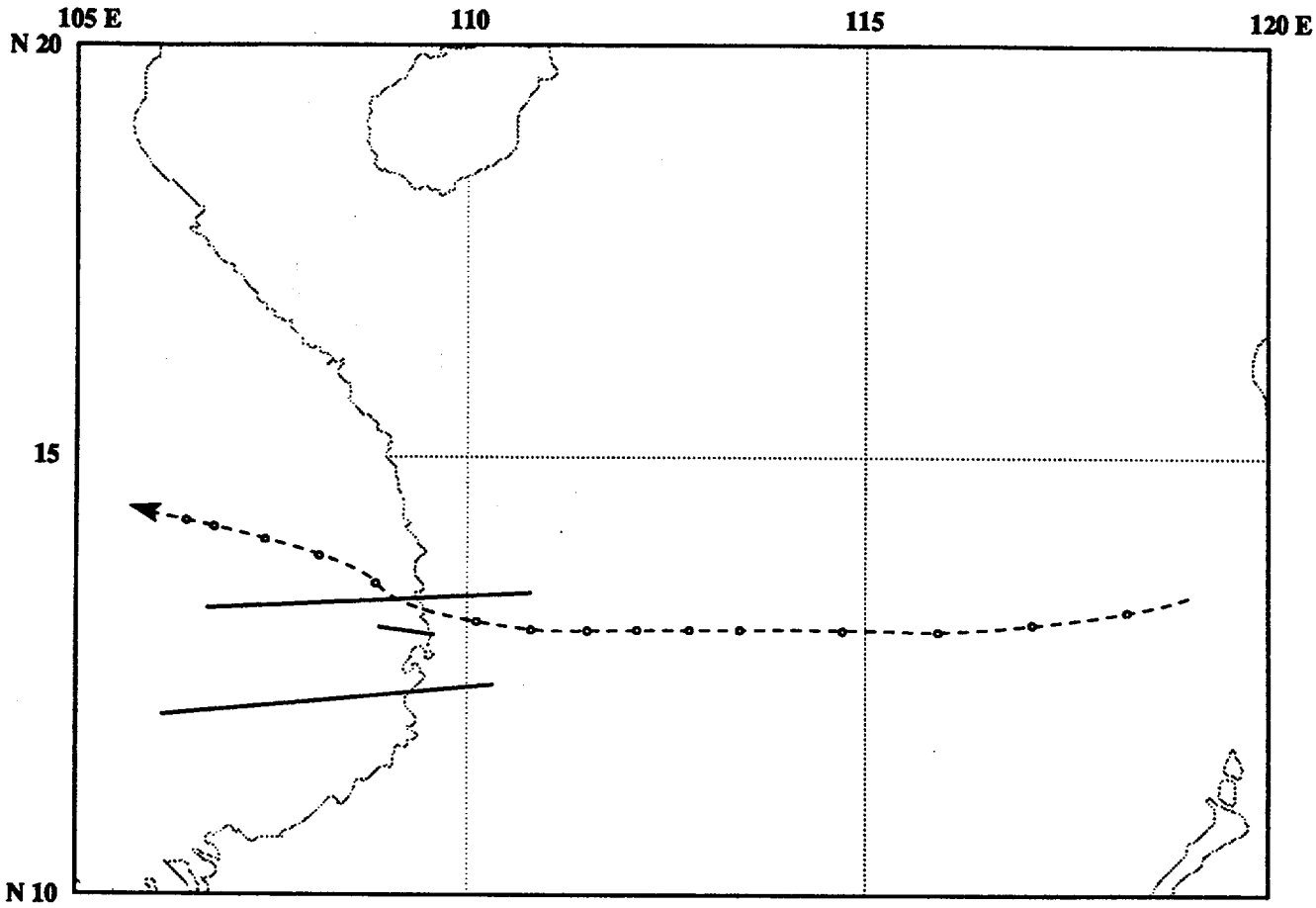

Figure 3-24-2. Summary of JTWC forecasts (solid lines) for Jeana superimposed on the final best track (dashed line).

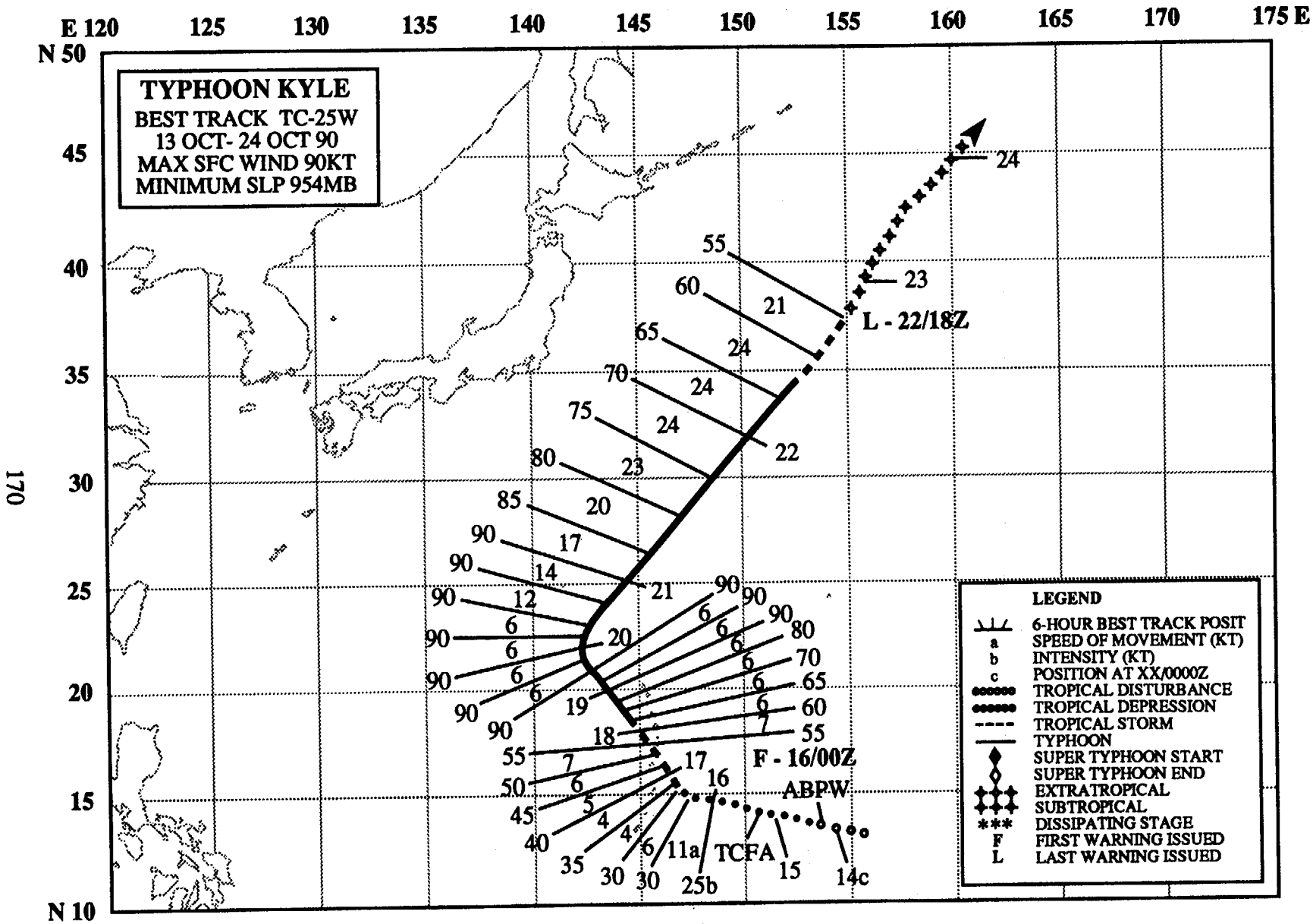
TYPHOON KYLE
BEST TRACK TC-25W
13 OCT- 24 OCT 90
MAX SFC WIND 90KT
MINIMUM SLP 954MB
E 120
125
130
135
140
145
150
155
160
165
170
175 E
N 50
45
40
35
30
25
20
15
N 10
170
L - 22/18Z
F - 16/00Z
ABPW
TCFA
LEGEND
6-HOUR BEST TRACK POSIT
SPEED OF MOVEMENT (KT)
INTENSITY (KT)
POSITION AT XX/0000Z
TROPICAL DISTURBANCE
TROPICAL DEPRESSION
TROPICAL STORM
TYPHOON
SUPER TYPHOON START
SUPER TYPHOON END
EXTRATROPICAL
SUBTROPICAL
DISSIPATING STAGE
FIRST WARNING ISSUED
LAST WARNING ISSUED

TYPHOON KYLE (25W)

I. HIGHLIGHTS

Kyle generated from a disturbance in the monsoon trough 600 nm (1110 km) east of Guam. Separating from the trough, the cloud system gained organization and began to track along the southern edge of the subtropical ridge to its northeast. The subtropical ridge and a series of fast moving mid-latitude short-wave troughs strongly influenced Kyle's track. The tropical cyclone passed through the northern Mariana Islands, causing minimal damage, intensified into a typhoon, and recurved several hundred miles east of Japan.

II. CHRONOLOGY OF EVENTS

140600Z - First mentioned on the Significant Tropical Weather Advisory as having fair potential for development due to its favorable location east of a TUTT cyclone.
150500Z - Tropical Cyclone Formation Alert issued based on first Dvorak intensity estimate of CI 1.0.
160000Z - First warning issued following intensity estimate of CI 1.5.
161800Z - Upgraded to tropical storm due to Dvorak current intensity estimate of 2.5.
180600Z - Upgrade to typhoon based on a CI 4.0 and weaker vertical shear.
190000Z - Peak intensity - 90 kt (45 m/sec) - followed on Dvorak current intensity of 5.0.
221200Z - Downgraded to tropical storm after the eye disappeared and interaction began with mid-latitude trough to the north.
221800Z - Final warning issued as Kyle underwent extratropical transition.

III. TRACK AND MOTION

Kyle formed at the eastern end of the monsoon trough. As the circulation consolidated and separated from the trough, it began to track west-northwestward under the influence of the mid-tropospheric subtropical ridge. On 16 October Kyle was headed directly towards the island of Saipan, which is located 100 nm (185 km) north-northeast of Guam. A mid-latitude short-wave trough approaching from Asia weakened the subtropical ridge and caused the tropical cyclone to slow and turn northwestward over the northern Marianas. The tropical cyclone continued to track northwestward along the western edge of the ridge and recurved on 20 October. Kyle maintained its tropical characteristics until extratropical transition occurred on 22 October.

IV. INTENSITY

Until 16 October, Kyle encountered upper-level wind shear which restricted its outflow to the west. Then the vertical wind shear lessened, Kyle intensified and interlocking cloud bands formed. A small eye was briefly observed on the 18 October satellite images, but disappeared into the ragged central dense overcast as the short wave approached from the northwest. Twenty-four hours later, after the short wave exited the area, the eye reappeared. As Kyle moved into higher latitudes, its eye became elongated due to pressure from increasing westerly winds aloft. Gradual weakening accompanied this interaction (Figure 3-25-1) and Kyle become extratropical on 22 October.

V. FORECASTING PERFORMANCE

JTWC beat all the objective aids with overall errors of 98 nm (181 km), 166 nm (307 km), and 196 nm (363 km) at 24, 48 and 72 hours, respectively. However, JTWC forecasters missed the turning point to the northwest on 16 October (Figure 3-25-2). The half persistence/half climatology model, HPAC, suggested a sharper turn than that predicted by the dynamical models, OTCM and FBAM. JTWC relied on the guidance from OTCM, since the ridge was not anticipated to weaken as drastically as it did. Later, JTWC forecasters accurately predicted the time and point of recurvature on 20 October,

achieving 72-hour forecast errors of less than 100 nm (185 km) for 3 consecutive warnings, beginning 60 hours prior to the event.

VI. IMPACT

No information was received.

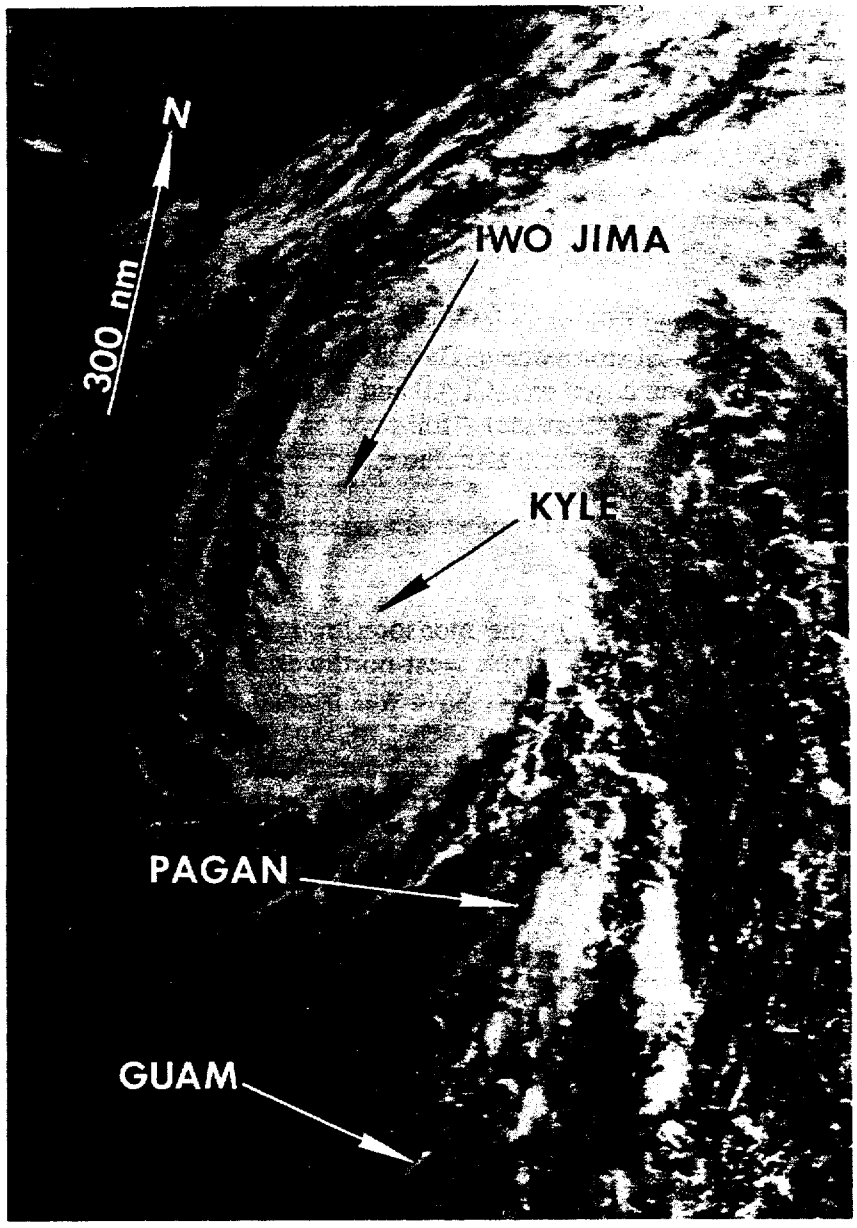

Figure 3-25-1. Typhoon Kyle with elongated eye begins to interact with a frontal system moving southeastward from Japan (200439Z October NOAA visual imagery).

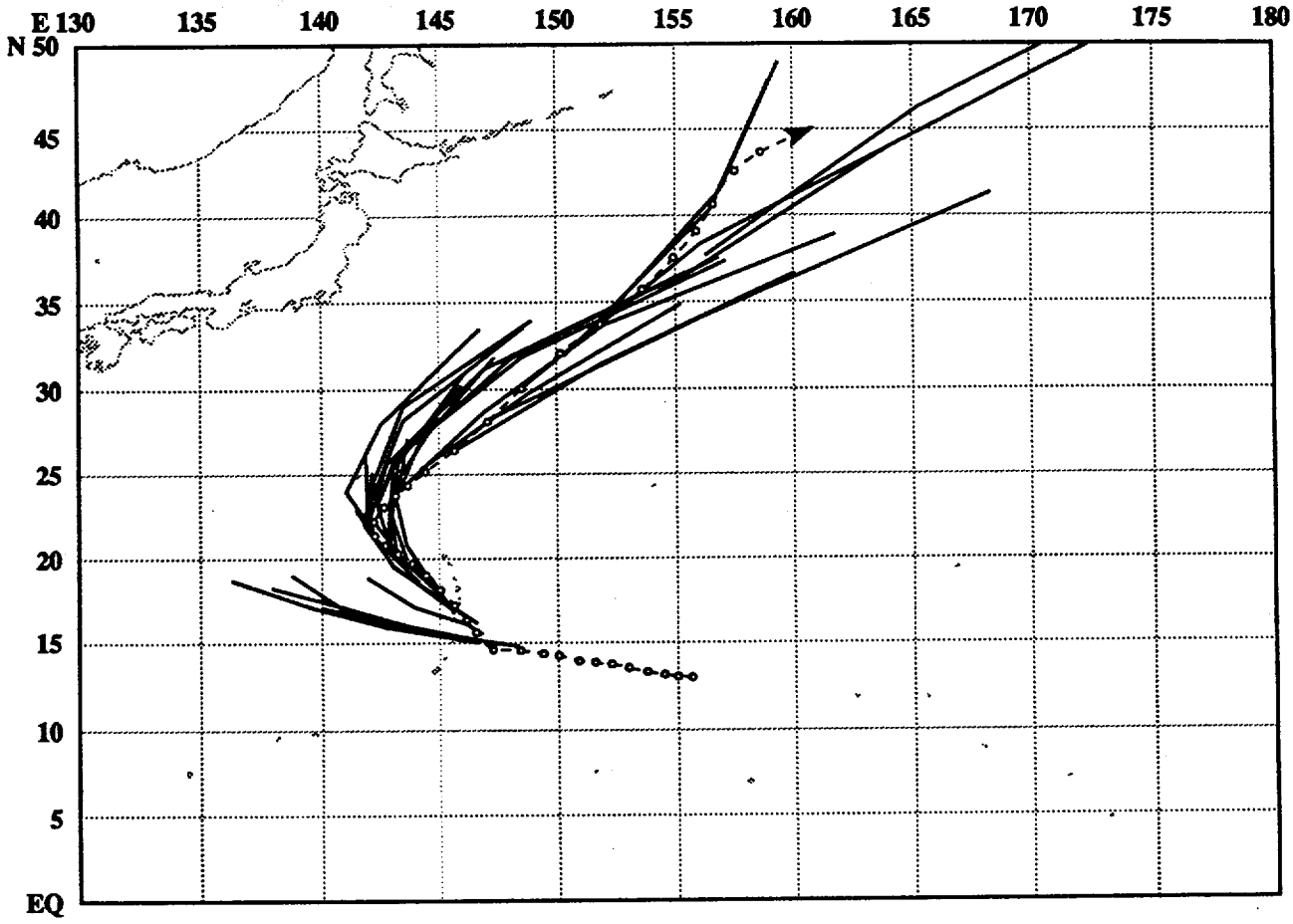

Figure 3-25-2. The overall JTWC forecast performance (solid lines) is superimposed on the final best track (dashed line).

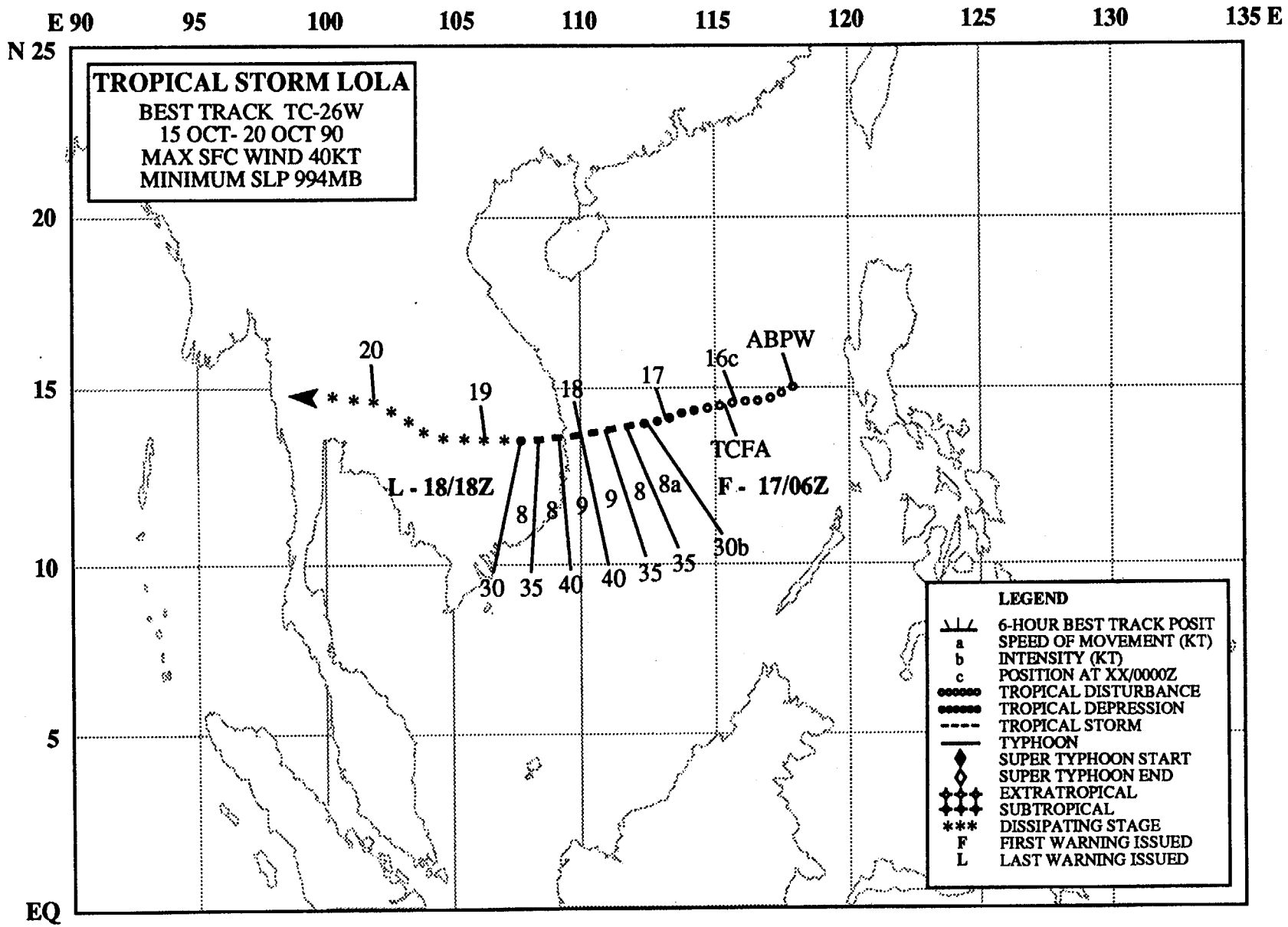
TROPICAL STORM LOLA
BEST TRACK TC-26W
15 OCT- 20 OCT 90
MAX SFC WIND 40KT
MINIMUM SLP 994MB
E 90
95
100
105
110
115
120
125
130
135 E
N 25
20
15
10
5
EQ
20
19
18
17
16c
ABPW
TCFA
L - 18/18Z
F - 17/06Z
8
8
9
9
8
8a
30b
30
35
40
40
35
35
LEGEND
6-HOUR BEST TRACK POSIT
a SPEED OF MOVEMENT (KT)
b INTENSITY (KT)
c POSITION AT XX/0000Z
TROPICAL DISTURBANCE
TROPICAL DEPRESSION
TROPICAL STORM
TYPHOON
SUPER TYPHOON START
SUPER TYPHOON END
EXTRATROPICAL
SUBTROPICAL
*** DISSIPATING STAGE
F FIRST WARNING ISSUED
L LAST WARNING ISSUED

TROPICAL STORM LOLA (26W)

I. HIGHLIGHTS

Lola, the last of four tropical cyclones to develop in October, formed in the South China Sea. It tracked westward along the same path taken by Tropical Storm Jeana (24W) four days earlier.

II. CHRONOLOGY OF EVENTS

150600Z - First mentioned on the Significant Tropical Weather as an area of convection associated with a weak low-level cyclonic circulation underneath a weak upper-level anticyclone.

160530Z - Tropical Cyclone Formation Alert based on increased organization associated with a surge of northeasterly winds coming off the coast of China.

170600Z - First Tropical Depression Warning issued due to a continued increase in organization as the system moved into an area of weaker vertical wind shear.

171200Z - Upgraded to a tropical storm due to an increase in organization associated with less vertical wind shear.

180000Z - Peak intensity - 40 kt (21 m/sec) - followed a small improvement in organization and an intensity estimate of 2.5.

181800Z - Final warning issued as Lola dissipated over land.

III. TRACK AND MOTION

Lola started in the monsoon trough on 15 October and tracked south of a narrow mid-level subtropical ridge for the next five days. Until landfall on the coast of Vietnam on 18 October, the track was consistently south of west because of the strong northeasterly low-level surge across the northern portion of the South China Sea.

IV. INTENSITY

Lola developed when a strong northeasterly surge spun up the low-level circulation. Reaching minimal tropical storm intensity on 17 October, Lola continued to intensify very slowly until it made landfall a day later (Figure 3-26-1). After landfall, the low-level cyclonic circulation persisted, as it crossed into Thailand, and dissipated just before entering the Bay of Bengal.

V. FORECASTING PERFORMANCE

Overall JTWC forecast performance is shown in Figure 3-26-2. Objective aid guidance and mid-level steering flow was used by forecasters; however, due to the strong low-level northeasterly surge Lola consistently tracked south of the forecasts.

VI. IMPACT

No information received.

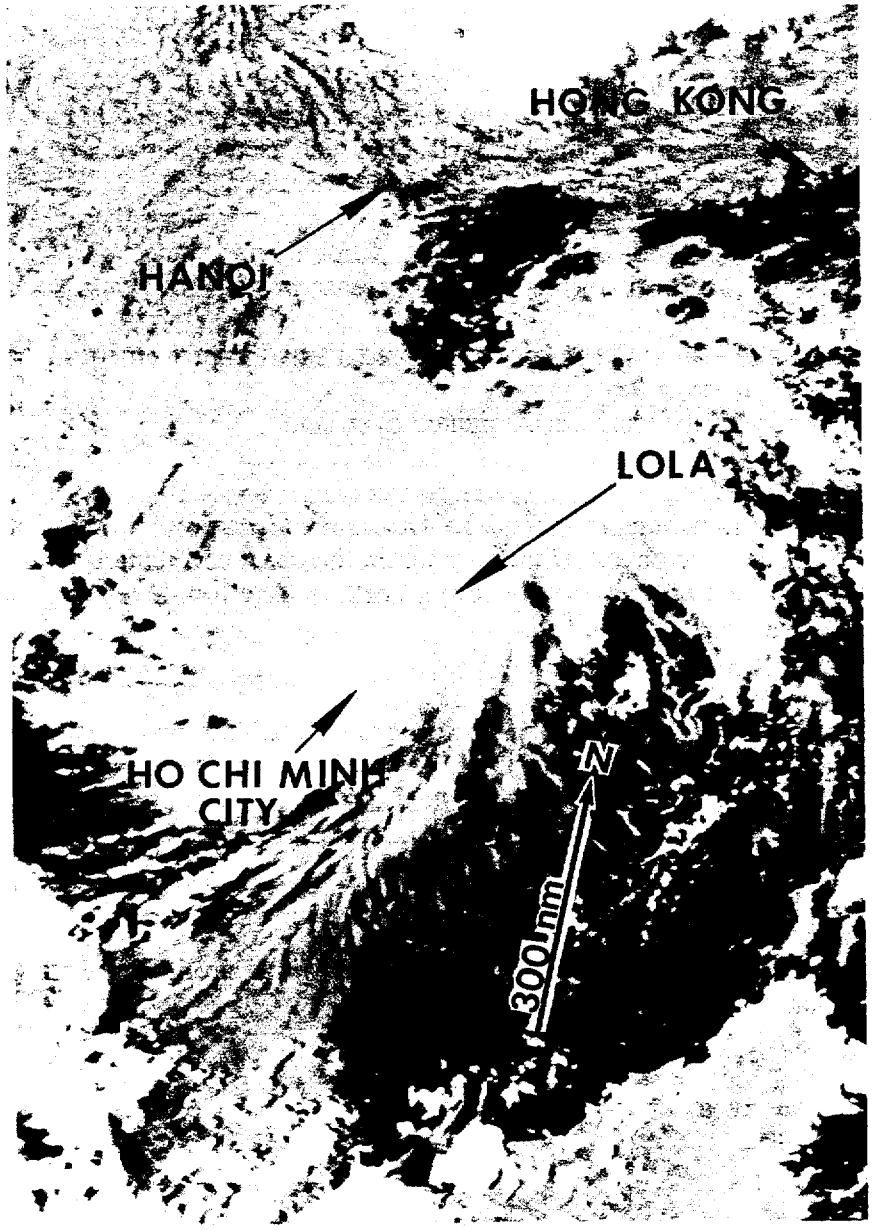

Figure 3-26-1. Lola at maximum intensity (180643Z October DMSP visual imagery).

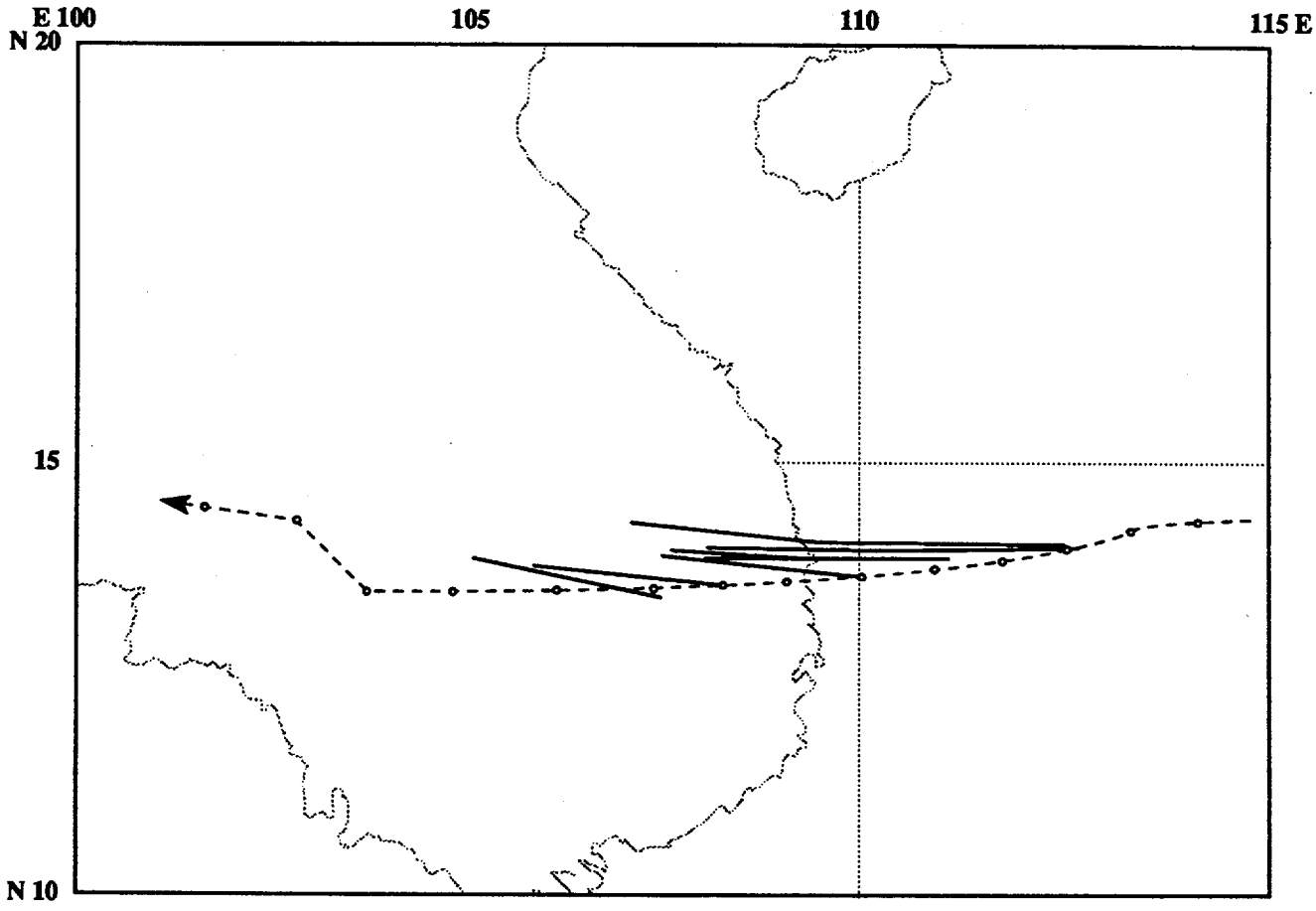

Figure 3-26-2. Summary of JTWC forecasts (solid lines) for Lola is superimposed on the final best track (dashed line).

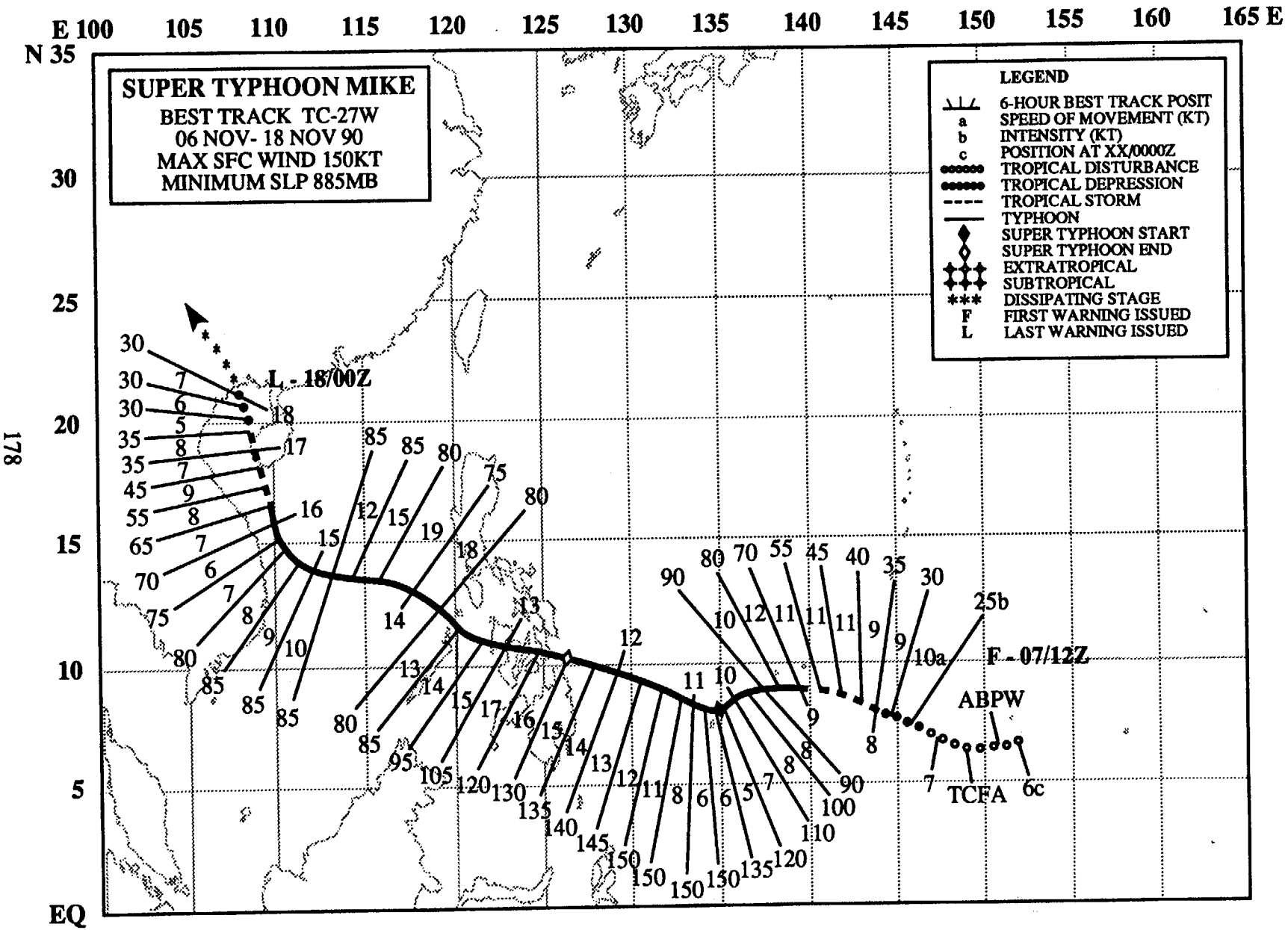
SUPER TYPHOON MIKE
BEST TRACK TC-27W
06 NOV- 18 NOV 90
MAX SFC WIND 150KT
MINIMUM SLP 885MB
LEGEND
6-HOUR BEST TRACK POSIT
SPEED OF MOVEMENT (KT)
INTENSITY (KT)
POSITION AT XX/0000Z
TROPICAL DISTURBANCE
TROPICAL DEPRESSION
TROPICAL STORM
TYPHOON
SUPER TYPHOON START
SUPER TYPHOON END
EXTRATROPICAL
SUBTROPICAL
DISSIPATING STAGE
FIRST WARNING ISSUED
LAST WARNING ISSUED
L - 18/00Z
F - 07/12Z
ABPW
TCFA
E 100
105
110
115
120
125
130
135
140
145
150
155
160
165 E
N 35
30
25
20
15
10
5
EQ
178

SUPER TYPHOON MIKE (27W)

I. HIGHLIGHTS

Mike, one of the most intense and destructive tropical cyclones of 1990, caused havoc in western Carolines and in the central Philippine islands. Although basically a west-northwestward "straight runner," it posed numerous forecast challenges due to frequent direction, speed and intensity changes. As a result of the devastation and death in the Republic of the Philippines, Super Typhoon Mike's name was retired from the JTWC naming list.

II. CHRONOLOGY OF EVENTS

060600Z – First mentioned on Significant Tropical Weather Advisory as an area of persistent convection with an estimated minimum sea-level pressure of 1008 mb.

061530Z – Tropical Cyclone Formation Alert based on rapidly improving outflow and curvature, an increase in central convection, and a CI 1.0 estimate.

071200Z – First warning issued due to continued increase in convection and good outflow in all quadrants. Synoptic data indicated minimum sea-level pressure of 1002 mb.

080000Z – Upgraded to tropical storm because synoptic data indicated 35 kt (18 m/sec) around the system.

090000Z – Upgraded to typhoon due to formation of an eye and a CI 4.5 estimate.

101200Z – Upgraded to super typhoon based on a Dvorak current intensity of 7.0, a small 15 nm (24 km) diameter symmetrical eye, and good outflow in all quadrants.

101800Z - Peak intensity - 150 kt (77 m/sec) - established with a CI 7.5.

121200Z – Downgraded from super typhoon status due to interaction with land, the eye had become ragged and cloud-filled, and the temperature at the top of the convection around the eye had warmed.

161200Z – Downgraded to tropical storm based on interaction with Vietnam coast and degraded satellite cloud signature due to increased vertical wind shear.

171200Z – Downgraded to tropical depression due to synoptic reports of weak winds and rising surface pressures, and disorganized cloud signature.

180000Z - Final warning (dissipated over land).

III. TRACK AND MOTION

Mike initially tracked west-northwestward under the influence of the mid-tropospheric subtropical ridge to the north. While undergoing rapid intensification on 9 November, it slowed and tracked west-southwestward (Figure 3-27-1). The reason for this change was not apparent, but could be related to the temporary effect of rapid intensification on the environment, and conversely the environment's adjustment to the massive release of latent heat. At 101200Z, Mike resumed its west-northwestward track which took it across the central Philippine islands and into the South China Sea. On 15 November, it turned north-northwestward toward a weakness in the subtropical ridge (Figure 3-27-2). This track took Mike across the western side of Hainan Dao and into southern China, where it dissipated.

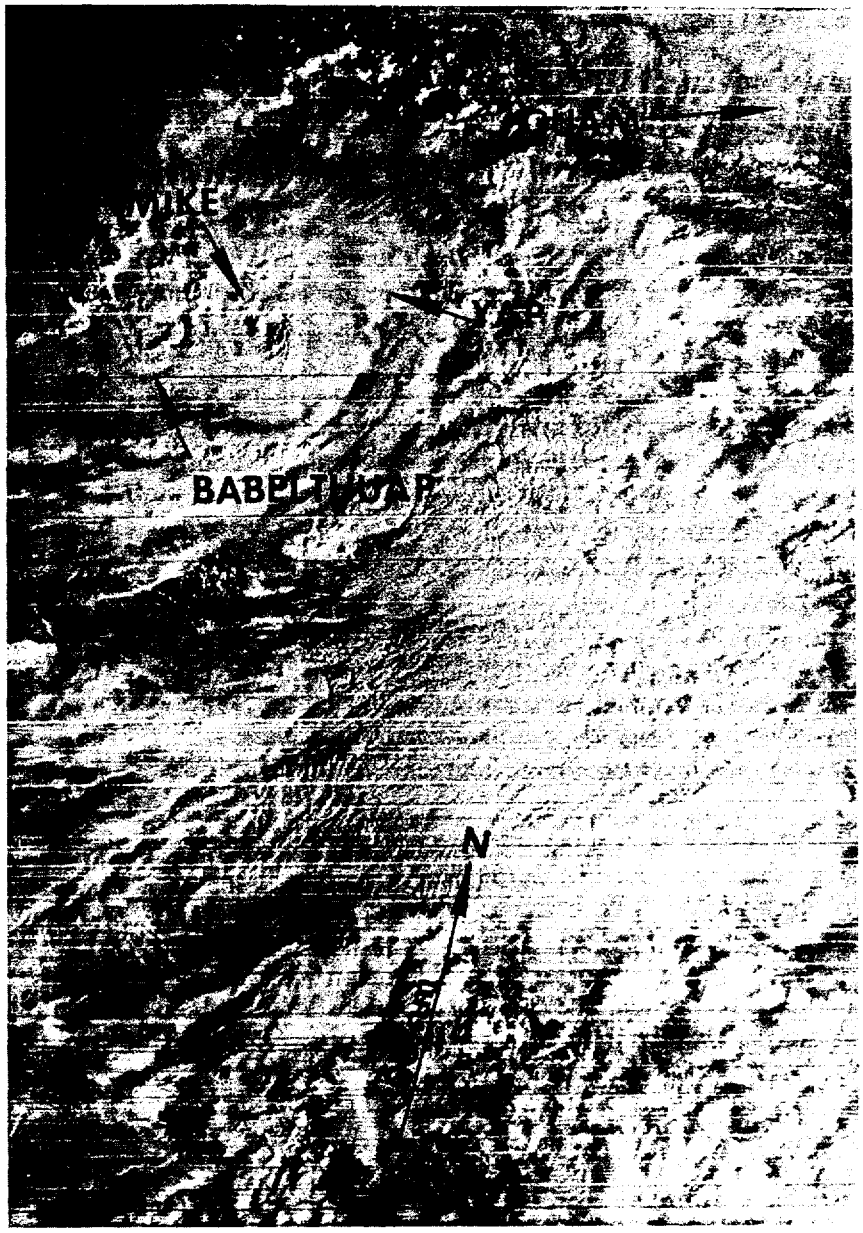

Figure 3-27-1. Mike is rapidly intensifying into a super typhoon as it passes through the western Caroline Islands (092106Z November DMSP visual imagery).

IV. INTENSITY

Mike intensified at a normal rate of T-number per day until reaching moderate tropical storm status at 081200Z. Then intensification accelerated and reached a peak of 150 kt (77 m/sec) at 101800Z. The maximum sustained surface winds increased an additional 95 kt and the estimated minimum sea-level pressure fell 99 mb to 885 mb (Figure 3-27-3) during this 48-hour period. A 200-mb trough to the northeast and broad cross equatorial flow to the south and southwest of Mike provided dual outflow channels that efficiently supported intensification. As Super Typhoon Mike approached landfall in the central Philippine Islands on 12 November, it weakened to just under super typhoon intensity at 121800Z due to the disruptive affects of the mountainous island chain across its path. After further weakening to 80 kt (40 m/sec), the typhoon reintensified to 85 kt (42 m/sec) at 141200Z over the open waters of the South China Sea. As Mike turned north-northwestward off the coast of Vietnam, increased vertical shear started the weakening process again. Dissipation followed on 18 November over southern China.

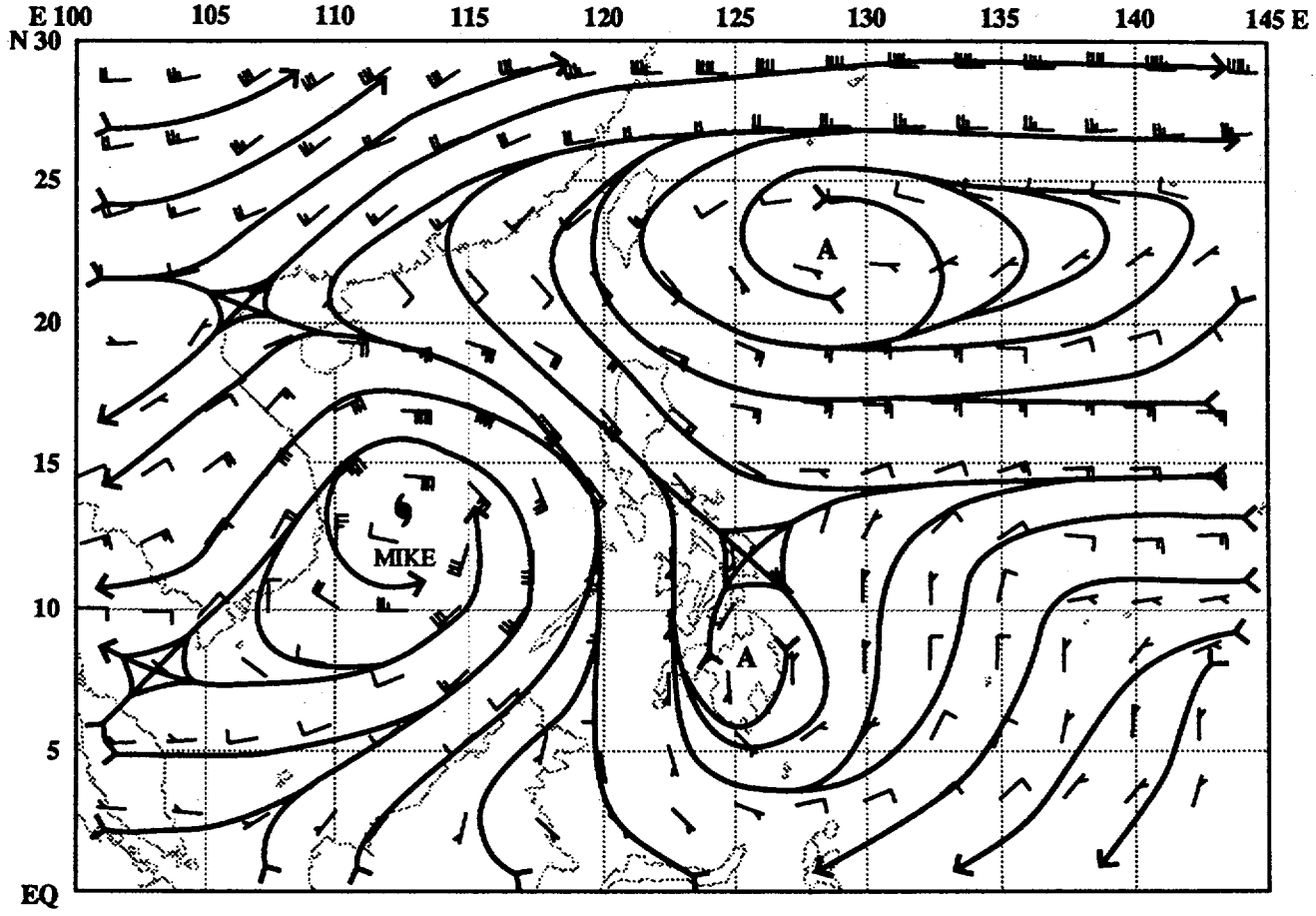

Figure 3-27-2. The deep layer mean analysis for 150000Z November shows Mike and the weakness in the subtropical ridge to the northwest.

V. FORECASTING PERFORMANCE

The overall JTWC forecast performance with respect to the best track is shown in Figure 3-27-4. Initially, JTWC forecast the tropical cyclone to move towards the northwest into the central Philippine Sea. At 091200Z, JTWC introduced a moderate probability alternate scenario of movement across the Philippine Islands, although the NOGAPS prognostic series continued to indicate that a weakness would develop in the ridge just east of Luzon. At 100000Z, it was apparent that Typhoon Mike was moving west-southwestward as the system approached Palau. Mike was expected to resume its west-northwestward track within 24 hours. The prognostic series continued to indicate a weakness in the subtropical ridge, and JTWC continued to forecast northwest motion. However, at the 120000Z, the NOGAPS prognostics changed to reflect a stronger subtropical ridge north of Mike, and subsequently JTWC forecasts reflected motion across the central Philippines, rather than up the east coast of Luzon. As Mike continued west-northwestward into the South China Sea, forecasters expected it to make landfall in Vietnam. Again, the models provided erroneous guidance. The prognostic series failed to predict the weakness that eventually developed in the subtropical ridge to the north (see again Figure 3-27-2).

Mike's favorable outflow pointed to rapid intensification, which was in fact forecast. Despite the fact that there are no objective aids, or hard and fast rules of thumb, to predict the exact rate or peak intensity, the forecast of 130 kt (67 m/sec) maximum was made 48 hours before Mike actually peaked at 150 kts (77 m/sec). Later as Mike approached the Philippine Islands, preliminary results from a climatological study of tropical cyclones crossing the Philippines correctly indicated that it would weaken to 85 kt (44 m/sec), enabling JTWC to issue a perfect 72-hour intensity forecast.

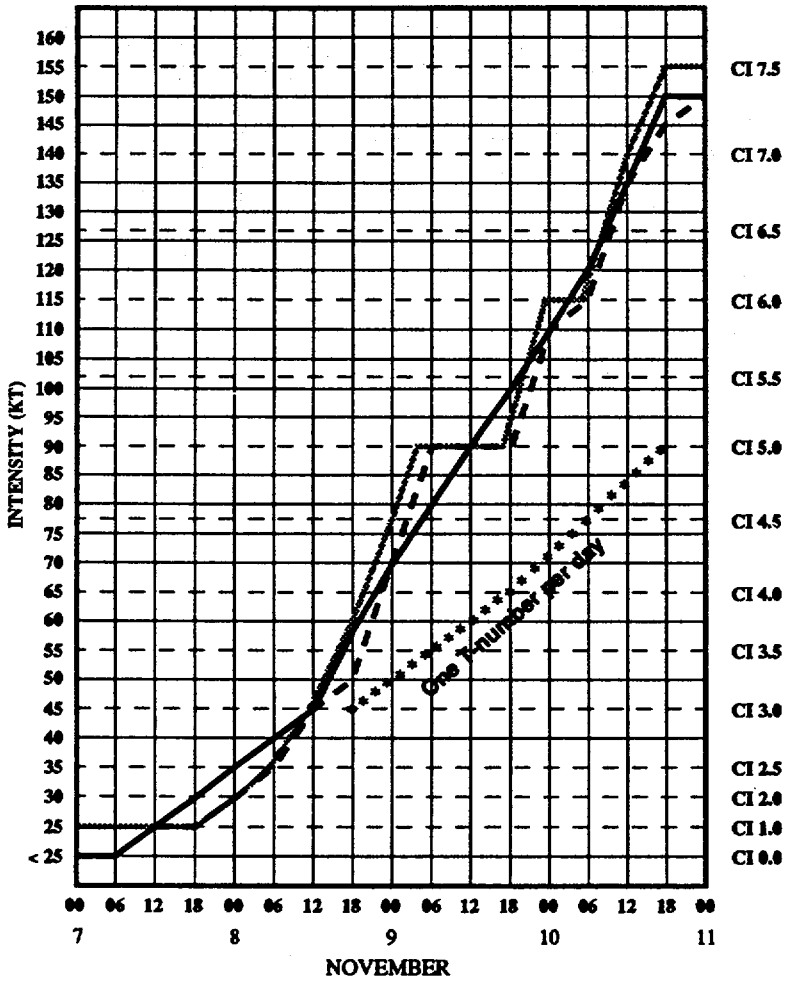

Figure 3-27-3. Plots of the satellite current intensity values (gray line), actual warning intensities (dashed line), and final best track (solid line) on a time-intensity comparison chart depict Mike's greater than normal rate of intensification after 081200Z. The normal development of one T-number per day (starred line) is included as a reference.

VI. IMPACT

Super Typhoon Mike was extremely destructive to the western Carolines and central Philippine Islands. On Koror, 45 nm (85 km) south of Mike's center, many roofs were lost and extensive damage occurred to boats, greenhouses, aquiculture projects, fruit trees and vegetable gardens. Fortunately there were no fatalities and only one serious injury was reported. Power, water and telephone services were completely out and roads were blocked by fallen trees. The National Weather Service Office at Koror (WMO 91408) recorded maximum wind gusts to 72 kt (36 m/sec), a minimum sea-level pressure of 980.5 mb and 9.8 inches (250 mm) of rain. Closer to Mike's center, where maximum wind gusts were estimated to range from 135 to 165 kt (69 to 85 m/sec), Kayangel Island just to the north of Babelthuap was almost totally devastated. Many people lost everything. Most trees used for subsistence were destroyed, with some, such as breadfruit, expected to take up to ten years to replace.

Super Typhoon Mike became the most powerful typhoon to strike the Philippine Islands this year and was reported to be the most devastating to hit the country since 1981. In the central Philippine islands at least 250 people were reported dead or missing, mostly from landslides, and 2 million people were forced from their homes into temporary shelters. Over 37,000 houses were destroyed, and at least $14 million worth of damage was recorded. Cebu city, the commercial and transportation capital of the region, was severely damaged and more than 57 water craft, mostly in the port of Cebu, sank.

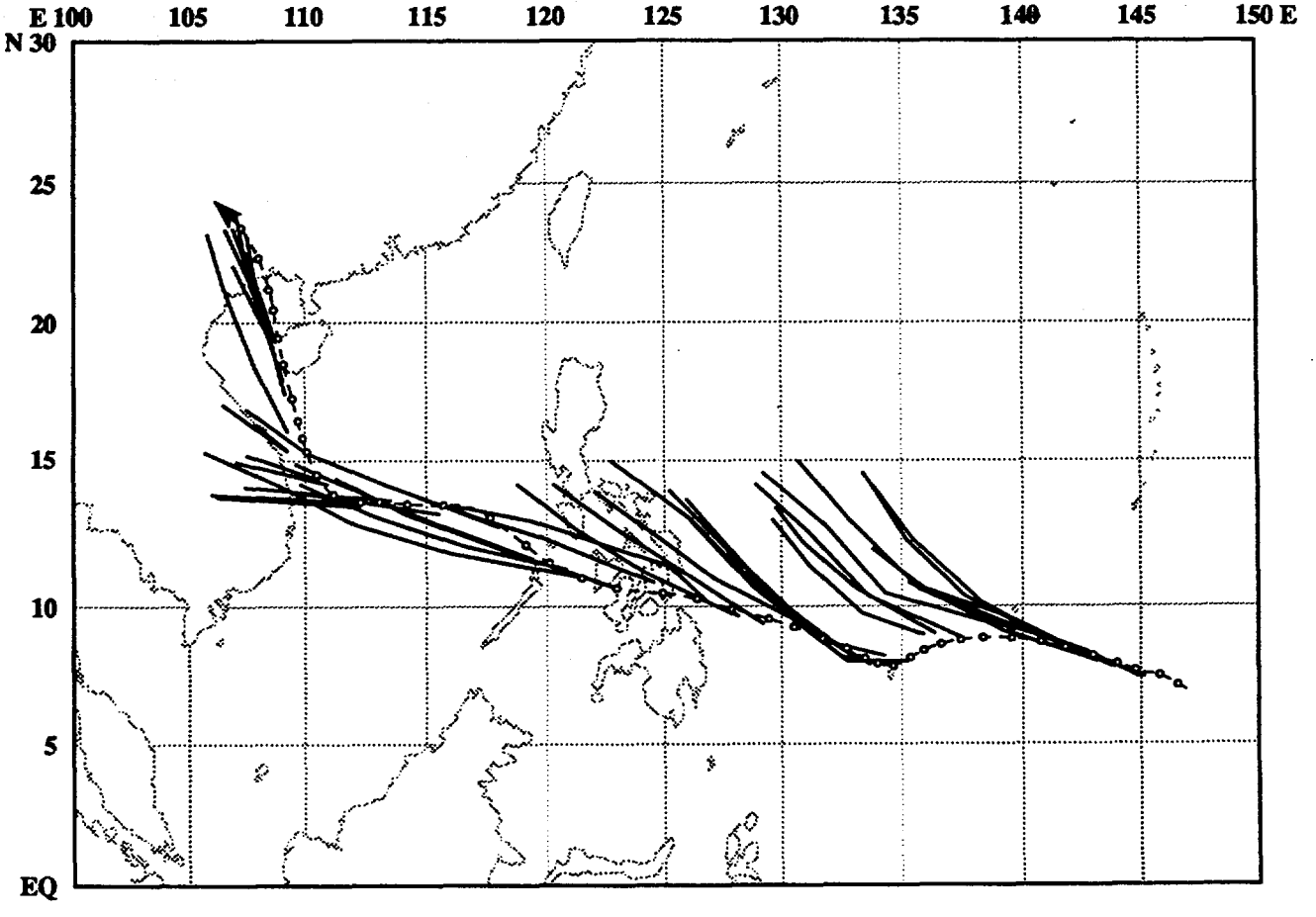

Figure 3-27-4. The JTWC forecasts (solid lines) for Mike superimposed on the final best track (dashed line).

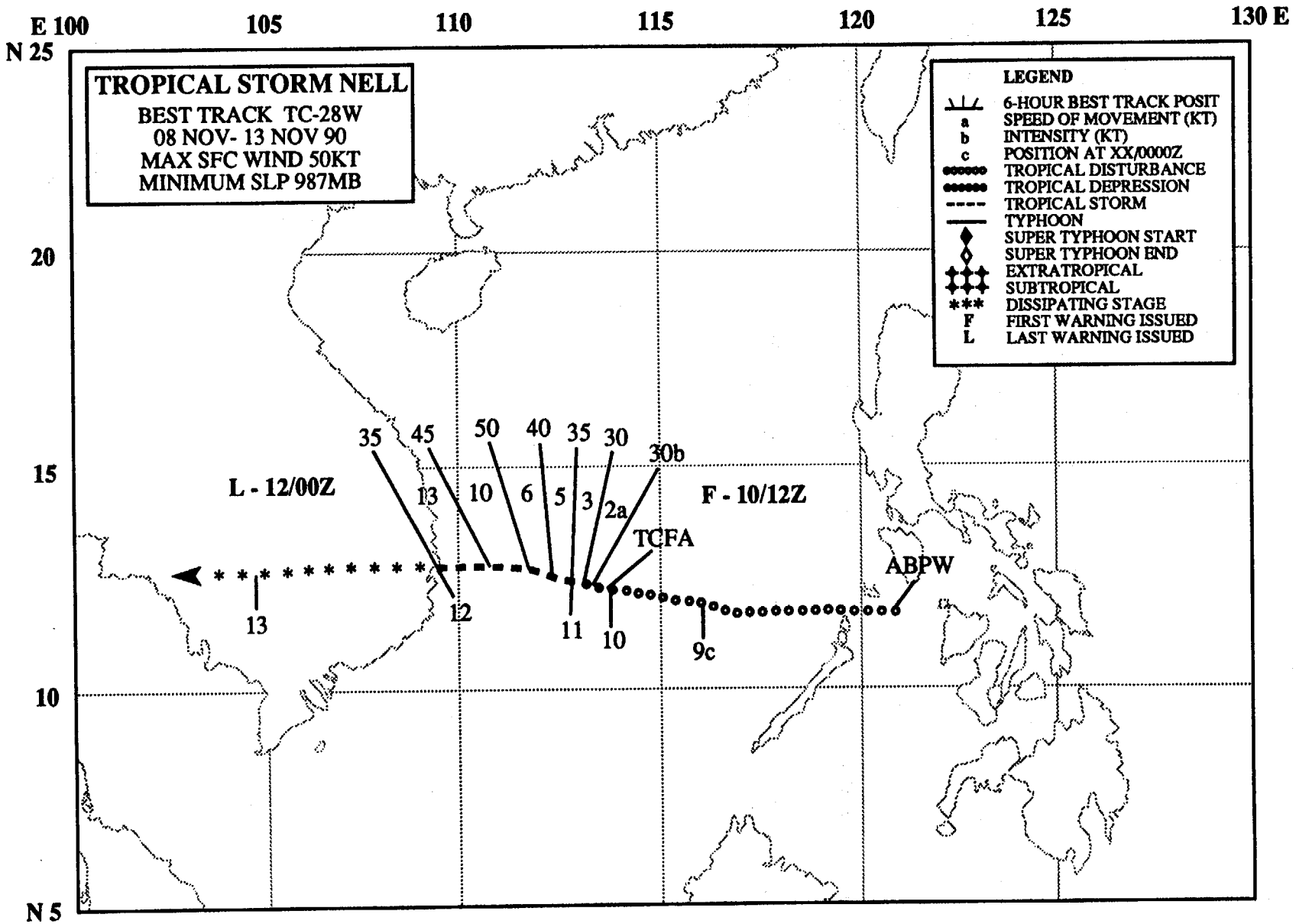
E 100
105
110
115
120
125
130 E
N 25
20
15
10
N 5
TROPICAL STORM NELL
BEST TRACK TC-28W
08 NOV- 13 NOV 90
MAX SFC WIND 50KT
MINIMUM SLP 987MB
LEGEND
6-HOUR BEST TRACK POSIT
a SPEED OF MOVEMENT (KT)
b INTENSITY (KT)
c POSITION AT XX/0000Z
TROPICAL DISTURBANCE
TROPICAL DEPRESSION
TROPICAL STORM
TYPHOON
SUPER TYPHOON START
SUPER TYPHOON END
EXTRATROPICAL
SUBTROPICAL
*** DISSIPATING STAGE
F FIRST WARNING ISSUED
L LAST WARNING ISSUED
35
45
50
40
35
30
30b
13
10
6
5
3
2a
TCFA
L - 12/00Z
F - 10/12Z
ABPW
13
12
11
10
9c

TROPICAL STORM NELL (28W)

I. HIGHLIGHTS

Nell, the second of four November tropical cyclones, intensified in the South China Sea and tracked westward, making landfall in Vietnam.

II. CHRONOLOGY OF EVENTS

080600Z - First mentioned on Significant Tropical Weather Advisory as a disturbance with a persistent area of convection with estimated minimum sea-level pressure of 1005 mb.
100330Z - Tropical Cyclone Formation Alert issued due to increased convective organization.
101200Z - First warning issued due to surface synoptic reports of 25-30 kt (13-15 m/sec) winds.
110000Z - Upgrade to tropical storm based on a synoptic report of 996 mb sea-level pressure and 35 kt (18 m/sec) surface wind.
111200Z - Peak intensity of 50 kt (25 m/sec) based on ship reports.
120000Z - Final warning issued as Nell moved over land and began to dissipate in Vietnam.

III. TRACK AND MOTION

Nell formed west of the central Philippine Islands and tracked across the South China Sea south of the subtropical ridge which remained near 20° north latitude. After landfall, the low-level cyclonic circulation moved westward into Thailand.

IV. INTENSITY

Nell developed in association with a surge in the northeast monsoon, reached tropical storm intensity (Figure 3-28-1) on 11 November, and peaked at 50 kt (25 m/sec) despite indications of strong vertical shear.

V. FORECASTING PERFORMANCE

Initially, fix position uncertainties and the strength of the surge in the northeast monsoon led forecasters to believe Nell would move south-southwestward. Later forecasts reflected the movement to the west (Figure 3-28-2).

VI. IMPACT

No information received.

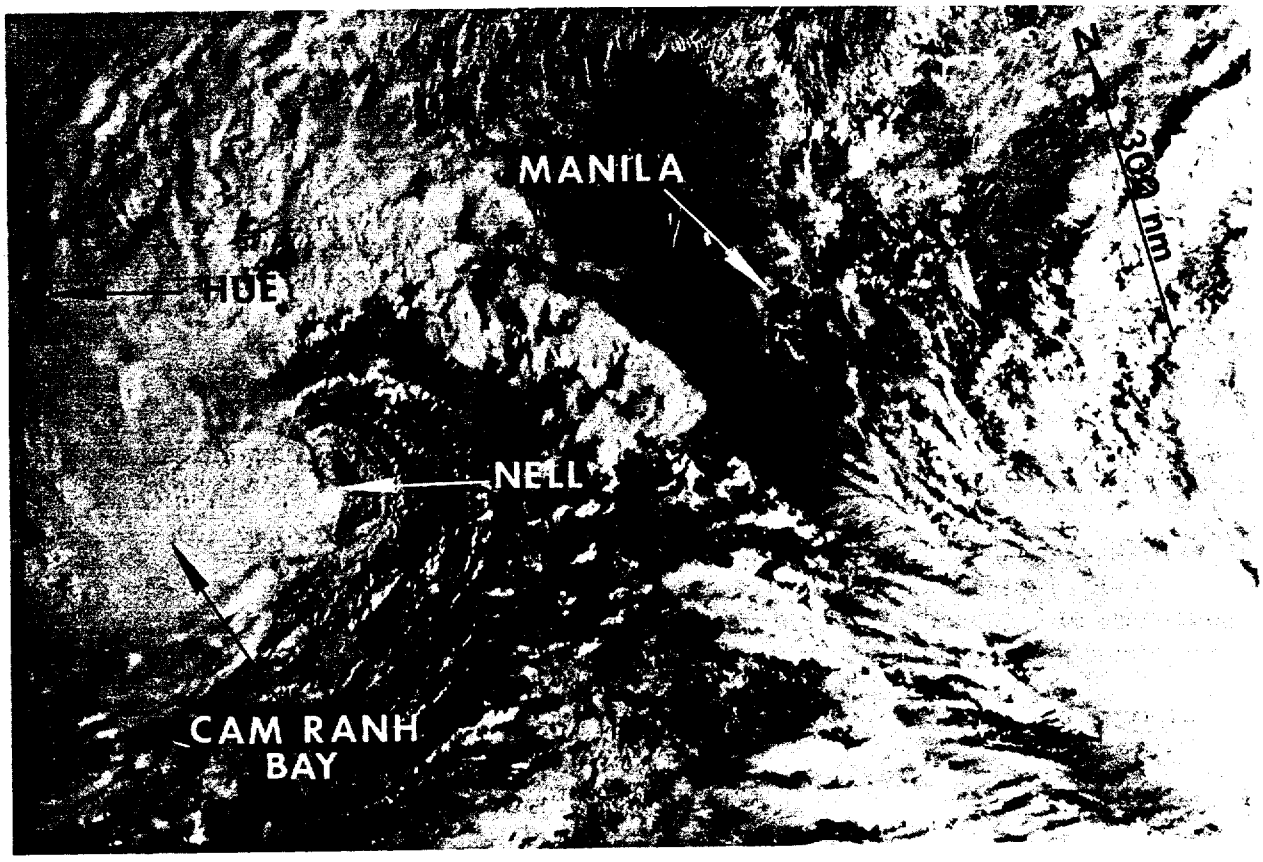

Figure 3-28-1. Just before reaching tropical storm intensity, Nell's LLCC is partially exposed (102335Z November NOAA visual imagery)

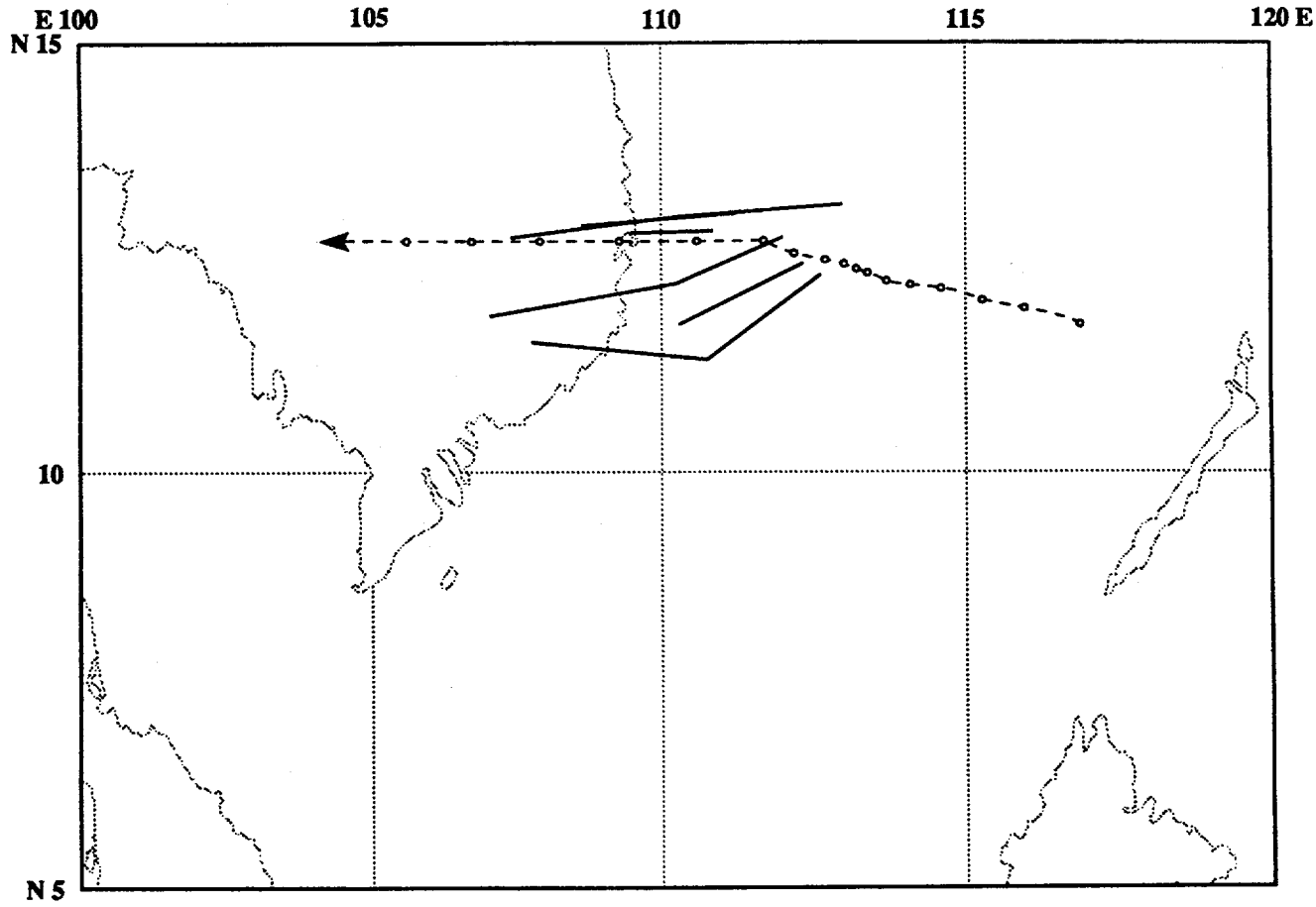

Figure 3-28-2. Summary of JTWC forecasts (solid lines) for Nell is superimposed on the final best track (dashed line).

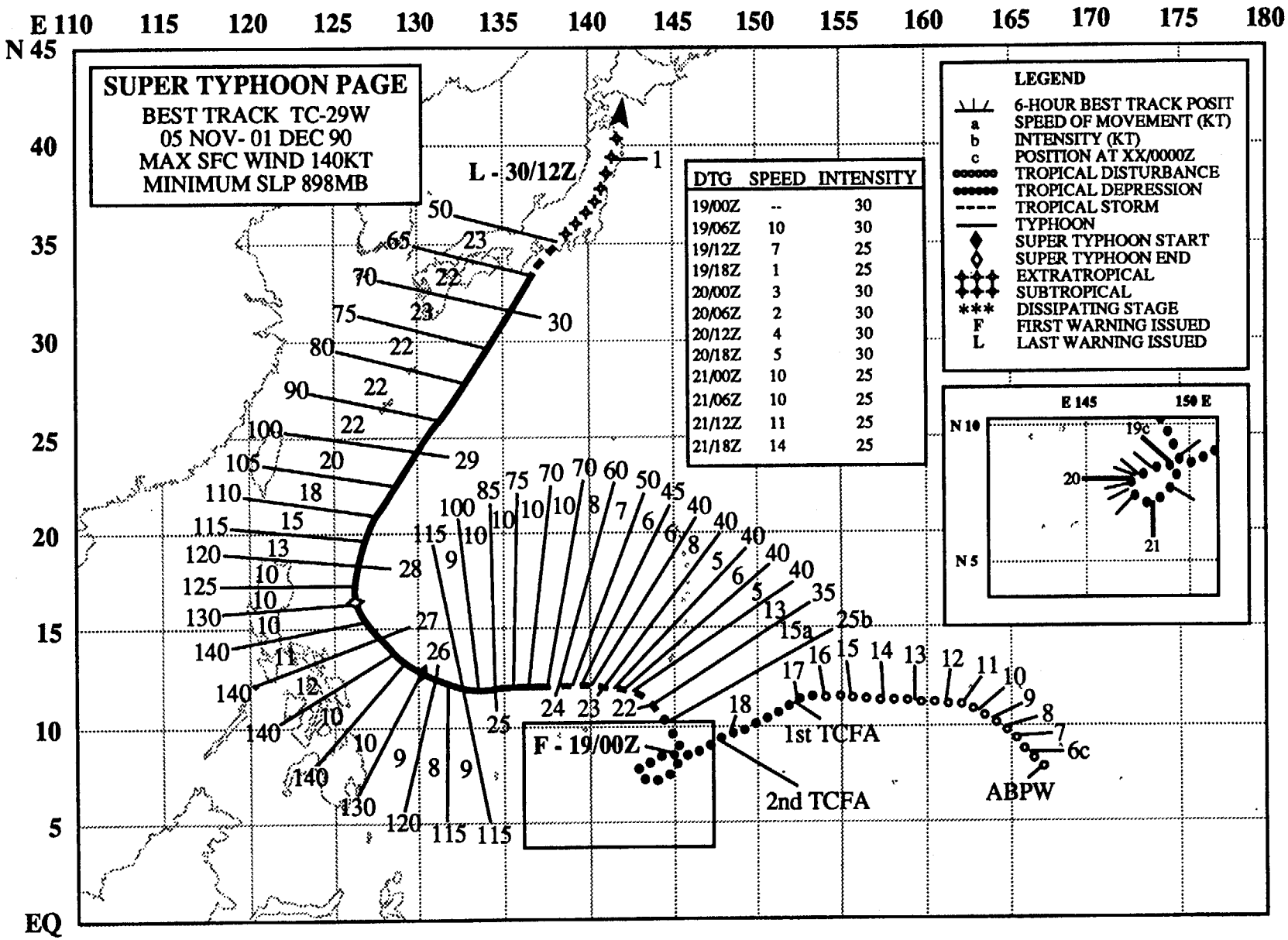
E 110 115 120 125 130 135 140 145 150 155 160 165 170 175 180
N 45 40 35 30 25 20 15 10 5 EQ
SUPER TYPHOON PAGE
BEST TRACK TC-29W
05 NOV- 01 DEC 90
MAX SFC WIND 140KT
MINIMUM SLP 898MB
L - 30/12Z
F - 19/00Z
1st TCFA
2nd TCFA
ABPW
DTG SPEED INTENSITY
19/00Z -- 30
19/06Z 10 30
19/12Z 7 25
19/18Z 1 25
20/00Z 3 30
20/06Z 2 30
20/12Z 4 30
20/18Z 5 30
21/00Z 10 25
21/06Z 10 25
21/12Z 11 25
21/18Z 14 25
LEGEND
6-HOUR BEST TRACK POSIT
a SPEED OF MOVEMENT (KT)
b INTENSITY (KT)
c POSITION AT XX/0000Z
TROPICAL DISTURBANCE
TROPICAL DEPRESSION
TROPICAL STORM
TYPHOON
SUPER TYPHOON START
SUPER TYPHOON END
EXTRATROPICAL
SUBTROPICAL
*** DISSIPATING STAGE
F FIRST WARNING ISSUED
L LAST WARNING ISSUED
E 145 150 E
N 10
N 5

SUPER TYPHOON PAGE (29W)

I. HIGHLIGHTS

Page was the third of four tropical cyclones to form in November, the second super typhoon of the month, and part of the three-storm outbreak which included a pair of tropical cyclones near the date line: Owen (30W) in the northern hemisphere and Sina (TC 03P) in the southern hemisphere. Persisting as a discrete disturbance for nearly two weeks before the first warning was issued, Page took only three days to intensify to 140 kt (70 m/sec) once development commenced.

II. CHRONOLOGY OF EVENTS

050600Z - First mentioned on the Significant Tropical Weather Advisory as an area of persistent convection with an estimated minimum sea-level pressure of 1008 mb.

170300Z - First Tropical Cyclone Formation Alert based on better convective organization with increased low-level inflow, indications in the NOGAPS prognostic series of a decrease in vertical wind shear over the area, and a CI 1.5 estimate.

180300Z - Second Tropical Cyclone Formation Alert based on a broadening low-level circulation with decreasing vertical wind shear and a surge in the easterlies north of the disturbance.

190000Z - First warning issued due to the low-level circulation center moving under the edge of the central cloud mass, a developing upper-level anticyclone, and a current intensity estimate of CI 2.0.

220000Z - Upgraded to a tropical storm after convective curvature increased, upper-level outflow improved, and the first intensity estimate of CI 2.5.

240600Z - Upgraded to typhoon intensity after formation of an eye wall and intensity estimates of CI 4.0.

260600Z - Upgrade to a super typhoon followed the development of a well defined 40 nm (75 km) diameter eye and intensity estimates of CI 6.5.

271800Z - Downgraded to a typhoon after a decrease in central convection, visible loss of eye wall definition and an intensity estimate of CI 6.0.

300600Z - Downgrade to tropical storm based on increased vertical wind shear and the start of extratropical transition.

301200Z - Final warning based on a combination of land interaction with Honshu and extratropical transition.

III. TRACK AND MOTION

Page formed in the Marshall Islands near Kwajalein Atoll and tracked slowly westward on the south side of the subtropical ridge. As the disturbance passed south of Guam on 19 November, it interacted with enhanced low-level equatorial westerlies supporting a multiple cyclone outbreak further eastward near the date line (Figure 3-29-1). Page executed a counterclockwise loop which took two days to complete and then the resumed a westward track on 22 November . As Page neared 125° east longitude, it tracked northward through a break in the subtropical ridge, recurved on 27 November, and accelerated northeastward.

IV. INTENSITY

Page's swirl of low-level cloudiness remained intact, but poorly organized, for two weeks beneath strong easterly flow aloft which restricted vertical development (Figure 3-29-2). On 23 November, the tropical cyclone began steady intensification in an area of lower vertical wind shear. Over the next three days, Page (Figure 3-29-3) underwent several periods of rapid intensification to reach a peak of 140 kt (72 m/sec) on 26 November. During this 72-hour period, the estimated sea-level pressure (Atkinson-Holliday, 1977) dropped 93 mb to a minimum of 898 mb with a subsequent 95 kt (50 m/sec) increase in the maximum winds. After maintaining peak intensity for a day, Page began to weaken due to increasing vertical wind shear as it encountered the mid-latitude westerlies. Extratropical transition occurred over Honshu on 30 November.

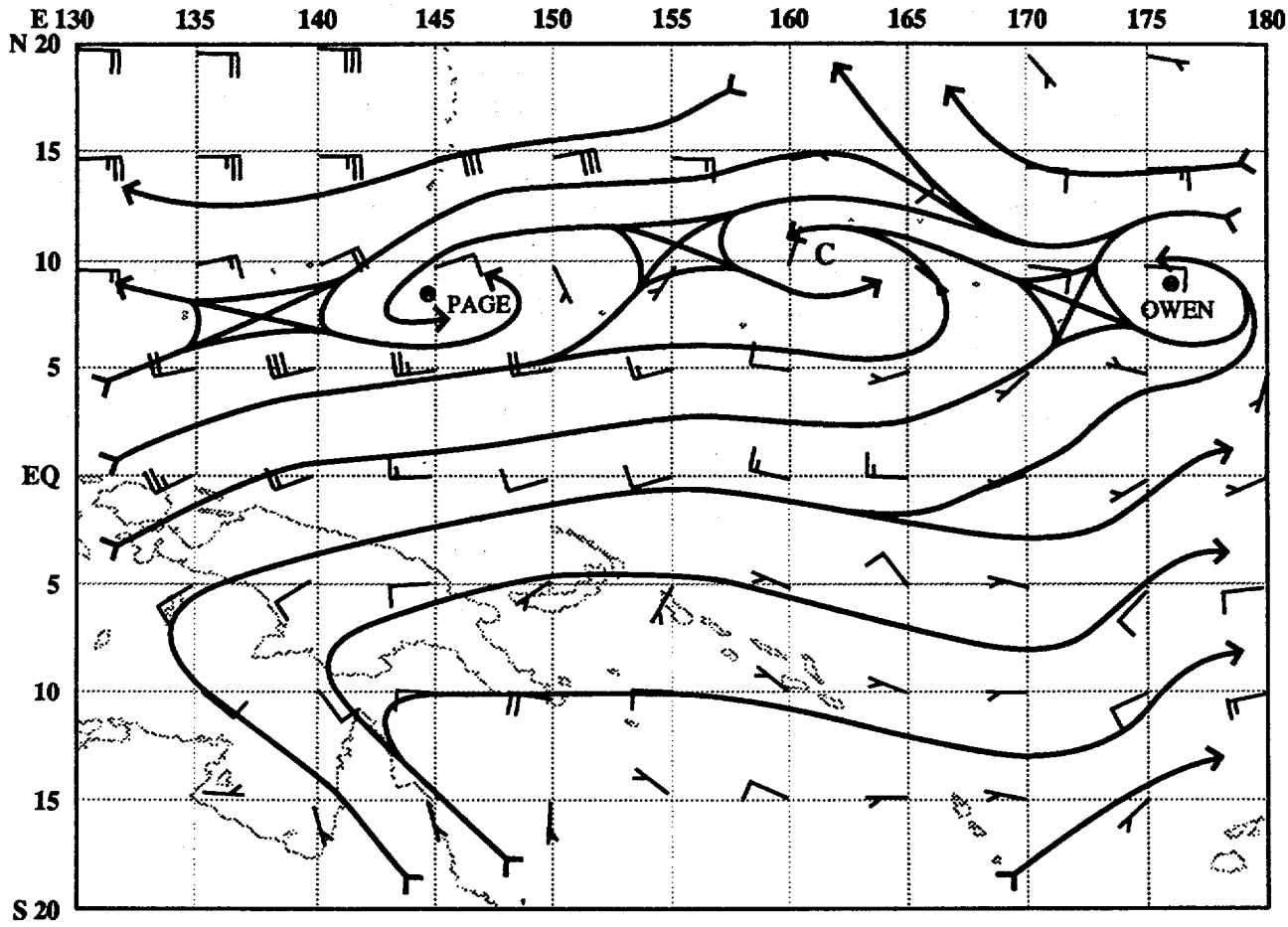

Figure 3-29-1. The 190000Z November NOGAPS 850-mb analysis shows enhanced low-latitude flow, extending eastward to the dateline where Owen (30W) was developing.

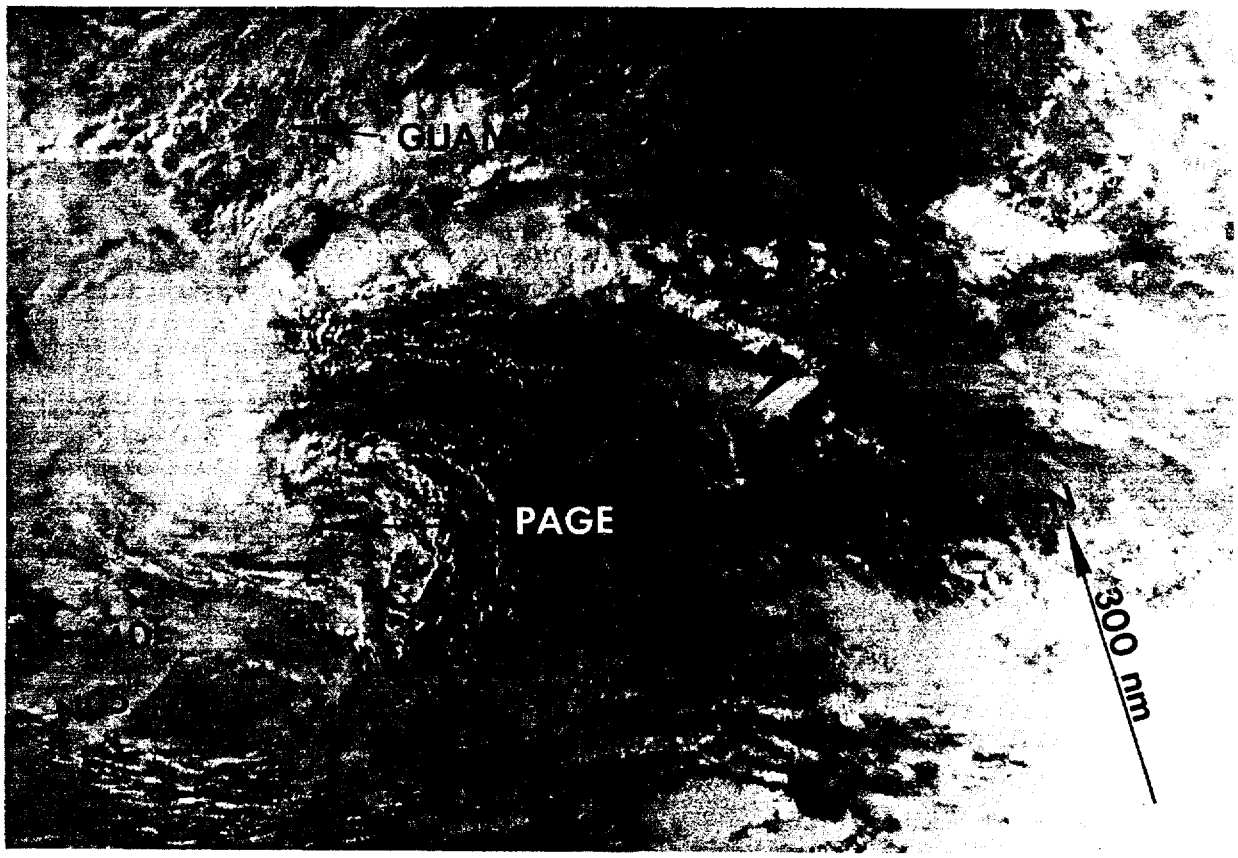

Figure 3-29-2. The exposed low-level circulation center associated with TD 29W as it loops south of Guam (202124Z November NOAA visual imagery).

Figure 3-29-3. Super Typhoon Page near its peak intensity (250443Z November NOAA visual imagery).

V. FORECASTING PERFORMANCE

Overall JTWC forecast performance is shown in Figure 3-29-4. The difficulties came from two sources: first the loop south of Guam was unexpected, and second the NOGAPS prognostic series maintained a weak mid-level ridge over the Philippine Sea to the north of Page, supporting a west-northwestward track into the northern Philippines. At 250000Z, a moderate probability alternate scenario was formulated calling for Page to recurve east of the Philippines in response to a developing weakness in the subtropical ridge associated with a passing shortwave trough. This alternate became the primary forecast at 260000Z, as the ridge broke and recurvature followed.

VI. IMPACT

Guam received peak gusts to 46 kt (23 m/sec) at the International Airport (WMO 91212) on 23 November and over 5 inches (125 mm) of rain, which resulted in some localized flooding. No information was received about Page's passage over Honshu.

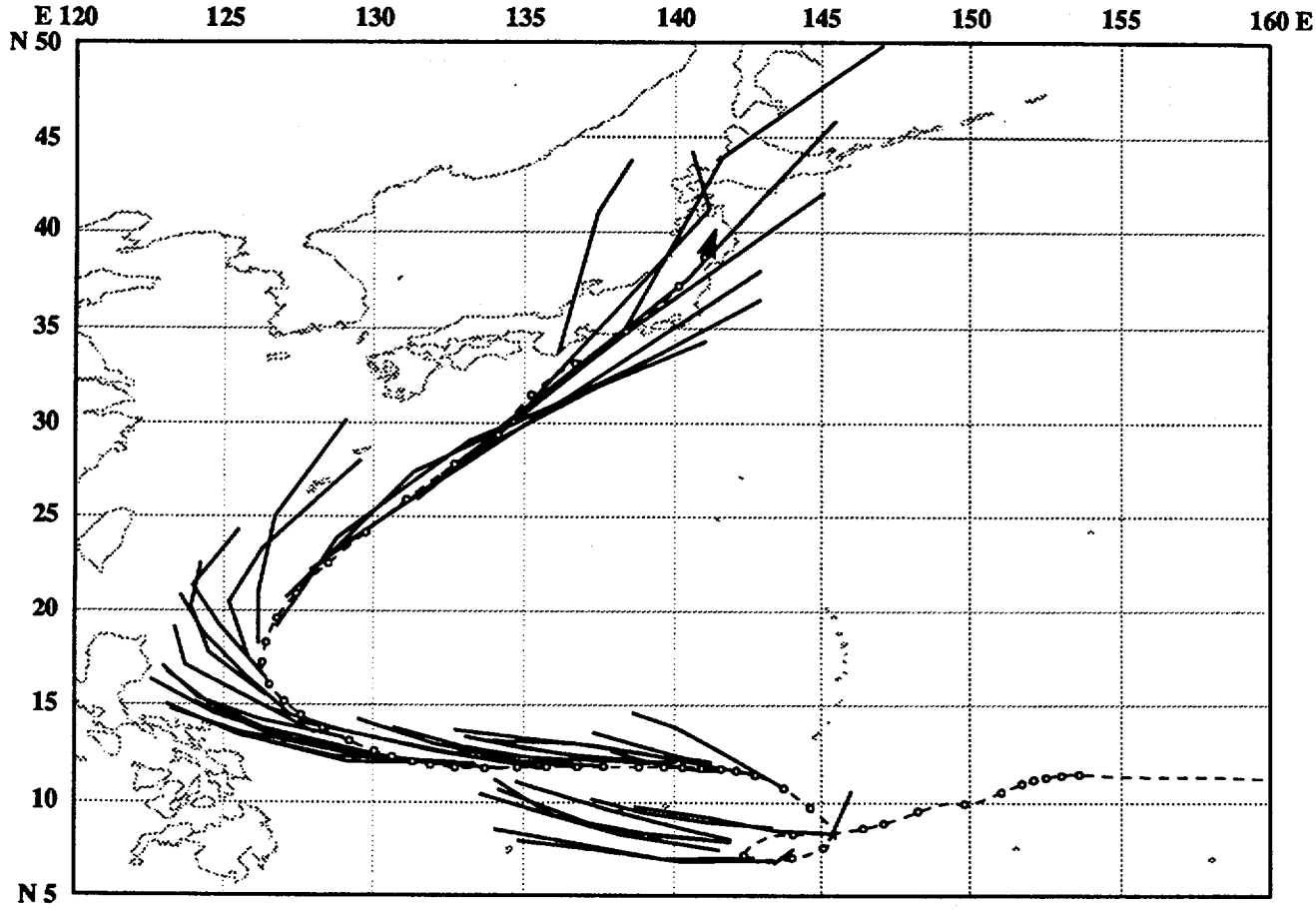

Figure 3-29-4. Summary of JTWC forecasts (solid lines) for Page superimposed on the final best track (dashed line).

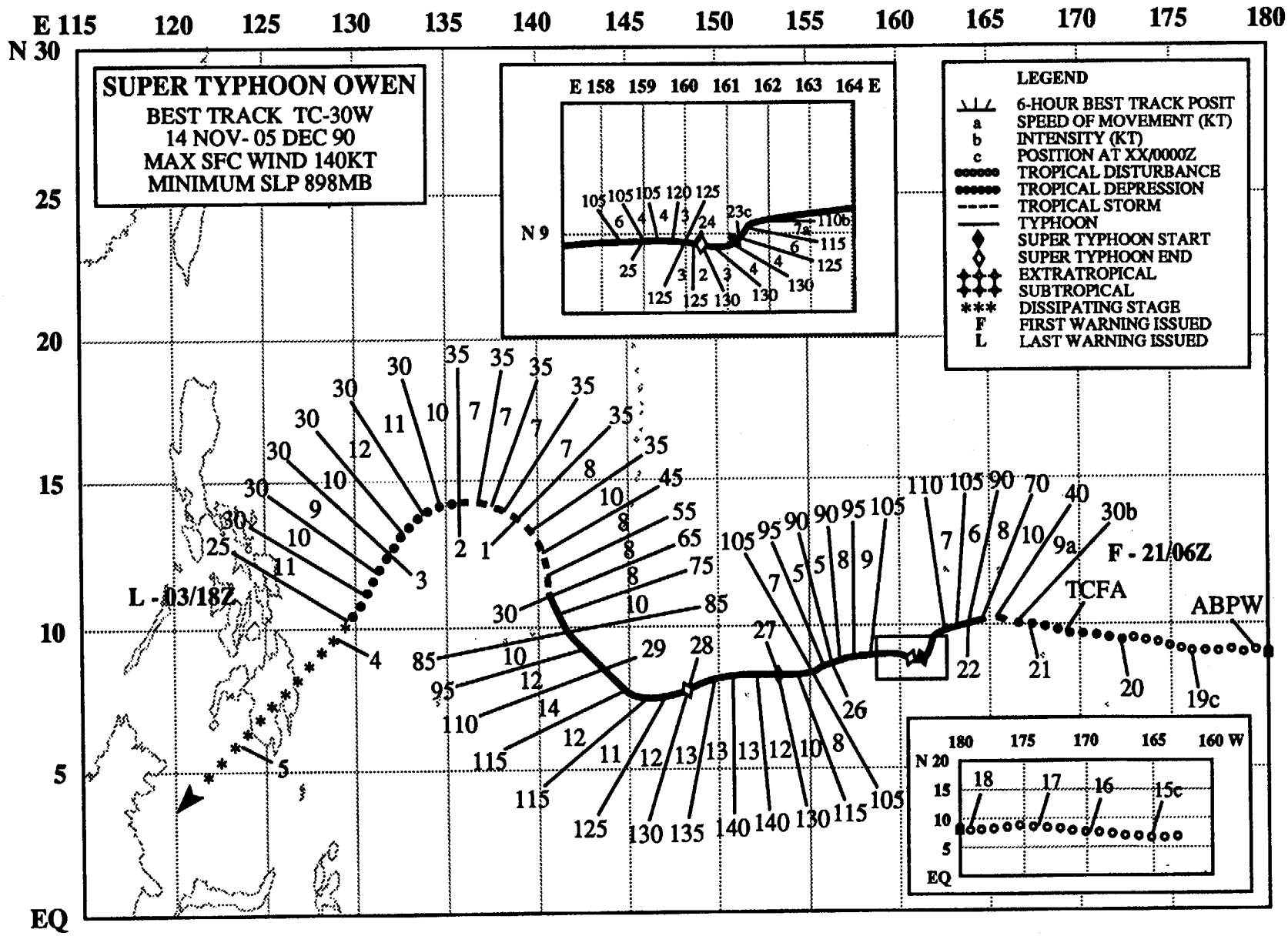
SUPER TYPHOON OWEN
BEST TRACK TC-30W
14 NOV- 05 DEC 90
MAX SFC WIND 140KT
MINIMUM SLP 898MB
LEGEND
6-HOUR BEST TRACK POSIT
SPEED OF MOVEMENT (KT)
INTENSITY (KT)
POSITION AT XX/0000Z
TROPICAL DISTURBANCE
TROPICAL DEPRESSION
TROPICAL STORM
TYPHOON
SUPER TYPHOON START
SUPER TYPHOON END
EXTRATROPICAL
SUBTROPICAL
DISSIPATING STAGE
FIRST WARNING ISSUED
LAST WARNING ISSUED
L - 03/18Z
F - 21/06Z
TCFA
ABPW
E 115 120 125 130 135 140 145 150 155 160 165 170 175 180
N 30 25 20 15 10 5 EQ
E 158 159 160 161 162 163 164 E
N 9
180 175 170 165 160 W
N 20 15 10 5 EQ

SUPER TYPHOON OWEN (30W)

I. HIGHLIGHTS

Owen was both the longest lasting and one of the most interesting tropical cyclones of 1990. It started to rapidly intensify while still a tropical depression, explosively deepened to super typhoon intensity, weakened and then reintensified to a super typhoon. Owen started as a discrete cloud mass southwest of Hawaii, maintained its integrity as it tracked westward in the trade wind trough, but did not intensify until it crossed the date line and passed north of Kwajalein in the Marshall Islands. It then reached typhoon intensity in less than 18 hours and continued westward over the central Caroline Islands where it weakened and reintensified. Its deep convection sheared away southeast of Ulithi Island in the western Carolines. The exposed low-level remained organized for six more days as it moved north, then west, and finally southwestward before dissipating over the Celebes Sea after crossing Mindanao.

II. HIGHLIGHT OF EVENTS

180600Z - First mentioned on Significant Tropical Weather Advisory as an area of persistent convection with maximum sustained surface winds estimated at 10-15 kt (5-7 m/sec) and a minimum sea-level pressure estimated at 1006 mb.

201400Z - Tropical Cyclone Formation Alert based on increased organization of central convection and improved outflow.

210600Z - First warning due to improved upper- and lower-level organization, increased deep convection, increasing wind speeds in the synoptic data, and a CI 2.5.

211200Z - Upgrade to tropical storm based on continued improvement in organization, increased deep convection, and good symmetrical outflow in all quadrants.

211800Z - Upgraded to typhoon following development of a 20 nm (35 km) diameter circular eye, continued rapid intensification, and a CI 4.0.

230600Z - Upgrade to a super typhoon based on continued warming of eye temperature and a CI 6.5.

240000Z - Downgrade to typhoon intensity based on observed vertical wind shear and restricted outflow in all quadrants except the southwest.

270000Z - Upgrade to super typhoon intensity based on warm eye temperature, cold surrounding convective cloud tops and a Dvorak current intensity estimate of 6.5.

280000Z - Downgrade to typhoon intensity based on increased vertical wind shear and restricted outflow to the east.

300600Z - Downgraded to a tropical storm due to increased vertical wind shear and exposed low-level circulation.

020600Z - (December) Downgrade to a tropical depression based on lack of deep central convection and decreased organization.

031800Z - Final warning followed further decrease in cloud organization and associated convection.

III. TRACK & MOTION

Owen developed out of a convective cluster 860 nm (1590 km) southwest of Hawaii near Palmyra Island, and was initially mentioned on a CPHC advisory. The system tracked westward across the central Pacific embedded in the tradewinds south of the subtropical ridge. It continued on this track until it reached the western Marshall Islands. Owen then slowed and tracked southwestward on 22 and 23 November as it approached an anticyclone located to the northwest (Figure 3-30-1). By 24 November, the omega block near the date line had dissipated and the mid-latitude westerlies returned to a more zonal flow. Owen then tracked west-southwestward along the

southern side of the subtropical ridge until 28 November. At that time, the typhoon entered an area dominated by broad low-level westerlies flowing into the recurving Typhoon Page (29W) (Figure 3-30-2). Owen's deep convection sheared apart late on 29 November and revealed an exposed low-

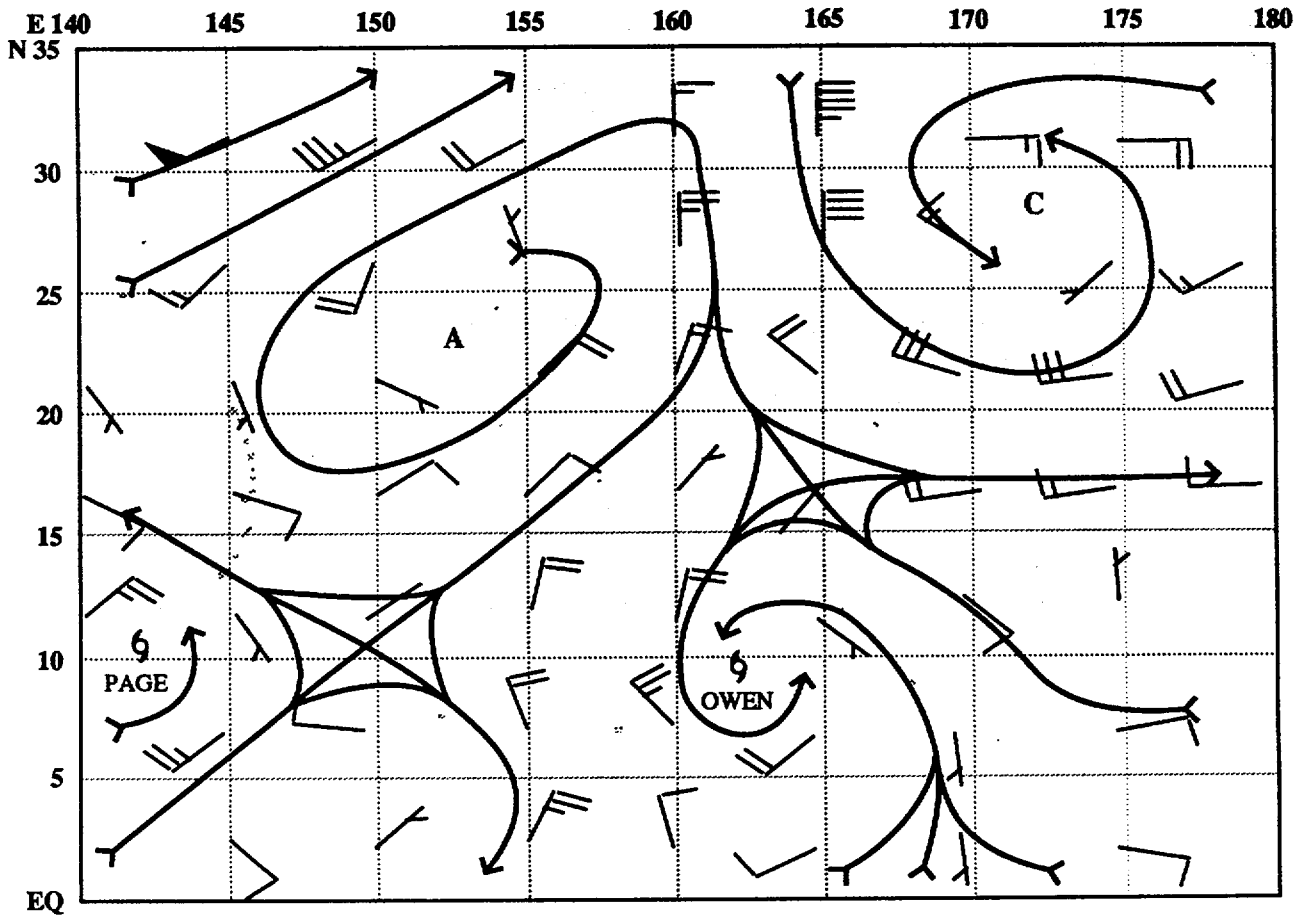

Figure 3-30-1. The 221200Z November NOGAPS 500-mb analysis shows an anticyclone to the northwest of Owen. The cyclonic circulation to the northeast of Owen is part of an omega block.

level circulation to the east of the major convection (Figure 3-30-3). This low-level circulation then tracked around the western periphery of the subtropical high until it encountered a shear line. Then, it turned southwestward, tracked down the shear line, and dissipated over the Celebes Sea on 05 December.

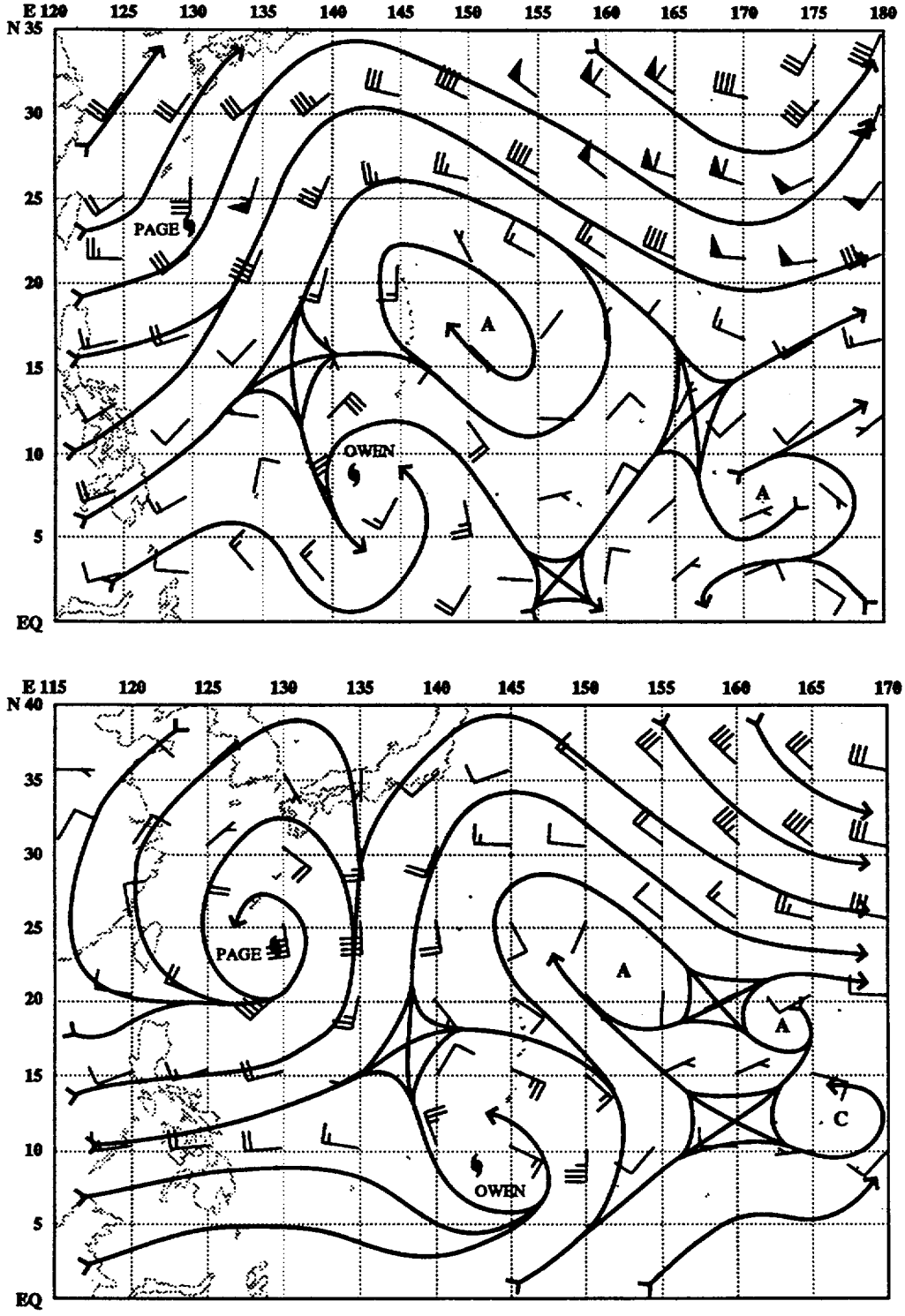

Figure 3-30-2. The 290000Z November NOGAPS analyses: a) for 500 mb depicting Owen near the western periphery of the subtropical high, and b) for 700 mb showing the deep westerly flow associated with Page (29W) which is located to the northwest of Owen.

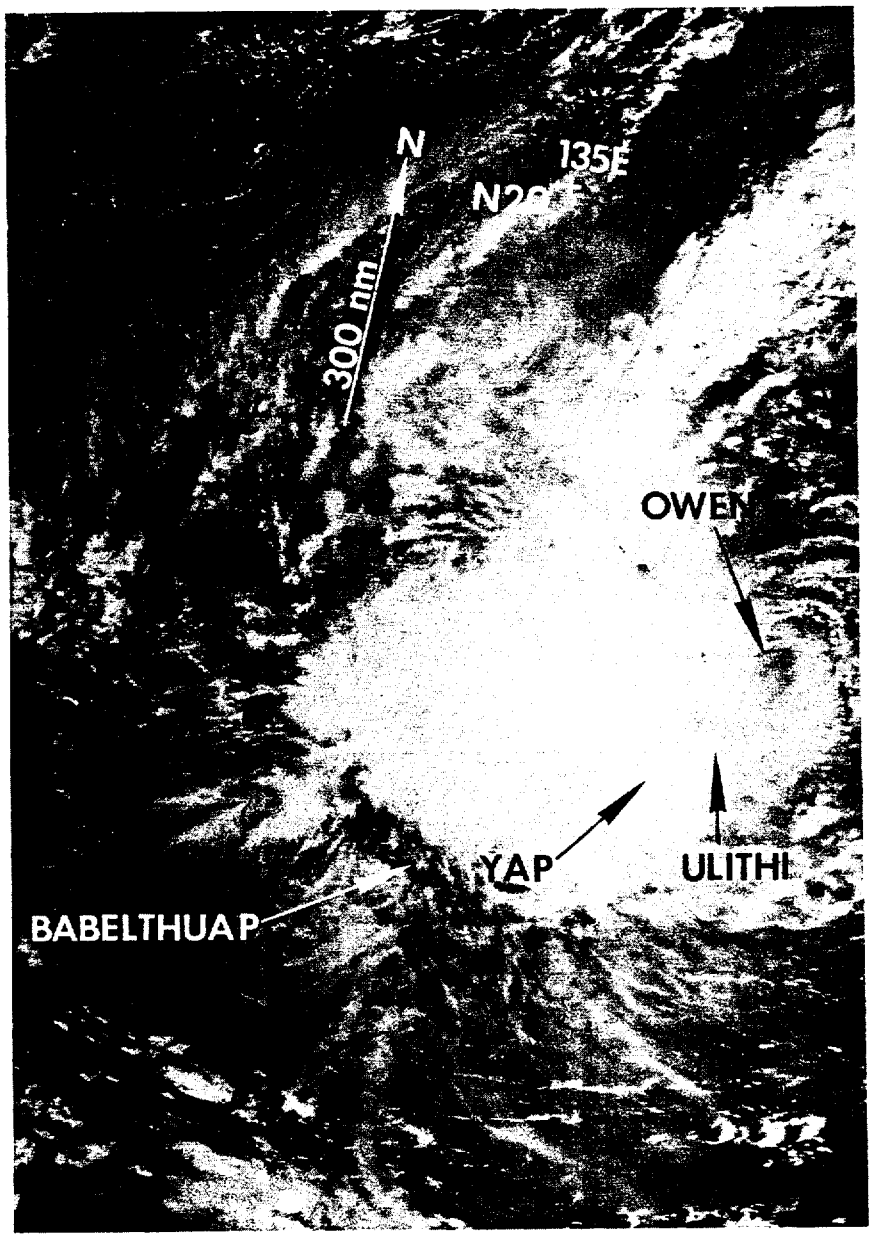

Figure 3-30-3. As Owen shears apart, the low-level circulation center appears to the east of the deep convective mass (300529Z November NOAA visual imagery).

IV. INTENSITY

The convective cloud mass that eventually became Owen formed southwest of Hawaii near Palmyra Island and maintained its continuity as it tracked across the central Pacific and past the date line. A discernible low-level circulation persisted, but the upper-levels did not favor further development. On 20 November, the convection flared and the overall organization started to improve as Owen entered an area of upper-level divergence and lighter winds (Figure 3-30-4). By 21 November, there were signs of an upper-level anticyclone forming over the disturbance and by the time of the second warning, surface pressures started dropping rapidly (Figures 3-30-5). By warning number 3, Owen had developed a 20 nm (35 km) diameter symmetric eye (Figure 3-30-6) and was well into its explosive intensification phase. Although tropical cyclones normally experience explosive intensification after reaching near typhoon intensity (Dunnavan, 1981), Owen commenced explosive intensification as a tropical depression, experiencing a drop in central pressure of 62 mb in 24 hours. Early stage development was supported by surface observations in

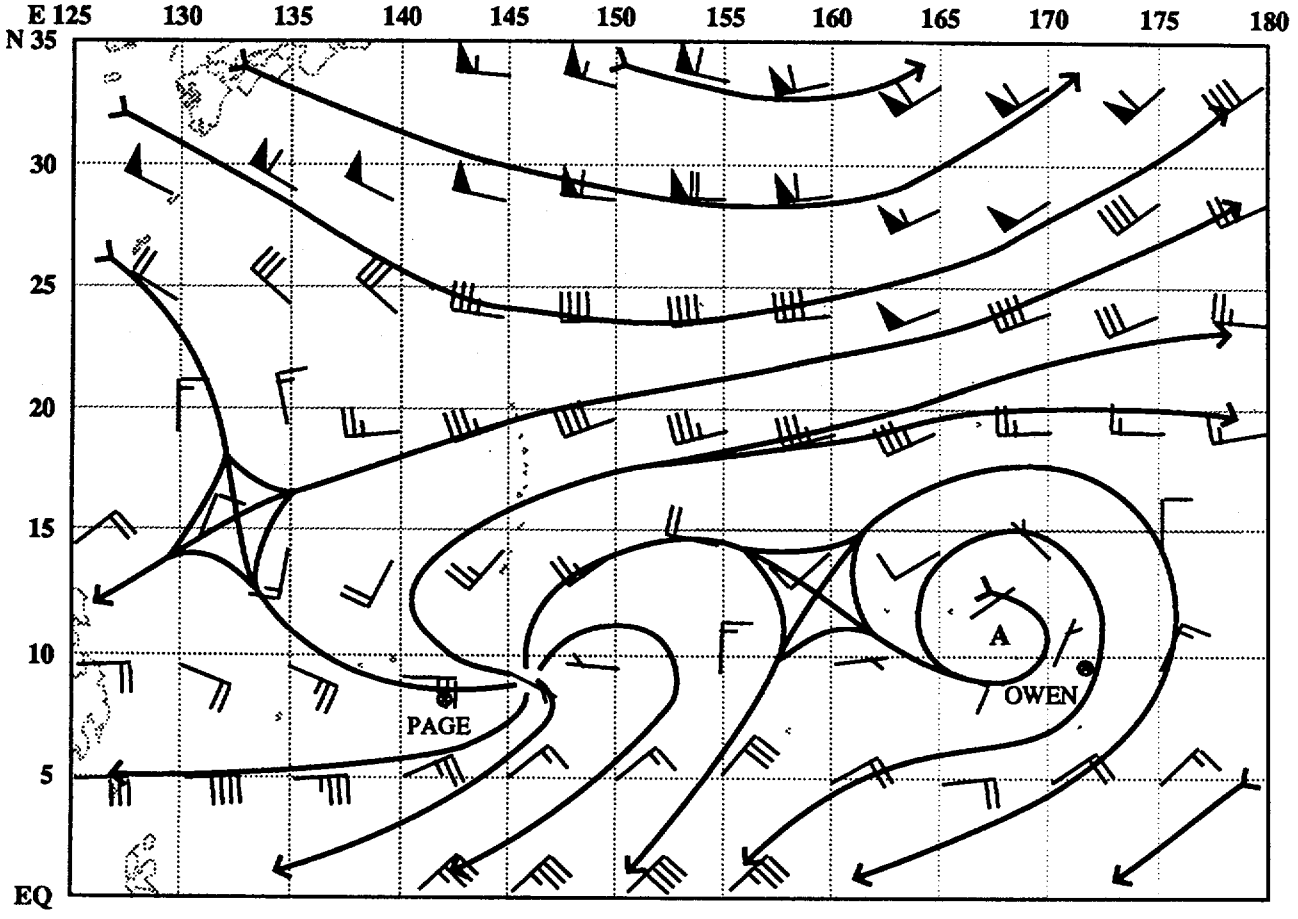

Figure 3-30-4. The 200000Z November 200-mb analysis shows Owen entering an area of lighter winds aloft.

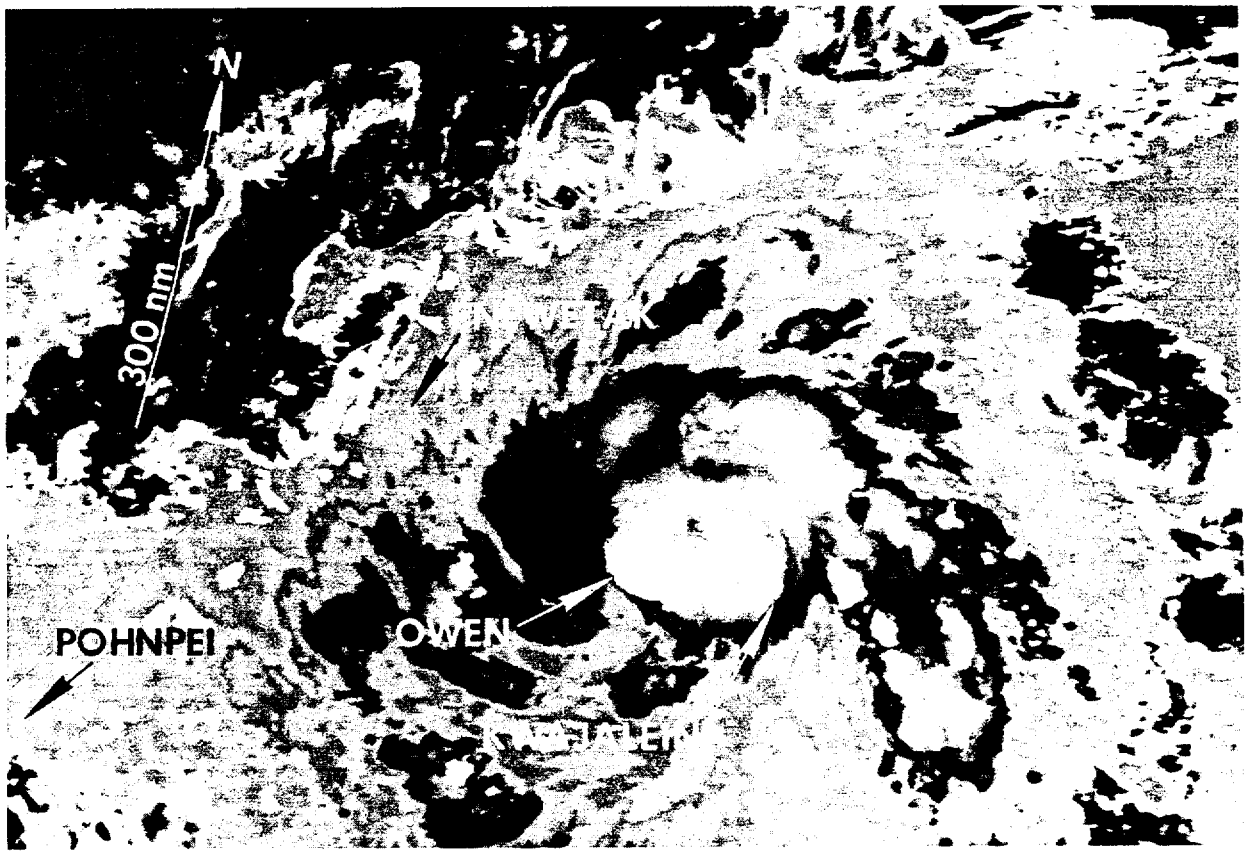

Figure 3-30-5. Tropical Storm Owen starting its explosive intensification phase (210822Z November DMSP enhanced infrared imagery).

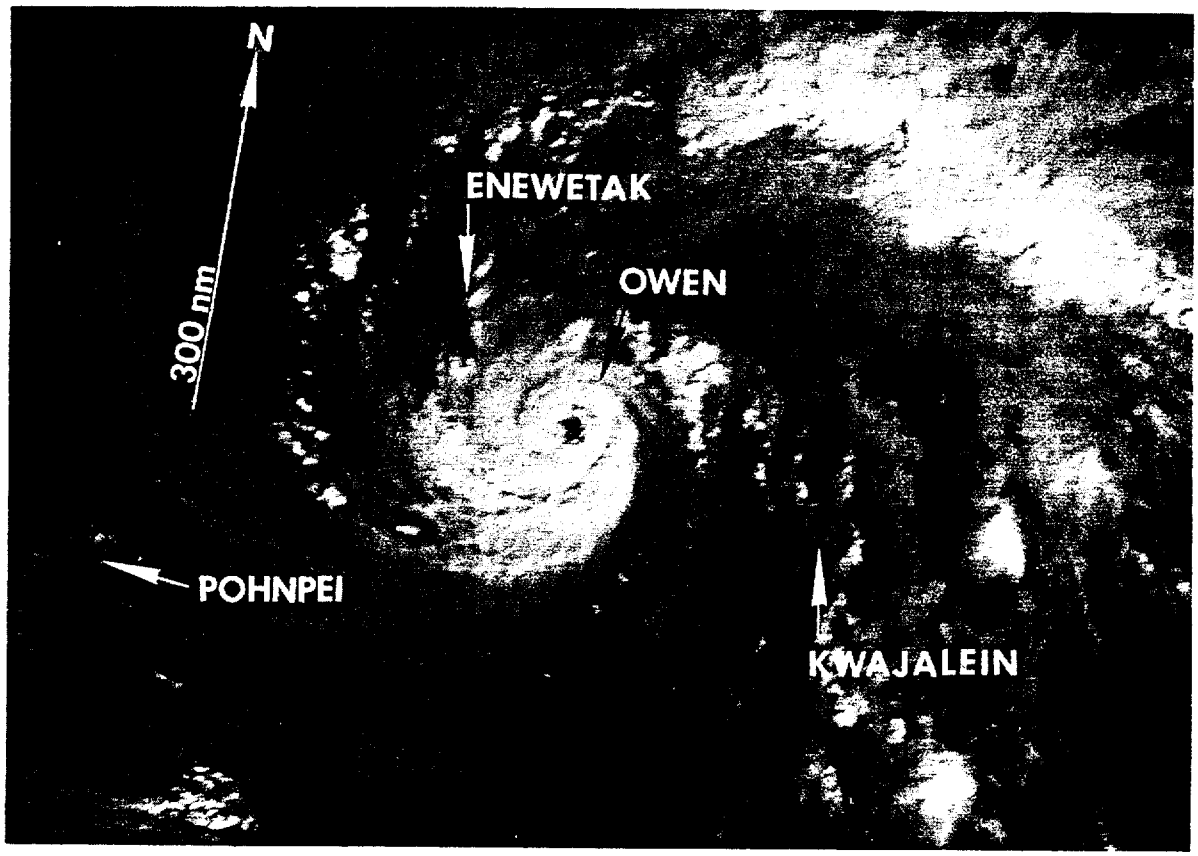

Figure 3-30-6. Fourteen hours after Figure 3-30-5, Owen has a symmetrical 20 nm (35 km) diameter eye and has reached typhoon intensity (212229Z November DMSP visual imagery).

the Marshall Islands and by radar observations from Kwajalein. Owen intensified from 30 kt (15 m/sec) to 105 kt (54 m/sec) in 24 hours, and peaked at 130 kt (67 m/sec) in 48 hours (Figure 3-30-7). Upon reaching super typhoon intensity (Figure 3-30-8), Owen moved into an area of increasing vertical wind shear and its outflow channel to the north was suppressed and eventually cut off by the convergence associated with a passing mid-latitude trough and the eastern side of the anticyclone located between Owen and Typhoon Page (29W). The vertical wind shear eased on 26 November

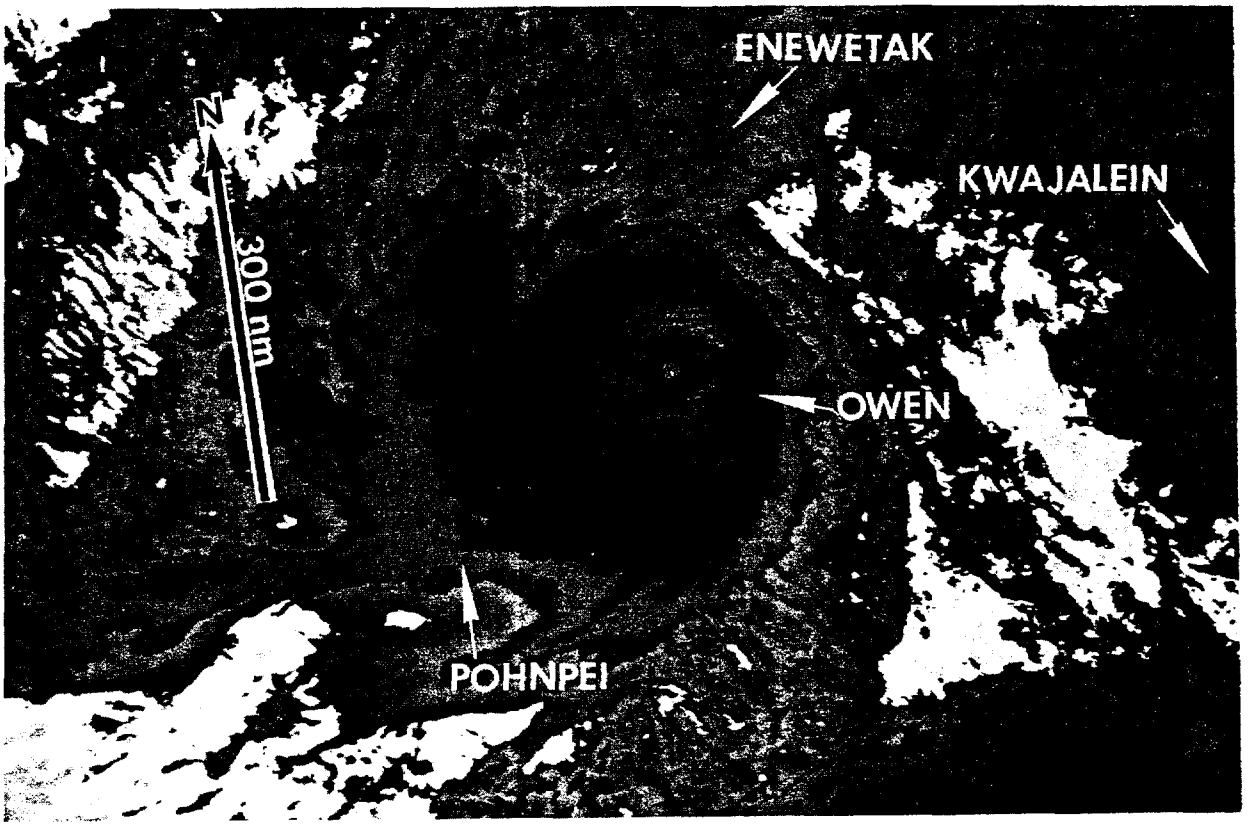

Figure 3-30-7. Super Typhoon Owen near its first peak in intensity (231048Z November DMSP enhanced infrared imagery).

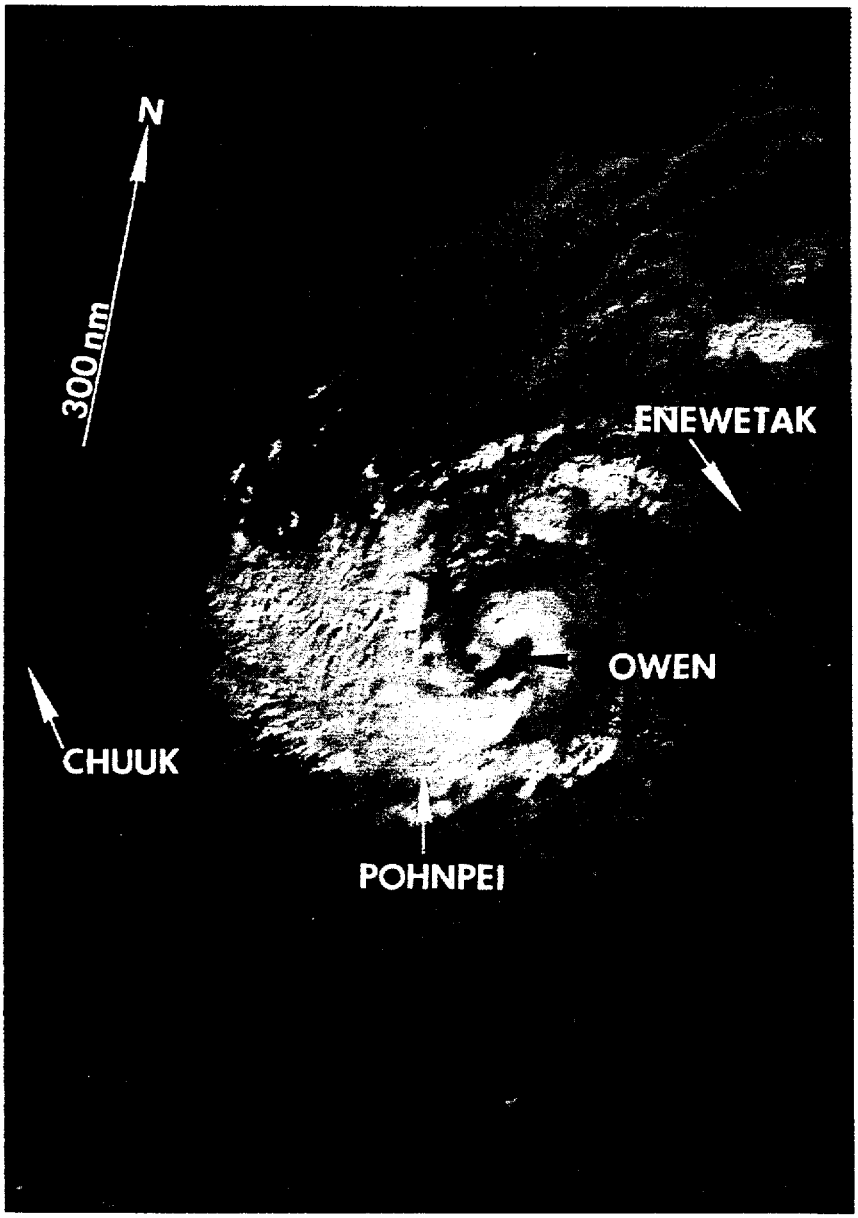

Figure 3-30-8. Shear from the northeast and restricted outflow to the north are evident, as Typhoon Owen weakens (242307Z November DMSP visual imagery).

permitting Owen to reintensify (Figure 3-30-9). The peak intensity of 140 kt (72 m/sec) was reached on 29 November and there was a significant shift in the position of the upper-level anticyclone (Figure 3-30-10). As the anticyclone shifted position, the upper-level shear from the east increased dramatically from approximately 10 kt to 40 kt. This environment persisted until Owen sheared apart late on 29 November with the upper-level convection continuing west-northwestward and the low-level circulation center moving north-northwestward. Owen never moved back into a environment favorable for redevelopment and only maintained scattered convection until it dissipated in the Celebes Sea (Figure 3-30-11).

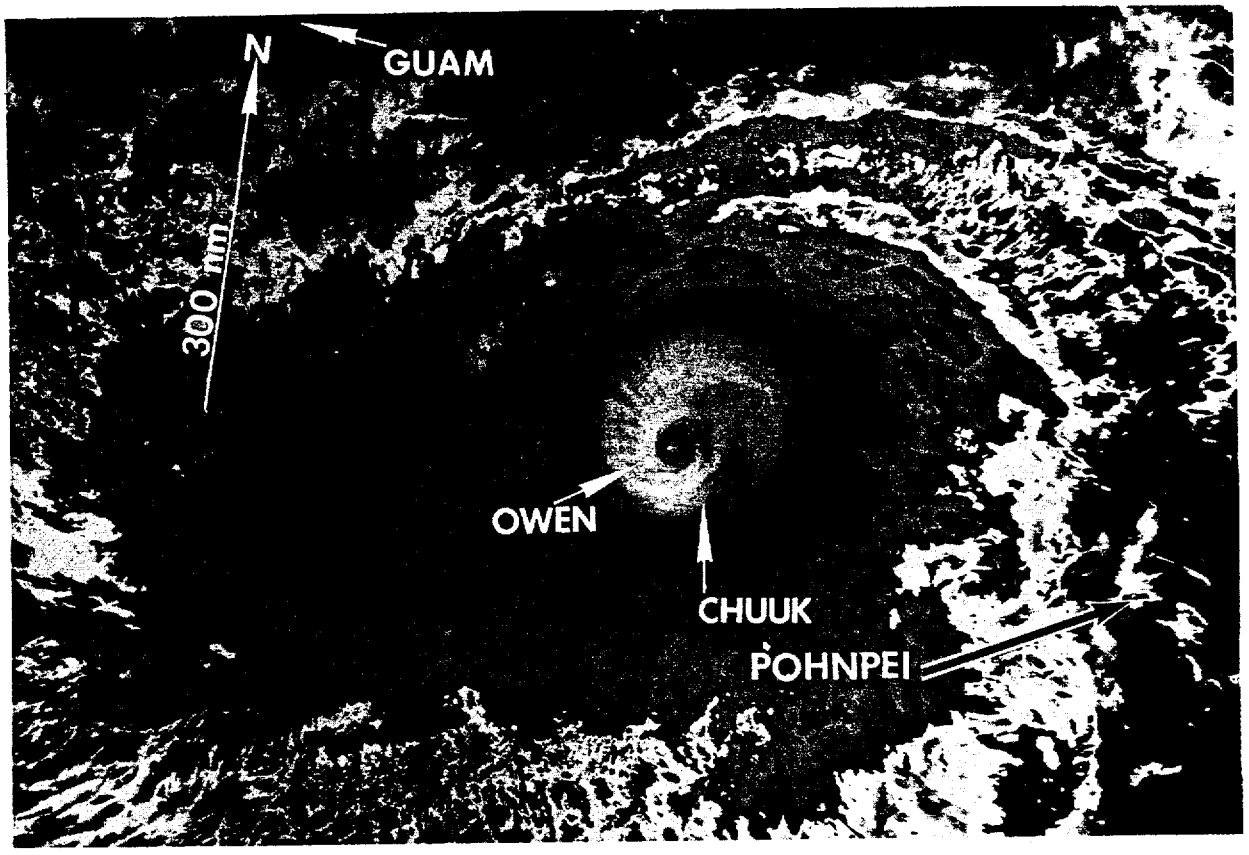

Figure 3-30-9. Owen after reintensifying to super typhoon intensity for a second time (270925Z November NOAA enhanced infrared imagery).

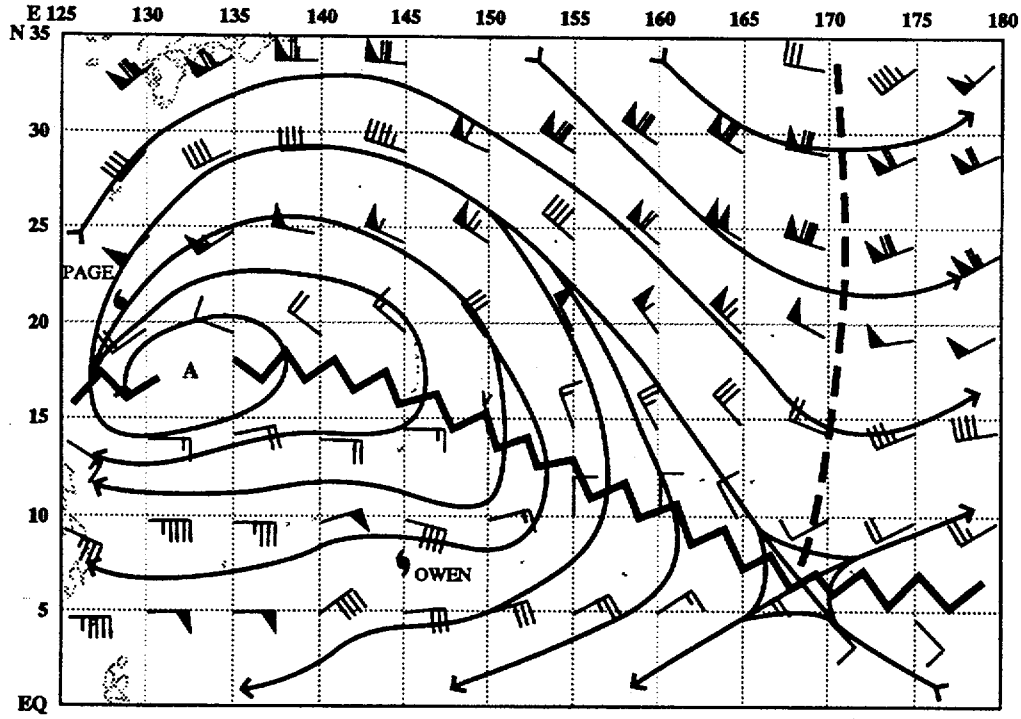

a)

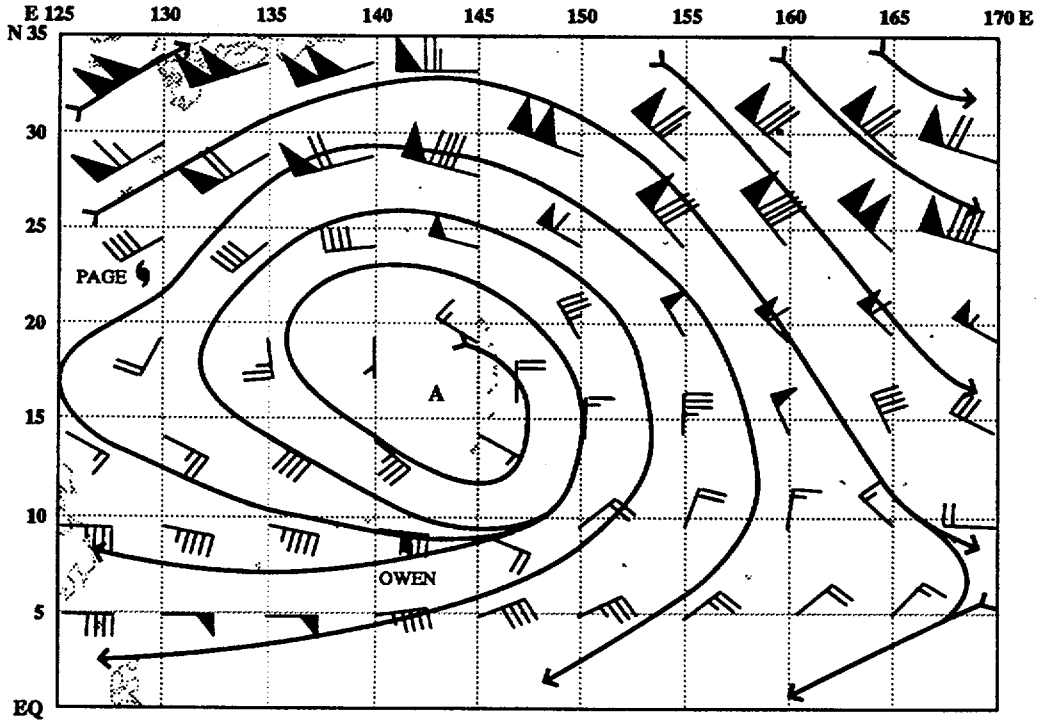

b)

Figure 3-30-10. The November NOGAPS 200-mb analyses: a) for 281200Z November showing Page (29W) and the center of the anticyclone to the northwest of Owen, and b) for 290000Z November showing the relocation of the center of the anticyclone to the north of Owen.

V. FORECASTING PERFORMANCE

JTWC's forecast performance is shown in Figure 3-30-12. Overall errors for this system were well below the long term average because JTWC did well forecasting the speed and speed changes exhibited by Owen. JTWC forecasts were generally right of track until 28 November for a number of reasons. First, the usually dependable NOGAPS deep layer mean provided guidance that indicated northwestward movement. Second, Owen took an anomalous track to the west-southwest. Finally, NOGAPS after 26 November consistently forecast the anticyclone steering Owen to reposition itself east of Guam sooner than the 29 November timeframe when the shift actually occurred. JTWC forecast recurvature early as a result, and the recurvature forecast had to be adjusted back to the west. Once Owen sheared, forecast guidance was based on the NOGAPS 700 mb and lower levels. JTWC accurately forecast the initial peak intensity and the subsequent weakening. The reintensification was correctly reflected in the forecasts, but the maximum intensity was under forecast. Since Owen was not forecast to shear apart, the final weakening trend was significantly faster than forecast.

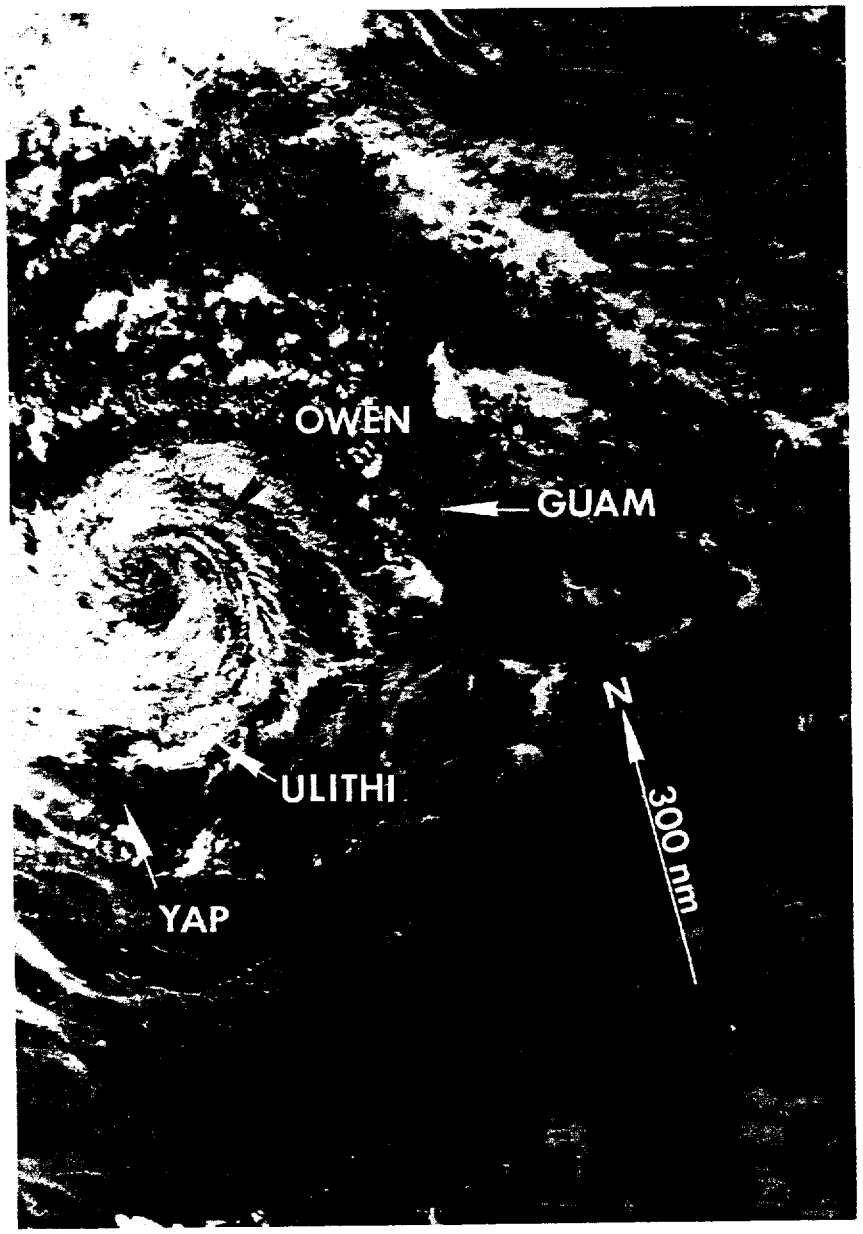

Figure 3-30-11. Owen's low-level circulation is fully exposed (301632Z November NOAA infrared imagery).

VI. IMPACT

POHNPEI	- 2 killed when a live power line fell and struck them.
CHUUK STATE	- declared a U.S. federal disaster area, 1000 people left homeless, major power failures.
HALL ISLANDS	- extensive crop damage, nearly all homes destroyed, all food crops destroyed.
NAMONUITO ATOLL	- extensive crop damage, nearly all homes destroyed, all food crops destroyed.
PULAP ATOLL	- extensive crop damage, 99 percent of homes destroyed.
YAP STATE	- declared a U. S. federal disaster area.
SATAWAL ISLAND	- reported winds in excess of 100 mph, 95 percent food crop destroyed, 90 percent homes damaged, all power lost.
LAMOTREK ATOLL	- reported winds in excess of 100 mph, 85 percent homes destroyed, 95 percent food crop destroyed, all power lost.
ELATO ATOLL	- 99 percent dwellings destroyed, 90 percent food crops destroyed.
IFALIK ATOLL	- dwellings - no report, 95 percent food crops destroyed, 20 percent land eroded.
WOLEAI ATOLL	- 85 percent dwellings, 90 percent food crops destroyed.
FARAULEP ATOLL**	- 20 percent dwellings, 100 percent canoes, 100 percent food crops destroyed, 20 - 30 percent land eroded.
ULITHI ISLAND	- 30 percent dwellings and government buildings, 100 percent food crops destroyed.

** NOTE: AMOS site on Faraulep was lost during passage of Owen. The shore was completely eroded away leaving the tower on its side in 10 feet of water and 20 yards off the beach. Site is now abandoned.

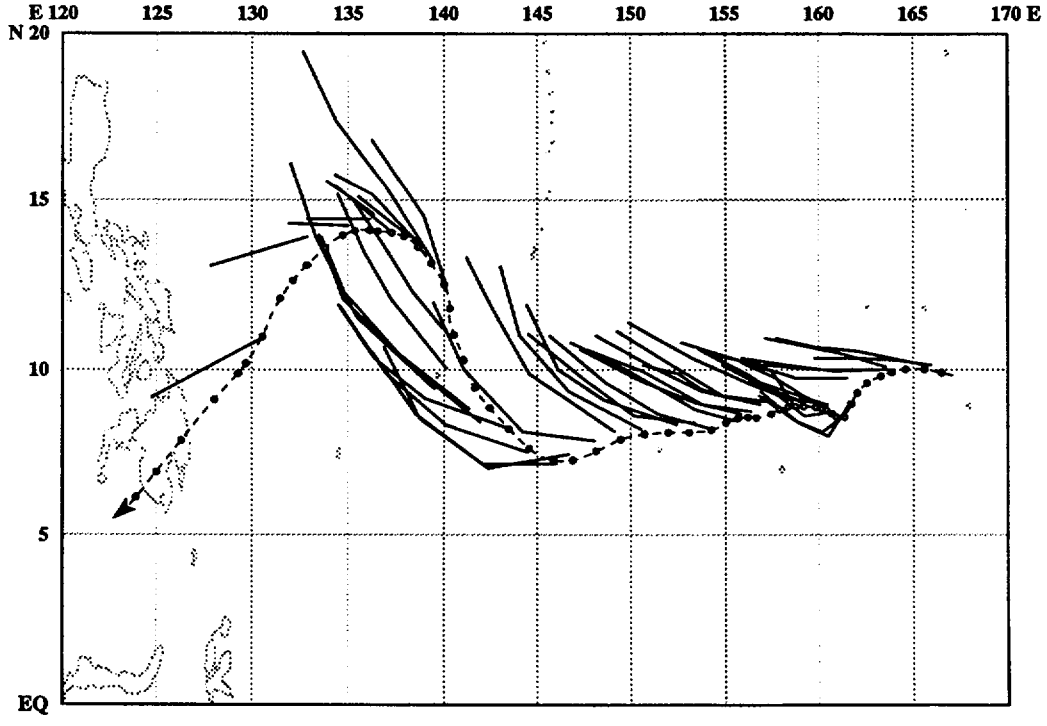

Figure 3-30-12. The JTWC forecast tracks (solid lines) for Owen superimposed on the final best track (dashed line).

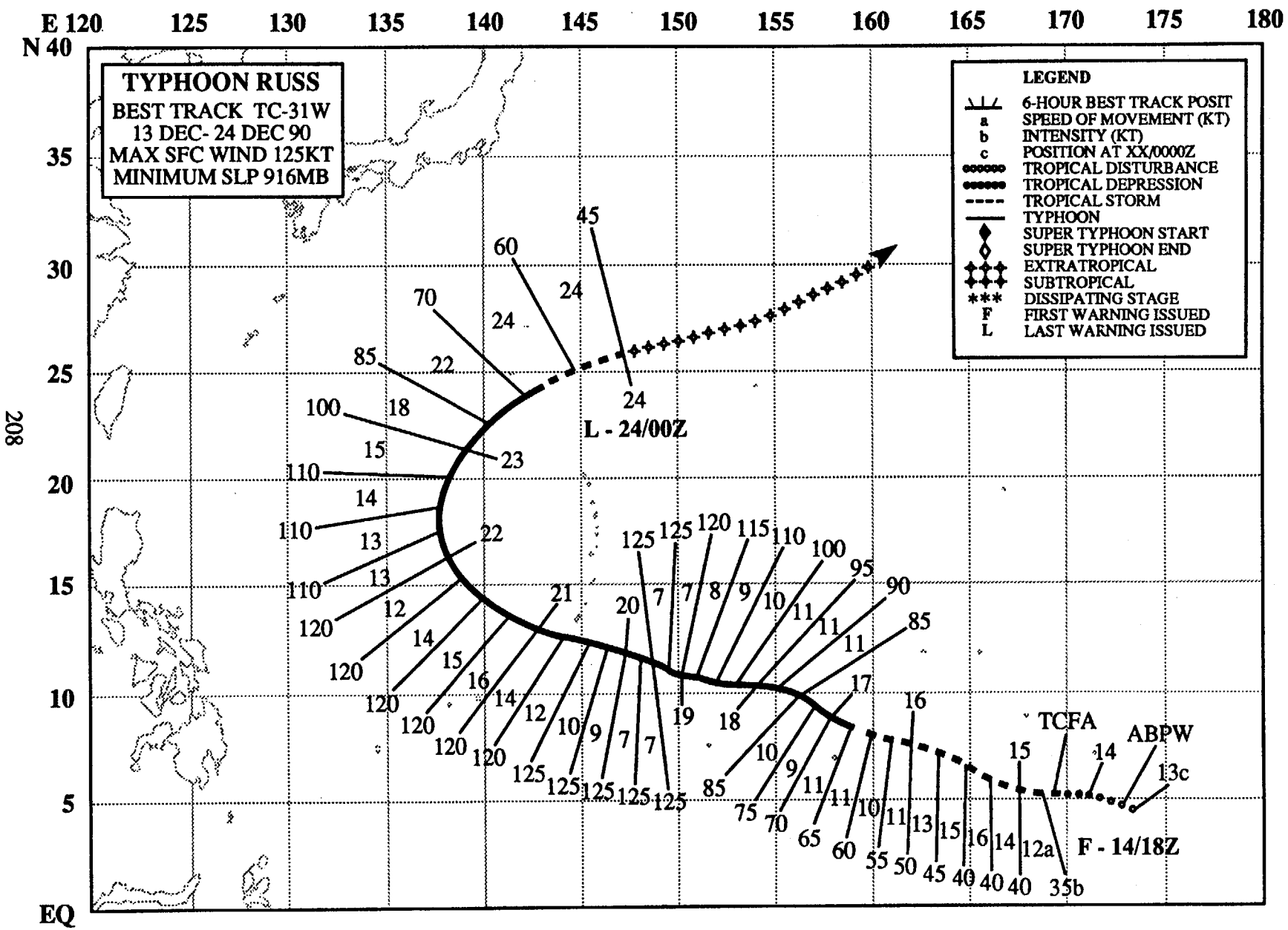
E 120
125
130
135
140
145
150
155
160
165
170
175
180
N 40
35
30
25
20
15
10
5
EQ
208
TYPHOON RUSS
BEST TRACK TC-31W
13 DEC- 24 DEC 90
MAX SFC WIND 125KT
MINIMUM SLP 916MB
LEGEND
6-HOUR BEST TRACK POSIT
a SPEED OF MOVEMENT (KT)
b INTENSITY (KT)
c POSITION AT XX/0000Z
TROPICAL DISTURBANCE
TROPICAL DEPRESSION
TROPICAL STORM
TYPHOON
SUPER TYPHOON START
SUPER TYPHOON END
EXTRATROPICAL
SUBTROPICAL
*** DISSIPATING STAGE
F FIRST WARNING ISSUED
L LAST WARNING ISSUED
L - 24/00Z
TCFA
ABPW
F - 14/18Z

TYPHOON RUSS (31W)

I. HIGHLIGHTS

Russ, the last western North Pacific tropical cyclone of 1990, was the most severe to strike Guam in 14 years. Damage was estimated as high as 120 million dollars. Russ formed in the Marshall Islands, tracked west-northwestward and intensified to near super typhoon intensity as it approached Guam. The typhoon passed within 30 nm (55 km) of the southern tip of Guam and brought typhoon force winds which caused extensive damage, especially to the southern portion of the island. After leaving Guam, Russ slowly weakened, recurved and became an extratropical cyclone.

II. CHRONOLOGY OF EVENTS

130600Z - First mentioned on a Significant Tropical Weather Advisory as an area of persistent convection associated with a low-level cyclonic circulation and an estimated minimum sea-level pressure of 1004 mb. The potential for significant tropical cyclone development was assessed as poor.

140600Z - Second mention on a Significant Tropical Weather Advisory due to persistent convection with an anticyclone developing aloft. Potential for development upgraded to fair.

141330Z - Tropical Cyclone Formation Alert issued based on increased curvature in the spiral cloud bands and a 35 kt (13 m/sec) surface wind report from Jaluit Atoll (WMO 91369).

141800Z - First Warning issued and Russ upgraded to tropical storm intensity prompted by rapid increase in amount and organization of the central convection.

161800Z - Upgraded to a typhoon based on anticipated appearance of an eye and a satellite intensity estimate of 65 kt (35 m/sec).

190600Z - Peak intensity - 125 kt (65 m/sec) - followed observation of further drying and warming within the 30 nm (55 km) diameter eye and a satellite intensity estimate of 125 kt.

240000Z - Final warning issued with Russ downgraded to tropical storm intensity and transitioning to an extratropical cyclone after the loss of its persistent central dense overcast.

III. TRACK AND MOTION

Russ developed in the near-equatorial trough in the southern Marshall Islands. The tropical cyclone followed a basic recurvature track, passing just south of Guam and recurving through the axis of the subtropical ridge to the northwest of Guam. Although Russ maintained an essentially west-northwestward direction of motion as it approached Guam, significant changes in speed of motion occurred. Beginning on 18 December, Russ began to decelerate in response to the passage of a mid-latitude short wave passing to the north of the subtropical ridge. By 19 December, the typhoon had slowed to 7 kt (13 km/hr) - almost half the 13 kt (24 km/hr) speed expected from climatology. Once the short wave passed to the northeast, the subtropical ridge and the steering flow strengthened, and on 20 December, Russ started to accelerate. Fortunately for Guam, this reduced the time of exposure to Russ' damaging winds. By the time Russ entered the Philippine Sea, another short wave had moved eastward from Asia and caused a break in the subtropical ridge to the northwest of Guam. Russ recurved through this break, accelerated and became an extratropical cyclone on 24 December.

IV. INTENSITY

Russ' initial intensification was surprisingly rapid. As a result, Russ was at minimal tropical storm intensity when the first warning was issued. Although satellite imagery showed poorly

organized convection with multiple circulations (Figure 3-31-1), surface wind reports from Jaluit Atoll (WMO 91369) in the southern Marshall Islands of 35 and 40 kt (17 and 20 m/sec) at 141200Z and 150000Z respectively, revealed that the tropical cyclone was consolidating. After this sudden initial development (Figure 3-31-2), Russ intensified (Figure 3-31-3) at a normal rate until it reached 125 kt (64 m/sec) at 190600Z. The passage of a mid-latitude short wave trough, which weakened the subtropical ridge and caused Russ to slow down, aided intensification by enhancing the typhoon's

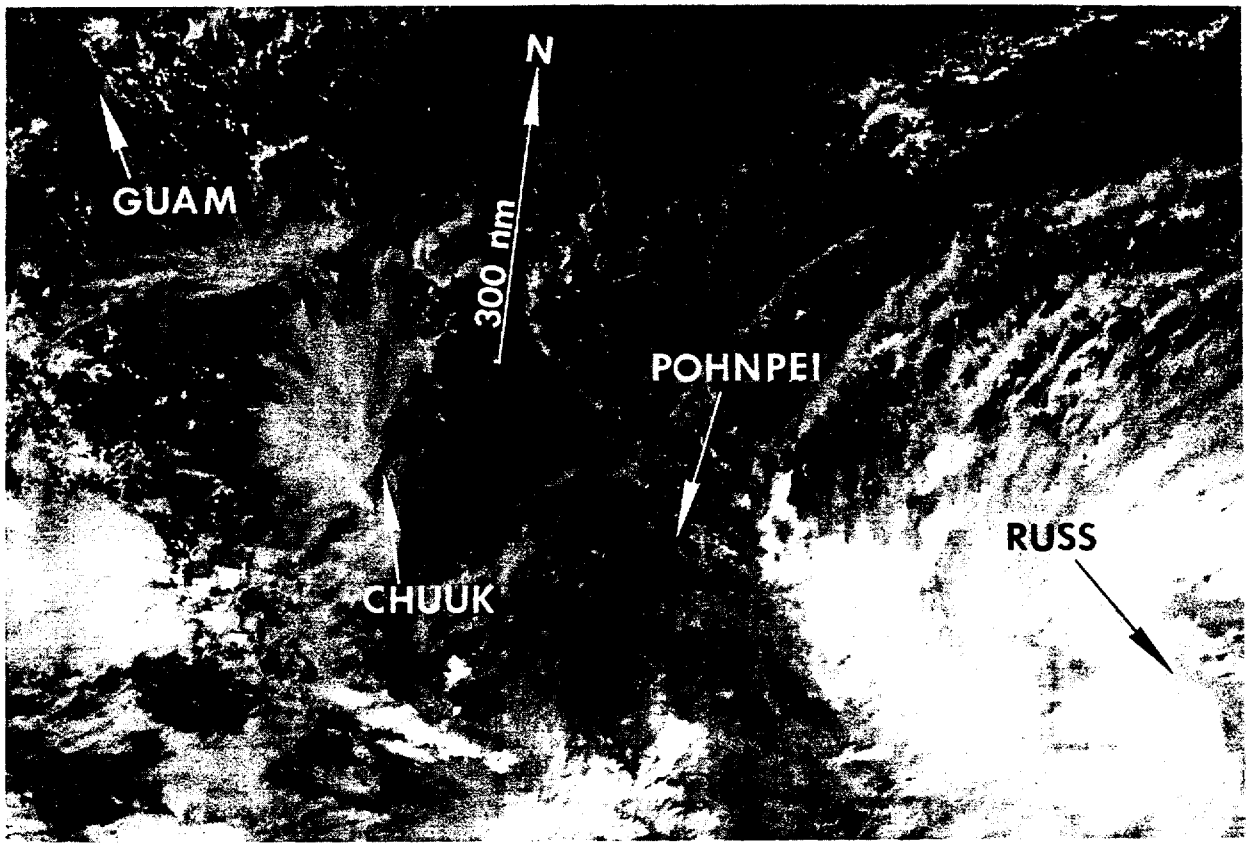

Figure 3-31-1. Russ after reaching tropical storm intensity. Central convection and outflow are well organized (142250Z December DMSP visual imagery).

outflow aloft into the polar westerlies (Figure 3-31-4). The tropical cyclone remained near its peak intensity for three days. During this time, it passed within 30 nm (55 km) of the southern tip of Guam (Figure 3-31-5). The closest point of approach at 201700Z (210300 local time on Guam) was reflected in the lowest pressure (Figure 3-31-6), increased wind (Figure 3-31-7), and increased seas (Figure 3-31-8). Maximum sustained winds experienced on the island, which is only 30 nm (55 km) in length, varied from minimum typhoon intensity in the north to almost double that in the south (Figure 3-31-9).

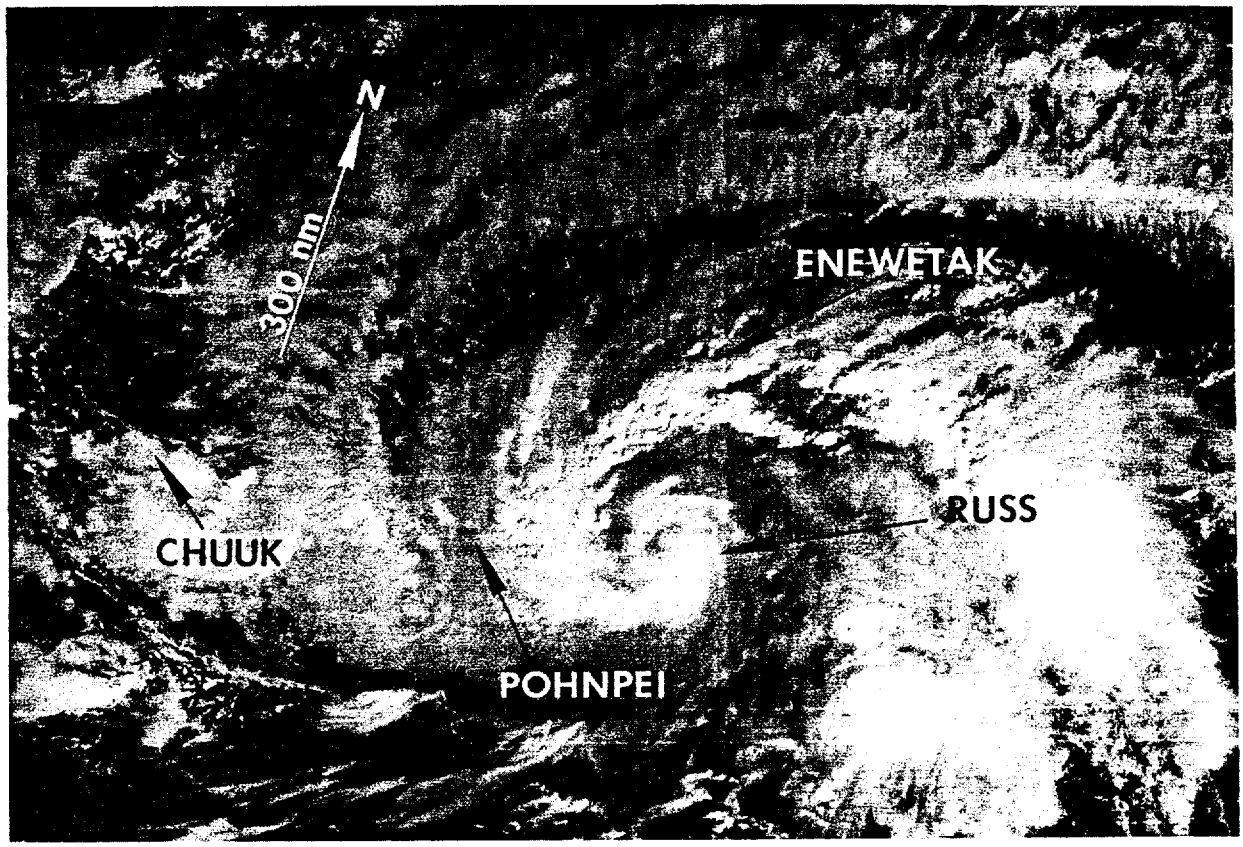

Figure 3-31-2. Spiral cloud band curvature increases as Russ intensifies (152229Z December DMSP visual imagery).

After passing to the west of Guam and into the Philippine Sea, Russ started to slowly weaken as it turned more to the north and interacted with the stronger polar westerly winds aloft (Figure 3-31-10). The typhoon's compact central convection resisted the increased vertical wind shear until 24 December, a day after recurvature. By then, the supporting deep convection was displaced to the north and east of the low-level circulation center and the cyclone (Figure 3-31-11) was extratropical.

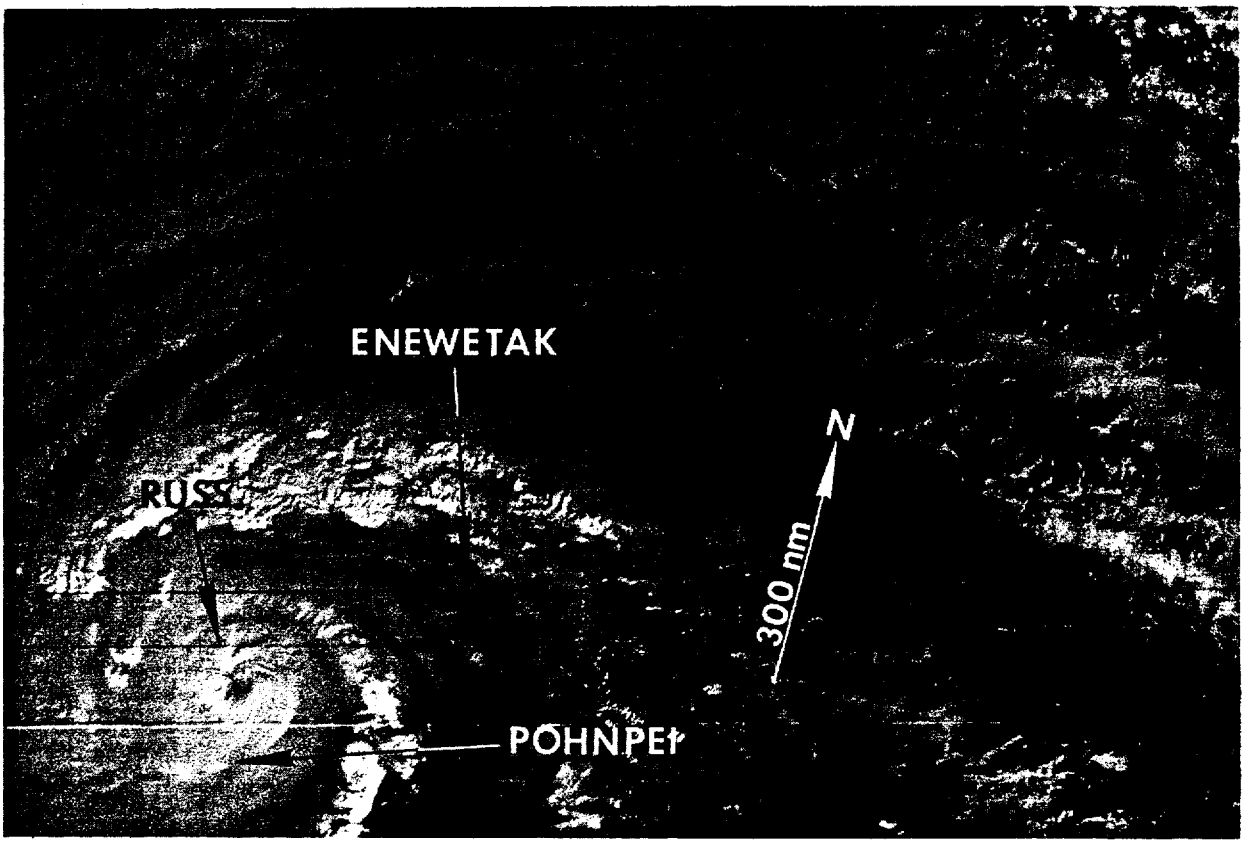

Figure 3-31-3. Russ develops an eye and reaches typhoon intensity (162207Z December DMSP visual imagery).

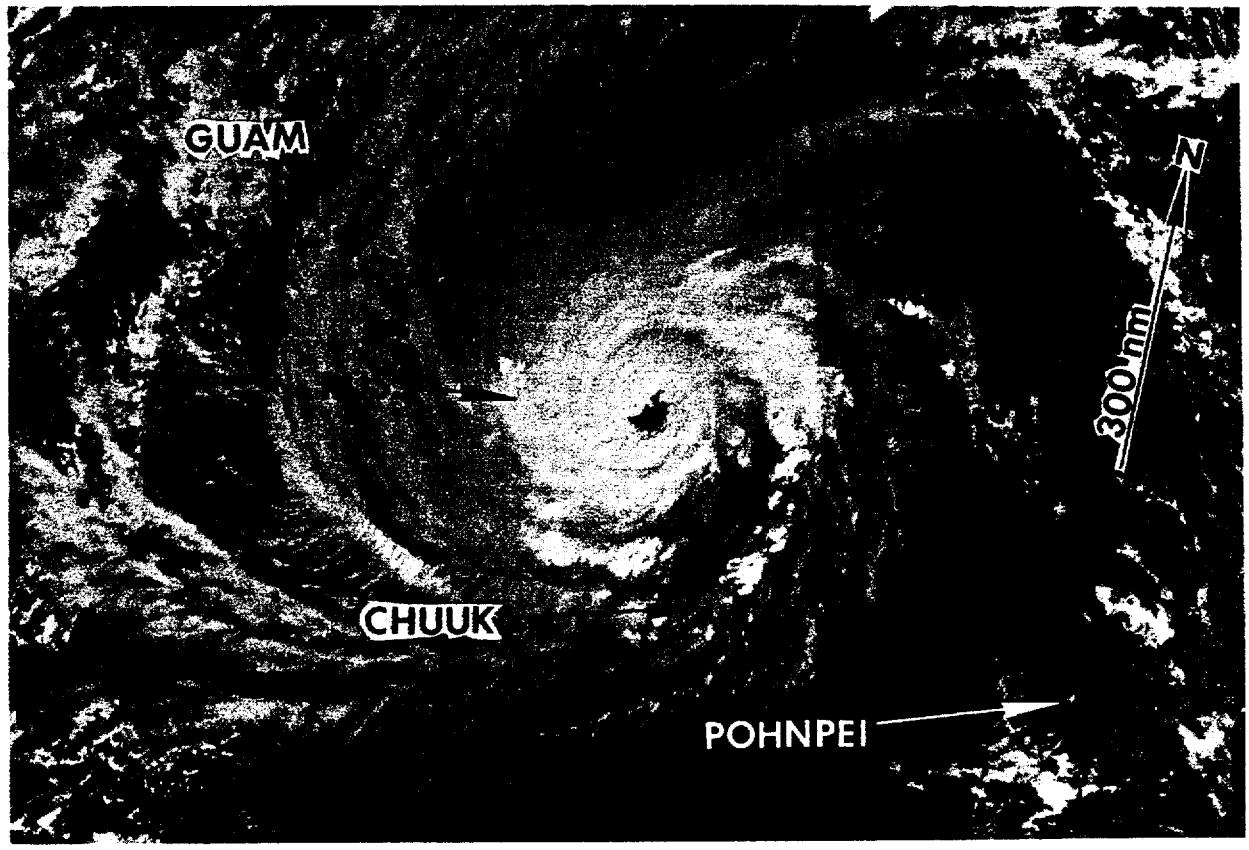

Figure 3-31-4. Russ at near peak intensity after the passage of a mid-latitude short wave to the north enhanced its outflow aloft (182307Z December DMSP visual imagery).

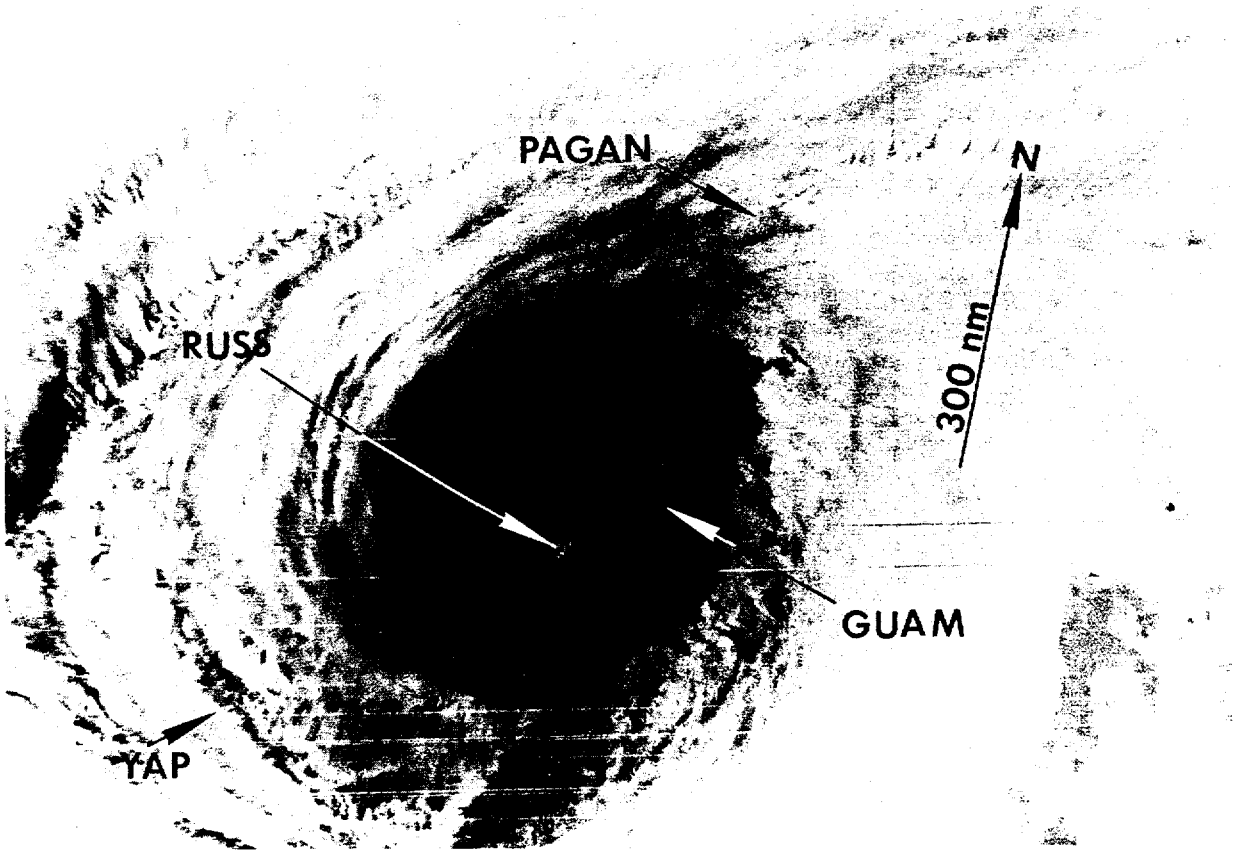

Figure 3-31-5. Russ after its closest point of approach to Guam (202014Z December DMSP infrared imagery).

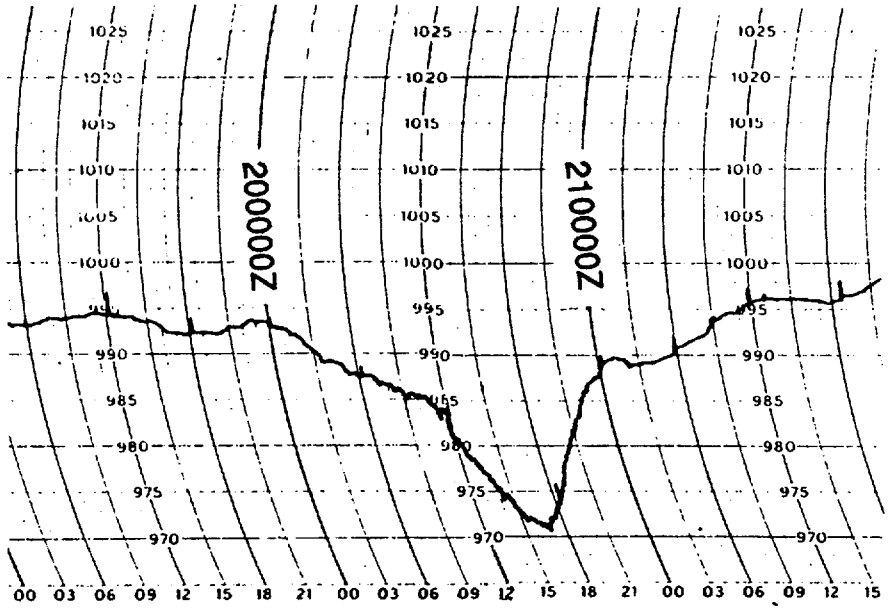

Figure 3-31-6. The microbarograph trace from Naval Air Station (WMO 91212), Agana, Guam shows its lowest pressure of 971 mb, at 201700Z, as Russ is near its closest point of approach to Guam.

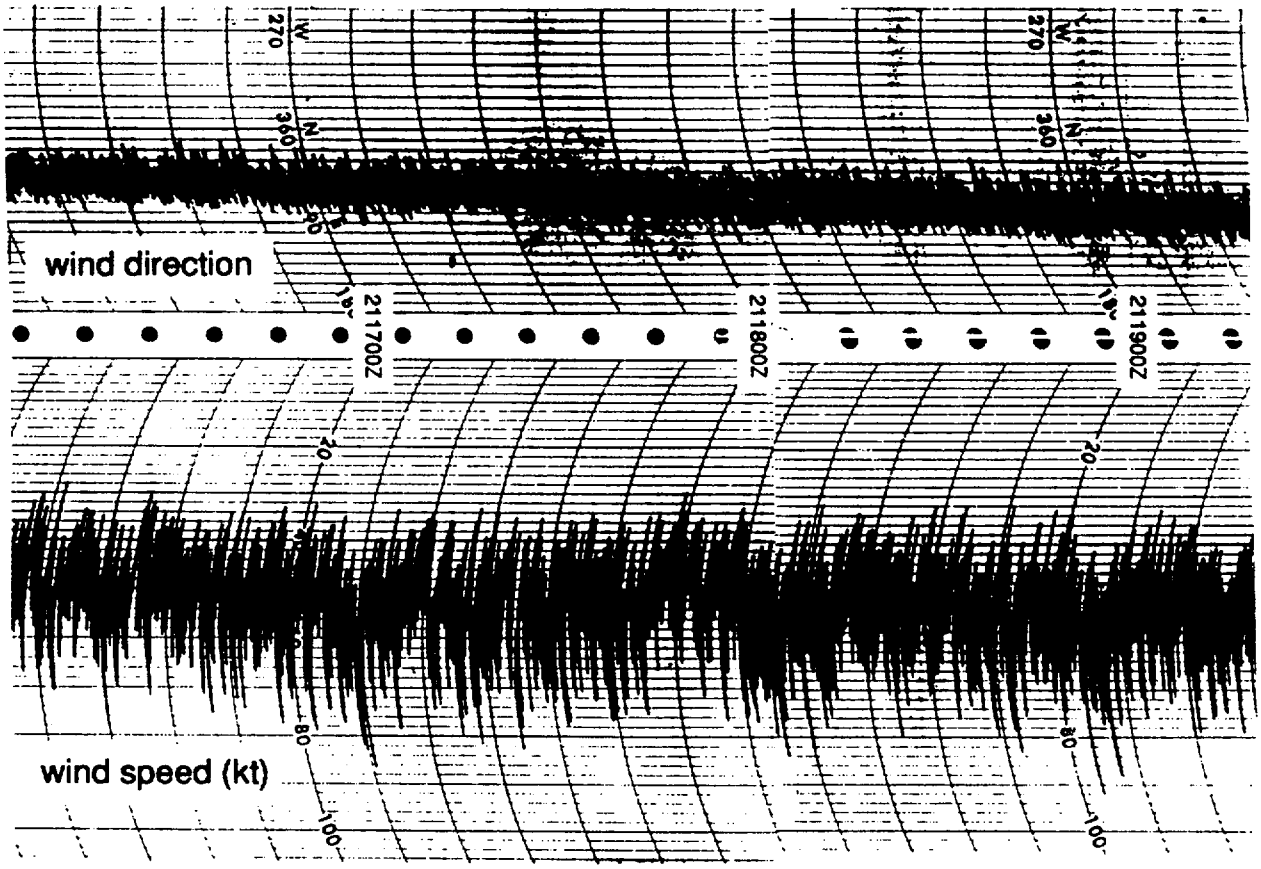

Figure 3-31-7. The wind record from Naval Air Station (WMO 91212), Agana, Guam reflects a steady increase from 211500Z through 211700Z as Russ approaches.

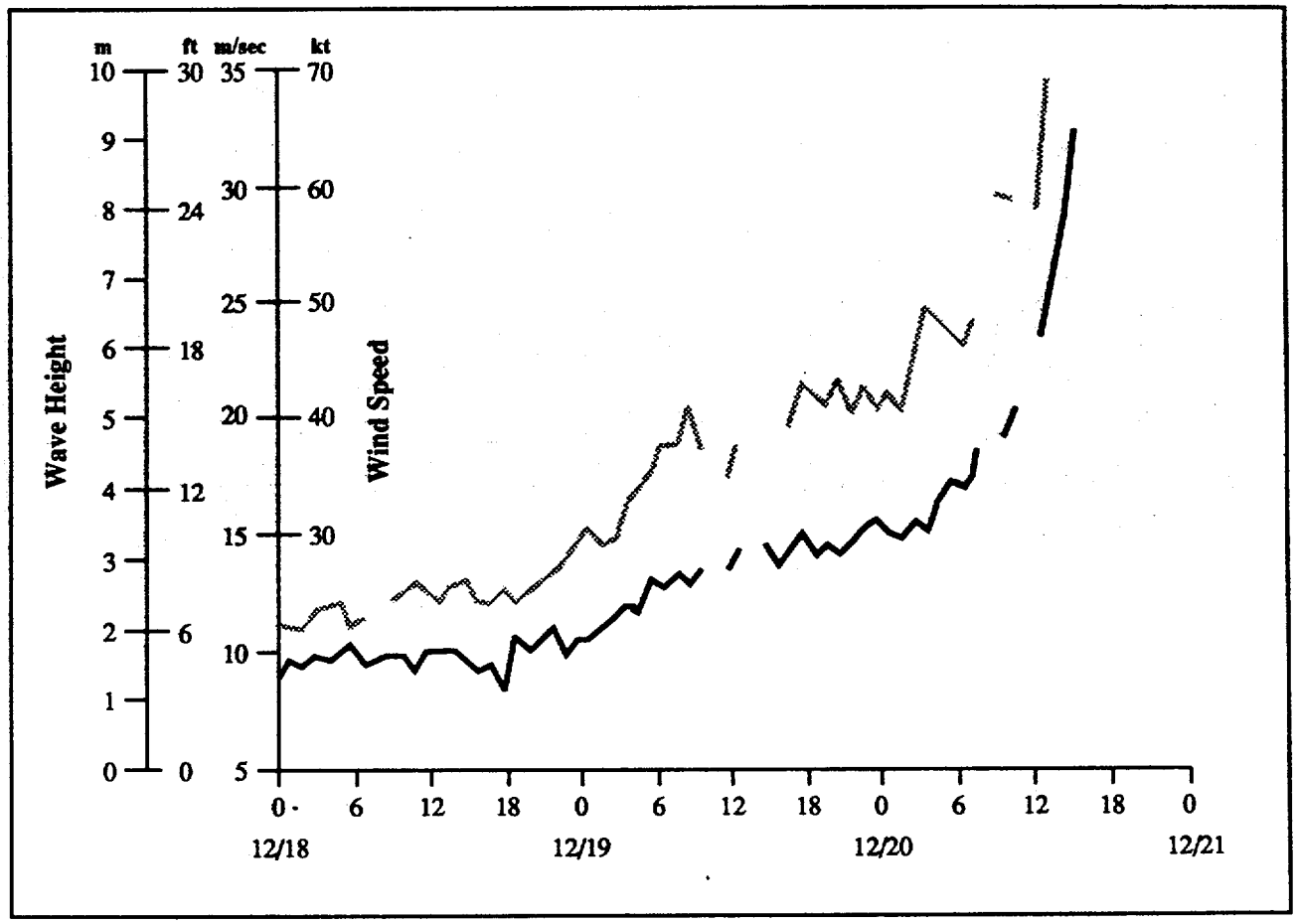

Figure 3-31-8. Time series plot of wave height (gray line) and wind speeds (black line) from a buoy moored 7 nm (13 km) west of the southern tip of Guam shows 30 ft (10 m) seas and 65 kt (33 m/sec) winds. The buoy was in the lee of Guam, but was lost shortly before Russ' CPA. (Data courtesy of the National Data Buoy Center)

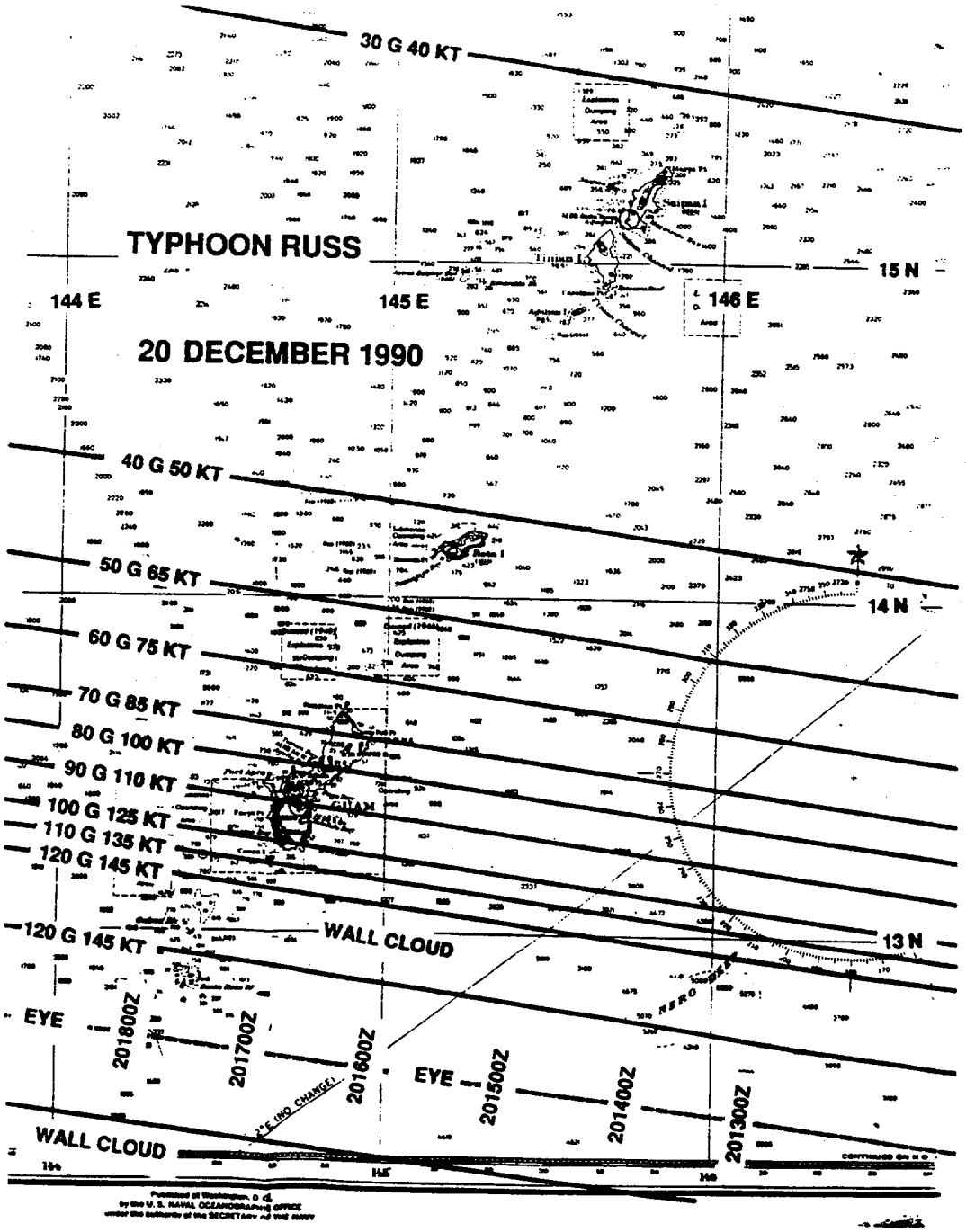

Figure 3-31-9. The post-analysis of the over water winds associated with Russ on 20 and 21 December while its track was nearest Guam. Note the rapid increase of winds near the eye wall.

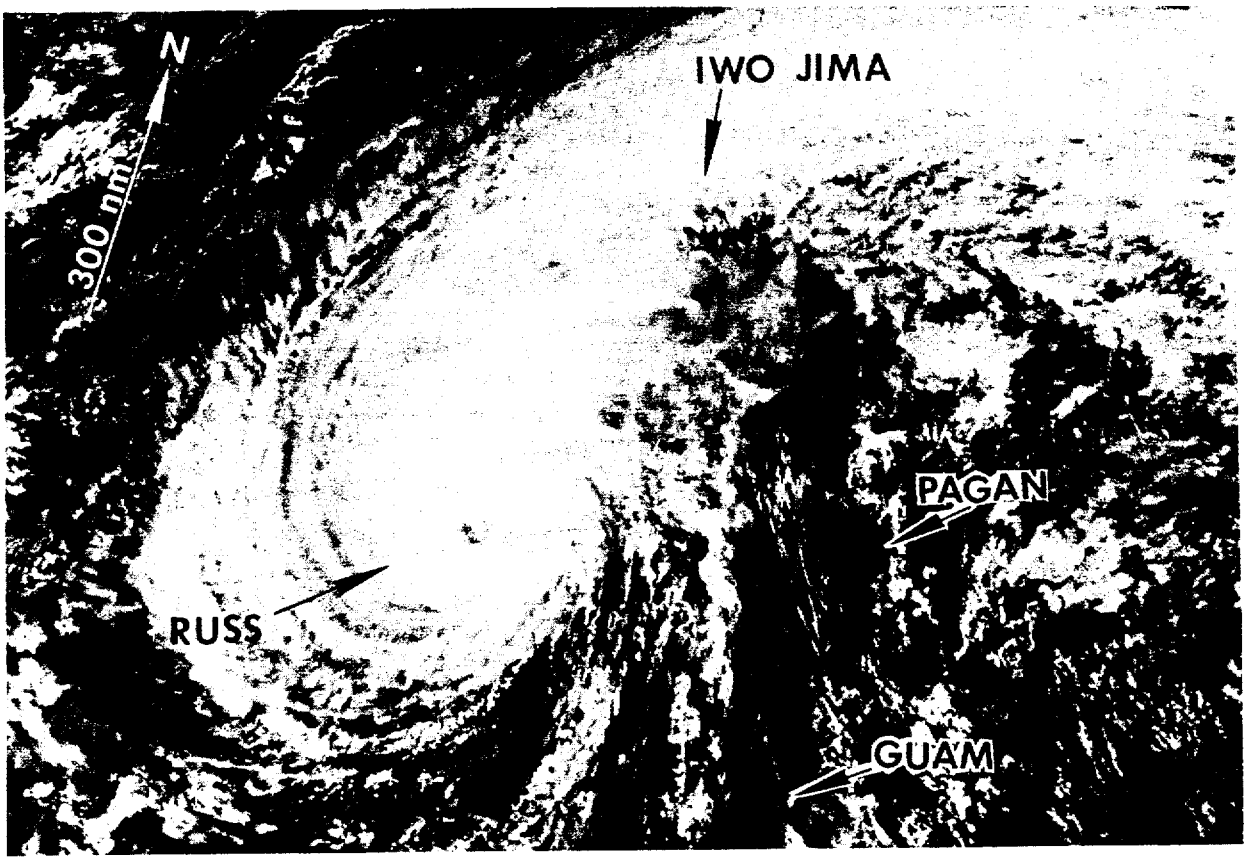

Figure 3-31-10. As Russ starts to move northward, it interacts with the polar westerlies aloft. The eye is still present in a compact central dense overcast, but the typhoon is weakening (220445Z December NOAA visual imagery).

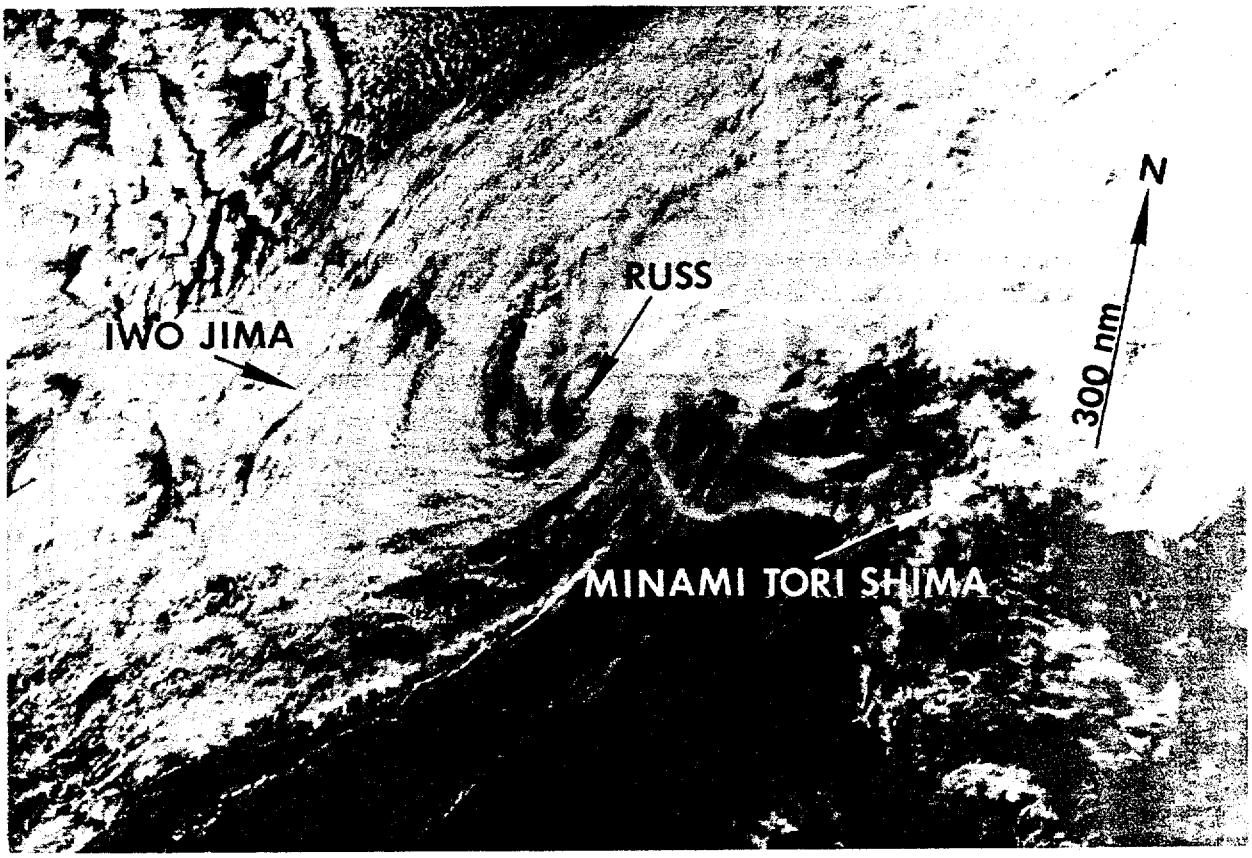

Figure 3-31-11. With the central dense overcast gone, Russ' low-level circulation center is exposed (232302Z December DMSP visual imagery).

V. FORECASTING PERFORMANCE

Overall JTWC forecast performance is shown in Figure 3-31-12. The clustering of the forecasts about the best track indicated that JTWC had a good handle on Russ' direction of motion. The mean cross track (direction) error was roughly one half the magnitude of the along track (speed) errors. This larger mean along track (speed) error was due to problems forecasting slowing and acceleration of Russ east of Guam and its acceleration after recurvature.

Russ influenced JTWC's operations. However, the day before Russ arrived JTWC had anticipated that damage might occur and had transferred all its tropical cyclone data files to the Alternate Joint Typhoon Warning Center (AJTWC) at Pearl Harbor, Hawaii. This transfer paid off because as Russ approached, JTWC began, after 201200Z, to lose most of its data base, including meteorological satellite imagery, analytic and prognostic fields, and objective guidance from Fleet Numerical Oceanography Center at Monterey, California. The increasing winds destroyed the geostationary satellite antenna, the polar orbiting satellite receiver lost power when the back up generator failed and off-island communications were interrupted. In addition, the Andersen AFB weather radar failed at this time, leaving the Federal Aviation Administration's air traffic control radar at Mount Santa Rosa as the only remaining on-island source of fixes. Rather than operate in a degraded mode, JTWC transferred responsibility for warnings to the AJTWC at Pearl Harbor, Hawaii, after the 201800Z warning. A half a day later, JTWC was able to resume normal operations and take the warning responsibility back from AJTWC.

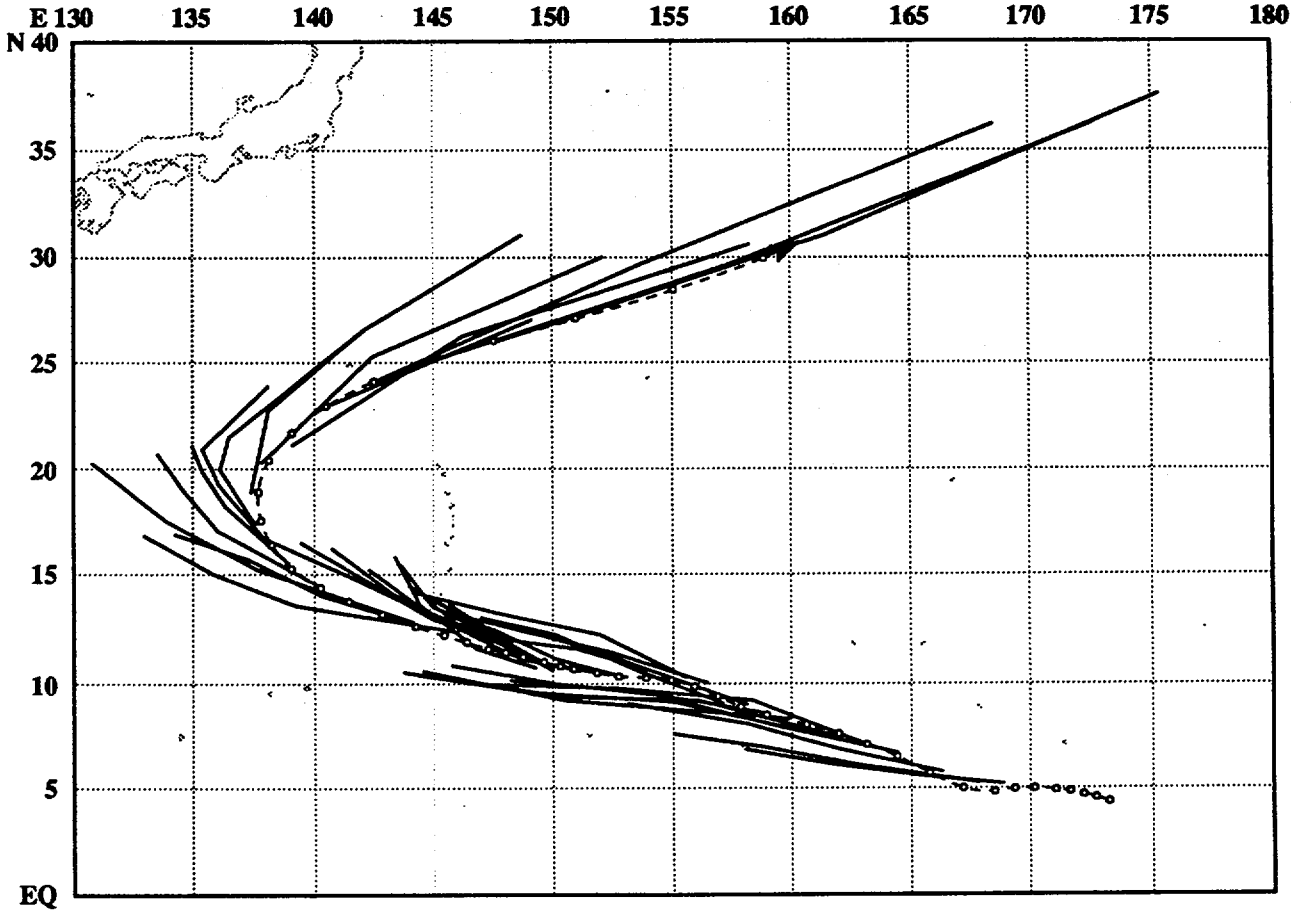

Figure 3-31-12. JTWC forecasts (solid lines) overlaid on the best track (dashed line). The clustering of forecasts shows that the general understanding of the motion toward Guam and of the recurvature track taken by Russ was good.

VI. IMPACT

Russ was the most severe tropical cyclone to hit Guam in 14 years. The island was declared a national disaster area by President Bush on 24 December, and damage estimates were as high as 120 million dollars. Miraculously, no fatalities occurred on Guam and only minor injuries were reported. This was a great credit to the disaster preparedness agencies and communications media which heightened public awareness. At sea, however, one crew member was lost from a Japanese fishing vessel that foundered southeast of Guam, and ten crew members from a South Korean fishing vessel were lost at sea after their 65 ft (20 m) boat apparently broke down south of Guam, directly in the typhoon's path.

The southern end of the Guam experienced the highest sustained winds and the most damage. Russ' winds uprooted many of the island's trees and defoliated much of the island's foliage. Two thousand houses were considered uninhabitable due to unsafe or unhealthy conditions. Of these, 341 houses were destroyed, 460 suffered major damage, and 1210 suffered minor damage. In addition, 10% of the island's total structures sustained some damage. Russ also left most of the island without power and water for several days. On the southern end of Guam, many residences were without power (Figure 3-31-13) and water for more than one week; some experienced outages for several weeks. Most telephones remained in service throughout the typhoon; however, the cable TV network sustained extensive damage. In some place on the southern and southeastern end of the island the combination of storm surge and wave run-up reached levels of 8 to 9 ft (2 to 3 m) above normal and extended inland 240-300 ft (75-90 m). For Guam, Russ was a relatively dry typhoon because the eye wall with its torrential rains passed just to the south, and rain bands were oriented north-south allowing the heavy rain to pass rapidly across the island. Thus, the inhabited part of the island was spared extensive flooding and additional damage.

An estimated 20 million dollars damage was done to civilian housing and 5 million dollars to the infrastructure. Government buildings incurred another estimated 20 million dollars in damage, including an estimated 300,000 dollars at the Oceanview High School to replace the roofing on three classrooms and other school property. The Port Authority of Guam recorded 107,000 dollars in property damage to port service equipment, primarily generators and gantry cranes. Private businesses estimated damage at 31 million dollars. This included 28 million dollars damage to the Cocos Island Resort, located on a small island on the fringing reef at the south end of Guam. The resort will have to be completely rebuilt. In addition, two ships broke their moorings and went aground on the breakwater in Apra Harbor. One of vessels was a three masted dinner cruise ship (Figure 3-31-14); the other was a 220 ft (65 m) commercial fishing vessel. Military losses (Figure 3-31-15) were estimated at over 6.5 million dollars, including 2 million dollars to military housing. It would be months before Guam fully recovered from the fury of Typhoon Russ (Figure 3-31-16).

Figure 3-31-13. Splintered utility pole bares mute testimony to Russ' high winds and termites that never sleep. (Photo courtesy of COMNAVMAR Public Affairs/PH1 Jon Hockersmith)

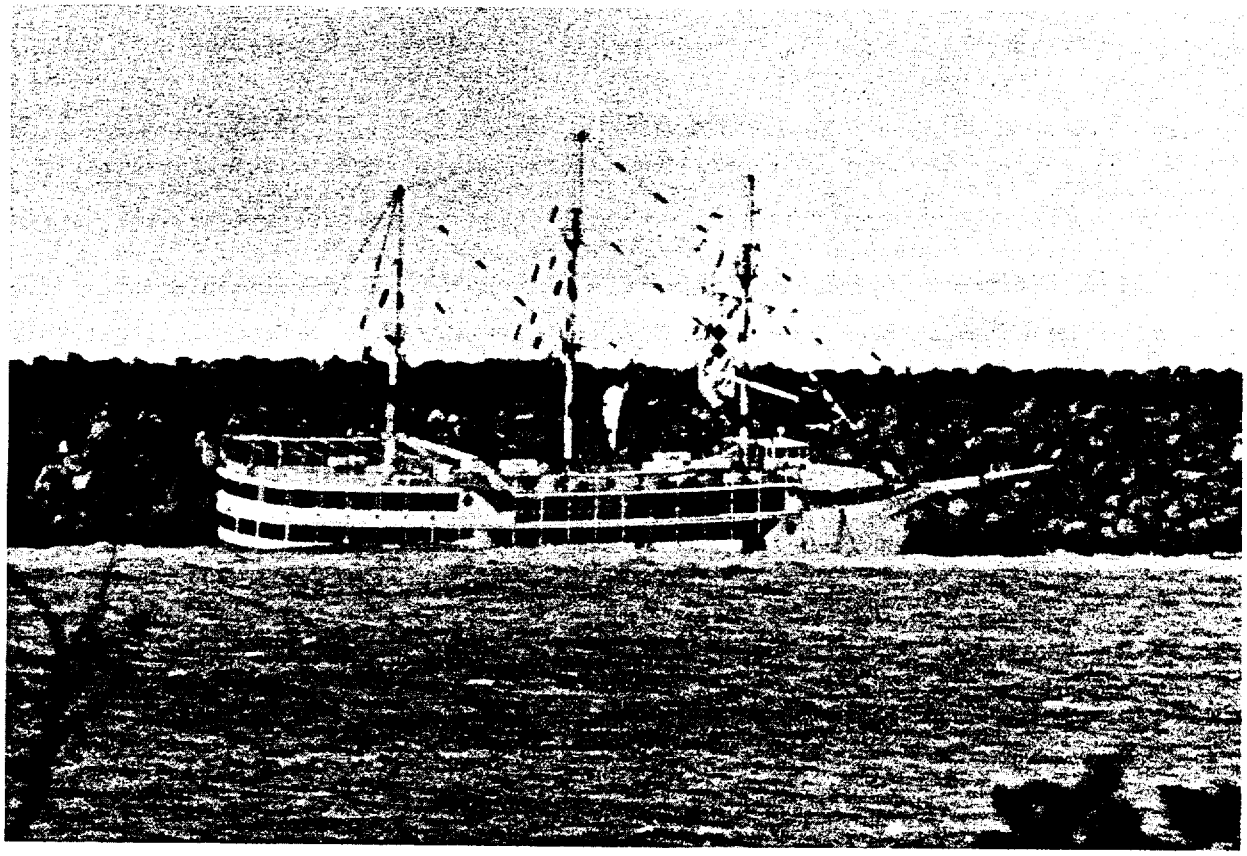

Figure 3-31-14. Dinner cruise ship Courageous aground on the Glass breakwater in Apra Harbor, Guam. (Photo courtesy of COMNAVMAR Public Affairs/PH1 Jon Hockersmith)

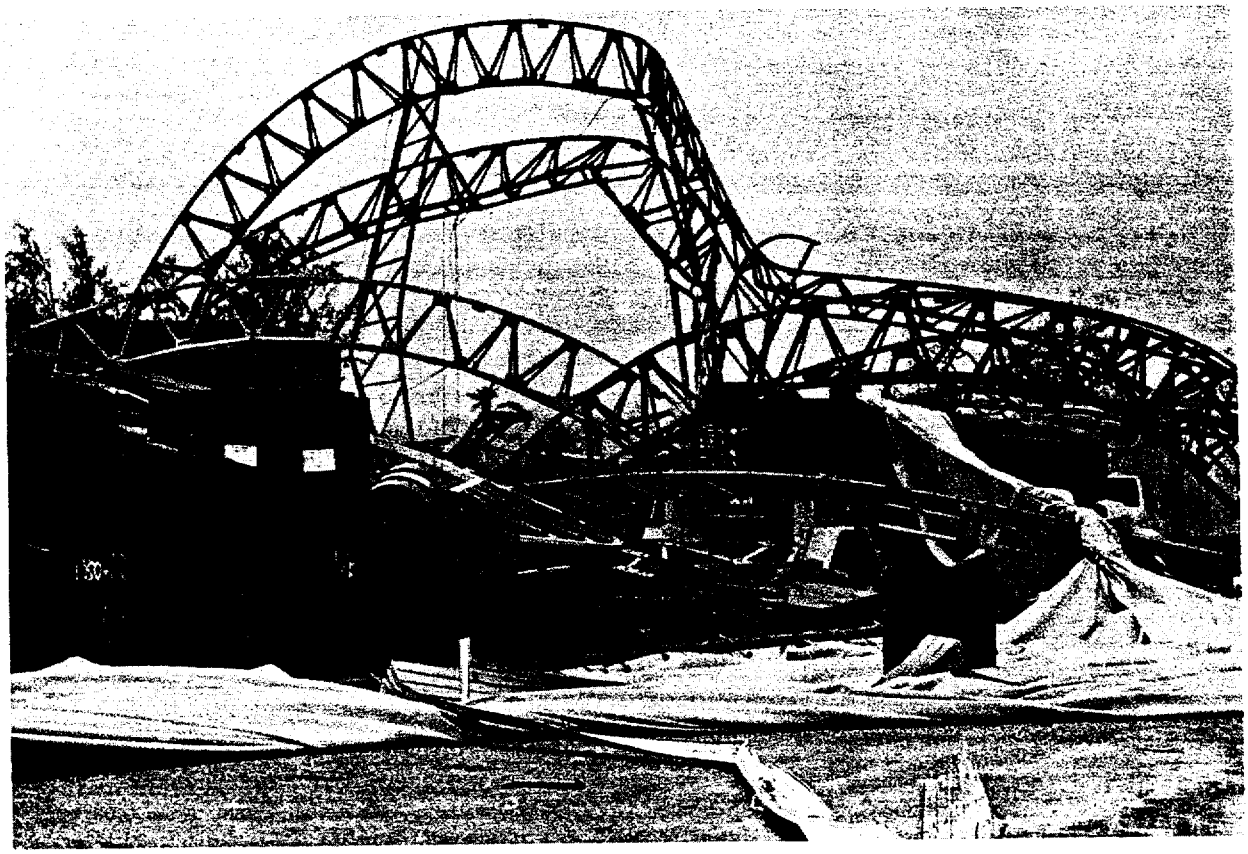

Figure 3-31-15. The steel girders of this temporary warehouse on Naval Station, Guam were twisted by the high winds and collapsed during Russ' passage.

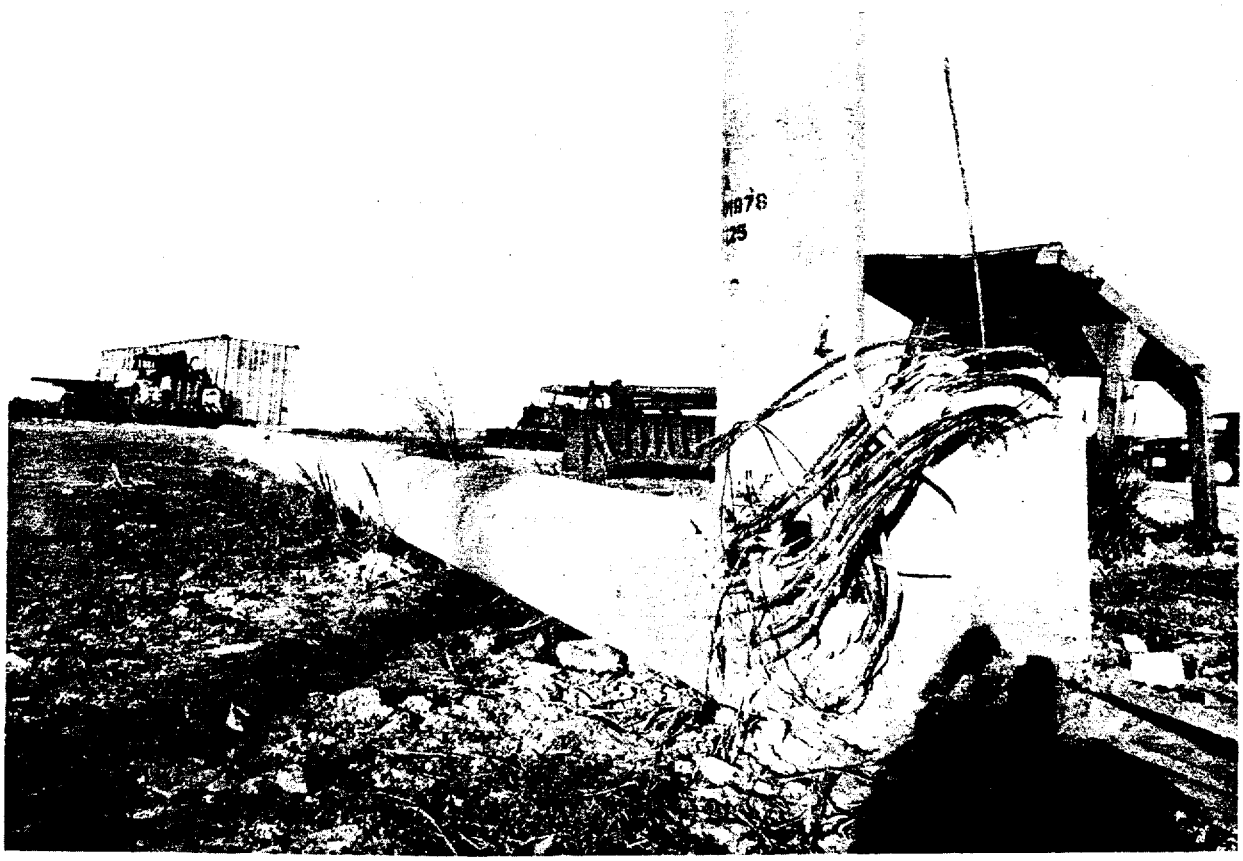

Figure 3-31-16. Concrete power pole on the highway north of Talofofo, Guam. The pole snapped about 5 feet above the ground and fell across the road. It was later pushed out of the road to enable traffic to pass. (Photo courtesy of Det 1, 1 Weather Wing/1Lt Joe Hanser)

3.3 NORTH INDIAN OCEAN TROPICAL CYCLONES

Spring and fall in the North Indian Ocean are periods of transition between major climatic controls and the most favorable seasons for tropical cyclone activity (Tables 3-5 and 3-6). Two significant tropical cyclones developed in the spring and two in the fall in the Bay of Bengal, however none occurred in the Arabian Sea. This activity was slightly below the 16-year average of five. Tropical Cyclone 02B was unusually intense - 125 kt (64 m/sec) - and like Tropical Cyclone 32W in 1989 occurred in November.

TABLE 3-5. 1990 SIGNIFICANT TROPICAL CYCLONES
NORTH INDIAN OCEAN

TROPICAL CYCLONE	PERIOD OF WARNING	NUMBER OF WARNINGS ISSUED	MAXIMUM SURFACE WINDS-KT (M/SEC)	ESTIMATED MSLP (MB)
TC 01B	18 APR - 18 APR	2	25 (13)	1002
TC 02B	05 MAY - 11 MAY	25	125 (64)	916
TC 03B	02 NOV - 03 NOV	6	30 (15)	1000
TC 04B	15 DEC - 18 DEC	14	45 (23)	991
	TOTAL:	47		

TABLE 3-6. NORTH INDIAN OCEAN
TROPICAL CYCLONES DISTRIBUTION

YEAR	JAN	FEB	MAR	APR	MAY	JUN	JUL	AUG	SEP	OCT	NOV	DEC	TOTAL
1971*	-	-	-	-	-	0	0	0	0	1	1	0	2
1972*	0	0	0	1	0	0	0	0	2	0	1	0	4
1973*	0	0	0	0	0	0	0	0	0	1	2	1	4
1974*	0	0	0	0	0	0	0	0	0	0	1	0	1
1975	1	0	0	0	2	0	0	0	0	1	2	0	6
1976	0	0	0	1	0	1	0	0	1	1	0	1	5
1977	0	0	0	0	1	1	0	0	0	1	2	0	5
1978	0	0	0	0	1	0	0	0	0	1	2	0	4
1979	0	0	0	0	1	1	0	0	2	1	2	0	7
1980	0	0	0	0	0	0	0	0	0	0	1	1	2
1981	0	0	0	0	0	0	0	0	0	1	1	1	3
1982	0	0	0	0	1	1	0	0	0	2	1	0	5
1983	0	0	0	0	0	0	0	1	0	1	1	0	3
1984	0	0	0	0	1	0	0	0	0	1	2	0	4
1985	0	0	0	0	2	0	0	0	0	2	1	1	6
1986	1	0	0	0	0	0	0	0	0	0	2	0	3
1987	0	1	0	0	0	2	0	0	0	1	2	2	8
1988	0	0	0	0	0	1	0	0	0	1	2	1	5
1989	0	0	0	0	1	1	0	0	0	0	1	0	3
1990**	0	0	0	1	1	0	0	0	0	0	1	1	4
(1975-1990) AVERAGE:	0.1	0.1	0.0	0.1	0.7	0.5	0.0	0.1	0.2	0.9	1.4	0.5	4.6
TOTAL:	2	1	0	2	11	8	0	1	3	14	23	8	73

* JTWC WARNING RESPONSIBILITY BEGAN ON 4 JUNE 1971 FOR THE BAY OF BENGAL, EAST OF 90° EAST LONGITUDE. AS DIRECTED BY CINCPAC, JTWC ISSUED WARNINGS ONLY FOR THOSE TROPICAL CYCLONES THAT DEVELOPED OR TRACKED THROUGH THAT PART OF THE BAY OF BENGAL. COMMENCING WITH THE 1975 TROPICAL CYCLONE SEASON, JTWC'S AREA OF RESPONSIBILITY WAS EXTENDED WESTWARD TO INCLUDE THE WESTERN PART OF THE BAY OF BENGAL AND THE ENTIRE ARABIAN SEA.
** JTWC ISSUED EIGHT TROPICAL CYCLONE FORMATION ALERTS. FORMATION ALERTS WERE ISSUED FOR ALL OF THE SIGNIFICANT TROPICAL CYCLONES THAT DEVELOPED IN 1990.

WARNINGS: NUMBER OF CALENDAR WARNING DAYS: 11
THERE WERE NO CALENDAR WARNING DAYS WITH TWO OR MORE TROPICAL CYCLONES.

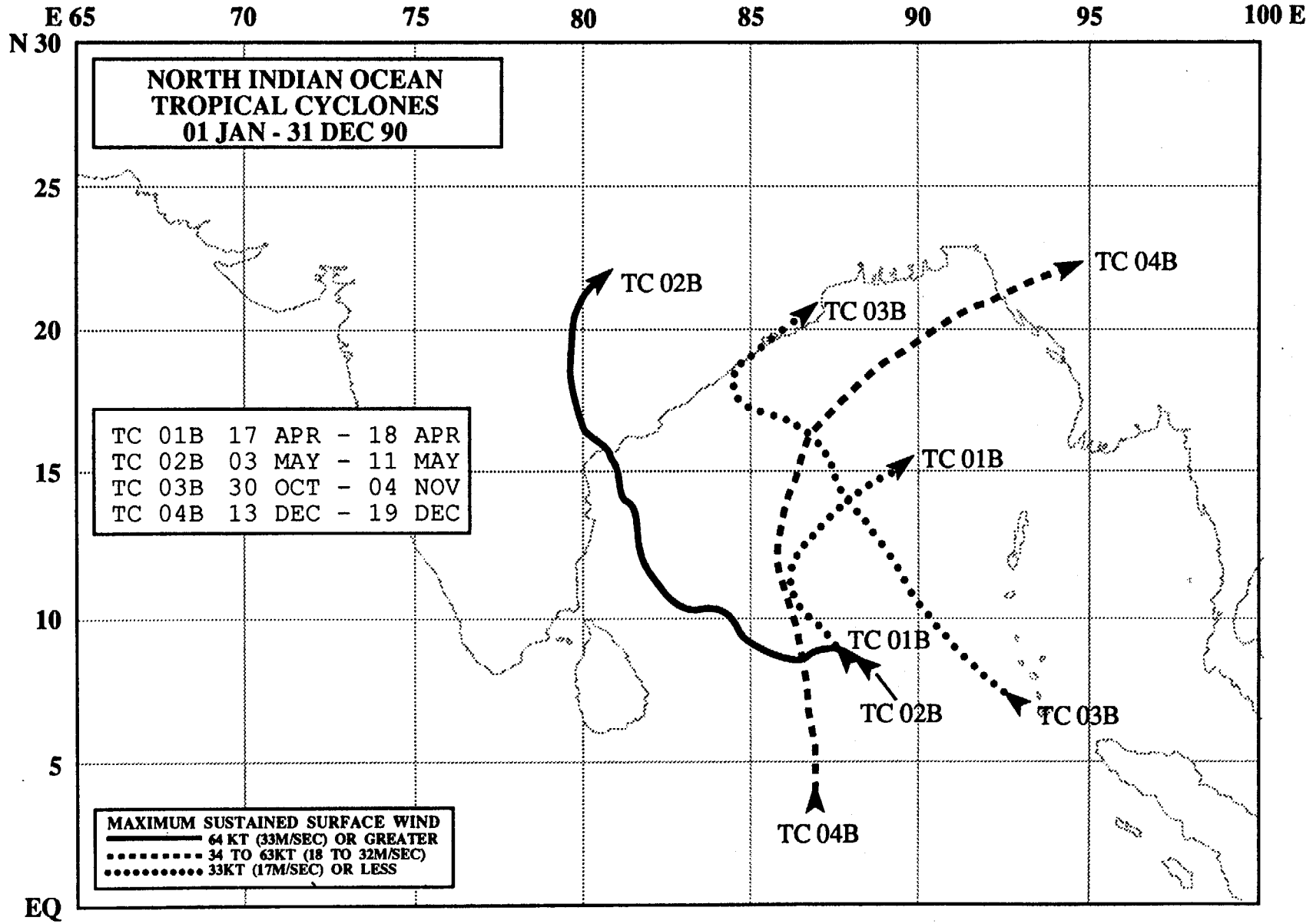
NORTH INDIAN OCEAN
TROPICAL CYCLONES
01 JAN - 31 DEC 90
TC 01B 17 APR - 18 APR
TC 02B 03 MAY - 11 MAY
TC 03B 30 OCT - 04 NOV
TC 04B 13 DEC - 19 DEC
MAXIMUM SUSTAINED SURFACE WIND
64 KT (33M/SEC) OR GREATER
34 TO 63KT (18 TO 32M/SEC)
33KT (17M/SEC) OR LESS
E 65
70
75
80
85
90
95
100 E
N 30
25
20
15
10
5
EQ
TC 02B
TC 03B
TC 04B
TC 01B
TC 01B
TC 02B
TC 03B
TC 04B

TROPICAL CYCLONE 01B

Tropical cyclone 01B was the first of two systems that formed in the Bay of Bengal during the spring transition season. It organized quite rapidly, having existed for less than 12 hours as a region of persistent convective activity, before becoming the subject of a TCFA issued at 171630Z. The brief period of northward motion followed by a short recurvature track to the northeast was related to the cyclone's formation near the axis of the subtropical ridge. The proximity of strong upper-level westerlies to the north, inhibited development beyond tropical depression intensity and brought about the rapid dissipation of 01B over water. Only two tropical depression warnings were issued on the system at 180000Z and 181200Z. Tropical cyclone 01B had no reported impact on military or civilian vessels.

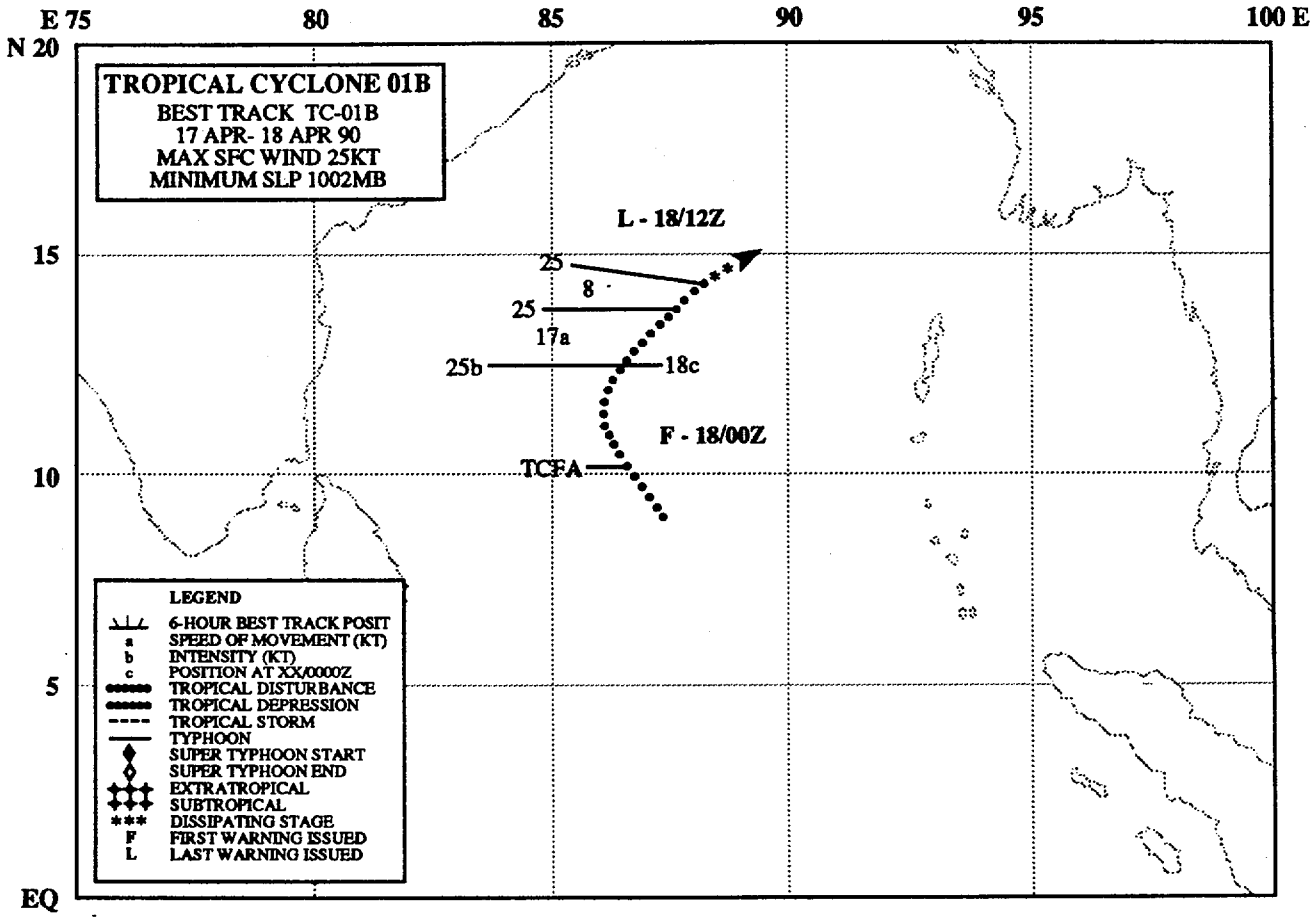

TROPICAL CYCLONE 02B

In stark contrast to its predecessor, Tropical Cyclone 01B, Tropical Cyclone 02B achieved near-super typhoon intensity, and had a major impact on the civilian populace of India. Existing as a discrete disturbance for about 36 hours before becoming the subject of a TCFA, the cyclone followed a sinuous west-northwest track under the mid-level subtropical ridge. Although TC02B had good outflow into the upper-level easterlies, landfall in southern India was expected by about 72 hours, prompting early forecasts of intensification to only nominal typhoon intensity followed by weakening due to the approach of landfall. Because of a weakness in the subtropical ridge, a moderate turn toward the northwest was expected, however the actual track change turned out to be much more northward than anticipated. This permitted the cyclone to stay off-shore and to establish strong outflow into the upper-level southwesterlies of a passing 200-mb short-wave trough. As the northward turn began, JTWC modified the intensity forecast to one of rapid deepening beginning with the 070000Z warning. The rapid deepening did in fact occur beginning at 061800Z with a 60 kt (30 m/sec) intensity and peaking at 125 kt (65 m/sec) by 080600Z: an increase of 65 kt (33 m/sec) in 36 hours. At 091200Z, the cyclone, with winds of 100 kt (50 m/sec) made landfall 165 nm (305 km) north of Madras in the vicinity of Machilipatnam in Andra Pradesh State.

In impact of this cyclone on India was substantial. An estimated 150,000 people were evacuated in preparation for landfall. Over 100 villages were destroyed resulting in at least 510 human fatalities. The cyclone also wreaked havoc on the rich agriculture industry of the region killing more than 100,000 farm animals and causing more than $600 million in damage to crops. Local officials reported that Tropical Cyclone 02B was the worst disaster for southern India since the 1977 cyclone that killed an estimated 10,000 people.

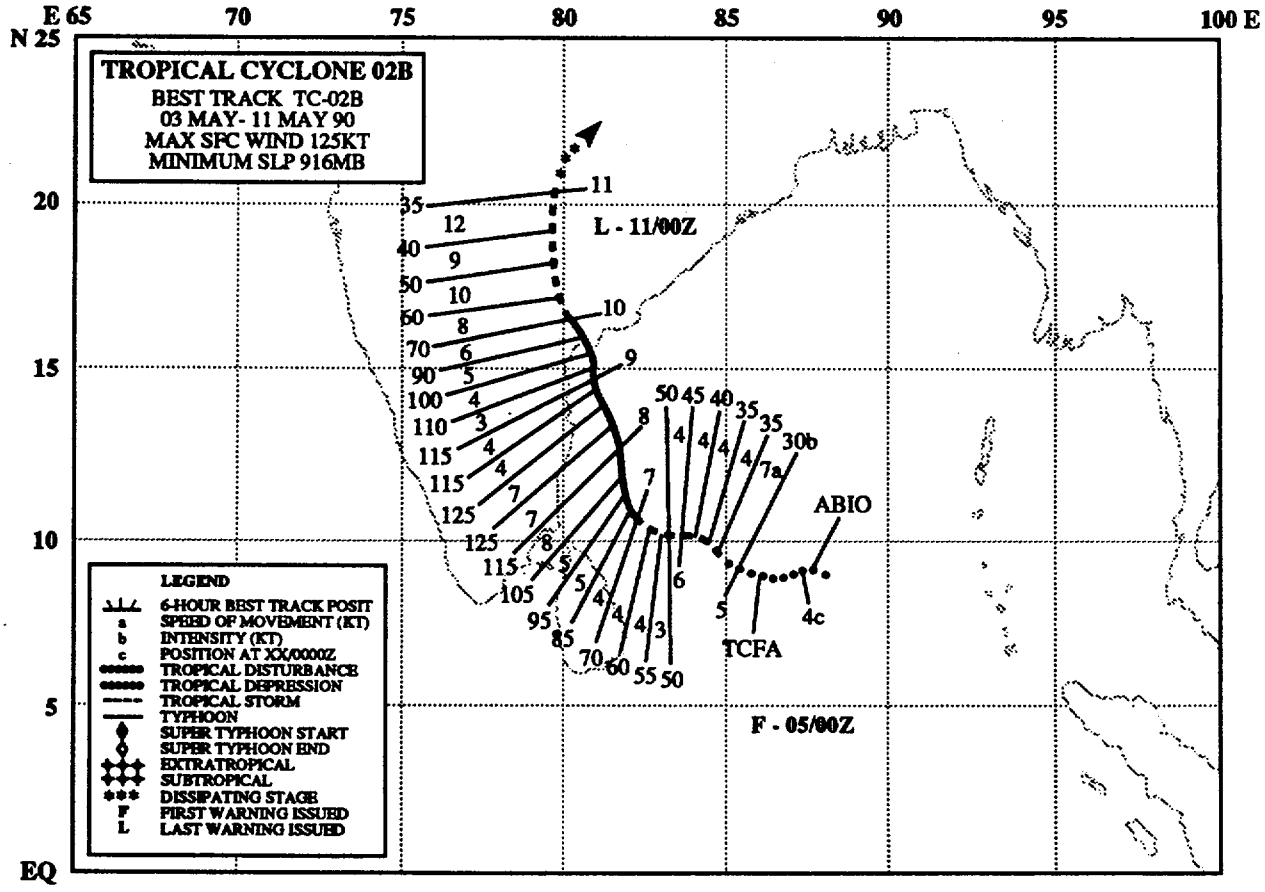

TROPICAL CYCLONE 03B

Tropical Cyclone 03B was the first of two systems that occurred the Bay of Bengal during the fall transition season. The system formed and remained under upper-level east-southeasterly wind shear associated with a 200-mb ridge circulation well to the northeast. Thus, development was strongly inhibited and TC03B never exceeded tropical depression intensity. The cyclone tracked north-northwestward along the western periphery of a broad mid-level subtropical ridge circulation centered over Indochina. It reached the axis of the ridge as it made landfall, then skirted the coast of India on a northeastward track as it dissipated. No reports of impact were received.

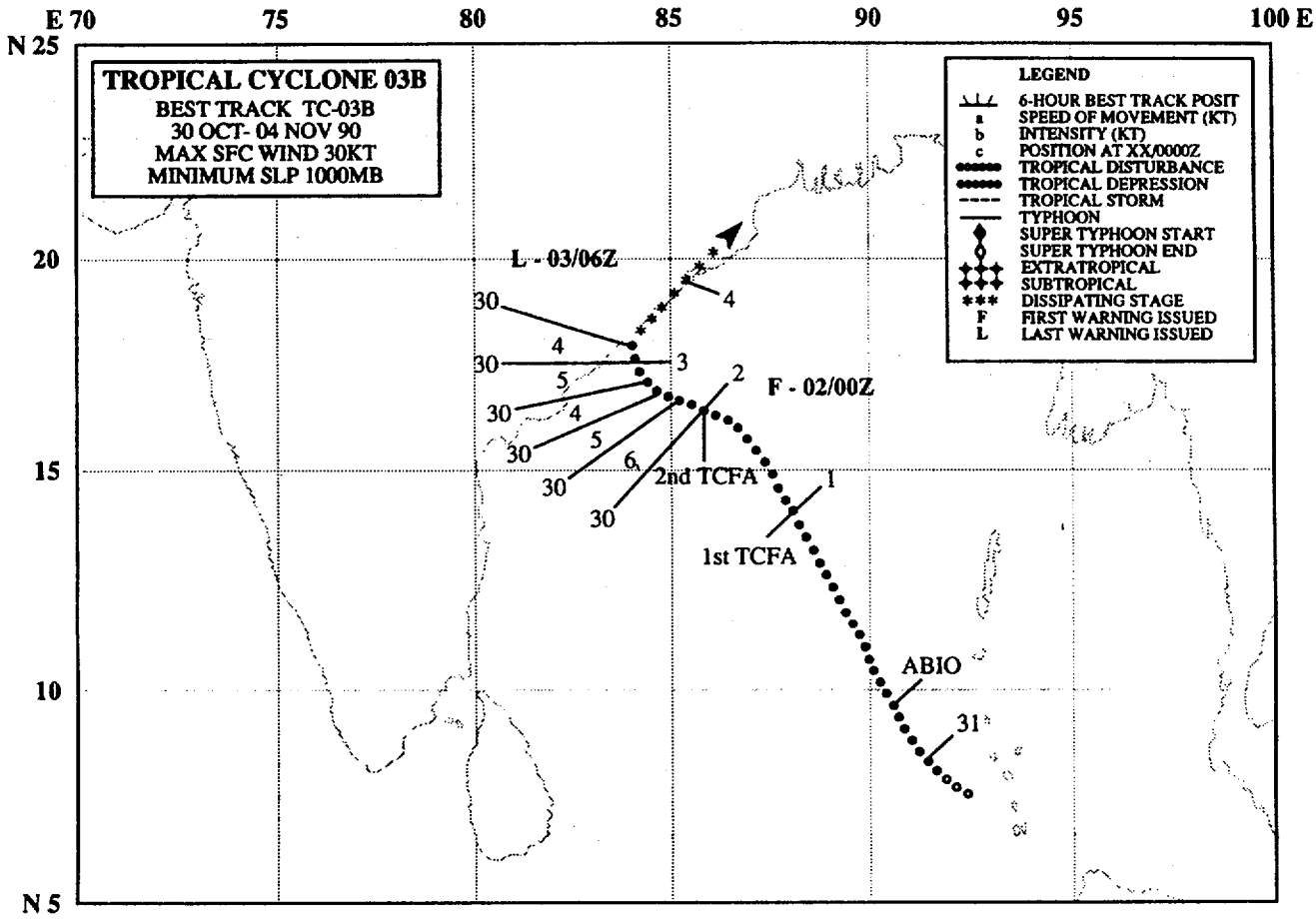

TROPICAL CYCLONE 04B

Tropical Cyclone 04B, the final system for the North Indian Ocean for the year, formed just to the south of a col in the mid-level subtropical ridge that typically extends across the Bay of Bengal between semi-permanent ridge circulations over Indochina and the Northeast African/Arabian Sea region. As a result, the cyclone tracked through the break in the subtropical ridge and followed a recurvature track that resulted in landfall in the area between Bangladesh and Burma. The development of TC04B into a significant tropical cyclone coincided with its movement into an area of relatively weak upper-level winds, however further intensification was restricted to a maximum of moderate tropical storm intensity. As the cyclone moved northeastward, it began to encounter increasing upper-level wind shear associated with the mid-latitude westerlies and weakened by the time landfall occurred. No reports of impact were received.

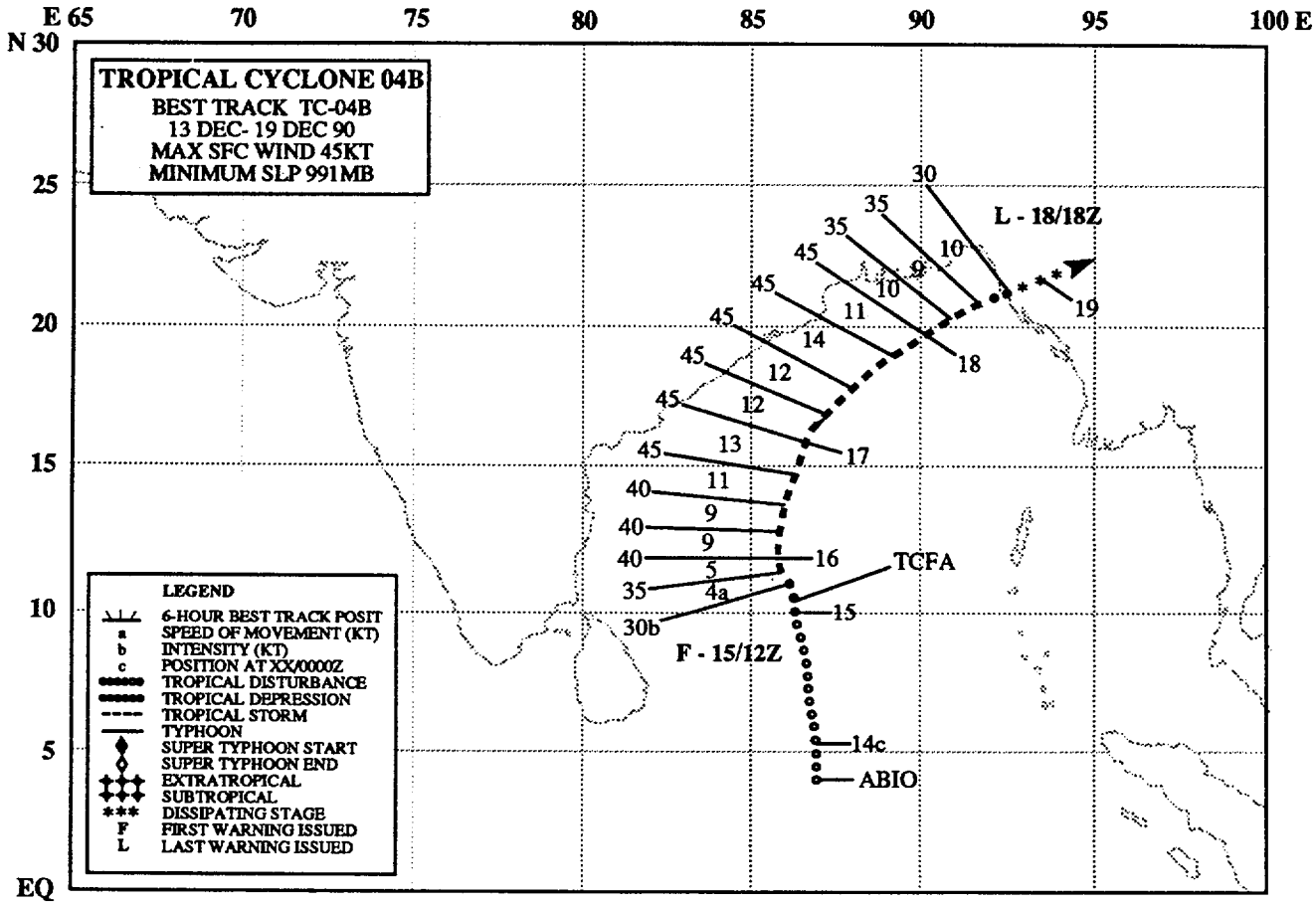

Intentionally left blank.

4. SUMMARY OF SOUTH PACIFIC AND SOUTH INDIAN OCEAN TROPICAL CYCLONES

4.1 GENERAL

On 1 October 1980, JTWC's area of responsibility (AOR) was expanded to include the Southern Hemisphere from 180° longitude westward to the coast of Africa. Details on Southern Hemisphere tropical cyclones and JTWC warnings from July 1980 through June 1982 are contained in Diercks et al. (1982) and from July 1982 through June 1984, in Wirfel and Sandgathe (1986). Information on Southern Hemisphere tropical cyclones after June 1984 can be found in the applicable Annual Tropical Cyclone Report.

The Naval Western Oceanography Center (NWOC) Pearl Harbor, HI issues warnings on tropical cyclones in the South Pacific east of 180° longitude. Tropical cyclones in NWOC's AOR are included in this and previous Annual Tropical Cyclone Reports.

In accordance with USCINCPACINST 3140.1 (series), Southern Hemisphere tropical cyclones are numbered sequentially from 1 July through 30 June. This convention is established to encompass the Southern Hemisphere tropical cyclone season, which primarily occurs from January through April. There are two ocean basins for warning purposes - the South Indian (west of 135° east longitude) and the South Pacific (east of 135° east longitude) - which are identified by appending the suffixes "S" and "P" respectively to the tropical cyclone number.

Intensity estimates for Southern Hemisphere tropical cyclones are derived from the interpretation of satellite imagery using the Dvorak technique (Dvorak, 1984) and in rare instances from surface observations. The Dvorak technique relates specific cloud signatures to maximum sustained one-minute average wind speeds. The conversion from maximum sustained winds to minimum sea-level pressure is obtained from the Atkinson and Holliday (1977) relationship (Table 4-1).

4.2. SOUTH PACIFIC AND SOUTH INDIAN OCEAN TROPIAL CYCLONES

As in 1989, tropical cyclone activity in 1990 (Table 4-2) approached the climatological mean of 28 storms (Table 4-3). An unusually large number of tropical cyclones occurred in the South Indian Ocean (Table 4-4). The number of storms near Australia was slightly below average, and there were only half the normal number east of 165° E. The activity began early, with two tropical cyclones in July, a month which rarely sees any. By November, six tropical cyclones had developed, three reaching

TABLE 4-1 MAXIMUM SUSTAINED SURFACE WINDS AND EQUIVALENT MINIMUM SEA-LEVEL PRESSURE (ATKINSON AND HOLLIDAY, 1977)

MAXIMUM SUSTAINED SURFACE WIND (KT)	MINIMUM SEA-LEVEL PRESSURE (MB)
30	1000
35	997
40	994
45	991
50	987
55	984
60	980
65	976
70	972
75	967
80	963
85	958
90	954
95	948
100	943
105	938
110	933
115	927
120	922
125	916
130	910
135	906
140	898
145	892
150	885
155	879
160	872
165	865
170	858
175	851
180	844

tropical storm intensity and one typhoon intensity. Tropical cyclone activity was almost continuous from December through March (Figure 4-1), with several instances of multiple outbreaks. For two days in March, five tropical cyclones were active simultaneously. Two systems in 1990 reached super typhoon intensity - Alibera (08S) and Alex (24S). Alibera (08S) was not only the most intense system, it also lasted the longest, being in warning status for two weeks. Plots of the tropical cyclone best tracks appear in Figures 4-2 and 4-3.

TABLE 4-2 **SOUTH PACIFIC AND SOUTH INDIAN OCEAN 1990 SIGNIFICANT TROPICAL CYCLONES (1 July 1989 - 30 June 1990)**

TROPICAL CYCLONE	PERIOD OF WARNING	NUMBER WARNINGS ISSUED	MAXIMUM SURFACE WINDS-KT (M/SEC)	ESTIMATED MSLP (MB)
01S ----	10 Jul - 11 Jul	4	25(13)	1002
02S ----	14 Jul - 16 Jul	6	35(18)	997
03S ----	25 Sep - 27 Sep	5	30(15)	1000
04S ----	13 Oct - 14 Oct	4	30(15)	1000
05S ----	31 Oct - 02 Nov	8	35(18)	997
06S Pedro	08 Nov - 12 Nov	9	65(33)	976
07P Felicity	15 Dec - 16 Dec	3	60(31)	980
07P Felicity*	17 Dec - 18 Dec	3	55(28)	984
08S Alibera	19 Dec - 02 Jan	31	135(69)	904
09S Bavomavo	02 Jan - 07 Jan	13	85(44)	958
10S Sam	13 Jan - 18 Jan	11	50(26)	987
11S Tina	25 Jan - 28 Jan	6	45(23)	991
12P Nancy	29 Jan - 02 Feb	8	65(33)	976
13P Ofa**	31 Jan - 08 Feb	17	115(59)	927
14S Cezera	01 Feb - 09 Feb	16	80(41)	963
15S Dety	02 Feb - 08 Feb	12	95(49)	949
16P Peni**	13 Feb - 17 Feb	9	60(31)	980
17S Vincent	01 Mar - 06 Mar	11	70(36)	972
18S Edisaona	01 Mar - 07 Mar	14	100(51)	944
19P Greg	03 Mar - 05 Mar	5	30(15)	1000
20S Walter	04 Mar - 06 Mar	6	30(15)	1000
21P Hilda	04 Mar - 07 Mar	7	60(31)	980
22S Felana	08 Mar - 15 Mar	13	45(23)	991
23S Gregoara	13 Mar - 22 Mar	18	110(57)	933
24S Alex	16 Mar - 24 Mar	17	130(67)	910
25P Ivor	16 Mar - 22 Mar	14	75(39)	968
26P Rae	22 Mar - 23 Mar	4	40(21)	994
27S ----	13 Apr - 14 Apr	3	45(23)	991
28S Bessi	16 Apr - 17 Apr	3	40(21)	994
29S Ikonjo	12 May - 20 May	18	55(28)	984
	Total:	**298**		

* Regenerated

** Warnings Issued by NWOC

NOTE: Names of Southern Hemisphere Tropical Cyclones are given by the Regional Warning Centers (Nadi, Brisbane, Darwin, Perth, Reunion and Mauritius) and are appended to JTWC Warnings, when available.

TABLE 4-3 **MONTHLY DISTRIBUTION OF SOUTH PACIFIC AND SOUTH INDIAN OCEAN TROPICAL CYCLONES**

YEAR	JUL	AUG	SEP	OCT	NOV	DEC	JAN	FEB	MAR	APR	MAY	JUN	TOTAL
(1959-1978) AVERAGE*	-	-	-	0.4	1.5	3.6	6.1	5.8	4.7	2.1	0.5	-	24.7
1981	0	0	0	1	3	2	6	5	3	3	1	0	24
1982	1	0	0	1	1	3	9	4	2	3	1	0	25
1983	1	0	0	1	1	3	5	6	3	5	0	0	25
1984	1	0	0	1	2	5	5	10	4	2	0	0	30
1985	0	0	0	0	1	7	9	9	6	3	0	0	35
1986	0	0	1	0	1	1	9	9	6	4	2	0	33
1987	0	1	0	0	1	3	6	8	3	4	1	1	28
1988	0	0	0	0	2	3	5	5	3	1	2	0	21
1989	0	0	0	0	2	1	5	8	6	4	2	0	28
1990	2	0	1	1	2	2	4	4	10	2	1	0	29
TOTAL CASES:	5	1	2	5	16	30	63	68	46	31	10	1	278
(1981-1990) AVERAGE:	0.5	0.1	0.2	0.5	1.6	3.0	6.3	6.8	4.6	3.1	1.0	0.1	27.8

* (Gray, 1979)

TABLE 4-4 **ANNUAL VARIATION OF SOUTHERN HEMISPHERE TROPICAL CYCLONES BY OCEAN BASIN**

YEAR	SOUTH INDIAN (WEST OF 105°E)	AUSTRALIAN (105°E - 165°E)	SOUTH PACIFIC (EAST OF 165°E)	TOTAL
(1959-1978) AVERAGE*	8.4	10.3	5.9	24.7
1981	13	8	3	24
1982	12	11	2	25
1983	7	6	12	25
1984	14	14	2	30
1985	14	15	6	35
1986	14	16	3	33
1987	9	8	11	28
1988	14	2	5	21
1989	12	9	7	28
1990	18	8	3	29
TOTAL CASES:	127	97	54	278
(1981-1989) AVERAGE:	12.7	9.7	5.4	27.8

* (Gray, 1979)

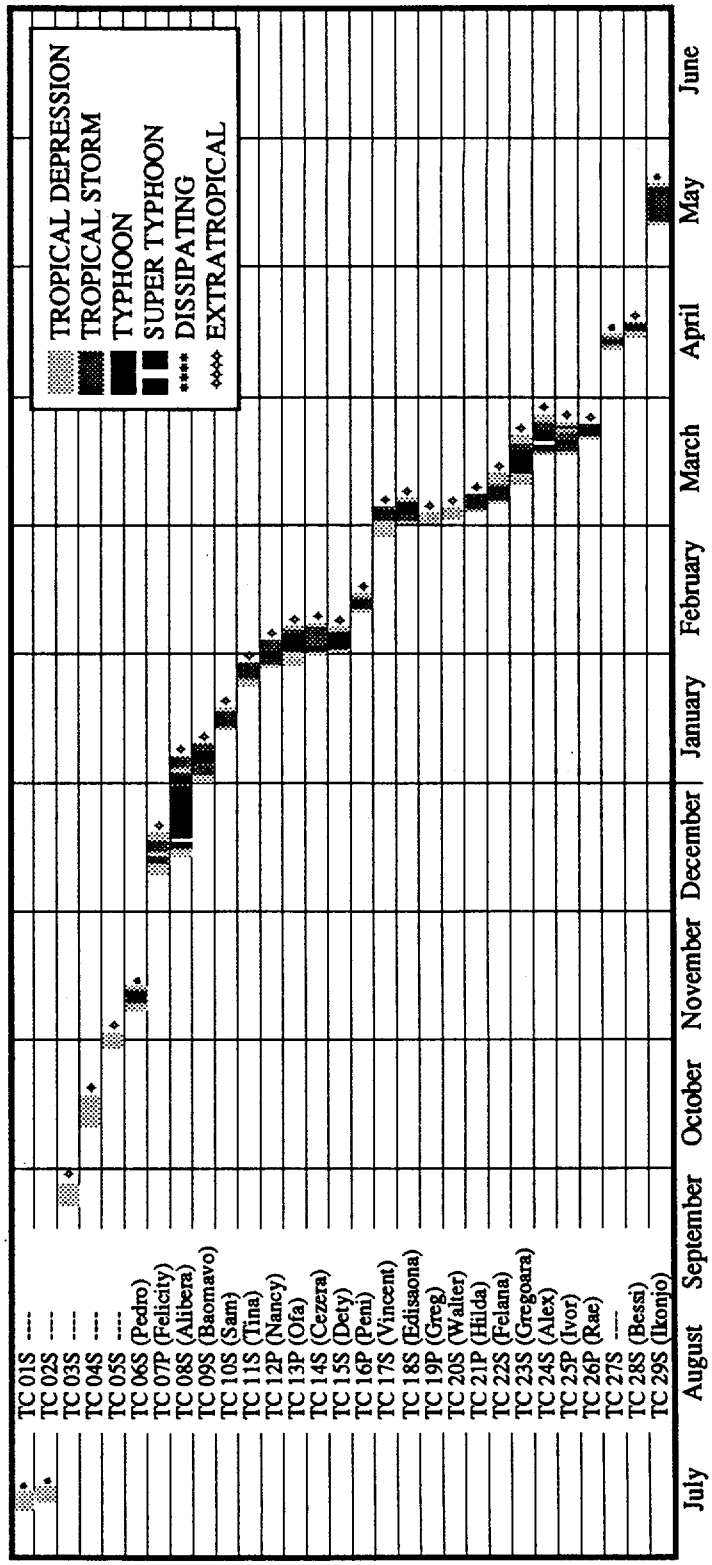

Figure 4-1. Chronology of South Pacific and South Indian Ocean tropical cyclones for 1990.

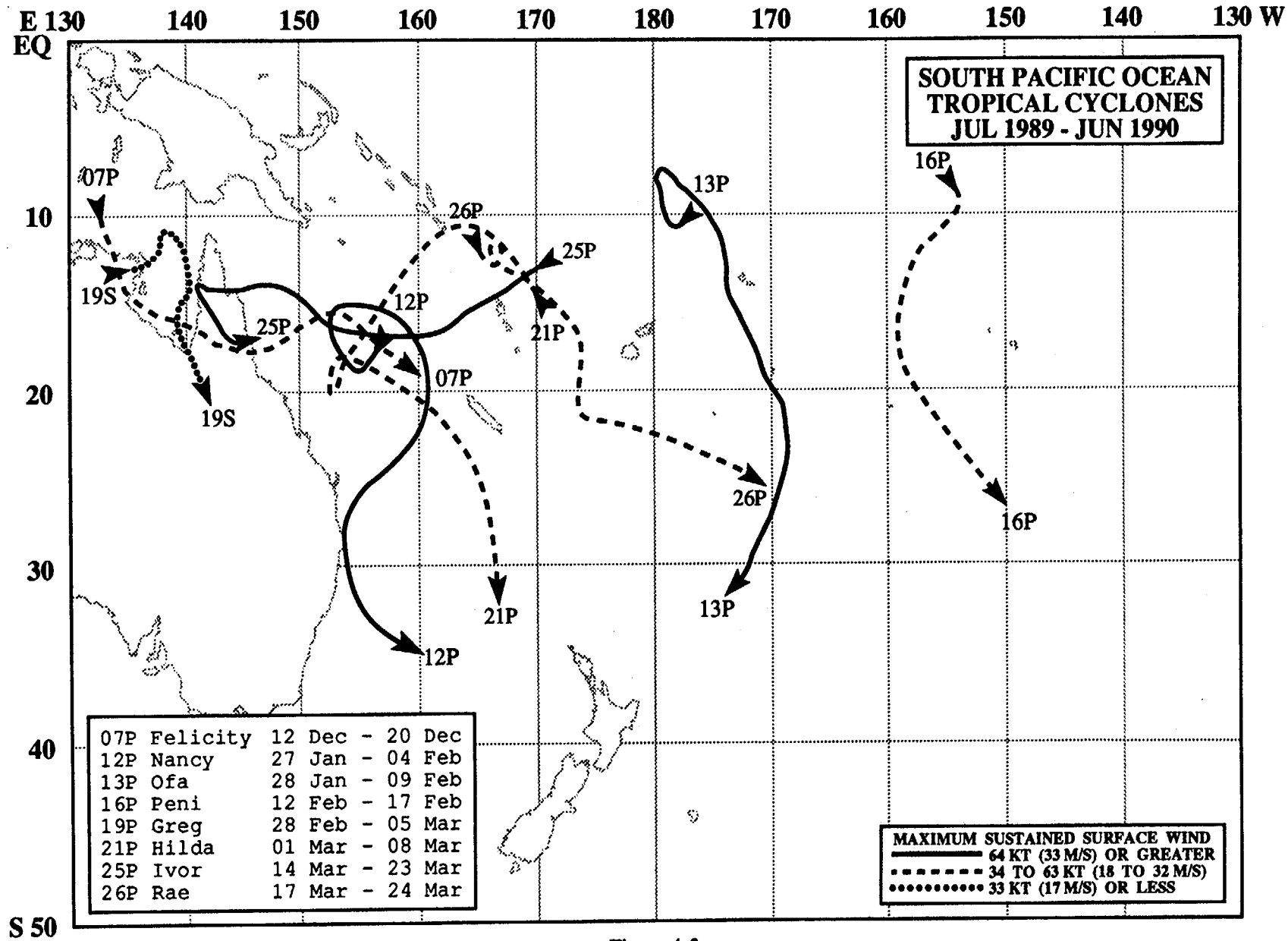
E 130
140
150
160
170
180
170
160
150
140
130 W
EQ
10
20
30
40
S 50
SOUTH PACIFIC OCEAN
TROPICAL CYCLONES
JUL 1989 - JUN 1990
07P
19S
26P
25P
12P
21P
07P
19S
25P
13P
16P
26P
16P
21P
13P
12P
07P Felicity 12 Dec - 20 Dec
12P Nancy 27 Jan - 04 Feb
13P Ofa 28 Jan - 09 Feb
16P Peni 12 Feb - 17 Feb
19P Greg 28 Feb - 05 Mar
21P Hilda 01 Mar - 08 Mar
25P Ivor 14 Mar - 23 Mar
26P Rae 17 Mar - 24 Mar
MAXIMUM SUSTAINED SURFACE WIND
64 KT (33 M/S) OR GREATER
34 TO 63 KT (18 TO 32 M/S)
33 KT (17 M/S) OR LESS

Figure 4-3.

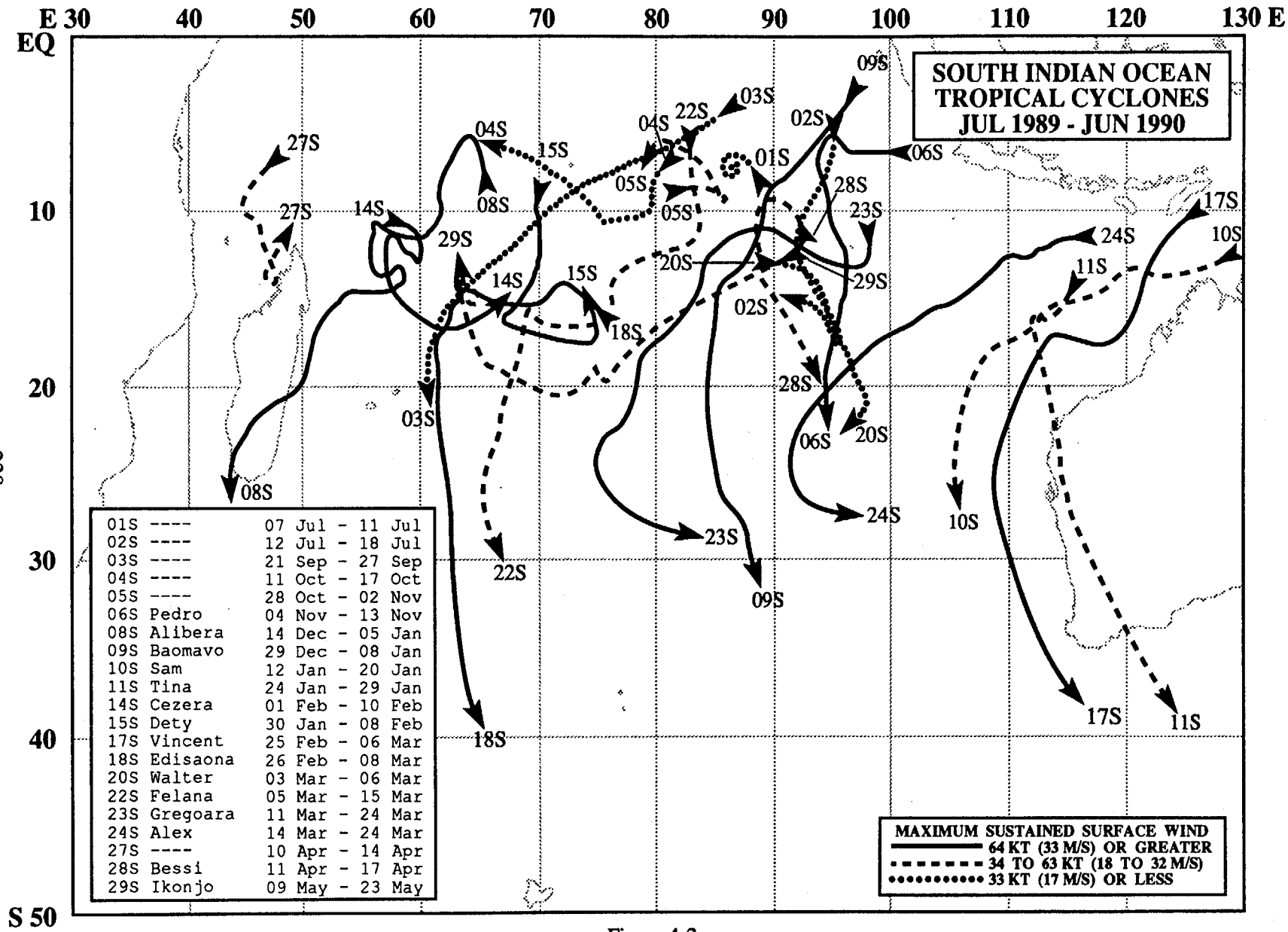
SOUTH INDIAN OCEAN
TROPICAL CYCLONES
JUL 1989 - JUN 1990
E 30
40
50
60
70
80
90
100
110
120
130 E
EQ
10
20
30
40
S 50
01S ---- 07 Jul - 11 Jul
02S ---- 12 Jul - 18 Jul
03S ---- 21 Sep - 27 Sep
04S ---- 11 Oct - 17 Oct
05S ---- 28 Oct - 02 Nov
06S Pedro 04 Nov - 13 Nov
08S Alibera 14 Dec - 05 Jan
09S Baomavo 29 Dec - 08 Jan
10S Sam 12 Jan - 20 Jan
11S Tina 24 Jan - 29 Jan
14S Cezera 01 Feb - 10 Feb
15S Dety 30 Jan - 08 Feb
17S Vincent 25 Feb - 06 Mar
18S Edisaona 26 Feb - 08 Mar
20S Walter 03 Mar - 06 Mar
22S Felana 05 Mar - 15 Mar
23S Gregoara 11 Mar - 24 Mar
24S Alex 14 Mar - 24 Mar
27S ---- 10 Apr - 14 Apr
28S Bessi 11 Apr - 17 Apr
29S Ikonjo 09 May - 23 May
MAXIMUM SUSTAINED SURFACE WIND
64 KT (33 M/S) OR GREATER
34 TO 63 KT (18 TO 32 M/S)
33 KT (17 M/S) OR LESS

Figure 4-2.

5. SUMMARY OF FORECAST VERIFICATION

5.1 ANNUAL FORECAST VERIFICATION

5.1.1 TRACK FORECAST VERIFICATION

5.1.1.1 NORTHWEST PACIFIC OCEAN — Verification of warning positions at initial, 24-, 48- and 72-hour forecast periods was made against the final best track. The (scalar) track forecast, along-track and cross-track errors (illustrated in Figure 5-1) were then calculated for each tropical cyclone and are presented in Tables 5-1A, 5-1B, 5-1C and 5-1D as appropriate. Table 5-2 includes mean along-track and cross-track forecast errors for 1978-1990. The frequency distributions of errors for warning positions and 24-hour, 48-hour, and 72-hour forecasts are in Figures 5-2A through 5-2D, respectively. A comparison of the annual mean track forecast errors for all tropical cyclones as compared to those tropical cyclones that reached typhoon intensity can be seen in Table 5-3. The mean track forecast errors for 1990 as compared to the previous twenty-one years are illustrated graphically in Figure 5-3.

5.1.1.2 NORTH INDIAN OCEAN — The positions given for warning times and those at the 24-, 48-, and 72-hour forecast times were verified for tropical cyclones in the North Indian Ocean by the same methods used for the Northwest Pacific. Table 5-4 summarizes the initial, track forecast, along-track and cross-track errors for the North Indian Ocean. Forecast errors are plotted in Figure 5-4 (72-hour forecast errors were evaluated for the first time in 1979). There were no verifying 72-hour forecasts in 1983 and 1985. Table 5-5 contains a summary of the annual mean forecast errors for each year.

5.1.1.3 SOUTH PACIFIC AND SOUTH INDIAN OCEANS — The positions given for warning times and those at the 24- and 48-hour forecast times were verified for tropical cyclones in the Southern Hemisphere by the same methods used for the western North Pacific. Table 5-6A is the summary of the initial, track forecast, along-track and cross-track errors for the Southern Hemisphere. Table 5-6B shows the number of warnings verified at each forecast period. Forecast errors are plotted in Figure 5-5. Table 5-7 contains a summary of the annual mean forecast errors since 1981, when JTWC first began warning in the Southern Hemisphere.

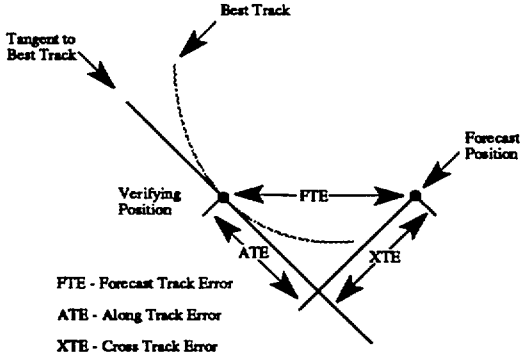

Figure 5-1. Definition of cross-track error (XTE), along-track error (ATE) and forecast track error (FTE). In this example, the XTE is positive (to the right of the best track) and the ATE is negative (behind or slower than the best track).

TABLE 5-1A **INITIAL POSITION ERRORS (NM)**
NORTHWEST PACIFIC OCEAN
1990 SIGNIFICANT TROPICAL CYCLONES

TROPICAL CYCLONE	ERROR (NM)	NUMBER OF WARNINGS
(01W) TY Koryn	35	19
(02W) TS Lewis	16	16
(03W) TY Marian	12	17
(04W) TD 04W	79	4
(05W) TS Nathan	27	14
(06W) TY Ofelia	23	31
(07W) TY Percy	17	36
(08W) TS Robyn	19	18
(09W) TY Steve	12	31
(10W) TS Tasha	20	12
(11W) TY Vernon	17	39
(12W) TY Winona	27	20
(01C) TS Aka	45	32
(13W) TY Yancy	26	31
(14W) TY Zola	24	23
(15W) TY Abe	22	36
(16W) TY Becky	13	25
(17W) TY Dot	27	25
(18W) TS Cecil	29	5
(19W) TY Ed	17	40
(20W) STY Flo	13	31
(21W) TY Gene	15	30
(22W) TY Hattie	21	31
(23W) TS Ira	33	6
(24W) TS Jeana	78	6
(25W) TY Kyle	17	28
(26W) TS Lola	8	7
(27W) STY Mike	17	43
(28W) TS Nell	31	7
(29W) STY Page	24	45
(30W) STY Owen	16	48
(31W) TY Russ	20	38
	Mean: 21	**Total:** 794

TABLE 5-1B

24-HOUR FORECAST ERRORS (NM)
NORTHWEST PACIFIC OCEAN
1990 SIGNIFICANT TROPICAL CYCLONES

TROPICAL CYCLONE			FORECAST ERROR (NM)	ALONG-TRACK ERROR MEAN*	ALONG-TRACK ERROR MEDIAN	CROSS-TRACK ERROR MEAN*	CROSS-TRACK ERROR MEDIAN	SAMPLE SIZE
(01W)	TY	Koryn	129	72	-50	95	-48	14
(02W)	TS	Lewis	146	97	57	89	-53	8
(03W)	TY	Marian	117	76	-96	75	-75	13
(04W)	TD	04W	173	139	-83	101	-80	3
(05W)	TS	Nathan	179	110	-84	101	13	10
(06W)	TY	Ofelia	125	73	-44	78	-25	28
(07W)	TY	Percy	113	72	-34	66	7	32
(08W)	TS	Robyn	94	79	-81	43	-35	14
(09W)	TY	Steve	114	68	-42	84	-67	27
(10W)	TS	Tasha	136	102	-95	78	-71	11
(11W)	TY	Vernon	73	41	-12	50	-33	34
(12W)	TY	Winona	133	113	-117	59	26	16
(01C)	TS	Aka	98	75	-64	50	-36	24
(13W)	TY	Yancy	87	57	-7	54	1	26
(14W)	TY	Zola	145	122	-113	56	28	19
(15W)	TY	Abe	102	74	-48	55	-14	32
(16W)	TY	Becky	98	74	-40	49	12	21
(17W)	TY	Dot	80	60	-36	40	-5	18
(18W)	TS	Cecil	40	9	9	39	-39	1
(19W)	TY	Ed	82	55	-28	45	33	36
(20W)	STY	Flo	78	50	-31	49	-15	27
(21W)	TY	Gene	53	32	10	39	-35	25
(22W)	TY	Hattie	79	54	-36	42	-28	26
(23W)	TS	Ira	64	46	2	31	24	3
(24W)	TS	Jeana	151	89	90	100	-100	2
(25W)	TY	Kyle	98	62	-23	60	-10	23
(26W)	TS	Lola	65	62	-71	18	16	3
(27W)	STY	Mike	120	81	-61	74	2	39
(28W)	TS	Nell	104	91	18	35	-11	3
(29W)	STY	Page	134	102	-62	67	-17	41
(30W)	STY	Owen	102	67	-42	65	26	45
(31W)	TY	Russ	102	84	-60	43	-7	34
		Mean:	103	72	-44	60	-12	
							Total:	658

* The mean was computed from absolute values.

NOTE:

1. The mean is the sum of all the values divided by the number of observations.
2. The median is the middle value of the sample.
3. The along-track error component is how far the warning position was displaced ahead or behind the best track position. The sample consists of two parts: The mean (distance) and the median (negative values were behind track or slow, and positive values were ahead of track or fast).
4. The cross-track error component is how far the warning position was displaced to the left or right of the best track position. The sample consists of two parts: The mean (distance) and the median (negative values were left of track and positive values were right of track).

TABLE 5-1C

48-HOUR FORECAST ERRORS (NM)
NORTHWEST PACIFIC OCEAN
1990 SIGNIFICANT TROPICAL CYCLONES

TROPICAL CYCLONE	FORECAST ERROR (NM)	ALONG-TRACK ERROR MEAN*	ALONG-TRACK ERROR MEDIAN	CROSS-TRACK ERROR MEAN*	CROSS-TRACK ERROR MEDIAN	SAMPLE SIZE
(01W) TY Koryn	261	164	-187	175	-168	10
(02W) TS Lewis	245	141	35	176	104	8
(03W) TY Marian	315	100	-312	287	-97	9
(04W) TD 04W	**	**	**	**	**	**
(05W) TS Nathan	255	222	-125	100	-118	3
(06W) TY Ofelia	255	183	-153	132	-112	24
(07W) TY Percy	229	137	-84	144	69	27
(08W) TS Robyn	289	268	-278	91	-81	10
(09W) TY Steve	291	146	-112	238	-261	23
(10W) TS Tasha	239	183	-236	133	-129	7
(11W) TY Vernon	152	90	-27	94	-51	30
(12W) TY Winona	246	224	-214	88	17	10
(01C) TS Aka	189	165	-148	71	32	20
(13W) TY Yancy	98	50	-4	73	32	22
(14W) TY Zola	282	210	-196	176	141	13
(15W) TY Abe	210	128	-53	128	35	28
(16W) TY Becky	159	128	-95	75	31	17
(17W) TY Dot	178	155	-135	69	-16	14
(18W) TS Cecil	**	**	**	**	**	**
(19W) TY Ed	178	122	-81	111	99	32
(20W) STY Flo	137	98	-37	86	-71	23
(21W) TY Gene	107	84	34	47	-25	21
(22W) TY Hattie	140	117	-97	66	-58	22
(23W) TS Ira	**	**	**	**	**	**
(24W) TS Jeana	**	**	**	**	**	**
(25W) TY Kyle	166	110	-16	103	-75	19
(26W) TS Lola	**	**	**	**	**	**
(27W) STY Mike	221	163	-128	110	77	28
(28W) TS Nell	**	**	**	**	**	**
(29W) STY Page	280	224	-142	126	-37	35
(30W) STY Owen	172	126	-76	97	58	40
(31W) TY Russ	219	193	-93	72	54	30
Mean:	203	148	-97	110	8	**Total:** 525

* The mean was computed from absolute values.
** Forecasts were not issued or did not verify.

NOTE:
1. Negative median along-track value denotes behind-track or slow.
2. Negative median cross-track value denotes left of track.

See Table 5-1B for explanations of the terms mean, median, and along-track and cross-track error.

TABLE 5-1D

72-HOUR FORECAST ERRORS (NM)
NORTHWEST PACIFIC OCEAN
1990 SIGNIFICANT TROPICAL CYCLONES

TROPICAL CYCLONE	FORECAST ERROR (NM)	ALONG-TRACK ERROR MEAN*	ALONG-TRACK ERROR MEDIAN	CROSS-TRACK ERROR MEAN*	CROSS-TRACK ERROR MEDIAN	SAMPLE SIZE
(01W) TY Koryn	609	493	-459	270	-276	6
(02W) TS Lewis	517	185	-94	446	474	6
(03W) TY Marian	657	650	-653	85	47	5
(04W) TD 04W	**	**	**	**	**	**
(05W) TS Nathan	330	324	324	61	61	1
(06W) TY Ofelia	382	299	-263	165	-128	19
(07W) TY Percy	340	235	-18	213	142	26
(08W) TS Robyn	489	471	-453	93	-65	6
(09W) TY Steve	556	306	-376	437	-388	19
(10W) TS Tasha	278	212	-191	178	-188	3
(11W) TY Vernon	233	149	-15	143	-68	26
(12W) TY Winona	424	410	-438	87	48	6
(01C) TS Aka	314	299	-253	72	54	16
(13W) TY Yancy	108	65	-16	75	41	18
(14W) TY Zola	512	311	-322	358	367	9
(15W) TY Abe	303	167	-85	206	90	24
(16W) TY Becky	216	156	-89	129	110	13
(17W) TY Dot	255	245	-266	57	-66	10
(18W) TS Cecil	**	**	**	**	**	**
(19W) TY Ed	304	208	-99	203	225	28
(20W) STY Flo	220	166	-36	119	-124	19
(21W) TY Gene	195	155	26	97	-106	17
(22W) TY Hattie	226	211	-190	75	-28	18
(23W) TS Ira	**	**	**	**	**	**
(24W) TS Jeana	**	**	**	**	**	**
(25W) TY Kyle	196	97	-42	154	-137	15
(26W) TS Lola	**	**	**	**	**	**
(27W) STY Mike	324	216	-177	192	197	27
(28W) TS Nell	**	**	**	**	**	**
(29W) STY Page	414	382	-191	125	-58	31
(30W) STY Owen	220	148	-78	136	107	38
(31W) TY Russ	287	231	-115	144	88	26
Mean:	310	225	-143	168	24	**Total:** 432

* The mean was computed from absolute values.
** Forecasts were not issued or did not verify.

NOTE:
1. Negative median along-track value denotes behind-track or slow.
2. Negative median cross-track value denotes left of track.

See Table 5-1B for explanations of the terms mean, median, and along-track and cross-track error.

TABLE 5-2. JTWC ANNUAL INITIAL POSITION AND FORECAST POSITION ERRORS (NM) 1978-1990 FOR THE NORTHWEST PACIFIC OCEAN

YEAR	NUMBER OF WARNINGS	INITIAL POSITION	NUMBER OF FORECASTS	24-HOUR TRACK	24-HOUR ALONG	24-HOUR CROSS	NUMBER OF FORECASTS	48-HOUR TRACK	48-HOUR ALONG	48-HOUR CROSS	NUMBER OF FORECASTS	72-HOUR TRACK	72-HOUR ALONG	72-HOUR CROSS
1978	696	21	556	126	87	71	420	274	194	151	295	411	296	218
1979	695	25	589	125	81	76	469	227	146	138	366	316	214	182
1980	590	28	491	127	86	76	369	244	165	147	267	391	266	230
1981	584	25	466	124	80	77	348	221	146	131	246	334	206	219
1972	786	19	666	113	74	70	532	238	162	142	425	342	223	211
1983	445	16	342	117	76	73	253	260	169	164	184	407	259	263
1984	611	22	492	117	84	64	378	232	163	131	286	363	238	216
1985	592	18	477	117	80	68	336	231	153	138	241	367	230	227
1986	743	21	645	126	85	70	535	261	183	151	412	394	276	227
1987	657	18	563	107	71	64	465	204	134	127	389	303	198	186
1988	465	23	373	114	85	58	262	216	170	103	183	315	244	159
1989	710	20	625	120	83	69	481	231	162	127	363	350	265	177
TOTALS:	7574		6285				4848				3657			
AVERAGE 78-89:	631	21	524	120	81	70	404	237	162	138	305	355	242	211
1990	794	21	658	103	72	60	525	203	148	110	432	310	225	168
TOTALS:	8368		6943				5373				4089			
AVERAGE 78-90:	644	21	534	118	80	69	413	234	161	135	314	354	242	206

SOURCES: 1978-85 24-, 48-, 72-hour errors are from Tsui and Miller (1986)
Initial position and 1986-1990 errors are from the ATCR

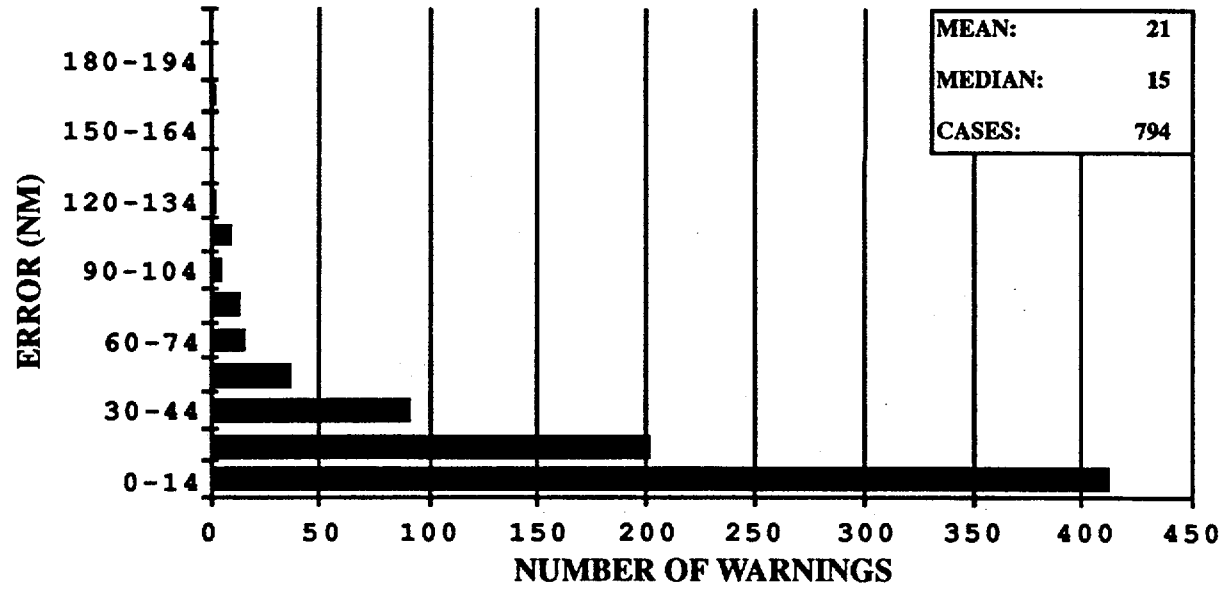

Figure 5-2A. Frequency distribution of initial position errors (15 nm increments) for the Northwest Pacific in 1990.

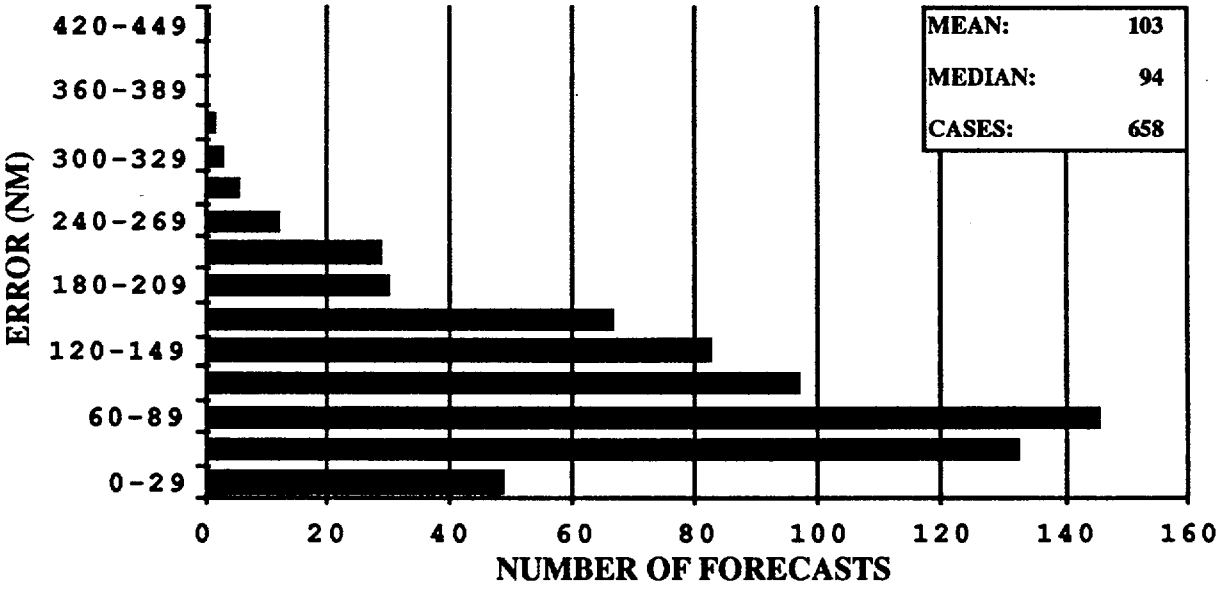

Figure 5-2B. Frequency distribution of 24-hour forecast errors (30 nm increments) for the Northwest Pacific in 1990.

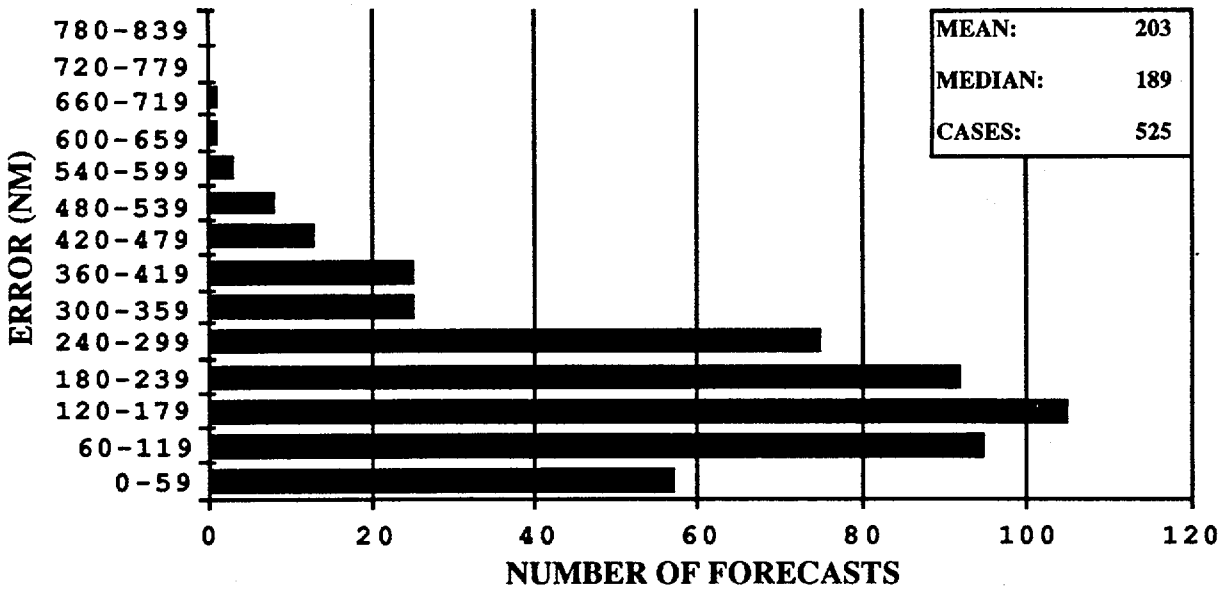

Figure 5-2C. Frequency distribution of 48-hour forecast errors (60 nm increments) for the Northwest Pacific in 1989.

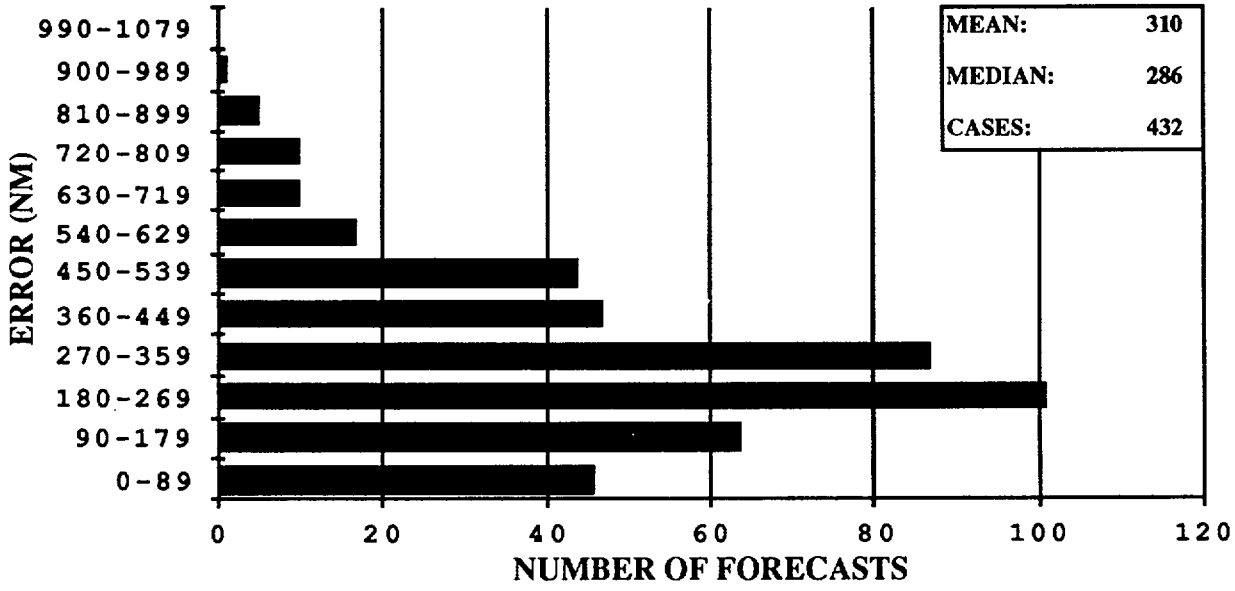

Figure 5-2D. Frequency distribution of 72-hour forecast errors (90 nm increments) for the Northwest Pacific in 1989.

TABLE 5-3 **ANNUAL MEAN FORECAST ERRORS (NM)**
NORTHWEST PACIFIC OCEAN

YEAR	24-HOUR ALL	24-HOUR / TYPHOONS*	48-HOUR ALL	48-HOUR / TYPHOONS*	72-HOUR ALL	72-HOUR / TYPHOONS*
1960		177 **		354 **		
1961		136		274		
1962		144		287		476
1963		127		246		374
1964		133		284		429
1965		151		303		418
1966		136		280		432
1967		125		276		414
1968		105		229		337
1969		111		237		349
1970	104	98	190	181	279	272
1971	111	99	212	203	317	308
1972	117	116	245	245	381	382
1973	108	102	197	193	253	245
1974	120	114	226	218	348	357
1975	138	129	288	279	450	442
1976	117	117	230	232	338	336
1977	148	140	283	266	407	390
1978	127	120	271	241	410	459
1979	124	113	226	219	316	319
1980	126	116	243	221	389	362
1981	123	117	220	215	334	342
1982	113	114	237	229	341	337
1983	117	110	259	247	405	384
1984	117	110	233	228	363	361
1985	117	112	231	228	367	355
1986	121	117	261	261	394	403
1987	107	101	204	211	303	318
1988	114	107	216	222	315	327
1989	120	107	231	214	350	325
1990	103	98	203	191	310	299

* Forecasts were verified when the tropical cyclone intensities were at least 35 kt (18 m/sec).

** Forecast positions north of 35 degrees north latitude were not verified.

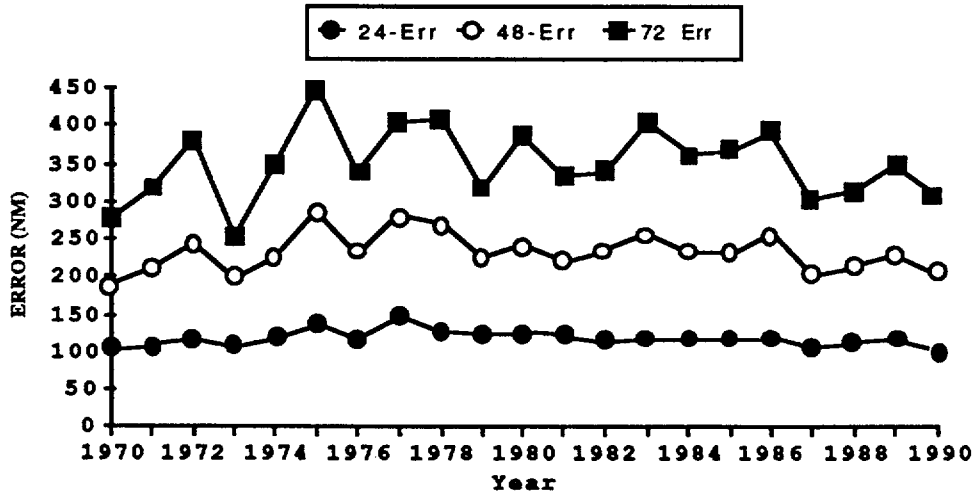

Figure 5-3. Annual mean forecast errors (nm) for all significant tropical cyclones in the Northwest Pacific Ocean.

TABLE 5-4

INITIAL POSITION AND FORECAST ERRORS (NM)
FOR THE NORTH INDIAN OCEAN
1990 SIGNIFICANT TROPICAL CYCLONES

TROPICAL CYCLONE	INITIAL POSITION ERROR (NM)	NUMBER OF WARNINGS
TC 01B	66	2
TC 02B	21	24
TC 03B	36	6
TC 04B	42	14
Mean:	31	**Total:** 46

24-HOUR FORECASTS

TROPICAL CYCLONE	FCST ERROR	ALONG-TRACK ERROR MEAN*	ALONG-TRACK ERROR MEDIAN	CROSS-TRACK ERROR MEAN	CROSS-TRACK ERROR MEDIAN	SAMPLE SIZE
TC 01B	**	**	**	**	**	**
TC 02B	81	62	-21	41	-7	22
TC 03B	156	142	144	61	-2	4
TC 04B	123	111	-18	41	-33	10
Mean:	101	85	-16	43	-17	**Total:** 36

48-HOUR FORECASTS

TROPICAL CYCLONE	FCST ERROR	ALONG-TRACK ERROR MEAN*	ALONG-TRACK ERROR MEDIAN	CROSS-TRACK ERROR MEAN	CROSS-TRACK ERROR MEDIAN	SAMPLE SIZE
TC 01B	**	**	**	**	**	**
TC 02B	116	86	-43	70	-38	17
TC 03B	**	**	**	**	**	**
TC 04B	221	192	-128	57	-30	7
Mean:	146	117	-68	67	-44	**Total:** 24

72-HOUR FORECASTS

TROPICAL CYCLONE	FCST ERROR	ALONG-TRACK ERROR MEAN*	ALONG-TRACK ERROR MEDIAN	CROSS-TRACK ERROR MEAN	CROSS-TRACK ERROR MEDIAN	SAMPLE SIZE
TC 01B	**	**	**	**	**	**
TC 02B	162	97	-97	117	-89	14
TC 03B	**	**	**	**	**	**
TC 04B	292	286	-218	44	-45	3
Mean:	185	130	-120	104	-82	**Total:** 17

* The mean was computed from absolute values.
** Forecasts were not issued or did not verify.

NOTE:
1. Negative median along-track value denotes behind-track or slow.
2. Negative median cross-track value denotes left of track.

See Table 5-1B for explanations of the terms mean, median, and along-track and cross-track error.

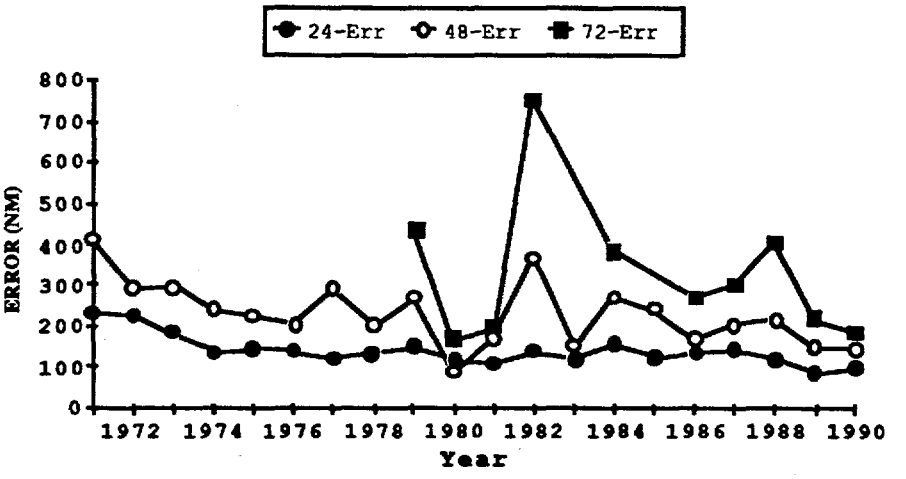

Figure 5-4. Annual mean forecast errors (nm) for all significant tropical cyclones in the North Indian Ocean.

TABLE 5-5 **ANNUAL MEAN FORECAST ERRORS (NM) FOR THE NORTH INDIAN OCEAN**

YEAR	24-HOUR FORECAST	24-HOUR RIGHT-ANGLE	48-HOUR FORECAST	48-HOUR RIGHT-ANGLE	72-HOUR FORECAST	72-HOUR RIGHT-ANGLE
1971*	232	---	410	---	---	---
1972*	224	101	292	112	---	---
1973*	182	99	299	160	---	---
1974*	137	81	238	146	---	---
1975	145	99	228	144	---	---
1976	138	108	204	159	---	---
1977	122	94	292	214	---	---
1978	133	86	202	128	---	---
1979	151	99	270	202	437	371
1980	115	73	93	87	167	126
1981**	109	65	176	103	197	73
1982**	138	66	368	175	762	404
1983**	117	46	153	67	---	---
1984**	154	71	274	127	388	159
1985**	123	51	242	109	---	---
1986***	134	53	168	80	269	180
1987***	144	100	205	140	305	188
1988***	120	63	219	176	409	303
1989***	84	50	146	86	216	111
1990***	101	43	146	67	185	104

* The Western Bay of Bengal and Arabian Sea were not included in the JTWC area of responsibility until 1975.

** The technique for calculating right-angle error was revised in 1981. therefore, a direct comparison in right-angle error statistics cannot be made between errors computed before 1981 and those computed since 1981.

*** In 1986, right-angle error was replaced by cross-track error.

See Table 5-1B for the definition of cross-track error.

TABLE 5-6A **INITIAL POSITION AND FORECAST ERRORS (NM) FOR THE SOUTH PACIFIC AND SOUTH INDIAN OCEANS 1990 SIGNIFICANT TROPICAL CYCLONES (1 JULY 1989 - 30 JUNE 1990)**

TROPICAL CYCLONE	INITIAL POSIT ERROR	24-HR FCST ERROR	24-HR ALONG-TRACK MEAN*	24-HR ALONG-TRACK MEDIAN	24-HR CROSS-TRACK MEAN*	24-HR CROSS-TRACK MEDIAN	48-HR FCST ERROR	48-HR ALONG-TRACK MEAN*	48-HR ALONG-TRACK MEDIAN	48-HR CROSS-TRACK MEAN*	48-HR CROSS-TRACK MEDIAN
TC 01S	31	56	48	30	30	30	**	**	**	**	**
TC 02S	50	182	149	-34	74	22	453	345	-345	294	294
TC 03S	25	110	94	-92	50	37	323	306	-306	105	-105
TC 04S	26	95	16	-2	94	-73	215	77	52	200	-173
TC 05S	16	177	125	-90	120	-90	303	176	-176	247	-247
TC 06S	25	118	60	16	96	-46	295	60	-20	282	-179
TC 07P	13	106	69	-47	59	35	183	168	-168	72	-72
TC 08S	19	96	61	-28	63	-26	199	123	-56	140	-48
TC 09S	29	143	97	-68	87	36	329	281	-291	152	126
TC 10S	27	93	59	-33	66	-29	168	105	-28	100	-37
TC 11S	21	152	84	18	110	57	423	362	-443	184	212
TC 12P	48	228	189	-167	109	-10	436	202	-184	342	62
TC 13P	25	110	90	-3	51	6	203	92	-34	164	12
TC 14S	21	139	104	-96	73	46	294	233	-212	130	-62
TC 15S	69	171	127	-103	99	38	360	208	-214	240	72
TC 16P	33	169	121	-9	92	-108	297	252	-184	122	-111
TC 17S	15	154	117	-84	65	-4	213	132	-90	144	-107
TC 18S	29	153	106	-52	79	27	285	202	-51	144	134
TC 19P	39	91	84	-52	25	-5	242	230	-230	76	76
TC 20S	22	83	75	-39	30	15	59	7	8	58	59
TC 21P	28	238	193	-182	90	15	511	280	-239	389	393
TC 22S	27	100	74	-12	50	4	155	123	-137	84	71
TC 23S	28	105	72	-24	66	10	150	118	-6	73	51
TC 24S	17	101	84	-63	45	4	197	181	-150	63	42
TC 25P	17	120	84	-62	67	12	233	155	-106	137	-67
TC 26P	23	218	186	-152	92	110	453	367	-367	266	266
TC 27S	26	83	54	-54	62	40	**	**	**	**	**
TC 28S	55	402	235	235	326	-326	**	**	**	**	**
TC 29S	29	126	60	-25	102	-58	234	117	-40	170	-134
MEAN	**27**	**143**	**105**	**-44**	**74**	**-8**	**263**	**178**	**-138**	**152**	**18**

* The mean was computed from absolute values.
** Not enough warnings were issued to verify the forecast.

NOTE:
1. Negative median along-track value denotes behind-track or slow.
2. Negative median cross-track value denotes left-of-track.

See Table 5-1B for explanations of the mean, median, and along-track and cross-track error.

TABLE 5-6B

NUMBER OF WARNINGS
SOUTH PACIFIC AND SOUTH INDIAN OCEAN
(1 JUL 1989 - 30 JUN 1990)

TROPICAL CYCLONE	INITIAL POSITION	24-HOUR FORECAST	48-HOUR FORECAST
TC 01S ----	4	2	0
TC 02S ----	6	4	1
TC 03S ----	5	3	1
TC 04S ----	4	3	3
TC 05S ----	8	4	1
TC 06S Pedro	9	8	6
TC 07P Felicity	6	4	1
TC 08S Alibera	31	30	28
TC 09S Baomavo	13	12	10
TC 10S Sam	11	10	9
TC 11S Tina	6	5	3
TC 12P Nancy	8	6	6
TC 13P Ofa*	17	16	16
TC 14S Cezera	16	15	13
TC 15S Dety	12	10	8
TC 16P Peni*	9	7	5
TC 17S Vincent	11	9	7
TC 18S Edisaona	14	13	11
TC 19P Greg	5	3	1
TC 20S Walter	6	4	2
TC 21P Hilda	7	6	4
TC 22S Felana	13	9	6
TC 23S Gregoara	18	17	15
TC 24S Alex	17	15	13
TC 25P Ivor	14	13	11
TC 26P Rae	4	3	1
TC 27P ----	3	2	0
TC 28S Bessi	3	1	0
TC 29S Ikonjo	18	17	16
Total:	**298**	**251**	**198**

* Naval Western Oceanography Center Pearl Harbor, Hawaii, forecast systems.

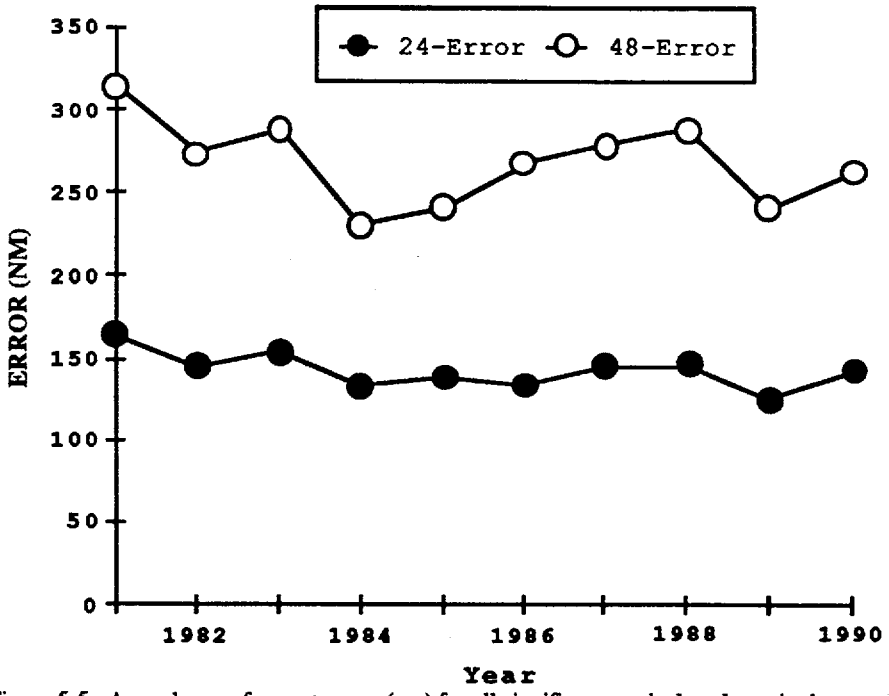

Figure 5-5. Annual mean forecast errors (nm) for all significant tropical cyclones in the South Pacific and South Indian Oceans.

Table 5-7 **ANNUAL MEAN FORECAST ERRORS (NM)**
SOUTH PACIFIC AND SOUTH INDIAN OCEANS

	24-Hour		48-Hour	
Year	Forecast	Right-Angle	Forecast	Right-Angle
1981	165	119	315	216
1982	144	91	274	174
1983	154	84	288	150
1984	133	73	231	124
1985	138	78	242	133
1986*	133	**	268	**
1987*	145	90	280	161
1988*	146	83	290	144
1989*	125	73	242	137
1990*	142	74	263	152

* In 1986, Right-angle error was replaced by cross-track error.
** Data not available
See Table 5-1B for an explanation of cross-track error.

5.1.2 INTENSITY — The mean intensity forecast errors for each Northwest Pacific tropical cyclone are presented in Table 5-8. A comparison of the annual mean intensity forecast errors in the Northwest Pacific for the past twenty years is shown in Figure 5-6. Table 5-9 summarizes intensity forecast errors for the North Indian Ocean. Table 5-10 contains a summary of intensity forecast errors for each tropical cyclone in the Southern Hemisphere.

5.2 COMPARISON OF OBJECTIVE TECHNIQUES

5.2.1 GENERAL — JTWC uses a variety of objective techniques as guidance in the warning development process. Multiple techniques are required, because each technique has particular strengths and weaknesses which vary by basin, time of year, synoptic situation and forecast period.

The accuracy of objective aid forecasts depends on both the specified position and the past motion of the tropical cyclone as determined by the working best track. For nearly a decade, standard procedure was to request objective technique forecasts based on the 6-hour old working best track position. For example, the 0600Z JTWC forecast was based on objective technique forecasts initialized with the 0000Z position. This approach avoided the use of the generally less accurate extrapolated position that would coincide with the upcoming warning. Thus, objective techniques that incorporate past storm motion (persistence) were better initialized, and lower 24-hour forecasts errors generally resulted. However, recent analysis based on the work of DeMaria (1985) indicated that an objective technique forecast based on a 6-hour old best track position can differ significantly at 72-hours (up to 500 nm (925 km)) from a forecast by the same technique initialized at the correct warning position. This is due to the tendency for tracks to diverge in a spatially and temporally variable environment, especially when significant turning (e.g., recurvature) is anticipated.

In July 1990, JTWC began initializing objective techniques using the extrapolated warning position. Although a small increase in 24-hour forecast error was noted, a significant improvement in official forecast errors at 48- and 72-hours resulted. Not only did JTWC's absolute forecast error decrease, but also JTWC's forecast standing relative to the objective techniques improved significantly for the second half of 1990 in the Northwest Pacific compared to the first half. The improvement in forecast accuracy, particularly at the 72-hour point, outweighed the degradation at 24-hours. Thus, JTWC procedures have been modified to use the extrapolated warning position when computing objective technique forecasts. Current best track procedures emphasize the importance of conservatively integrating new fixes with 12-hr persistence to minimize degradation of 24-hour forecast accuracy due to "chasing" the fixes.

Two existing objective techniques have been retired from service. The CYCLone OPerational Steering (CYCLOPS) model, which is based on an antiquated geostrophic steering concept, was documented by Tsui and Miller (1986) as JTWC's least accurate aid. CYCLOPS performance has also shown further deterioration with the introduction of the NOGAPS 3.2 in August 1989. Since more accurate windfield-based steering models are presently available, an attempt to update and fix CYCLOPS was not considered worthwhile. The CYCLOPS Objective Steering Model Output Statistics (COSMOS) model, which was intended to use CYCLOPS forecasts generated from the Primitive Equation Global Model, has also been retired. This decision was motivated by serious degradations in the performance of COSMOS after the switch to NOGAPS 3.2, and by the ineffectiveness that would result from updating CYCLOPS and recomputing COSMOS regression coefficients.

5.2.2 DESCRIPTION OF OBJECTIVE TECHNIQUES — Unless stated otherwise, all the objective techniques discussed below run in all basins covered by JTWC's AOR and provide forecast positions at 24-, 48-, and 72-hours unless the technique aborts prematurely during

TABLE 5-8 **ANNUAL MEAN INTENSITY FORECAST ERRORS (KT) NORTHWEST PACIFIC OCEAN**

TROPICAL CYCLONE	MAXIMUM INTENSITY	24-HOUR FORECAST ERROR KT (M/SEC)	48-HOUR FORECAST ERROR KT (M/SEC)	72-HOUR FORECAST ERROR KT (M/SEC)
(01W) TY Koryn	75(39)	8(4)	14(7)	38(20)
(02W) TS Lewis	35(18)	10(5)	17(9)	14(7)
(03W) TY Marian	90(46)	14(7)	15(8)	25(13)
(04W) TD 04W	30(15)	10(5)	*	*
(05W) TS Nathan	55(28)	8(4)	7(4)	15(8)
(06W) TY Ofelia	90(46)	10(5)	15(8)	16(8)
(07W) TY Percy	115(59)	14(7)	17(9)	19(10)
(08W) TS Robyn	45(23)	3(2)	8(4)	22(11)
(09W) TY Steve	115(59)	9(5)	18(9)	21(11)
(10W) TS Tasha	55(28)	6(3)	14(7)	17(9)
(11W) TY Vernon	95(49)	8(4)	10(5)	8(4)
(12W) TY Winona	65(33)	4(2)	4(2)	16(8)
(01C) TS Aka	45(23)	9(5)	15(8)	20(10)
(13W) TY Yancy	90(46)	9(5)	10(5)	9(5)
(14W) TY Zola	100(51)	8(4)	13(7)	14(7)
(15W) TY Abe	90(46)	8(4)	20(10)	27(14)
(16W) TY Becky	70(36)	8(4)	11(6)	15(8)
(17W) TY Dot	80(41)	10(5)	14(7)	8(4)
(18W) TS Cecil	45(23)	20(10)	*	*
(19W) TY Ed	90(46)	6(3)	11(6)	16(8)
(20W) STY Flo	145(75)	13(7)	23(12)	28(14)
(21W) TY Gene	80(41)	8(4)	11(6)	5(3)
(22W) TY Hattie	90(46)	9(5)	21(11)	28(14)
(23W) TS Ira	35(18)	10(5)	*	*
(24W) TS Jeana	35(18)	12(6)	*	*
(25W) TY Kyle	90(46)	4(2)	9(5)	8(4)
(26W) TS Lola	40(21)	12(6)	*	*
(27W) STY Mike	150(77)	17(9)	23(12)	27(14)
(28W) TS Nell	50(26)	12(6)	*	*
(29W) STY Page	140(72)	10(5)	18(9)	24(12)
(30W) STY Owen	140(72)	18(9)	32(16)	44(23)
(31W) TY Russ	125(64)	9(5)	11(6)	10(5)
	Average:	**10(5)**	**16(8)**	**20(10)**

* Forecast was not issued or did not verify.

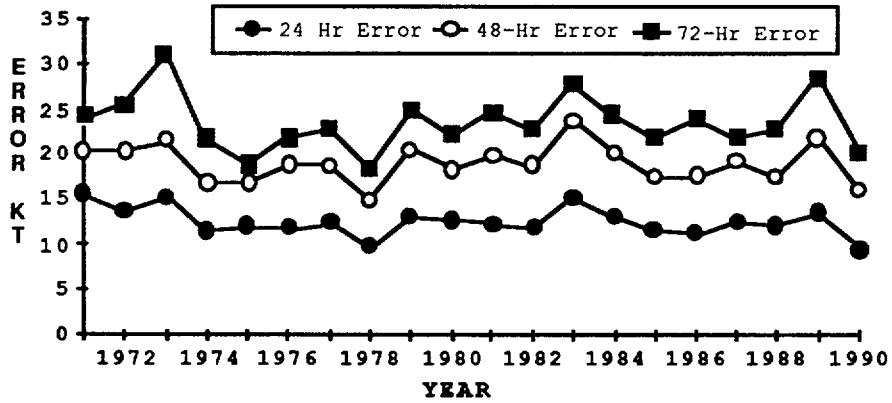

Figure 5-6. Annual mean intensity forecast errors (kt) for all significant tropical cyclones in the Northwest Pacific Ocean. 1971-1989 errors from Mundell (1990).

TABLE 5-9

ANNUAL MEAN INTENSITY
FORECAST ERRORS (KT) NORTHERN INDIAN OCEAN

TROPICAL CYCLONE	MAXIMUM INTENSITY	24-HOUR FORECAST ERROR KT (M/SEC)	48-HOUR FORECAST ERROR KT (M/SEC)	72-HOUR FORECAST ERROR KT (M/SEC)
01B ----	25(13)	*	*	*
02B ----	125(64)	12	28	50
03B ----	30(15)	0	*	*
04B ----	45(23)	8	16	42
	Average:	**9(5)**	**24(13)**	**48(25)**

*Forecast was not issued or did not verify.

TABLE 5-10

ANNUAL MEAN INTENSITY
FORECAST ERRORS (KT) SOUTHERN HEMISPHERE

TROPICAL CYCLONE	MAXIMUM INTENSITY	24-HOUR FORECAST ERROR KT (M/SEC)	48-HOUR FORECAST ERROR KT (M/SEC)
01S ----	25(13)	5	*
02S ----	35(18)	1	5
03S ----	30(15)	5	15
04S ----	30(15)	7	12
05S ----	35(18)	8	15
06S Pedro	65(33)	8	12
07P Felicity	60(31)	6	0
08S Alibera	135(69)	12	16
09S Bavomavo	85(44)	8	16
10S Sam	50(26)	10	19
11S Tina	45(23)	5	8
12P Nancy	65(33)	9	6
13P Ofa	115(59)	16	20
14S Cezera	80(41)	10	16
15S Dety	95(49)	16	21
16P Peni	60(31)	9	20
17S Vincent	70(36)	4	9
18S Edisaona	100(51)	15	24
19P Greg	30(15)	8	35
20S Walter	30(15)	4	8
21P Hilda	60(31)	11	8
22S Felana	45(23)	6	18
23S Gregoara	110(57)	15	18
24S Alex	130(67)	11	21
25P Ivor	75(39)	7	14
26P Rae	40(21)	3	10
27S ----	45(23)	5	*
28S Bessi	40(21)	0	*
29S Ikonjo	55(28)	10	16
	Average:	**10(5)**	**16(8)**

*Forecast was not issued or did not verify.

computations. An initiative is presently underway to convert most of the objective techniques that currently run on mainframe computers at FNOC to desktop computer versions that run on ATCF workstations. These will eventually replace the FNOC-generated techniques. As of this writing, three of these new aids have been received and are under evaluation.

5.2.2.1 EXTRAPOLATION (XTRP) — Past speed and direction are computed using the rhumb line distance between the current and 12-hour old positions of the tropical cyclone. Extrapolation from the current warning position is used to compute forecast positions.

5.2.2.2 CLIMATOLOGY (CLIM, PCLM) — JTWC has access to three climatology objective techniques at present. Two run on the ATCF. They are: 1) CLIM which continues to run operationally at FNOC, and 2) PCLM which is the PC-based version. The historical data base for both has been recently updated to 1945-1981 for the Northwest Pacific, and 1900 to 1989 for the rest of JTWC's AOR. Both techniques employ time and location windows relative to the current position of the storm to determine which historical storms will be used to compute the forecast. PCLM differs from CLIM in that it looks symmetrically in time about the current best track position and corrects CLIM's tendency to place more weight on slow-moving historical storms. The third climatology-based technique exists on JTWC's Macintosh®™ II computers. It employs data bases from 1945 to 1989 and from 1970 to 1989. The latter is referred to as the satellite-era data base. Objective intensity forecasts are available from these data bases. Scatter diagrams of expected tropical cyclone motion at bifurcation points are also available from these data bases.

5.2.2.3 HALF PERSISTENCE AND CLIMATOLOGY (HPAC, PCHP) — Forecast positions are generated by equally weighting the forecasts given by XTRP and CLIM in the case of HPAC, and by XTRP and PCLM in the case of PCHP.

5.2.2.4 ANALOGS — JTWC's analog and climatology techniques use the same historical data base, except that the analog approach imposes more restrictions on which storms will be used to compute the forecast positions. Analogs in all basins must satisfy time, location, speed, and direction windows, although the window definitions are distinctly different in the Northwest Pacific. In this basin, acceptable analogs are also ranked in terms of a similarity index that includes the above parameters and: storm size and size change, intensity and intensity change, and heights and locations of the 700-mb subtropical ridge and upstream midlatitude trough. In other basins, all acceptable analogs receive equal weighting and a persistence bias is explicitly added to the forecast. Inside the Northwest Pacific, analog weighting is varied using the similarity index, and a persistence bias is implicitly incorporated by rotating the analog tracks so that they initially match the 12-hr old motion of the current storm. In the Northwest Pacific, a forecast based on all acceptable analogs called TOTL, as well as a forecast based only on historical recurvers called RECR are available. Outside this basin, only the TOTL technique is available.

5.2.2.5 CLIMATOLOGY AND PERSISTENCE (CLIP) — This is a statistical regression technique that is based on climatology, current position and 12-hour and 24-hour past movement. This technique is used as a crude baseline against which to measure the forecast skill of other more sophisticated techniques. CLIP in the Northwest Pacific uses third-order regression equations and is based on the work of Xu and Neuman (1985). CLIP has been available outside this basin only since mid-1990, and it uses second-order equations developed by Neuman and Randrianarison (1976) with regression coefficients recently recomputed by FNOC based on the updated 1900-1989 data base.

5.2.2.6 COLORADO STATE UNIVERSITY MODEL (CSUM) — CSUM is a statistical-

dynamical technique based on the work of Matsumoto (1984). Predictor parameters include the current and 24-hr old position of the storm, heights from the current and 24-hr old NOGAPS 500-mb analyses, and heights from the 24-hr and 48-hr NOGAPS 500 mb prognoses. Height values from 200-mb fields are substituted for storms that have an intensity exceeding 90 knots and are located north of the subtropical ridge. Three distinct sets of regression equations are used depending on whether the storm's direction of motion falls into "below," "on," or "above" the subtropical ridge categories. During the development of the regression equation coefficients for CSUM, the so-called "perfect prog" approach was used, in which verifying analyses were substituted for the numerical prognoses that are used when CSUM is run operationally. Thus, CSUM was not "tuned" to any particular version of NOGAPS, and in fact, the performance of CSUM should presumably improve as new versions of NOGAPS improve. CSUM runs only in the Northwest Pacific, South China Sea, and North Indian Ocean basins.

5.2.2.7 NOGAPS VORTEX TRACKING ROUTINE (NGPS) — This objective technique follows the movement of the point of minimum height on the 1000 mb pressure surface analyzed and predicted by NOGAPS. A search in the expected vicinity of the storm is conducted every six hours through 72 hours, even if the tracking routine temporarily fails to discern a minimum height point. Explicit insertion of a tropical cyclone bogus via data provided over TYMNET by JTWC began in mid-1990, and should improve the ability of the NOGAPS technique to track the vortex.

5.2.2.8 ONE-WAY INFLUENCE TROPICAL CYCLONE MODEL (OTCM) — This technique is a coarse resolution (205 km grid), three layer, primitive equation model with a horizontal domain of 6400 x 4700 km. OTCM is initialized using 6-hour or 12-hour prognostic fields from the latest NOGAPS run, and the initial fields are smoothed and adjusted in the vicinity of the storm to induce a persistence bias into OTCM's forecast. A symmetric bogus vortex is then inserted, and the boundaries updated every 12 hours by NOGAPS fields as the integration proceeds. The bogus vortex is maintained against frictional dissipation by an analytical heating function. The forecast positions are based on the movement of the vortex in the lowest layer of the model (effectively 850-mb).

5.2.2.9 FNOC BETA AND ADVECTION MODEL (FBAM) — This model is an adaptation of the Beta and Advection model used by NMC. The forecast motion results from a calculation of environmental steering and an empirical correction for the observed vector difference between that steering and the 12-hour old storm motion. The steering is computed from the NOGAPS Deep Layer Mean (DLM) wind fields which are a weighted average of the wind fields computed for the 1000-mb to 100-mb levels. The difference between past storm motion and the DLM steering is treated as if the storm were a Rossby wave with an "effective radius" propagating in response to the horizontal gradient of the coriolis parameter, Beta. The forecast proceeds in one-hour steps, recomputing the effective radius as Beta changes with storm latitude, and blending in a persistence bias for the first 12 hours.

5.2.2.10 COMBINED CONFIDENCE WEIGHTED FORECASTS (CCWF) — An optimal blend of objective techniques produced by the ATCF. The ATCF blends the selected techniques by using the inverse of the covariance matrices computed from historical and real-time cross-track and along-track errors as the weighting function.

5.2.2.11 DVORAK — An estimation of a tropical cyclone's current and 24-hour forecast intensity is made from the interpretation of satellite imagery (Dvorak, 1984) . These intensity estimates are used with other intensity related data and trends to forecast short-term tropical cyclone intensity.

5.2.2.12 MARTIN/HOLLAND — The tech-

nique adapts an earlier work (Holland, 1980) and specifically addresses the need for realistic 30-kt, 50-kt and 100-kt wind radii around tropical cyclones. It solves equations for basic gradient wind relations within the tropical cyclone area, using input parameters obtained from enhanced infrared satellite imagery. The diagnosis also includes an asymmetric area of winds caused by tropical cyclone movement. Satellite-derived size and intensity parameters are also used to diagnose internal steering components of tropical cyclone motion known collectively as "beta-drift".

5.2.2.13 Navy Operational Regional Prediction System (NRPS) — The Advanced Tropical Cyclone Model (ATCM) produced from NORAPS fields.

5.3 TESTING AND RESULTS

A comparison of selected techniques is included in Tables 5-11A and 5-11B for all Northwest Pacific tropical cyclones; Table 5-12 for all North Indian Ocean tropical cyclones and Table 5-13 for the Southern Hemisphere. In these tables, " x-axis " refers to techniques listed vertically. For example (Table 5-11A) in the 748 cases available for a (homogeneous) comparison, the average forecast error at 24 hours was 161 nm (298 km) for CLIM and 129 nm (239 km) for HPAC. The difference of 32 nm (59 km) is shown in the lower right. (Differences are not always exact, due to computational round-off which occurs for each of the cases available for comparison).

TABLE 5-11A 1990 ERROR STATISTICS FOR SELECTED OBJECTIVE TECHNIQUES IN THE NORTHWEST PACIFIC (1 JAN 1990 - 31 DEC 1990)

24-HOUR MEAN FORECAST ERROR (NM)

	JTWC	OTCM	FBAM	CLIP	HPAC	CLIM	XTRP	CSUM	TOTL	RECR
JTWC	658 103 104 0									
OTCM	616 102 109 7	744 117 117 0								
FBAM	583 100 121 21	687 118 125 7	712 129 129 0							
CLIP	622 102 115 13	734 117 123 6	710 129 124 -5	759 125 125 0						
HPAC	619 102 123 21	729 117 128 11	706 129 130 1	754 125 131 6	755 131 131 0					
CLIM	616 102 158 56	728 114 159 45	700 126 158 32	747 122 161 39	748 129 161 32	756 162 162 0				
XTRP	611 102 131 29	720 114 134 20	697 126 138 12	744 122 138 16	741 129 138 9	741 161 138 -23	745 138 138 0			
CSUM	599 102 115 13	703 117 123 6	678 130 125 -5	724 123 125 2	724 132 125 -7	718 162 122 -40	711 138 122 -16	728 125 125 0		
TOTL	594 102 125 21	687 114 130 16	656 126 127 1	697 120 131 11	694 127 131 4	694 156 129 -27	686 134 128 -6	675 120 131 11	707 132 132 0	
RECR	561 103 124 21	648 116 134 18	625 127 133 6	658 120 135 15	658 128 135 7	661 156 133 -23	652 134 132 -2	659 120 134 14	668 131 135 4	668 135 135 0

Number of Cases	X-Axis Technique Error
Y-Axis Technique Error	Error Difference (Y-X)

CLIM - Climatology
CLIP - Climatology/Persistence
CSUM - Colorado State University Model
FBAM - FNOC Beta and Advection Model
HPAC - Half Persistence and Climatology
JTWC - Offical JTWC Forecast
OTCM - One-Way Tropical Cyclone Model
RECR - Recurve Analog
TOTL - Total Analog
XTRP - Extrapolation

TABLE 5-11B

1990 ERROR STATISTICS FOR SELECTED OBJECTIVE TECHNIQUES IN THE NORTHWEST PACIFIC (1 JAN 1990 - 31 DEC 1990)

48-HOUR MEAN FORECAST ERROR (NM)

	JTWC	OTCM	FBAM	CLIP	HPAC	CLIM	XTRP	CSUM	TOTL	RECR
JTWC	525 203 203 0									
OTCM	483 199 203 4	642 219 219 0								
FBAM	468 197 247 50	591 221 248 27	628 257 257 0							
CLIP	503 199 229 30	632 219 240 21	626 256 242 -14	670 243 243 0						
HPAC	500 199 233 34	626 219 245 26	622 257 247 -10	663 242 250 8	664 250 250 0					
CLIM	496 200 286 86	626 216 293 77	617 253 294 41	657 239 297 58	658 247 297 50	666 299 299 0				
XTRP	493 200 276 76	620 216 289 73	615 252 293 41	657 240 295 55	652 246 295 49	652 297 295 -2	658 295 295 0			
CSUM	484 199 229 30	603 220 239 19	595 259 243 -16	636 235 243 8	634 250 243 -7	629 297 240 -57	625 295 240 -55	640 243 243 0		
TOTL	490 200 253 53	601 214 264 50	589 250 261 11	625 241 266 25	622 246 266 20	622 292 265 -27	614 289 263 -26	604 238 268 30	635 267 267 0	
RECR	464 201 246 45	566 218 259 41	557 253 259 6	589 234 260 26	589 247 260 13	592 292 259 -33	583 292 258 -34	591 239 259 20	599 269 262 -7	599 262 262 0

Number of Cases	X-Axis Technique Error
Y-Axis Technique Error	Error Difference (Y-X)

72-HOUR MEAN FORECAST ERROR (NM)

	JTWC	OTCM	FBAM	CLIP	HPAC	CLIM	XTRP	CSUM	TOTL	RECR
JTWC	432 310 310 0									
OTCM	388 303 317 14	524 340 340 0								
FBAM	384 300 364 64	481 344 383 39	528 386 386 0							
CLIP	414 301 341 40	515 341 367 26	526 385 370 -15	565 370 370 0						
HPAC	410 300 327 27	510 342 360 18	521 385 362 -23	559 365 364 -1	560 364 364 0					
CLIM	407 302 385 83	511 337 402 65	517 382 406 24	554 362 408 46	555 362 408 46	562 409 409 0				
XTRP	406 302 435 133	507 338 471 133	519 382 477 95	556 367 479 112	552 361 479 118	552 408 479 71	557 479 479 0			
CSUM	399 302 339 37	492 345 356 11	495 391 360 -31	531 348 358 10	531 365 358 -7	527 405 355 -50	524 482 356 -126	535 359 359 0		
TOTL	412 302 386 84	503 336 419 83	503 386 412 26	537 369 416 47	533 362 418 56	534 405 415 10	530 473 414 -59	516 356 424 68	547 416 416 0	
RECR	391 302 376 74	474 345 404 59	473 393 408 15	505 351 405 54	505 365 405 40	509 403 402 -1	502 481 401 -80	507 359 403 44	515 421 406 -15	515 406 406 0

CLIM - Climatology
CLIP - Climatology/Persistence
CSUM - Colorado State University Model
FBAM - FNOC Beta and Advection Model
HPAC - Half Persistence and Climatology
JTWC - Offical JTWC Forecast
OTCM - One-Way Tropical Cyclone Model
RECR - Recurve Analog
TOTL - Total Analog
XTRP - Extrapolation

TABLE 5-12 **1990 ERROR STATISTICS FOR SELECTED OBJECTIVE TECHNIQUES IN THE NORTH INDIAN OCEAN**

24-HOUR MEAN FORECAST ERROR (NM)

	JTWC	OTCM	FBAM	HPAC	CLIM	XTRP	CSUM	TOTL
JTWC	36 101 101 0							
OTCM	28 100 99 -1	30 99 99 0						
FBAM	25 98 150 52	27 101 151 50	27 151 151 0					
HPAC	28 100 88 -12	30 99 91 -8	27 151 93 -58	30 91 91 0				
CLIM	28 100 86 -14	30 99 88 -11	27 151 91 -60	30 91 88 -3	30 88 88 0			
XTRP	27 101 112 11	29 100 115 15	26 153 118 -35	29 93 115 22	29 91 115 24	29 115 115 0		
CSUM	25 92 222 130	27 101 229 128	25 152 226 74	27 87 229 142	27 85 229 144	26 108 229 121	27 229 229 0	
TOTL	28 100 91 -9	29 99 91 -8	26 151 92 -59	29 88 91 3	29 84 91 7	28 114 93 -21	26 224 86 -138	29 91 91 0

Number of Cases	X-Axis Technique Error
Y-Axis Technique Error	Error Difference (Y-X)

48-HOUR MEAN FORECAST ERROR (NM)

	JTWC	OTCM	FBAM	HPAC	CLIM	XTRP	CSUM	TOTL
JTWC	24 146 146 0							
OTCM	18 135 166 31	22 157 157 0						
FBAM	19 152 261 109	19 153 243 90	23 251 251 0					
HPAC	21 146 150 4	22 157 149 -8	23 251 171 -80	26 162 162 0				
CLIM	21 146 174 28	22 157 159 2	23 251 185 -66	26 162 171 9	26 171 171 0			
XTRP	20 144 183 39	21 158 198 40	22 251 216 -35	25 163 210 47	25 175 210 35	25 210 210 0		
CSUM	21 146 582 436	19 163 602 439	21 261 588 327	23 156 594 438	23 183 594 411	22 187 589 402	23 594 594 0	
TOTL	21 146 146 0	21 158 146 -12	22 250 147 -103	25 155 149 -6	25 161 149 -12	24 208 150 -58	22 583 142 -441	25 149 149 0

72-HOUR MEAN FORECAST ERROR (NM)

	JTWC	OTCM	FBAM	HPAC	CLIM	XTRP	CSUM	TOTL
JTWC	17 185 185 0							
OTCM	12 174 192 18	16 183 183 0						
FBAM	13 208 410 202	13 163 323 160	17 389 389 0					
HPAC	15 198 209 11	16 183 204 21	17 389 262 -127	20 248 248 0				
CLIM	15 198 257 59	16 183 217 34	17 389 277 -112	20 248 262 14	20 262 262 0			
XTRP	14 195 286 91	15 187 308 121	16 383 361 -22	19 251 343 92	19 270 343 73	19 343 343 0		
CSUM	15 198 1033 835	13 185 1126 941	15 407 1043 636	17 226 1037 811	17 281 1037 756	16 293 1030 737	17 1037 1037 0	
TOTL	15 198 215 17	15 188 191 3	16 390 222 -168	19 241 220 -21	19 248 220 -28	18 347 221 -126	16 1023 220 -803	19 220 220 0

CLIM - Climatology
FBAM - FNOC Beta and Advection Model
HPAC - Half Persistence and Climatology Blend
JTWC - Official JTWC Forecast
OTCM - One-Way Tropical Cyclone Model
TOTL - Total Analog

TABLE 5-13 **1990 ERROR STATISTICS FOR SELECTED OBJECTIVE TECHNIQUES IN THE SOUTHERN HEMISPHERE (1 JULY 1989 - 30 JUNE 1990)**

24-HOUR MEAN FORECAST ERROR (NM)

	JTWC	OTCM	FBAM	HPAC	CLIM	TOTL
JTWC	251 143 143 0					
OTCM	105 148 159 11	348 144 144 0				
FBAM	84 157 147 -10	270 142 129 -13	279 131 131 0			
HPAC	94 151 152 1	308 146 141 -5	278 131 142 11	318 141 141 0		
CLIM	93 152 200 48	325 145 187 42	278 131 188 57	317 141 187 46	335 186 186 0	
TOTL	56 182 204 22	184 139 161 22	178 128 168 40	188 154 166 12	188 200 166 -34	188 166 166 0

Number of Cases	X-Axis Technique Error
Y-Axis Technique Error	Error Difference (Y-X)

48-HOUR MEAN FORECAST ERROR (NM)

	JTWC	OTCM	FBAM	HPAC	CLIM	TOTL
JTWC	198 263 263 0					
OTCM	81 277 271 -6	281 256 256 0				
FBAM	69 294 239 -55	219 251 230 -21	238 233 233 0			
HPAC	73 285 257 -28	243 261 245 -16	233 228 243 15	264 243 243 0		
CLIM	73 285 309 24	260 261 301 40	233 228 294 66	264 243 297 54	282 299 299 0	
TOTL	44 329 366 37	146 246 309 63	146 229 308 79	155 267 304 37	155 312 304 -8	155 304 304 0

72-HOUR MEAN FORECAST ERROR (NM)

	OTCM	FBAM	HPAC	CLIMO	TOTL
OTCM	223 348 348 0				
FBAM	174 327 319 -8	197 332 332 0			
HPAC	192 347 314 -33	193 324 314 -10	218 319 319 0		
CLIM	208 350 378 28	193 324 370 46	218 319 382 63	236 387 387 0	
TOTL	118 306 388 82	118 320 388 68	124 321 385 64	124 361 385 24	124 385 385 0

CLIM - Climatology
FBAM - FNOC Beta and Advection Model
HPAC - Half Persistence and Climatology Blend
JTWC - Offiacial JTWC Forecast
OTCM - One-Way Tropical Cyclone Model
TOTL - Total Analog

Intentionally left blank.

6. TROPICAL CYCLONE SUPPORT SUMMARY

TROPICAL CYCLONES AFFECTING THE PHILIPPINE ISLANDS

Capt. Daniel Shoemaker, USAF
Detachment 1, 1 Weather Wing

Two early 1970's studies on the climatology of tropical cyclones striking the Philippine Islands have been updated. The previous studies involved manual interpretation of a small data base; now, with computer processing, a much larger data base is used. The computer study provides quantitative output, including standard deviations. This study looks at tropical cyclone intensity change, track change, occurrence climatology, and various other parameters. It allows the typhoon forecaster to more accurately anticipate changes in intensity and motion of tropical cyclones interacting with the Philippine Islands.

DVORAK FORECAST INTENSITY STUDY

MSgt Charles Bonini, USAF
Detachment 1, 1 Weather Wing

A study to compare forecast intensity (FI) to the actual JTWC best track verification showed that some minor modifications to the Dvorak model would make FI more accurate. These modifications were incorporated into a flow chart the analysts now use to determine FI. Improvements include the ability to lower FI if a peaking day is determined, the ability to more accurately reflect FI when the forecast track brings the system over land, and the ability to keep the FI stable when short-term fluctuations to the Dvorak T-number occur.

DVORAK INTENSITY ANALYSIS OVER LAND STUDY

MSgt Charles Bonini, USAF
Detachment 1, 1 Weather Wing

A recent paper, Improved Utilization of Satellite Imagery in Tropical Cyclone Analysis (Takemura, 1989), addressed tropical cyclone intensity estimation over land. In its current state, the Dvorak analysis scheme does not allow analysis overland. Thus, when a tropical cyclone moves back over water there is a break in the intensity trend. A local study was initiated using satellite images of tropical cyclones over land. Analysts were required to derive a Dvorak T-number for the cloud systems while they were over land. Compilation of results showed that all intensity analyses from Detachment 1 satellite analysts were within an acceptable error margin of 0.5 T-number establishing that analysts could derive with consistent T-numbers for tropical cyclones over land. The next part of this study will associate the T-number over land with actual tropical cyclone intensities. This will allow satellite analysts to provide over-land current intensity numbers to JTWC.

SOUTHERN HEMISPHERE TROPICAL CYCLONE CLIMATOLOGY

Capt. Daniel Shoemaker, USAF
Detachment 1, 1 Weather Wing

Detachment 1 expanded its interactive tropical cyclone climatology data base (currently complete for the western North Pacific) to include the Southern Hemisphere. Data includes position, intensity, speed, intensity change and speed change. The Bay of Bengal and the Arabian Sea will be included in the next data base expansion.

NOGAPS STEERING MODEL (NSM)

LCDR Les Carr, USN
Joint Typhoon Warning Center

Since May 1990, JTWC has been developing and testing a locally run steering model known as the NOGAPS Steering Model (NSM). It is designed to replace the CYCLone Operational Prediction System (CYCLOPS) and

to overcome a number of weaknesses inherent in that model. These include i) use of NOGAPS 500- and 700-mb wind fields to compute steering directly, whereas CYCLOPS uses height fields to compute steering geostrophically, and ii) steering from unsmoothed NOGAPS data over an annular region around the tropical cyclone, whereas CYCLOPS uses the heavily smoothed SR height fields that tend to miss weak synoptic features that nevertheless affect storm motion. Although it has been tested for only portions of the 1990 Northwest Pacific tropical cyclone season, NSM has shown skill in forecasting movement of small cyclones and in detecting sudden turns (NSM uses no persistence). The model performs poorly on large tropical cyclones, presumably due to misplaced vortex effects and annulus size. NSM will be modified in 1991 to include an additional, larger steering flow annulus to better determine the environmental steering around large systems.

TROPICAL CYCLONE MOTION FIELD EXPERIMENT

Russell L. Elsberry
Technical Director for TCM-90
Naval Postgraduate School
Monterey, California

The Tropical Cyclone Motion (TCM-90) field experiment was conducted in the Northwest Pacific during August and September 1990. TCM-90 was the culmination of a five-year Accelerated Research Initiative of the Office of Naval Research Marine Meteorology Program (Dr. Robert Abbey, Jr., Program Director). The TCM-90 field experiment was coincident in time with three other separate field experiments, which made this effort one of the largest experiments on typhoons ever attempted. The World Meteorological Organization Typhoon Committee sponsored a real-time prediction experiment called SPECTRUM (SPecial Experiment Concerning Typhoon Recurvature and Unusual Motion). A USSR oceanographic expedition called TYPHOON-90 provided meteorological observations over the Philippine Sea. Finally, the Taiwan Area Typhoon Experiment (TATEX) studied the interaction of typhoons with the Taiwan orography.

TCM-90 was organized around Intensive Observing Periods (IOP) of 36-48 hours duration when 6-hour rawinsondes were launched and other special observations were collected. Seven IOP'S involving six typhoons were conducted, and will provide data sets to test several hypotheses that were developed during the research phase leading to TCM-90. Complex interactions with the subtropical ridge occurred during all seven IOP's. Documentation of the physical mechanisms by which the typhoon can affect the adjacent ridge, and thus affect the track, is expected to be one of the major results of the research initiative.

Perhaps the most impressive early result of TCM-90 was the detailed documentation of the complexity of the environmental flow fields observed in the western North Pacific. Interactions with the monsoon trough, midlatitude troughs and Tropical Upper Tropospheric Trough (TUTT) cells were observed in various IOP's. In some cases, the troughs changed the typhoon track. In other cases, the typhoon continued to track steadily along. Documenting these effects, and when they occur, should provide a solid scientific result that will also contribute to improvements in forecasting.

Five other tropical cyclones occurred during August and September that were not the subject of an IOP due to timing or location. These cases will provide additional examples for study. Comparisons of track predictions during these storms will indicate the benefits of the additional observations collected during the TCM-90 IOP's. Other data sensitivity studies (withholding certain sites or data types from the complete set) should indicate the crucial locations for observations to improve track predictions.

TROPICAL CYCLONE FORECASTER'S REFERENCE GUIDE

Miller, R.J., J-H. Chu, and C.R. Sampson
NOARL West
Monterey, California

Development of a Tropical Cyclone Forecaster's Reference Guide continues. The reference guide will contain a section covering tropical meteorology in general, as well as the formation, motion, structure, and dissipation of tropical cyclones. Satellite case studies and descriptions of forecast aids will also be included. Future plans are to put the guide on a computer as an information management system.

AUTOMATED TROPICAL CYCLONE FORECASTING SYSTEM (ATCF) UPGRADE

Roesser, D. M., R. J. Miller, and C. R. Sampson
NOARL West
Monterey, California

The ATCF has been operational at JTWC since August 1988. The system runs on an IBM-AT compatible machine using the MS-DOS operation system. This current configuration limits the capabilities of the ATCF. For this reason, NOARL is currently adapting the ATCF software to a UNIX environment. UNIX advantages include more power, multi-tasking, and portability. The X-Windows/Motif system will serve as the user interface, allowing the user to run all ATCF functions in a windows environment.

TROPICAL CYCLONE EXPERT SYSTEM

Sampson, C. R., J-H. Chu and, R.W. Fett
NOARL West
Monterey, California

NOARL is developing an expert system for tropical cyclone forecasting. Using forecasting thumb rules and research results such as objective technique error statistics, the expert system will objectively weigh the information based upon the current forecast situation and assist the forecaster in making decisions.

PC-BASED TROPICAL CYCLONE TRACK CLIMATOLOGY FORECAST AID

Sampson, C.R., R.E. Kreitner, and R. J. Miller
NOARL West
Monterey, California

The traditional climatology track forecast aid has been developed for use on a desktop PC. The aid uses a global climatology data base from 1945 to present. New best track information can easily be added to the data base. A graphical display shows the past positions used in formulating the forecast. This facilitates evaluation of the fit of the climatology to the forecast track.

TROPICAL CYCLONES AFFECTING TAIWAN

Capt. Bruce Thompson, USAF
Joint Typhoon Warning Center

The study done by Brand and Blelloch in 1973 on the climatology of tropical cyclones affecting Taiwan has been updated using computer processing and a significantly larger data set. It examines tropical cyclone intensity change, speed of movement change, tracks, and occurrence. It provides a guide to the satellite analysts and typhoon forecasters for forecasting changes in intensity and motion of tropical cyclones interacting with Taiwan.

NEW METHODS IN FORECASTING INTENSITY OF TROPICAL CYCLONES

Capt. Bruce Thompson, USAF
Joint Typhoon Warning Center

New methods have been developed to assist typhoon forecasters with intensity forecasts using the NOGAPS 200-mb prognostic charts and intensity climatology. The 200-mb NOGAPS charts are used to assess the synoptic

pattern and determine if the tropical cyclone will move into a favorable or unfavorable area for intensification within the next 72 hours. The assessment generally considers the amount of vertical shear and outflow channel(s). In addition, a tropical cyclone climatology data base is used to develop a specially tailored intensity climatology for a specific tropical cyclone. The intensity climatology can be stratified by time of year, latitude, longitude, intensity trend, and a number of other parameters. Using the 200-mb NOGAPS prognostic charts and the intensity climatology, the "normal" one T-number per day intensification scheme developed by Dvorak (1984) can be modified to produce a customized intensity forecast.

A CLIMATOLOGY OF VERY INTENSE TYPHOONS: OR WHERE HAVE ALL THE SUPER TYPHOONS GONE?

LT. R. H. Bouchard, USN
Joint Typhoon Warning Center

Introduction. The term super typhoon is a classification applied to tropical cyclones that reach 130 kt sustained one-minute average wind speed. The term is not a World Meteorological Organization (WMO) standard, but is used by JTWC. A Climatological Study of Super Typhoons was published in the 1970 Annual Typhoon Report (ATR, the predecessor of the ATCR) (JTWC, 1970), and included the years 1959-1970. Figures from that climatological study have been republished in various individual storm write-ups in succeeding ATR's/ATCR's and the study is frequently used in intensity forecasting. This article provides a long-needed update to the earlier study.

At the outset such an update seemed fairly simple. By using an interactive climatology of tropical cyclones of the western North Pacific developed by the Technique Development Group, Detachment 1, First Weather Wing, all tropical cyclones meeting the 130-kt criterion from 1971 through 1988 where identified. The 1970 Study identified 70 super typhoons during the period 1959-1970 for an average of 5.8 per year. The 1989 climatological search identified 48 for the period 1971-1988 for an average of 2.7 - less than half the number for the earlier period. Where had all the super typhoons gone?

Background. The 1970 Study identified super typhoons by applying the equation developed by Fletcher (1955) which correlated maximum sustained winds with recorded minimum sea-level pressure. The equation gives 944 mb as the equivalent sea-level pressure corresponding to 130 kt. Since aircraft estimates of surface wind speeds in excess of 100 kt are subjective, the conservative nature of sea-level pressure makes it the optimum parameter to use in classifying super typhoons.

The most often cited part of the 1970 Study is the figure depicting 5°x 5° squares containing the frequency of first occurrence of first super typhoon intensity (Figure 6-1). The 1970 Study found two maxima between the Philippine and the northern Mariana Islands. The super typhoon maxima were downstream from the minimum sea-level pressure double maxima found by Fung (1970). The 1970 Study also showed that super typhoon occurrence was normally distributed about the peak reached in September.

Subsequently Atkinson and Holliday (1975) developed a relationship between tropical cyclone minimum sea-level pressure and maximum sustained winds. That relationship (reinforced by the results of (Lubeck and Shewchuck (1980))has become the standard relationship used by JTWC since. That relationship equates 130 kt with approximately 910 mb.

Pressure was routinely available because of the availability of aircraft reconnaissance. Gradually satellite surveillance augmented, and ultimately, replaced aircraft reconnaissance in 1987. Subsequent determinations of intensity have been made either by satellite imagery using the procedures of Dvorak (1973, 1984), or by the occasional surface observation. Because pressure was no longer measured, intensities where determined from the Dvorak scale and then converted to pressure using the Atkinson-Holliday relationship.

Methodology. Because of the advantage of using sea-level pressure cited by the 1970 Study, this study also used sea-level pressure to determine intensity. The Atkinson-Holliday threshold of 910 mb was used as the criterion for selecting super typhoons. However, because the term super typhoon is based on intensities of at least 130 kt, the term - Very Intense Typhoons (VIT) will be used in this study to indicate the use of pressure vice wind criteria.

Aircraft reconnaissance and satellite surveillance data were extracted from the Individual and Consolidated Typhoon Reports from 1950 through 1958 and the ATR's and ATCR's thereafter. Each instance of a tropical cyclone reaching a central pressure of 910 mb was classified as a VIT. No attempt was made to determine the location of the first occurrence of 910 mb to other than 5°x 5° square unless fix data crossed square boundaries. In those cases the fix data were linearly interpolated to locate the appropriate square. If only aircraft fix data were available, either the measured central pressure from dropsonde data, or a derived-pressure obtained from the relationship:

$$SLP = 645 + .115\,x$$

x = *700 mb height in meters*

was used. When aircraft data became scarce, the first occurence of super typhoon intensity was equated to 910 mb using satellite derived intensities and the Atkinson-Holliday relationship.

Results. By using the more restrictive criterion of 910 mb, 83 tropical cyclones were classified as VIT's for the period 1950 through

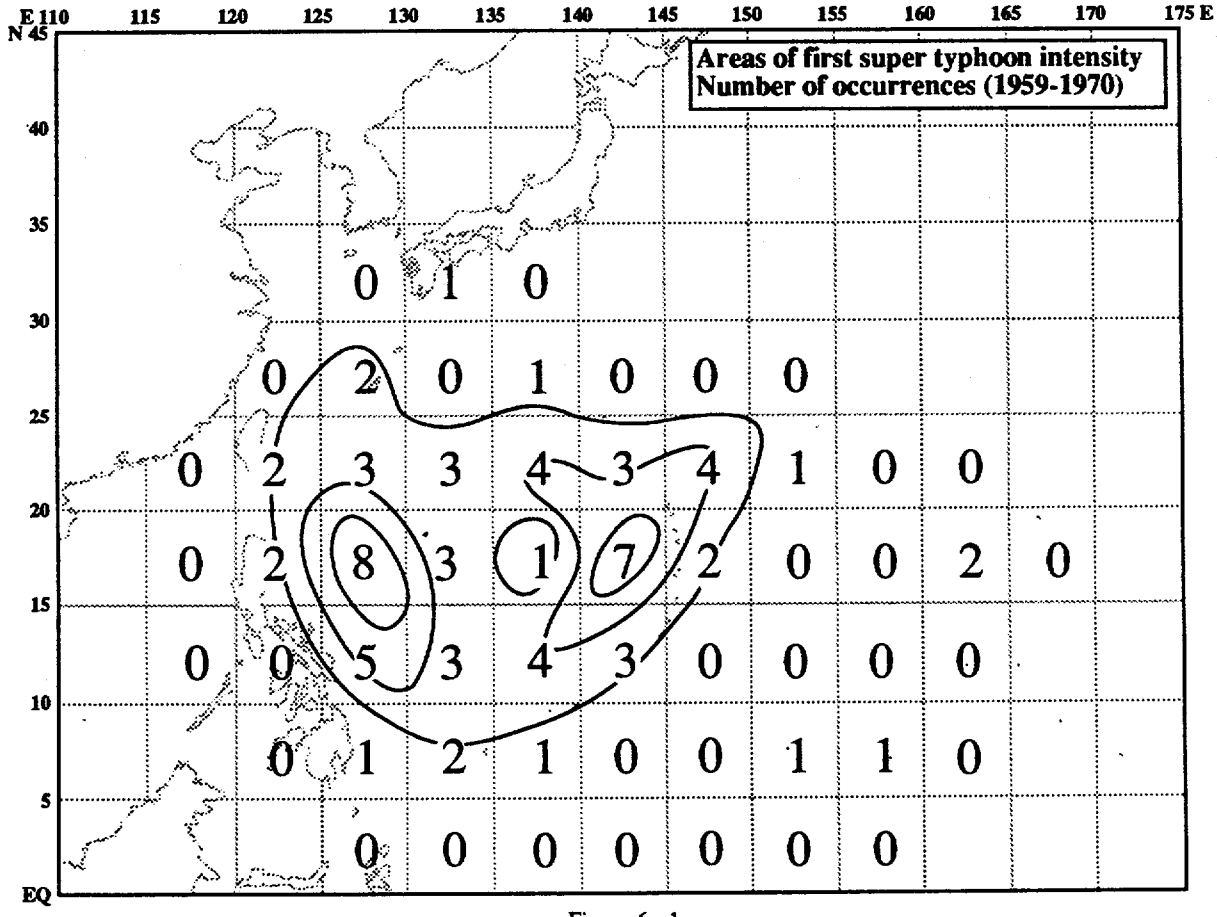

Figure 6 - 1

1989. This is an average of 2.2 per year. While the double maxima is no longer evident (Figure 6-2), an axis of maximum occurrence remains between 15°- 20° north latitudes. The primary area is west of 135°. The axis of maximum occurrence corresponds to the axis of the Sub-Equatorial Ridge (SER) and is east of the East Asian Trough (EAT) (Guard, 1977).

The 1970 Study had found super typhoons normally distributed about a peak in September. The peak in VIT occurrence is in October (Figures 6-3 and 6-4).

There appears to be some consistency in the VIT classification. Despite the changing fix platforms and procedures, the decadal average of VIT's remains relatively constant with the 60's being a below average decade and the 80's an above average decade and the 50's and 70's near average (Figure 6-5). However, since 1975 at least one VIT has occurred every year. This may be attributable to the the advent of the operational availability of satellite derived intensities (Dvorak, 1973).

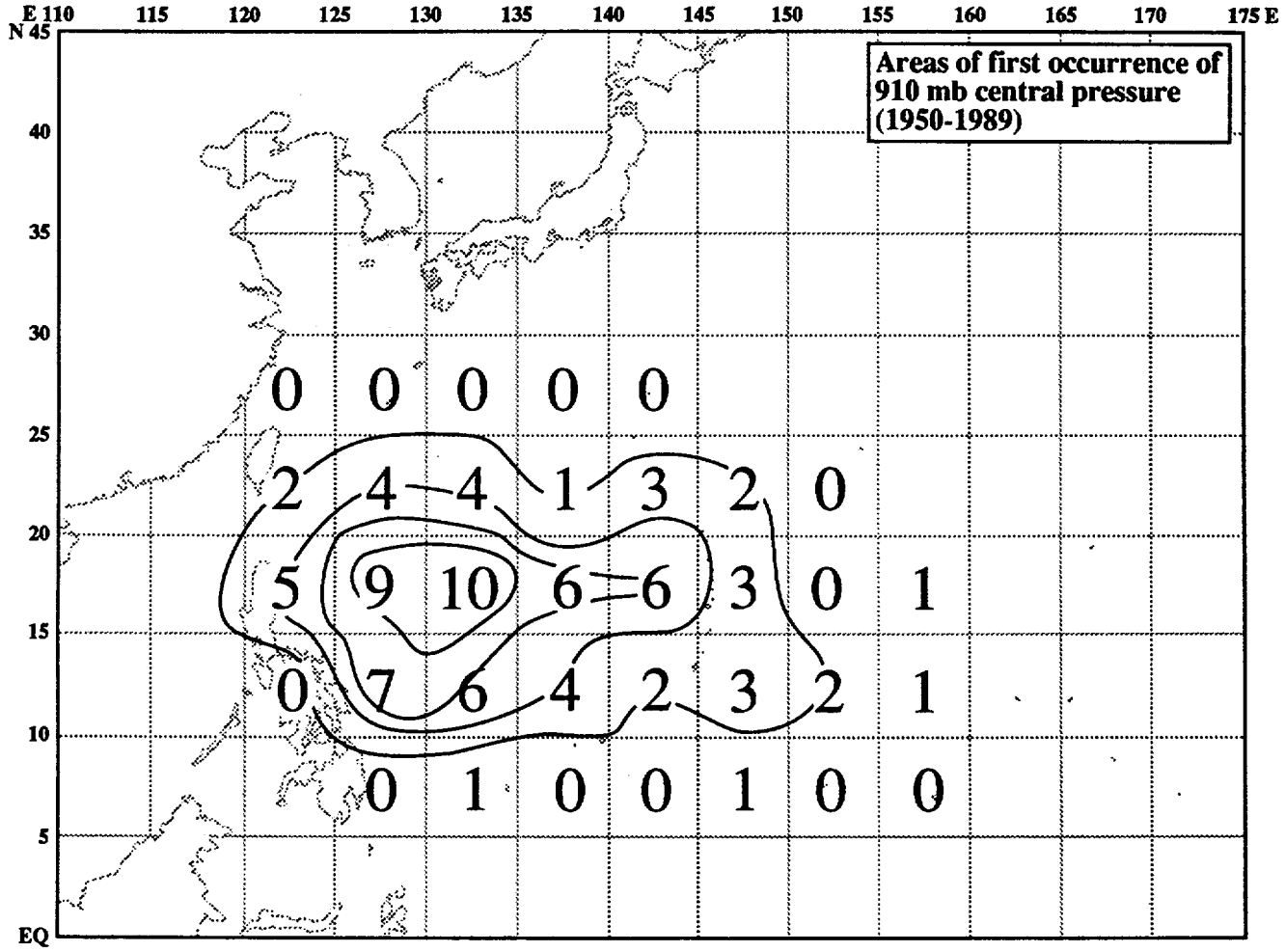

Figure 6 - 2

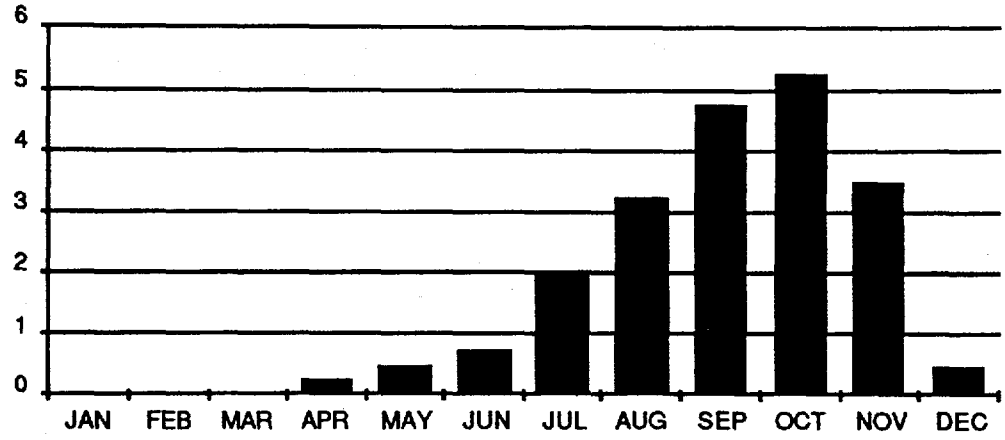

Figure 6 - 3

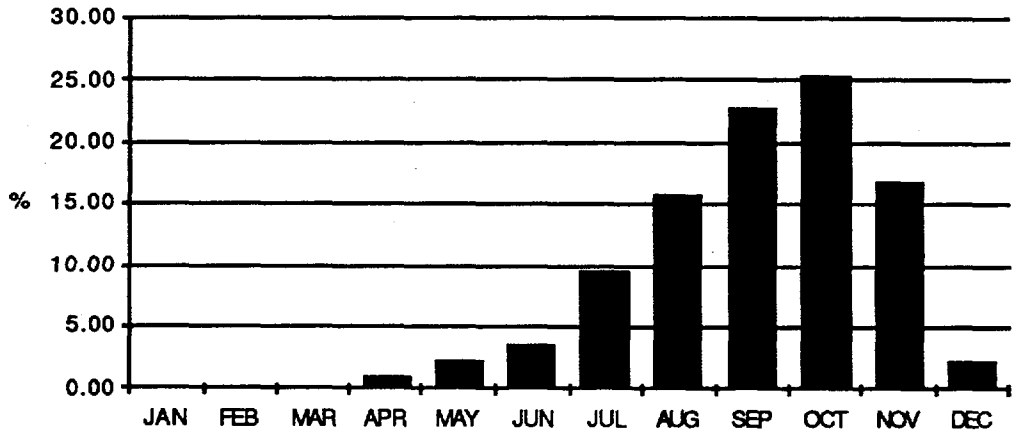

Figure 6 - 4

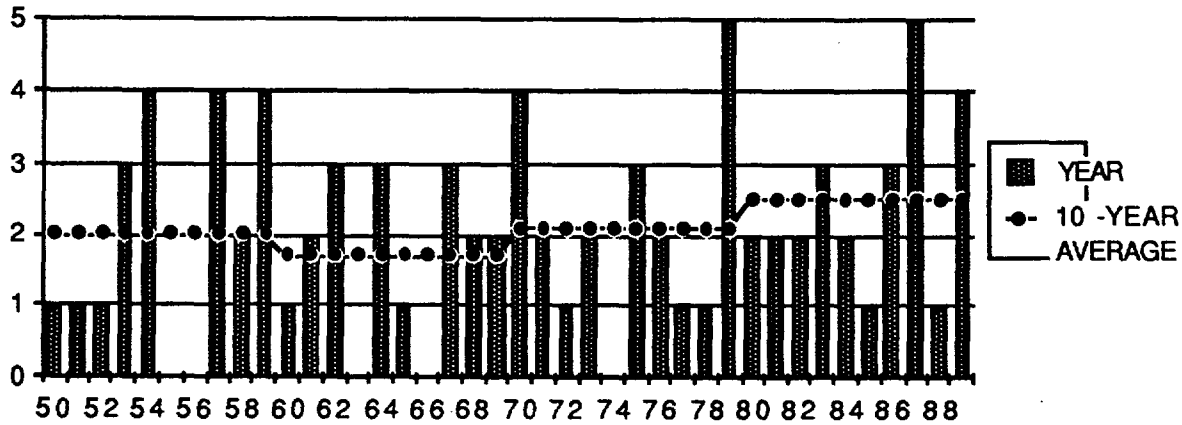

Figure 6 - 5

BIBLIOGRAPHY

Allen, R. L., 1984: COSMOS: CYCLOPS Objective Steering Model Output Statistics. Postprints, 15th Conference on Hurricanes and Tropical Meteorology. Miami, FL, January 9-13, 1984, pp. 14-20.

Atkinson, G. D. and C. R. Holliday, 1977: Tropical Cyclone Minimum Sea-Level Pressure and Maximum Sustained Wind Relationship for the Western North Pacific. *Monthly Weather Review*, Vol. 105, No. 4, pp. 421-427 (also FLEWEACEN TECH NOTE: JTWC 75-1).

Brand, S., 1970: Interaction of Binary Tropical Cyclones of the Western North Pacific Ocean. *Journal of Applied Meteorology*, Vol. 9, pp. 433-441.

Brand, S. and J. W. Blelloch, 1973: Changes in the Characteristics of Typhoons Crossing the Island of Taiwan. ENVPREDRSCHFAC Technical Paper No. 8-73, 21 pp.

Brand, S. and C. P. Guard, 1978: Extratropical Storm Evolution from Tropical Cyclones in the Western North Pacific Ocean. NAVENVPREDRSCHFAC, TR78-02, 24 pp.

Diercks, J. M., R. C. Weir and M. K. Kopper, 1982: Forecast Verification and Reconnaissance Data for Southern Hemisphere Tropical Cyclones (July 1980 through June 1982). NAVOCEANCOMCEN/JTWC TECH NOTE 82-1, 77 pp.

Dong, K. and C. J. Neumann, 1983: On the Relative Motion of Binary Tropical Cyclones. *Monthly Weather Review*, Vol. 111, pp. 945-953.

Dunnavan, G. M., 1981: Forecasting Intense Tropical Cyclones Using 700 mb Equivalent Potential Temperature and Central Sea-Level Pressure. NAVOCEACOMCEN/JTWC TECH NOTE 81-1, 12 pp.

Dvorak, V.F., 1973: A Technique for the Analysis and Forecasting of Tropical Cyclone Intensities from Satellite Pictures. NOAA Technical-memorandum NESS45, 19pp.

Dvorak, V. F., 1984: Tropical Cyclone Intensity Analysis Using Satellite Data. NOAA Technical Report NESDIS 11, U. S. Department of Commerce, National Oceanic and Atmospheric Administration, National Earth Satellite Service, Washington, D. C., 20233, 46 pp.

Fletcher, R., 1955: Computation of Maximum Winds in Hurricanes. *Bulletin of the American Meteorological Society*, 36, pp. 247-250.

Guard, C. P., 1983: A Study of Western North Pacific Tropical Storms and Typhoons that Intensify after Recurvature. 1WW/TN-83/002, 28 pp.

Herbert, P. H. and K. O. Poteat, 1975: A Satellite Classification Technique for Subtropical Cyclones. NOAA Technical Memorandum NWS SR-83, 25 pp.

Holland, G. R., 1980: An Analytical Model of Wind and Pressure Profiles in Hurricanes. *Monthly Weather Review*, Vol. 108, No. 8, pp. 1212-1218.

Holliday, C. R. and A. H. Thompson, 1979: Climatological Characteristics of Rapidly Intensifying Typhoons. *Monthly Weather Review*, Vol. 107, pp. 1022-1034.

Lewis, B.M. and H.F. Hawkins, 1982: Polygonal Eye Walls and Rainbands in Hurricanes. *Bulletin of the American Meteorological Society*, Vol. 63, No. 11, pp. 1294-1300.

Matsumoto, C. R., 1984: A Statistical Method for One-to Three-Day Tropical Cyclone Track Prediction. Atmospheric Science Paper 379, Department of Atmospheric Science, Colorado State University, Fort Collins, Colorado, 201 pp.

Sadler, J. C., 1974: A Role Of Tropical Upper Tropospheric Trough in the Early Season Typhoon Development. NAVENVPREDRSCHFAC Technical Paper No. 2-76, 104 pp.

Sadler, J. C., 1979: Tropical Cyclone Initiation by the Upper-Tropospheric Trough. Naval Environmental Prediction Research Facility Technical Paper No. 2-76, 103 pp.

Sikora, C. R., 1976: A Reevaluation of the Changes in Speed and Intensity of Tropical Cyclones Crossing the Philippines, FLEWEACEN TECH NOTE: JTWC 76-2, 11 pp.

Takemura, Y., 1989: Improved Utilization of Satellite Imagery in Tropical Cyclone Observation. Part I of paper for Economic and Social Commission for Asia and the Pacific and the World Meteorological Organization, Typhoon Committee, Tokyo, pp. 1-10.

Tsui, T. L. and R. J. Miller, 1986: Evaluation of JTWC Tropical Cyclone Objective Forecast Aids (1978-85). Naval Environmental Prediction Research Facility Technical Report, TR 86-05, 44 pp.

Wirfel, W. P. and S. A. Sandgathe, 1986: Forecast Verification and Reconnaissance Data for Southern Hemisphere Tropical Cyclones (July 1982 through June 1984). NAVOCEANCOMCEN/JTWC TECH NOTE 86-1, 102 pp.

Xu, Y. and C. J. Neumann, 1985: A Statistical Model for the Prediction of Western North Pacific Tropical Cyclone Motion. NOAA Technical Memorandum NWS NHC 28, 30 pp.

APPENDIX A
DEFINITIONS

BEST TRACK - A subjectively smoothed path, versus a precise and very erratic fix-to-fix path, used to represent tropical cyclone movement.

CENTER - The vertical axis or core of a tropical cyclone. Usually determined by cloud vorticity patterns, wind and/or pressure distribution.

EPHEMERIS - Position of a body (satellite) in space as a function of time; used for gridding satellite imagery. Since ephemeris gridding is based solely on the predicted position of the satellite, it is susceptible to errors from vehicle wobble, orbital eccentricity and the oblateness of the Earth.

EXPLOSIVE DEEPENING - A decrease in the minimum sea-level pressure of a tropical cyclone of 2.5 mb/hr for 12 hours or 5.0 mb/hr for six hours (Dunnavan, 1981).

EXTRATROPICAL - A term used in warnings and tropical summaries to indicate that a cyclone has lost its "tropical" characteristics. The term implies both poleward displacement from the tropics and the conversion of the cyclone's primary energy source from the release of latent heat of condensation to baroclinic processes. It is important to note that cyclones can become extratropical and still maintain winds of typhoon or storm force.

EYE - The central area of a tropical cyclone when it is more than half surrounded by wall cloud.

FUJIWHARA EFFECT - A binary interaction where tropical cyclones within about 750 nm (1390 km) of each other begin to rotate about one another. When tropical cyclones are within about 400 nm (740 km) of each other, they may also begin to be drawn closer to one another (Brand, 1970) (Dong and Neumann, 1983).

INTENSITY - The maximum sustained 1-minute mean surface wind speed, typically within one degree of the center of a tropical cyclone.

MAXIMUM SUSTAINED WIND - The highest surface wind speed averaged over a one-minute period of time. (Peak gusts over water average 20 to 25 percent higher than sustained winds.)

RAPID DEEPENING - A decrease in the minimum sea-level pressure of a tropical cyclone of 1.75 mb/hr or 42 mb for 24-hours (Holliday and Thompson, 1979).

RECURVATURE - The turning of a tropical cyclone from an initial path toward the west and poleward to east and poleward.

SIGNIFICANT TROPICAL CYCLONE - A tropical cyclone becomes "significant" with the issuance of the first numbered warning by the responsible warning agency.

SIZE - The areal extent of a tropical cyclone, usually measured radially outward from the center to the outermost closed isobar.

STRENGTH - The average wind speed of the surrounding low-level wind flow, usually measured within one to three degrees of the center of a tropical cyclone.

SUBTROPICAL CYCLONE - a low pressure system that forms over the ocean in the subtropics and has some characteristics of a tropical circulation, but not a central dense overcast. Although of upper cold low or low-level baroclinic origins, the system can transition to a tropical cyclone.

SUPER TYPHOON - A typhoon with maximum sustained 1-minute mean surface winds of 130 kt (67 m/sec) or greater.

TROPICAL CYCLONE - A non-frontal, migratory low-pressure system, usually of synoptic scale, originating over tropical or subtropical waters and having a definite organized circulation.

TROPICAL DEPRESSION - A tropical cyclone with maximum sustained 1-minute mean surface winds of 33 kt (17 m/sec) or less.

TROPICAL DISTURBANCE - A discrete system of apparently organized convection, generally 100 to 300 nm (185 to 555 km) in diameter, originating in the tropics or subtropics, having a non-frontal, migratory character and having maintained its identity for 12- to 24-hours. It may or may not be associated with a detectable perturbation of the wind field. It is the basic generic designation which, in successive stages of development, may be classified as a tropical depression, tropical storm, typhoon or super typhoon.

TROPICAL STORM - A tropical cyclone with maximum sustained surface winds in the range of 34 to 63 kt (17 to 32 m/sec) inclusive.

TROPICAL UPPER-TROPOSPHERIC TROUGH (TUTT) - A dominant climatological system and a daily upper-level synoptic feature of the summer season, over the tropical North Atlantic, North Pacific and South Pacific Oceans (Sadler, 1979).

TYPHOON (HURRICANE) - A tropical cyclone with maximum sustained 1-minute mean surface winds of 64 to 129 kt (33 to 66 m/sec). West of 180 degrees longitude they are called typhoons and east of 180 degrees longitude hurricanes.

WALL CLOUD - An organized band of cumuliform clouds that immediately surrounds the central area of a tropical cyclone. The wall cloud may entirely enclose or partially surround the center.

APPENDIX B

NAMES FOR TROPICAL CYCLONES IN THE WESTERN NORTH PACIFICAND SOUTH CHINA SEA

Column 1	Column 2	Column 3	Column 4
ANGELA	ABE	AMY	AXEL
BRIAN	BECKY	BRENDAN	BOBBIE
COLLEEN	CECIL	CAITLIN	CHUCK
DAN	DOT	DOUG	DEANNA
ELSIE	ED	ELLIE	ELI
FORREST	FLO	FRED	FAYE
GAY	GENE	GLADYS	GARY
HUNT	HATTIE	HARRY	HELEN
IRMA	IRA	IVY	IRVING
JACK	JEANA	JOEL	JANIS
KORYN	KYLE	KINNA	KENT
LEWIS	LOLA	LUKE	LOIS
MARIAN	*MANNY	MIREILLE	MARK
NATHAN	NELL	NAT	NINA
OFELIA	OWEN	ORCHID	OMAR
PERCY	PAGE	PAT	POLLY
ROBYN	RUSS	RUTH	RYAN
STEVE	SHARON	SETH	SIBYL
TASHA	TIM	THELMA	TED
VERNON	VANESSA	VERNE	VAL
WINONA	WALT	WILDA	WARD
YANCY	YUNYA	YURI	YVETTE
ZOLA	ZEKE	ZELDA	ZACK

* The name Manny replaces Mike which was retired due to the impact of Super Typhoon Mike (27W).

NOTE: Names are assigned in rotation and alphabetically. When the last name in Column 4 (ZACK) has been used, the sequence will begin again with the first name in Column 1 (ANGELA).

SOURCE: CINCPACINST 3140.1T

APPENDIX C
CONTRACTIONS

AB	Air Base
ABIO	Significant Tropical Weather Advisory for the Indian Ocean
ABPW	Significant Tropical Weather Advisory for the Western Pacific Ocean
ACFT	Aircraft
ADP	Automated Data Processing
AFB	Air Force Base
AFGWC	Air Force Global Weather Central
AFTN	Airfield Fixed Telecommuncation Network
AIREP	Aircraft (Weather) Report (Commercial and Military)
AMOS	Automatic Meteorological Observing Station
AOR	Area of Responsibility
APT	Automatic Picture Transmission
ARGOS	International Service for Drifting Buoys
ATCF	Automated Tropical Cyclone Forecast System
ATCM	Advanced Tropical Cyclone Model
AUTODIN	Automated Digital Network
AWDS	Automated Weather Distribution System
AWN	Automated Weather Network
CCWF	Combined Confidence Wieghted Forecast
CDO	Central Dense Overcast
CI	Cirriform Cloud or Cirrus (or) Current Intensity (Dvorak)
CINCPAC	Commander-in-Chief Pacific AF - Air Force, FLT - Navy
CLD	Cloud
CLIM	Climatology
CLIP or CLIPER	Climatology and Persistence Technique
CM	Centimeter(s)
CNOC	Commander Naval Oceanography Command
COSM or COSMOS	Cyclops Objective Steering Model Output Statistics
CPA	Closest Point of Approach
CPHC	Central Pacific Hurricane Center
CSC	Cloud System Center
CSUM	Colorado State University Model
CYCLOPS	Tropical Cyclone Steering Program (HATTRACK and MOHATT)
DDN	Defense Data Network
DEG	Degree(s)
DFS	Digital Facsimile System
DMSP	Defense Meteorological Satellite Program
DOD	Department of Defense
DSAT	Digital Satellite Acquitition System
DSN	Defense Switched Network
DWIPS	Digital Weather Image Processing System
FBAM	FNOC Beta Advection Model
FI	Forecast Intensity (Dvorak)
FNOC	Fleet Numerical Oceanography Center
FT	Feet
GMT	Greenwich Mean Time
GOES	Geostationary Operational Environmental Satellite
GTS	Global Telecommunications System
HATTRACK	Hurricane and Typhoon Tracking and Steering Program
HPAC	Mean of XTRP and CLIM Techniques (Half Persistence and Climatology)
HR	Hour(s)
ICAO	International Civil Aviation Organization
INIT	Initial
INST	Instruction
IR	Infrared
JTWC	Joint Typhoon Warning Center
KM	Kilometer(s)
KT	Knot(s)
LAN	Local Area Network
LLCC	Low-Level Circulation Center
LUT	Local User Terminal
LVL	Level
M	Meter(s)
MAX	Maximum
MB	Millibar(s)
MET	Meteorological
MIN	Minimum
MM	Millimeter(s)
MOHATT	Modified HATTRACK
MOVG	Moving
MSLP	Minimum Sea-level Pressure
NARDAC	Naval Regional Data Automation Center
NAS	Naval Air Station
NASA	National Aeronautics and Space Administration

NEDN	Naval Environmental Data Network
NEDS	Naval Environmental Display Station
NEPRF	Naval Environmental Prediction Research Facility
NESDIS	NationalEnvironmental Satellite, Data, an Information Service
NESN	Naval Environmental Satellite Network
NM	Nautical Mile(s)
NMC	National Meteorological Center
NOAA	National Oceanic and Atmospheric Administration
NOARL	Naval Oceanographic and Atmospheric Research Laboratory
NOCC	Naval Oceanography Command Center
NODDES	Naval Environmental Data Network Oceanographic Data Distribution and Expansion System
NODDS	Navy/NOAA Oceanographic Data Distribution System
NOGAPS	Navy Operational Global Atmospheric Prediction System
NRPS or NORAPS	Navy Operational Regional Atmospheric Prediction System
NSDS	Naval Satellite Display System
NSDS-G	Naval Satellite Display System - Geostationary
NWOC	Naval Western Oceanography Center
NWS	National Weather Service
NR	Number
NRL	Naval Research Laboratory
NTCC	Naval Telecommunications Center
OBS	Observations
ONR	Office of Naval Research
OTCM	One Way (Interactive) Tropical Cyclone Model
PACAF	Pacific Air Force
PACDIGS	Pacific Digital Information Graphics System
PACMEDS	Pacific Meteorological Data System
PACOM	Pacific Command
PCN	Position Code Number
PDN	Public Data Network
PIREP	Pilot Weather Report(s)
RADOB	Radar Observation
RECON	Reconnaissance
RRDB	Reference Roster Data Base
RSDB	Raw Satellite Data Base
SAT	Satellite
SEC	Second
SDHS	Satellite Data Handling System
SFC	Surface
SGDB	Satellite Global Data Base
SLP	Sea-Level Pressure
SSM/I	Special Sensor Microwave/ Imager
SST	Sea Surface Temperature
STNRY	Stationary
ST	Subtropical
STR	Subtropical Ridge
STY	Super Typhoon
TAPT	Typhoon Acceleration Prediction Technique
TC	Tropical Cyclone
TCFA	Tropical Cyclone Formation Alert
TCM-90	Tropical Cyclone Motion Field Experiment
TD	Tropical Depression
TDA	Typhoon Duty Assistant
TDO	Typhoon Duty Officer
TIROS	Television Infrared Observational Satellite
TOGA	Tropical Ocean Global Atmosphere
TS	Tropical Storm
TUTT	Tropical Upper-Tropospheric Trough
TY	Typhoon
TYAN	Typhoon Analog (Program)
TYMNET	Time-Sharing Network: Commercial wide area network connecting micro- and main-frame computers
ULAC	Upper-Level Anticyclone
ULCC	Upper-Level Circulation Center
US	United States
USAF	United States Air Force
USN	United States Navy
UTC	Universial Time Coordinated
VIS	Visual
WESTPAC	Western (North) Pacific
WMO	World Meteorological Organization
WRNG	Warning(s)
WW	Weather Wing
XTRP	Extrapolation
Z	Zulu Time (UTC)

APPENDIX D

PAST ANNUAL TROPICAL CYCLONE REPORTS

Copies of the past Annual Tropical Cyclone Reports for DOD agencies or contractors can be obtained through:

Defense Technical Information Center
ATTN:FDAC
Cameron Station
Alexandria, VA.
22304-6145

Copies for non-DOD agencies or users can be obtained from:

National Technical Information Service
5285 Port Royal Road
Springfield, Virginia
22161

Refer to the following numbers when ordering:

YEAR	ACQUISITION NUMBER	YEAR	ACQUISITION NUMBER
1959	AD 786147	1975	AD A023601
1960	AD 786148	1976	AD A038484
1961	AD 786149	1977	AD A055512
1962	AD 786128	1978	AD A070904
1963	AD 786208	1979	AD A082071
1964	AD 786209	1980	AD A094668
1965	AD 786210	1981	AD A112002
1966	AD 785891	1982	AD A124860
1967	AD 785344	1983	AD A137836
1968	AD 785251	1984	AD A153395
1969	AD 785178	1985	AD A168284
1970	AD 785252	1986	AD A184082
1971	AD 768333	1987	AD A191883
1972	AD 768334	1988	AD A207206
1973	AD 777093	1989	AD A232469
1974	AD 010271		

APPENDIX E
DISTRIBUTION LIST

1 COPY
ANALYSIS AND PROCESSING CENTER, INDONESIA
BARRETT CONSULTING GROUP
BRUNEI SHELL PETROLEUM CO
CATHOLIC UNIVERSITY OF AMERICA
CAF WEATHER CENTRAL, TAIWAN
CENTRAL MET OBSERVATORY, BEIJING
CENTRAL METEOROLOGICAL OFFICE, SEOUL
CHULALONGKORN UNIVERSITY, BANGKOK
CHUNG CHENG INSTITUTE, TAIWAN
CITIES SERVICES OIL GAS CORP
CITY POLYTECHNIC OF HONG KONG
CIUDAD UNIVERSITARIA, MEXICO
CIVIL DEFENSE, BELAU
CIVIL DEFENSE, MAJURO
CIVIL DEFENSE, POHNPEI
CIVIL DEFENSE, SAIPAN
CIVIL DEFENSE, TRUK
CIVIL DEFENSE, YAP
CINCPACFLT
CNO (OP-096)
CNO (OP-096T)
CNO (OP-981D)
CNO (OP-943G)
COLORADO STATE UNIVERSITY LIBRARY
COMMONWEALTH NORTHERN MARIANAS ISLANDS
COMNAVFOR PHILIPPINES
COMNAVMAR
COMNAVOCEANCOM
COMNAVSURFGRU WESTPAC
COMNAVSURFPAC
COMPATRECFOR
COMPHIBGRU ONE
COMSC
COMSEVENTHFLT
COMSPAWARSYSCOM
COMSUBGRU SEVEN
COMTHIRDFLT
CONGRESSIONAL INFORMATION SERVICE, MD
DCA GUAM
DET 2, 20 WS/CC
DET 4, 20 WS/CC
DET 5, 20 WS/CC
DET 7, 20 WS/CC
DET 8, 20 WS/CC
DET 10, 30 WS/CC
DET 13, 20 WS/CC
DET 15, 30 WS/CC
DET 18, 30 WS/CC
DET 19, 30 WS/CC
DET 20, 30 WS/CC
DISASTER CONTROL OFFICE, SAIPAN
ECMWF, BERKSHIRE, UK
FAIRECONRON ONE
FIJI METEOROLOGICAL SERVICE
GEOLOGICAL FLUID DYNAMICS LAB, PRINCETON, NJ
GEOLOGICAL SURVEY, GUAM
GEOPHYSICS LAB/LYS
GIFU METEOROLOGICAL OFFICE, JAPAN
GODDARD SPACE FLIGHT CENTER
GUAM COMMUNITY COLLEGE
GUAM PUBLIC LIBRARY
HORIZON MARINE, INC
HQ AWS/DO
HQ AWS/DOOF
HQ AWS/XT
HQ MAC/DOOS
HQ USAF/XOORZ
HUGHES AIRCRAFT CO
INDIAN INSTITUTE OF TROPICAL METEOROLOGY
INSTITUO DE GEOFISICA, MEXICO
JAPAN AIR LINES
JCS ENV SERVICES DIV (J3(OES))
JET PROPULSION LAB, PASADENA
LISD CAMP SPRINGS CENTER, MD
LOS ANGELES PUBLIC LIBRARY
MAURITIUS METEOROLOGICAL SERVICE
MASS INST OF TECH
MCAS FUTENMA
MCAS IWAKUNI
MCAS KANEOHE BAY HI
METEOROLOGICAL DEPARTMENT, PAKISTAN
METEOROLOGICAL OFFICE, BRACKNELL
METEOROLOGICAL SERVICE, FRENCH POLYNESIA
METEOROLOGICAL SERVICE, MAURITIUS
METEOROLOGICAL SERVICE, REUNION
METEOROLOGY SOCIETY OF NEW SOUTH WALES, AUST
MIL ASST ENV SCI (R & AT / E &LS)
MOBIL OIL GUAM, INC
MONASH UNIVERSITY, AUSTRALIA
MOUNTAIN STATES WEATHER SERVICES
NASA
NATIONAL DATA BUOY CENTER
NATIONAL METEOROLOGICAL CENTER
NATIONAL RESOURCES INSTITUTE, INC
NATIONAL TAIWAN UNIVERSITY
NATIONAL TECHNICAL INFORMATION SERVICE
NATIONAL WEATHER SERVICE, PAPUA NEW GUINEA
NAVAL ACADEMY
NAVAL CIVIL ENG LAB, PORT HUENEME, CA
NAVAL RESEARCH LAB
NAVEASTOCEANCEN NORFOLK
NAVHISTCEN
NAVOCEANCOMCEN ROTA
NAVOCEANCOMDET AGANA
NAVOCEANCOMDET ALAMEDA
NAVOCEANCOMDET ASHEVILLE
NAVOCEANCOMDET ATSUGI
NAVOCEANCOMDET BARBERS POINT
NAVOCEANCOMDET KADENA
NAVOCEANCOMDET MONTEREY
NAVOCEAN COMFAC JACKSONVILLE
NAVOCEANCOMFAC YOKOSUKA
NAVOCEANO
NAVAL POST GRADUATE SCHOOL LIBRARY
NAVPOLAROCEANCEN SUITLAND
NEW ZEALAND MET SERVICE
NOAA/ACQUISITION SECTION, ROCKVILLE, MD
NOAA/AOML, HRD, MIAMI, FL
NOAA/HYDROMETEOROLOGY BR, SILVER SPRINGS, MD
NOAA/NESDIS, HONOLULU, HI
WEATHER SERVICE FORECAST OFFICE REDWOOD CITY, CA
NOAA/PMEL, SEATTLE, WA

NOAA ENVIRONMENTAL RESEARCH LAB
NOAA LIBRARY, SEATTLE, WA
NOARL ATMOSPHERIC DIRECTORATE
NOBEL DENTON
OCEANO SERVICES INC. LIBRARY
OCEANWEATHER, INC.
OFFICE OF FEDERAL COORDINATOR METEOROLOGY
OFFICE OF NAVAL RESEARCH
OFFICE OF THE NAVAL DEPUTY, NOAA
PACAF/DOW
PACAF/WSU
PACIFIC STARS & STRIPES
PACNAVFACENGCOM
PENNSYLVANIA STATE UNIVERSITY
REUNION METEOROLOGICAL SERVICE
RUCH WEATHER SERVICE, INC
SAINT LOUIS UNIVERSITY
SAT APPL LAB, NOAA/NESDIS, WASHINGTON, DC
SHANGHAI TYPHOON INSTITUTE
SRI LANKA METEOROLOGICAL SOCIETY
SRI LIBRARY
TAO PROJECT OFFICE
TEXAS A & M UNIVERSITY
UNIVERSITY OF CHICAGO
UNIVERSITY OF GUAM, BIOLOGY DEPT
UNIVERSITY OF HAWAII LIBRARY
UNIVERSITY OF WASHINGTON
USAFETAC/DN
USCINCPAC
USCINCPAC REP GUAM
USCINCPAC REP FIJI
USCINCPAC REP PHILIPPINES
USNA (OCEANOGRAPHY DEPT/LIBRARY)
USS AMERICA (CV 66)
USS BELLEAU WOOD (LHA 3)
USS CARL VINSON (CVN 70)
USS CONSTELLATION (CV 64)
USS CORAL SEA (CV 43)
USS EISENHOWER (CVN 69)
USS ENTERPRISE (CVN 65)
USS FORRESTAL (CV 59)
USS INDEPENDENCE (CV 62)
USS J. F. KENNEDY (CV 67)
USS KITTY HAWK (CV 63)
USS LINCOLN (CVN 72)
USS MIDWAY (CV 41)
USS MISSOURI (BB 63)
USS NEW JERSEY (BB 62)
USS NEW ORLEANS (LPH 11)
USS NIMITZ (CVN 68)
USS OKINAWA (LPH 3)
USS PELELIU (LHA 5)
USS RANGER (CV 61)
USS SARATOGA (CV 60)
USS TARAWA (LHA 1)
USS TRIPOLI (LPH 10)
USS T. ROOSEVELT (CVN 71)
USS WISCONSIN (BB 64)
VANUATU METEOROLOGICAL SERVICE
WORLD DATA CENTER B1, MOSCOW
AFGWC/WFM
5WW/CC
7WW/OL-A
9WS/DO
20 WS/DO
30WS/DO
3350 TCHTG/TTMV-S

2 COPIES
AFGWC/WFMP
AWS TECH LIBRARY
BUREAU OF METEOROLOGY, BRISBANE
BUREAU OF METEOROLOGY, DARWIN
BUREAU OF METEOROLOGY, MELBOURNE
BUREAU OF METEOROLOGY, PERTH
BUREAU OF PLANNING, GUAM
CIVIL DEFENSE, GUAM
DEFENSE TECHNICAL INFORMATION CENTER
DEPARTMENT OF COMMERCE
ESCAP LIBRARY, BANGKOK
FLENUMOCEANCEN MONTEREY
FLORIDA STATE UNIVERSITY
HQ AWS GP, JAPAN
INSTITUTE OF PHYSICS, TAIWAN
MARATHON OIL CO, TX
MARINERS WEATHER LOG
MET RESEARCH INST LIBRARY, TOKYO
MICRONESIAN RESEARCH CENTER UOG, GUAM
NATIONAL CLIMATIC DATA CENTER
NATIONAL METEOROLOGICAL LIBRARY,
BRACKNELL, UK
NATIONAL WEATHER SERVICE, HONOLULU
NAVOCEANCOMDET DIEGO GARCIA
NAVOCEANCOMDET MISAWA
NAVOCEANCOMFAC CUBI PT
NAVWESTOCEANCEN PEARL HARBOR
NOAA CORAL GABLES LIBRARY
NOAA GUAM
NORA 1570 DALLAS, TX
OKINAWA METEOROLOGY OBSERVATORY
SAT APPL LAB, NOAA/NESDIS, CAMP SPRINGS, MD
TYPHOON COM SECR, MANILA
UNIVERSITY OF PHILIPPINES
US ARMY, FORT SHAFTER
WORLD DATA CENTER A, NOAA
1WW/DN
17 WS/DON
23 AF/HQ
73 WEATHER GROUP, ROK AF

3 COPIES
CENTRAL WEATHER BUREAU, TAIWAN
INDIA METEOROLOGICAL DEPT
INOSHAC, DDGM (WF)
JAPAN METEOROLOGICAL AGENCY
NATIONAL HURRICANE CENTER, MIAMI
NAVPGSCOL DEPT OF METEOROLOGY
UNIVERSITY OF HAWAII, METEOROLOGY DEPT
WEATHER CENTRAL, CAF

4 COPIES
COLORADO STATE UNIVERSITY
METEOROLOGY DEPT, BANGKOK

5 COPIES
PAGASA WEATHER BUREAU, RP
R & D UNIT, NHC, MIAMI
ROYAL OBSERVATORY HONG KONG

6 COPIES
NOARL WEST
NATIONAL WEATHER ASSOCIATION

UNCLASSIFIED
SECURITY CLASSIFICATION OF THIS PAGE

REPORT DOCUMENTATION PAGE

Form Approved
OMB No. 0704-0188

1a. REPORT SECURITY CLASSIFICATION UNCLASSIFIED	1b. RESTRICTIVE MARKINGS
2a. SECURITY CLASSIFICATION AUTHORITY	3. DISTRIBUTION/AVAILABILITY OF REPORT AS IT APPEARS IN THE REPORT? DISTRIBUTION UNLIMITED
2b. DECLASSIFICATION/DOWNGRADING SCHEDULE	
4. PERFORMING ORGANIZATION REPORT NUMBER(S)	5. MONITORING ORGANIZATION REPORT NUMBER(S)
6a. NAME OF PERFORMING ORGANIZATION NAVOCEANCOMCEN/JTWC 6b. OFFICE SYMBOL (If applicable)	7a. NAME OF MONITORING ORGANIZATION NAVOCEANCOMCEN/JTWC
6c. ADDRESS (City, State, and ZIP Code) COMNAVMAR BOX 12 FPO SAN FRANCISCO 96630-2926	7b. ADDRESS (City, State, and ZIP Code) COMNAVMAR BOX 12 FPO SAN FRANCISCO 96630-2926
8a. NAME OF FUNDING/SPONSORING ORGANIZATION NAVOCEANCOMCEN/JTWC 8b. OFFICE SYMBOL (If applicable)	9. PROCUREMENT INSTRUMENT IDENTIFICATION NUMBER
8c. ADDRESS (City, State, and ZIP Code) COMNAVMAR BOX 12 FPO SAN FRANCISCO 96630-2926	10. SOURCE OF FUNDING NUMBERS PROGRAM ELEMENT NO. / PROJECT NO. / TASK NO. / WORK UNIT ACCESSION NO.
11. TITLE (Include Security Classification) 1990 ANNUAL TROPICAL CYCLONE REPORT	
12. PERSONAL AUTHOR(S)	
13a. TYPE OF REPORT ANNUAL	13b. TIME COVERED FROM JAN 90 TO DEC 90
14. DATE OF REPORT (Year, Month, Day) 1990	15. PAGE COUNT 278 plus i thru vi
16. SUPPLEMENTARY NOTATION	

17. COSATI CODES		
FIELD	GROUP	SUB-GROUP
04	02	

18. SUBJECT TERMS (Continue on reverse if necessary and identify by block number)
TROPICAL CYCLONES
TROPICAL STORMS
TROPICAL DEPRESSIONS
TYPHOONS/SUPER TYPHOONS
TROPICAL CYCLONE RESEARCH
METEOROLOGICAL SATELLITES

19. ABSTRACT (Continue on reverse if necessary and identify by block number)

ANNUAL PUBLICATION SUMMARIZING TROPICAL CYCLONE ACTIVITY IN THE WESTERN NORTH PACIFIC, BAY OF BENGAL, ARABIAN SEA, WESTERN SOUTH PACIFIC AND SOUTH INDIAN OCEANS. A BEST TRACK IS PROVIDED FOR EACH SIGNIFICANT TROPICAL CYCLONE. A BRIEF NARRATIVE IS GIVEN FOR ALL TROPICAL CYCLONES IN THE WESTERN NORTH PACIFIC AND NORTH INDIAN OCEANS. ALL RECONNAISSANCE AND FIX DATA USED TO CONSTRUCT THE BEST TRACKS ARE PROVIDED, UPON REQUEST, ON FLOPPY DISKETTES. FORECAST VERIFICATION DATA AND STATISTICS FOR THE JOINT TYPHOON WARNING CENTER (JTWC) ARE SUBMITTED.

20. DISTRIBUTION/AVAILABILITY OF ABSTRACT ☒ UNCLASSIFIED/UNLIMITED ☒ SAME AS RPT. ☐ DTIC USERS	21. ABSTRACT SECURITY CLASSIFICATION UNCLASSIFIED
22a. NAME OF RESPONSIBLE INDIVIDUAL FRANK H. WELLS	22b. TELEPHONE (Include Area Code) 671-344-5240 / 22c. OFFICE SYMBOL NOCC/JTWC

DD Form 1473, JUN 86 *Previous editions are obsolete.*

BLOCK 18 CONTINUED

RADAR
AUTOMATIC METEOROLOGICAL OBSERVING STATIONS
SYNOPTIC DATA
TROPICAL CYCLONE INTENSITY
TROPICAL CYCLONE BEST TRACK DATA
TROPICAL CYCLONE FORECASTING
TROPICAL CYCLONE RECONNAISSANCE
TROPICAL CYCLONE STEERING MODELS
OBJECTIVE FORECASTING TECHNIQUES
TROPICAL CYCLONE FIX DATA
MICROWAVE IMAGERY
DRIFTING BUOYS

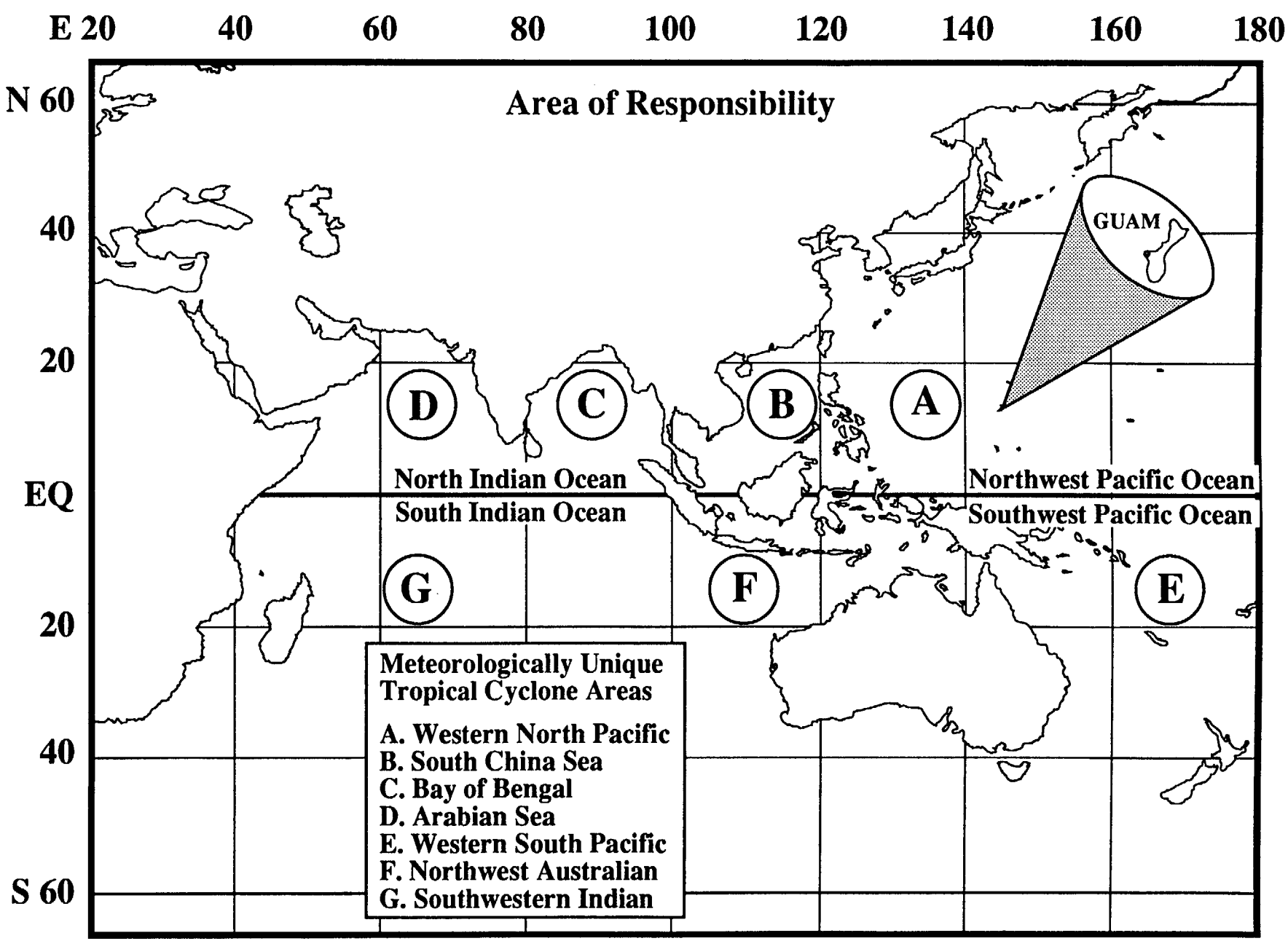
E 20
40
60
80
100
120
140
160
180
N 60
40
20
EQ
20
40
S 60
Area of Responsibility
GUAM
D
C
B
A
North Indian Ocean
South Indian Ocean
Northwest Pacific Ocean
Southwest Pacific Ocean
G
F
E
Meteorologically Unique
Tropical Cyclone Areas
A. Western North Pacific
B. South China Sea
C. Bay of Bengal
D. Arabian Sea
E. Western South Pacific
F. Northwest Australian
G. Southwestern Indian